frontiers | Research Topics

# Multiple abiotic stresses: Molecular, physiological, and genetic responses and adaptations in cereals

**Edited by**
Sindhu Sareen, Nabin Bhusal, Ranjeet Ranjan Kumar and Pradeep Sharma

**Published in**
Frontiers in Plant Science

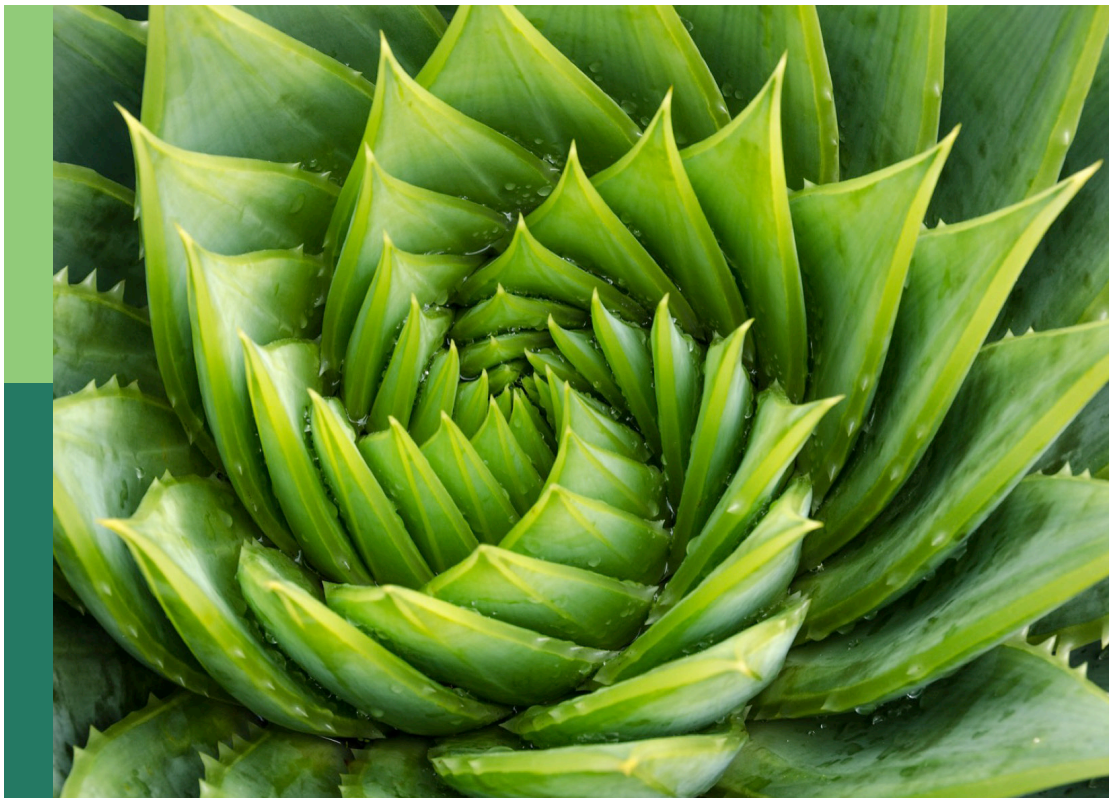

ISSN 1664-8714
ISBN 978-2-83251-831-1
DOI 10.3389/978-2-83251-831-1

## About Frontiers

Frontiers is more than just an open access publisher of scholarly articles: it is a pioneering approach to the world of academia, radically improving the way scholarly research is managed. The grand vision of Frontiers is a world where all people have an equal opportunity to seek, share and generate knowledge. Frontiers provides immediate and permanent online open access to all its publications, but this alone is not enough to realize our grand goals.

## Frontiers journal series

The Frontiers journal series is a multi-tier and interdisciplinary set of open-access, online journals, promising a paradigm shift from the current review, selection and dissemination processes in academic publishing. All Frontiers journals are driven by researchers for researchers; therefore, they constitute a service to the scholarly community. At the same time, the *Frontiers journal series* operates on a revolutionary invention, the tiered publishing system, initially addressing specific communities of scholars, and gradually climbing up to broader public understanding, thus serving the interests of the lay society, too.

## Dedication to quality

Each Frontiers article is a landmark of the highest quality, thanks to genuinely collaborative interactions between authors and review editors, who include some of the world's best academicians. Research must be certified by peers before entering a stream of knowledge that may eventually reach the public - and shape society; therefore, Frontiers only applies the most rigorous and unbiased reviews. Frontiers revolutionizes research publishing by freely delivering the most outstanding research, evaluated with no bias from both the academic and social point of view. By applying the most advanced information technologies, Frontiers is catapulting scholarly publishing into a new generation.

## What are Frontiers Research Topics?

Frontiers Research Topics are very popular trademarks of the *Frontiers journals series*: they are collections of at least ten articles, all centered on a particular subject. With their unique mix of varied contributions from Original Research to Review Articles, Frontiers Research Topics unify the most influential researchers, the latest key findings and historical advances in a hot research area.

Find out more on how to host your own Frontiers Research Topic or contribute to one as an author by contacting the Frontiers editorial office: frontiersin.org/about/contact

# Multiple abiotic stresses: Molecular, physiological, and genetic responses and adaptations in cereals

**Topic editors**

Sindhu Sareen — Indian Institute of Wheat and Barley Research (ICAR), India
Nabin Bhusal — Agriculture and Forestry University, Nepal
Ranjeet Ranjan Kumar — Division of Biochemistry, Indian Agricultural Research Institute (ICAR), India
Pradeep Sharma — Indian Institute of Wheat and Barley Research (ICAR), India

**Citation**

Sareen, S., Bhusal, N., Kumar, R. R., Sharma, P., eds. (2023). *Multiple abiotic stresses: Molecular, physiological, and genetic responses and adaptations in cereals*. Lausanne: Frontiers Media SA. doi: 10.3389/978-2-83251-831-1

# Table of contents

frontiers | Frontiers in Plant Science

TYPE Editorial
PUBLISHED 21 February 2023
DOI 10.3389/fpls.2023.1146326



OPEN ACCESS

EDITED BY
Luisa M. Sandalio,
Department of Biochemistry, Cell and Molecular Biology of Plants, (CSIC), Spain

REVIEWED BY
Rosa M. Rivero,
Center for Edaphology and Applied Biology of Segura (CSIC), Spain

*CORRESPONDENCE
Sindhu Sareen
sareen9@hotmail.com

SPECIALTY SECTION
This article was submitted to Plant Abiotic Stress, a section of the journal Frontiers in Plant Science

RECEIVED 17 January 2023
ACCEPTED 31 January 2023
PUBLISHED 21 February 2023

CITATION
Bhusal N, Sharma P, Kumar RR and Sareen S (2023) Editorial: Multiple abiotic stresses: Molecular, physiological, and genetic responses and adaptations in cereals. *Front. Plant Sci.* 14:1146326. doi: 10.3389/fpls.2023.1146326



# Editorial: Multiple abiotic stresses: Molecular, physiological, and genetic responses and adaptations in cereals

Nabin Bhusal[1], Pradeep Sharma[2], Ranjeet Ranjan Kumar[3] and Sindhu Sareen[2]*

[1]Department of Genetics & Plant Breeding, Agriculture and Forestry University, Bharatpur, Nepal, [2]Crop Improvement Division, Indian Institute of Wheat and Barley Research (ICAR), Karnal, India, [3]Division of Biochemistry, Indian Agricultural Research Institute (ICAR), New Delhi, India

KEYWORDS

**abiotic stress, molecular response, physiological response, genetic response, adaptation, cereals**

Editorial on the Research Topic
Multiple abiotic stresses: Molecular, physiological, and genetic responses and adaptations in cereals

Cereal crops provide approximately 40% of the energy and protein components of the human diet and are vital to the food security of the world (Dunwell, 2014). With the increasing incidence of global warming (expected 1.2–1.9°C higher than ambient during 2021–2040) and extreme weather events, the intensity of various climatic constraints is expected to accelerate, ultimately affecting global cereal crop production (IPCC, 2021). Most of the climatic constraints are abiotic stresses (drought, heat, cold, waterlogging, salinity, mineral deficiency, heavy metal stress, and ultraviolet-B (UV-B), etc.) causing extensive yield losses (Paul et al., 2019; Chaudhry and Sidhu, 2021; Rivero et al., 2022). Estimates have shown that each degree Celsius rise in the global mean temperature may lead to yield losses of 6.0, 3.2, and 7.4% in major cereals, i.e., wheat, rice, and maize, respectively, without effective adaptation and genetic improvement (Zhao et al., 2017).

The occurrence of abiotic stresses singly has less effect than when occurring in combination at different growth stages (Mittler, 2006; Suzuki et al., 2014; Shaar-Moshe et al., 2017). Under field conditions, frequently occurring combined stresses are drought and heat (Mittler, 2006; Lamaoui et al., 2018; Lawas et al., 2018; Nasser et al., 2020), drought and salinity (Paul et al., 2019; Abobatta, 2020), and salinity and waterlogging (Lamaoui et al., 2018; Lawas et al., 2018). The effect of these stresses in combination on crop plants depends on the nature of the interactions between them (Ramu et al., 2016). These multiple stresses induce unique mechanisms (morphophysiological, biochemical, molecular, and genetic) in crop plants for adaptations and cannot be predicted by simply studying each of the different stresses (Suzuki et al., 2014; Zandalinas et al., 2021). Understanding the mechanisms of plant response to multiple stresses is crucial to unravel the complexities of plant responses to stress combinations

for the development of climate-resilient crops for future food security (Rivero et al., 2022). Therefore, keeping the above under consideration, the present Research Topic has been designed to demonstrate the current level of research and progress in the study of molecular, physiological, and genetic responses and adaptation strategies toward multiple abiotic stresses in cereals. The insights of this Research Topic are divided into the following headings:

## 1 Genetic studies and genome-wide association mapping

Characterization and identification of the differential responses of crop plants are one of the major essential steps for the development of climate-resilient crop plants. Amro et al. studied the growth responses and genetic variation among wheat genotypes for salinity tolerance (seawater) and identified a high genetic diversity among the studied genotypes, which could be utilized for breeding programs. Likewise, Radha et al. reviewed the individual and interactive effects of various abiotic stresses (drought, salinity, high temperature, eCO2, submergence, nutrient deficiency) and their combined effect on rice physiology with the possible adaptation strategies for improving grain quality parameters and yield traits. With the advancement of various tools in system biology (high-throughput phenotyping and genome sequencing), different approaches have been developed, such as quantitative trait locus (QTL) mapping, candidate gene association studies, and genome-wide association studies (GWAS), in order to link phenotypes and genotypes in crop plants for the identification of genetic factors associated with the various traits under consideration (Mir et al., 2019). Among them, GWAS is one of the most powerful tools for investigating complex traits associated with single or multiple abiotic stresses. It detects marker–trait association (MTA) using conserved linkage disequilibrium (LD) present in the selected panel of accessions (Myles et al., 2009; Saini et al., 2022). GWAS has a high capacity to identify small-effect genes/MTAs on a genome-wide scale by efficiently using the multiple historical crossover events that occur in the diverse association panel used (Saini et al., 2022; Xiao et al., 2022). In the present Research Topic, Devate et al. used a 35k SNP wheat breeder's genotyping array to identify 57 unique markers associated with various traits across the locations for drought and heat tolerance in wheat. Out of these associations, 23 MTAs were deemed to be stable. Similarly, in another study, Devate et al. identified six unique marker–trait associations for grain iron (GFeC), zinc (GZnC) contents, and thousand-grain weight (TGW) under drought and heat stress conditions in wheat. These identified MTAs could be utilized in the breeding program after validation through marker-assisted selection (MAS).

## 2 Marker-assisted selection and abiotic stresses

The trait-specific markers (linked markers) allow the efficient introgression of targeted genomic loci from the donor genotype into an elite breeding line, facilitate indirect selection for difficult traits (i.e., root traits under drought stress conditions), and cut the number of genes/QTL into a single genotype using the marker-assisted selection approach (Pandurangan et al., 2022; Rai and Pandey-Rai, 2021). This method is very rapid and cost-effective for genetic improvement after the identification of tightly linked markers associated with the trait under consideration. It is effectively implemented for the improvement of multiple abiotic stress tolerance in various crops, i.e., rice (heat tolerance (Lang et al., 2015); submergence and drought tolerance (Kumar et al., 2020); drought, salinity, and submergence (Muthu et al., 2020); drought and heat stress (Withanawasam et al., 2022), wheat (drought tolerance (Ciucă et al., 2009; Merchuk-Ovnat et al., 2016; Rai et al., 2018; Gautam et al., 2021), and maize (drought (Ribaut and Ragot, 2007)). Similarly, in the present Research Topic, Sunilkumar et al. introgressed the rust resistance gene Lr24 and QTLs linked to moisture deficit stress tolerance in the background of HD3086 (a high-yielding, stress-susceptible genotype of wheat) from the HI1500 donor genotype.

## 3 Omics-based approaches and transgenics for multiple abiotic stresses

Understanding differential levels of plant mechanisms under multiple stress conditions is essential for combating their effect. Adopting different omics approaches (genomics, transcriptomics, proteomics, and metabolomics) and understanding their overall phenotypic effects on crop plants under abiotic stress conditions are crucial to developing strategies for designing crops with superior tolerance mechanisms (Bhardwaj et al., 2021; Jeyasri et al., 2021). Among the different omics approaches, transcription factors (TFs) are crucial for recognizing the appropriate molecular processes and pathways under stress conditions (Muthuramalingam et al., 2018; Muthuramalingam et al., 2020). In the present Research Topic, Annum et al. studied a phospholipase C (PLC) signaling pathway in spring wheat and evaluated its four AtPLC5 overexpressed (OE)/transgenic lines under heat and osmotic stresses through $^{32}$Pi radioactive labeling. The results indicate that heat stress and osmotic stress activate several lipid responses in wild-type and transgenic wheat conforming to osmotic stress tolerance. Kumar et al. studied the differential transcript expression of K+ transport genes in different tissues (root, stem, and leaf) under different abiotic stresses, such as salt, drought, heat, and cold, to elucidate their role in ion homeostasis and stress tolerance mechanisms in sorghum. Maheshwari et al. reviewed paclobutrazol (PBZ) as a plant growth regulator and multistress protectant; they discussed current findings and the prospective application of PBZ in regulating crop growth and ameliorating abiotic stresses. In another study, Kumar et al. used the 20S proteasome gene family in rapeseed and identified 20S proteasome genes for α- (PA) and β-subunits (PB) through systematically performed gene structure analysis. Out of 82 BnPA/PB genes, three exhibited high expression under abiotic stresses. Likewise, Ahmed et al. proposed a novel activation function, the Gaussian Error Linear Unit with Sigmoid (SIELU), for the deep learning (DL) model along with other hyperparameters for the classification of unknown abiotic stress protein sequences from cereal crops.

The papers presented in the current Research Topic are associated with the multiple abiotic stresses on various crops and show wider scope to understand the molecular, physiological, and genetic responses of multiple abiotic stresses. At the same time, the findings of the papers presented show a wide range of advanced scientific approaches and research ideas to understand and identify the effects of multiple abiotic stress and the implementation of their adaptation strategies for the development of climate-resilient crop plants.

## Author contributions

NB wrote the draft editorial. All authors edited it. All authors contributed to the article and approved the submitted version.

## Conflict of interest

The authors declare that the research was conducted in the absence of any commercial or financial relationships that could be construed as a potential conflict of interest.

## Publisher's note



## References

Abobatta, W. F. (2020). "Plant responses and tolerance to combined salt and drought stress," in *Salt and drought stress tolerance in plants* (Cham: Springer), 17–52.

Bhardwaj, A., Devi, P., Chaudhary, S., Rani, A., Jha, U. C., Kumar, S., et al. (2021). 'Omics' approaches in developing combined drought and heat tolerance in food crops. *Plant Cell Rep.* 41, 699–739. doi: 10.1007/s00299-021-02742-0

Chaudhry, S., and Sidhu, G. P. S. (2021). Climate change regulated abiotic stress mechanisms in plants: a comprehensive review. *Plant Cell Rep.* 41, 1–31. doi: 10.1007/s00299-021-02759-5

Ciucă, M., Todorvska, E., Kolev, S., Nicolae, R., Guinea, I., and Saulescu, N. (2009). Marker-assisted selection (MAS) for drought tolerance in wheat using markers associated with membrane stability. *FUNDULEA* 12, 7–12.

Dunwell, J. M. (2014). Transgenic cereals: Current status and future prospects. *J. Cereal Sci.* 59 (3), 419–434. doi: 10.1016/j.jcs.2013.08.008

Gautam, T., Saripalli, G., Kumar, A., Gahlaut, V., Gadekar, D. A., Oak, M., et al. (2021). Introgression of a drought insensitive grain yield QTL for improvement of four Indian bread wheat cultivars using marker assisted breeding without background selection. *J. Plant Biochem. Biotechnol.* 30 (1), 172–183. doi: 10.1007/s13562-020-00553-0

IPCC (2021). "Summary for policymakers," in *Climate change 2021: The physical science basis. contribution of working group I to the sixth assessment report of the intergovernmental panel on climate change*. Eds. V. Masson-Delmotte, P. Zhai, A. Pirani, S. L. Connors, C. Péan, S. Berger, et al (Cambridge University Press).

Jeyasri, R., Muthuramalingam, P., Satish, L., Pandian, S. K., Chen, J. T., Ahmar, S., et al. (2021). An overview of abiotic stress in cereal crops: Negative impacts, regulation, biotechnology and integrated omics. *Plants* 10 (7), 1472. doi: 10.3390/plants10071472

Kumar, A., Sandhu, N., Venkateshwarlu, C., Priyadarshi, R., Yadav, S., Majumder, R. R., et al. (2020). Development of introgression high-yielding semi-dwarf genetic backgrounds to enable improvement of modern rice varieties for tolerance to multiple abiotic stresses free from undesirable linkage drag. *Sci. Rep.* 10 (1), 1–13. doi: 10.1038/s41598-020-70132-9

Lamaoui, M., Jemo, M., Datla, R., and Bekkaoui, F. (2018). Heat and drought stresses in crops and approaches for their mitigation. *Front. Chem.* 6. doi: 10.3389/fchem.2018.00026

Lang, N. T., Ha, P. T. T., Tru, P. C., Toan, T. B., Buu, B. C., and Cho, Y. C. (2015). Breeding for heat tolerance rice based on marker-backcrossing in Vietnam. *Plant Breeding and Biotechnology* 3, 274–281. doi: 10.9787/PBB.2015.3.3.274

Lawas, L. M. F., Zuther, E., Jagadish, S. K., and Hincha, D. K. (2018). Molecular mechanisms of combined heat and drought stress resilience in cereals. *Curr. Opin. Plant Biol.* 45, 212–217. doi: 10.1016/j.pbi.2018.04.002

Merchuk-Ovnat, L., Barak, V., Fahima, T., Ordon, F., Lidzbarsky, G. A., Krugman, T., et al. (2016). Ancestral QTL alleles from wild emmer wheat improve drought resistance and productivity in modern wheat cultivars. *Front. Plant Sci.* 7. doi: 10.3389/fpls.2016.00452

Mir, R. R., Reynolds, M., Pinto, F., Khan, M. A., and Bhat, M. A. (2019). High-throughput phenotyping for crop improvement in the genomics era. *Plant Sci.* 282, 60–72. doi: 10.1016/j.plantsci.2019.01.007

Mittler, R. (2006). Abiotic stress, the field environment, and stress combination. *Trends Plant Sci.* 11 (1), 15–19. doi: 10.1016/j.tplants.2005.11.002

Muthu, V., Abbai, R., Nallathambi, J., Rahman, H., Ramasamy, S., Kambale, R., et al. (2020). Pyramiding QTLs controlling tolerance against drought, salinity, and submergence in rice marker-assisted breeding. *PloS One* 15 (1), e0227421. doi: 10.1371/journal.pone.0227421

Muthuramalingam, P., Jeyasri, R., Bharathi, R. K. A. S., Suba, V., Pandian, S. T. K., and Ramesh, M. (2020). Global integrated omics expression analyses of abiotic stress signaling HSF transcription factor genes in oryza sativa l.: An in-silico approach. *Genomics* 112 (1), 908–918. doi: 10.1016/j.ygeno.2019.06.006

Muthuramalingam, P., Krishnan, S. R., Saravanan, K., Mareeswaran, N., Kumar, R., and Ramesh, M. (2018). Genome-wide identification of major transcription factor superfamilies in rice identifies key candidates involved in abiotic stress dynamism. *J. Plant Biochem. Biotechnol.* 27 (3), 300–317. doi: 10.1007/s13562-018-0440-3

Myles, S., Peiffer, J., Brown, P. J., Ersoz, E. S., Zhang, Z., Costich, D. E., et al. (2009). Association mapping: critical considerations shift from genotyping to experimental design. *Plant Cell* 21 (8), 2194–2202. doi: 10.1105/tpc.109.068437

Nasser, L. M., Badu-Apraku, B., Gracen, V. E., and Mafouasson, H. N. (2020). Combining ability of early-maturing yellow maize inbreds under combined drought and heat stress and well-watered environments. *Agronomy* 10 (10), 1585. doi: 10.3390/agronomy10101585

Pandurangan, S., Workman, C., Nilsen, K., and Kumar, S. (2022). *Introduction to marker-assisted selection in wheat breeding. in accelerated breeding of cereal crops* (New York, NY: Humana), 77–117.

Paul, K., Pauk, J., Kondic-Spika, A., Grausgruber, H., Allahverdiyev, T., Sass, L., et al. (2019). Co-Occurrence of mild salinity and drought synergistically enhances biomass and grain retardation in wheat. *Front. Plant Sci.* 10. doi: 10.3389/fpls.2019.00501

Rai, N., Bellundagi, A., Kumar, P. K., Kalasapura Thimmappa, R., Rani, S., Sinha, N., et al. (2018). Marker-assisted backcross breeding for improvement of drought tolerance in bread wheat (Triticum aestivum l. em thell). *Plant Breed.* 137 (4), 514–526. doi: 10.1111/pbr.12605

Rai, S. K., and Pandey-Rai, S. (2021). "Marker-assisted breeding for abiotic stress tolerance in horticultural crops," in *Stress tolerance in horticultural crops* (Woodhead Publishing), 63–74.

Ramu, V. S., Paramanantham, A., Ramegowda, V., Mohan-Raju, B., Udayakumar, M., and Senthil-Kumar, M. (2016). Transcriptome analysis of sunflower genotypes with contrasting oxidative stress tolerance individual and combined biotic-biotic and abiotic stress tolerance mechanisms. *PloS One* 11 (6), e0157522. doi: 10.1371/journal.pone.0157522

Ribaut, J. M., and Ragot, M. (2007). Marker-assisted selection to improve drought adaptation in maize: the backcross approach, perspectives, limitations, and alternatives. *J. Exp. Bot.* 58 (2), 351–360. doi: 10.1093/jxb/erl214

Rivero, R. M., Mittler, R., Blumwald, E., and Zandalinas, S. I. (2022). Developing climate-resilient crops: improving plant tolerance to stress combination. *Plant J.* 109 (2), 373–389. doi: 10.1111/tpj.15483

Saini, D. K., Chopra, Y., Singh, J., Sandhu, K. S., Kumar, A., Bazzer, S., et al. (2022). Comprehensive evaluation of mapping complex traits in wheat using genome-wide association studies. *Mol. Breed.* 42 (1), 1–52. doi: 10.1007/s11032-021-01272-7

Shaar-Moshe, L., Blumwald, E., and Peleg, Z. (2017). Unique physiological and transcriptional shifts under combinations of salinity, drought, and heat. *Physiologyysiology* 174 (1), 421–434. doi: 10.1104/pp.17.00030

Suzuki, N., Rivero, R. M., Shulaev, V., Blumwald, E., and Mittler, R. (2014). Abiotic and biotic stress combinations. *New Phytol.* 203 (1), 32–43. doi: 10.1111/nph.12797

Withanawasam, D. M., Kommana, M., Pulindala, S., Eragam, A., Moode, V. N., Kolimigundla, A., et al. (2022). Improvement of grain yield under moisture and heat stress conditions through marker-assisted pedigree breeding in rice (Oryza sativa l.). *Crop Pasture Sci.* 73 (4), 356–369. doi: 10.1071/CP21410

Xiao, Q., Bai, X., Zhang, C., and He, Y. (2022). Advanced high-throughput plant phenotyping techniques for genome-wide association studies: A review. *J. Advanced Res.* 35, 215–230. doi: 10.1016/j.jare.2021.05.002

Zandalinas, S. I., Fritschi, F. B., and Mittler, R. (2021). Global warming, climate change, and environmental pollution: recipe for a multifactorial stress combination disaster. *Trends Plant Sci.* 26 (6), 588–599. doi: 10.1016/j.tplants.2021.02.011

Zhao, C., Liu, B., Piao, S., Wang, X., Lobell, D. B., Huang, Y., et al. (2017). Temperature increase reduces global yields of major crops in four independent estimates. *Proc. Natl. Acad. Sci.* 114 (35), 9326–9331. doi: 10.1073/pnas.1701762114

frontiers | Frontiers in Plant Science

ORIGINAL RESEARCH
published: 14 June 2022
doi: 10.3389/fpls.2022.881188

# $^{32}P_i$ Labeled Transgenic Wheat Shows the Accumulation of Phosphatidylinositol 4,5-bisphosphate and Phosphatidic Acid Under Heat and Osmotic Stress

*Nazish Annum[1], Moddassir Ahmed[1]*, Khadija Imtiaz[1], Shahid Mansoor[1], Mark Tester[2] and Nasir A. Saeed[1]*

*[1] Wheat Biotechnology Lab, Agricultural Biotechnology Division, National Institute for Biotechnology and Genetic Engineering, Constituent College Pakistan Institute of Engineering and Applied Sciences, Faisalabad, Pakistan, [2] Center for Desert Agriculture, King Abdullah University of Science and Technology, Thuwal, Saudi Arabia*

OPEN ACCESS

**Edited by:**
*Nabin Bhusal, Agriculture and Forestry University, Nepal*

**Reviewed by:**
*Girish Mishra, University of Delhi, India*
*Jasdeep Chatrath Padaria, Indian Council of Agricultural Research, India*

***Correspondence:**
*Moddassir Ahmed*
*cmmanibge@yahoo.co.uk*

**Specialty section:**
*This article was submitted to Plant Abiotic Stress, a section of the journal Frontiers in Plant Science*

**Received:** *22 February 2022*
**Accepted:** *16 May 2022*
**Published:** *14 June 2022*

**Citation:**
*Annum N, Ahmed M, Imtiaz K, Mansoor S, Tester M and Saeed NA (2022) $^{32}P_i$ Labeled Transgenic Wheat Shows the Accumulation of Phosphatidylinositol 4,5-bisphosphate and Phosphatidic Acid Under Heat and Osmotic Stress. Front. Plant Sci. 13:881188. doi: 10.3389/fpls.2022.881188*

The ensuing heat stress drastically affects wheat plant growth and development, consequently compromising its grain yield. There are many thermoregulatory processes/mechanisms mediated by ion channels, lipids, and lipid-modifying enzymes that occur in the plasma membrane and the chloroplast. With the onset of abiotic or biotic stresses, phosphoinositide-specific phospholipase C (PI-PLC), as a signaling enzyme, hydrolyzes phosphatidylinositol 4,5-bisphosphate ($PIP_2$) to generate inositol 1,4,5-trisphosphate ($IP_3$) and diacylglycerol (DAG) which is further phosphorylated into phosphatidic acid (PA) as a secondary messenger and is involved in multiple processes. In the current study, a phospholipase C (PLC) signaling pathway was investigated in spring wheat (*Triticum aestivum* L.) and evaluated its four *AtPLC5* overexpressed (OE)/transgenic lines under heat and osmotic stresses through $^{32}P_i$ radioactive labeling. Naturally, the wheat harbors only a small amount of $PIP_2$. However, with the sudden increase in temperature (40°C), $PIP_2$ levels start to rise within 7.5 min in a time-dependent manner in wild-type (*Wt*) wheat. While the Phosphatidic acid (PA) level also elevated up to 1.6-fold upon exposing wild-type wheat to heat stress (40°C). However, at the anthesis stage, a significant increase of ∼4.5-folds in $PIP_2$ level was observed within 30 min at 40°C in *AtPLC5* over-expressed wheat lines. Significant differences in $PIP_2$ level were observed in *Wt* and *AtPLC5-OE* lines when treated with 1200 mM sorbitol solution. It is assumed that the phenomenon might be a result of the activation of PLC/DGK pathways. Together, these results indicate that heat stress and osmotic stress activate several lipid responses in wild-type and transgenic wheat and can explain heat and osmotic stress tolerance in the wheat plant.

**Keywords: heat stress, osmotic stress, PA, $PIP_2$, $^{32}P_i$, wheat**

**Abbreviations:** DAG, diacylglycerol; DGK, diacylglycerol kinase; $IP_3$, inositol 1,4,5 trisphosphate; IPP, inositol polyphosphate; OE, overexpression; PA, phosphatidic acid; PIP, phosphatidylinositol monophosphate; $PIP_2$, phosphatidylinositol 4,5-bisphosphate; PIPK, phosphatidylinositol phosphate kinase; PI-PLC, phosphoinositide specific phospholipase C; PLD, phospholipase D.

## INTRODUCTION

Sustainability in agriculture depends on growing suitable crops for a particular climate in the defined areas. Prolonged exposure to high temperatures drastically affects crop productivity. Elevated temperatures also result in osmotic stress from the water evaporation within the soil causing excessive salt accumulation. Heat, drought, and salt are the major abiotic stresses affecting crop yield. These stresses in combination are becoming quite common in heat and drought-hit areas. Among cereals, wheat is domesticated first and considered a major staple food crop globally (Tack et al., 2015; Abhinandan et al., 2018). Heat negatively affects the wheat grain yield. It is estimated that every 1°C rise in temperature results in 6% yield losses in wheat crops; however, it depends on the specific growth stage of the crop, time, duration, and intensity. An increase in temperature above the optimum value before and during anthesis results in embryo abortion in developing seeds, reducing the grain number/ear without affecting the grain weight, whereas, after anthesis, the onset of high temperature does not affect the number of grains per ear but reduce the grain size and weight by hampering grain filling ultimately affecting the crop yield (Foulkes et al., 2002; Weldearegay et al., 2012; Schmidt et al., 2020).

Plants are sessile eukaryotes and are very sensitive to even slight changes in their environment. There are some receptors present on the plant cell membrane that perceive stress (abiotic/biotic) signals and transduce this information downstream for the activation of certain stress-responsive genes. The ultimate product of coordinated action of these genes results in signal transcription/proteins synthesis, protein modification like ubiquitination, glycosylation, methylation, adaptors attachment, and subsequently scaffolding of the plants to adapt/survive under harsh environmental conditions (Trewavas and Malho, 1997; McCarty and Chory, 2000; Gilroy and Trewavas, 2001; Mahajan and Tuteja, 2005; Tuteja, 2007; Tuteja and Sopory, 2008).

Under extreme temperatures, plants tend to maintain their membrane integrity and fluidity, acting as a permeable barrier. According to a rough estimate, the membrane surface of a plant cell is recycled every 90–120 min (Munnik et al., 2021). These lipids have amphipathic properties and can be differentiated as sphingolipids, glycerolipids, and sterols based on their unique chemical structure and biophysical properties (Enrique Gomez et al., 2017). Among glycerolipids, phospholipids are predominantly present in the mitochondrial envelope and plasma membrane (PM), which play a vital role in the development of the plant, regulating their responses against particular environmental stimuli (Dubots et al., 2012; Niu and Xiang, 2018; Wang X. et al., 2020). Plant phospholipases are involved in the hydrolysis of phospholipids and can be divided into four categories, that is, *PLA 1* (phospholipase A1), *PLA 2* (phospholipase A2), *PLC* (phospholipase C), and *PLD* (phospholipase D). Within each category, there are subfamilies with different structures, substrates, and binding sites (Wang X. et al., 2020). Three types of PLCs are reported based on their cellular function and substrates specificity: (1) PI-PLC (Phosphatidylinositol-specific PLCs) hydrolyzes phosphoinositide (PPI); (2) *PC-PLC/NPC* (phosphatidylcholine-specific *PLC*/Non-specific phospholipase C) hydrolyzes the commonly present phospholipids like PC and PE; and (3) *GPI-PLC* (Glycosyl phosphatidylinositol PLC) hydrolyzes the proteins attached to the glycosylphosphatidylinositol (GPI) (Hong et al., 2016).

Extracellular signals activate the *PLC*s responsible for the production of inositol 1,4,5 trisphosphate (InsP3) and diacylglycerol (DAG). InsP3 travels to the cytoplasm to bind and activate the ligand-gated calcium channel also known as the InsP3 receptor to release $Ca^{+2}$ from intracellular channels, whereas, DAG deals with the protein kinase C (PKC) family which has a C1 conserved domain. Massive intracellular processes due to increase or decrease in calcium and phosphorylation levels result in the activation and deactivation of various target proteins to respond against extracellular changes (Shiva et al., 2020; Hayes et al., 2021).

The signaling pathway of plant PI-PLC is somewhat different from mammals, for example, in plants, inositol 1, 4, and 5 trisphosphates (InsP3) could phosphorylate further to inositol hexakisphosphate (InsP6), which is responsible for the release of calcium ions from intracellular calcium reserves and similarly, phosphatidic acid (PA) which is a product of diacylglycerol (DAG) might act as a second messenger in this pathway (Munnik, 2014). $PIP_2$ is presumably a substrate of PLC, hardly found in the plasma membrane of flowering plants (Simon et al., 2014; Zhang et al., 2018c). PLC hydrolyze PIP (Phosphatidylinositol 4 monophosphate), that is, also known as the precursor of PLC and can be found in abundance in the plasma membrane, but to date, the typical precursor of PLC in plants is unknown in *in vivo* analysis (Munnik, 2014). Likewise, DGPP (Diacylglycerol pyrophosphate) can function as an attenuator of PA signaling and as a generator of new signals, but it needs to be investigated further (van Schooten et al., 2006).

Plants tend to upregulate many *PLC* genes upon the onset of various biotic and abiotic stresses. In *Arabidopsis thaliana*, 9 *PI-PLCs* and 6 *NPC*s genes (Munnik, 2014), 4 *PI-PLC* and 5 *NPCs* in *Oryza sativa* (Rice) (Singh et al., 2013), 12 *PI-PLCs* and 9 *NPC*s genes in *Gossypium* spp. (Cotton) (Zhang et al., 2018a), 5 *PI-PLC* and 4 *NPC*s genes in *Zea mays* L. (Maize), while 12 *PLC* genes in *Glycine max* (Soybean) (Wang F. et al., 2015) are reported. An increase in $PIP_2$ and PA had been observed in response to heat, salt, cold, drought, and ABA stresses (Alcázar-Román and Wente, 2008; Darwish et al., 2009; Mishkind et al., 2009; Arisz et al., 2013; Balogh et al., 2013; Simon et al., 2014; Zhang et al., 2018c). Earlier it is reported that *PLC* is involved in plant growth and development, for example, *PLC1* is known to contribute to pollen tube growth in tobacco and petunia (Dowd et al., 2006; Helling et al., 2006), over-expression of the *PLC2* gene can increase drought tolerance and regulate phytochrome level in *Brassica napus* (Das et al., 2005; Nokhrina et al., 2014), *PLC3* and *PLC9* contributing in generating thermotolerance in *Arabidopsis thaliana* (Zheng et al., 2012; Gao et al., 2014), upregulation of *AtPLC5* in response to drought stress could lead to subsequent novel phenotype including stunted root hair growth, reduced lateral root development, stomatal closure, and inhibition/reduction of seed germination (Zhang et al., 2018b,c).

These findings are inconsistent with previous studies as reported on maize, tomato, and potato (Apone et al., 2003; Apostolakos et al., 2008; Wang et al., 2008; Vossen et al., 2010).

PI-PLC was initially reported in wheat in root plasma membrane vesicles (Melin et al., 1992). Based on their subfamily, genomic homology, and chromosomal position, a total of 26 *TaPLC* genes including 7 *NPC* genes have been reported in *Triticum aestivum* (wheat) which are located unevenly on 14 chromosomes (Wang X. et al., 2020), but to date, *TaPLC1* (Zhang et al., 2014; Wang X. et al., 2021) and *TaPI-PLC1-2B* have been cloned and investigated for salt, drought, heat, and cold stress (Khalil et al., 2011; Wang X. et al., 2020). However, *TaPLC5* has yet to be reported in the already identified wheat PLCs. There is growing evidence that phosphoinositide signaling is a major element of stress responses. It proposes that changes in the lipid signal levels are one of the early consequences of abiotic stresses. Therefore, this study focuses on investigating signaling phospholipids levels in response to high temperature and osmotic stresses. We observed that *AtPLC5* over-expression causes a dramatic increase in $PIP_2$ and PA levels at tillering and anthesis stages. These are the crucial stages for wheat grain development at various duration in varying intensity levels of heat and osmotic stresses.

# MATERIALS AND METHODS

## Plant Material

Seeds of local wheat cultivar Faisalabad-2008 was used as wild-type (*Wt*) and four transgenic wheat lines over-expressing (OE) *AtPLC5* gene were used in the current study. The transgenic lines *OE1* and *OE2* were processed under *CaMV35S* promoter, while lines *OE3* and *OE4* contained *UBQ10* promotor. These transgenic wheat lines were obtained through *Agrobacterium*-mediated plant transformation method using immature embryos as explant (Ishida et al., 2015), and putative transgenic wheat lines were screened out based on PCR, quantitative PCR, and antibiotic leaf dip assay. Nevertheless, morpho-physiologically best representative lines were selected and used in this study (unpublished data). Plants were grown in small pots containing peat moss in a greenhouse with a 16/8 h day length regime at 20°C. Leaf samples from transgenic wheat lines were collected from the greenhouse and processed for further experimentation.

## RNA Extraction and Q-PCR

The expression level of *AtPLC5* (At5g58690) transgene in wheat was measured using primer pairs: 5'GT CGCTTTCAACATGCAGGG3' and 5'TGGGTAACTTCGCTTT CGGG3'. Trizol reagent (Invitrogen, United States) was used for the extraction of RNA followed by DNases treatment. RevertAid First-strand cDNA synthesis kit (ThermoFisher Scientific, EU, Luthiana) was used for cDNA synthesis. A comparative threshold cycle value was used to determine the relative expression of the gene. Actin gene (AB181991.1) with primer pair 5'AA CTGGGATGACATGGGGAA3' and 5'TTTTCTCTCTGTTGG CCTTGGG3' was used for normalization of transcript level.

## $^{32}P_i$ Labeling and Heat and Osmotic Stress Treatment

Leaf discs of 0.5 cm in size were taken from the center of collected leaf samples with the help of a vertical leaf disc puncher (**Supplementary Figure 1**). Two leaf discs for every replicate were taken. Leaf discs were metabolically labeled using labeling buffer 200 μl (MES-KOH 2.5 mM, pH 5.8, KCl 1 mM) containing carrier-free $PO_4^{-3}$ (5–10 μCi) in 2 ml Eppendorf tubes for overnight incubation, as described by Munnik et al. (1998) and Darwish et al. (2009). For PLD activity assay, n-butanol (0.5% v/v) was used as transphosphatidylation substrate (Darwish et al., 2009).

### Heat Treatment

After overnight incubation for $^{32}P_i$ labeling, samples were subjected to heat stress at 40°C using a heat block for the mentioned period of time, that is, 0, 7.5, 15, 30, and 60 min.

### Osmotic Stress Treatment

For osmotic stress, 3–4-week-old leaf samples were treated with/without sorbitol by adding 200 μl of sorbitol in MES labeling buffer for 30 min and at 0, 600, and 1200 mM concentrations.

## Lipid Extraction and Analysis

Treatments were stopped by adding PCA (Perchloric acid) to the Eppendorf tubes and centrifuged at 13,000 rpm for 30 s. Leaving behind the leaf tissues in the tube, all the remaining material was discarded carefully, then 400 μl CMH [$CHCL_3$/MeOH/HCl (50:100:1, by volume)] was added in the same tube and shook them for 5 min (until tissues turned colorless). By adding 400 μl of $CHCL_3$ and 200 μl of NaCl (0.9% w/v), two-phase system was induced followed by 2 min centrifugation at 13,000 rpm. The rest of the lipid extraction and isolation was carried out by Munnik and Zarza (2013). Heat-activated K-oxalate ($KOX^-$) impregnated TLC plates, using an alkaline solvent containing $CHCL_3$, MeOH, 25% $NH_3$ and $H_2O$ [90:70:4:16] constituents or an ethyl acetate system containing: EtAc/iso-octane/HCOOH/H2O (12:2:3:10, by vol.) were used to separate radioactive lipids (Munnik et al., 1998). Radioactively labeled phospholipids were visualized on an autoradiograph by overnight exposure of TLC plate to autoradiography film and quantified by using phosphoimaging (Typhon FLA 7000, GE Healthcare).

## Performance of Transgenic Lines of Wheat Under Heat and Combination of Stresses

Wild-type and transgenic lines (*AtPLC5OE*) of wheat were grown in pots under optimum conditions. These plants were subjected to heat stress (40°C) and drought together with heat stress (500 ml $H_2O$ + 40°C) in combination at the anthesis stage for 3 h daily for 14 days. Wild-type and transgenic lines of wheat were also grown at optimum temperature (25°C) as a control. Stay green character was recorded based on visual observation and leaf greenness. Data were recorded and analyzed in percentages.

# RESULTS

## Expression of *AtPLC5* in Wheat Under Heat Stress

The expression level of wild-type and *AtPLC5 OE* lines of wheat were determined by Q-PCR, relative to the expression of actin gene. For this, wild-type and transgenic lines (*AtPLC5 OE*) of wheat were subjected to heat stress at 40°C for 3 h at the anthesis stage. Leaf samples were collected immediately and stored in liquid nitrogen for further processing. Little to no expression was observed in *Wt*. Relative expression of *AtPLC5* shows a significant increase in all four over-expression transgenic lines of wheat (**Figure 1A**). The transgenic lines *OE1* and *OE2* showed 9.9X and 12.3X, while *OE3* and *OE4* lines showed 36.1X and 27.3X significant increase in the expression levels in comparison to the wild-type.

## Heat Stress Rapidly Stimulates Phosphatidylinositol 4,5-bisphosphate and Phosphatidic Acid Accumulation

To study the effect of the heat stress in wheat, the leaf disc of *Wt* was labeled with $^{32}P$ isotope by keeping the leaf discs for overnight incubation in MES buffer and exposed to 20°C and 40°C by using heat block for 0, 7.5, 15, 30, and 60 min. Then, Perchloric acid (2.4% final concentration) was added to stop the reaction and crude lipids were extracted. Alkaline TLC (thin layer chromatography) plates were used to separate the lipids that were further quantified by phosphoimaging.

To investigate how fast the $PIP_2$ and PA start to produce when subjected to heat stress, leaf discs of 4-week-old seedlings of wheat were exposed to heat stress for different time durations. The results of the time course experiment are presented in **Figure 1B**. The $PIP_2$ and PA responses increased with the increase in duration of exposure to heat stress in a time-dependent manner (Mishkind et al., 2009), expression of $PIP_2$ increased up to 2.2-fold, and PA increased up to 1.6-fold (**Figure 1C**) depending on the time of exposure.

### Assay for Phospholipase D Activity

An experiment was carried out to investigate the distinct route of heat-induced PA generation. Either it occurs through PLC which cleaves $PIP_2$ into IP3 and DAG that are further phosphorylated by DGK enzyme to generate PA or PA generation directly through PLD. Therefore, transphosphatidylation activity of PLD was employed. For this, pre-labeled leaf discs were subjected to heat stress (20°C and 40°C) at said time intervals in the presence of n-butanol (0.5% v/v). Ethyl acetate TLC was used to separate lipids and to track PLD-catalyzed phosphatidyl butanol (PBut) formation by phosphoimaging. Under these conditions, a small increase was observed in the PBut level at some time points, while a decrease in PA level was observed. In contrast, a simultaneous decrease in the accumulation of PBut level was observed during subsequent incubation at 40°C with an increase in the level of PA (**Figure 1D**).

## Mature Leaves Accumulate More Phosphatidylinositol 4,5-bisphosphate

Differential response of leaves of the same tiller of the same wheat plant was analyzed for accumulation of $PIP_2$ upon exposure to heat stress. An experiment was designed to investigate which leaf (either younger or mature leaves) responds more efficiently to heat stress by producing a sufficient amount of $PIP_2$, PIP, and PA, and four different leaves including the newly emerged leaf of the same tiller of Faisalabad-2008 wheat cultivar were taken and labeled radioactively by overnight incubation. $^{32}P_i$ labeled leaf discs of four different leaves were subjected to heat stress at 21°C and 40°C for 15 min (**Figure 2A**). The results demonstrated a considerable gradual increase in $PIP_2$ and PA levels among leaves with the increase in temperature, while the level of PIP declined (**Figure 2B**) upon receiving heat stress as described previously (Mishkind et al., 2009). The mature leaves showed a 3.3-fold increase in $PIP_2$ and a 2.6-fold in PA but a 1-fold gradual decrease in PIP production was observed as compared to younger leaves (**Figure 2C**; Wang X. et al., 2021).

## Phosphatidylinositol 4,5-bisphosphate Level Increases at Anthesis Stage in Response to Heat Stress

The wheat anthesis stage is very sensitive to high temperatures. A rise in temperature beyond 25°C drastically affects pollen viability, decreases the chances of seed setting, and results in lesser crop yield. The lipid profile of transgenic wheat plants containing two different promoters and their response to heat stress at the anthesis stage was determined by subjecting their labeled leaf discs to 40°C for 30 min (**Figure 3A**). The lipid profile patterns showed a rise in $PIP_2$ levels in response to heat stress in transgenic and wild-type wheat plants (**Figure 3B**). The $PIP_2$ level revealed a significant increase in the transgenic lines under different promotors in comparison to the wild-type. While the wild-type showed little to no increase, the transgenic lines, *OE1* and *OE2*, depicted a 2.0- to 2.5-fold increase, whereas, *OE3* and *OE4* transgenic plants showed ∼4.5-fold and 4-fold increase in $PIP_2$ production, respectively (**Figure 3C**).

## Osmotic Stress Triggers the Phosphatidylinositol 4,5-bisphosphate Production in *AtPLC5* Over-Expressing Wheat Lines

The role of osmotic stress in the production of lipid was analyzed in *Wt* and *AtPLC5* over-expressing wheat lines. $^{32}P_i$ labeling of 4-week-old plant leaf discs was performed to test various concentrations of sorbitol to mimic water stress. Leaf discs were treated with 0, 600, and 1200 mM sorbitol pre-dissolved in MES labeling buffer for 30 min before extraction. Five percent perchloric acid (PCA) was used to stop preceding the reaction further and crude lipids were extracted. Potassium oxalate ($KOX^-$)-treated TLC plates were used to separate the lipids and phosphoimaged for quantification purposes (**Figure 4A**).

Under control conditions, the amount of $PIP_2$ remained the same among *AtPLC5 OE* lines and wild-type (**Figure 4B**).

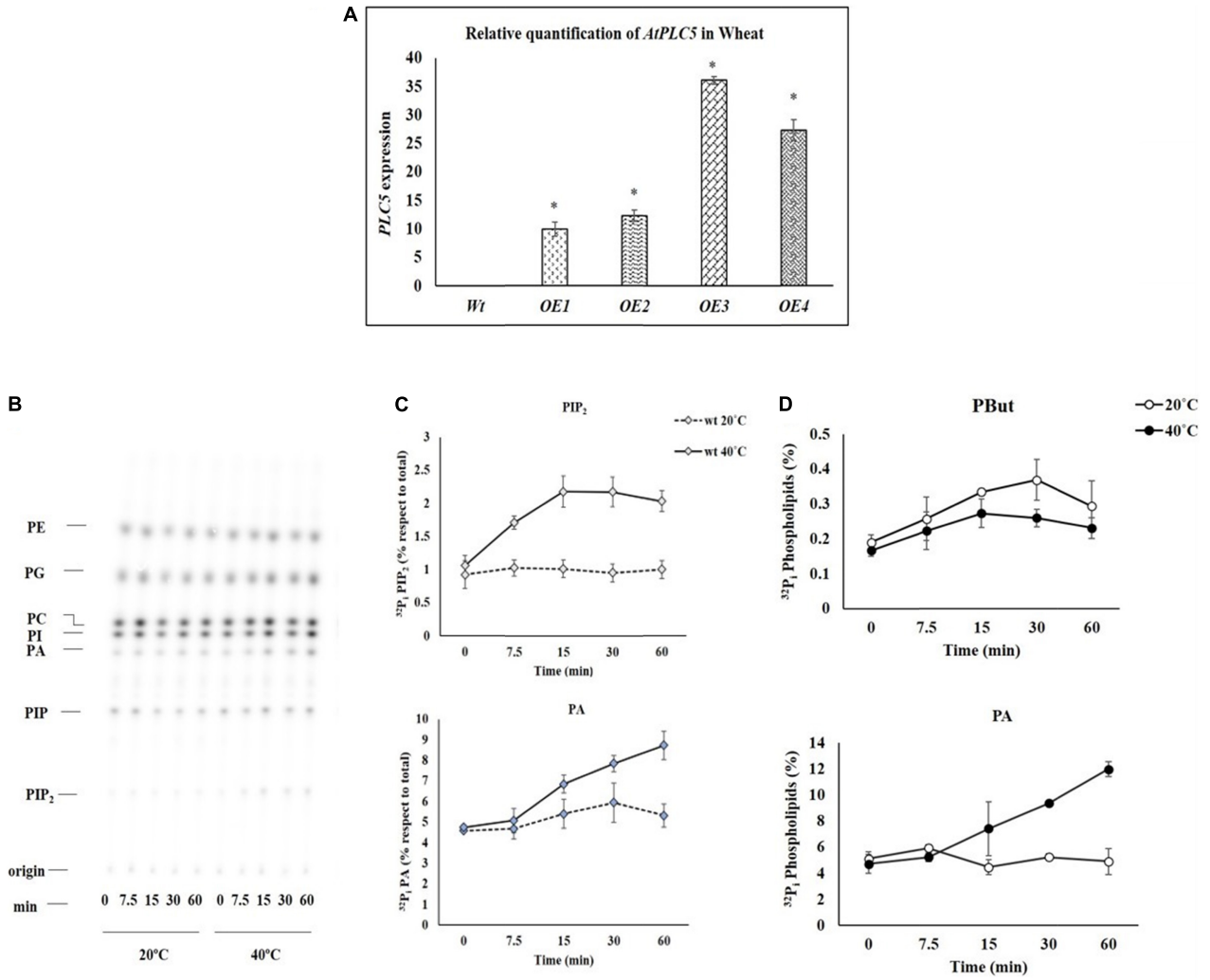


**FIGURE 1 | (A)** The relative expression of *AtPLC5* transgenes in wheat normalized with actin gene determined through Q-PCR with a significant level $P < 0.05$ (*). **(B)** Heat stress excitation of $PIP_2$ and PA formation in a time-dependent manner. Wheat leaf discs labeled with $^{32}P_i$ and tested at 20°C (control) and 40°C (heat stress) for 0, 7.5, 15, 30, and 60 min time periods. An autoradiograph of a time-course experiment with two different temperatures, each lane representing extract (1/5th) of two leaf discs of two different leaves. **(C)** Quantification of $PIP_2$ and PA, respectively, after heat treatment for said time. The experiment was independently repeated two times and similar results were obtained. **(D)** PLD activity. Pre-labeled wheat leaf discs were subjected to heat stress for said time periods in the presence of n-butanol (0.5% v/v). Lipids were extracted and separated by EtAc TLC. Quantification of PBut and PA levels was done by phosphoimaging. Abbreviations: $PIP_2$, Phosphatidylinositol 4,5-bisphosphate; PIP, Phosphatidylinositol phosphate; PA, Phosphatidic acid; PI, Phosphatidylinositol; PC, Phosphatidylcholine; PE, Phosphatidylethanolamine; PG, Phosphatidylglycerol; CL, Cardiolipin.

A relative significant [$P < 0.05$ (*), $P < 0.01$ (**)] increase in $PIP_2$ level was observed in *AtPLC5 OE* lines (*OE*1, *OE2*, *OE3*, and *OE4*) under different promoters at 600 mM sorbitol concentration, while a non-significant increase was observed in wild-type. Upon sorbitol treatment of 1200 mM, a significant increase in $PIP_2$ level was observed in wild-type (∼2.7-fold) and *AtPLC5* over-expression lines (∼3.3-fold) as compared to control condition, whereas non-significant differences were observed between the wild-type and *AtPLC5-OE* lines at 600 mM and 1200 mM sorbitol concentrations. However, the *AtPLC5 OE4* line showed a significant ($P < 0.05$) increase (∼1.8 and ∼3.2-fold) in the $PIP_2$ level at 600 mM and 1200 mM sorbitol treatment, respectively. The PA and PIP responses in wild-type and *AtPLC5 OE* lines appeared to be almost similar (a slight increase was observed in *AtPLC5* over-expression lines) at said levels of sorbitol concentrations.

## Combination of Heat and Osmotic Stress Elicit Phosphatidylinositol 4,5-bisphosphate Accumulation in *AtPLC5* Over-Expression Line

Usually, owing to the duration of the wheat cultivation, the crop faces several stresses at the same time. The occurrence of more than one stress in combination severely affects plant growth and development. Moreover, any visible symptom of

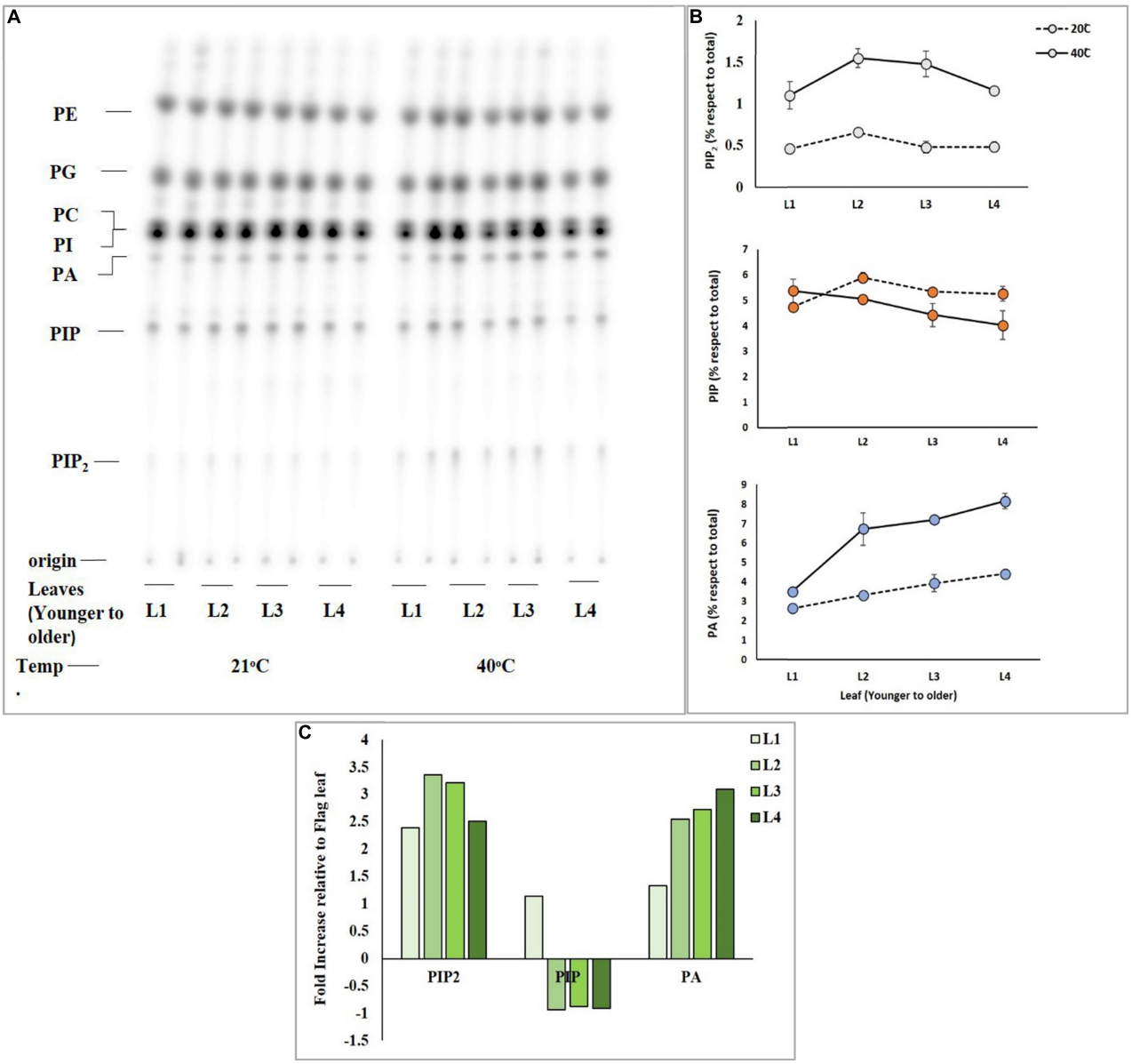


**FIGURE 2 |** High temperature triggers the rapid accumulation of $PIP_2$ and PA in mature leaves. Wheat leaf discs were pre-labeled overnight with $^{32}PO_4^{3-}$, incubated for 15 min at 21°C and 40°C, and lipid extraction and separation were carried out by using alkaline TLC. Panel **(A)** shows autoradiograph of lipid TLC. **(B)** $PIP_2$, PIP, and PA levels were quantified by densitometry of autoradiograph shown in panel **(A)**. **(C)** Summary of fold increase in levels of $PIP_2$, PIP, and PA relative to $t = 0$. The experiment was repeated three times independently and similar results were obtained. See **Figure 1** for the definition of abbreviation.

heat and osmotic stress cannot be detected at the early stages of plant growth. To determine the response of *AtPLC5* in transgenic wheat under the combination of heat and osmotic stress conditions, 4-week-old plantlets were tested at 40°C and 600 mM sorbitol for 30 min simultaneously.

The amount of $PIP_2$ under control/non-treated conditions was observed (**Figure 5A**) to be the same among the *AtPLC5 OE4* line and wild-type (**Figure 5B**). A relative increase in $PIP_2$ was observed at a significance level of $P < 0.05$ (*) in wild-type and *AtPLC5 OE* lines (containing *UBQ10* promoter) at 600 mM sorbitol concentration at 40°C temperature when compared to the control condition. Under co-stress conditions, a significant increase of 2.8-folds in $PIP_2$ was observed in wild-type and 3.5-folds in *AtPLC5* over-expression line in a controlled environment.

## Performance of *AtPLC5* Overexpression Line Under Abiotic Stress

To check the contribution of *AtPLC5* overexpression in wheat physiology or its agronomic performance, two different experimental conditions were set up. First, we tested the physical response of *AtPLC5 OE* lines under heat stress at 40°C and

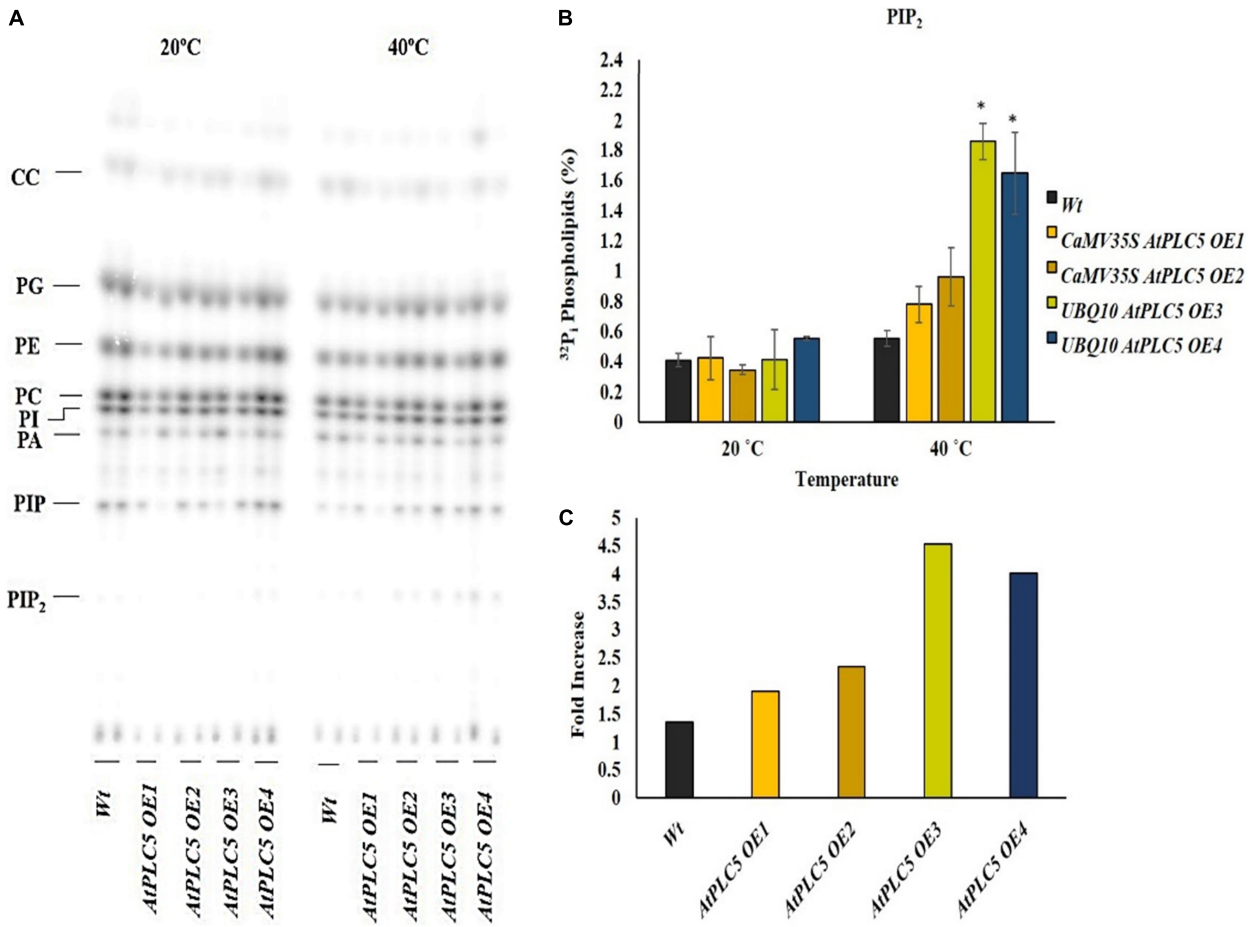


**FIGURE 3 |** Heat stress increases the production of $PIP_2$ at the anthesis stage. A small section (~0.5 cm) of leaf disc of transgenic wheat lines and wild-type were taken at the anthesis stage, radioactively labeled O/N with $^{32}P_i$, and incubated for 30 min at 20°C and 40°C using a heat block. **(A)** An autoradiograph of alkaline TLC showing a complete lipid profile. **(B)** Quantified level of $PIP_2$ after heat treatment at 20°C and 40°C. **(C)** Summary of fold increase transgenic lines show with respect to wild-type. Student *t*-test was used to determine significant differences between wild-type and transgenic lines of *AtPLC5* at a significance level of $P < 0.05$ (*).

second, when stress was applied in combination, such as heat with drought stress (40°C + 500 ml $H_2O$). After the treatment of 2 weeks, we observed the stay-green character in *Wt* and *AtPLC5* transgenics of wheat. We observed that at optimum conditions (32°C), *Wt* possesses ~32%, while *AtPLC5* transgenics possess ~40% greenness (**Figure 6**). When stress was applied in combination with heat (40°C) and drought (500 ml water), we observed visible leaf necrosis in *Wt* (~5% greenness) and *AtPLC5* transgenic plants of wheat (~25% greenness). Interestingly, we found that the transgenic plants of wheat that received treatment of heat stress (40°C) show the ~70% stay-green character as compared to *Wt*.

## DISCUSSION

Abiotic stresses can elicit a series of plant responses. Membrane plays an important role in vesicle transport and cell signaling not only through host-specific proteins but also provides a substrate for the production of lipid (as a second messenger). In addition to the role of lipids as components of membrane structure, they also work as a signal transducer, component of coordinated regulatory activator, and stimulate the expression of specialized proteins and trigger cellular responses to environmental cues (Hou et al., 2016; Kosová et al., 2018; Munnik et al., 2021). Phospholipases on the plasma membrane are the first receptors to receive environmental signals and respond accordingly. PLCs due to their regulatory roles in stress management have been extensively investigated in different plant species. It has been established that stress causes a synergistic increase in $PIP_2$ levels and free calcium, which enhances $IP_3$ synthesis and further releases cytosolic calcium through PI-PLC activity (Hunt et al., 2004; Gao et al., 2014; Zhang et al., 2014). Heat shock induces a rapid increase of $Ca^{+2}$ in the cytoplasm, probably from intracellular reserves and extracellular sources. It is reported that $Ca^{+2}$/calmodulin pathway is involved in thermotolerance. It is logical to claim that $Ca^{+2}$ channels could be used as a thermosensor (Gao et al., 2012; Hayes et al., 2021). However, it

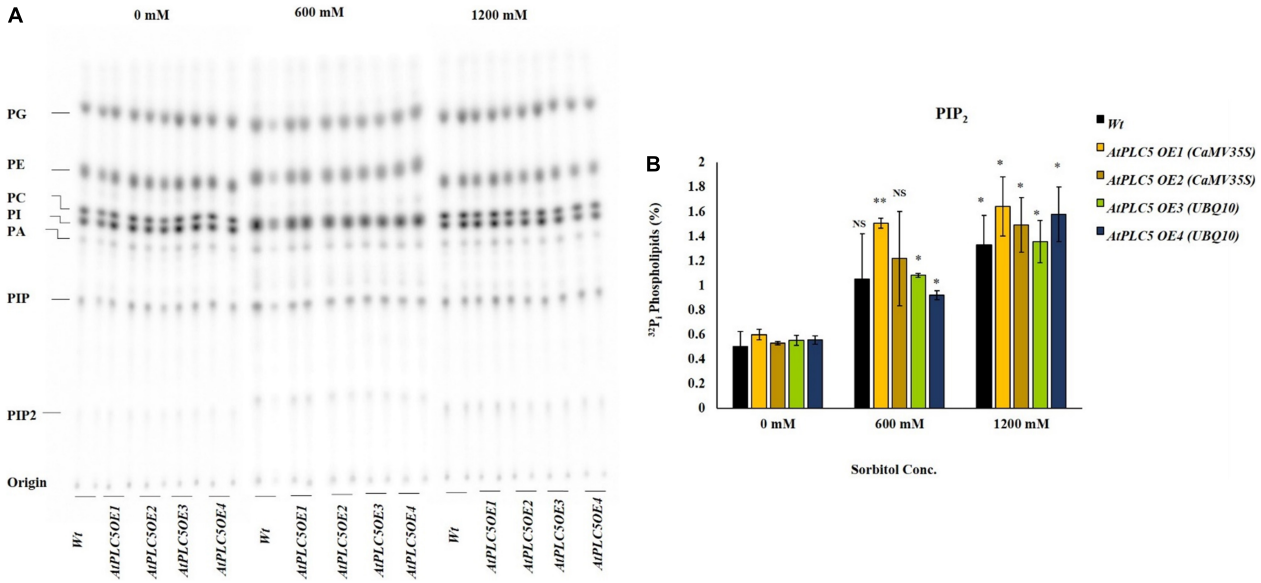


**FIGURE 4 |** $PIP_2$ accumulation in wheat *AtPLC5 OE* lines at different levels of osmotic stress. Overnight labeled leaf disc treated with different concentrations of sorbitol (0 mM, 600 mM, 1200 mM) dissolve in MES buffer for 30 min. Lipids were extracted, separated, and quantified by phosphoimaging. **(A)** A typical autoradiograph of structural lipids with each lane containing lipid extract of two leaf discs. **(B)** $^{32}P_i$ level of $PIP_2$ of the wild-type and *AtPLC5 OE* transgenic lines of wheat under control conditions and at said sorbitol concentrations. Data represented as means ± SD ($n = 2$). Two independent experiments were carried out with similar results obtained. Statistically significant differences at $P < 0.05$ (*) and at $P < 0.01$ (**) were observed in *AtPLC5 OE* of wheat at different sorbitol concentrations, based on the student's *t*-test.

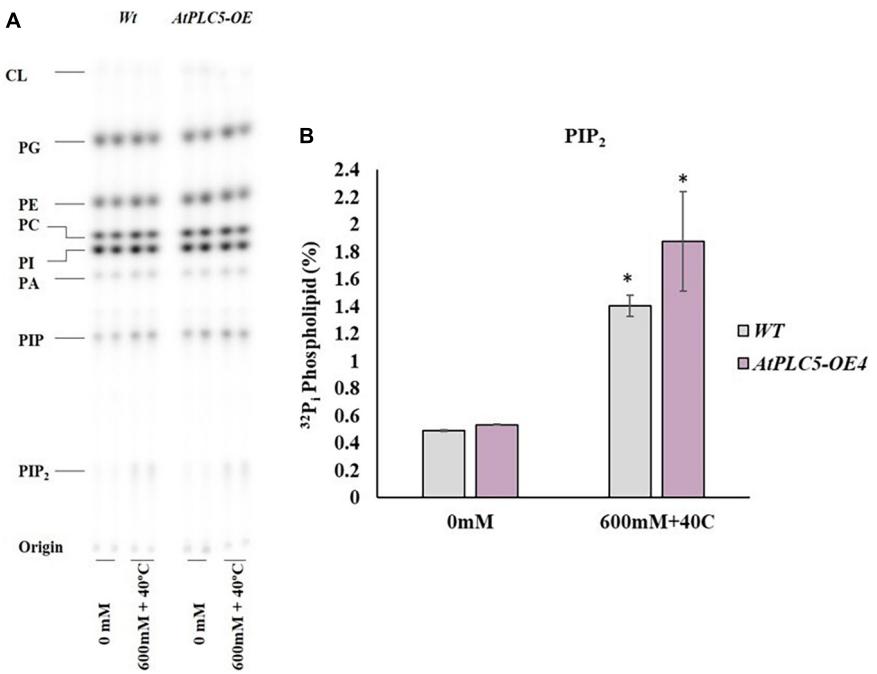


**FIGURE 5 |** The occurrence of stresses in combination elicits $PIP_2$ accumulation in *AtPLC5 OE4* lines in wheat. Radioactively labeled leaf discs were treated with 600 mM sorbitol at 40°C for 30 min. Lipids were extracted, separated by Thin Layer Chromatography plates, and quantified by phosphoimaging. **(A)** A typical autoradiograph of lipids with each lane containing 1/5th lipid extract of two leaf discs. **(B)** $^{32}P_i$ level of $PIP_2$ of the wild-type and *AtPLC5 OE4* line under control conditions and at co-stress of heat and osmotic stress situation. Data represented as means ± SD ($n = 2$). Two independent experiments were carried out with similar results. Statistically significant differences at $P < 0.05$ (*) were observed between the *AtPLC5 OE4* line of wheat and wild-types under said stress conditions, based on the student's *t*-test.

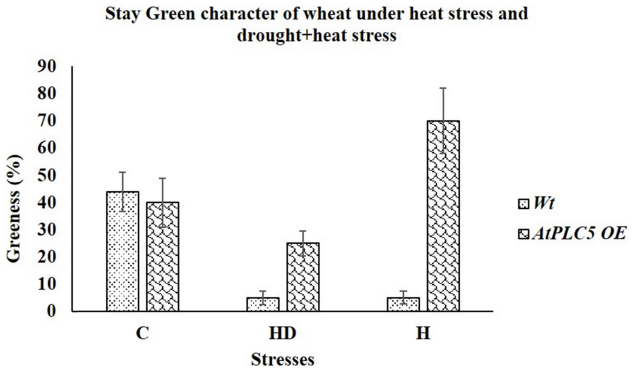


**FIGURE 6 |** Morphological evaluation of *Wt* and *AtPLC5* overexpression lines of wheat under heat stress and under the combined effect of heat and drought stress. Stay green character was recorded based on visual observation and leaf greenness. Data ($n$ = 26, ±SD) were recorded and analyzed in percentage.

is still a challenging task to identify the primary heat-activated $Ca^{+2}$ channel.

Previously, $PIP_2$ and PA abundance had been observed in *Arabidopsis* within 2 min of onset of heat (40°C) stress, and it was mediated by PLD and PIPK (Mishkind et al., 2009). In the current study, we investigated the stimulation of heat-induced $PIP_2$ and PA accumulation in *Triticum aestivum* L. and observed that their induction proceeded in a time-dependent manner. The rapid rise in $PIP_2$ level was evident with the onset of heat (40°C) that reached 2.2-folds in just 15 min and continue to increase with the increase in the duration of heat stress. However, after 60 min, the $PIP_2$ level started to decline, which might indicate the stress-induced damage caused to the plasma membrane. In the current study, it was observed that the PA accumulation started just after 7.5 min of the onset of heat stress, and kept on increasing continuously with the increase in the duration of heat stress. The quick abundance of $PIP_2$ and PA indicates the synthesis of these signaling lipids associated with thermosensing. Although it is still unclear how the elevated temperature activates these lipid-modifying enzymes, this increase in $PIP_2$ and PA is either caused by PIP5K, PLC, or PLD activity, which is yet to be determined. It is reported previously that PA induction is closely associated with the activation of PLD under heat stress (Shiva et al., 2020; Hayes et al., 2021); however, it has been observed that in wheat at 40°C, PBut level seems to decrease while the total PBut content remains in lower limit. In contrast, PA level seems to increase in a time-dependent manner. It is still unknown which other factors are involved in the generation of PA through PLD or PLC. Similarly, it is yet to be explored what circumstances help in the activation/inhibition of PLD or PLC.

Plant leaves serve as a sensor for biotic and abiotic stresses. A slight change in the surrounding temperature is usually sensed by the plant through their leaves. The present study investigated $PIP_2$ and PA responses in younger to older leaves against heat stress. We also observed PIP (Phosphatidylinositol monophosphate) response. Upon onset of heat stress (40°C), the young leaves depicted minor elevation in $PIP_2$, PIP, and PA and contributed accordingly to stress responses as compared to mature leaves which showed a gradual increase up to 3.4-folds in $PIP_2$ and PA accumulation, while illustrated 1-fold decrease in PIP level. Therefore, it could be suggested that although the younger leaves have actively dividing cells, they are quite sensitive to heat stress Zhang et al. (2014) reported a 16-fold increase in *TaPLC1* expression level in older leaves upon salt and drought stress. This could be implied that an increase in expression in response to environmental changes might be considered an adaptive mechanism to manage abiotic stresses.

In the current study, $PIP_2$ response was observed to be similar in wild-type (Faisalabad-2008) and *AtPLC5* over-expressing lines of wheat under normal conditions (20°C). However, heat stress (40°C) at the anthesis stage caused a stronger and significant rise in $PIP_2$ level in *AtPLC5* over-expression lines (**Figure 3B**) as compared to wild-type that ultimately helped the plant to adapt/tolerate fluctuations in temperature and grain formation sustaining the crop yield. We also compared the strength of two constitutive promoters (*CaMV35S* and *UBQ10*). *UBQ10* promoter indicated relatively higher expression of *AtPLC5* in *OE3* and *OE4* lines with a consequent significant increase of ∼4.5-folds in $PIP_2$ accumulation as compared to *AtPLC5* expression driven under *CaMV35S* promoter in *OE1* and *OE2* transgenic wheat. Zhang et al. (2018c) reported a 12-fold increase in $PIP_2$ level at the onset of osmotic stress in *PLC5OE* lines containing *UBQ10* promoter in 6-day-old seedlings of *Arabidopsis thaliana* (Zhang et al., 2018c), which is in agreement with our findings and increase in PLC activity.

PI-PLC as a stress mediator had been reported along with their isoforms in many plants including maize (Apostolakos et al., 2008), rice (Darwish et al., 2009; Singh et al., 2013), tobacco (Helling et al., 2006), tomato (Vossen et al., 2010), cotton (Zhang et al., 2018a), soybean (Wang F. et al., 2015), brassica (Das et al., 2005), *Arabidopsis* (Gao et al., 2014), and wheat (Wang X. et al., 2021). Recent findings illustrated the over-expression of *TaPLC1* aided in improved salt, drought, heat, and cold stress tolerance in wheat (Khalil et al., 2011; Wang Y. et al., 2020; Wang X. et al., 2021). $PIP_2$, as a PLC substrate is hardly detected in plants' plasma membrane under normal conditions, while its level significantly increased under osmotic stress, for example, cold, salinity, or heat stress (Darwish et al., 2009; Mishkind et al., 2009; Arisz et al., 2013; Munnik, 2014; Zhang et al., 2014). In the present study, it was observed that the lines that showed more $PIP_2$ accumulation also revealed more transcript levels through real-time quantitative PCR. In addition, we also observed that these lines retained their stay green character relatively for a longer period of time when exposed continuously for 14 days to heat stress.

The structural lipids like PC (Phosphatidylcholine), PG (Phosphatidylglycerol), and PA (Phosphatidic acid) at the anthesis stage of wheat were reported to drop under high temperatures (Narayanan et al., 2016; Djanaguiraman et al., 2020). Likewise, we also observed a slight decrease in PA in our

*AtPLC5* over-expression lines of wheat during anthesis at 40°C. However, ∼2.2-fold increase in PA accumulation was observed in the wild when subjected to heat stress (40°C for 30 min). This increase might reflect the activity of PLD as previously reported by Hayes et al. (2021).

Upon rising environmental temperature, plants with sufficient water resources transpire more rapidly to keep their leaves cool, while on water scarcity in hot conditions, leaves close their stomata to prevent water loss through evaporation and to maintain their cells membrane integrity. Lee et al. (2007) reported $PIP_2$ to be an important precursor for stomatal opening, as detected previously in the closed stomata phenotype of the *PLC5OE* line in *Arabidopsis*. In this study, sorbitol was used to mimic drought/osmotic stress in wheat and to observe its effect on the $PIP_2$ level. Interestingly, a significant increase in $PIP_2$ level was observed upon osmotic stress in *AtPLC5* overexpression lines of wheat, this might result in the enhanced hydrolytic activity of *PLC5* which might lead to an increase in $PIP_2$ hydrolysis resulting in a subsequent increase in $IP_3$ that might further be metabolized into $IP_6$ which facilitate the stomatal closure by activating the release of $Ca^{+2}$ from intracellular channels (Zhang et al., 2018b,c). In addition, in the current study, we observed that wheat transgenic lines containing *CaMV35S* promoter induced significantly higher $PIP_2$ that matched with findings previously reported by Zhai et al. (2013). It is explained that *ZmPI-PLC1* expressed under *CaMV35S* promoter induced drought tolerance in transgenic tobacco (Ruelland et al., 2015).

However, a detailed phosphoimager-based densitometry study demonstrated a meager decrease in PI and PE levels and a slight increase in PC and PG levels, when exposed to osmotic stresses. An increase in the level of cardiolipin (CL) was observed in *OE* lines of transgenic wheat. In plants, PG (phosphatidylglycerol) was found to be mainly present in the thylakoid membrane of chloroplast and supposed to be involved in the photosynthetic electron transport chain (Hagio et al., 2002; Kobayashi et al., 2017). Previous reports have suggested the prerequisite presence of PG for chloroplast biogenesis, as its deficiency yielded a pale-yellow green phenotype, indicating the failure of establishing thylakoid membrane networks inside leaf chloroplast (Haselier et al., 2010; Kobayashi et al., 2015). Interestingly, an increase in PG level of overexpressor lines of wheat was observed, which means they remained photosynthetically active when exposed to abiotic stress and could accumulate more synthates, more synthates mean more nutrients available to be assimilated during grain filling leading to enhanced crop productivity, which might ultimately yield higher grain and biomass.

Phosphatidylinositol 4,5-bisphosphate is claimed to be a PLC substrate in animals, its concentration is relatively hard to detect in the plasma membrane of plants where PLC activity mostly resides (Van Leeuwen et al., 2007; Munnik, 2014). In contrast to $PIP_2$, PI4P is 20–30 times more abundant in plasma membrane under normal conditions. Under stress conditions such as abscisic acid (ABA), salinity, heat, or hyperosmotic stress, the level of $PIP_2$ increased (Darwish et al., 2009; Mishkind et al., 2009; Zhang et al., 2018b), while the level of PI4P has been reported to drop in response to these stresses (Arisz et al., 2013). But does it go down due to conversion into $PIP_2$ or PIP is an assumed substrate of PLC in the plant? Also, it remained debatable, whether this reflected the hydrolysis by phosphatase or a PLC or is a result of PIP5K activation. Further research is needed to decipher the exact role of PLC in wheat and the downstream process of PA, PPIs, and IPPs production and accumulation.

## DATA AVAILABILITY STATEMENT

The original contributions presented in the study are included in the article/ **Supplementary Material**, further inquiries can be directed to the corresponding author.

## AUTHOR CONTRIBUTIONS

NA, MA, and NS conceived and designed the research. NA conducted the research experiments. NA and KI evaluated the data. MA, NS, and MT provided the research material. NA and MA wrote the manuscript. SM, MT, and NS critically reviewed and edited the manuscript. All authors contributed to the article and approved the submitted version.

## FUNDING

This work was supported by the International Research Support Initiative Program (IRSIP) fellowship to Ph.D. scholar funded by Higher Education Commission (HEC), Pakistan IRSIP Fellowship No. (PIN) IRSIP 39, BMS 43, the National Research Program for Universities entitled "Improvement of heat tolerance in wheat under climate change scenario" Project No. 7202, and the Center for Desert Agriculture, King Abdullah University of Science and Technology (KAUST), Saudi Arabia, NIBGE-KAUST Grant No. ORS#2375.

## ACKNOWLEDGMENTS

We would like to thank Teun Munnik, Research Cluster Green Life Sciences, Section Plant Cell Biology, Swammerdam Institute for Life Sciences, University of Amsterdam, Netherlands, for providing excellent learning and experimental environment, technical guidance, and support for this study.

## SUPPLEMENTARY MATERIAL

The Supplementary Material for this article can be found online at: https://www.frontiersin.org/articles/10.3389/fpls.2022.881188/full#supplementary-material

## REFERENCES


Abhinandan, K., Skori, L., Stanic, M., Hickerson, N. M. N., Jamshed, M., and Samuel, M. A. (2018). Abiotic stress signaling in wheat – an inclusive overview of hormonal interactions during abiotic stress responses in wheat. *Front. Plant Sci.* 9:734. doi: 10.3389/fpls.2018.00734

Alcázar-Román, A. R., and Wente, S. R. (2008). Inositol polyphosphates: a new frontier for regulating gene expression. *Chromosoma* 117, 1–13. doi: 10.1007/s00412-007-0126-4

Apone, F., Alyeshmerni, N., Wiens, K., Chalmers, D., Chrispeels, M. J., and Colucci, G. (2003). The G-protein-coupled receptor GCR1 regulates DNA synthesis through activation of phosphatidylinositol-specific phospholipase C. *Plant Physiol.* 133, 571–579. doi: 10.1104/pp.103.026005

Apostolakos, P., Panteris, E., and Galatis, B. (2008). The involvement of phospholipases C and D in the asymmetric division of subsidiary cell mother cells of *Zea mays*. *Cell Motil. Cytoskeleton* 65, 863–875. doi: 10.1002/cm.20308

Arisz, S. A., van Wijk, R., Roels, W., Zhu, J. K., Haring, M. A., and Munnik, T. (2013). Rapid phosphatidic acid accumulation in response to low temperature stress in *Arabidopsis* is generated through diacylglycerol kinase. *Front. Plant Sci.* 4:1. doi: 10.3389/fpls.2013.00001

Balogh, G., Péter, M., Glatz, A., Gombos, I., Török, Z., Horváth, I., et al. (2013). Key role of lipids in heat stress management. *FEBS Lett.* 587, 1970–1980. doi: 10.1016/j.febslet.2013.05.016

Darwish, E., Testerink, C., Khalil, M., El-Shihy, O., and Munnik, T. (2009). Phospholipid signaling responses in salt-stressed rice leaves. *Plant Cell Physiol.* 50, 986–997. doi: 10.1093/pcp/pcp051

Das, S., Hussain, A., Bock, C., Keller, W. A., and Georges, F. (2005). Cloning of *Brassica napus* phospholipase C2 (BnPLC2), phosphatidylinositol 3-kinase (BnVPS34) and phosphatidylinositol synthase1 (BnPtdIns S1)–comparative analysis of the effect of abiotic stresses on the expression of phosphatidylinositol signal transduction-related genes in B. *napus*. *Planta* 220, 777–784. doi: 10.1007/s00425-004-1389-0

Djanaguiraman, M., Narayanan, S., Erdayani, E., and Prasad, P. V. V. (2020). Effects of high temperature stress during anthesis and grain filling periods on photosynthesis, lipids and grain yield in wheat. *BMC Plant Biol.* 20:268. doi: 10.1186/s12870-020-02479-0

Dowd, P. E., Coursol, S., Skirpan, A. L., Kao, T.-h., and Gilroy, S. (2006). *Petunia* phospholipase c1 is involved in pollen tube growth. *Plant cell* 18, 1438–1453. doi: 10.1105/tpc.106.041582

Dubots, E., Botté, C., Boudière, L., Yamaryo-Botté, Y., Jouhet, J., Maréchal, E., et al. (2012). Role of phosphatidic acid in plant galactolipid synthesis. *Biochimie* 94, 86–93. doi: 10.1016/j.biochi.2011.03.012

Enrique Gomez, R., Joubès, J., Valentin, N., Batoko, H., Satiat-Jeunemaître, B., and Bernard, A. (2017). Lipids in membrane dynamics during autophagy in plants. *J. Exp. Bot.* 69, 1287–1299. doi: 10.1093/jxb/erx392

Foulkes, M. J., Scott, R. K., and Sylvester-Bradley, R. (2002). The ability of wheat cultivars to withstand drought in UK conditions: formation of grain yield. *J. Agric. Sci.* 138, 153–169. doi: 10.1017/s0021859601001836

Gao, F., Han, X., Wu, J., Zheng, S., Shang, Z., Sun, D., et al. (2012). A heat-activated calcium-permeable channel–*Arabidopsis* cyclic nucleotide-gated ion channel 6–is involved in heat shock responses. *Plant J.* 70, 1056–1069. doi: 10.1111/j.1365-313X.2012.04969.x

Gao, K., Liu, Y. L., Li, B., Zhou, R. G., Sun, D. Y., and Zheng, S. Z. (2014). *Arabidopsis thaliana* phosphoinositide-specific phospholipase C isoform 3 (AtPLC3) and AtPLC9 have an additive effect on thermotolerance. *Plant Cell Physiol.* 55, 1873–1883. doi: 10.1093/pcp/pcu116

Gilroy, S., and Trewavas, A. (2001). Signal processing and transduction in plant cells: the end of the beginning? *Nat. Rev. Mol. Cell Biol.* 2, 307–314. doi: 10.1038/35067109

Hagio, M., Sakurai, I., Sato, S., Kato, T., Tabata, S., and Wada, H. (2002). Phosphatidylglycerol is essential for the development of thylakoid membranes in *Arabidopsis thaliana*. *Plant Cell Physiol.* 43, 1456–1464. doi: 10.1093/pcp/pcf185

Haselier, A., Akbari, H., Weth, A., Baumgartner, W., and Frentzen, M. (2010). Two closely related genes of *Arabidopsis* encode plastidial cytidinediphosphate diacylglycerol synthases essential for photoautotrophic growth. *Plant Physiol.* 153, 1372–1384. doi: 10.1104/pp.110.156422

Hayes, S., Schachtschabel, J., Mishkind, M., Munnik, T., and Arisz, S. A. (2021). Hot topic: thermosensing in plants. *Plant Cell Environ.* 44, 2018–2033. doi: 10.1111/pce.13979

Helling, D., Possart, A., Cottier, S. p., Klahre, U., and Kost, B. (2006). Pollen tube tip growth depends on plasma membrane polarization mediated by tobacco PLC3 activity and endocytic membrane recycling. *Plant Cell* 18, 3519–3534. doi: 10.1105/tpc.106.047373

Hong, Y., Zhao, J., Guo, L., Kim, S. C., Deng, X., Wang, G., et al. (2016). Plant phospholipases D and C and their diverse functions in stress responses. *Prog. Lipid Res.* 62, 55–74. doi: 10.1016/j.plipres.2016.01.002

Hou, Q., Ufer, G., and Bartels, D. (2016). Lipid signalling in plant responses to abiotic stress. *Plant Cell Environ.* 39, 1029–1048. doi: 10.1111/pce.12666

Hunt, L., Otterhag, L., Lee, J. C., Lasheen, T., Hunt, J., Seki, M., et al. (2004). Gene-specific expression and calcium activation of *Arabidopsis thaliana* phospholipase C isoforms. *New Phytol.* 162, 643–654. doi: 10.1111/j.1469-8137.2004.01069.x

Ishida, Y., Tsunashima, M., Hiei, Y., and Komari, T. (2015). "Wheat (*Triticum aestivum* L.) transformation using immature embryos," in *Agrobacterium Protocols*, ed. K. Wang (New York, NY: Springer), 189–198. doi: 10.1007/978-1-4939-1695-5_15

Khalil, H. B., Wang, Z., Wright, J. A., Ralevski, A., Donayo, A. O., and Gulick, P. J. (2011). Heterotrimeric Galpha subunit from wheat (*Triticum aestivum*), GA3, interacts with the calcium-binding protein, Clo3, and the phosphoinositide-specific phospholipase C, PI-PLC1. *Plant Mol. Biol.* 77, 145–158. doi: 10.1007/s11103-011-9801-1

Kobayashi, K., Endo, K., and Wada, H. (2017). Specific distribution of phosphatidylglycerol to photosystem complexes in the thylakoid membrane. *Front. Plant Sci.* 8:1991. doi: 10.3389/fpls.2017.01991

Kobayashi, K., Fujii, S., Sato, M., Toyooka, K., and Wada, H. (2015). Specific role of phosphatidylglycerol and functional overlaps with other thylakoid lipids in *Arabidopsis* chloroplast biogenesis. *Plant Cell Rep.* 34, 631–642. doi: 10.1007/s00299-014-1719-z

Kosová, K., Vítámvás, P., Urban, M. O., Prášil, I. T., and Renaut, J. (2018). Plant abiotic stress proteomics: the major factors determining alterations in cellular proteome. *Front. Plant Sci.* 9:122. doi: 10.3389/fpls.2018.00122

Lee, Y., Kim, Y. W., Jeon, B. W., Park, K. Y., Suh, S. J., Seo, J., et al. (2007). Phosphatidylinositol 4,5-bisphosphate is important for stomatal opening. *Plant J.* 52, 803–816. doi: 10.1111/j.1365-313X.2007.03277.x

Mahajan, S., and Tuteja, N. (2005). Cold, salinity and drought stresses: an overview. *Arch. Biochem. Biophys.* 444, 139–158. doi: 10.1016/j.abb.2005.10.018

McCarty, D. R., and Chory, J. (2000). Conservation and innovation in plant signaling pathways. *Cell* 103, 201–209. doi: 10.1016/S0092-8674(00)00113-6

Melin, P. M., Pical, C., Jergil, B., and Sommarin, M. (1992). Polyphosphoinositide phospholipase C in wheat root plasma membranes. Partial purification and characterization. *Biochim. Biophys. Acta* 24, 163–169. doi: 10.1016/0005-2760(92)90107-7

Mishkind, M., Vermeer, J. E., Darwish, E., and Munnik, T. (2009). Heat stress activates phospholipase D and triggers PIP accumulation at the plasma membrane and nucleus. *Plant J.* 60, 10–21. doi: 10.1111/j.1365-313X.2009.03933.x

Munnik, T. (2014). "PI-PLC: phosphoinositide-phospholipase C in plant signaling," in *Phospholipases in Plant Signaling*, Vol. 20, ed. X. Wang (Berlin: Springer), 27–54.

Munnik, T., and Zarza, X. (2013). Analyzing plant signaling phospholipids through 32Pi-labeling and TLC. *Methods Mol. Biol.* 1009, 3–15. doi: 10.1007/978-1-62703-401-2_1

Munnik, T., Irvine, R., and Musgrave, A. (1998). Phospholipid signalling in plants. *Biochim. Biophys. Acta (BBA) Lipids Lipid Metab.* 1389, 222–272.

Munnik, T., Mongrand, S., Zársky, V., and Blatt, M. (2021). Dynamic membranes—the indispensable platform for plant growth, signaling, and development. *Plant Physiol.* 185, 547–549. doi: 10.1093/plphys/kiaa107

Narayanan, S., Tamura, P. J., Roth, M. R., Prasad, P. V., and Welti, R. (2016). Wheat leaf lipids during heat stress: I. High day and night temperatures result in major lipid alterations. *Plant Cell Environ.* 39, 787–803. doi: 10.1111/pce.12649

Niu, Y., and Xiang, Y. (2018). An overview of biomembrane functions in plant responses to high-temperature stress. *Front. Plant Sci.* 9:915. doi: 10.3389/fpls.2018.00915

Nokhrina, K., Ray, H., Bock, C., and Georges, F. (2014). Metabolomic shifts in *Brassica napus* lines with enhanced BnPLC2 expression impact their response to low temperature stress and plant pathogens. *GM Crops Food* 5, 120–131. doi: 10.4161/gmcr.28942

Ruelland, E., Kravets, V., Derevyanchuk, M., Martinec, J., Zachowski, A., and Pokotylo, I. (2015). Role of phospholipid signalling in plant environmental responses. *Environ. Exp. Bot.* 114, 129–143.

Schmidt, J., Claussen, J., Wörlein, N., Eggert, A., Fleury, D., Garnett, T., et al. (2020). Drought and heat stress tolerance screening in wheat using computed tomography. *Plant Methods* 16:15. doi: 10.1186/s13007-020-00565-w

Shiva, S., Samarakoon, T., Lowe, K. A., Roach, C., Vu, H. S., Colter, M., et al. (2020). Leaf lipid alterations in response to heat stress of *Arabidopsis thaliana*. *Plants* 9:845. doi: 10.3390/plants9070845

Simon, M. L., Platre, M. P., Assil, S., van Wijk, R., Chen, W. Y., Chory, J., et al. (2014). A multi-colour/multi-affinity marker set to visualize phosphoinositide dynamics in *Arabidopsis*. *Plant J.* 77, 322–337. doi: 10.1111/tpj.12358

Singh, A., Kanwar, P., Pandey, A., Tyagi, A. K., Sopory, S. K., Kapoor, S., et al. (2013). Comprehensive genomic analysis and expression profiling of phospholipase C gene family during abiotic stresses and development in rice. *PLoS One* 8:e62494. doi: 10.1371/journal.pone.0062494

Tack, J., Barkley, A., and Nalley, L. L. (2015). Effect of warming temperatures on US wheat yields. *Proc. Natl. Acad. Sci. U.S.A.* 112, 6931–6936. doi: 10.1073/pnas.1415181112

Trewavas, A. J., and Malho, R. (1997). Signal perception and transduction: the origin of the phenotype. *Plant Cell* 9, 1181–1195. doi: 10.1105/tpc.9.7.1181

Tuteja, N. (2007). Mechanisms of high salinity tolerance in plants. *Methods Enzymol.* 428, 419–438. doi: 10.1016/S0076-6879(07)28024-3

Tuteja, N., and Sopory, S. K. (2008). Chemical signaling under abiotic stress environment in plants. *Plant Signal. Behav.* 3, 525–536. doi: 10.4161/psb.3.8.6186

Van Leeuwen, W., Vermeer, J. E., Gadella, T. W. Jr., and Munnik, T. (2007). Visualization of phosphatidylinositol 4, 5-bisphosphate in the plasma membrane of suspension-cultured tobacco BY-2 cells and whole *Arabidopsis* seedlings. *Plant J.* 52, 1014–1026. doi: 10.1111/j.1365-313X.2007.03292.x

van Schooten, B., Testerink, C., and Munnik, T. (2006). Signalling diacylglycerol pyrophosphate, a new phosphatidic acid metabolite. *Biochim. Biophys. Acta* 2, 151–159. doi: 10.1016/j.bbalip.2005.12.010

Vossen, J. H., Abd-El-Haliem, A., Fradin, E. F., van den Berg, G. C., Ekengren, S. K., Meijer, H. J., et al. (2010). Identification of tomato phosphatidylinositol-specific phospholipase-C (PI-PLC) family members and the role of PLC4 and PLC6 in HR and disease resistance. *Plant J.* 62, 224–239. doi: 10.1111/j.1365-313X.2010.04136.x

Wang, C. R., Yang, A. F., Yue, G. D., Gao, Q., Yin, H. Y., and Zhang, J. R. (2008). Enhanced expression of phospholipase C 1 (ZmPLC1) improves drought tolerance in transgenic maize. *Planta* 227, 1127–1140. doi: 10.1007/s00425-007-0686-9

Wang, F., Deng, Y., Zhou, Y., Dong, J., Chen, H., Dong, Y., et al. (2015). Genome-wide analysis and expression profiling of the phospholipase C gene family in soybean (*Glycine max*). *PLoS One* 10:e0138467. doi: 10.1371/journal.pone.0138467

Wang, X., Liu, Y., Li, Z., Gao, X., Dong, J., Zhang, J., et al. (2020). Genome-wide identification and expression profile analysis of the phospholipase C gene family in wheat (*Triticum aestivum* L.). *Plants* 9:885. doi: 10.3390/plants9070885

Wang, X., Yao, X., Zhao, A., Yang, M., Zhao, W., LeTourneau, M. K., et al. (2021). Phosphoinositide-specific phospholipase C gene involved in heat and drought tolerance in wheat (*Triticum aestivum* L.). *Genes Genomics* 43, 1167–1177. doi: 10.1007/s13258-021-01123-x

Wang, Y., Zhang, X., Huang, G., Feng, F., Liu, X., Guo, R., et al. (2020). Dynamic changes in membrane lipid composition of leaves of winter wheat seedlings in response to PEG-induced water stress. *BMC Plant Biol.* 20:84. doi: 10.1186/s12870-020-2257-1

Weldearegay, D. F., Yan, F., Jiang, D., and Liu, F. (2012). Independent and combined effects of soil warming and drought stress during anthesis on seed set and grain yield in two spring wheat varieties. *J. Agron. Crop Sci.* 198, 245–253. doi: 10.1111/j.1439-037X.2012.00507.x

Zhai, S., Gao, Q., Liu, X., Sui, Z., and Zhang, J. (2013). Overexpression of a *Zea mays* phospholipase C1 gene enhances drought tolerance in tobacco in part by maintaining stability in the membrane lipid composition. *Plant Cell Tissue Organ Cult. (PCTOC)* 115, 253–262.

Zhang, Q., van Wijk, R., Zarza, X., Shahbaz, M., van Hooren, M., Guardia, A., et al. (2018c). Knock-Down of *Arabidopsis* PLC5 reduces primary root growth and secondary root formation while overexpression improves drought tolerance and causes stunted root hair growth. *Plant Cell Physiol.* 59, 2004–2019. doi: 10.1093/pcp/pcy120

Zhang, B., Wang, Y., and Liu, J. Y. (2018a). Genome-wide identification and characterization of phospholipase C gene family in cotton (*Gossypium* spp.). *Sci. China Life Sci.* 61, 88–99. doi: 10.1007/s11427-017-9053-y

Zhang, K., Jin, C., Wu, L., Hou, M., Dou, S., and Pan, Y. (2014). Expression analysis of a stress-related phosphoinositide-specific phospholipase C gene in wheat (*Triticum aestivum* L.). *PLoS One* 9:e105061. doi: 10.1371/journal.pone.0105061

Zhang, Q., van Wijk, R., Shahbaz, M., Roels, W., Schooten, B. V., Vermeer, J. E. M., et al. (2018b). *Arabidopsis* phospholipase C3 is involved in lateral root initiation and ABA responses in seed germination and stomatal closure. *Plant Cell Physiol.* 59, 469–486. doi: 10.1093/pcp/pcx194

Zheng, S. Z., Liu, Y. L., Li, B., Shang, Z. L., Zhou, R. G., and Sun, D. Y. (2012). Phosphoinositide-specific phospholipase C9 is involved in the thermotolerance of *Arabidopsis*. *Plant J.* 69, 689–700. doi: 10.1111/j.1365-313X.2011.04823.x

**Conflict of Interest:** The authors declare that the research was conducted in the absence of any commercial or financial relationships that could be construed as a potential conflict of interest.

**Publisher's Note:** All claims expressed in this article are solely those of the authors and do not necessarily represent those of their affiliated organizations, or those of the publisher, the editors and the reviewers. Any product that may be evaluated in this article, or claim that may be made by its manufacturer, is not guaranteed or endorsed by the publisher.

frontiers | Frontiers in Plant Science

TYPE Original Research
PUBLISHED 16 August 2022
DOI 10.3389/fpls.2022.943033



OPEN ACCESS

EDITED BY
Nabin Bhusal,
Agriculture and Forestry University, Nepal

REVIEWED BY
Karansher Singh Sandhu,
Bayer Crop Science, United States
Yawen Zeng,
Yunnan Academy of Agricultural Sciences, China

*CORRESPONDENCE
Hari Krishna
harikrishna.agri@gmail.com
Pradeep Kumar Singh
pksinghiari@gmail.com

SPECIALTY SECTION
This article was submitted to Plant Abiotic Stress, a section of the journal Frontiers in Plant Science

RECEIVED 13 May 2022
ACCEPTED 25 July 2022
PUBLISHED 16 August 2022

CITATION
Devate NB, Krishna H, Parmeshwarappa SKV, Manjunath KK, Chauhan D, Singh S, Singh JB, Kumar M, Patil R, Khan H, Jain N, Singh GP and Singh PK (2022) Genome-wide association mapping for component traits of drought and heat tolerance in wheat. *Front. Plant Sci.* 13:943033. doi: 10.3389/fpls.2022.943033



# Genome-wide association mapping for component traits of drought and heat tolerance in wheat

Narayana Bhat Devate[1], Hari Krishna[1]*, Sunil Kumar V. Parmeshwarappa[1], Karthik Kumar Manjunath[1], Divya Chauhan[1], Shweta Singh[1], Jang Bahadur Singh[1], Monu Kumar[2], Ravindra Patil[3], Hanif Khan[4], Neelu Jain[1], Gyanendra Pratap Singh[4] and Pradeep Kumar Singh[1]*

[1]Division of Genetics, ICAR-Indian Agricultural Research Institute, New Delhi, India, [2]Division of Genetics and Plant Breeding, ICAR-Indian Agricultural Research Institute, Gauria Karma, India, [3]Genetics and Plant Breeding Group, Agharkar Research Institute, Pune, India, [4]ICAR-Indian Institute of Wheat and Barley Research, Karnal, India

Identification of marker trait association is a prerequisite for marker-assisted breeding. To find markers linked with traits under heat and drought stress in bread wheat (*Triticum aestivum* L.), we performed a genome-wide association study (GWAS). GWAS mapping panel used in this study consists of advanced breeding lines from the IARI stress breeding programme produced by pairwise and complex crosses. Phenotyping was done at multi locations namely New Delhi, Karnal, Indore, Jharkhand and Pune with augmented-RCBD design under different moisture and heat stress regimes, namely timely sown irrigated (IR), timely sown restricted irrigated (RI) and late sown (LS) conditions. Yield and its component traits, *viz.*, Days to Heading (DH), Days to Maturity (DM), Normalized Difference Vegetation Index (NDVI), Chlorophyll Content (SPAD), Canopy temperature (CT), Plant Height (PH), Thousand grain weight (TGW), Grain weight per spike (GWPS), Plot Yield (PLTY) and Biomass (BMS) were phenotyped. Analysis of variance and descriptive statistics revealed significant differences among the studied traits. Genotyping was done using the 35k SNP Wheat Breeder's Genotyping Array. Population structure and diversity analysis using filtered 10,546 markers revealed two subpopulations with sufficient diversity. A large whole genome LD block size of 7.15 MB was obtained at half LD decay value. Genome-wide association search identified 57 unique markers associated with various traits across the locations. Twenty-three markers were identified to be stable, among them nine pleiotropic markers were also identified. *In silico* search of the identified markers against the IWGSC ref genome revealed the presence of a majority of the SNPs at or near the gene coding region. These SNPs can be used for marker-assisted transfer of genes/QTLs after validation to develop climate-resilient cultivars.

KEYWORDS

**genome-wide association study (GWAS), wheat, drought, heat, single nucleotide polymorphism (SNPs)**

## Introduction

Wheat (*Triticum aestivum* L.) is the staple food crop of one-third of the world population (Guo et al., 2018). To meet the food requirements, it has become mandatory to increase its production with limited resources. The development of high-yielding varieties became utmost important to meet the demand. Decades of breeding in wheat through conventional and molecular approaches enhanced the wheat productivity to ever-reached heights. Enormous improvement in the productivity of wheat has been attained by understanding the genetic principles and phenotypic evaluation and selection through conventional breeding methods (Pingali, 2012).

However, enhancing productivity under global climatic change is a challenging task. Abiotic stresses impact wheat production and tend to the shortage of food supply due to unpredictable crop loss. Among all the abiotic stresses curtailing wheat productivity, drought and heat are the most important and have detrimental effects (Zhang et al., 2018; Gajghate et al., 2020). The impact of drought and heat increased due to increment in global temperature and dry spells in arable land. The terminal drought that occurs at the time of grain filling will decrease the spike weight and the yield (Amiri et al., 2013; Saeidi and Abdoli, 2015). Hence, climate-resilient wheat cultivars are the ultimate means of safeguarding the crop against adverse effects of heat and drought and to fulfill future food needs.

An essential component of the Indian wheat improvement effort is breeding for resilience to abiotic stresses like drought and terminal heat. The interrelationship among breeding, molecular biology and physiology is the foundation of the breeding approach for drought and heat tolerance (Sukumaran et al., 2021), with an emphasis on precise dissection of morpho-physiological traits by precision phenotyping (Lopes et al., 2012). Physiological traits like Canopy Temperature (CT) and grain yield under drought stress environments have a well-established relationship (Gautam et al., 2015; Rehman et al., 2021; Munawar et al., 2022; Singh et al., 2022), and drought and heat tolerance are correlated with lower canopy temperature (CT) (Pinto et al., 2010). Maintenance of lower canopy temperature indirectly attributes to higher transpiration and deep root system in the variety to absorb water from the deeper soil horizon. CT influences the stay-green of leaves, a drought-adaptive trait characterized by a distinct green leaf phenotype during grain filling during terminal drought (Borrell et al., 2014). Drought and heat stress have a significant impact on leaf chlorophyll content (Barboričová et al., 2022). The level of chlorophyll in flag leaves is measured by a portable equipment (SPAD meter), which is thought to be a sign of 'stay-green' or delayed senescence (Lopes et al., 2012). In the post-anthesis phase, "Stay-green" is reported to be associated with drought tolerance in wheat (Kumar et al., 2021) and is utilized for breeding drought tolerant varieties in wheat along with NDVI (normalized difference vegetative index) (Christopher et al., 2015; Rutkoski et al., 2016; Singh et al., 2016). In crop canopies, NDVI is sensitive to biomass and nitrogen (N) variability, both of which are regulated by stress experienced by the crop. Tools for proximal canopy sensing, like Green Seeker (Trimble Navigation Limited, Sunnyvale, California, USA), can detect reflected light from the crop canopy to capture vegetation indices, such as the simple ratio or the NDVI (Naser et al., 2020). For high throughput screening of drought and heat tolerance in wheat, CT, chlorophyll content (SPAD) and NDVI have been successfully integrated into breeding programmes (Singh et al., 2016; Phuke et al., 2020).

Drought and heat tolerance are complex traits that are influenced by a number of genes and have a complex genetic inheritance (Phuke et al., 2020; Saini et al., 2022). Due to its polygenic inheritance and genotype by environment interaction, drought and heat tolerance typically has low heritability (Blum, 2010; Khakwani et al., 2012). Genetic improvement under abiotic stress can be achieved by identifying sources of stress-tolerant traits, as well as introgress, and mobilize the genes underlying the desired traits into locally adapted cultivars (Edae et al., 2014). The challenges in implementing this method in breeding programmes determine the most appropriate target traits for various stress scenarios in a timely and cost-effective manner (Passioura, 2012). Recent advances in high-throughput genotyping and phenotyping have increased our understanding of the physiological and genetic basis of complex characteristics like drought (Mir et al., 2012; Sinclair, 2012) and heat tolerance (Paliwal et al., 2012). One of the most important tools for understanding the genetic architecture of complex characteristics in plants is QTL mapping (Holland, 2007; Xu et al., 2017). However, QTL mapping utilizing biparental populations can only explain a limited percentage of a trait's genetic architecture. Low-mapping resolution, population specificity of discovered QTL and the requirement of a long time to establish mapping populations are further constraints of biparental populations (Edae et al., 2014).

Precise improvement of the complex quantitative trait for adaption to the particular environmental condition like drought and heat needs identification of related genomic regions like QTLs. For the identification of genes/QTLs based on the linkage disequilibrium (LD), GWAS is one of the effective methods. For the prediction of candidate genes, GWAS has been widely used in several crops using genome-wide dense markers (Liu et al., 2018; Srivastava et al., 2020; Alseekh et al., 2021; Tiwari et al., 2022), including wheat (Negisho et al., 2022; Zhang et al., 2022). Advantages of GWAS is, QTLs for several traits can be found with high resolution in one go. Since association mapping uses diverse germplasm, making the procedure more efficient and less expensive than bi-parental QTL mapping (Ersoz et al., 2009; Jin et al., 2016). The resolution and power of association studies, however, depend on the extent of linkage disequilibrium (LD) across the genome. LD needs to be determined in each study

as it is affected by several factors, such as population history, recombination frequency and mating system (Edae et al., 2014).

Association mapping has been used successfully to detect marker trait associations and QTLs in wheat for various traits. There are few studies targeting traits under abiotic stress (Sukumaran et al., 2018; Li H. et al., 2019; Shokat et al., 2020; Abou-Elwafa and Shehzad, 2021; Ahmed A. A. et al., 2021; Ahmed et al., 2022a). High-density SNPs markers used for genome-wide association study (GWAS) can inspect large gene pools representative of diverse breeding reservoirs. GWAS is the most suitable approach to locate robust QTLs that show effect in both normal and stressed conditions (Jamil et al., 2019; Ahmed H. G. M. D. et al., 2021; Saini et al., 2022). Hence, genome-wide association studies (GWAS) have developed into a powerful and ubiquitous tool for the investigation of complex traits (Tibbs Cortes et al., 2021).

In the Indian context, improving wheat cultivars for drought and heat stress resistance is critical for the country's food security. In this study, SNPs markers associated with component traits of drought and heat tolerance were mapped in the advanced breeding lines of Indian hexaploid wheat with the genome-wide markers using the Axiom Wheat Breeder's Genotyping Array (Affymetrix, Santa Clara, CA, United States) having 35,143 SNPs and well suited for high-throughput genotyping in hexaploid wheat (Allen et al., 2017). The aim here is to identify the genomic regions related to yield- and stress-related traits under multi-location stress conditions.

# Materials and methods

## Plant material

The association panel under study was constituted by pairwise and multi-parent crosses of the selected Indian varieties, cultivars, superior breeding lines and exotic introductions. The crosses were advanced with the modified bulk pedigree method and each line was maintained with the respective pedigree record (Supplementary Table 1), and finally, 295 diverse advanced lines were used in the current investigation. However, 282 lines were retained after matching with the obtained genotyping data for further analysis.

## Phenotyping

The phenotypic evaluation was conducted at multiple locations, namely, IARI, New Delhi—DL (28.6550° N, 77.1888° E, MSL 228.61 m), ARI, Pune—PUNE (18.5204° N, 73.8567° E, MSL 560 m), IIWBR, Karnal—IIWBR (29.6857° N, 76.9905°E, MSL 243 m), IARI, Jharkhand—JR (24.1929° N, 85.3756° E, MSL 580 m) and IARI RS, Indore—IND (22.7196° N, 75.8577° E, MSL 553 m). Irrigated trials (IR) were conducted in *rabi* season in 2019 in Delhi and in 2020 in Delhi, Karnal and Pune. Whereas Restricted irrigation (RI) trials were conducted in 2019 in Delhi and in 2020 in Delhi, Indore, Pune and Jharkhand. LS trial was conducted only in IARI New Delhi in the years 2019 and 2020 (Table 1). A total of six irrigations were given for irrigated trials, whereas only 1 irrigation was given (21 days after sowing besides pre-sowing irrigation) in restricted irrigation trials to induce the terminal drought stress. Heat stress was induced by sowing the crop (Late sown—LS) in the second fortnight of December. The experiment was planned with an augmented RCBD design (Federer, 1956, 1961; Searle, 1965) with 295 genotypes and 4 checks replicated twice in 6 blocks. Lines and checks were randomized and sown in plots in three lines of 1 m with a 30 cm inter-line distance. All agronomic practices were carried out according to the recommended package of practices at each location.

The standard procedure for data collection was followed as given in the manual 'Wheat Physiological Breeding II: A Field Guide to Wheat Phenotyping' (Pask et al., 2012). Data were collected for traits like Days to heading (DH), Days to maturity (DM), Normalized Difference Vegetation Index (NDVI) at anthesis and grain filling stage, chlorophyll content (SPAD) of flag leaf at the post-anthesis stage, Plant height (PH), Canopy temperature (CT), Grain weight per spike (GWPS), Thousand Grain weight (TGW), Plot Yield (PLTY) and Biomass.

## Genotyping

DNA isolation was carried out using the leaves of 7-days-old seedlings grown under controlled conditions. DNA was extracted using the CTAB method (Murray and Thompson, 1980) with minor modifications. DNA quality was checked with the 0.8% agarose gel electrophoresis and 20 ng/μl DNA was used for further SNP genotyping. Out of 295 DNA samples, 282 passed the quality check step and were used for further genotyping. The remaining 13 genotypes were excluded from genotyping due to poor DNA quality. Hybridisation-based SNP chip genotyping of 282 genotypes was performed using the 35K Axiom® Wheat Breeder's Array of Affymetrix GeneTitan® system according to the procedure described by Affymetrix. Allele calling was carried out using the Affymetrix proprietary software package Axiom Analysis Suite, following the Axiom® Best Practices Genotyping Workflow (https://media.affymetrix.com/support/downloads/manuals/axiom_analysis_suite_user_guide.pdf). SNP marker data were obtained in the Hap Map format. The chip had 35,143 SNPs; however, after filtration for monomorphic alleles, minor allele frequency (MAF) was >0.05, missing data frequency was >0.2 and heterozygote frequency >0.25; a total of 10,546 SNPs were retained for GWAS analysis.

TABLE 1 Details of sowing conditions, locations and year of experiment along with abbreviations.

| Treatment | Location | GPS location | Year | Abbreviation |
|---|---|---|---|---|
| Irrigated–(IR) | ICAR-Indian Agricultural Research Institute (IARI)-New Delhi | 28.6550° N, 77.1888° E, MSL 228.61 m | 2019 | DL_IR_2019 |
| | | | 2020 | DL_IR_2020 |
| | Agharkar Research Institute-ARI, Pune | 18.5204° N, 73.8567° E with MSL 560 m | 2020 | PUNE_IR_2020 |
| | Indian Institute of Wheat and Barley Research-IIWBR, Karnal | 29.6857° N, 76.9905°E, MSL 243 m | 2020 | IIWBR_IR_2020 |
| Restricted irrigated–(RI) | ICAR-Indian Agricultural Research Institute (IARI)-New Delhi | 28.6550° N, 77.1888° E, MSL 228.61 m | 2019 | DL_RI_2019 |
| | | | 2020 | DL_RI_2020 |
| | Agharkar Research Institute-ARI, Pune | 18.5204° N, 73.8567° E with MSL 560 m | 2020 | PUNE_RI_2020 |
| | ICAR-Indian Agricultural Research Institute, Regional station-IARI RS, Indore | 22.7196° N, 75.8577° E, MSL 553 m | 2020 | IND_RI_2020 |
| | ICAR-Indian Agricultural Research Institute-IARI, Jharkhand | 24.1929° N, 85.3756° E, MSL 580 m | 2020 | JR_RI_2020 |
| Late Sown–(LS) | ICAR-Indian Agricultural Research Institute (IARI)-New Delhi | 28.6550° N, 77.1888° E, MSL 228.61 m | 2019 | DL_LS_2019 |
| | | | 2020 | DL_LS_2020 |

## Analysis of data

Phenotypic data at each location and condition (IR, RI and LS) were analyzed using the r package 'augmentedRCBD' (Aravind et al., 2021) for ANOVA, and adjusted means for each genotype under study were estimated based on Federer (1956, 1961). Calculated adjusted mean eliminating block effect at each environment is used further in all the analyses, including GWAS. The adjusted mean of each block was calculated with the formula (Federer, 1961):

$$Vi = ui - bj$$

where
Vi is the adjusted mean of $i^{th}$ variety
*ui* is the unadjusted mean of $i^{th}$ variety
*bj* is $j^{th}$ block effect.

Principal component analysis was carried out using the R package "FactoMineR version 2.4" (Multivariate Exploratory Data Analysis and Data Mining) by Husson et al. (2016). Graphical representation of PCA results was done with the R package "factoextra version 1.0.7" (Kassambara, 2020). Pearson's correlation was calculated among the studied traits and figures were drawn.

A total of 5,480 SNPs equally spaced around 1 MB distance throughout the genome were filtered and used for the estimation of population structure using the STURUCTURE software (Pritchard et al., 2010). The parameters, *viz*., burn-in cycles and MCMC (Monte Carlo Markov Chains) were set to 100,000. Three iterations for each *k* value ranging from 1 to 7 were conducted to determine the population structure. The ideal number of delta K (subpopulations) was found out by the Evanno method (Evanno et al., 2005) using Structure Harvester (http://taylor0.biology.ucla.edu/structureHarvester/). Furthermore, the filtered 10,546 SNPs were analyzed using TASSEL 5.0 (Trait Analysis by Association, Evolution and Linkage) (Bradbury et al., 2007) to construct the neighbor-joining dendrogram. SNP marker-based PCA and Kinship analysis were conducted with GAPIT (Lipka et al., 2012).

## Association analysis

The filtered SNP markers were utilized for determining marker-trait associations using TASSEL v 5.0. The $r^2$ values between marker pairs were obtained and filtered for pairs within each chromosome. LD decay curve was drawn for each A, B and D genomes along with whole the genome. LD block size was estimated by plotting the $r^2$ value against the distance in base pairs (bp) and the distance at the half LD Decay point was noted.

The filtered 10,546 SNPs and the location-wise "adjusted mean" for each trait were used for the genome-wide association analysis using GAPIT v3 in R with PCA 3 and default parameters (https://zzlab.net/GAPIT/gapit_help_document.pdf) using the "BLINK" (Bayesian-information and Linkage-disequilibrium Iteratively Nested Keyway) model. The BLINK model is presumed to be superior in identifying QTNs and avoiding false positives to decipher true associations (Huang et al., 2019). Quality of association model fitting was found out using a Q-Q plot drawn with expected vs. observed $-log10(p)$ value. Stringent selection of MTAs was done using the Bonferroni correction (*p*-value cut-off at 0.05/total number of markers) to avoid false positives and a Manhattan plot was drawn to represent MTAs. Stable MTAs across the location were found out with a significant *p*-value cut-off at 0.001. Pleiotropic SNPs having association with more than one trait were also found out. Stable and pleiotropic SNPs

were compared with the IWGSC Reference genome using BLAST search in the ensemble plants platform (http://plants.ensembl.org/Triticum_aestivum/Tools/Blast). To identify the candidate genes associated with significant SNPs, gene coding regions located within the 10 KB flanking region of the MTAs were considered.

# Results

## Phenotypic evaluation

There was high variability in means and range for each trait at the respective location. Mean DH and PLTY were highest in Delhi as compared to other locations, and Pune had the least. Late sown trials planted for heat stress had lower DH, DM, PH, GWPS, TGW, BIOMASS and PLTY as compared to IR and RI trials (Table 2). NDVI had a similar pattern across the environments except in the late sown where it had lower NDVI values. CT at anthesis was highest in RI trials followed by LS and IR. Jharkhand and Indore locations displayed higher TGW as compared to Delhi. IR trials at Delhi had higher TGW compared to RI and LS due to shrinkage of grains under drought and heat stress (Table 2). Descriptive statistics like minimum, maximum, average, standard deviation, coefficient of variation and critical difference of all the studied traits in each environment were calculated (Supplementary Table 2).

Analysis of variance indicated a significant difference between the studied traits at 5% and 1% as noted in Supplementary Table 2. The frequency distribution curve indicated the near normal distribution for the majority of the traits in Delhi under all three conditions and a similar pattern was observed at other locations too (Figure 1; Supplementary Figure 1). There was the least variation for days to heading in Delhi under irrigated condition (0.78%) followed by NDVI_1 (0.89%) at the late sown condition in Delhi. Being high environmental responsive traits, plot yield, biomass, NDVI_3 and GWPS were the highly variable traits having higher CV values compared to other traits in all the locations.

## Correlation- and phenotype-based PCA

There was a positive correlation among the traits like NDVI, SPAD, DH, DM and PH in all the three conditions at the Delhi location and a similar trend was observed in all other locations. Similarly, yield-related traits like GWPS, TGW and PLTY also showed a positive correlation across the studied locations and treatment conditions. CT was negatively correlated with all the studied traits (Figure 2; Supplementary Figure 2).

PCA based on phenotypic data indicated that in Delhi irrigated condition, the first principal component was contributing 32.7% variation; the major contributors were DM, DH and NDVI (Figure 3), whereas the second dimension represents 17.2% variation receiving contribution from yield-related traits, *viz.*, PLTY, TGW, CT, GWPS and BIOMASS (Figure 3). The traits DH, DM and NDVI are clustered together with an acute angle indicating a positive correlation among them. Similarly, TGW, PLTY, GWPS and BIOMASS were clustered together. Whereas CT indicated a negative correlation to all the studied traits. Similarly, PCA analysis under RI and LS conditions at Delhi indicated that dimension 1 was explaining 28.6 and 25.3%; dimension 2 was explaining 21 and 15.6% variation, respectively. Variation explained by both the dimension (i.e. Dim-1 and Dim-2) of PCA from other locations were also found out using PCA analysis viz., IIWBR (Dim1-31.8%, Dim2-25%), PUNE_IR (Dim1-25.3%, Dim2-19.5%), PUNE_RI (Dim1-20.9%, Dim2-18.6%) and JR (Dim1-37.2%, Dim2-21.9%) locations (Supplementary Figure 3).

## Genotyping

Out of 35,143 SNPs screened over 282 genotypes, 10,546 SNPs were retained after filtering. Genome-wide SNP distribution analysis showed 3,350, 4,083 and 3,113 SNPs in A, B and D genomes, respectively. Having 777 SNPs, 2B was the chromosome containing the highest number of polymorphic SNPs followed by 2D having 767. Chromosome 4D had the lowest number of polymorphic SNPs (184) (Table 3).

## Population structure and diversity

Population structure was determined with burn-in and MCMC of 100,000 with three iterations using STRUCTURE HARVESTER. The best *K*-value obtained was 2 indicating 2 subpopulations in the GWAS panel (Figure 4A). The subpopulations 1 and 2 had 133 and 135 genotypes, respectively, whereas 14 genotypes were considered as the admixtures population (Supplementary Table 3). The result was verified with the PCA analysis based on SNP marker data; two clusters were also obtained in a marker-based PCA plot (Figure 4B), indicating two subpopulations in the panel. Kinship and neighbor-joining cluster analysis verified the presence of two clusters as shown in Figures 4C,D.

## Linkage disequilibrium (LD) block

To estimate LD, the $r^2$ (squared allele frequency correlation) value was calculated among all the possible pairs of SNPs in each chromosome using TASSEL 5.0 (Bradbury et al., 2007). LD decay map was constructed by plating $r^2$ values against genetic distance in bp for each genome and whole genome. LD block size at half LD decay was 5.24, 5.26, and

TABLE 2 A summary of yield and stress related traits in GWAS panel evaluated across the different environment.

| Condition | Environment | DH | PH | DM | NDVI_1 | NDVI_2 | NDVI_3 | SPAD | CT | GWPS | BIOMASS | PLTY | TGW |
|---|---|---|---|---|---|---|---|---|---|---|---|---|---|
| **IR** | DL-2019 | 94.1 ± 6.32 | 107.48 ± 7.21 | – | 0.8 ± 0.01 | 0.7 ± 0.35 | 0.71 ± 0.04 | – | – | 2.29 ± 0.74 | – | 350.96 ± 75.79 | – |
| | | (79.24–112.76) | (75.06–128.06) | | (0.71–0.82) | (0.54–6.66) | (0.56–0.81) | | | (0.49–4.48) | | (75.12–477.56) | |
| | PUNE-2020 | 63.12 ± 3.78 | – | – | 0.86 ± 0.04 | 0.83 ± 0.04 | – | – | 26.91 ± 1.17 | 1.47 ± 0.13 | – | 186.5 ± 45.68 | 42.99 ± 3.52 |
| | | (51.02–72.02) | | | (0.71–0.96) | (0.69–0.94) | | | (24.07–29.98) | (1.05–1.82) | | (41.45–321.8) | (31.83–50.36) |
| | DL-2020 | 94.99 ± 6.45 | 108.12 ± 6.25 | 133.23 ± 3.84 | 0.68 ± 0.05 | 0.59 ± 0.06 | 0.21 ± 0.09 | 46.66 ± 4.02 | 27.46 ± 1.48 | 1.98 ± 0.44 | 1661.34 ± 332.87 | 484.53 ± 103.21 | 38.82 ± 4.43 |
| | | (75.21–113.96) | (87.91–125.12) | (123.81–144.81) | (0.54–0.8) | (0.43–0.74) | (0.06–0.5) | (33.76–56.84) | (23.19–30.68) | (0.71–4.06) | (337.62–2775.25) | (101.77–708.65) | (24.16–57.28) |
| | IIWBR-2020 | 88.08 ± 2.51 | – | 123.56 ± 1.66 | 0.6 ± 0.09 | – | – | – | – | 2.07 ± 0.32 | – | 261.68 ± 83.68 | 36.83 ± 5.03 |
| | | (81.9–100.02) | | (118.98–127.98) | (0.26–0.82) | | | | | (1.32–3.09) | | (46.55–485.27) | (23.63–53.33) |
| **LS** | DL-2019 | 93.3 ± 2.99 | – | – | 0.81 ± 0.02 | 0.96 ± 4.14 | 0.4 ± 0.12 | – | 21.97 ± 0.87 | 1.39 ± 0.31 | – | 291.41 ± 64.32 | – |
| | | (85.5–100.5) | | | (0.71–0.85) | (0.55–72.01) | (0.07–0.72) | | (19.91–24.51) | (1.1–2.75) | | (80.69–441.52) | |
| | DL-2020 | 82.99 ± 2.7 | 87.23 ± 6.31 | 109.41 ± 3.05 | 0.57 ± 0.05 | 0.42 ± 0.07 | 0.2 ± 0.07 | 49.75 ± 4.32 | 29.01 ± 1.39 | 1.68 ± 0.3 | 995.87 ± 344.44 | 340.12 ± 110.94 | 36.28 ± 4.06 |
| | | (77.69–93.44) | (69.4–103.98) | (101.44–120.06) | (0.38–0.72) | (0.22–0.6) | (0.09–0.56) | (36.55–60.79) | (26.27–39.02) | (0.95–2.9) | (55.9–2267.6) | (53.88–597.63) | (23.15–48.15) |
| **RI** | DL-2019 | 94.38 ± 6.49 | – | – | 0.8 ± 0.01 | 0.65 ± 0.04 | – | – | – | 2.49 ± 0.56 | – | – | – |
| | | (75.5–107.5) | | | (0.71–0.83) | (0.53–0.76) | | | | (1.14–4.54) | | | |
| | PUNE-2020 | 58.36 ± 2.95 | – | – | 0.85 ± 0.05 | 0.81 ± 0.04 | – | – | 27.93 ± 1.06 | 1.66 ± 0.15 | – | 92.31 ± 33.67 | 40.85 ± 3.45 |
| | | (50.48–68.48) | | | (0.68–0.97) | (0.68–0.97) | | | (25.43–30.24) | (1.23–2.01) | | (19.04–215.16) | (31.13–49.01) |
| | JR-2020 | 78.06 ± 3.52 | 90.61 ± 7.08 | 112.18 ± 3.99 | – | – | – | – | – | 2.2 ± 0.34 | 320.49 ± 98.54 | 163.85 ± 48.18 | 43.38 ± 3.87 |
| | | (61.53–87.53) | (64.74–112.74) | (101.67–124.94) | | | | | | (0.9–3.21) | (42.75–627.75) | (13.48–286) | (29.47–58.86) |
| | DL-2020 | 97.84 ± 6.37 | 101.41 ± 6.62 | 130.43 ± 3.46 | 0.64 ± 0.05 | 0.53 ± 0.05 | 0.21 ± 0.08 | 52.31 ± 4.71 | 32.54 ± 1.17 | 1.74 ± 0.36 | 1199.13 ± 321.87 | 300.78 ± 86.3 | 32.99 ± 4.91 |
| | | (77.71–115.46) | (77.47–119.97) | (120.52–140.4) | (0.51–0.82) | (0.38–0.67) | (0.07–0.52) | (35.34–62.24) | (29.51–36.21) | (0.85–3.2) | (30.2–1937.15) | (34.58–560.21) | (20.98–50.1) |
| | IND-2020 | – | – | – | – | – | – | – | – | – | – | 301.16 ± 64.6 | 44.38 ± 3.15 |
| | | | | | | | | | | | | (82.73–466.83) | (36–53.62) |

*DL-Delhi, PUNE-Pune, IIWBR-Karnal, JR-Jharkhand, IND-Indore. IR, Irrigated; RI, Restricted irrigated; LS, Late sown.

**(Mean ± SD) with (Min–Max) values are given in brackets for each trait.

***DH, Days to Heading; PH, Plant Height; DM, Days to maturity; NDVI – Normalized difference vegetation index, SPAD, Chlorophyll content; CT, Canopy Temperature; GWPS, Grain Weight per Spike; BIOMASS – Biomass; PLTY, Plot yield; TGW, Thousand grain weight.



10.3389/fpls.2022.943033

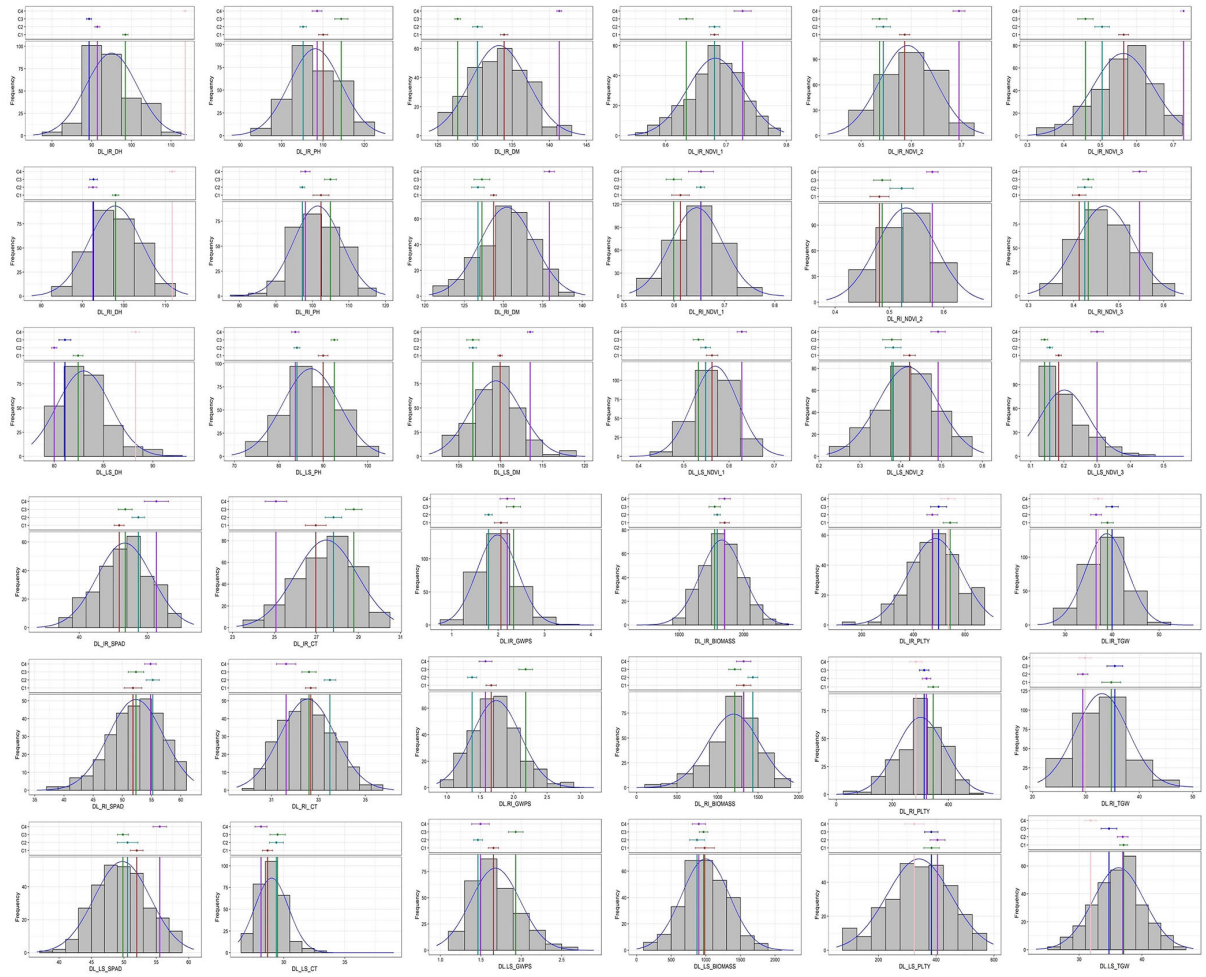

FIGURE 1
Frequency distribution of studied traits in GWAS panel evaluated at IARI Delhi under three conditions *viz*., IR, RI and LS during 2020–2021.

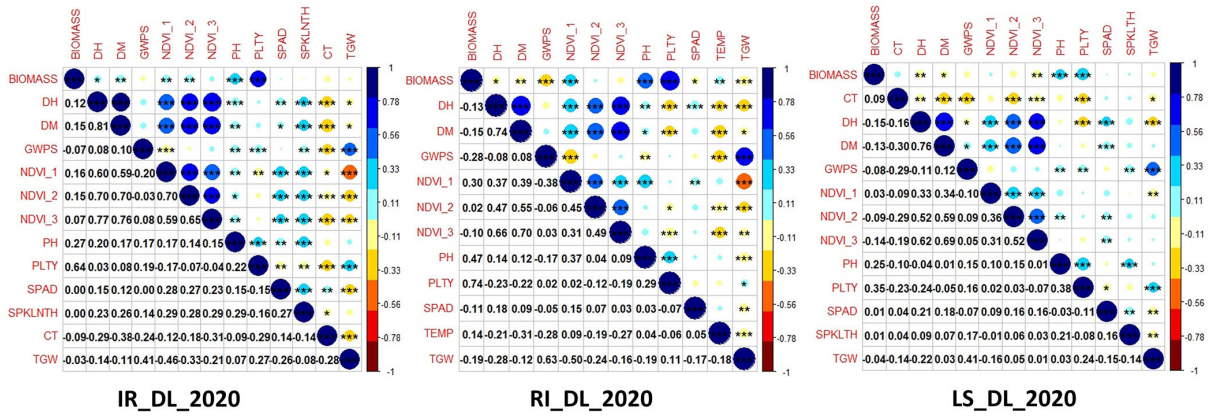


FIGURE 2
Correlation among the studied traits in the GWAS panel evaluated at IARI Delhi under three conditions, *viz*., IR, RI and LS during 2020–2021.

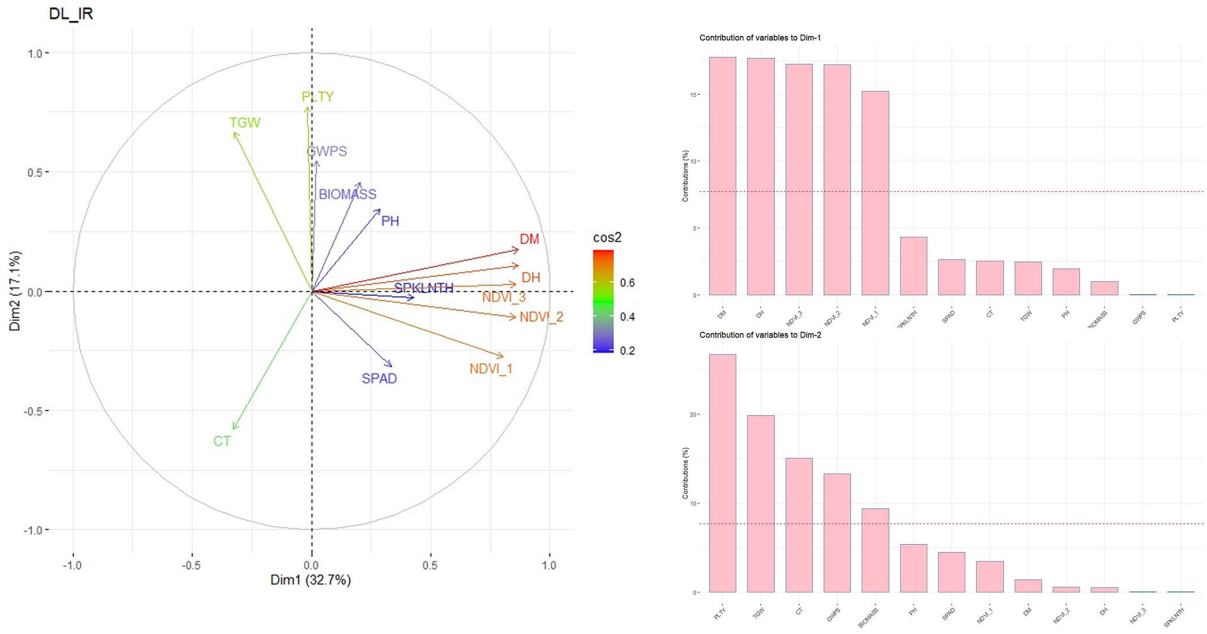


FIGURE 3
PCA biplot and contribution of studied traits to dimension 1 and dimension 2 in GWAS panel evaluated at IARI Delhi under IR condition during 2020–2021.

TABLE 3 Chromosome wise distribution of SNP markers on the three sub genomes of wheat.

| Chromosome | Sub genome | | |
|---|---|---|---|
| | A | B | D |
| 1 | 489 | 705 | 616 |
| 2 | 628 | 777 | 767 |
| 3 | 432 | 499 | 348 |
| 4 | 397 | 299 | 184 |
| 5 | 477 | 652 | 433 |
| 6 | 404 | 570 | 323 |
| 7 | 523 | 581 | 442 |
| Total | 3,350 | 4,083 | 3,113 |

9.22 MB for A, B and D genomes, respectively (Figure 5). Whole genome LD decay was observed to be 7.15 MB, indicating any SNPs within this distance are said to behave as inheritance block.

## Marker trait associations (MTAs)

For all the studied traits together across the location with different treatment conditions, *viz.*, IR, RI and LS, a total of 761 MTAs were identified with a significance $-log_{10}(p)$ value of >3. The highest number of SNPs were obtained for the trait NDVI (242 MTAs) and the lowest for the SPAD (19 MTAs). Associated SNPs identified for each trait under different conditions are listed with their respective *p*-values (Supplementary Table 4). MTAs were filtered with Bonferroni correction value ($-log_{10}(p)$ >5.32) to increase the stringency of selection, and 57 SNPs were obtained that were located on 18 different chromosomes (Figure 6). Out of 57 SNPs, 28 were identified under IR condition, which were linked with BIOMASS, DH, DM, GWPS NDVI, PH and TGW. Under RI condition, 16 SNPs linked with DH, GWPS, NDVI and PH were obtained. Thirteen significant associations were obtained under LS conditions for traits, *viz.*, CT, DH, DM, GWPS, NDVI and PLTY (Table 3). Pictorial representation of some significant SNPs identified at Delhi and other locations for the studied traits were depicted with Manhattan plots along with QQ plots (Figure 7; Supplementary Figure 4). The details of MTAs above Bonferroni correction with their position in the genome are noted down (Table 4). Among them, 22 SNPs were stable and pleiotropic and were associated with six different traits, namely, DH, DM, NDVI, TGW, PH and BIOMASS. NDVI and DH were showing the highest number of stable MTAs, i.e., 7, followed by DM and TGW having 3 and 2 MTAs, respectively. Whereas BIOMASS and PH were having one stable association each (Table 5). Percent phenotypic variation explained ($r^2$) by the stable MTAs ranged from 3.87% in PH to 19.22% in DM (Table 4).

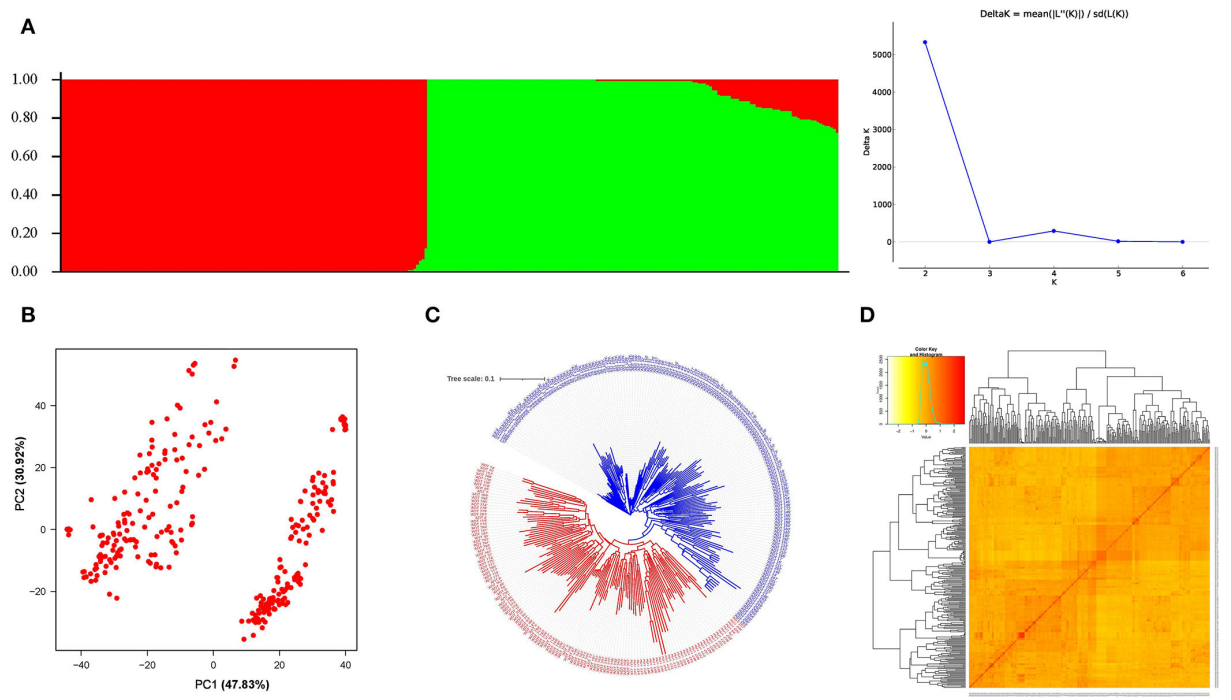


FIGURE 4
Population groupings in the GWAS panel from different models. **(A)** Population structure-based grouping of genotype from STUCTURE analysis. **(B)** The 2D plot of the principal component-based grouping. **(C)** Neighbor-joining tree-based diversity. **(D)** Heat map of pair-wise kinship matrix.

We identified nine pleiotropic MTAs having associations with different traits (Table 5). The SNP marker AX-94490240 and AX-94463626 were associated with DM, NDVI and DH, whereas AX-94598030 and AX-94759710 were linked with TGW and NDVI. Similarly, GWPS and DH were associated with AX-94988124 and AX-94466450 with BIOMASS and PLTY. However, their strength of association differs depending on traits and location (Table 5).

## *In silico* analysis

BLAST analysis of stable SNPs against the IWGSC reference genome of *Triticum aestivum* revealed the location of SNPs in the gene-rich region of the genome. Almost all SNPs were near to one or the other transcript coding for some proteins or transcription factors except SNP AX-94466450. SNPs were located near the genes coding for proteins like peroxisomal membrane protein, ran binding protein, augmin family, etc. (Table 6). SNPs AX-94762983 and AX-95133267 were located in a protein-coding region whose protein is still unknown. The SNPs markers like AX-94578563, AX-94941121 and AX-94631711 were linked to the genes governing the traits like endosperm, ascorbate content and root growth, and are helpful in the heading of the wheat. Similarly, SNPs like AX-94759710 and AX-94598030 linked are to TGW and are present near the gene coding region for endosperm development and resistance to oxidative stress (Table 6).

# Discussion

Drought and heat have the greatest influence on wheat varieties, therefore identifying the genomic region using genome-wide SNP markers is a smart way to gain knowledge, which can then be used to create climate-resilient varieties. The goal of this study is to identify a new region of the wheat genome that is responsible for drought and heat stress resistance. The use of elite breeding material for GWAS invariably reduces the number of significant SNPs compared with other studies, where diverse plant materials with high diversity and larger phenotypic differences were used (Bordes et al., 2014; Zanke et al., 2015). In such material QTL with large effects on the traits may be fixed in the breeding lines, and will therefore not be detectable (Kristensen et al., 2018). However, the utilization of an advanced breeding line will help to explore untouched parts of the genome having minor effects on the target traits by avoiding the influence of major QTL regions during the study that are already fixed. Furthermore, advanced breeding lines are ready to use the material in the breeding programme as a parent

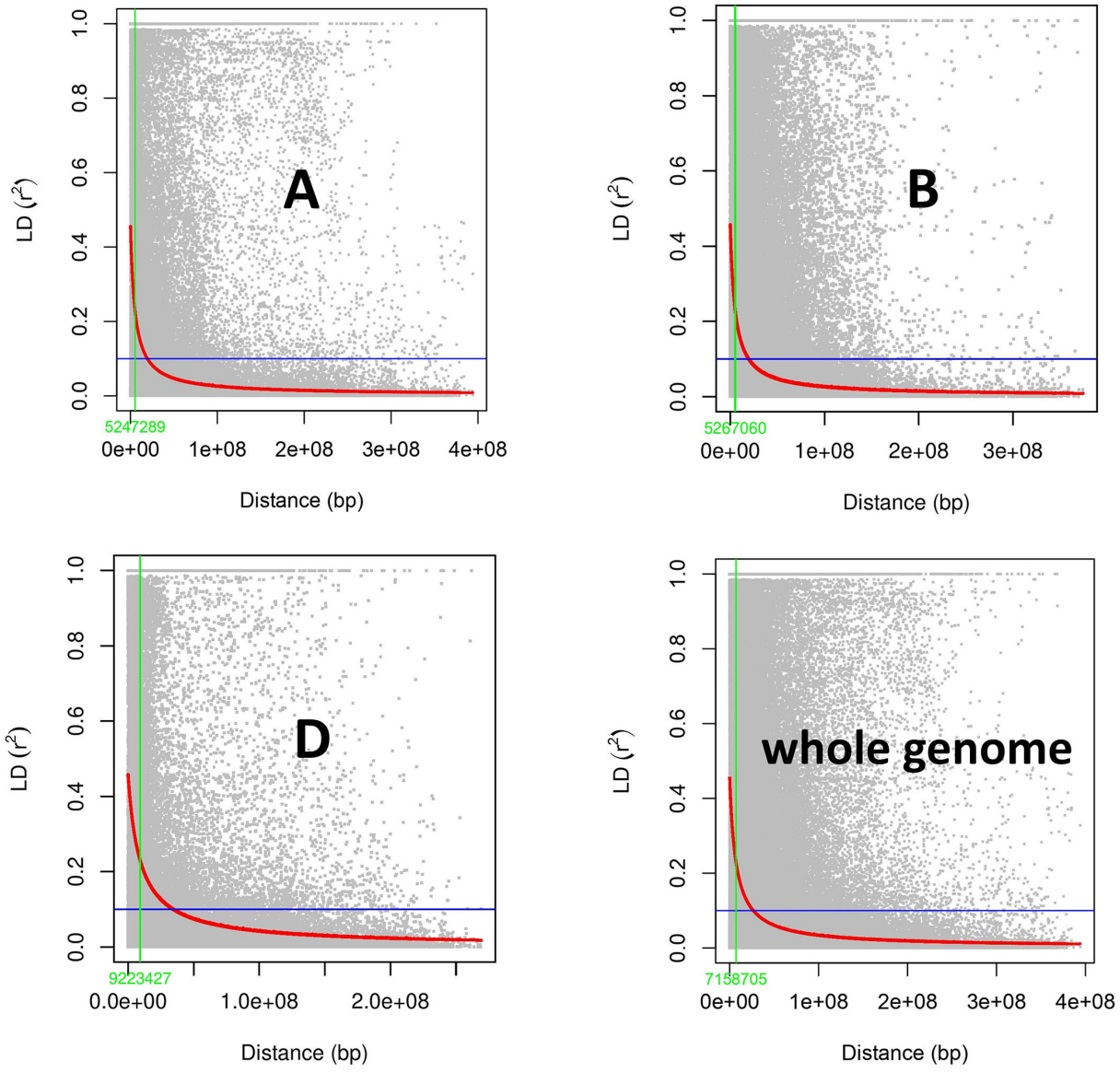


FIGURE 5
Subgenome and whole genome-wide linkage disequilibrium (LD) decay in GWAS panel of 282 diverse bread wheat genotypes.

(Kristensen et al., 2018) with preferred qualities and having a meager problem of linkage drag.

In this study, the near normal distribution among all the studied traits (Figure 1) indicated the polygenic nature of the studied traits. Significant variation was observed from the analysis of variance indicating the data can be used for further analysis. The coefficient of variation was low for the traits, such as DH, DM and NDVI, whereas high CV was observed for biomass and plot yield which was due to the high influence of environmental factors. To nullify the effect of environmental influence, multi-location and multi-year data were used to find out stable associations.

In GWAS analysis, population structure might be a confounding factor that must be addressed to avoid false associations. STRUCTURE and PCA are two popular approaches for inferring the population structure of the genome-wide association panel using high-density SNPs (Abraham and Inouye, 2014). The use of genotypes from Indian and exotic introduction in the study might be the reason for clear-cut two subpopulations (Figure 4A) in the mapping panel. As many as 14 admixture genotypes carrying genomic regions from both the subpopulations were observed, which is due to the advanced breeding line developed from common founding parents used in their crossing plan. AM

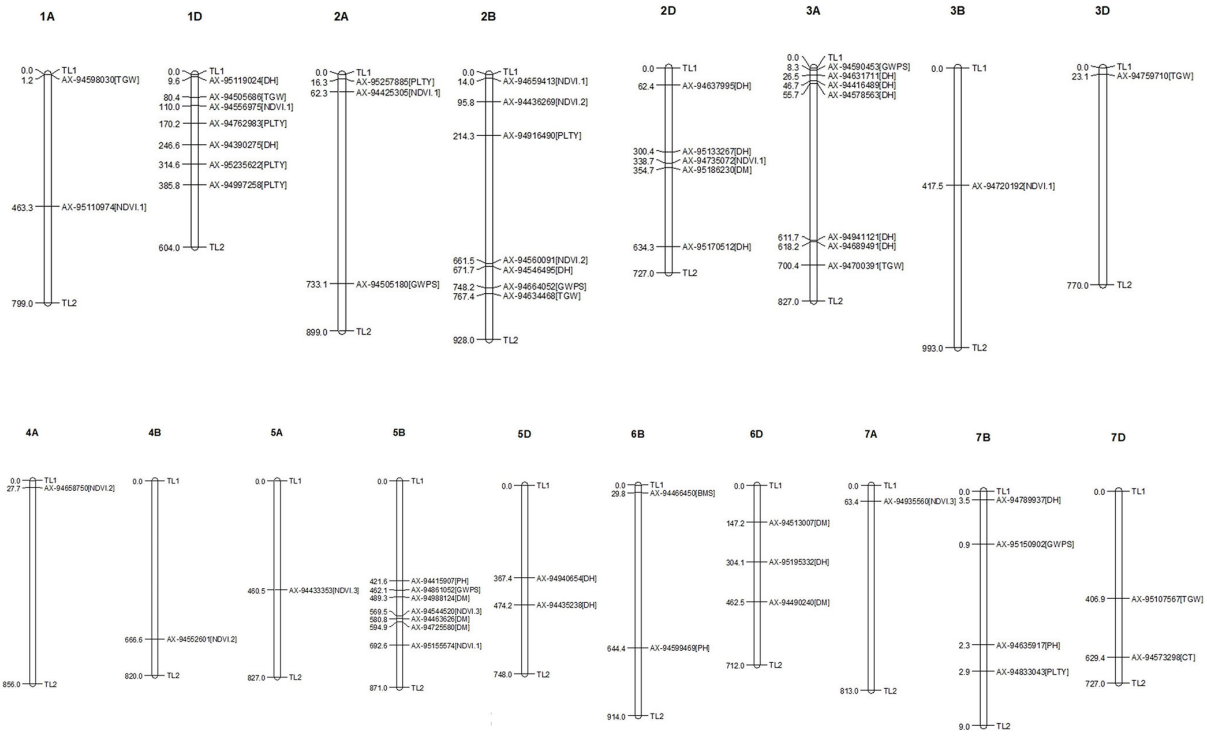


FIGURE 6
Distribution and position of identified MTAs (*-log(p)* above 5.32) at their respective chromosome.

panels with subpopulations were used efficiently by using either PCA-based grouping (Odilbekov et al., 2019; Rathan et al., 2022) or with the uses of the Q matrix from the STRUCTURE analysis as covariates (Beyer et al., 2019; Luján Basile et al., 2019; Danakumara et al., 2021; Alotaibi et al., 2022). Apart from that, suitable diversity for GWAS study among the genotypes in AM panel was confirmed by neighbor-joining clustering from the distance matrix. The use of a diverse panel of genotypes can provide more valuable inference compared to bi-parental populations (Vos-Fels et al., 2017) by taking advantage of maximum allelic diversity (Ayalew et al., 2018; Onyemaobi et al., 2018). The present study material being developed from multiple crossing ensures the required diversity for the association study, and estimation is based on neighbor-joining clusters and kinship-based heat map (Figure 4D).

In outcrossing crop species like maize, LD block was observed at a short distance and thus decays were faster, and in the case of self-pollinated crops longer distance is attributed to a lower decay rate as in wheat (Yu et al., 2014; Roncallo et al., 2021). For example, the genome-wide LD decay distance is ∼100 kb in rice and ∼2 kb in maize (Huang and Han, 2014); however, in wheat, up to 30.4 mb LD decay was observed in Argentinian germplasm collection (Roncallo et al., 2021). LD is important in population genetics and crop improvement using molecular techniques (Gupta et al., 2005). The number of markers required for association mapping is determined by the extent of LD decay, based on the genetic distance between markers (Mather et al., 2007). LD decay varies widely among wheat populations. In this study, LD at half LD decay (Figure 5) varies for each genome with larger whole genome LD of 7.15 Mb, inferring the lower decay for the advanced breeding materials. Similarly, a large LD block size of 4.4 MB was observed by Pang et al. (2020). As much as 9.22 Mb distance was observed for the D genome inferring lower decay, which is in accordance with the previous study (Ogbonnaya et al., 2017; Jamil et al., 2019; Li G. et al., 2019; Pang et al., 2020). In contrast, faster LD decay in the D genome was observed; comparable to the A and B genomes in a study using breeding lines developed from synthetics, driving more recombination in the D genome (Ledesma-Ramírez et al., 2019). The significant variations in LD decay rates among the A, B and D genomes imply that the three genomes and their donors, *T. turgidum* (A and B) and *Ae. tauschii* (D), might have evolved independently and under different selection pressures throughout the domestication and modern breeding objectives (Mirzaghaderi and Mason, 2017). LD decay depends on cultivation patterns, breeding methods, breeding history and evolutionary history. Wheat is grown once a year, hence has a much slower rate of evolution, and

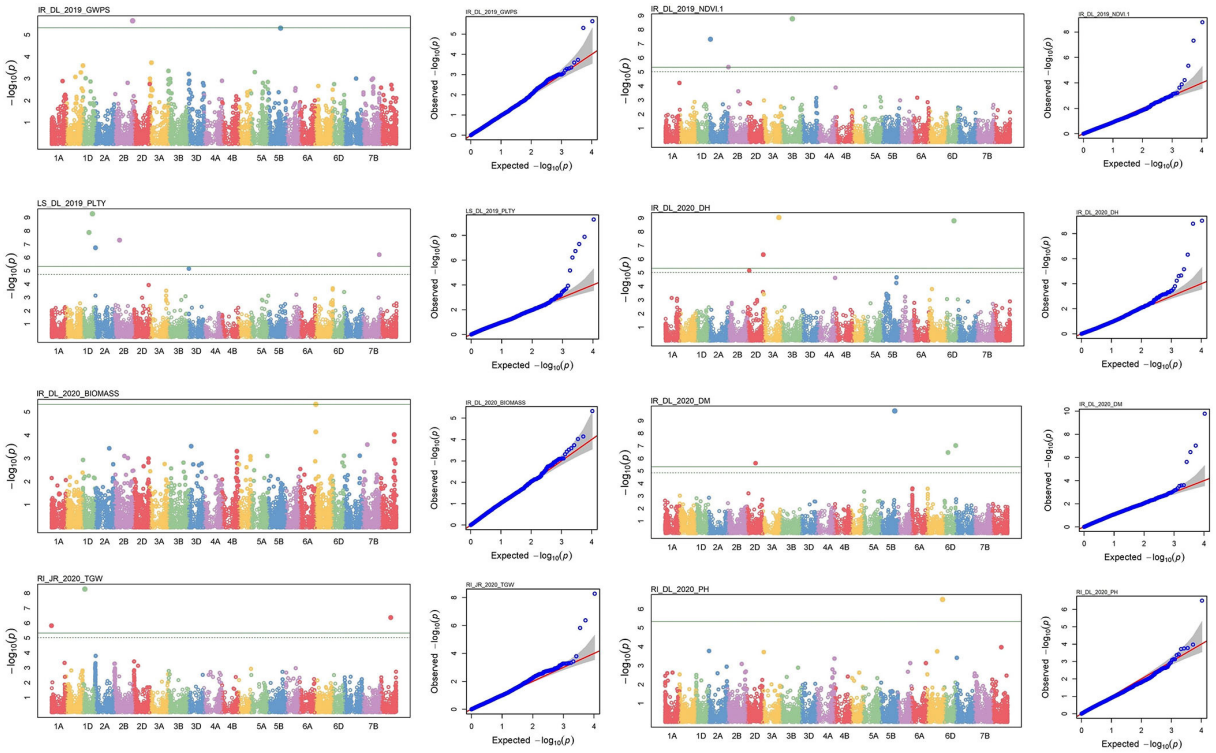


FIGURE 7
Manhattan and respective-QQ plots of significant associations at IR_Delhi_2019 for GWPS, LS_DL_2019 for PLTY, IR_DL_2020 for BIOMASS and RI_JR_2020 for TGW, IR_DL_2019 for NDVI, IR_DL_2020 for DH, IR_DL_2020 for DM and IR_DL_2020 for PH.

likely accumulated far fewer historical recombination events and mutations, resulting in a slower LD decay than in other self-pollinated crops like rice (Pang et al., 2020).

At a significant $p < 0.001$, a total of 761 SNPs were identified to be associated with traits under investigation. Such a huge number of MTAs can be justifiable for high-throughput genotyping data and with the cut-off *p-value* of 0.001, similar to earlier reports for various agronomic traits (Ma et al., 2018; Pang et al., 2020). A huge number of SNPs obtained for yield-related traits under stress conditions may include many of the false positives due to lower threshold values. To avoid such biasness, a stringent selection procedure of Bonferroni correction was applied like Kumar et al. (2018), and in total 57 MTAs were retained. If geographical and environmental variation among different locations was significantly high, a location-wise association study was carried out to avoid flattening of the genetic variation as mentioned in previous references (Pujar et al., 2020; Rathan et al., 2022). MTAs observed in more than one location with Bonferroni corrected *p-value* in at least one location (Stable MTAs) are presumed to be the true association, which is supported by the presence of the candidate gene (Table 6).

NDVI is an indicator of vegetation response to drought based on the relationships between NDVI and drought index (Rutkoski et al., 2016; Singh et al., 2016). In our study, as many as 242 SNPs were linked with NDVI at an LOD score of 3. When we observe the stable expressing SNPs across the environment, 10 SNPs belonging to NDVI indicated a true association with it. The reason might be drought and heat conditions applied by restricted irrigation and late sown conditions have induced the drought and heat tolerant genotypes to exhibit related traits and associated SNPs were identified. Susceptibility indices of drought and heat could be a potential targeting trait to encounter consistent yield in the stress breeding programme (Devi et al., 2022; Mutari et al., 2022). An extensive analysis of susceptibility indices could be our further target to dissect the genomic regions concerned with drought and heat tolerant traits.

A total of 22 stable SNPs were found for different traits having major number of MTAs for NDVI (10) and DH (11). Easy phenotyping and having high accuracy might lead to a greater number of associations between DH and NDVI. DH-linked SNPs were detected on chromosomes 3A, 2D, 1D, 5D, 3A, 5B, and 6D are on par with earlier reports like the presence of VRN genes responsible for flowering on chromosomes 5A, 5B and 5D (Ogbonnaya et al., 2017). Markers linked with the DH were also found on chromosomes 1D, 2A, 4A, 5B, 5D, 6A, 6B, and 7A (Jamil et al., 2019). It is notable that we got clusters of markers on chromosome 5B for DM, GWPS, NDVI and PH that might be influenced by the presence of the *vrn B-1* gene on 5B. Earlier reports denote 29.1% of phenotypic variations for heading date

TABLE 4 Significant marker trait associations at Bonferroni corrected *p value* for traits under study at each environment.

| Trait | Condition/location | SNP | Chromosome | Position in MB | *P*-value | R square | $-log_{10}(P)$ |
|---|---|---|---|---|---|---|---|
| BIOMASS | IR_DL_2020 | AX-94466450 | 6B | 29.84924 | 4.67E-06 | 0.071452 | 5.33089 |
| CT | LS_DL_2019 | AX-94573298 | 7D | 629.4069 | 3.01E-06 | 0.20653 | 5.521182 |
| DH | LS_DL_2020 | AX-94416489 | 3A | 46.7133 | 1.51E-06 | 0.081693 | 5.820014 |
| | IR_PUNE_2020 | AX-94435238 | 5D | 474.2051 | 3.92E-09 | 0.098932 | 8.407157 |
| | RI_PUNE_2020 | AX-94435238 | 5D | 474.2051 | 7.68E-10 | 0.097184 | 9.114737 |
| | IR_IIWBR_2020 | AX-94546495 | 2B | 671.7411 | 1.26E-08 | 0.069093 | 7.900783 |
| | IR_PUNE_2020 | AX-94578563 | 3A | 55.74342 | 1.40E-08 | 0.087051 | 7.852822 |
| | RI_PUNE_2020 | AX-94578563 | 3A | 55.74342 | 1.78E-07 | 0.080392 | 6.749976 |
| | IR_PUNE_2020 | AX-94631711 | 3A | 26.46988 | 3.07E-06 | 0.08455 | 5.513009 |
| | IR_DL_2020 | AX-94689491 | 3A | 618.1646 | 9.18E-10 | 0.137955 | 9.037012 |
| | IR_IIWBR_2020 | AX-94789937 | 7B | 33.53386 | 4.13E-07 | 0.076708 | 6.384131 |
| | LS_DL_2020 | AX-94940654 | 5D | 367.436 | 4.17E-06 | 0.104355 | 5.379682 |
| | IR_PUNE_2020 | AX-94941121 | 3A | 611.7026 | 3.28E-11 | 0.110475 | 10.48453 |
| | RI_DL_2019 | AX-94941121 | 3A | 611.7026 | 2.34E-09 | 0.13456 | 8.630091 |
| | RI_PUNE_2020 | AX-94941121 | 3A | 611.7026 | 2.77E-10 | 0.095057 | 9.557035 |
| | RI_DL_2019 | AX-95119024 | 1D | 9.592365 | 1.21E-06 | 0.135519 | 5.917904 |
| | RI_DL_2019 | AX-95133267 | 2D | 300.437 | 1.71E-06 | 0.138337 | 5.766205 |
| | IR_DL_2020 | AX-95170512 | 2D | 634.3167 | 4.74E-07 | 0.129128 | 6.323975 |
| | IR_DL_2020 | AX-95195332 | 6D | 304.1167 | 1.59E-09 | 0.119489 | 8.798271 |
| | RI_JR_2020 | AX-95235622 | 1D | 314.5742 | 3.25E-10 | 0.111089 | 9.488192 |
| DM | IR_DL_2020 | AX-94463626 | 5B | 580.8401 | 1.66E-10 | 0.189125 | 9.780337 |
| | IR_DL_2020 | AX-94490240 | 6D | 462.537 | 9.50E-08 | 0.192265 | 7.022311 |
| | IR_DL_2020 | AX-94513007 | 6D | 147.2393 | 3.43E-07 | 0.183054 | 6.465213 |
| | IR_IIWBR_2020 | AX-94725580 | 5B | 594.8691 | 3.20E-08 | 0.085151 | 7.494575 |
| | LS_DL_2020 | AX-94725580 | 5B | 594.8691 | 2.69E-08 | 0.09407 | 7.570521 |
| | IR_DL_2020 | AX-95186230 | 2D | 354.7437 | 2.43E-06 | 0.15434 | 5.615057 |
| GWPS | LS_DL_2019 | AX-94505180 | 2A | 733.0912 | 1.64E-07 | 0.108636 | 6.785046 |
| | RI_DL_2019 | AX-94590453 | 3A | 8.325489 | 2.69E-08 | 0.141871 | 7.569559 |
| | IR_DL_2019 | AX-94664052 | 2B | 748.1526 | 2.30E-06 | 0.081038 | 5.637959 |
| | IR_DL_2019 | AX-94988124 | 5B | 489.2835 | 4.97E-06 | 0.077532 | 5.303543 |
| | RI_DL_2019 | AX-95150902 | 7B | 200.9228 | 2.36E-07 | 0.133409 | 6.62789 |
| NDVI.1 | IR_DL_2019 | AX-94425305 | 2A | 62.27144 | 4.79E-08 | 0.089911 | 7.319923 |
| | IR_DL_2019 | AX-94659413 | 2B | 14.04945 | 4.53E-06 | 0.10992 | 5.343983 |
| | IR_DL_2019 | AX-94720192 | 3B | 417.493 | 1.69E-09 | 0.110884 | 8.771124 |
| | IR_DL_2020 | AX-94735072 | 2D | 338.6773 | 3.35E-07 | 0.078254 | 6.474963 |
| | LS_DL_2019 | AX-94762983 | 1D | 170.2247 | 1.57E-11 | 0.098748 | 10.80411 |
| | LS_DL_2019 | AX-95110974 | 1A | 463.2904 | 2.06E-08 | 0.107363 | 7.685398 |
| | LS_DL_2019 | AX-95155574 | 5B | 692.565 | 1.31E-06 | 0.116167 | 5.883924 |
| NDVI.2 | RI_DL_2019 | AX-94436269 | 2B | 95.79736 | 6.06E-10 | 0.115805 | 9.21725 |
| | LS_DL_2020 | AX-94552601 | 4B | 666.5719 | 3.51E-08 | 0.093756 | 7.454121 |
| | RI_DL_2020 | AX-94560091 | 2B | 661.4501 | 1.64E-08 | 0.078829 | 7.784441 |
| | RI_DL_2020 | AX-94658750 | 4A | 27.67354 | 3.91E-07 | 0.059888 | 6.407471 |
| NDVI.3 | LS_DL_2019 | AX-94433353 | 5A | 460.5185 | 5.61E-10 | 0.110697 | 9.251103 |
| | IR_DL_2020 | AX-94463626 | 5B | 580.8401 | 1.9E-08 | 0.121709 | 7.720863 |
| | LS_DL_2019 | AX-94935560 | 7A | 63.38946 | 9.13E-09 | 0.132109 | 8.039646 |
| PH | IR_JR_2020 | AX-94415907 | 5B | 421.6436 | 2.25E-07 | 0.038779 | 6.648635 |
| | RI_DL_2020 | AX-94599469 | 6B | 644.4316 | 3.15E-07 | 0.116949 | 6.501722 |

*(Continued)*

TABLE 4 Continued

| Trait | Condition/location | SNP | Chromosome | Position in MB | *P*-value | R square | $-log_{10}(P)$ |
|---|---|---|---|---|---|---|---|
| PLTY | LS_DL_2019 | AX-94390275 | 1D | 246.6495 | 1.32E-08 | 0.187926 | 7.878685 |
| | LS_DL_2019 | AX-94833043 | 7B | 682.8865 | 6.12E-07 | 0.200662 | 6.212957 |
| | LS_DL_2019 | AX-94916490 | 2B | 214.2827 | 4.97E-08 | 0.20182 | 7.303398 |
| | LS_DL_2019 | AX-94997258 | 1D | 385.8051 | 5.22E-10 | 0.21241 | 9.282206 |
| | LS_DL_2019 | AX-95257885 | 2A | 16.25963 | 1.86E-07 | 0.203534 | 6.731365 |
| TGW | RI_JR_2020 | AX-94505686 | 1D | 80.44586 | 5.32E-09 | 0.124761 | 8.273984 |
| | RI_JR_2020 | AX-94598030 | 1A | 1.159536 | 1.51E-06 | 0.117123 | 5.822309 |
| | IR_PUNE_2020 | AX-94634468 | 2B | 767.3743 | 1.52E-07 | 0.073127 | 6.817671 |
| | IR_IIWBR_2020 | AX-94700391 | 3A | 700.422 | 6.70E-08 | 0.084706 | 7.173684 |
| | RI_JR_2020 | AX-95107567 | 7D | 406.8963 | 4.32E-07 | 0.12292 | 6.364986 |

TABLE 5 List of stable SNPs expressed at more than one environment and Pleiotropic* SNPs (Bold ones) linked to more than one traits.

| SNP | Chromosome | Position | Trait | Location | *-log10(p)* Value |
|---|---|---|---|---|---|
| **AX-94466450** | 6B | 3E+07 | BIOMASS, PLTY | DL.IR / DL.IR | 5.33 / 4.46 |
| AX-94631711 | 3A | 2.6E+07 | DH | PUNE IR / PUNE RI | 5.51 / 3.86 |
| AX-94578563 | 3A | 5.6E+07 | DH | PUNE IR / PUNE RI | 7.85 / 6.75 |
| AX-94637995 | 2D | 6.2E+07 | DH | DL.IR / DL.2019.LS | 5.16 / 3.21 |
| AX-95133267 | 2D | 3E+08 | DH | DL.2019.RI / DL.2019.RI / DL.2019.LS | 5.77 / 5.23 / 3.42 |
| AX-95235622 | 1D | 3.1E+08 | DH | JR.RI / DL.RI / DL.2019LS / DL.LS | 9.49 / 3.99 / 3.4 / 3.24 |
| AX-94435238 | 5D | 4.7E+08 | DH | PUNE RI / PUNE IR | 9.11 / 8.41 |
| AX-94941121 | 3A | 6.1E+08 | DH | PUNE IR / PUNE RI / DL.2019.RI | 10.48 / 9.56 / 8.63 |
| **AX-94725580** | 5B | 5.9E+08 | DM, DM, DH | DL.LS / IIWBR / DL.LS | 7.57 / 7.49 / 4.72 |
| **AX-94490240** | 6D | 4.6E+08 | DM, NDVI, DH | DL.IR / DL.IR / DL.IR | 7.02 / 3.3 / 3.04 |
| **AX-94463626** | 5B | 5.8E+08 | DM, NDVI, DH, NDVI, NDVI | DL.IR / DL.IR / DL.IR / DL.IR / DL. LS | 9.78 / 7.72 / 4.66 / 3.11 / 3 |
| **AX-94513007** | 6D | 1.5E+08 | DM, TGW | DL.IR / IIWBR | 6.47 / 3.21 |
| **AX-94988124** | 5B | 4.9E+08 | GWPS, DH | DL.2019.IR / DL.2019.LS | 5.3 / 4.07 |
| AX-94552601 | 4B | 6.7E+08 | NDVI | DL.LS / DL.RI | 7.45 / 3.03 |
| AX-94436269 | 2B | 9.6E+07 | NDVI | DL.2019.RI / DL.IR | 9.22 / 3.04 |
| **AX-94560091** | 2B | 6.6E+08 | NDVI, DH | DL.RI / DL.2019.LS | 7.78 / 3.64 |
| AX-95155574 | 5B | 6.9E+08 | NDVI | DL.2019.LS | 5.88 / 3.14 |
| AX-94433353 | 5A | 4.6E+08 | NDVI | DL.2019.LS / DL.2020.LS / DL.2019.LS.NDVI.3 | 9.25 / 4.2 / 3.73 |
| AX-94762983 | 1D | 1.7E+08 | NDVI | DL.2019.LS / DL.2019.LS | 10.8 / 3.01 |
| AX-94415907 | 5B | 4.2E+08 | PH | JR.RI / IIWBR | 6.65 / 3.41 |
| **AX-94598030** | 1A | 1159536 | TGW, NDVI | JR.RI / DL.IR | 5.82 / 3.36 |
| **AX-94759710** | 3D | 2.3E+07 | TGW, NDVI | PUNE RI | 5.3 / 3.16 |

*Bold one are pleiotropic MTAs.

from this region (Rivera-Burgos et al., 2022). Previous studies confirmed the influence of the chromosome 5B on flowering and the presence of *VRN* genes at 5B, influencing the vegetative and reproductive traits (Kiseleva et al., 2016; Huang et al., 2018). For NDVI, MTAs were obtained on chromosomes 1A and 5A on the A genome, 2B, 4B, and 5B on the B genome and 1D, 3D, and 6D on the D genome. The MLM-Q+K-based analysis detected unique NDVI QTLs on chromosomes 1A, 1B, 2B, 4A, 4B, 5A, 6A, 6B, and 7A in a study conducted by Condorelli et al. (2018). Similarly, NDVI-related MTAs on 1A and 7A were found out by Ward et al. (2019). As argued by Paliwal et al. (2012), a chromosomal region on 2B is of prime importance for heat stress. We obtained a stable SNP on the 2B chromosome for NDVI with an 11.5% variation explained. Apart from these, MTAs, *viz.*, AX-94466450 (6B), AX-94988124 (5B) and AX-94415907 (5B) were linked stably to the traits, plot yield, GWPS and PH, respectively. Three SNPs, AX-94513007, AX-94598030 and AX-94759710, were identified for TGW on chromosomes 1A, 3D and 6D. In previous studies, markers linked with TGW were observed in 6D (Wang et al., 2012; Chen et al., 2016),

10.3389/fpls.2022.943033

TABLE 6 Putative candidate genes identified at the 10 kb region of Linked SNPs along with their molecular functions.

| Trait | SNP | Gene | Position | Protein | Role | Reference |
|---|---|---|---|---|---|---|
| DH | AX-94637995 | TraesCS2D02G112700.1 | 2D: 62,401,570-62,405,841 | AIG1-type guanine nucleotide-binding (G) domain | | |
| | AX-94631711 | TraesCS3A02G050211.2 | 3A: 26,472,148-26,482,725 | Wall-associated receptor kinase, galacturonan-binding domain | Regulation of root growth | Kaur et al., 2013 |
| | AX-95133267 | TraesCS2D02G328100LC.1 | 2D: 300,439,172-300,440,223 | Protein coding | | |
| | AX-94578563 | TraesCS3A02G086500.1 | 3A: 55,743,110-55,743,857 | Invertase/pectin methylesterase inhibitor domain superfamily | Early development of wheat grain endosperm and outer layers | Mehdi et al., 2020 |
| | AX-94941121 | TraesCS3A02G363000.1 | 3A: 611,700,692-611,703,172 | SUGAR-1-PHOSPHATE GUANYL TRANSFERASE | L-galactose guanyltransferase, increases leaf ascorbate content | Laing et al., 2007 |
| | AX-94435238 | TraesCS5D02G410900.1 | 5D: 474,200,732-474,205,422 | AUGMIN FAMILY | Centrosome cycle spindle assembly | Hotta et al., 2012 |
| | AX-95235622 | TraesCS1D02G226200.1 | 1D: 314,573,418-314,574,779 | RAN BINDING PROTEIN | | |
| DM | AX-94513007 | TraesCS6D02G166200.1 | 6D: 147,236,496-147,241,863 | RNA recognition motif domain | | |
| | AX-94490240 | TraesCS6D02G383800.1 | 6D: 462,536,412-462,540,932 | ZINC FINGER, RING/FYVE/PHD-TYPE | | |
| | AX-94725580 | TraesCS5B02G418600.1 | 5B: 594,867,010-594,872,193 | Inosine-5'-monophosphate dehydrogenase | Regulation of cell growth. | Uniprot |
| NDVI | AX-95155574 | TraesCS5B02G536500.1 | 5B: 692,559,588-692,565,223 | Serine/threonine-protein kinase, active site | Flag leaf width, plant height and water-soluble carbohydrates under drought conditions | Zhang et al., 2013 |
| | AX-94552601 | TraesCS4B02G390400.1 | 4B: 666,571,620-666,572,590 | Ubiquitin-like domain | | |
| | AX-94463626 | TraesCS5B02G405200.1 | 5B: 580,830,088-580,840,255 | ALPHA-N-ACETYLGLUCOSAMINIDASE | Fertilization and seed development in Arabidopsis | Ronceret et al., 2008 |
| | AX-94560091 | TraesCS2A02G444900.1 | 2A: 694,905,983-694,909,467 | Peptidase S8 and S53 | Integrin-mediated signaling pathway, calcium ion binding | Uniport |
| | AX-94436269 | TraesCS2B02G127800.1. | 2B: 95,794,615-95,797,096 | AP2/ERF DOMAIN-CONTAINING PROTEIN | Ethylene-responsive transcription factor | Djemal and Khoudi, 2015 |
| | AX-94433353 | TraesCS5A02G246700.1 | 5A: 460,516,405-460,520,083 | Protein kinase, ATP binding site | | |
| | AX-94762983 | TraesCS1D02G197500LC.1 | 1D: 170,223,005-170,223,304 | Protein coding | | |
| PH | AX-94415907 | TraesCS5B02G241800.1 | 5B: 421,643,604-421,643,664 | ACTIN T1-LIKE PROTEIN | | |
| TGW | AX-94759710 | TraesCS3D02G055400.1 | 3D: 23,057,692-23,061,395 | Glycosyl transferase, family 1 | Development of Rice Endosperm | Yang et al., 2021 |
| | AX-94598030 | TraesCS1A02G001900.6 | 1A: 1,162,817-1,166,405 | PEROXISOMAL MEMBRANE PROTEIN | Plant proteases, protein degradation, and oxidative stress | Palma et al., 2002 |

1A (Ogbonnaya et al., 2017) and pleiotropic regions affecting kernel weight-related traits on chromosomes 1B, 2A and 3A (Chen et al., 2016). Contrary to this, stable SNPs for TGW were observed on chromosomes 5A (Wang et al., 2017), 1D and 7A (Edae et al., 2014). SNPs location on 1A, 3D and 6D were novel in our study.

Stable expression along the different locations and conditions is presumed to be the real association of these

markers with the studied traits. Significant SNPs detected in this study for grain yield parameter can be indirectly selected under drought and heat condition having an influence on the stress tolerance mechanism and pathway involved in abiotic stress tolerance, which is also observed by Schmidt et al. (2020). Hence, it is common to find markers to be associated with more than one trait, i.e. pleiotropic influence. Significant pleiotropic loci were detected for yield and stress tolerance-related traits showing yield and stress tolerant traits have an influence on one another as reported by Mathew et al. (2018). Similarly, we found nine different stable MTAs showing pleiotropic effects between different yield related and stress-tolerant traits as depicted in Table 5. Important yield trait like TGW linked SNPs, *viz*., AX-94598030 and AX-94759710 were pleiotropic with NDVI, an important drought tolerant trait. Pleiotropy between yield related and NDVI was found in a QTL mapping study by Shi et al. (2017). SNP, AX-94513007, was having pleiotropy between TGW and DM, a stay-green trait was helpful in heat and drought tolerance. It is clear that markers, *viz*., AX-94725580, AX-94490240, AX-94560091 and AX-94463626 exhibit pleiotropy among traits DH, DM and NDVI. Due to the interdependence on one another they are bound to share genes in common and the results can also be supported by the presence of positive correlation among these traits (Figure 2). Pleiotropy between NDVI and TGW observed by the markers AX-94598030 and AX-94759710 indicates the collinearity between stress tolerant and yield-related traits under stress condition. Markers such as AX-94560091 located near to the transcript TraesCS1A02G001900 related to Integrin-mediated signaling pathway and calcium ion-binding protein obviously having multiple roles in drought tolerance in plant system (Lü et al., 2007; Takahashi et al., 2020). Pleiotropic maker AX-94598030 was mapped near the proteins involved in stress tolerance, such as peroxisomal membrane protein (Table 6), which are involved in the mitigation of protein degradation and oxidative stress tolerance (Palma et al., 2002), in turn may have influence on yield parameters in stress. The pleiotropic effect between stress tolerance and grain traits are previously reported in many studies (Ahmed et al., 2022b). Markers such as AX-94578563 and AX-94941121 associated with DH were present near the gene coding for Invertase/pectin methylesterase inhibitor domain superfamily and sugar-1-phosphate guanyl transferase, respectively. The first has a role in early development of wheat grain endosperm and outer layers (Mehdi et al., 2020), which is related to flowering fertilization in flowering plants. Whereas the second one has a role in L-galactose guanyl-transferase, which increases leaf ascorbate content that induces early flowering (Laing et al., 2007). These findings found out that novel MTAs that are detected here can be evaluated further for the validation of the markers.

Furthermore, such markers can be utilized for marker assisted breeding for genes related to drought and heat tolerance along with high yield. MTAs that are stable across the environment have great potential to be deployed in developing new wheat varieties through molecular breeding. Marker validation and pathway followed by the genes associated with markers can be analyzed for further evidence to support the reliability of associations, thereby have utilization in breeding programmes. As the plant materials used in the study are advanced breeding lines that are used for further evaluation to release variety or can be directly used as parents in breeding programmes.

## Conclusion

Genetic dissection of the genomic region responsible for drought and heat tolerance is having immense importance in the development of climate-resilient varieties. A total of 295 advanced breeding lines used in GWAS panel showed continuous variation for most of the studied traits. Sufficient genetic diversity was observed in AM panel with structured two subpopulations. A large LD block size of 7.15 MB was found out showing reliable linkage of markers with the trait of interest for more generations. Fifty-seven high-confident markers associated with drought and heat tolerance and yield related traits, *viz.,* DH, DM, NDVI, PH and TGW were discovered in this study. Many of the identified MTAs were located near the putative candidate gene and protein coding transcript influencing the traits of interest. A total of 22 stable MTAs identified across the locations were having practical utilization in future wheat breeding programmes.

## Data availability statement

The original contributions presented in the study are included in the article/Supplementary material, and in the DRYAD repository, accessible at https://datadryad.org/stash/share/SwCnD0OA5Pi0oa96xplZAv3k51QMn0FFU_0kEZNFpn0 further inquiries can be directed to the corresponding author/s.

## Author contributions

PS, NJ, GS, and HKr conceptualized the investigation and edited the manuscript. PS supervised the conduct of the experiment. ND conducted the investigation and prepared the draft of the manuscript. ND, SP, MK, HKh, RP, and JS generated the phenotypic data. HKr, SS, DC, and KM contributed in the generation of genotyping data. ND and HKr did the statistical and GWAS analysis. PS, HKr, MK, HKh, RP, and JS conducted field trials and provided help in recording observations. All authors contributed to the article and approved the submitted version.

## Funding

This study was supported by funding provided by the Indian Council of Agricultural Research (ICAR) and the Bill & Melinda Gate Foundation (BMGF) under the project ICAR-BMGF (Grant number: OPP1194767).

## Acknowledgments

ND acknowledges the Council of Scientific and Industrial Research (CSIR), New Delhi and the ICAR—Indian Agricultural Research Institute (IARI), New Delhi for scholarships to complete this work as part of Ph.D. thesis.

## Conflict of interest

The authors declare that the research was conducted in the absence of any commercial or financial relationships that could be construed as a potential conflict of interest.

## Publisher's note

All claims expressed in this article are solely those of the authors and do not necessarily represent those of their affiliated organizations, or those of the publisher, the editors and the reviewers. Any product that may be evaluated in this article, or claim that may be made by its manufacturer, is not guaranteed or endorsed by the publisher.

## Supplementary material

The Supplementary Material for this article can be found online at: https://www.frontiersin.org/articles/10.3389/fpls.2022.943033/full#supplementary-material

## References

Abou-Elwafa, S. F., and Shehzad, T. (2021). Genetic diversity, GWAS and prediction for drought and terminal heat stress tolerance in bread wheat (Triticum aestivum L.). *Genet. Resour. Crop Evol.* 68, 711–728. doi: 10.1007/s10722-020-01018-y

Abraham, G., and Inouye, M. (2014). Fast principal component analysis of large-scale genome-wide data. *PLoS ONE.* 9, e93766. doi: 10.1371/journal.pone.0093766

Ahmed, A. A., Mohamed, E. A., Hussein, M. Y., and Sallam, A. (2021). Genomic regions associated with leaf wilting traits under drought stress in spring wheat at the seedling stage revealed by GWAS. *Environ. Exp. Bot.* 184, 104393. doi: 10.1016/j.envexpbot.2021.104393

Ahmed, H. G. M. D., Iqbal, M. N., Iqbal, M. A., Zeng, Y., Ullah, A., Iqbal, M., et al. (2021). Genome-wide association mapping for stomata and yield indices in bread wheat under water limited conditions. *Agronomy.* 11, 1646. doi: 10.3390/agronomy11081646

Ahmed, H. G. M. D., Naeem, M., Zeng, Y., Rashid, M. A. R., Ullah, A., Saeed, A., et al. (2022a). Genome-wide association mapping for high temperature tolerance in wheat through 90k SNP array using physiological and yield traits. *PLoS ONE*. 17, e0262569. doi: 10.1371/journal.pone.0262569

Ahmed, H. G. M. D., Zeng, Y., Iqbal, M., Rashid, M. A. R., Raza, H., Ullah, A., et al. (2022b). Genome-wide association mapping of bread wheat genotypes for sustainable food security and yield potential under limited water conditions. *PLoS ONE.* 17, e0263263. doi: 10.1371/journal.pone.0263263

Allen, A. M., Winfield, M. O., Burridge, A. J., Downie, R. C., Benbow, H. R., Barker, G. L., et al. (2017). Characterization of a Wheat Breeders' Array suitable for high-throughput SNP genotyping of global accessions of hexaploid bread wheat (Triticum aestivum). *Plant Biotechnol. J.* 15, 390–401. doi: 10.1111/pbi.12635

Alotaibi, F. S., Al-Qthanin, R. N., Aljabri, M., Shehzad, T., Albaqami, M., and Abou-Elwafa, S. F. (2022). Identification of genomic regions associated with agronomical traits of bread wheat under two levels of salinity using GWAS. *Plant Mol. Biol. Rep.* 1–15. doi: 10.1007/s11105-022-01341-x

Alseekh, S., Kostova, D., Bulut, M., and Fernie, A. R. (2021). Genome-wide association studies: assessing trait characteristics in model and crop plants. *Cell. Mol. Life Sci.* 78, 5743–5754. doi: 10.1007/s00018-021-03868-w

Amiri, R., Bahraminejad, S., and Jalali-Honarmand, S. (2013). Effect of terminal drought stress on grain yield and some morphological traits in 80 bread wheat genotypes. *Int. J. Agric. Crop Sci.* 5, 1145.

Aravind, J., Mukesh Sankar, S., Wankhede, D. P., and Kaur, V. (2021). *augmentedRCBD: Analysis of Augmented Randomised Complete Block Designs. R package version 0.1.5.9000.* Avvailable online at: https://aravind-j.github.io/augmentedRCBD/; https://cran.rproject.org/package=augmentedRCBD (accessed January 18, 2022).

Ayalew, H., Liu, H., Borner, A., Kobiljski, B., Liu, C., and Yan, G. (2018). Genome-wide association mapping of major root length QTLs under PE and induced water stress in wheat. *Front Plant Sci.* 9, 1759–1763. doi: 10.3389/fpls.2018.01759

Barboričová, M., Filaček, A., Vysoká, D. M., Gašparovič, K., Živčák, M., and Brestic, M. (2022). Sensitivity of fast chlorophyll fluorescence parameters to combined heat and drought stress in wheat genotypes. *Plant Soil Environ* 68, 309–316. doi: 10.17221/87/2022-PSE

Beyer, S., Daba, S., Tyagi, P., Bockelman, H., Brown-Guedira, G., and Mohammadi, M. (2019). Loci and candidate genes controlling root traits in wheat seedlings—a wheat root GWAS. *Funct. Integr. Genomics* 19, 91–107. doi: 10.1007/s10142-018-0630-z

Blum, A. (2010). *Plant Breeding for Water-Limited Environments*. London: Springer. p. 1–210. doi: 10.1007/978-1-4419-7491-4_1

Bordes, J., Goudemand, E., Duchalais, L., Chevarin, L., Oury, F. X., Heumez, E., et al. (2014). Genome-wide association mapping of three important traits using bread wheat elite breeding populations. *Mol. Breed.* 33, 755–768. doi: 10.1007/s11032-013-0004-0

Borrell, A. K., Mullet, J. E., George-Jaeggli, B., van Oosterom, E. J., Hammer, G. L., Klein, P. E., et al. (2014). Drought adaptation of stay green sorghum is associated with canopy development, leaf anatomy, root growth and water uptake. *J. ExpBot.* 65, 6251–6263. doi: 10.1093/jxb/eru232

Bradbury, P. J., Zhang, Z., Kroon, D. E., Casstevens, T. M., Ramdoss, Y., and Buckler, E. S. (2007). TASSEL: Software for association mapping of complex traits in diverse samples. *Bioinformatics.* 23:2633–2635. doi: 10.1093/bioinformatics/btm308

Chen, G., Zhang, H., Deng, Z., Wu, R., Li, D., Wang, M., et al. (2016). Genome-wide association study for kernel weight-related traits using SNPs in a Chinese winter wheat population. *Euphytica.* 212, 173–185. doi: 10.1007/s10681-016-1750-y

Christopher, J., Richard, C., Chenu, K., Christopher, M., Borrell, A., and Hickey, L. (2015). Integrating rapid phenotyping and speed breeding to improve stay-green

and root adaptation of wheat in changing, water limited, Australian environments. *Procedia Environ. Sci.* 29:175–176. doi: 10.1016/j.proenv.2015.07.246

Condorelli, G. E., Maccaferri, M., Newcomb, M., Andrade-Sanchez, P., White, J. W., French, A. N., et al. (2018). Comparative aerial and ground based high throughput phenotyping for the genetic dissection of NDVI as a proxy for drought adaptive traits in durum wheat. *Front. Plant Sci.* 9, 893. doi: 10.3389/fpls.2018.00893

Danakumara, T., Kumari, J., Singh, A. K., Sinha, S. K., Pradhan, A. K., Sharma, S., et al. (2021). Genetic dissection of seedling root system architectural traits in a diverse panel of hexaploid wheat through multi-locus genome-wide association mapping for improving drought tolerance. *Int. J. Mol. Sci.* 22, 7188. doi: 10.3390/ijms22137188

Devi, K., Chahal, S., Pandey, G. C., and Tiwari, R. (2022). Utilization of Heat Susceptibility Index for Comparative Evaluation of Consistent Yield Performance in Wheat Under Heat Stress. *Nat. Academy Sci. Lett.* 1–5. doi: 10.1007/s40009-022-01125-7

Djemal, R., and Khoudi, H. (2015). Isolation and molecular characterization of a novel WIN1/SHN1 ethylene-responsive transcription factor *TdSHN1* from durum wheat (*Triticum turgidum*. L. subsp. *durum*). *Protoplasma*. 252, 1461–1473. doi: 10.1007/s00709-015-0775-8

Edae, E. A., Byrne, P. F., Haley, S. D., Lopes, M. S., and Reynolds, M. P. (2014). Genome-wide association mapping of yield and yield components of spring wheat under contrasting moisture regimes. *Theor. Appl. Genet.* 127, 791–807. doi: 10.1007/s00122-013-2257-8

Ersoz, E., Yu, J., and Buckler, E. (2009). "Applications of linkage disequilibrium and association mapping in maize," in *Molecular genetic approaches to maize improvement 173, vol. 63. Biotechnology in Agriculture and Forestry,* Kriz A. L., Larkins, B. A. (eds). doi: 10.1007/978-3-540-68922-5_13

Evanno, G., Regnaut, S., and Goudet, J. (2005). Detecting the number of clusters of individuals using the software structure: a simulation study. *Mol. Ecol.* 14, 2611–2620. doi: 10.1111/j.1365-294X.2005.02553.x

Federer, W. T. (1956). "Augmented (or Hoonuiaku) designs." *The Hawaiian Planters' Record*, LV(2). p. 191–208. Available online at: https://ecommons.cornell.edu/handle/1813/32841

Federer, W. T. (1961). Augmented designs with one-way elimination of heterogeneity. *Biometrics*. 17, 447–473. doi: 10.2307/2527837

Gajghate, R., Chourasiya, D., and Sharma, R. K. (2020). "Plant morphological, physiological traits associated with adaptation against heat stress in wheat and maize," in *Plant Stress Biology*. Singapore: Springer. p. 51–81. doi: 10.1007/978-981-15-9380-2_3

Gautam, A., Sai Prasad, S. V., Jajoo, A., and Ambati, D. (2015). Canopy temperature as a selection parameter for grain yield and its components in durum wheat under terminal heat stress in late sown conditions. *Agricultural Res.* 4, 238–244. doi: 10.1007/s40003-015-0174-6

Guo, J., Shi, W. P., Zhang, Z., Cheng, J. Y., Sun, D. Z., Yu, J., et al. (2018). Association of yield-related traits in founder genotypes and derivatives of common wheat (Triticum aestivum L.). *BMC Plant Biol*. 18:38. doi: 10.1186/s12870-018-1234-4

Gupta, P. K., Rustgi, S., and Kulwal, P. L. (2005). Linkage disequilibrium and association studies in higher plants: present status and future prospects. *Plant Mol. Biol.* 57, 461–485. doi: 10.1007/s11103-005-0257-z

Holland, J. B. (2007). Genetic architecture of complex traits in plants. *Curr. Opin. Plant Biol.* 10:156–161. doi: 10.1016/j.pbi.2007.01.003

Hotta, T., Kong, Z., Ho, C. M. K., Zeng, C. J. T., Horio, T., Fong, S., et al. (2012). Characterization of the *Arabidopsis* augmin complex uncovers its critical function in the assembly of the acentrosomal spindle and phragmoplast microtubule arrays. *Plant Cell*. 24, 1494–1509. doi: 10.1105/tpc.112.096610

Huang, M., Liu, X., Zhou, Y., Summers, R. M, and Zhang, Z. (2019). BLINK: a package for the next level of genome wide association studies with both individuals and markers in the millions. *Gigascience*. 8:giy154. doi: 10.1093/gigascience/giy154

Huang, M., Mheni, N., Brown-Guedira, G., McKendry, A., Griffey, C., Van Sanford, D., et al. (2018). Genetic analysis of heading date in winter and spring wheat. *Euphytica*. 214, 1–18. *doi: 10.1007/s10681-018-2199-y*

Huang, X., and Han, B. (2014). Natural variations and genome-wide association studies in crop plants. *Annu. Rev. Plant Biol.* 65, 531–551. doi: 10.1146/annurev-arplant-050213-035715

Husson, F., Josse, J., Le, S., Mazet, J., and Husson, M. F. (2016). Package 'factominer'. *An R package.* 96, 698.

Jamil, M., Ali, A., Gul, A., Ghafoor, A., Napar, A. A., Ibrahim, A. M., et al. (2019). Genome-wide association studies of seven agronomic traits under two sowing conditions in bread wheat. *BMC Plant Biol.* 19, 1–18. doi: 10.1186/s12870-019-1754-6

Jin, H., Wen, W., Liu, J., Zhai, S., Zhang, Y., Yan, J., et al. (2016). Genome-wide QTL mapping for wheat processing quality parameters in a Gaocheng 8901/Zhoumai 16 recombinant inbred line population. *Front. Plant Sci.* 7, 1032. doi: 10.3389/fpls.2016.01032

Kassambara, A. (2020). Mundt F. factoextra: Extract and visualize the results of multivariate data analyses. *2020; R package version* 1.0.7.

Kaur, R., Singh, K., and Singh, J. (2013). A root-specific wall-associated kinase gene, HvWAK1, regulates root growth and is highly divergent in barley and other cereals. *Func. Intergr. Genom.* 13, 167–177. doi: 10.1007/s10142-013-0310-y

Khakwani, A., Dennett, M., Munir, M., and Abid, M. (2012). Growth and yield response of wheat varieties to water stress at booting and anthesis stages of development. *Pak. J. Bot.* 44, 879–886.

Kiseleva, A. A., Shcherban, A. B., Leonova, I. N., Frenkel, Z., and Salina, E. A. (2016). Identification of new heading date determinants in wheat 5B chromosome. *BMC Plant Biol.* 16, 35–46. *doi: 10.1186/s12870-015-0688-x*

Kristensen, P. S., Jahoor, A., Andersen, J. R., Cericola, F., Orabi, J., Janss, L. L., et al. (2018). Genome-wide association studies and comparison of models and cross-validation strategies for genomic prediction of quality traits in advanced winter wheat breeding lines. *Front. Plant Sci.* 9, 69. doi: 10.3389/fpls.2018.00069

Kumar, J., Saripalli, G., Gahlaut, V., Goel, N., Meher, P. K., Mishra, K. K., et al. (2018). Genetics of Fe, Zn, β-carotene, GPC and yield traits in bread wheat (Triticum aestivum L.) using multi-locus and multi-traits GWAS. *Euphytica.* 214, 1–17. doi: 10.1007/s10681-018-2284-2

Kumar, R., Harikrishna, H., Ghimire, O., Barman, D., Chinnusamy, V., Singh, P. K., et al. (2021). Stay-green trait ameliorates combined heat and drought stress in wheat. *Indian J. Agri. Sci.* 91.

Laing, W. A., Wright, M. A., Cooney, J., and Bulley, S. M. (2007). The missing step of the L-galactose pathway of ascorbate biosynthesis in plants, an L-galactose guanyltransferase, increases leaf ascorbate content. *Proc. Nat. Acad. Sci.* 104, 9534–9539. doi: 10.1073/pnas.0701625104

Ledesma-Ramírez, L., Solís-Moya, E., Iturriaga, G., Sehgal, D., Reyes-Valdes, M. H., Montero-Tavera, V., et al. (2019). GWAS to identify genetic loci for resistance to yellow rust in wheat pre-breeding lines derived from diverse exotic crosses. *Front. Plant Sci.* 1390. doi: 10.3389/fpls.2019.01390

Li, G., Xu, X., Tan, C., Carver, B. F., Bai, G., Wang, X., et al. (2019). Identification of powdery mildew resistance loci in wheat by integrating genome-wide association study (GWAS) and linkage mapping. *Crop J.* 7, 294–306. doi: 10.1016/j.cj.2019.01.005

Li, H., Zhou, Y., Xin, W., Wei, Y., Zhang, J., and Guo, L. (2019). Wheat breeding in northern China: achievements and technical advances. *Crop J.* 7, 718–729 doi: 10.1016/j.cj.2019.09.003

Lipka, A. E., Tian, F., Wang, Q., Peiffer, J., Li, M., et al. (2012). GAPIT: genome association and prediction integrated tool. *Bioinformatics*. 28, 2397–2399. doi: 10.1093/bioinformatics/bts444

Liu, J., Feng, B., Xu, Z. B., Fan, X. L., Jiang, F., Jin, X. F., et al. (2018). A genomewide association study of wheat yield and quality-related traits in southwest China. *Mol. Breed.* 38, 1. doi: 10.1007/s11032-017-0759-9

Lopes, M. S., Reynolds, M. P., Jalal-Kamali, M. R., Moussa, M., Feltaous, Y., Tahir, I. S. A., et al. (2012). The yield correlations of selectable physiological traits in a population of advanced spring wheat lines grown in warm and drought environments. *Field Crops Res.* 128, 129–136. doi: 10.1016/j.fcr.2011.12.017

Lü, B., Chen, F., Gong, Z. H., Xie, H., and Liang, J. S. (2007). Integrin-like protein is involved in the osmotic stress-induced abscisic acid biosynthesis in Arabidopsis thaliana. *J. Integr. Plant Biol.* 49, 540–549. doi: 10.1111/j.1744-7909.2007.00439.x

Luján Basile, S. M., Ramírez, I. A., Crescente, J. M., Conde, M. B., Demichelis, M., Abbate, P., et al. (2019). Haplotype block analysis of an Argentinean hexaploid wheat collection and GWAS for yield components and adaptation. *BMC Plant Biol.* 19, 1–16. doi: 10.1186/s12870-019-2015-4

Ma, F., Xu, Y., Ma, Z., Li, L., and An, D. (2018). Genome-wide association and validation of key loci for yield-related traits in wheat founder parent Xiaoyan 6. *Mol. Breed.* 38, 1–15. doi: 10.1007/s11032-018-0837-7

Mather, K. A., Caicedo, A. L., Polato, N. R., Olsen, K. M., McCouch, S., and Purugganan, M. D. (2007). The extent of linkage disequilibrium in rice (*Oryza sativa* L.). *Genetics.* 177, 2223–2232. doi: 10.1534/genetics.107.079616

Mathew, I., Shimelis, H., Mwadzingeni, L., Zengeni, R., Mutema, M., and Chaplot, V. (2018). Variance components and heritability of traits related to root: shoot biomass allocation and drought tolerance in wheat. *Euphytica*. 214, 225–237. doi: 10.1007/s10681-018-2302-4

Mehdi, C., Virginie, L., Audrey, G., Axelle, B., Colette, L., Hélène, R., et al. (2020). Cell wall proteome of wheat grain endosperm and outer layers at two key stages of early development. *Int. J. Mol. Sci.* 21, 239. doi: 10.3390/ijms21010239

Mir, R., Zaman-Allah, M., Sreenivasulu, N., Trethowan, R., and Varshney, R. (2012). Integrated genomics, physiology and breeding approaches for improving drought tolerance in crops. *Theor. Appl. Genet*. doi: 10.1007/s00122-012-1904-9

Mirzaghaderi, G., and Mason, A. S. (2017). Revisiting pivotal-differential genome evolution in wheat. *Trends Plant Sci*. 22:674–684. doi: 10.1016/j.tplants.2017.06.003

Munawar, N., Nijabat, A., Hussain, R., Shah, A. I., Nawaz, S., Nazir, A., et al. (2022). Influence Of heat stress on physiological and yield potential of promising bread wheat cultivars. *Plant Cell Biotechnol. Mol. Biol.* 87–95.

Murray, M. G., and Thompson, W. F. (1980). Rapid isolation of high molecularweight plant DNA. *Nucleic Acids Res.* 8, 4321–4325. doi: 10.1093/nar/8.19.4321

Mutari, B., Sibiya, J., Gasura, E., Matova, P. M., Simango, K., and Kondwakwenda, A. (2022). Genetic analysis of grain yield and yield-attributing traits in navy bean (Phaseolus vulgaris L.) under drought stress. *Euphytica.* 218, 1–20. doi: 10.1007/s10681-022-03001-3

Naser, M. A., Khosla, R., Longchamps, L., and Dahal, S. (2020). Using NDVI to differentiate wheat genotypes productivity under dryland and irrigated conditions. *Remote Sens.* 12, 824. doi: 10.3390/rs12050824

Negisho, K., Shibru, S., Matros, A., Pillen, K., Ordon, F., and Wehner, G. (2022). Genomic dissection reveals QTLs for grain biomass and correlated traits under drought stress in Ethiopian durum wheat (Triticum turgidum ssp. durum). *Plant Breed*. doi: 10.1111/pbr.13010

Odilbekov, F., Armonien,é, R., Koc, A., Svensson, J., and Chawade, A. (2019). GWAS-assisted genomic prediction to predict resistance to Septoria tritici blotch in Nordic winter wheat at seedling stage. *Front. Genet.* 10, 1224. doi: 10.3389/fgene.2019.01224

Ogbonnaya, F. C., Rasheed, A., Okechukwu, E. C., Jighly, A., Makdis, F., Wuletaw, T., et al. (2017). Genome-wide association study for agronomic and physiological traits in spring wheat evaluated in a range of heat prone environments. *Theor. Appl. Genet.* 130, 1819–1835. doi: 10.1007/s00122-017-2927-z

Onyemaobi, I., Ayalew, H., Liu, H., Siddique, K. H., and Yan, G. (2018). Identification and validation of a major chromosome region for high grain number per spike under meiotic stage water stress in wheat (Triticum aestivum L.). *PloS ONE*. 13, e0194075. doi: 10.1371/journal.pone.0194075

Paliwal, R., Röder, M. S., Kumar, U., Srivastava, J. P., and Joshi, A. K. (2012). QTL mapping of terminal heat tolerance in hexaploid wheat (T. aestivum L.). *Theor. Appl. Genet*. 125, 561–575. doi: 10.1007/s00122-012-1853-3

Palma, J. M., Sandalio, L. M., Corpas, F. J., Romero-Puertas, M. C., McCarthy, I., and Luis, A. (2002). Plant proteases, protein degradation, and oxidative stress: role of peroxisomes. *Plant Physiol. Biochem.* 40, 521–530. doi: 10.1016/S0981-9428(02)01404-3

Pang, Y., Liu, C., Wang, D., Amand, P. S., Bernardo, A., Li, W., et al. (2020). High-resolution genome-wide association study identifies genomic regions and candidate genes for important agronomic traits in wheat. *Mol. Plant* 13, 1311–1327. doi: 10.1016/j.molp.2020.07.008

Pask, AJD., Pietragalla, J., Mullan, D. M., and Reynolds, MP. (2012). *Physiological Breeding II: A Field Guide to Wheat Phenotyping.* Mexico, D.F.: CIMMYT.

Passioura, J. B. (2012). Phenotyping for drought tolerance in grain crops: when is it useful to breeders? *Funct. Plant Biol.* 39:851–859. doi: 10.1071/FP12079

Phuke, R. M., Ambati, D., Singh, J., Prasad, S., Singh,10, G. P., Prabhu,11, K. V., et al. (2020). Genetic variability, Genotype× Environment interaction for grain yield of wheat (Triticum aestivum) backcross inbred lines population under different moisture regimes. *Indian J. Agric. Sci*. 90, 1678–1684.

Pingali, P. L. (2012). Green revolution: impacts, limits, and the path ahead. *Proc. Natl. Acad. Sci.* 109, 12302–12308. doi: 10.1073/pnas.0912953109

Pinto, R. S., Reynolds, M. P., Mathews, K. L., McIntyre, C. L., Olivares-Villegas, J. J., and Chapman, S. C. (2010). Heat and drought adaptive QTL in a wheat population designed to minimize confounding agronomic effects. *Theor. Appl. Genetics.* 121, 1001–1021 doi: 10.1007/s00122-010-1351-4

Pritchard, J. K., Wen, W., and Falush, D. (2010). *Documentation for STRUCTURE Software: Version 2.* Chicago, IL: University of Chicago.

Pujar, M., Gangaprasad, S., Govindaraj, M., Gangurde, S. S., Kanatti, A., and Kudapa, H. (2020). Genome-wide association study uncovers genomic regions associated with grain iron, zinc and protein content in pearl millet. *Sci. Rep.* 10, 1–15. doi: 10.1038/s41598-020-76230-y

Rathan, N. D., Krishna, H., Ellur, R. K., Sehgal, D., Govindan, V., Ahlawat, A. K., et al. (2022). Genome-wide association study identifies loci and candidate genes for grain micronutrients and quality traits in wheat (Triticum aestivum L.). *Sci. Rep.* 12, 1–15. doi: 10.1038/s41598-022-10618-w

Rehman, H. U., Tariq, A., Ashraf, I., Ahmed, M., Muscolo, A., Basra, S. M., et al. (2021). Evaluation of physiological and morphological traits for improving spring wheat adaptation to terminal heat stress. *Plants*. 10, 455. doi: 10.3390/plants10030455

Rivera-Burgos, L. A., Brown-Guedira, G., Johnson, J., Mergoum, M., and Cowger, C. (2022). Accounting for heading date gene effects allows detection of small-effect QTL associated with resistance to Septoria nodorum blotch in wheat. *PLoS ONE*. 17, e0268546. *doi: 10.1371/journal.pone.0268546*

Roncallo, P. F., Larsen, A. O., Achilli, A. L., Pierre, C. S., Gallo, C. A., Dreisigacker, S., et al. (2021). Linkage disequilibrium patterns, population structure and diversity analysis in a worldwide durum wheat collection including Argentinian genotypes. *BMC Genomics.* 22, 1–17. doi: 10.1186/s12864-021-07519-z

Ronceret, A., Gadea-Vacas, J., Guilleminot, J., and Devic, M. (2008). The alpha-N-acetyl-glucosaminidase gene is transcriptionally activated in male and female gametes prior to fertilization and is essential for seed development in Arabidopsis. *J. Exper. Biol*. 59, 3649–3659. doi: 10.1093/jxb/ern215

Rutkoski, J., Poland, J., Mondal, S., Autrique, E., Pérez, L. G., Crossa, J., et al. (2016). Canopy temperature and vegetation indices from high-throughput phenotyping improve accuracy of pedigree and genomic selection for grain yield in wheat. *G3: Genes, Genomes, Genetics.* 6, 2799–2808. doi: 10.1534/g3.116.032888

Saeidi, M., and Abdoli, M. (2015). Effect of drought stress during grain filling on yield and its components, gas exchange variables, and some physiological traits of wheat cultivars. *J. Agric. Sci.* 17, 885–898.

Saini, D. K., Chopra, Y., Singh, J., Sandhu, K. S., Kumar, A., Bazzer, S., et al. (2022). Comprehensive evaluation of mapping complex traits in wheat using genome-wide association studies. *Mol. Breed.* 42, 1–52. doi: 10.1007/s11032-021-01272-7

Schmidt, J., Tricker, P. J., Eckermann, P., Kalambettu, P., Garcia, M., and Fleury, D. (2020). Novel alleles for combined drought and heat stress tolerance in wheat. *Front. Plant Sci.* 10, 1800. doi: 10.3389/fpls.2019.01800

Searle, S. R. (1965). "Computing Formulae for Analyzing Augmented Randomized Complete Block Designs." Technical Report BU-207-M. New York: Cornell University.

Shi, S., Azam, F. I., Li, H., Chang, X., Li, B., and Jing, R. (2017). Mapping QTL for stay-green and agronomic traits in wheat under diverse water regimes. *Euphytica.* 213, 1–19. doi: 10.1007/s10681-017-2002-5

Shokat, S., Sehgal, D., Liu, F., and Singh, S. (2020). GWAS analysis of wheat pre-breeding germplasm for terminal drought stress using next generation sequencing technology. Life Sci. 2020, 2020020272. doi: 10.20944/preprints202002.0272.v1

Sinclair, T. R. (2012). Is transpiration efficiency a viable plant trait in breeding for crop improvement? *Funct. Plant Biol.* 39:359–365. doi: 10.1071/FP11198

Singh, G. P., Jain, N., Singh, P. K., Sai Prasad, S. V., Ambati, D., Das, T. R., et al. (2016). Physiological characterization and grain yield stability analysis of RILs under different moisture stress conditions in wheat (Triticum aestivum L.). *Indian Journal of Plant Physiology* 21, 576–582. doi: 10.1007/s40502-016-0257-9

Singh, S. K., Barman, M., Prasad, J. P., and Bahuguna, R. N. (2022). Phenotyping diverse wheat genotypes under terminal heat stress reveal canopy temperature as critical determinant of grain yield. *Plant Physiol. Rep*. 1–10. doi: 10.1007/s40502-022-00647-y

Srivastava, R. K., Singh, R. B., Pujarula, V. L., Bollam, S., Pusuluri, M., Chellapilla, T. S., et al. (2020). Genome-wide association studies and genomic selection in Pearl Millet: advances and prospects. *Front. Genet.* 10, 1389. doi: 10.3389/fgene.2019.01389

Sukumaran, S., Krishna, H., Singh, K., Mottaleb, K. A., and Reynolds, M. (2021). Progress and prospects of developing climate resilient wheat in south asia using modern pre-breeding methods. *Curr. Genomics.* 22, 440–449. doi: 10.2174/1389202922666210705125006

Sukumaran, S., Reynolds, M. P., and Sansaloni, C. (2018). Genome-wide association analyses identify QTL hotspots for yield and component traits in durum wheat grown under yield potential, drought, and heat stress environments. *Front. Plant Sci.* 9, 81. doi: 10.3389/fpls.2018.00081

Takahashi, F., Kuromori, T., Urano, K., Yamaguchi-Shinozaki, K., and Shinozaki, K. (2020). Drought stress responses and resistance in plants: from cellular responses to long-distance intercellular communication. *Front. Plant Sci.* 11, 556972. doi: 10.3389/fpls.2020.556972

Tibbs Cortes, L., Zhang, Z., and Yu, J. (2021). Status and prospects of genome-wide association studies in plants. *Plant Genome* 14, e20077. doi: 10.1002/tpg2.20077

Tiwari, A., Choudhary, S., Padiya, J., Ubale, A., Mikkilineni, V., and Char, B. (2022). "Recent Advances and Applicability of GBS, GWAS, and GS in Maize," in *Genotyping by Sequencing for Crop Improvement*. p. 188–217. doi: 10.1002/9781119745686.ch9

Vos-Fels, K. P., Qian, L., Parra-Londono, S., Uptmoor, R., Frisch, M., Keeble-Gagnère, G., et al. (2017). Linkage drag constrains the roots of modern wheat. *Plant Cell Environ*. 40, 717–25. doi: 10.1111/pce.12888

Wang, L., Ge, H., Hao, C., Dong, Y., and Zhang, X. (2012). Identifying loci influencing 1,000-kernel weight in wheat by microsatellite screening for evidence of selection during breeding. *PLoS ONE*. 7, e29432. doi: 10.1371/journal.pone.0029432

Wang, S. X., Zhu, Y. L., Zhang, D. X., Shao, H., Liu, P., Hu, J. B., et al. (2017). Genome-wide association study for grain yield and related traits in elite wheat varieties and advanced lines using SNP markers. *PLoS ONE*. 12, e0188662. doi: 10.1371/journal.pone.0188662

Ward, B. P., Brown-Guedira, G., Kolb, F. L., Van Sanford, D. A., Tyagi, P., Sneller, C. H., et al. (2019). Genome-wide association studies for yield-related traits in soft red winter wheat grown in Virginia. *PLoS ONE*. 14, e0208217. doi: 10.1371/journal.pone.0208217

Xu, Y., Li, P., Yang, Z., and Xu, C. (2017). Genetic mapping of quantitative trait loci in crops. *Crop J.* 5, 175–184. doi: 10.1016/j.cj.2016.06.003

Yang, H., Liu, L., Wu, K., Liu, S., Liu, X., Tian, Y., et al. (2021). Floury and shrunken endosperm6 encodes a glycosyltransferase and is essential for the development of rice endosperm. *J. Plant Biol.* 65, 187–198. doi: 10.1007/s12374-020-09293-z

Yu, H., Deng, Z., Xiang, C., and Tian, J. (2014). Analysis of diversity and linkage disequilibrium mapping of agronomic traits on B-genome of wheat. *J. Genomics*. 2, 20–30. doi: 10.7150/jgen.4089

Zanke, C. D., Ling, J., Plieske, J., Kollers, S., Ebmeyer, E., Korzun, V., et al. (2015). Analysis of main effect QTL for thousand grain weight in european winter wheat (*Triticum Aestivum L.*) by genome-wide association mapping. *Front. Plant Sci.* 6:644. doi: 10.3389/fpls.2015.00644

Zhang, H., Cui, F., Wang, L., Li, J., Ding, A., Zhao, C., et al. (2013). Conditional and unconditional QTL mapping of drought-tolerance-related traits of wheat seedling using two related RIL populations. *J. Genet*. 92, 213–231. doi: 10.1007/s12041-013-0253-z

Zhang, J., Zhang, S., Cheng, M., Jiang, H., Zhang, X., Peng, C., et al. (2018). Effect of drought on agronomic traits of rice and wheat: a meta-analysis. *Int. J. Environ. Res. Public Health* 15, 839. doi: 10.3390/ijerph15050839

Zhang, P., Li, L., Zhang, C., Liu, Y., Liu, J., Wang, Q., et al. (2022). Genome-wide association study of yunnan-specific wheat varieties under conditions of drought stress. *Pak. J. Bot.* 54, 1715–1731. doi: 10.30848/PJB2022-5(43)

frontiers | Frontiers in Plant Science

TYPE Original Research
PUBLISHED 02 September 2022
DOI 10.3389/fpls.2022.965530



OPEN ACCESS

EDITED BY
Sindhu Sareen,
Indian Institute of Wheat and Barley Research (ICAR), India

REVIEWED BY
Ram Singh Purty,
Guru Gobind Singh Indraprastha University, India
Adnan Aydin,
Iğdır Üniversitesi, Turkey
Rakesh Singh,
National Bureau of Plant Genetic Resources (ICAR), India

*CORRESPONDENCE
P. B. Kavi Kishor
pbkavi@yahoo.com
Ramesh Katam
ramesh.katam@gmail.com

†These authors have contributed equally to this work and share senior authorship

SPECIALTY SECTION
This article was submitted to Plant Abiotic Stress, a section of the journal Frontiers in Plant Science

RECEIVED 09 June 2022
ACCEPTED 04 August 2022
PUBLISHED 02 September 2022

CITATION
Anil Kumar S, Hima Kumari P, Nagaraju M, Sudhakar Reddy P, Durga Dheeraj T, Mack A, Katam R and Kavi Kishor PB (2022) Genome-wide identification and multiple abiotic stress transcript profiling of potassium transport gene homologs in *Sorghum bicolor*.
*Front. Plant Sci.* 13:965530.
doi: 10.3389/fpls.2022.965530



# Genome-wide identification and multiple abiotic stress transcript profiling of potassium transport gene homologs in *Sorghum bicolor*

S. Anil Kumar[1,2], P. Hima Kumari[2], Marka Nagaraju[3], Palakolanu Sudhakar Reddy[4], T. Durga Dheeraj[1], Alexis Mack[2,5], Ramesh Katam[2*†] and P. B. Kavi Kishor[1*†]

[1]Department of Biotechnology, Vignan's Foundation for Science, Technology & Research (Deemed to be University), Guntur, India, [2]Department of Biological Sciences, Florida A&M University, Tallahassee, FL, United States, [3]Biochemistry Division, National Institute of Nutrition, Hyderabad, India, [4]International Crops Research Institute for the Semi-Arid Tropics (ICRISAT), Patancheru, India, [5]Department of Biology, Florida State University, Tallahassee, FL, United States

Potassium ($K^+$) is the most abundant cation that plays a crucial role in various cellular processes in plants. Plants have developed an efficient mechanism for the acquisition of $K^+$ when grown in $K^+$ deficient or saline soils. A total of 47 $K^+$ transport gene homologs (27 HAKs, 4 HKTs, 2 KEAs, 9 AKTs, 2 KATs, 2 TPCs, and 1 VDPC) have been identified in *Sorghum bicolor*. Of 47 homologs, 33 were identified as $K^+$ transporters and the remaining 14 as $K^+$ channels. Chromosome 2 has been found as the hotspot of $K^+$ transporters with 9 genes. Phylogenetic analysis revealed the conservation of sorghum $K^+$ transport genes akin to *Oryza sativa*. Analysis of regulatory elements indicates the key roles that $K^+$ transport genes play under different biotic and abiotic stress conditions. Digital expression data of different developmental stages disclosed that expressions were higher in milk, flowering, and tillering stages. Expression levels of the genes *SbHAK27* and *SbKEA2* were higher during milk, *SbHAK17*, *SbHAK11*, *SbHAK18*, and *SbHAK7* during flowering, *SbHAK18*, *SbHAK10*, and 23 other gene expressions were elevated during tillering inferring the important role that $K^+$ transport genes play during plant growth and development. Differential transcript expression was observed in different tissues like root, stem, and leaf under abiotic stresses such as salt, drought, heat, and cold stresses. Collectively, the in-depth genome-wide analysis and differential transcript profiling of $K^+$ transport genes elucidate their role in ion homeostasis and stress tolerance mechanisms.

KEYWORDS

**HAK/KT/KUP, KEA, $K^+$ channels, $K^+$ transporters, *Sorghum*, Trk/HKT**

## Introduction

Potassium ($K^+$) is an essential macronutrient and most ubiquitous monovalent cation in plants. It contributes up to 10% of total plant dry weight and plays an overriding role in diverse cellular processes such as ion homeostasis, plant growth, development, transport, and signaling (Feng et al., 2019; Hussain et al., 2021). Despite its abundance, $K^+$ is not readily available to plants since they absorb it in the ionic form only, and the concentrations at the root surface often fall below or up to μM range (Ashley et al., 2006). $K^+$ uptake in plants is mediated by two mechanisms: a low affinity system that functions when extracellular $K^+$ concentration is high (> 200 μM to mM) and a high affinity system that functions when extracellular concentration is low (20 μM $Rb^+$) (Gierth et al., 2005). $Na^+$ competes with $K^+$ but does not fulfill the physiological functions, and higher $K^+/Na^+$ is critical in maintaining electro-neutrality of the cells (Hussain et al., 2021). $K^+$ transport occurs through five major families, classified under 2 categories as $K^+$ transporters and channels. The transporters include HAK (high-affinity $K^+$)/KUP ($K^+$ uptake)/KT ($K^+$ transporter) family, Trk/HKT family, and KEA ($K^+$ efflux anti-porter) family, while the $K^+$ channels include the shakers/voltage-gated channels (AKT and KAT) and non-voltage-gated [tandem-pore $K^+$ (TPK) and two-pore (TPC)] channels (Hedrich, 2012). HAK/KUP/KT transporters are critical in maintaining osmotic potential and salt tolerance (Feng et al., 2019) and are the largest family of $K^+$ transporters (Ahn et al., 2004). While HKTs are involved in the uptake of $K^+$ during short-term $K^+$ starvation (Riedelsberger et al., 2021), KEAs are implicated in the regulation of thylakoid and stromal pH (Sánchez-McSweeney et al., 2021). Abiotic stresses like salt, drought, heat, and cold impair the final yields (Teklić et al., 2021). But $K^+$ is a vital regulator of plant responses and imparts tolerance to the abiotic stresses (Hasanuzzaman et al., 2018; Sardans and Peñuelas, 2021). $K^+$ reduces the adverse effects of drought stress tolerance alongside maintaining turgor pressure at low water potentials, alleviates salt stress by achieving homeostatic balance, enhances seed yield during heat stress by reducing the silique canopy, improves freezing tolerance by accumulation of osmolytes (Assaha et al., 2017; Aksu and Altay, 2020; Hu et al., 2021; Saadati et al., 2021).

Genome-wide analyses have been widely performed in HAK/KUP/KT family, but studies were limited to $K^+$ transporters. Analysis of HAK/KUP/KT transporters on a genome scale has been carried out in *Oryza sativa* (Banuelos et al., 2002), *Arabidopsis thaliana* (Ahn et al., 2004), *Populus trichocarpa* (He et al., 2012), *Zea mays* (Zhang et al., 2012), *Solanum lycopersicum* (Hyun et al., 2014), *Prunus persica* (Song et al., 2015), *Triticum aestivum* (Cheng et al., 2018), *Pyrus betulifolia* (Li Y. et al., 2018), *Manihot esculenta* (Ou et al., 2018), *Nicotiana tabacum* (Song et al., 2019), *Saccharum spontaneum* (Feng et al., 2020b), *Gossypium* (Yang X. et al., 2020), and *Ipomoea batatas* (Jin et al., 2021). Genome-wide analysis of $K^+$ transport gene family has been reported in *Oryza sativa* (Amrutha et al., 2007), *Glycine max* (Rehman et al., 2017), *Cicer arietinum* (Azeem et al., 2018), *Cajanus cajan* (Siddique et al., 2021), and *Gossypium raimondii* (Azeem et al., 2022) but not in *Sorghum bicolor*.

Sorghum, a moderately drought stress-tolerant crop is the fifth most important cereal. It is the staple food for human populations in arid regions and a good source of feed and fuel in the global agronomics and economics. It is a self-pollinated, $C_4$ photosynthetic plant with a smaller genome size of 730 Mb (Paterson et al., 2009). In the present study, the discovery, and identification of $K^+$ transport gene homologs in *Sorghum bicolor* were conducted including their expression profiles in different tissues under various abiotic stresses. Further, chromosomal locations, gene characterization, protein modeling, conserved motifs analysis, cellular localization, promoter analysis, evolutionary relationship, and protein-protein interactions were investigated, resulting in the characterization of candidate genes.

## Materials and methods

### *In silico* prediction, identification, and characterization of $K^+$ transport gene homologs

All the 49 rice full-length cDNA sequences of $K^+$ encoding genes were collected from rice (Amrutha et al., 2007). The homology search of the collected FASTA sequences was performed by BLASTN against Sorghum genome in the Gramene database with default settings.[1] The coding sequences (CDS) and corresponding protein sequences were retrieved from the BLAST output using GENSCAN web server.[2] To check the presence of the $K^+$ domain, Conserved Domain Database search and SMART were employed.[3], [4] For analysis of transmembrane, TMHMM (Moller et al., 2001), for prediction of gene structure, Gene Structure Display Server,[5] for prediction of subcellular localization of the protein, WoLFPSORT,[6] for isoelectric point (pI) molecular weight (MW), GRAVY (grand average of hydropathy) instability, and aliphatic indexes, ProtParam software,[7] for identification of phosphorylation sites, NetPhos 3.1[8] for amino acid composition and net charge,

1 http://www.gramene.org/
2 http://genes.mit.edu/GENSCAN.html
3 https://www.ncbi.nlm.nih.gov/Structure/cdd/wrpsb.cgi
4 http://smart.embl-heidelberg.de/
5 http://gsds.gao-lab.org/
6 https://wolfpsort.hgc.jp/
7 http://web.expasy.org/protparam/
8 https://services.healthtech.dtu.dk/service.php?NetPhos-3.1

pepcalc[9] for conserved motifs, MEME[10] with parameters like 10 number of motifs, 2–20 motif sites, 6–20 wide motif width were used. The genes on the chromosomes were mapped based on their physical location using MG2C[11] tool.

## Prediction of *cis*-elements, protein modeling and protein-protein interactions

Promoter elements were identified for all the transporter and channel genes by taking 2 kb sequence upstream to all the sorghum $K^+$ transport homologs using PLACE tools.[12] The 3D structures of all the $K^+$ transport proteins were predicted using SWISS-MODEL server (Biasini et al., 2014). The predicted 3D structures of proteins were evaluated for stability using protein structure verification server (PSVS).[13] The stability of the proteins was analyzed by Ramachandran plots. The predicted protein-protein interaction (PPI) map of sorghum $K^+$ transport homologs was generated from the STRING database.[14]

## Phylogenetic analysis and generation of synteny maps

A phylogenetic tree was constructed with amino acid sequences of *Sorghum bicolor* (Sb), *Oryza sativa* (Os), and *Arabidopsis thaliana* (At) using MEGA 10.0 software, by Neighbor-Joining method with 1000 bootstrap replicates (Kumar et al., 2018). Evolutionary analysis of orthologs and paralogs was performed by calculating synonymous (dS) and non-synonymous (dN) substitution rates using the PAL2NAL program.[15] Synonymous (dS) and non-synonymous (dN) substitution rates were calculated by codeml in the PAML package. Synteny and collinearity were analyzed to identify $K^+$ homologs using TBtools (Chen et al., 2020).

## Digital and qRT-PCR analysis of $K^+$ transport gene homologs under different abiotic stresses

For digital expression profiling of $K^+$ transport genes, Genevestigator[16] was used. The mRNA-seq data were used for analysis. The data are available for all the 46 genes (except SbHAK26) for 2 stress conditions (cold and drought) in 3 tissues (root, shoot, and leaf), and 4 developmental stages (milk stage, seedling stage, tillering stage, and flowering stage). Using hierarchical clustering, heat maps were generated separately for anatomical, developmental, and perturbations. Seeds of *Sorghum bicolor* L. BTx623 genotype were collected from the International Crops Research Institute for the Semi-Arid Tropics and used. Seventy-five-day-old seedlings maintained in green house at 28/20°C day/night temperatures were treated with salt (200 mM NaCl), drought (200 mM mannitol), heat (42°C), and cold (4°C) stresses for 4 h. Control (without any stress) plants were treated with tap water. Root, stem, and leaftissue samples were collected immediately, snap frozen in liquid nitrogen and stored at −80°C. Total RNA was isolated from all the samples using Macherey-Nagel NucleoSpin RNA plant kit (740949.50) by following the instructions manual. Total RNA (2 μg) was taken as a template for first strand cDNA synthesis using RevertAid First Strand cDNA Synthesis Kit (#K1622, Thermo Scientific EU, Reinach, Switzerland). The relative expression levels of $K^+$ gene homologs were studied using Mx3000p (Agilent) with 2X applied biosystems (ABI) Master Mix with gene specific primers (**Supplementary Table 1**) with the following thermal cycles: 1 cycle at 95°C for 10 min, followed by 40 cycles alternatively at 95°C for 15 s and 60°C for 1 min. The expression of each gene in various samples was normalized with *ACTIN* gene. The experiment was performed with two biological replicates and for each sample three technical replicates were used. The comparative $2^{-\Delta\Delta CT}$ method was used to calculate the relative quantities of each transcript in the samples (Schmittgen and Livak, 2008).

# Results

## Discovery, identification and characterization of $K^+$ gene homologs

A total of 47 $K^+$ transport homologs have been identified in sorghum (**Table 1** and **Supplementary Table 2**). Of the 47 transport homologs 27 belong to HAKs (*SbHAK1* to *SbHAK27*), 4 HKTs (*SbHKT2*, *SbHAT3*, *SbHKT4*, and *SbHKT5*), 9 AKTs (*SbAKT1* to *SbAKT9*), 2 KEAs (*SbKEA1* and *SbKEA2*), 2 KATs (*SbKAT1* and *SbKAT2*), 2 TPKs (*SbTPC1* and *SbTPC2*), and 1 VDPC (*SbVDPC1*) (**Table 1**). Homologs of *OsHKTs* (*OsHKT1*, *OsHKT6*, and *OsHKT7*) and *OsKEA3* are not available in *Sorghum bicolor*. $K^+$ transporter and channel domains like K-trans, TrK, voltage-dependent $K^+$ channel, KHA, Two pore potassium channel, and $K^+$-efflux system protein have been identified (**Table 1**). Predicted amino acid sequences were used to identify the number of transmembrane segments. While the number of transmembrane domains for $K^+$ transporters varies from

9 https://pepcalc.com/
10 https://meme-suite.org/meme/tools/meme
11 http://mg2c.iask.in/mg2c_v2.1/
12 https://www.dna.affrc.go.jp/PLACE/?action=newplace
13 https://montelionelab.chem.rpi.edu/PSVS/PSVS/
14 https://string-db.org/
15 http://www.bork.embl.de/pal2nal/
16 https://genevestigator.com/gv

TABLE 1 Characterization of *Sorghum bicolor* potassium transport gene homologs.

| Gene | Gene id | Cds | Aa | Chr | Domain | TMHMM | Exons | Localization |
|---|---|---|---|---|---|---|---|---|
| > SbHAK1 | SORBI_3006G061300 | 2316 | 771 | 6 | K-trans | 12 | 7 | PM |
| > SbHAK2 | SORBI_3003G418100 | 2163 | 720 | 3 | K-trans | 10 | 8 | PM |
| > SbHAK3 | SORBI_3003G164400 | 2367 | 788 | 3 | K-trans | 11 | 5 | PM |
| > SbHAK4 | SORBI_3007G153001 | 2124 | 707 | 7 | K-trans | 9 | 4 | PM |
| > SbHAK5 | SORBI_3003G413700 | 2412 | 803 | 3 | K-trans | 10 | 11 | PM |
| > SbHAK6 | SORBI_3007G209900 | 2121 | 706 | 7 | K-trans | 8 | 9 | N |
| > SbHAK7 | SORBI_3002G411500 | 2517 | 838 | 2 | K-trans | 8 | 11 | PM |
| > SbHAK8 | SORBI_3001G379900 | 1983 | 660 | 1 | K-trans | 9 | 6 | PM |
| > SbHAK9 | SORBI_3002G417500 | 2604 | 867 | 2 | K-trans | 11 | 9 | PM |
| > SbHAK10 | SORBI_3010G197500 | 2511 | 836 | 10 | K-trans | 6 | 11 | PM |
| > SbHAK11 | SORBI_3006G213500 | 2340 | 779 | 6 | K-trans | 13 | 10 | PM |
| > SbHAK12 | SORBI_3007G075100 | 1860 | 619 | 7 | K-trans | 8 | 9 | PM |
| > SbHAK13 | SORBI_3010G224400 | 2784 | 927 | 10 | K-trans | 9 | 12 | PM |
| > SbHAK14 | SORBI_3002G313900 | 2313 | 770 | 2 | K-trans | 10 | 7 | PM |
| > SbHAK15 | SORBI_3006G210700 | 3261 | 1086 | 6 | K-trans | 3 | 14 | N |
| > SbHAK16 | SORBI_3001G184000 | 2781 | 926 | 1 | K-trans | 9 | 11 | PM |
| > SbHAK17 | SORBI_3002G220600 | 2160 | 719 | 2 | K-trans | 13 | 8 | PM |
| > SbHAK18 | SORBI_3002G130800 | 1986 | 661 | 2 | K-trans | 10 | 6 | PM |
| > SbHAK19 | SORBI_3004G160000 | 2217 | 738 | 4 | K-trans | 10 | 6 | PM |
| > SbHAK20 | SORBI_3006G062100 | 2154 | 717 | 6 | K-trans | 10 | 8 | PM |
| > SbHAK21 | SORBI_3001G183700 | 2457 | 818 | 1 | K-trans | 11 | 13 | PM |
| > SbHAK22 | SORBI_3002G001800 | 2379 | 792 | 2 | K-trans | 9 | 5 | PM |
| > SbHAK23 | SORBI_3002G188600 | 2316 | 771 | 2 | K-trans | 10 | 7 | PM |
| > SbHAK24 | SORBI_3010G112800 | 3339 | 1112 | 10 | K-trans | 10 | 17 | PM |
| > SbHAK25 | SORBI_3004G250700 | 2007 | 668 | 4 | K-trans | 7 | 7 | PM |
| > SbHAK26 | Unknown | 1587 | 528 | 3 | K-trans | 5 | 4 | PM |
| > SbHAK27 | SORBI_3001G184300 | 2217 | 738 | 1 | K-trans | 11 | 9 | PM |
| > SbHKT2 | SORBI_3004G059800 | 1749 | 582 | 4 | Trk | 3 | 8 | PM |
| > SbHKT3 | SORBI_3006G208100 | 1692 | 563 | 6 | Trk | 7 | 3 | PM |
| > SbHKT4 | SORBI_3003G145800 | 2046 | 681 | 3 | Trk | 8 | 5 | PM |
| > SbHKT5 | SORBI_3010G251700 | 2145 | 714 | 10 | Trk | 7 | 7 | PM |
| > SbAKT1 | SORBI_3003G237900 | 2625 | 874 | 3 | VDPC | 5 | 10 | C |
| > SbAKT2 | SORBI_3002G049700 | 2607 | 868 | 2 | VDPC | 0 | 8 | C |
| > SbAKT3 | SORBI_3004G107500 | 1899 | 632 | 4 | VDPC | 3 | 9 | PM |
| > SbAKT4 | SORBI_3003G300600 | 1518 | 505 | 3 | VDPC | 4 | 10 | PM |
| > SbAKT5 | SORBI_3009G146800 | 2196 | 731 | 9 | VDPC | 2 | 6 | ER |
| > SbAKT6 | SORBI_3003G278200 | 1968 | 655 | 3 | VDPC | 5 | 6 | PM |
| > SbAKT7 | SORBI_3004G193100 | 1926 | 641 | 4 | KHA | 4 | 2 | PM |
| > SbAKT8 | SORBI_3010G102800 | 2565 | 854 | 10 | VDPC | 5 | 11 | PM |
| > SbAKT9 | SORBI_3006G201000 | 1926 | 641 | 6 | KHA | 4 | 2 | PM |
| > SbKAT1 | SORBI_3009G147500 | 2280 | 759 | 9 | VDPC | 3 | 8 | M |
| > SbKAT2 | SORBI_3009G147200 | 2319 | 772 | 9 | VDPC | 3 | 8 | ER |
| > SbTPC1 | SORBI_3001G086900 | 1044 | 347 | 1 | TPC | 6 | 2 | PM |
| > SbTPC2 | SORBI_3002G162400 | 1572 | 523 | 2 | TPC | 5 | 3 | PM |
| > SbVDPC1 | SORBI_3006G093400 | 2241 | 746 | 6 | VDPC | 4 | 11 | PM |
| > SbKEA1 | SORBI_3006G271800 | 2046 | 681 | 6 | KEFC | 10 | 16 | PM |
| > SbKEA2 | SORBI_3008G173800 | 2136 | 711 | 8 | KEFC | 7 | 15 | C |

Cds, Coding sequence; Aa, amino acid length; Chr, chromosomal location; TMHMM, transmembrane domain; Sb, *Sorghum bicolor*; HAK, high affinity potassium; VDPC, voltage-dependent potassium channel; TPC, two-pore channels; KEA, $K^+$ efflux antiporter; K-trans, $K^+$ transport; KEFC, $K^+$-efflux system protein; PM, Plasma membrane; N, Nucleus; ER, Endoplasmic reticulum; C, Chloroplast; M, Mitochondria.

0 (*SbAKT2*) to 13 (*SbHAK11* and *SbHAK17*) (Table 1), the number of exons varies from 2 (*SbAKT7*, *SbAKT9*, and *SbTPC1*) to 17 (*SbHAK24*) in sorghum (Table 1 and Figure 1). Most of the $K^+$ transport gene homologs are localized on the plasma membrane, followed by chloroplast, nucleus, endoplasmic reticulum, and mitochondria. SbHAK6 and HAK15 are localized on nucleus, SbAKT1, SbAKT2, and SbKEA on chloroplast, SbAKT5 and SbKAT2 on endoplasmic reticulum, and SbKAT1 on mitochondria (Table 1). The pI, MW, GRAVY, instability, aliphatic indexes (Supplementary Table 3), amino acid and net charge (Supplementary Table 4) have also been tabulated. Kinases play an important role in phosphorylation and $K^+$ gene homologs showed 18 different serine, threonine, and tyrosine kinases (Supplementary Table 5). The consensus motif GVVYGDLGTSPLY was identified in all the HAK transporter proteins except HAK5, HAK12, and HAK22 (Figure 2). Another signature sequence like GGTFALYSLLCR has been observed in all the HAK transporters leaving out HAK7, HAK15, and HAK22. The motif SLVFWTLTLIPLLKYVFIVL has been detected in all the HAK transporters excluding HAK12 (Figure 2). The motifs, VEMEDFSSAQLLVLTLLM, FSVFTTVSTFSNCGFLPTNE, GEKLVNALFMAVNSRHAGE, and DLSTLASAILVLYVLMMYLP were noticed in all the sorghum HKT $K^+$ transporter proteins (Figure 2). The KEA family displayed FFMTVGMSIDPKLLJREWP and KAFPNVKIFVRAKDLDH motifs (Figure 2). The sorghum $K^+$ channel (AKT, KAT, TPK, and VDPC) proteins displayed the motif YWSITTLTTVGYGDLHAENP (Figure 2).

## Promoter, 3D protein structures, and PPI analysis

Promoter analysis revealed the presence of biotic, abiotic, and phytohormone-responsive putative *cis*-elements (Supplementary Table 6). Different abiotic stress elements like DRE, CRT, CCAAT, MYB, MYC, LTRE, CBHFV, and IBOX have been identified (Figure 3). MYB represented the highest number of elements in all the transporters indicating their involvement in the stress tolerance. WBOX, the biotic stress-responsive element has also been recognized in all the $K^+$ transporters. Most transporters have phytohormone-responsive elements like ABRE, WRKY, DPBF, ARR1, and GARE. ARR1, the cytokinin-responsive elements have been found as the highest number of elements among the phytohormone-responsive elements and identified in all the transporter and channel gene homologs (Figure 3). Such *cis*-element studies are essential since they might contribute to find out the functional regulation of KT/HAK/KUP gene family members in sorghum. 3D structures of $K^+$ transport proteins were predicted with the best PDB templates (Figure 4). The template PDB id, template description, chain, model of the oligomer, and their structure validations are represented in the Supplementary Table 7. 3D structures of SbHAK26, SbAKT1, SbAKT2, SbAKT3, SbAKT4, SbAKT5, SbAKT6, SbAKT7, SbAKT8, SbAKT9, SbKAT1, SbKAT2, and SbVDPC1 proteins displayed significant sequence similarity percent ranging from 30.77% (SbHAK26) to 68.61% (SbAKT4). 3D structures of other $K^+$ transport proteins did not show any significant ($< 30\%$) sequence similarity (Supplementary Table 7). All the generated Ramachandran plots for structure validation are represented as Supplementary Figure 1. In the predicted PPI map, sorghum $K^+$ proteins displayed interactions with several other $K^+$ proteins. A total of 46 $K^+$ proteins, except SbAKT9 were found in the PPI map (Figure 5). All the 46 proteins have been displayed as 46 nodes with 193 edges. Each protein showed more than one interactant (Supplementary Table 8). SbTPC1, SbTPC2, SbHAK23, SbHKT3, SbHKT4, SbAKT1, SbKEA1, SbHAK8, SbKAT1, and SbKAT2 have been found to be the major interacting proteins. SbHAK15 and SbVDPC1 did not show any interactions (Figure 5). All the STRING protein names used for PPIs are available in Supplementary Table 8.

## Evolutionary divergence, chromosomal location and synteny

The phylogenetic tree revealed the evolutionary relationship of $K^+$ transport homologs of *Sorghum bicolor* with *Oryza sativa* and *Arabidopsis thaliana* (Figure 6 and Supplementary Table 9). A total of 9 paralogs have been identified (Figure 7), 1 recognized as regional (SbHAK3 and SbHAK26) and 8 as segmental (SbHAK24 and SbHKT4, SbHAK6 and SbHAK13, SbHAK7 and SbKEA1, SbHAK18 and SbHAK20, SbHAK21 and SbKAT2, SbHKT2 and SbHKT3, SbAKT7 and SbAKT9, and SbAKT8 and SbAKT5) duplications. Sorghum showed 21 ortholog pairs (Figure 6), 18 with *Oryza* (SbHAK1 and OsHAK1, SbAKT2 and OsVDPC1, SbHAK2 and OsHAK16, SbHAK4 and OsHAK4, SbHAK5 and OsHAK26, SbHAK14 and OsHAK15, SbHAK10 and OsHAK13, SbHAK16 and OsAKT3, SbHAK12 and OsHAK20, SbHAK15 and OsHAK14, SbTPC1 and OsTPC1, SbHAK19 and OsHAK19, SbHAK27 and OsHAK27, SbKEA2 and OsKEA2, SbKAT1 and OsHKT2, SbAKT3 and OsAKT4, SbAKT4 and OsVDPC2, and SbAKT6 and OsHAK11) and 3 with *Arabidopsis* (SbHAK8 and AtHAK8, SbHAK23 and AtTPK3, and SbHAK22 and AtKEA1). All the 9 sorghum paralogs (SbHAK3 and SbHAK26, SbHAK24 and SbHKT4, SbHAK6 and SbHAK13, SbHAK7 and SbKEA1, SbHAK18 and SbHAK20, SbHAK21 and SbKAT2, SbHKT2 and SbHKT3, SbAKT7 and SbAKT9, and SbAKT8 and SbAKT5) display substitution rate $< 1$. The lowest $d_N/d_S$ (0.0010) were observed in the regional paralog (SbHAK3 and SbHAK26) and the highest $d_N/d_S$ (0.3651) in segmental paralog (SbHAK24 and SbHKT4) gene pairs (Table 2) respectively. Sorghum


FIGURE 1
Characterization of $K^+$ transporter gene homologs. Exons are represented as red boxes and introns as black lines. Sb, *Sorghum bicolor*; HAK, high affinity potassium; KEA, $K^+$ efflux antiporter; VDPC, voltage-dependent potassium channel; TPC, two-pore channels.

$K^+$ transport gene homologs have been mapped onto *Oryza* (Figure 8). *S. bicolor* chromosome 2 displays 9 (highest) homologs followed by chromosome 3 and 6 with 8 homologs each, chromosome 1, 4, and 10 with 5 homologs each, chromosome 7 and 9 with 3 homologs each, and chromosome 8 with 1 homolog respectively. Similarly, *O. sativa* displays 10 homologs on chromosome 1, followed by chromosome 4 with 8 homologs, chromosomes 6 and 7 with 6 homologs each, chromosomes 2 and 3 with 5 homologs each, chromosomes 8 and 9 with 3 homologs each, chromosome 12 with 2 homologs, and chromosome 5 with 1 homolog. *O. sativa* and *S. bicolor* chromosomes 1 and 2 show the highest number of homologs with 10 and 9, respectively (Figure 8). Chromosome 5 of sorghum, 10 and 11 of rice do not contain any of the $K^+$ gene homologs. A correspondence matrix was created and automated name-based and synteny maps were generated (Figure 8). The links on the chromosomes represent the gene homologs in sorghum and rice (Figure 8).

## Digital expressions and quantitative expression analysis of sorghum $K^+$ transport gene homologs under abiotic stress conditions in different tissues

Digital expression of all the 46 $K^+$ transport genes was analyzed in root, shoot, and leaf tissues exposed to cold

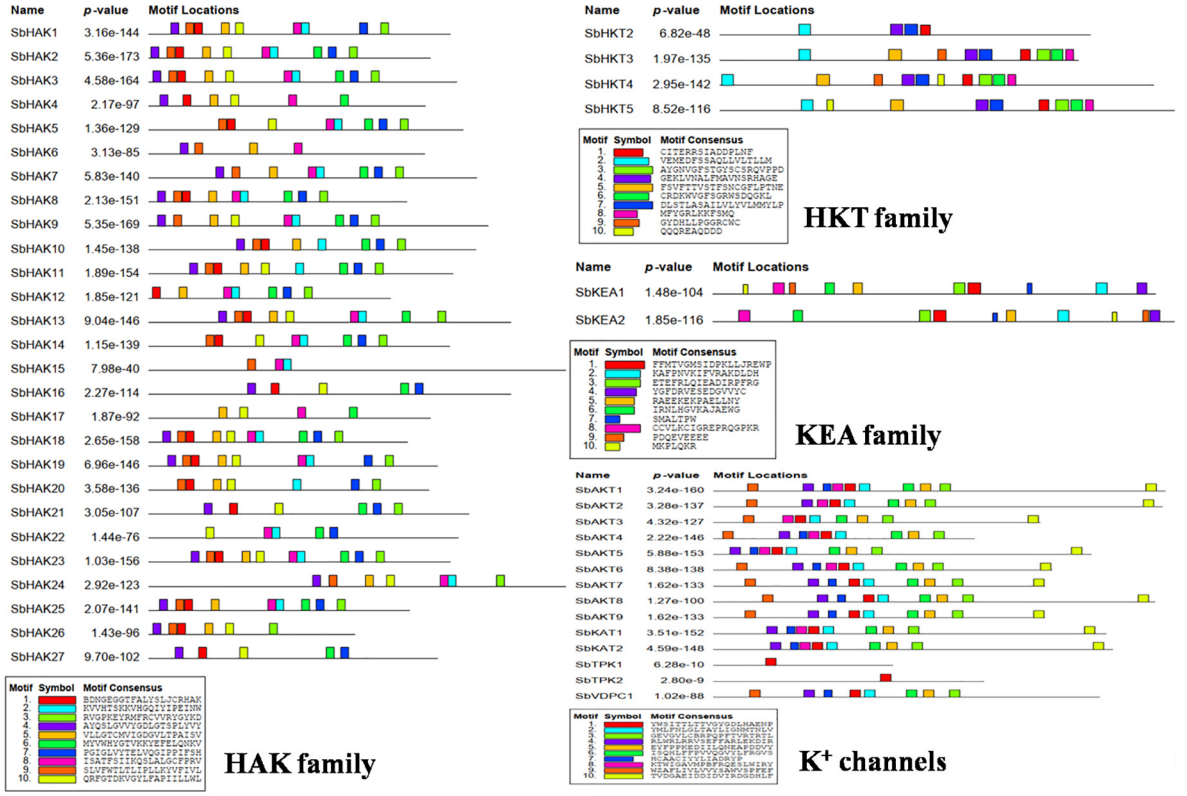


FIGURE 2
Conserved motif analysis of $K^+$ transporter (HAK, HKT, and KEA) and channel (AKT, KAT, VDPC, and TPC) proteins. The consensus motif GVVYGDLGTSPLY was identified in all the HAK transporters except HAK5, HAK12, and HAK22. The motifs, VEMEDFSSAQLLVLTLLM, FSVFTTVSTFSNCGFLPTNE, GEKLVNALFMAVNSRHAGE, and LSTLASAILVLYVLMMYLP were observed in all the sorghum HKT transport proteins. The KEA family displayed FFMTVGMSIDPKLLJREWP and KAFPNVKIFVRAKDLDH motifs. All the channel proteins displayed the motif YWSITTLTTVGYGDLHAENP. Sb, *Sorghum bicolor*; HAK, high affinity potassium; KEA, $K^+$ efflux antiporter; VDPC, voltage-dependent potassium channel; TPC, two-pore channels.

and drought stress conditions. In anatomical tissues, high expression levels of $K^+$ transport genes were noticed in root compared shoot, and leaf tissues (Figure 9A). In root tissues, *SbHAK7*, *SbHAK18*, *SbHAK10*, and *SbHAK25*, in shoot tissues, *SbHAK11*, *SbKEA1*, and *SbHAK22*, *SbHAK11*, *SbKEA1*, and *SbKEA2* displayed high expressions respectively (Figure 9A). In developmental stages high expression levels of $K^+$ transport genes were noticed in milk stage, flowering stage, tillering stage and seedling stage (Figure 9B). In milk stage *SbHAK27* and *SbKEA2*, in the flowering stage *SbHAK17*, *SbHAK11*, *SbHAK18*, and *SbHAK7*, in tillering stage *SbHAK18*, *SbHAK10*, and 23 genes displayed elevated expression levels than other transport genes (Figure 9B). Differential expression profile of $K^+$ transport genes was noticed in cold and drought conditions (Figure 9C). Higher expression levels were noticed in cold stress compared to drought stress. *SbAKT1*, *SbHAK7*, *SbHKT5*, *SbHAK25*, and *SbAKT7* genes have higher expression levels in cold stress. SbHAK5 and SbHAK17 genes have higher expression in drought stress (Figure 9C).

Expression levels of only 32 $K^+$ transport gene homologs (*SbHAK1*, *SbHAK2*, *SbHAK3*, *SbHAK4*, *SbHAK5*, *SbHAK6*, *SbHAK7*, *SbHAK8*, *SbHAK9*, *SbHAK10*, *SbHAK11*, *SbHAK12*, *SbHAK13*, *SbHAK14*, *SbHAK15*, *SbHAK17*, *SbHAK18*, *SbHAK19*, *SbHAK20*, *SbHAK21*, *SbHAK22*, *SbHAK23*, *SbHAK24*, *SbHAK25*, *SbHAK26*, *SbHAK27*, *SbHKT2*, *SbHKT3*, *SbHKT4*, *SbHKT5*, *SbKEA1*, and *SbKEA2*) were analyzed in sorghum root, stem, and leaf tissues subjected to salt, drought, heat, and cold stresses and shown in the heat map (Figure 10). qRT-PCR for other 15 $K^+$ transport gene homologs could not be performed due to high sequence similarity. The homologs displayed differential gene expression in different tissues (Supplementary Table 10). *SbHAK2*, *SbHAK20*, *SbHAK5*, and *SbHAK3* showed markedly increased expressions under salt, heat, drought and cold stresses respectively. Among the stress treatments, a 13.86-fold increase in transcript levels was observed in *SbHAK3* in cold-stressed roots, followed by strong upregulation of *SbHAK2* (13.39-folds increase) under salt stress in the leaves. *SbHAK7* was enhanced by 11.95-folds in the

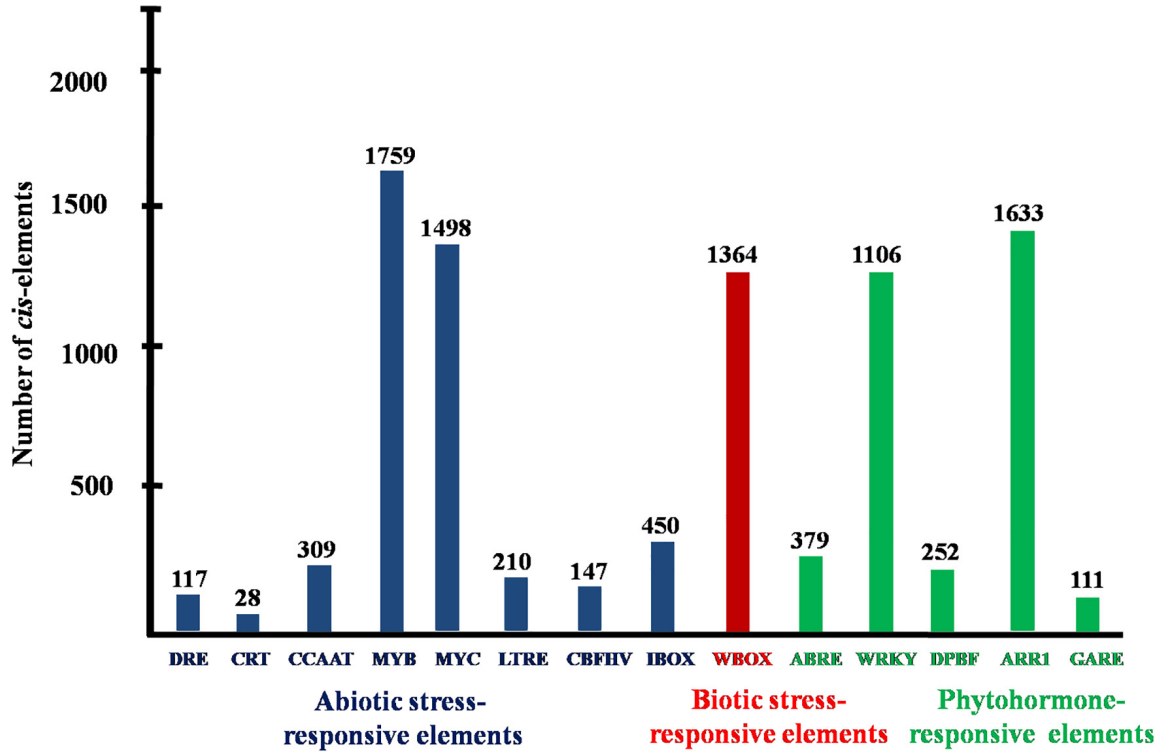


FIGURE 3
Conserved putative *cis*-acting elements of sorghum $K^+$ transport gene homologs. DRE, dehydration-responsive elements; CRT, low-temperature responsive element; CCAAT, promoter of heat shock protein; MYB, responsive to drought and ABA; MYC, response to drought, cold and ABA; LTRE, low temperature and cold-responsive; CBFHV, dehydration-responsive element; IBOX, light regulation; WBOX, transcriptional repressor ERF3 gene; ABRE, early responsive to dehydration; WRKY, transcriptional repressor of the gibberellin; DPBF, ABA; AAR1, cytokinin-regulated transcription factor; GARE, gibberellic acid-responsive elements.

leaves exposed to salt stress. Similarly, *SbHAK12*, *SbHAK20*, and *SbHAK21* displayed 10.19, 10.48, and 10.14-folds enhanced activity in stem tissues subjected to salt (SbHAK12) and heat stresses (*SbHAK20*, *SbHAK21*) respectively. While *SbHAK15* showed 9.36-fold increase in roots exposed to cold stress, *SbHAK8*, *SbHAK14*, and *SbHAK10* exhibited higher activities in stems treated with salt and cold stresses respectively. Out of all gene homologs, *SbHAK2*, *3*, *7*, *8*, *10*, *12*, *14*, *15*, *20*, *21*, and *14* recorded markedly high expressions in compared to other *SbHAK*, *SbHKT*, and *SbKEA* members. Transcripts *SbHAK7*, *SbHAK8*, *SbHAK9*, *SbHAK10*, *SbHAK11*, *SbHAK12*, *SbHAK13*, and *SbHAK14* are highly upregulated under salt, heat, and cold, while *SbHAK1*, *SbHAK4*, *SbHAK5*, *SbHAK18*, *SbHAK22*, and *SbHAK27* (4.55–7.94-folds) were well expressed under drought stress conditions. *SbHAK17* has the lowest level of expression among all the genes across different stresses and tissues (**Figure 10**). Transcript expressions were increased in stem and leaf tissues subjected to high temperature stress especially in most of *SbHAKs*. Among the *SbHKTs*, the transcript level of *SbHKT5* was superior (7.17-fold increase) in leaves exposed to salt stress. Similarly, *SbKEA1* expression was significantly high (10.14-folds) under salt stress in the stems of Sorghum. Activity of *SbKEA2* was 11.2-folds higher in salt-stressed leaves.

## Discussion

$K^+$ plays a pivotal role as a constituent of the plant structure, in ion homeostasis, salt tolerance, plant growth, development, transport, aside from acting as a signaling molecule (Feng et al., 2019; Hussain et al., 2021). It has a regulatory function in many physiological and biochemical processes such as protein synthesis, and activation of enzymes (Hasanuzzaman et al., 2018). $K^+$ is available to plants only in ionic form and higher $K^+/Na^+$ has been recognized unequivocally as a crucial molecule for maintaining electro-neutrality of the cells (Hussain et al., 2021). Under saline and water deficient conditions, $K^+$ maintains ion homeostasis and modulates the osmotic balance. Further, $K^+$ participates in stomatal regulation during drought stress and increases the antioxidative ability of the plants (Hasanuzzaman et al., 2018). Since many homologs have been detected in plants, we need to understand which of the homologs perform the crucial processes

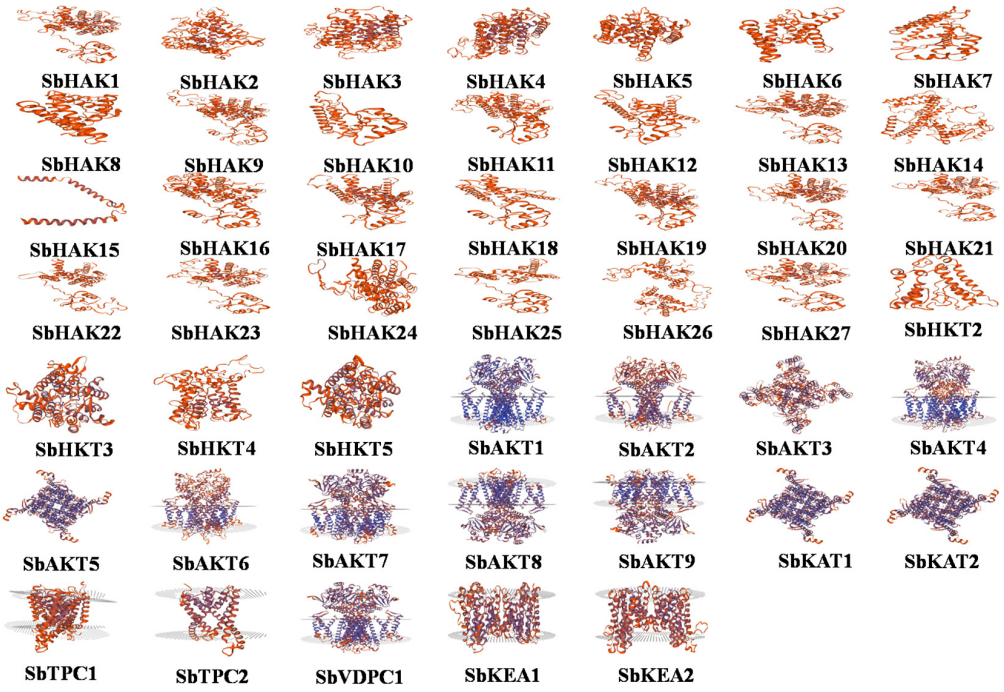


FIGURE 4
Structural analysis of 47 modeled sorghum $K^+$ transport proteins. Sb, *Sorghum bicolor*; HAK, high affinity potassium; KEA, $K^+$ efflux antiporter; VDPC, voltage-dependent potassium channel; TPC, two-pore channels.

of plant growth, abiotic stress, and under $K^+$ deprivation conditions (Hamamoto et al., 2008; Jiang et al., 2021). In the present investigation, a total of 47 $K^+$ transporter gene homologs (**Table 1**) were discovered in all including 33 $K^+$ transporters (27 HAKs, 4 HKTs, and 2 KEAs) and the remaining 14 (9 AKTs, 2 KATs, 2 TPCs, and 1 VDPC) as $K^+$ channels in *S. bicolor*.

## Characterization of $K^+$ transport gene homologs in sorghum

Sorghum has 47 $K^+$ transporter gene homologs (**Table 1** and **Figure 1**) in comparison with 43 in *Gossypium raimondii*, (Azeem et al., 2022), 39 in *Cajanus cajan* (Siddique et al., 2021), and 36 in *Cicer arietinum* (Azeem et al., 2018). Nevertheless, these numbers are lower than that of *Glycine max*, where 70 homologs have been detected (Rehman et al., 2017), and 49 in *Oryza sativa* (Amrutha et al., 2007). The 27 genes encoding HAK transporters in Sorghum (**Figure 1**) are similar in the number of HAK encoding genes detected in *Zea mays* and *Hordeum vulgare* (Zhang et al., 2012; Cai et al., 2021). *Triticum aestivum* and *Pyrus betulifolia* have 56 HAK transporters each (Cheng et al., 2018; Li Y. et al., 2018) followed by 41 in *Nicotiana tabacum* (Song et al., 2019), 31 in *Populus trichocarpa* (He et al., 2012), 30 in *Saccharum spontaneum* (Feng et al., 2020b), 29 in *Glycine max* (Rehman et al., 2017), 26 in *Oryza sativa* (Amrutha et al., 2007), 22 in *Salix purpurea* and *Ipomoea batatas* (Liang et al., 2020; Jin et al., 2021), 21 in *Populus trichocarpa*, *Prunus persica*, *Manihot esculenta*, and *Camellia sinensis* (He et al., 2012; Song et al., 2015; Ou et al., 2018; Yang T. et al., 2020), 19 in *Solanum lycopersicum* (Hyun et al., 2014), 17 in *Oryza sativa* and *Cajanus cajan* (Banuelos et al., 2002; Siddique et al., 2021), 16 in *Prunus persica* and *Gossypium raimondii* (Song et al., 2015; Azeem et al., 2022), and 13 in *Arabidopsis thaliana* (Ahn et al., 2004). These studies indicate that $K^+$ transport genes are highly conserved in plants during evolution. A total of 21, 24, 45, and 44 HAK/KUP/KT genes were identified in *Gossypium hirsutum*, *Gossypium barbadense*, *Gossypium raimondii*, and *Gossypium arboretum* genomes respectively (Yang X. et al., 2020). The higher number of $K^+$ transporter homologs in *Triticum* is due to its ploidy nature (Kyriakidou et al., 2018). Sorghum has shared 4 HKT encoding genes with *Glycine max* (Rehman et al., 2017). *Oryza sativa* has 8 HKTs, followed by 4 in *Sorghum bicolor* and *Glycine max*, 2 HKTs in *Gossypium raimondii*, *Cajanus cajan*, and *Cicer arietinum* (Amrutha et al., 2007; Rehman et al., 2017; Azeem et al., 2018, 2022; Siddique et al., 2021). *Glycine max* has the highest number of KEA transporters (12) (Rehman et al., 2017), followed by 7 KEAs in *Gossypium raimondii* (Azeem et al., 2022), 6 KEAs in *Cicer arietinum* and *Cajanus cajan* (Azeem et al., 2018; Siddique et al., 2021), but 2 KEAs in sorghum, and 1 KEA in *Oryza sativa* (Amrutha et al., 2007). The number of $K^+$ channels identified in sorghum corroborates the previously reported genomes. A total

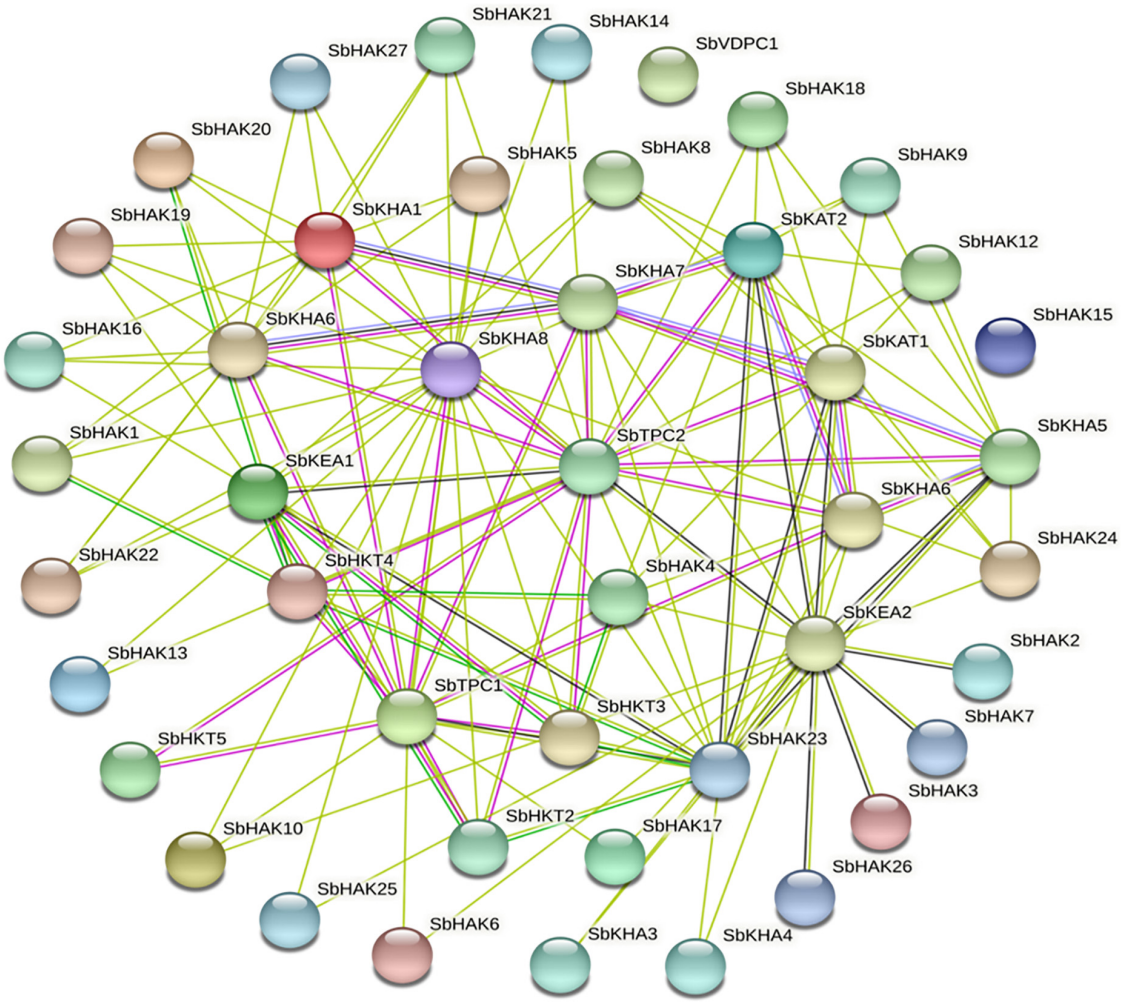


FIGURE 5
String analysis of sorghum $K^+$ transport homologs. All the proteins displayed the interacting partners except SbHAK15 and SbVDPC1. Sb, *Sorghum bicolor*; HAK, high affinity potassium; KEA, $K^+$ efflux antiporter; VDPC, voltage-dependent potassium channel; TPC, two-pore channels.

of 14 $K^+$ channels were identified in sorghum (9 AKTs, 2 KATs, 2TPKs, and 1 VDPC), an equal number in *Oryza sativa* (14 AKTS) (Amrutha et al., 2007), belonging to the same family. But *Cajanus cajan* has 9 shakers and 5 TPKs (Siddique et al., 2021). However, 25 $K^+$ channel gene homologs (16 VDPCs, 9 TPK/KCO) have been reported in *Glycine max* (Rehman et al., 2017) and 18 (11 shakers and 7 TPKs/KCO) in *Gossypium raimondii* (Azeem et al., 2022).

The conserved domains of $K^+$ transporter system *viz.*, K-trans, TrK, KEA, voltage-dependent $K^+$ channel, KHA, and Two Pore Potassium (TPK) channel were identified in sorghum (**Table 1**) which corroborates the identified $K^+$ genes in other plant genomes such as *Oryza sativa* (Amrutha et al., 2007), *Glycine max* (Rehman et al., 2017), *Cicer arietinum* (Azeem et al., 2018), *Cajanus cajan* (Siddique et al., 2021), and *Gossypium raimondii* (Azeem et al., 2022). The consensus motif GVVYGDLGTSPLY (Rodríguez-Navarro, 2000) was identified in all the sorghum HAK transporters except *SbHAK5*, *SbHAK12*, and *SbHAK22* (**Figure 2**). Similar results were also reported in *Oryza* (Amrutha et al., 2007), *Cicer arietinum* (Azeem et al., 2018), *Cajanus cajan* (Siddique et al., 2021), and *Gossypium raimondii* (Azeem et al., 2022). The motif GGTFALYSLLCR was detected in *Arabidopsis thaliana* (Ahn et al., 2004), *Cicer arietinum* (Azeem et al., 2018), *Cajanus cajan* (Siddique et al., 2021), *Gossypium* (Azeem et al., 2022) was also noticed in sorghum inferring its evolutionary conservation. The conserved $K^+$ channel motif GYGD (Kuang et al., 2015) has been observed in all the sorghum $K^+$ channels (**Figure 2**), identical to that of *Oryza sativa* (Amrutha et al., 2007), *Cicer arietinum* (Azeem et al., 2018), *Cajanus cajan* (Siddique et al., 2021), and *Gossypium* (Azeem et al., 2022). Most of the sorghum HAK transporters are localized on plasma membrane (**Table 1**) akin to

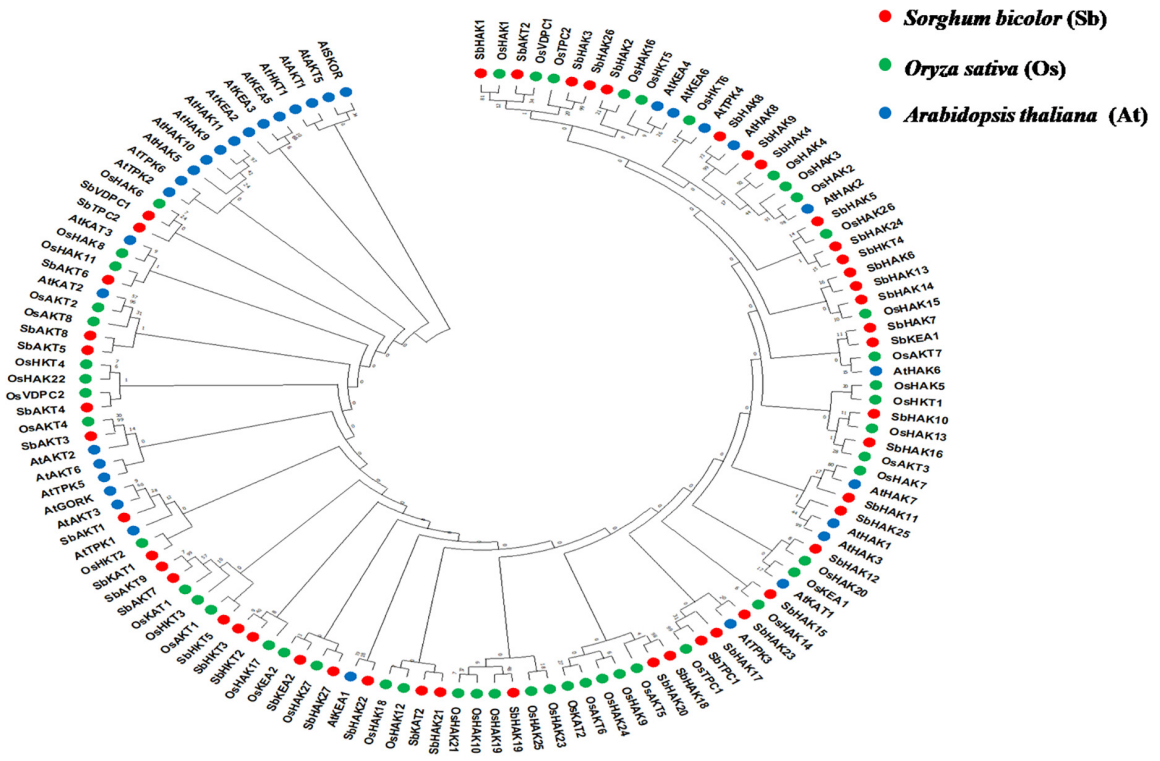


FIGURE 6
Phylogenetic tree of $K^+$ transport proteins between *Sorghum bicolor* (Sb), *Oryza sativa* (Os), and *Arabidopsis thaliana* (At). Predicted amino acid sequences were used for construction of the tree. The tree was constructed by the Neighbor Joining method using MEGA-X. Values indicate the number of times (as a percentage) that each branch topology was found during bootstrap analysis. Sb, *Sorghum bicolor*; HAK, high affinity potassium; KEA, $K^+$ efflux antiporter; VDPC, voltage-dependent potassium channel; TPC, two-pore channels.

*Triticum aestivum* (Cheng et al., 2018), *Saccharum spontaneum* (Feng et al., 2020b), *Salix purpurea* (Liang et al., 2020), *Camellia sinensis* (Yang T. et al., 2020), *Hordeum vulgare* (Cai et al., 2021), and *Ipomoea batatas* (Jin et al., 2021). *A. thaliana* AtHAK5 has been associated with the uptake of $Na^+$ (Wang Q. et al., 2015). This implies that these porters subscribe to the accumulation of $Na^+$ under saline conditions. Since restricting $Na^+$ uptake determines salt tolerance, care must be taken while breeding the crop plants for salt stress tolerance. Also, HKTs are involved in loading $Na^+$ into the xylem. Zhu et al. (2016) also noticed a link between SOS1 and HKT pathways for salt stress in wheat. These studies indicate the HKTs critical role during salt stress tolerance. $K^+$ efflux antiporters KEA1 and KEA2 have been found in inner envelop membrane in *A. thaliana,* and the loss of function mutants influence both ROS and reactive nitrogen species (RNS). Double knock-out mutants of *kea1kea2* elicited an alteration of the ROS homeostasis. However, nitric oxide (NO) content has negatively affected photosynthesis increasing photorespiratory activity (Sánchez-McSweeney et al., 2021). The studies infer that KEAs maintain chloroplast osmotic balance. In sorghum, SbKEA1 is localized on chloroplast membranes and is perhaps involved in the regulation of thylakoid and stromal pH (Sánchez-McSweeney et al., 2021).

## Analysis of putative *cis*-elements and 3D protein structures, and interactions

Hyun et al. (2014) and Assaha et al. (2017) reported the involvement of *cis*-regulatory elements in abiotic stress tolerance and in $K^+$ homeostasis. Similarly, analysis of promoter sequences of $K^+$ transport gene homologs in sorghum revealed the presence of *cis*-elements which may be involved in diverse abiotic stress tolerances. This prediction is in line with that of *Cicer arietinum* (Azeem et al., 2018), *Cajanus cajan* (Siddique et al., 2021), and *Gossypium raimondii* (Azeem et al., 2022). In the promoter regions, regulatory elements like ABRE, MYB, MYC, GARE, WBOX, LTRE, and CCAAT have been noticed in *Cicer arietinum* (Azeem et al., 2018), *Pyrus betulifolia* (Li Y. et al., 2018), *Manihot esculenta* (Ou et al., 2018), *Nicotiana tabacum* (Song et al., 2019), *Salix purpurea* (Liang et al., 2020), *Camellia sinensis* (Yang T. et al., 2020), *Hordeum vulgare* (Cai et al., 2021), *Cajanus cajan* (Siddique et al., 2021), *Ipomoea batatas* (Jin et al., 2021), and *Gossypium* species (Yang X. et al., 2020; Azeem et al., 2022) indicating the involvement of $K^+$ transport gene homologs in abiotic stress tolerance. Aside abiotic stress-responsive elements, promoter analysis also revealed the presence of biotic stress-responsive and phytohormone

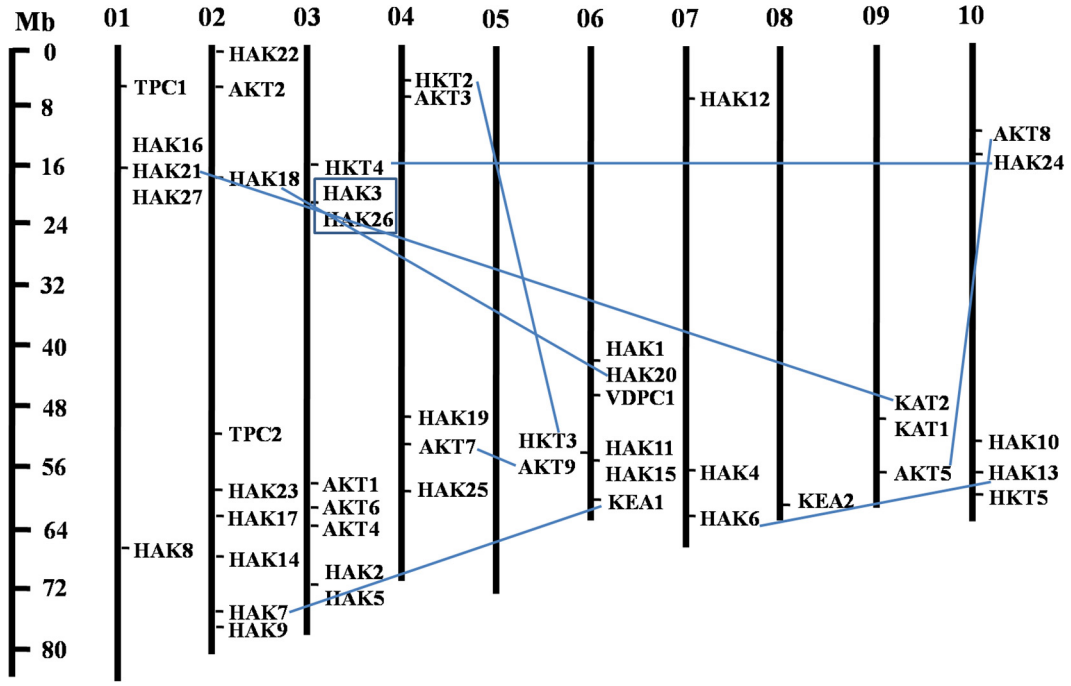


FIGURE 7
Physical mapping of sorghum $K^+$ transport gene homologs. The 9 paralog gene pairs are represented in blue color. Of the 9 paralogs, 8 have been identified as segmental (SbHAK24 and SbHKT4, SbHAK6 and SbHAK13, SbHAK7 and SbKEA1, SbHAK18 and SbHAK20, SbHAK21 and SbKAT2, SbHKT2 and SbHKT3, SbAKT7 and SbAKT9, and SbAKT8 and SbAKT5) represented as lines and 1 as regional (SbHAK3 and SbHAK26) represented as box. Sb, *Sorghum bicolor*; HAK, high affinity potassium; KEA, $K^+$ efflux antiporter; VDPC, voltage-dependent potassium channel; TPC, two-pore channels.

stress-responsive elements in sorghum (**Figure 3**). The predicted elements indicate that $K^+$ transporters are implicated in biotic stress response and their cross-talk with hormones during stress. Protein models (**Figure 4**) help to understand structure-function relationships (Rasheed et al., 2020). Protein-protein interactions (PPIs) of sorghum (**Figure 5**) displayed interaction with other $K^+$ transporters and channels like what has been noticed in *Cajanus cajan* (Siddique et al., 2021). The SbHAK transporters also interacted with other SbHAK transporters like *Ipomoea batatas* HAK transporters (Jin et al., 2021).

## Evolutionary divergence and comparative analysis

Phylogenetic analysis revealed the close relationship of *Sorghum bicolor* $K^+$ transporters with *Oryza sativa* (Amrutha et al., 2007) than to *Arabidopsis thaliana* (**Figure 6**). A comparative phylogenetic analysis of $K^+$ transporters has been carried out in *Oryza sativa* (Amrutha et al., 2007), *Glycine max* (Rehman et al., 2017), *Cicer arietinum* (Azeem et al., 2018), *Cajanus cajan* (Siddique et al., 2021), and *Gossypium raimondii* (Azeem et al., 2022). Similarly, comparative studies of HAK transporters have been reported in *Oryza sativa* (Banuelos et al., 2002), *Arabidopsis thaliana* (Ahn et al., 2004), *Populus trichocarpa* (He et al., 2012), *Zea mays* (Zhang et al., 2012), *Solanum lycopersicum* (Hyun et al., 2014), *Prunus persica* (Song et al., 2015), *Glycine max* (Rehman et al., 2017), *Triticum aestivum* (Cheng et al., 2018) and *Pyrus betulifolia* (Li Y. et al., 2018), *Manihot esculenta* (Ou et al., 2018), *Nicotiana tabacum* (Song et al., 2019), *Saccharum spontaneum* (Feng et al., 2020b), *Salix purpurea* (Liang et al., 2020), *Hordeum vulgare*

TABLE 2 Non-synonymous and synonymous substitution rates of sorghum paralog genes.

| Gene 1 | Gene 2 | $d_N$ | $d_S$ | $d_N/d_S$ |
|---|---|---|---|---|
| SbHAK3 | SbHAK26 | 0.0000 | 0.0067 | 0.0010 |
| SbHAK24 | SbHKT4 | 1.4970 | 4.1006 | 0.3651 |
| SbHAK6 | SbHAK13 | 0.8725 | 48.9776 | 0.0178 |
| SbHAK7 | SbKEA1 | 1.7874 | 41.0903 | 0.0435 |
| SbHAK18 | SbHAK20 | 0.6416 | 46.0156 | 0.0139 |
| SbHAK21 | SbKAT2 | 1.8058 | 33.4346 | 0.0540 |
| SbHKT2 | SbHKT3 | 11.1872 | 17.6762 | 0.6329 |
| SbAKT7 | SbAKT9 | 0.0000 | 0.0000 | 0.2325 |
| SbAKT8 | SbAKT5 | 0.7637 | 67.2009 | 0.0114 |

dS, synonymous substitution; dN, non-synonymous substitution; Sb, *Sorghum bicolor*; HAK, high affinity potassium; KEA, $K^+$ efflux antiporter.

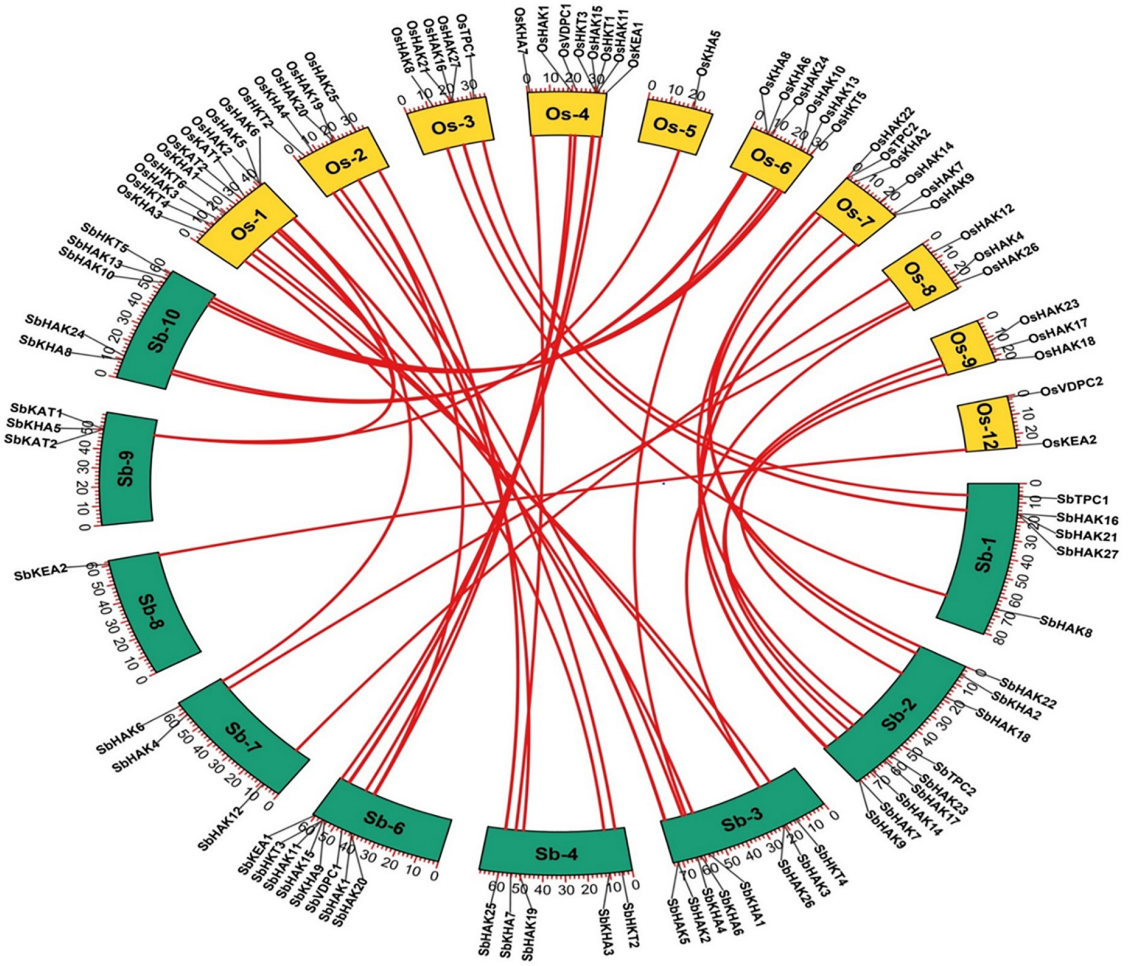


FIGURE 8
Synteny analysis of $K^+$ transporter genes in *Sorghum bicolor* and *Oryza sativa*. The map was built with TB tools software. Sb, *Sorghum bicolor*; Os, *Oryza sativa*; HAK, high affinity $K^+$; KEA, $K^+$ efflux antiporter; VDPC, voltage-dependent $K^+$ channel; TPC, two-pore channels.

(Cai et al., 2021), *Ipomoea batatas* (Jin et al., 2021), and *Camellia sinensis* (Yang T. et al., 2020). Most sorghum $K^+$ homologs showed high gene conservation with *Oryza sativa* (**Figure 6**) as both share common ancestor (Wang X. et al., 2015). The tree indicated 9 paralog and 21 ortholog (18 with *Oryza sativa* and 3 with *Arabidopsis thaliana*) groups. Chromosomal distribution and synteny analyses revealed the presence of 1 regional (*SbHAK3* and *SbHAK26*) and 8 segmental (*SbHAK24* and *SbHKT4*, *SbHAK6* and *SbHAK13*, *SbHAK7* and *SbKEA1*, *SbHAK18* and *SbHAK20*, *SbHAK21* and *SbKAT2*, *SbHKT2* and *SbHKT3*, *SbAKT7* and *SbAKT9*, and *SbAKT8* and *SbAKT5*) duplication gene pairs. Such gene duplication events have also been reported in *Ipomoea batatas* HAK transporters (Jin et al., 2021). All the 9 sorghum paralogs (*SbHAK3* and *SbHAK26*, *SbHAK24* and *SbHKT4*, *SbHAK6* and *SbHAK13*, *SbHAK7* and *SbKEA1*, *SbHAK18* and *SbHAK20*, *SbHAK21* and *SbKAT2*, *SbHKT2* and *SbHKT3*, *SbAKT7* and *SbAKT9*, and *SbAKT8* and *SbAKT5*) have the dN/dS value < 1 (**Table 2**), indicating a purifying Darwinian selection during the evolution of HAK genes (Bowers et al., 2003). The HAK family of *Saccharum spontaneum* (Feng et al., 2020b) and *Ipomoea batatas* (Jin et al., 2021) have also showed the non-synonymous/synonymous value < 1. Uneven distributions of $K^+$ transport gene homologs on different chromosomes have been observed in sorghum (**Figure 7**) similar to *Oryza sativa* (Amrutha et al., 2007), *Glycine max* (Rehman et al., 2017), *Cicer arietinum* (Azeem et al., 2018), *Cajanus cajan* (Siddique et al., 2021), and *Gossypium raimondii* (Azeem et al., 2022). Uneven distribution of HAK/KUP/KT homologs has been observed in angiosperms also (Nieves-Cordones et al., 2016). Gene order conservation of $K^+$ gene homologs across sorghum and rice has been identified by circos (**Figure 8**). $K^+$ transport homologs displayed very high conservation between sorghum and rice since they share a common ancestor (Wang X. et al., 2015). Chromosome 2 and 1

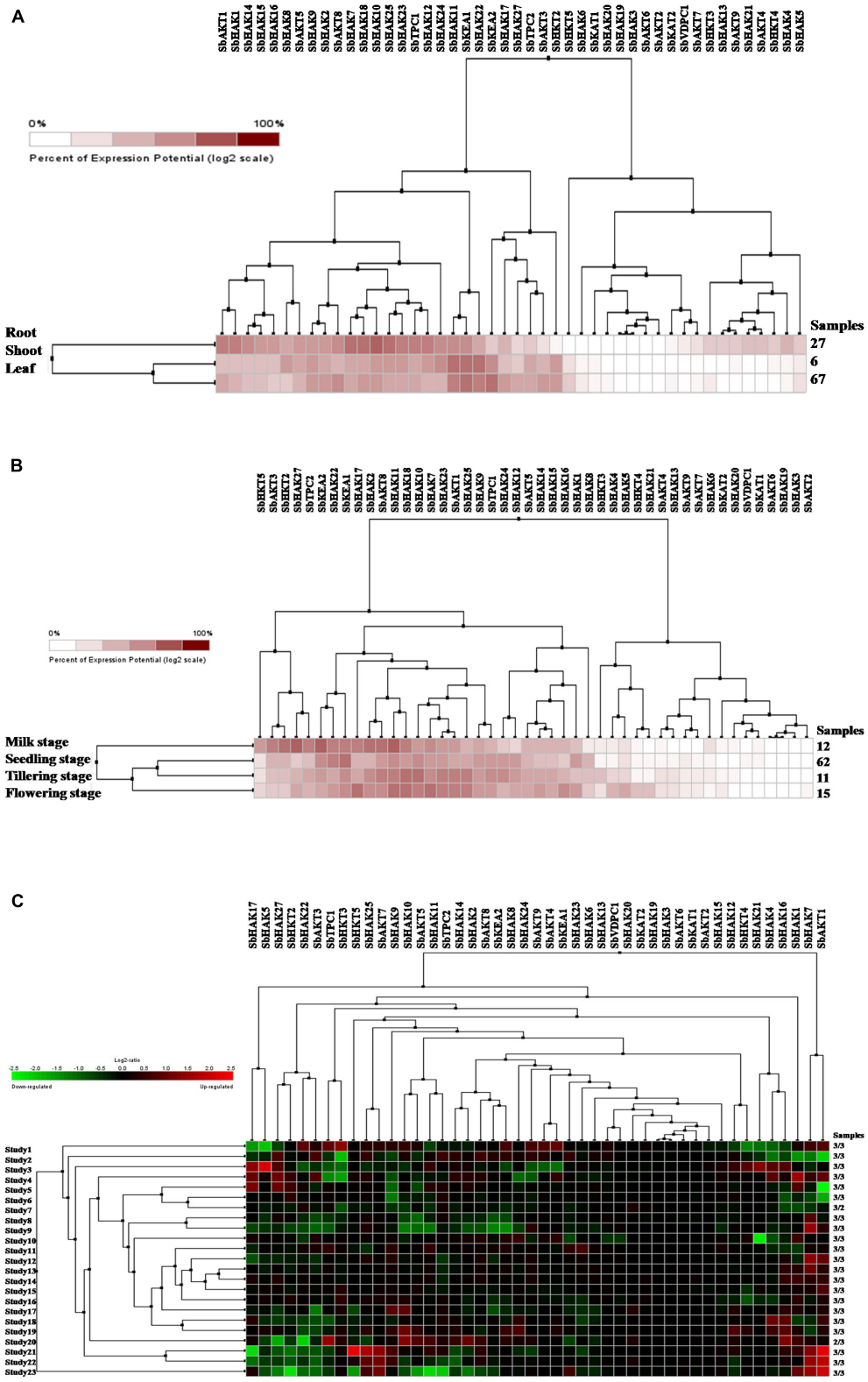


FIGURE 9
Digital expression profile of sorghum $K^+$ transport genes in different tissues, developmental stages under cold and drought stresses **(A)** $K^+$ transport in anatomical tissues, **(B)** $K^+$ transport in developmental stages, **(C)** $K^+$ transport gene expressions under cold and drought stresses. Sb, *Sorghum bicolor*; HAK, high affinity potassium; KEA, $K^+$ efflux antiporter; VDPC, voltage-dependent potassium channel; TPC, two-pore channels.

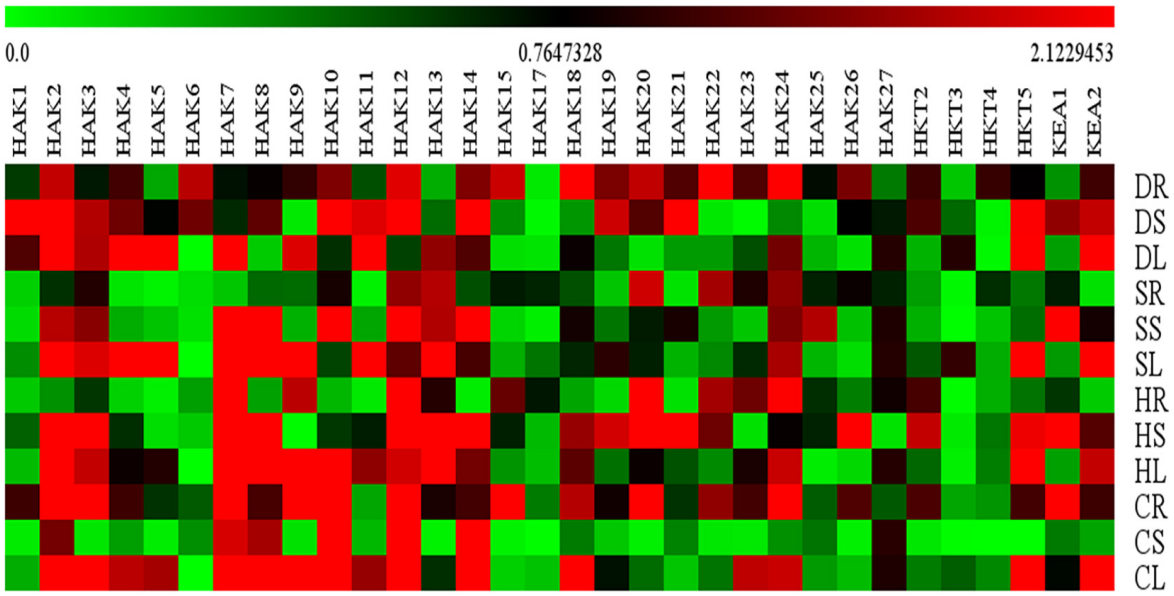


FIGURE 10
Relative expression analysis of sorghum $K^+$ transporter gene homologs. Sorghum transporter expressions during salt, drought, heat, and cold stresses. Relative expression of transporters is shown during different stress conditions compared to its corresponding controls. Values represent the expression levels obtained after normalizing against control tissues. All samples were analyzed in triplicate, in two independent experiments. Names on the vertical axis indicate the tissues and the horizontal axis represents various genes. R, root; S, stem; L, leaf; S, salt; D. drought; H, heat; C, cold. Each color represents the relative expression levels of the transcripts. Sb, *Sorghum bicolor*; HAK, high affinity potassium; KEA, $K^+$ efflux antiporter; VDPC, voltage-dependent potassium channel; TPC, two-pore channels.

of sorghum and rice displayed the highest number of homologs with 9 and 10, respectively. Also, an equal number (3) of $K^+$ transport gene homologs was observed on chromosome 9 of sorghum and rice (**Figure 8**).

## Digital and qRT-PCR transcript patterns of sorghum $K^+$ transport genes responding to abiotic stresses

Digital expression of $K^+$ transport genes have been identified in different tissues like root, shoot, and leaf (**Figure 9A**) and in different developmental stages like milk stage, seedling stage, tillering stage, and flowering stage (**Figure 9B**). Expression of sorghum $K^+$ transport genes has reported under cold and drought stresses (**Figure 9C**). Sorghum transcript analysis revealed that $K^+$ transport genes are responsive to different abiotic stresses. qRT-PCR results indicated differential gene expression of sorghum $K^+$ transport gene homologs in the root, stem, and leaf tissue treated with salt, drought, heat, and cold stresses (**Figure 10**). Such a differential gene expression of $K^+$ transporters and channels in diverse tissues and under abiotic stresses have been reported in *Triticum aestivum* (Cheng et al., 2018), *Cicer arietinum* (Azeem et al., 2018), *Saccharum spontaneum* (Feng et al., 2020b), *Cajanus cajan* (Siddique et al., 2021), *Ipomoea batatas* (Jin et al., 2021), and *Gossypium raimondii* (Azeem et al., 2022). Reports exist that HAK/KUP/KT family members ameliorate the plants from salt stress. In cotton, GhPOT5, a homolog of *OsHAK1* exhibited significantly higher expression under salt stress in comparison with other genes (Yang X. et al., 2020). Salinity reduces the uptake of $K^+$ as evident in rice mutants *Oshak1*, when the levels were below 0.05 mM. Overexpression of *HAK1* resulted in salt stress tolerance in rice (Chen et al., 2015). Hamamoto et al. (2015) noticed that *AtHKT1* provides protection to the leaves under salt stress. In line with this, *SbHKT5* displayed higher activity under salt stress in the present study. Similarly, $K^+$ transporter genes were upregulated in the present study under water deficit conditions. Under drought conditions, root growth is restricted and diffusion of $K^+$ toward the roots (Wang et al., 2013). Also, long-term exposure to water deficit conditions led to leaf damage due to ROS formation (Wang et al., 2013). In support of this, optimization of $K^+$ supply mitigates the damage caused due to the oxidative stress in barley exposed to drought stress (Tavakol et al., 2021). Silencing *HvAKT2* and *HvHAK1* in barley enhanced the ROS ($H_2O_2$) production in PEG-treated leaves (Feng et al., 2020a). In rice, overexpression of *OsHAK1* positively regulates drought stress, while the knockout lines accumulate less $K^+$ and more $H_2O_2$ with stunted growth of the plants and less tolerance to drought stress (Chen et al., 2017). These results point out that $K^+$ reduces the accumulation of $H_2O_2$ and thus helps the plants during

drought stress. Earlier studies also revealed that HAK/KUP/KT family genes improve drought stress tolerance in plants (Wang et al., 2013; Li W. et al., 2018). Further, under water deficit conditions, $K^+$ regulates opening of stomata and make the plants adaptive to drought (Tang et al., 2015). $K^+$ increases the antioxidant defense in plants under abiotic stress conditions (Wang et al., 2013; Amanullah et al., 2016). Under extreme temperatures, osmolytes accumulate and $K^+$ helps to maintain stomatal conductance and therefore avoids the damage (Azedo-Silva et al., 2004; Hasanuzzaman et al., 2018). These studies point out that $K^+$ transporter genes play pivotal roles during environmental adversities and impart tolerance to multiple abiotic stresses.

In conclusion, genome-wide analysis of sorghum has led to the identification of 47 $K^+$ transport gene homologs; 33 $K^+$ transporters (27 HAKs, 4 HKTs, and 2 KEAs) and 14 $K^+$ channels (9 AKTs, 2 KATs, 2 TPCs, and 1 VDPC). Gene characterization, conserved domains, motif identifications, localization, phylogenetic analysis revealed the close relation of *Sorghum bicolor* $K^+$ transport gene homologs with its relative *Oryza sativa*. Identification of *cis*-acting elements would be helpful to explore further and to manipulate $K^+$ porters as well as channels for designing better crops. Gene expression data indicate that such genes can be utilized effectively in breeding programs aimed at abiotic stress tolerance. The results bring forth precious information candidate gene identification for functional analyses and subsequent utilization in genetic engineering, and traditional breeding programs to improve sorghum for abiotic stress tolerance.

## Data availability statement

The datasets presented in this study can be found in online repositories. The names of the repository/repositories and accession number(s) can be found in the article/**Supplementary material**.

## Author contributions

SAK and PBK designed the experiments. PHK, MN, TDD, AM, and PSR carried out the bioinformatics analysis. SAK and MN performed the qRT-PCR experiments. SAK, PHK, MN, TDD, PSR, and PBK analyzed the data. SAK, RK, and PBK prepared the manuscript and refined it. All authors have read and approved the manuscript.

## Funding

RK and AM acknowledge the National Science Foundation REU (No. 15600349/2150087) grant.

## Acknowledgments

SAK acknowledge the SERB-NPDF fellowship (PDF/2015/000929) and PBK was thankful to VFSTR for the Emeritus fellowship.

## Conflict of interest

The authors declare that the research was conducted in the absence of any commercial or financial relationships that could be construed as a potential conflict of interest.

## Publisher's note

All claims expressed in this article are solely those of the authors and do not necessarily represent those of their affiliated organizations, or those of the publisher, the editors and the reviewers. Any product that may be evaluated in this article, or claim that may be made by its manufacturer, is not guaranteed or endorsed by the publisher.

## Supplementary material

The Supplementary Material for this article can be found online at: https://www.frontiersin.org/articles/10.3389/fpls.2022.965530/full#supplementary-material

**SUPPLEMENTARY FIGURE 1**
Ramachandran plot validation for 3D structures of $K^+$ transport proteins.

**SUPPLEMENTARY TABLE 1**
List of qRT-PCR primers used for transcript profiling of *Sb* $K^+$ transport genes.

**SUPPLEMENTARY TABLE 2**
Nucleotide and protein sequences of *Sb* $K^+$ transport homologs with ids.

**SUPPLEMENTARY TABLE 3**
The pI, MW, GRAVY, instability, and aliphatic indexes of *Sb* $K^+$ transport proteins.

**SUPPLEMENTARY TABLE 4**
Amino acid composition and net charge of the *Sb* $K^+$ transport genes.

**SUPPLEMENTARY TABLE 5**
Types of protein kinases in the phosphorylation of *Sb* $K^+$ transport genes.

**SUPPLEMENTARY TABLE 6**
Conserved *cis*-acting regulatory elements in *Sb* $K^+$ transport gene promoters.

**SUPPLEMENTARY TABLE 7**
Modeled *Sb* $K^+$ transport proteins using SWISS-MODEL server.

**SUPPLEMENTARY TABLE 8**
STRING ids of *Sb* $K^+$ transport proteins used for protein-protein interactions.

**SUPPLEMENTARY TABLE 9**
List of $K^+$ transport genes from *Sorghum bicolor, Oryza sativa*, and *Arabidopsis thaliana* used for construction of phylogenetic tree.

**SUPPLEMENTARY TABLE 10**
Relative expression analysis of $K^+$ transport gene homologs.

# References


Ahn, S. J., Shin, R., and Schachtman, D. P. (2004). Expression of KT/KUP genes in Arabidopsis and the role of root hairs in K+ uptake. *Plant Physiol.* 134, 1135–1145. doi: 10.1104/pp.103.034660

Aksu, G., and Altay, H. (2020). The effects of potassium applications on drought stress in sugar beet. *Sugar Tech* 22, 1092–1102. doi: 10.26900/jsp.4.013

Amanullah, Iqbal, A., and Hidayat, Z. (2016). Potassium management for improving growth and grain yield of maize (*Zea* mays L.) under moisture stress condition. *Sci. Rep.* 6, 1–12. doi: 10.1038/srep34627

Amrutha, R. N., Sekhar, P. N., Varshney, R. K., and Kavi Kishor, P. B. (2007). Genome-wide analysis and identification of genes related to potassium transporter families in rice (*Oryza sativa* L.). *Plant Sci.* 172, 708–721. doi: 10.1016/j.plantsci.2006.11.019

Ashley, M. K., Grant, M., and Grabov, A. (2006). Plant responses to potassium deficiencies: A role for potassium transport proteins. *J. Exp. Bot.* 57, 425–436. doi: 10.1093/jxb/erj034

Assaha, D. V., Ueda, A., Saneoka, H., Al-Yahyai, R., and Yaish, M. W. (2017). The role of Na+ and K+ transporters in salt stress adaptation in glycophytes. *Front. Physiol.* 8:509. doi: 10.3389/fphys.2017.00509

Azedo-Silva, J., Osório, J., Fonseca, F., and Correia, M. J. (2004). Effects of soil drying and subsequent re-watering on the activity of nitrate reductase in roots and leaves of *Helianthus annuus*. *Funct. Plant Biol.* 31, 611–621. doi: 10.1071/fp04018

Azeem, F., Ahmad, B., Atif, R. M., Ali, M. A., Nadeem, H., Hussain, S., et al. (2018). Genome-wide analysis of potassium transport-related genes in chickpea (*Cicer arietinum* L.) and their role in abiotic stress responses. *Plant Mol. Biol. Report.* 36, 451–468. doi: 10.1007/s11105-018-1090-2

Azeem, F., Zameer, R., Rashid, M. A. R., Rasul, I., Ul-Allah, S., Siddique, M. H., et al. (2022). Genome-wide analysis of potassium transport genes in *Gossypium raimondii* suggest a role of GrHAK/KUP/KT8, GrAKT2. 1 and GrAKT1. 1 in response to abiotic stress. *Plant Physiol. Biochem.* 170, 110–122. doi: 10.1016/j.plaphy.2021.11.038

Banuelos, M. A., Garciadeblasm, B., Cuberom, B., and Rodrıguez-Navarro, A. (2002). Inventory and functional characterization of the HAK potassium transporters of rice. *Plant Physiol.* 130, 784–795. doi: 10.1104/pp.007781

Biasini, M., Bienert, S., Waterhouse, A., Arnold, K., Studer, G., Schmidt, T., et al. (2014). SWISS-MODEL:modeling protein tertiary and quaternary structure using evolutionary information. *Nucl. Acids Res.* 42, W252–W258. doi: 10.1093/nar/gku340

Bowers, J. E., Chapman, B. A., Rong, J., and Paterson, A. H. (2003). Unravelling angiosperm genome evolution by phylogenetic analysis of chromosomal duplication events. *Nature* 422, 433–438. doi: 10.1038/nature01521

Cai, K., Zeng, F., Wang, J., and Zhang, G. (2021). Identification and characterization of HAK/KUP/KT potassium transporter gene family in barley and their expression under abiotic stress. *BMC Genom.* 22:317. doi: 10.1186/s12864-021-07633-y

Chen, C., Chen, H., Zhang, Y., Thomas, H. R., Frank, M. H., He, Y., et al. (2020). TBtools: An integrative toolkit developed for interactive analyses of big biological data. *Mol. Plant* 13, 1194–1202. doi: 10.1016/j.molp.2020.06.009

Chen, G., Hu, Q., Luo, L. E., Yang, T., Zhang, S., Hu, Y., et al. (2015). Rice potassium transporter OsHAK1 is essential for maintaining potassium-mediated growth and functions in salt tolerance over low and high potassium concentration ranges. *Plant Cell Environ.* 38, 2747–2765. doi: 10.1111/pce.12585

Chen, G., Liu, C., Gao, Z., Zhang, Y., Jiang, H., Zhu, L., et al. (2017). OsHAK1, a high-affinity potassium transporter, positively regulates responses to drought stress in rice. *Front. Plant Sci.* 8:1885. doi: 10.3389/fpls.2017.01885

Cheng, X., Liu, X., Mao, W., Zhang, X., Chen, S., Zhan, K., et al. (2018). Genome-wide identification and analysis of HAK/KUP/KT potassium transporters gene family in wheat (*Triticum aestivum* L.). *Int. J. Mol. Sci.* 19:3969. doi: 10.3390/ijms19123969

Feng, H., Tang, Q., Cai, J., Xu, B., Xu, G., and Yu, L. (2019). Rice OsHAK16 functions in potassium uptake and translocation in shoot, maintaining potassium homeostasis and salt tolerance. *Planta* 250, 549–561. doi: 10.1007/s00425-019-03194-3193

Feng, X., Wang, Y., Zhang, N., Wu, Z., Zeng, Q., Wu, J., et al. (2020b). Genome-wide systematic characterization of the HAK/KUP/KT gene family and its expression profile during plant growth and in response to low-K+ stress in *Saccharum*. *BMC Plant Biol.* 20:20. doi: 10.1186/s12870-019-2227-7

Feng, X., Liu, W., Qiu, C. W., Zeng, F., Wang, Y., Zhang, G., et al. (2020a). HvAKT2 and HvHAK1 confer drought tolerance in barley through enhanced leaf mesophyll H+ homoeostasis. *Plant Biotechnol. J.* 18, 1683–1696. doi: 10.1111/pbi.13332

Gierth, M., Maäser, P., and Schroeder, J. I. (2005). The potassium transporter AtHAK5 functions in K+ deprivation-induced high-affinity K+ uptake and AKT1 K+ channel contribution to K+ uptake kinetics in *Arabidopsis* roots. *Plant Physiol.* 137, 1105–1114. doi: 10.1104/pp.104.057216

Hamamoto, S., Horie, T., Hauser, F., Deinlein, U., Schroeder, J. I., and Uozumi, N. (2015). HKT transporters mediate salt stress resistance in plants: From structure and function to the field. *Curr. Opin. Biotechnol.* 32, 113–120. doi: 10.1016/j.copbio.2014.11.025

Hamamoto, S., Marui, J., Matsuoka, K., Higashi, K., Igarashi, K., Nakagawa, T., et al. (2008). Characterization of a tobacco TPK-type K+ channel as a novel tonoplast K+ channel using yeast tonoplasts. *J. Biol. Chem.* 283, 1911–1920. doi: 10.1074/jbc.m708213200

Hasanuzzaman, M., Bhuyan, M. H. M., Nahar, K., Hossain, M. D., Mahmud, J. A., Hossen, M., et al. (2018). Potassium: A vital regulator of plant responses and tolerance to abiotic stresses. *Agronomy* 8:31. doi: 10.3390/agronomy8030031

He, C., Cui, K., Duan, A., Zeng, Y., and Zhang, J. (2012). Genome-wide and molecular evolution analysis of the poplar KT/HAK/KUP potassium transporter gene family. *Ecol. Evol.* 2, 1996–2004. doi: 10.1002/ece3.299

Hedrich, R. (2012). Ion channels in plants. *Physiol. Rev.* 92, 1777–1811. doi: 10.1152/physrev.00038.2011

Hu, W., Lu, Z., Meng, F., Li, X., Cong, R., Ren, T., et al. (2021). Potassium fertilization reduces silique canopy temperature variation in *Brassica napus* to enhance seed yield. *Ind. Crops Prod.* 168:113604. doi: 10.1016/j.indcrop.2021.113604

Hussain, S., Hussain, S., Ali, B., Ren, X., Chen, X., Li, Q., et al. (2021). Recent progress in understanding salinity tolerance in plants: Story of Na+/K+ balance and beyond. *Plant Physiol. Biochem.* 160, 239–256. doi: 10.1016/j.plaphy.2021.01.029

Hyun, T. K., Rim, Y., Kim, E., and Kim, J. S. (2014). Genome-wide and molecular evolution analyses of the KT/HAK/KUP family in tomato (*Solanum lycopersicum* L.). *Genes Genom.* 36, 365–374. doi: 10.1007/s13258-014-0174-0

Jiang, M., Chen, H., Liu, J., Du, Q., Lu, S., and Liu, C. (2021). Genome-wide identification and functional characterization of natural antisense transcripts in *Salvia miltiorrhiza*. *Sci. Rep.* 11, 1–14. doi: 10.1038/s41598-021-83520-6

Jin, R., Jiang, W., Yan, M., Zhang, A., Liu, M., Zhao, P., et al. (2021). Genome-wide characterization and expression analysis of HAK K+ transport family in Ipomoea. *3 Biotech* 11, 1–18. doi: 10.1007/s13205-020-02552-3

Kuang, Q., Purhonen, P., and Hebert, H. (2015). Structure of potassium channels. *Cell. Mol. Life Sci.* 72, 3677–3693. doi: 10.1007/s00018-015-1948-5

Kumar, S., Stecher, G., Li, M., Knyaz, C., and Tamura, K. (2018). MEGA X: Molecular evolutionary genetics analysis across computing platforms. *Mol. Biol. Evol.* 35:1547. doi: 10.1093/molbev/msy096

Kyriakidou, M., Tai, H. H., Anglin, N. L., Ellis, D., and Strömvik, M. V. (2018). Current strategies of polyploid plant genome sequence assembly. *Front. Plant Sci.* 9:1660. doi: 10.3389/fpls.2018.01660

Li, Y., Peng, L., Xie, C., Shi, X., Dong, C., Shen, Q., et al. (2018). Genome-wide identification, characterization, and expression analyses of the HAK/KUP/KT potassium transporter gene family reveals their involvement in K+ deficient and abiotic stress responses in pear rootstock seedlings. *Plant Growth Regul.* 85, 187–198.

Li, W., Xu, G., Alli, A., and Yu, L. (2018). Plant HAK/KUP/KT K+ transporters: Function and regulation. *Semin. Cell Dev. Biol.* 74, 133–141. doi: 10.1016/j.semcdb.2017.07.009

Liang, M., Gao, Y., Mao, T., Zhang, X., Zhang, S., Zhang, H., et al. (2020). Characterization and expression of KT/HAK/KUP transporter family genes in willow under potassium deficiency, drought, and salt stresses. *BioMed Res. Int.* 2020:2690760. doi: 10.1155/2020/2690760

Moller, S., Croning, M. D., and Apweiler, R. (2001). Evaluation of methods for the prediction of membrane spanning regions. *Bioinformatics* 17, 646–653. doi: 10.1093/bioinformatics/17.7.646

Nieves-Cordones, M., Ródenas, R., Chavanieu, A., Rivero, R. M., Martinez, V., Gaillard, I., et al. (2016). Uneven HAK/KUP/KT protein diversity among angiosperms: Species distribution and perspectives. *Front. Plant Sci.* 7:127. doi: 10.3389/fpls.2016.00127

Ou, W., Mao, X., Huang, C., Tie, W., Yan, Y., Ding, Z., et al. (2018). Genome-wide identification and expression analysis of the KUP family under abiotic stress

in cassava (*Manihot esculenta Crantz*). *Front. Physiol.* 9:17. doi: 10.3389/fphys.2018.00017

Paterson, A. H., Bowers, J. E., Bruggmann, R., Dubchak, I., Grimwood, J., Gundlach, H., et al. (2009). The *Sorghum* bicolor genome and the diversification of grasses. *Nature* 457, 551–556. doi: 10.1038/nature07723

Rasheed, F., Markgren, J., Hedenqvist, M., and Johansson, E. (2020). Modeling to understand plant protein structure-function relationships-implications for seed storage proteins. *Molecules* 25:873. doi: 10.3390/molecules25040873

Rehman, H. M., Nawaz, M. A., Shah, Z. H., Daur, I., Khatoon, S., Yang, S. H., et al. (2017). In-depth genomic and transcriptomic analysis of five K+ transporter gene families in soybean confirm their differential expression for nodulation. *Front. Plant Sci.* 8:804. doi: 10.3389/fpls.2017.00804

Riedelsberger, J., Miller, J. K., Valdebenito-Maturana, B., Piñeros, M. A., González, W., and Dreyer, I. (2021). Plant HKT channels: An updated view on structure, function and gene regulation. *Int. J. Mol. Sci.* 22:1892. doi: 10.3390/ijms22041892

Rodríguez-Navarro, A. (2000). Potassium transport in fungi and plants. *Biochim. Biophys. Acta Rev. Biomembr.* 1469, 1–30. doi: 10.1016/s0304-4157(99)00013-1

Saadati, S., Baninasab, B., Mobli, M., and Gholami, M. (2021). Foliar application of potassium to improve the freezing tolerance of olive leaves by increasing some osmolyte compounds and antioxidant activity. *Sci. Hortic.* 276:109765. doi: 10.1016/j.scienta.2020.109765

Sánchez-McSweeney, A., González-Gordo, S., Aranda-Sicilia, M. N., Rodríguez-Rosales, M. P., Venema, K., Palma, J. M., et al. (2021). Loss of function of the chloroplast membrane K+/H+ antiporters AtKEA1 and AtKEA2 alters the ROS and NO metabolism but promotes drought stress resilience. *Plant Physiol. Biochem.* 160, 106–119. doi: 10.1016/J.PLAPHY.2021.01.010

Sardans, J., and Peñuelas, J. (2021). Potassium control of plant functions: Ecological and agricultural implications. *Plants* 10:419.

Schmittgen, T. D., and Livak, K. J. (2008). Analyzing real-time PCR data by the comparative CT method. *Nat. Protoc.* 3, 1101–1108. doi: 10.1038/nprot.2008.73

Siddique, M. H., Babar, N. I., Zameer, R., Muzammil, S., Nahid, N., Ijaz, U., et al. (2021). Genome-wide identification, genomic organization, and characterization of potassium transport-related genes in *Cajanus cajan* and their role in abiotic stress. *Plants* 10:2238. doi: 10.3390/plants10112238

Song, Z. Z., Ma, R. J., and Yu, M. L. (2015). Genome-wide analysis and identification of KT/HAK/KUP potassium transporter gene family in peach (*Prunus persica*). *Genet. Mol. Res.* 14, 774–787. doi: 10.4238/2015.january.30.21

Song, Z., Wu, X., Gao, Y., Cui, X., Jiao, F., Chen, X., et al. (2019). Genome-wide analysis of the HAK potassium transporter gene family reveals asymmetrical evolution in tobacco (*Nicotiana tabacum*). *Genome* 62, 267–278. doi: 10.1139/gen-2018-0187

Tang, Z. H., Zhang, A. J., Wei, M., Chen, X. G., Liu, Z. H., Li, H. M., et al. (2015). Physiological response to potassium deficiency in three sweet potato (*Ipomoea batatas* [L.] Lam.) genotypes differing in potassium utilization efficiency. *Acta Physiol. Plant.* 37, 1–10. doi: 10.1007/s11738-015-1901-0

Tavakol, E., Jákli, B., Cakmak, I., Dittert, K., and Senbayram, M. (2021). Optimization of potassium supply under osmotic stress mitigates oxidative damage in barley. *Plants* 11:55. doi: 10.3390/plants11010055

Teklić, T., Parađiković, N., Špoljarević, M., Zeljkovič, S., Lončarić, Z., and Lisjak, M. (2021). Linking abiotic stress, plant metabolites, biostimulants and functional food. *Ann. Appl. Biol.* 178, 169–191. doi: 10.1111/aab.12651

Wang, M., Zheng, Q., Shen, Q., and Guo, S. (2013). The critical role of potassium in plant stress response. *Int. J. Mol. Sci.* 14, 7370–7390. doi: 10.3390/ijms14047370

Wang, Q., Guan, C., Wang, P., Lv, M. L., Ma, Q., Wu, G. Q., et al. (2015). AtHKT1; 1 and AtHAK5 mediate low-affinity Na+ uptake in *Arabidopsis thaliana* under mild salt stress. *Plant Growth Regul.* 75, 615–623. doi: 10.1007/s10725-014-9964-2

Wang, X., Wang, J., Jin, D., Guo, H., Lee, T. H., Liu, T., et al. (2015). Genome alignment spanning major poaceae lineages reveals heterogeneous evolutionary rates and alters inferred dates for key evolutionary events. *Mol. Plant* 8, 885–898. doi: 10.1016/j.molp.2015.04.004

Yang, X., Zhang, J., Wu, A., Wei, H., Fu, X., Tian, M., et al. (2020). Genome-wide identification and expression pattern analysis of the HAK/KUP/KT gene family of cotton in fiber development and under stresses. *Front. Genet.* 11:566469. doi: 10.3389/fgene.2020.566469

Yang, T., Lu, X., Wang, Y., Xie, Y., Ma, J., Cheng, X., et al. (2020). HAK/KUP/KT family potassium transporter genes are involved in potassium deficiency and stress responses in tea plants (*Camellia sinensis* L.): Expression and functional analysis. *BMC Genom.* 21:556. doi: 10.1186/s12864-020-06948-6

Zhang, Z., Zhang, J., Chen, Y., Li, R., Wang, H., and Wei, J. (2012). Genome-wide analysis and identification of HAK potassium transporter gene family in maize (*Zea* mays L.). *Mol. Biol. Rep.* 39, 8465–8473.

Zhu, M., Shabala, L., Cuin, T. A., Huang, X., Zhou, M., Munns, R., et al. (2016). Nax loci affect SOS1-like Na+/H+ exchanger expression and activity in wheat. *J. Exp. Bot.* 67, 835–844. doi: 10.1093/jxb/erv493

frontiers | Frontiers in Plant Science

TYPE Original Research
PUBLISHED 14 October 2022
DOI 10.3389/fpls.2022.996538



OPEN ACCESS

EDITED BY
Sindhu Sareen,
Indian Institute of Wheat and Barley Research (ICAR), India

REVIEWED BY
Hossein Sadeghi,
Shiraz University, Iran
Veenu Kaul,
University of Jammu, India

*CORRESPONDENCE
Ahmed Sallam
sallam@ipk-gatersleben.de;
amsallam@aun.edu.eg

SPECIALTY SECTION
This article was submitted to Plant Abiotic Stress, a section of the journal Frontiers in Plant Science

RECEIVED 17 July 2022
ACCEPTED 22 August 2022
PUBLISHED 14 October 2022

CITATION
Amro A, Harb S, Farghaly KA, Ali MMF, Mohammed AG, Mourad AMI, Afifi M, Börner A and Sallam A (2022) Growth responses and genetic variation among highly ecologically diverse spring wheat genotypes grown under seawater stress.
*Front. Plant Sci.* 13:996538.
doi: 10.3389/fpls.2022.996538



# Growth responses and genetic variation among highly ecologically diverse spring wheat genotypes grown under seawater stress

Ahmed Amro[1], Shrouk Harb[2], Khaled A. Farghaly[3], Mahmoud M. F. Ali[2], Aml G. Mohammed[2], Amira M. I. Mourad[4,5], Mohamed Afifi[6], Andreas Börner[4] and Ahmed Sallam[2,4]*

[1]Department of Botany and Microbiology, Faculty of Science, Assiut University, Assiut, Egypt, [2]Department of Genetics, Faculty of Agriculture, Assiut University, Assiut, Egypt, [3]Department of Soil and Water Resources, Faculty of Agriculture, Assiut University, Assiut, Egypt, [4]Resources Genetics and Reproduction, Department Genebank, Leibniz Institute of Plant Genetics and Crop Plant Research (IPK), Gatersleben, Germany, [5]Department of Agronomy, Faculty of Agriculture, Assiut University, Assiut, Egypt, [6]Ultrasonic Laboratory, National Institute of Standards, Giza, Egypt

Most of the freshwaters worldwide are used for agriculture. Freshwater sources are expected to decline and will not suffice to support the food production needed for the growing population. Therefore, growing crops with seawater might constitute a solution. However, very little work has been done on the effect of seawater stress on wheat, an important cereal crop. The present study aimed to determine whether particular wheat genotypes provided better resistance to seawater stress. A set of 80 highly diverse spring wheat genotypes collected from different countries in Europe, Asia, Africa, North and South America was exposed to 50% seawater stress at the early growth stage. Four seeding shoot and root traits were scored for all genotypes. High genetic variations were found among all genotypes for the epicotyl length (EL), hypocotyl length (HL), number of radicles (NOR), and fresh weight (FW). Eight genotypes with high-performance scores of seedling traits were selected. The correlation analyses revealed highly significant correlations among all traits scored in this study. The strongest correlation was found between the NOR and the other seeding traits. Thus, the NOR might be an important adaptive trait for seawater tolerance. The genetic diversity among all genotypes was investigated based on genetic distance. A wide range of genetic distances among all genotypes was found. There was also a great genetic distance among the eight selected genotypes. In particular, the genetic distance between ATRI 5310 (France) and the other seven genotypes was the greatest. Such high genetic diversity might be utilized to select highly divergent genotypes for crossing in a future breeding program. The present study provides very useful information on the presence of different genetic resources in wheat for seawater tolerance.

KEYWORDS

***Triticum aestivum L.*, germination traits, salinity stress, breeding, genetic diversity**

# Introduction

Soil salinization is a global and dynamic problem that may increase in the future because of climate change scenarios, e.g., rise in temperature, rise in sea level and impact on coastal areas, and increase in evaporation (Kumar and Sharma, 2020). The predicted increase of the sea level due to the thermal expansion of seawater ranges from 31 to more than 100 cm by the year 2100 (Mimura, 2013). This will reduce the land areas and consequently increase the potential yield losses resulting from the soil salinity. Salinity condition in arid and semi-arid regions occurs due to scanty precipitation and high evaporation (Dehnavi et al., 2020). The deficit in the freshwater supply is compensated by pumping excess ground water, especially in coastal areas (Halder et al., 2022). This situation results in high soluble salt contents (saline soils) and/or high sodium ion ($Na^+$) levels (sodic or saline-sodic soils) beneath the crop rooting zone (soil horizon; Sadeghi and Rostami, 2017). This leads to stress that reduces the ability of plants (except halophytes and salt-tolerant crops) to take up water from the soil and causes soil degradation. Ultimately, a significant reduction in crop growth and productivity occurs (Food Agriculture Organization of the United Nations, 2022).

Several salinity management techniques have been deployed to improve the growth efficiency of economic crops under salt stress. Urgent solutions allowing the sustainable use of vital crop vegetation despite the harsh environmental situation are needed. The development of salinity-adapting crops is a realistic solution. Conducting research to find alternative ways to solve salinity problems is essential to meet current and future food demands. Suitable management practices to control salinity problems must be implemented in irrigated fields, irrigation projects, and geohydrologic systems (Tomaz et al., 2021). Among these practices, soil erosion control measures, rainwater harvesting, integrating appropriate plant species, and efficient irrigation methods are routine practices for obtaining suitable and sustainable results (Singh et al., 2018).

Egypt is a unique part of the Middle East located in an arid zone with large flat planes, salt-affected shores, and salt marshes facing the Red Sea and the Mediterranean coasts. These areas are integral components of the Egyptian coastal and inland ecosystems and can serve as important areas for food production. The main salt marshes in Egypt are located in the Red Sea coastal belt in South Sinai and east of the Eastern Desert (Amro et al., 2021). Consequently, the utilization of seawater in Egypt has been the latest endeavor to obtain satisfying agricultural yields and horticultural crops (Rady et al., 2016).

Crop species of Gramineae (including wheat and their cultivars) often differ in their tolerance to salinity. These differences can be assessed through germination percentage and seedling growth in saline conditions. This information is crucial for identifying a suitable salt-tolerant wheat cultivar for cultivation under salt stress conditions (Thabet et al., 2021b). Many studies investigated the response of wheat (*Triticum aestivum* L.) cultivars to salt stress at germination and early seedling-growth stages (Mujeeb-ur-Rahman et al., 2008). Wheat receives a lot of attention because it constitutes an important staple food for at least 36% of the world's population. Indeed, it provides 55% of the carbohydrates, 20% of the calories (Nahar et al., 2017; Seleiman et al., 2021), and essential micro- and macro-nutrients of the human diet. Considering that the international population is predicted to increase by 25% (to reach 10 billion) by 2050 (Halder et al., 2022), the current world production of wheat should be doubled (Food Agriculture Organization of the United Nations, 2022). Achieving this goal is particularly challenged by the greater frequency and number of climate change stressors including salinity.

The germination responses and emerging ability of seeds in a saline environment depend not only on the salt concentration but also on other various biological and genetic factors. Özyazici and Açikbaş (2021) stated that some plants are sensitive to salinity at the early seedling-growth stage because the mechanism of salinity tolerance is not fully developed yet. Salt stress also affects many biochemical characteristics such as antioxidant enzyme activity, proline, protein, and both K+ and Na+ contents in leaves (Ghanaatiyan and Sadeghi, 2015; Sadeghi and Rostami, 2017). The differential suppression of wheat genotypes in salinity conditions might originate from differences in metabolic efficiencies against stress-induced carbon deficit and activities of anti-oxidative enzymes as these have been positively correlated with stress tolerance (Srivastava et al., 2010). Differences in cell membrane stability and macromolecule stability induced by salinity might also be a cause for the different responses (Sadeghi and Robati, 2015).

Screening large germplasms of genotypes from different countries is very useful to identify the ones allowing salt tolerance. Once identified, these genotypes might be used as candidate parents in future breeding programs to produce high-yielding wheat cultivars with high tolerance to abiotic stress. Moreover, the analysis of genetic diversity based on DNA molecular markers might allow a precise selection of truly promising tolerant genotypes to accelerate the breeding programs.

The present study aimed to investigate the impact of genetic variations in highly diverse wheat genotypes collected from different countries on seawater tolerance and to select the one(s) performing the best under seawater stress for phenotypic selection and genetic diversity analysis.

# Materials and methods

## Seawater properties

The pH was measured in a 50% seawater sample using an electric pH meter (Hanna pH 211), and water electric conductivity (EC in $dS.m^{-1}$) was determined using a

conductivity meter (4310 JEN WAY). $Na^{+}$ and potassium ions ($K^{+}$) contents were determined with a flame-photometer (Carl-Zeiss DR-LANGE M7D). Methods described by Jackson (1973) were used to determine the concentration of calcium ($Ca^{+2}$), magnesium ($Mg^{2+}$), chloride ($Cl^{-}$), and soluble sulfates ($SO_4^{2-}$) ions. $Ca^{+2}$ and $Mg^{2+}$ contents were volumetrically determined by the titration method against 0.01 N EDTA, and $Cl^{-}$ contents were volumetrically determined against $AgNO_3$. The soluble $SO_4^{2-}$ content was estimated by the turbidity method against $BaCl_3$ according to the method published by Tabatabai and Bremner (1970).

## Plant material

A set of 48 highly diverse spring wheat genotypes were randomly selected from the population and tested in 10, 40, or 50% seawater stress conditions. This preliminary experiment showed high genetic variation in hypocotyl and epicotyl traits in 50% of seawater. Therefore, the whole population (80 genotypes) was tested in 50% seawater. The genotypes used in this study were highly diverse wheat genotypes collected from different parts of Europe (Supplementary Table 1).

## Experimental layout and trait scoring

In all experiments, 20 seeds/genotype were sown in Petri dishes in three replicates using a randomized complete block design. All experiments were conducted under controlled conditions. The seeds were sterilized using 0.5% Na-hypochlorite (for 2 min) and washed in sterilized water. Then, all genotypes were sown in different seawater concentrations. Finally, all Petri dishes were incubated in dark under normal laboratory conditions (21–23°C and 65–70% humidity) in a Heraeus incubator (Germany) for 10 days. On the 10th day, the epicotyl length (EL, cm), hypocotyl length (HL, cm), and number of radicles (NOR) were measured in at least 10 seeds/genotype. The epicotyl/hypocotyl ratio (EHR) was calculated as the ratio of EL to HL. The seedling's fresh weight (FW, mg) was determined by weighing the shoots of the germinated seeds.

## Statistical analysis

Data were analyzed using the SPSS package (v. 25). The differences in the genotype responses according to their spatial affinities (geographical distribution) and behavior (performance against salinity) were determined. The Shapiro–Wilk test of normality was employed to choose the proper comparison test, and the differences between means were considered significant at $p < 0.05$. Non-parametric tests, i.e., Mann–Whitney *U*-test for comparing two groups and Kruskal–Wallis *H*-test for comparing more than two groups, were used. Correlation analyses of grain germination parameters were carried out. Factorial ANOVA was performed to assess the effect of replication, genotypes, and seawater concentrations on seedling attributes and the effect of their interaction.

ANOVA of all phenotypic data and correlation analyses were carried out to estimate the variance and covariance using PLABSTAT software (Utz, 2011). All graphical presentations of the phenotypic data were performed using R software (R Core Team, 2014).

## Analysis of the genetic diversity

The DNA of the 80 genotypes was sent to Trait Genetics (Gatersleben, Germany) for genotyping-by-sequencing using a 25K Infinium iSelect array. Extensive details on the development of the 25K wheat Infinium array were reported by Aleksandrov et al. (2021). The array genotyping revealed 21,450 single-nucleotide polymorphisms (SNP) markers that were used to calculate the genetic distance among the selected genotypes using the R-package "ade4" as described by Dray and Dufour (2007). The genetic distance was calculated using a simple matching coefficient.

# Results

## Chemical properties of seawater

The analysis of the chemical composition of the 50% seawater sample revealed a high EC value (26.33 $dS.m^{-1}$) and high contents in $Na^{+}$ (6.8 $g.L^{-1}$) and $Cl^{-}$ (10.73 $g.L^{-1}$). According to FAO classification of irrigation water, these values corresponded to high-salinity seawater (Rhoades et al., 1992). Additionally, adequate content in essential nutrients (e.g., $Ca^{2+}$, $K^{+}$, and $SO_4^{2-}$) were measured.

## Variation in growth monitors

The analysis of variation in the selected traits (EL, HL, NOR EHR, and FW) for the 48 genotypes is presented in Table 1. Highly significant differences in all traits were found among the three seawater conditions (10, 40, and 50%). Moreover, the ANOVA revealed significant genetic differences among genotypes for all traits. Highly significant differences in all traits were found among the three seawater conditions (10, 40, and 50%; Figure 1 and Supplementary Table 2). All seedling traits decreased proportionally to the increase in seawater concentration. ELs decreased from 12.25 ± 1.63 cm in 10%

seawater to 4.04 ± 1.26 cm and 1.11 ± 0.55 cm when exposed to 40 and 50% seawater, respectively. The same trend was observed for the HL as the mean decreased from 16.63 ± 2.16 cm in 10% seawater to 4.66 ± 0.93 cm and 3.16 ± 0.42 cm in 40 and 50% seawater, respectively. The mean seedling FWs similarly decreased from 3.73 ± 0.23 g in 10% seawater to 0.37 ± 0.13 g in 40% seawater and 0.11 ± 0.05 g in 50% seawater. Interestingly, the NOR was not as much reduced by the different seawater treatments as the other traits were. Indeed, the average NOR was 4.61 in 10% seawater, whereas it was 4.51 and 3.70 in 40 and 50% seawater, respectively.

TABLE 1 The average value of the concentration of major ions contents, EC, and pH in dilute in 50% seawater.

| Property | Average |
|---|---|
| **pH** | 7.12 |
| **EC ($dS.m^{-1}$)** | 30.5 |
| **Cation ($g.L^{-1}$)** | |
| $Na^{+}$ | 6.80 |
| $K^{+}$ | 0.26 |
| $Ca^{+2}$ | 1.38 |
| $Mg^{+2}$ | 0.57 |
| **Anion ($g.L^{-1}$)** | |
| $Cl^{-}$ | 10.73 |
| $SO_4^{-2}$ | 1.07 |

The variations among the 80 genotypes were thoroughly investigated for 50% seawater. The results of the ANOVA of all previously mentioned traits for 80 genotypes exposed to 50% seawater are presented in Table 2 and supplementary Table 3. Highly significant differences were observed according to replication (R), except for FW. Additionally, highly significant differences were observed among genotypes (G) for all assessed traits. The broad-sense heritability ranged from 0.40 (FW) to 0.84 (HL). The difference in each trait after treatment with 50% seawater due to the genotypic variation is presented in Figure 2. The genotypes performing the best differed according to the trait. For example, ATRI 5692 (Iran) had the greatest EL (1.88 cm). The greatest HL was obtained for ATRI 4563 (Italy). ATRI 10340 (China) had the greatest NOR (4.66) and ATRI 4940 (USA) the greatest FW with 0.24 g.

To determine the best performing genotypes, the 20 genotypes bearing traits with higher values were chosen. Then, the genotypes figuring among these 20 for at least three traits were selected (Figure 3 and Table 3). These criteria were fulfilled by eight genotypes from seven countries: Nepal (2), India (1), Iran (1), France (1), Sweden (1), the USA (1), and Argentina (1). A set of three-common genotypes ATRI 5310 (France), ATRI

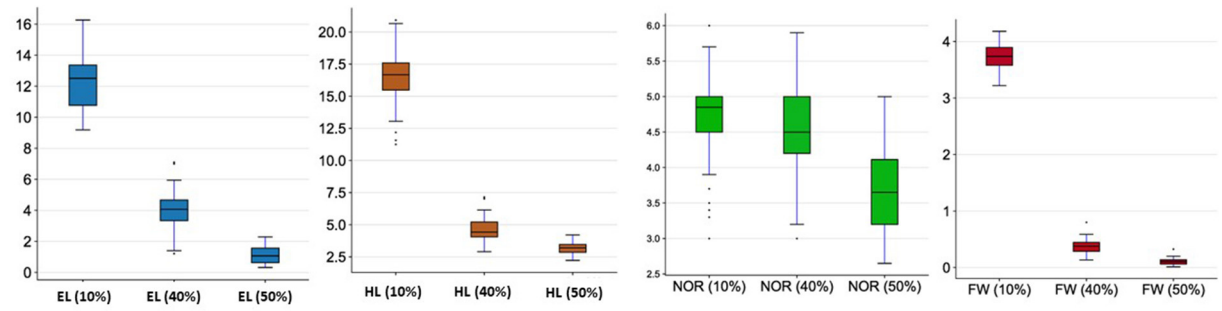


FIGURE 1
Seedling development under different seawater concentrations (10, 40, and 50%). For abbreviations see Table 1.

TABLE 2 Mean square (M.S.) of Epicotyl length (EL), Hypocotyl length (HL), number of roots (NOR), fresh weight (FW), and shoot length/root length ratio under three salt treatments with different concentrations (10, 40, and 50%) in a set of 48 wheat genotypes.

| Source of variance | EL | | HL | | NOR | | FW | | EL/HL | |
|---|---|---|---|---|---|---|---|---|---|---|
| | d.f. | M.S. | d.f. | M.S. | d.f. | M.S. | d.f. | M.S. | d.f. | M.S. |
| Treatments (T) | 2 | 1,598.40** | 2 | 2,618.26** | 2 | 12.93** | 2 | 196.20** | 2 | 3.53** |
| Genotypes (G) | 47 | 2.26** | 47 | 2.96** | 47 | 0.69** | 47 | 0.03** | 47 | 0.07** |
| TxG | 92 | 1.14 | 92 | 1.34 | 92 | 0.27 | 92 | 0.023 | 92 | 0.02 |
| Total | 141 | – | 141 | – | 141 | – | 141 | – | 141 | – |

*P < 0.05.
**P < 0.01.

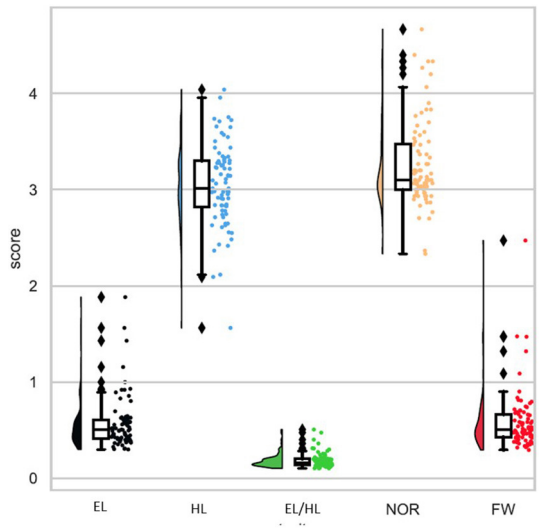


FIGURE 2
Distribution and variation among all genotypes under 50% seawater. For abbreviations see Table 1.

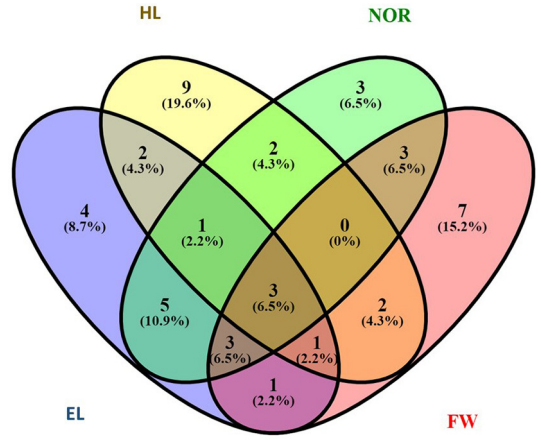


FIGURE 3
Number of genotypes with high performance.

5325 (Argentina), and ATRI 2679 (India) were identified as the best performing genotypes for all assessed traits when exposed to 50% seawater.

## Variation in seawater tolerance among continents

The comparison of seedling-growth attributes in response to 50% seawater according to their origin is represented in Figures 4A,B. Kruskal–Wallis *H*-test of non-parametric data (normal distribution not assumed) showed no significant differences among continents. The greatest mean HL (3.15 ± 0.12 cm) was measured in South American genotypes. The seedling FW increased in North American genotypes (73.50 ± 22.28 mg). The greatest mean EL and NOR (0.70 ± 0.09 cm and 3.40 ± 0.14, respectively) were recorded in seedlings with Asian genotypes. In contrast, a decrease in the seedling FW and NOR was found in European genotypes exposed to 50% seawater.

## Phenotypic correlation

The correlation analysis of traits after exposure to 50% seawater is presented in Figure 5. Significant positive correlations were found between EL and EHR ($r = 0.94^{**}$), EL and NOR ($r = 0.63^{**}$), and EL and FW ($r = 0.28^{*}$). There also was a significant positive correlation between HL and NOR ($r = 0.62^{**}$) and HL and FW ($r = 0.17^{*}$). Additionally, EHR was positively and significantly associated with NOR ($r = 0.63^{**}$) and FW ($r = 0.17^{*}$). NOR and FW were positively correlated ($r = 0.21^{*}$). The strongest positive correlations were found between EL and EHR, EL and NOR, and EHR and NOR.

## Genetic distances among genotypes

The genetic distance among the 80 genotypes was calculated to assess the level of genetic diversity in the population (Figure 6 and Supplementary Table 4). The dendrogram analysis revealed two main groups and one genotype, TRI10296 (Mexico). The genetic distance ranged from 0.0988 between TRI10654 and TRI10593 from Cyprus to 0.6696 between TRI3831 (Portugal) and TRI3631 (Canada).

When analyzing the best performing genotypes in a 50% seawater condition, eight genotypes (Table 3) were found in group II (G II.). Notably, TRI5310 (France) was highly distanced from the other selected genotypes. Generally, a high genetic distance was found among the eight selected genotypes and ranged from 0.354 between TRI5332 (USA) and TRI5325 (Argentina) to 00.62998 between TRI5310 (France) to TRI2679 (India).

# Discussion

## Genetic variation and seawater tolerance

Salt-affected soils are found in Australia, China, the former USSR, India, Iran, Bangladesh, Pakistan, Egypt, Iraq, Syria, Turkey Mexico, and the USA (Sanower Hossain and Sultan Ahmad Shah, 2019). More than 833 million hectares of subsoil (30–100 cm) are affected by salinity (Food Agriculture Organization of the United Nations, 2022).

Salinity stress induces a great extent of variations with respect to seed germination and physiological, anatomical,

TABLE 3 Mean square (M.S.) of epicotyl length (EL), hypocotyl length (HL), number of radicles (NOR), and fresh weight (FW) under 50% salt treatment in a set of 80 wheat genotypes.

| Source of variance | EL | | HL | | NOR | | FW | | EL/HL | |
|---|---|---|---|---|---|---|---|---|---|---|
| | d.f. | M.S. | d.f. | M.S. | d.f. | M.S. | d.f. | M.S. | d.f. | M.S. |
| Replication (R) | 2 | 0.26** | 2 | 5.13** | 2 | 1.45** | 2 | 8.34 | 2 | 0.04** |
| Genotypes (G) | 79 | 0.11** | 79 | 0.54** | 79 | 0.60** | 79 | 2.03** | 79 | 1.37** |
| RxG | 156 | 0.02 | 158 | 0.09 | 158 | 0.09 | 157 | 3.84 | 158 | 0.92 |
| Total | 237 | – | 239 | – | 239 | – | 238 | – | 239 | – |
| Heritability | 0.82 | | 0.84 | | 0.85 | | 0.52 | | 0.66 | |

*P < 0.05.
**P < 0.01.

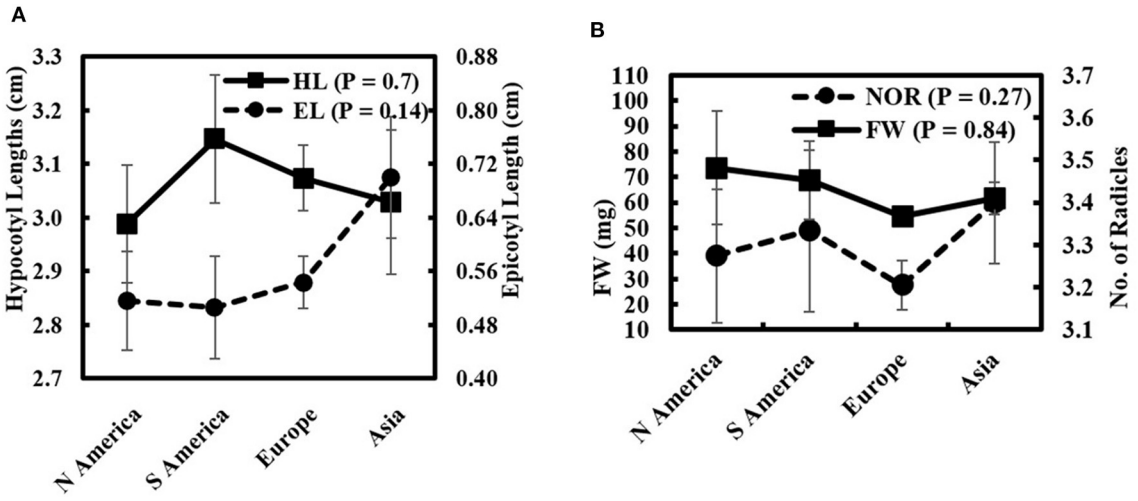


FIGURE 4
Wheat genotypes attributes means classified according to their global affinities for **(A)** EL and HL and **(B)** FW and NOR under salinity stress (50% seawater).

morphological, biochemical, molecular, and genetic impacts. Hence, salinity is one of the factors significantly decreasing wheat production per hectare (Hasseb et al., 2022). Additionally, early stages as germination and seedling growth are critical because they affect all the following stages including grain yield (Mourad et al., 2019; Sallam et al., 2019a; Moursi et al., 2020; Ahmed et al., 2021; Thabet et al., 2021a). It was reported that poor germination and weak seedling growth are major problems that lead to significant deterioration in yield (Sadeghi and Robati, 2015). Moreover, the use of seedlings is relatively simple and cost-effective (Ahmed et al., 2021).

Yildirim et al. (2004) showed that irrigation with seawater with an EC = 15 or 30 $dS.m^{-1}$ significantly decreases the seedling gas exchange and accelerates the respiratory carbon loss, which is coupled with rising in $CO_2$ compensation point and a reduction of the photosynthetic assimilation process. The present results revealed that the different seawater treatments had a great impact on all shoot traits scored for all 48 genotypes. Ragab and Taha (2016) reported that increasing salt concentrations decrease seedling shoot dry weight, shoot length, root dry weight, root length, and emergence index in nine Egyptian wheat cultivars. We observed an important and clear variation among seedling traits when using 50% seawater. Therefore, this seawater concentration was selected to test all genotypes of the population.

The high genetic variation among genotypes ($n = 80$) in all traits investigated in this study after exposure to 50% seawater provides great insight for plant breeders and agronomists to select highly performing genotypes in seawater stress conditions. The high broad-sense heritability for HL, EL, and NOR might allow improving these traits for better seawater tolerance. The heritability of FW was lower than that of the other traits. This high genetic variation that existed among genotypes was due to their being diverse and having originated from 33 countries spread on four continents. Screening highly diverse germplasms from semi-arid and arid regions, especially with salt-affected

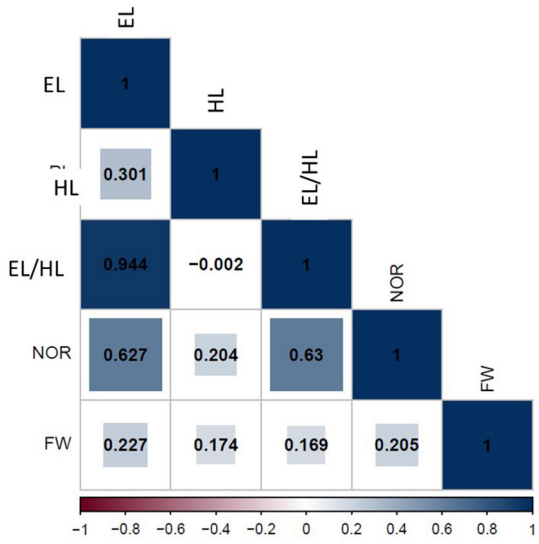


FIGURE 5
Phenotypic correlation among all traits scored under 50% seawater stress.

soils, has been highly recommended for selecting promising salt-tolerant genotypes (Sayed, 1985). The diversity in salt tolerance among different species of wheat was greater than that between ploidy levels (Singh and Chatrath, 2022).

As mentioned before, all genotypes in the present investigation were tested under seawater stress conditions. The analysis of 50% seawater indicated that all genotypes were exposed to a high level of $Na^+$, $K^+$, and $Ca^{2+}$. Most of the previous studies used NaCl to induce salt stress in wheat and other crops. Unfortunately, only a few studies used natural seawater to test the tolerance to salinity of wheat genotypes (Kingsbury and Epstein, 1984; Nassar et al., 2020; Hadia et al., 2022; Kulshreshtha et al., 2022). Two studies assessed the seawater tolerance of wheat genotypes at the germination and seedling stages (Kingsbury and Epstein, 1984; Hadia et al., 2022). Therefore, the present work provides very useful information on the tolerance to seawater stress at early growth stages and might contribute to improving seawater tolerance in wheat. Kingsbury and Epstein (1984), exposed a set of 312 hexaploid wheat varieties to 50% seawater and found 29 salt-resistant lines (9%) with vigorous germination. Here, all the 80 genotypes germinated, and no significant differences were found in the germination percentage after treatment. However, significant variation was observed in shoot and root traits. Out of the 80 genotypes, 8 (10%) showed vigorous growth under 50% seawater condition. Therefore, these eight genotypes might be used for developing seawater-tolerant strains.

Two wheat genotypes were tested for their tolerance to seawater at 0.75% = 13.053 $mS.cm^{-1}$, 1.5% = 24.695 $mS.cm^{-1}$, and 3% = 46.253 $mS.cm^{-1}$ by Hadia et al. (2022) who reported significant differences in coleoptile weight, radicle weight, NOR, coleoptile length, radicle length, radicle length to coleoptile length ratio, and total seedling length. The reduction of the radical number was less important than the reduction in other traits investigated in their study (Hadia et al., 2022). This agrees with the present results as the NOR was not as clearly reduced as the other traits. The more genotypes are investigated for target traits, the higher the genetic variation and, consequently, the better the selection. Therefore, the NOR might be an important trait for enhancing salt tolerance in wheat as it was the least affected by different concentrations of seawater. Shoot growth is more sensitive to salt stress than root growth because the accumulation of $Na^+$ and/or $Cl^-$ at toxic levels affects the photosynthetic capacity, resulting in less supply of carbohydrates to the young leaves and further reducing the shoot growth rate (Munns and Tester, 2008).

To precisely select the genotypes performing the best when exposed to 50% seawater, all genotypes were sorted from the highest to lowest values for each trait. Eight genotypes were found among the 20 genotypes with the highest values for at least three traits. The selection was based on the performances for multiple traits to identify true tolerant genotypes (Sallam et al., 2015, 2018; Bhavani et al., 2021; Ghazy et al., 2021; Mondal et al., 2021; Mourad et al., 2021; Hasseb et al., 2022). Interestingly, the eight selected genotypes displayed a good seawater tolerance and might be used as a basis for improving salt tolerance in wheat at early growth stages. It is recommended to perform the selection at early growth stages in controlled conditions rather than in field conditions because screening the germplasm at the seedling stage may reduce the number of lines to test at another growth stage (Sayed, 1985; Sallam et al., 2016; Abou-Zeid and Mourad, 2021).

Here, the genotypes originated from different geographical regions. Therefore, it was worth comparing the performances under seawater stress conditions of genotypes from one continent with those of genotypes originating from other continents. There were no significant differences in all traits among groups from different continents. However, Asian genotypes had, on average, the greatest NOR and EL compared to those from the continents. In the study from Sayed (1985) a set of 5,072 wheat germplasm lines at different ploidy levels was exposed at the seedling stage to different salt concentrations with different electrical conductivities of 0.8 (control), 12.5, 18.75, and 25.0 $dS.m^{-1}$. He found 442 genotypes with more than 70% surviving seedlings when tested for whole-life cycle survival. The largest groups of tolerant genotypes were from the USA and Egypt (Sayed, 1985). Furthermore, the widest variability among genotypes was observed in seedlings originating from the USA, Mexico, and Egypt.

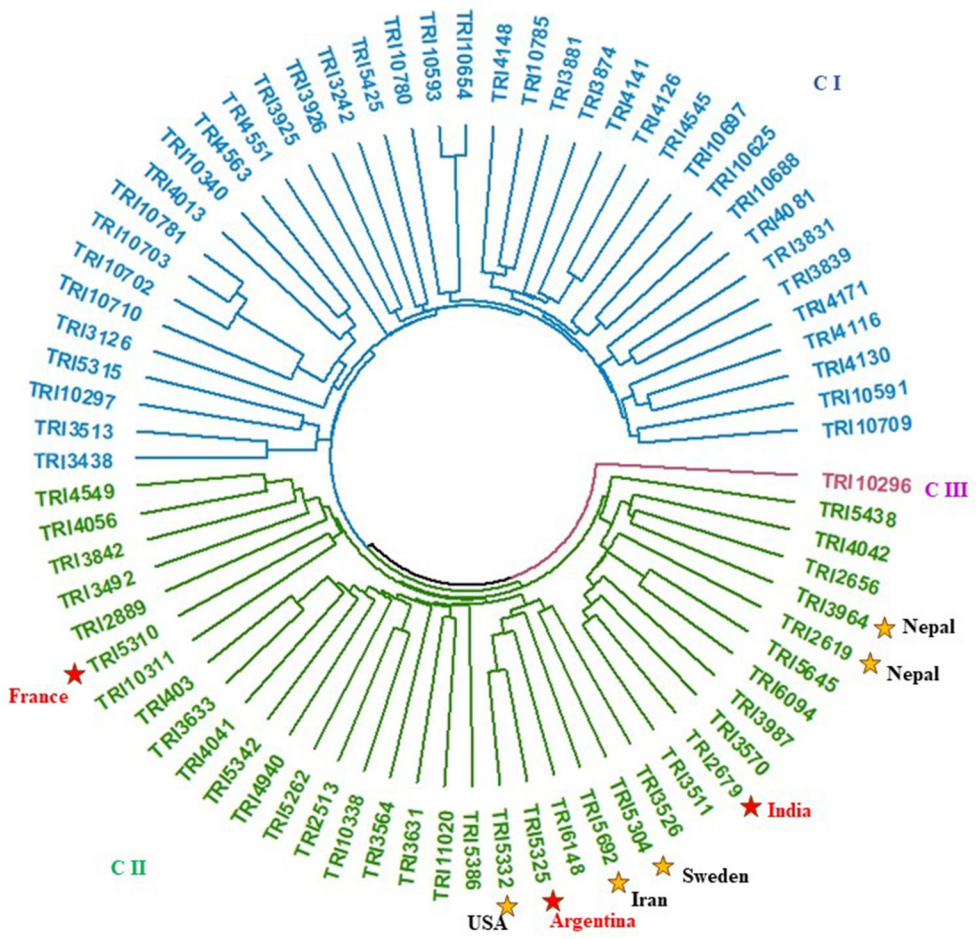


FIGURE 6
Dendrogram analysis based on genetic diversity among all genotypes.

## Phenotypic correlations

In the population ($N = 80$ genotypes) tested in the present study, important significant correlations among seedling traits were observed. Root traits were highly associated with shoot traits in the seawater stress condition. Compared with HL, the NOR was significantly more correlated with EL and FW. Therefore, the NOR seemed to be a trait less affected by seawater stress than HL. Breeding to increase the NOR as an adaptive trait might allow to improve seawater tolerance, especially as root traits play an important role in the ability of plants to survive irrigation with seawater (Trimble, 2020). It was reported that salt stress inhibit the growth and number of primary and lateral roots causing a significant decrease in the root zone (Julkowska et al., 2014; Koevoets et al., 2016). Julkowska et al. (2014) found that no effect of salt stress on lateral root density, suggesting that the reduction in the number of lateral roots is related to the inhibition of primary root growth (Julkowska et al., 2014).

The positive correlations among HL, EL, and FW suggested that shoot water gain or loss is a direct consequence of the water absorption capacity of the root systems because of the high osmotic potential coupled with salt stress around the plant rooting zone (Oyiga et al., 2018). This significant positive correlation among traits allowed the selection of genotypes with high seedling traits in 50% seawater conditions.

Hasseb et al. (2022) studied the correlation among shoot and root traits in a set of 138 wheat genotypes at early growth stages exposed to 175 mM NaCl. They found no or weak correlations among shoot and root traits in wheat. Additionally, no or weak correlations between shoot and root traits were reported in barley subjected to NaCl stress (Moursi et al., 2020). Thus, the correlation among traits may depend on the plant material and the salt concentration.

TABLE 4 List of superior genotypes based on at least three out of the four studied traits, Epicotyl length (EL) and Hypocotyl length (HL), number of roots (NOR), and fresh weight (FW).

| Genotype | Country | Superior studied trait | | | |
|---|---|---|---|---|---|
| | | EL | HL | NOR | FW |
| ATRI 5310* | France | 1.563$^{+}$ | 3.657$^{+}$ | 4.067$^{+}$ | 1.4713$^{+}$ |
| ATRI 5325* | Argentina | 0.920$^{+}$ | 3.310$^{+}$ | 4.400$^{+}$ | 0.796$^{+}$ |
| ATRI 2679* | India | 0.830$^{+}$ | 3.343$^{+}$ | 3.533$^{+}$ | 0.705$^{+}$ |
| ATRI 2619 | Nepal | 0.620$^{+}$ | 3.503$^{+}$ | 3.767$^{+}$ | 0.458$^{-}$ |
| ATRI 3964 | Nepal | 0.647$^{+}$ | 3.380$^{+}$ | 3.167$^{-}$ | 1.320$^{+}$ |
| ATRI 5692 | Iran | 1.883$^{+}$ | 3.257$^{-}$ | 4.267$^{+}$ | 0.814$^{+}$ |
| ATRI 5332 | USA | 1.000$^{+}$ | 3.277$^{-}$ | 3.500$^{+}$ | 0.808$^{+}$ |
| ATRI 5304 | Sweden | 0.803$^{+}$ | 3.073$^{-}$ | 4.333$^{+}$ | 0.717$^{+}$ |

*Genotypes that are superior based on all the four studied seedling traits. $^{+}$refers that the genotype was among the 15 highest performance genotypes under seawater stress for the respective trait.

## Using genetic diversity among genotypes to improve seawater tolerance

Understanding the level of genetic diversity existing among the genotypes of the germplasm is key to genetically improve target traits (Babu et al., 2014; Salem and Sallam, 2016; Eltaher et al., 2018; Sallam et al., 2019b; Mourad et al., 2020). The genetic distance among the 80 genotypes was calculated using 12,390 SNP markers. Different degrees, extending from low to high, of genetic diversity were found among the genotypes. The maximum genetic diversity was achieved when collections of germplasms with genetic variability were from widely different geographic origins. The genetic diversity among the eight wheat genotypes with the greatest traits under seawater stress ranged from 0.354 to 0.692. Although there were two genotypes from Nepal (TRI2619 and TRI2679) among these selected genotypes, the genetic distance among them was 0.508, which was greater than the minimum genetic distance of 0.354 found between TRI5332 (USA) and TRI5325 (Argentina). Thus, crossing between TRI5332 and TRI5325 might not be useful and other candidate genotypes might be selected. Interestingly, TRI5310 from France was highly distanced from all genotypes and including this genotype for crossing in breeding programs might be fruitful. Therefore, it is very important to estimate the genetic distance for a better selection of genotypes to cross. This high genetic diversity can be utilized to produce wheat cultivars with high tolerance to seawater stress, even to higher seawater concentrations, by crossing highly divergent genotypes (Eltaher et al., 2021).

Another important step included in the genetic analysis was to confirm the diversity of the genotypes in the target population. These genotypes were collected from farmers from different countries. As some genotypes were collected from different parts of a given country, they had different accession numbers. Thus, duplicate genotypes with the same genetic makeup could be found. The analysis of genetic diversity can detect such duplicates, and redundant genotypes can be excluded as they will affect the selection procedures for improving target traits.

The analysis of genetic diversity performed here was very useful in selecting true and promising high-performance genotypes with a high level of genetic diversity. Using these genotypes in breeding programs might accelerate and facilitate the achievement of goals such as obtaining strains resistant to seawater. Such selected genotypes (Table 4) with high performance under salt stress can be utilized in Egypt not only to improve seawater tolerance but also to expand the circle of genetic diversity of wheat in Egypt. The 80 genotypes tested in this study have good growing conditions in Egypt (Ahmed Sallam, personal communications).

In conclusion, analyzing germplasms with high genetic variation and different seawater tolerances is very useful in identifying genotypes that might be used in future breeding programs. Moreover, the evaluation of tolerance to seawater at early stages (i.e., seedling stage) will help to reduce screening efforts in field conditions. Seedling traits including shoots and roots allowed to distinguish between high- and low-performance genotypes in seawater stress conditions. Three genotypes had high-performance scores for all traits investigated in the present study. Incorporating the analysis of genetic diversity contributed to the selection of candidate parents for crossing to produce wheat cultivars having high tolerance to seawater. The present data provide useful information on seawater tolerance at the seedling stage in wheat, particularly as very few studies focused on this research point.

## Data availability statement

The original contributions presented in the study are included in the article/Supplementary materials, further inquiries can be directed to the corresponding author.

## Author contributions

AM designed the study, analyzed data, and wrote the manuscript. SH, MMA, and AGM collected the phenotypic data and helped in data analysis. KY analyzed seawater under different concentrations. AMIM helped in collecting data and analyzing the phenotypic data data. MA helped in data collection and analysis. AB provided the germplasm, discussed the results, and helped in editing the paper. AS designed the study, supervised the experiment, and wrote the manuscript. All authors contributed to the article and approved the submitted version.

## Funding

This paper is based upon work supported by Science, Technology and Innovation Funding Authority (STDF) under grant number 43694. Costs for open access publishing were partially funded by the Deutsche Forschung Gemeinschaft (DFG, German Research Foundation grant 491250510). This work was financially partial supported by Alexander von Humboldt Foundation.

## Conflict of interest

The authors declare that the research was conducted in the absence of any commercial or financial relationships that could be construed as a potential conflict of interest.

## Publisher's note

All claims expressed in this article are solely those of the authors and do not necessarily represent those of their affiliated organizations, or those of the publisher, the editors and the reviewers. Any product that may be evaluated in this article, or claim that may be made by its manufacturer, is not guaranteed or endorsed by the publisher.

## Supplementary material

The Supplementary Material for this article can be found online at: https://www.frontiersin.org/articles/10.3389/fpls.2022.996538/full#supplementary-material

## References

Abou-Zeid, M. A., and Mourad, A. M. I. (2021). Genomic regions associated with stripe rust resistance against the Egyptian race revealed by genome-wide association study. *BMC Plant Biol.* 21, 1–14. doi: 10.1186/s12870-020-02813-6

Ahmed, A. A. M., Mohamed, E. A., Hussein, M. Y., and Sallam, A. (2021). Genomic regions associated with leaf wilting traits under drought stress in spring wheat at the seedling stage revealed by GWAS. *Environ. Exp. Bot.* 184, 104393. doi: 10.1016/j.envexpbot.2021.104393

Aleksandrov, V., Kartseva, T., Alqudah, A. M., Kocheva, K., Tasheva, K., Börner, A., et al. (2021). Genetic diversity, linkage disequilibrium and population structure of bulgarian bread wheat assessed by genome-wide distributed SNP markers: from old germplasm to semi-dwarf cultivars. *Plants.* 10, 1–20. doi: 10.3390/plants10061116

Amro, A., Salama, F. M., Abd El-Ghani, M. M., El-Zohary, A. M., and El-Shazoly, R. M. (2021). Variations in community structure and plant species diversity with soil properties in a hyper-arid coastal desert of Egypt. *J. Anim. Plant Sci* 31, 2021. doi: 10.36899/JAPS.2021.6.0372

Babu, B. K., Meena, V., Agarwal, V., and Agrawal, P. K. (2014). Population structure and genetic diversity analysis of Indian and exotic rice (*Oryza sativa* L.) accessions using SSR markers. *Mol. Biol. Rep.* 41, 4329–39. doi: 10.1007/s11033-014-3304-5

Bhavani, S., Singh, P. K., Qureshi, N., He, X., Kumar Biswal, A., Juliana, P., et al. (2021). Globally important wheat diseases: status, challenges, breeding and genomic tools to enhance resistance durability. *Genom. Design. Biotic Stress Res. Cereal Crops* 2, 59–128. doi: 10.1007/978-3-030-75879-0_2

Dehnavi, A. R., Zahedi, M., Ludwiczak, A., Perez, S. C., and Piernik, A. (2020). Effect of salinity on seed germination and seedling development of sorghum (*Sorghum bicolor* (L.) moench) genotypes. *Agronomy* 10, 859. doi: 10.3390/agronomy10060859

Dray, S., and Dufour, A. B. (2007). The ade4 package: Implementing the duality diagram for ecologists. *J. Stat. Softw.* 22, 1–20. doi: 10.18637/JSS.V022.I04

Eltaher, S., Baenziger, P. S., Belamkar, V., Emara, H. A., Nower, A. A., Salem, K. F. M., et al. (2021). GWAS revealed effect of genotype × environment interactions for grain yield of Nebraska winter wheat. *BMC Genom.* 22, 1–14. doi: 10.1186/s12864-020-07308-0

Eltaher, S. S., Sallam, A., Belamkar, V., Emara, H., Nower, A., Salem, K. F. M., et al. (2018). Genetic diversity and population structure of F3:6 nebraska winter wheat genotypes using genotyping-by-sequencing. *Front. Gene.* 9, 76. doi: 10.3389/fgene.2018.00076

Food and Agriculture Organization of the United Nations (2022). *GlobalMap of Salt-affected Soils. FAO Soils Portal*. Available online at: https://www.fao.org/soils-portal/data-hub/soil-maps-and-databases/global-map-of-salt-affected-soils/en/ (accessed July 4, 2022).

Ghanaatiyan, K., and Sadeghi, H. (2015). Divergences in hormonal and enzymatic antioxidant responses of two chicory ecotypes to salt stress. *Planta Daninha* 34, 199–208. doi: 10.1080/15592324.2015.1052925

Ghazy, M. I., Salem, K. F. M., and Sallam, A. (2021). Utilization of genetic diversity and marker-trait to improve drought tolerance in rice (*Oryza sativa* L.). *Mol. Biol. Rep.* 48, 157–170. doi: 10.1007/s11033-020-06029-7

Hadia, E., Slama, A., Romdhane, L., Cheikh M'Hamed, H., Fahej, M. A. S., and Radhouane, L. (2022). Seed priming of bread wheat varieties with growth regulators and nutrients improves salt stress tolerance particularly for the local genotype. *J. Plant Growth Reg.* 3, 1–15. doi: 10.1007/s00344-021-10548-3

Halder, T., Choudhary, M., Liu, H., Chen, Y., Yan, G., and Siddique, K. H. M. (2022). Wheat proteomics for abiotic stress tolerance and root system architecture: current status and future prospects. *Proteomes* 10, 17. doi: 10.3390/proteomes10020017

Hasseb, N. M., Sallam, A., Karam, M. A., Gao, L., Wang, R. R., and Moursi, Y. S. (2022). High-LD SNP markers exhibiting pleiotropic effects on salt tolerance at germination and seedlings stages in spring wheat. *Plant Mol. Biol.* 108, 585–603. doi: 10.1007/s11103-022-01248-x

Jackson, M. L. (1973). *Soil Chemical Analysis*. Prentice hall of India Pvt. Ltd., New Delhi, 498. References–cientific Research Publishing. Available online at: https://www.scirp.org/(S(351jmbntvnsjt1aadkposzje))/reference/ReferencesPapers.aspx?ReferenceID=1453838 (accessed July 11, 2022).

Julkowska, M. M., Hoefsloot, H. C. J., Mol, S., Feron, R., de Boer, G. J., Haring, M. A., et al. (2014). Capturing arabidopsis root architecture dynamics with root-fit reveals diversity in responses to salinity. *Plant Physiol.* 166, 1387–1402. doi: 10.1104/pp.114.248963

Kingsbury, R. W., and Epstein, E. (1984). Selection for salt-resistant spring wheat1. *Crop Sci.* 24, 310–315. doi: 10.2135/cropsci1984.0011183X002400020024x

Koevoets, I. T., Venema, J. H., Elzenga, J. T. M., and Testerink, C. (2016). Roots withstanding their environment: exploiting root system architecture responses to abiotic stress to improve crop tolerance. *Front. Plant Sci.* 7, 1335. doi: 10.3389/fpls.2016.01335

Kulshreshtha, N., Kumar, A., Kumar, A., Lata, C., Kulshreshtha, N., and Kumar, A. (2022). Genetic interventions to improve salt and microelement toxicity tolerance in wheat. *New Horizons Wheat Barley Res.* 429–483. doi: 10.1007/978-981-16-4449-8_18

Kumar, P., and Sharma, P. K. (2020). Soil salinity and food security in India. *Front. Sust. Food Sys.* 4, 174. doi: 10.3389/fsufs.2020.533781

Mimura, N. (2013). Sea-level rise caused by climate change and its implications for society. Proceedings of the Japan Academy. *Series B. Phys. Biol. Sci.* 89, 281. doi: 10.2183/pjab.89.281

Mondal, S., Sallam, A., Sehgal, D., Sukumaran, S., Krishnan, J. N., Kumar, U., et al. (2021). "Advances in breeding for abiotic stress tolerance in wheat," in *Genomic Designing for Abiotic Stress Resistant Cereal Crops*, ed C. Kole (Cham: Springer), 71–103.

Mourad, A. M. I., Alomari, D. Z., Alqudah, A. M., Sallam, A., and Salem, K. F. M. (2019). Recent advances in wheat (spp.) breeding. *Adv. Plant Breed. Strat. Cereals* 5, 559–593. doi: 10.1007/978-3-030-23108-8_15

Mourad, A. M. I., Amin, A. E. E. A. Z., and Dawood, M. F. A. (2021). Genetic variation in kernel traits under lead and tin stresses in spring wheat diverse collection. *Environ. Exp. Bot.* 192, 104646. doi: 10.1016/j.envexpbot.2021.104646

Mourad, A. M. I., Belamkar, V., and Baenziger, P. S. (2020). Molecular genetic analysis of spring wheat core collection using genetic diversity, population structure, and linkage. Disequilibrium. *BMC Genom.* 21, 1–12. doi: 10.1186/s12864-020-06835-0

Moursi, Y. S., Thabet, S. G., Amro, A., Dawood, M. F. A., Stephen Baenziger, P., and Sallam, A. (2020). Detailed genetic analysis for identifying QTLs associated with drought tolerance at seed Germination and seedling stages in Barley. *Plants* 9, 1–22. doi: 10.3390/plants9111425

Mujeeb-ur-Rahman, Ali Soomro, U., Zahoor-ul-Haq, M., and Gul, S. (2008). Effects of NaCl salinity on wheat (*Triticum aestivum* L.) cultivars. *World J. Agri. Sci.* 4, 398–403. Available online at: https://www.idosi.org/wjas/wjas4(3)/18.pdf

Munns, R., and Tester, M. (2008). Mechanisms of salinity tolerance. *Ann. Rev. Plant Biol.* 59, 651–681. doi: 10.1146/annurev.arplant.59.032607.092911

Nahar, K., Hasanuzzaman, M., Alam, M. M., and Protoplasma, A. R. (2017). *Undefined 2017 Insights Into Spermine-Induced Combined High Temperature and Drought Tolerance in Mung Bean: Osmoregulation and Roles of Antioxidant and Glyoxalase*. Berlin: Springer. Available online at: https://idp.springer.com/authorize/casa?redirect_uri=https://link.springer.com/article/10.1007/s00709-016-0965-zandcasa_token=ntPe5CnNbooAAAAA:sj4lQNu6jO4WEyRvDqpb1ZVkhAPvEuUQsMjSsRLPIR0yMHLoRCZT5PbqNcGpmVCAP1PEX9k_i4VU4GeDS2k

Nassar, R. M. A., Kamel, H. A., Ghoniem, A. E., Alarcón, J. J., Sekara, A., Ulrichs, C., et al. (2020). Physiological and anatomical mechanisms in wheat to cope with salt stress induced by seawater. *Plants* 9, 237. doi: 10.3390/plants9020237

Oyiga, B. C., Ogbonnaya, F. C., Sharma, R. C., Baum, M., Léon, J., and Ballvora, A. (2018). Genetic and transcriptional variations in NRAMP-2 and OPAQUE1 genes are associated with salt stress response in wheat. *Theor. App. Gene.* 132, 323–346. doi: 10.1007/s,00122-018-3220-5

Özyazici, M. A., and Açikbaş, S. (2021). Effects of different salt concentrations on germination and seedling growth of some sweet sorghum [*Sorghum bicolor* var. saccharatum (L.) mohlenbr] cultivars. *Turkish J. Agri. Res.,* 8, 133–143. doi: 10.19159/tutad.769463

R Core Team (2014). *R: A Language and Environment for Statistical Computing*. Vienna: R Foundation for Statistical Computing. Available online at: http://www.R-project.org/

Rady, M. M., Semida, W. M., Hemida, K. A., and Abdelhamid, M. T. (2016). The effect of compost on growth and yield of *Phaseolus vulgaris* plants grown under saline soil. *Int. J Recycling Org. Waste Agri.* 5, 311–321. doi: 10.1007/s40093-016-0141-7

Ragab, K. E., and Taha, N. I. (2016). Evaluation of nine egyptian bread wheat cultivars for salt tolerance at seedling and adult-plant stages. *J. Plant Prod. Mansoura Univ.* 7, 147–159. doi: 10.21608/jpp.2016.45248

Rhoades, J. D., Kandiah, A., and Mashali, A. M. (1992). *The Use of Salirle Waters for Crop Production*. Available online at: https://halophyteskh.biosaline.org/sites/default/files/content/BestPractices_MWManagement/FAO48.pd (accessed July 11, 2022).

Sadeghi, H., and Robati, Z. (2015). Response of *Cichorium intybus* L. to eight seed priming methods under osmotic stress conditions. *Biocatalysis Agri. Biotechnol.* 4, 443–448. doi: 10.1016/j.bcab.2015.08.003

Sadeghi, H., and Rostami, L. (2017). Changes in biochemical characteristics and Na and K content of caper (*Capparis spinosa* L.) seedlings under water and salt stress. *J. Agri. Rural Dev. Tropics Subtropics* 118, 119–206. Available online at: https://scirange.com/pdf/irjbs.2019.1.3.pdf

Salem, K. F. M., and Sallam, A. (2016). Analysis of population structure and genetic diversity of Egyptian and exotic rice (*Oryza sativa* L.) genotypes. *Comp. Rendus Biol.* 339, 1–9. doi: 10.1016/j.crvi.2015.11.003

Sallam, A., Alqudah, A. M., Dawood, M. F. A., Baenziger, P. S., and Börner, A. (2019a). Drought stress tolerance in wheat and barley: advances in physiology, breeding and genetics research. *Int. J. of Mol. Sci.* 20, 3137. doi: 10.3390/ijms20133137

Sallam, A., Amro, A., Elakhdar, A., Dawood, M. F. A., Kumamaru, T., and Stephen Baenziger, P. (2019b). Correction to: genetic diversity and genetic variation in morpho-physiological traits to improve heat tolerance in Spring barley. *Mol. Biol. Rep.* 46, 2441–2453. doi: 10.1007/s11033-018-4410-6

Sallam, A., Dhanapal, A. P., and Liu, S. (2016). Association mapping of winter hardiness and yield traits in faba bean (*Vicia faba* L.). *Crop Pasture Sci.* 67, 55–68. doi: 10.1071/CP15200

Sallam, A., Martsch, R., and Moursi, Y. S. (2015). Genetic variation in morpho-physiological traits associated with frost tolerance in faba bean (*Vicia faba* L.). *Euphytica* 205, 395–408. doi: 10.1007/s10681-015-1395-2

Sallam, A., Mourad, A. M. I., Hussain, W., and Stephen Baenziger, P. (2018). Genetic variation in drought tolerance at seedling stage and grain yield in low rainfall environments in wheat (*Triticum aestivum* L.). *Euphytica* 214, 1–18. doi: 10.1007/s10681-018-2245-9

Sanower Hossain, M., and Sultan Ahmad Shah, J. (2019). Present scenario of global salt affected soils, its management and importance of salinity research article information. *Int. Res. J. Biol. Sci. Pers.* 1, 2663–5976. Available online at: https://scirange.com/pdf/irjbs.2019.1.3.pdf

Sayed, H. I. (1985). Diversity of salt tolerance in a germplasm collection of wheat (*Triticum* spp.). *Theor. App. Gene.* 69, 651–657. doi: 10.1007/BF00251118

Seleiman, M. F., Aslam, M. T., Alhammad, B. A., Hassan, M. U., Maqbool, R., Chattha, M. U., et al. (2021). Salinity stress in wheat: effects, mechanisms and management strategies. *Phyton* 91, 667. doi: 10.32604/phyton.2022.017365

Singh, A., Sharma, D. K., Kumar, R., Kumar, A., Yadav, R. K., and Gupta, S. K. (2018). "Soil salinity management in fruit crops: a review of options and challenges," in *Engineering Practices for Management of Soil Salinity*, eds S. K. Gupt, M. R. Goyal, A. Singh (Cambridge, MA: Apple Academic Press), 81–128.

Singh, K. N., and Chatrath, R. (2022). *Genetic Divergence in Bread Wheat (Triticum aestivum L. em thell) Under Sodic Soil Conditions*. Available online at: https://agris.fao.org/agris-search/search.do?recordID=JP19940117693 (accessed July 5, 2022).

Srivastava, A. K., Suprasanna, P., Srivastava, S., and D'Souza, S, F. (2010) Thiourea mediated regulation in the expression profile of aquaporins and its impact on water homeostasis under salinity stress in Brassica juncea roots. *Plant Sci.* 178, 517–522.

Tabatabai, M. A., and Bremner, J. M. (1970). A simple turbidimetric method of determining total sulfur in plant materials. *Agron. J.* 62, 805–806. doi: 10.2134/agronj1970.00021962006200060038x

Thabet, S. G., Moursi, Y. S., Sallam, A., Karam, M. A., and Alqudah, A. M. (2021a). Genetic associations uncover candidate SNP markers and genes associated with salt tolerance during seedling developmental phase in barley. *Environ. Exp. Bot.* 188, 104499. doi: 10.1016/j.envexpbot.2021.104499

Thabet, S. G., Sallam, A., Moursi, Y. S., Karam, M. A., Alqudah, A. M., Wu, H., et al. (2021b). Genetic factors controlling nTiO$_2$ nanoparticles stress tolerance in barley (*Hordeum vulgare*) during seed germination and seedling development. *Function. Plant Biol.* 48, 1288–1301. doi: 10.1071/FP21129

Tomaz, A., Costa, M. J., Coutinho, J., Dôres, J., Catarino, A., Martins, I., et al. (2021). Applying risk indices to assess and manage soil salinization and sodification in crop fields within a mediterranean hydro-agricultural area. *Water* 13, 3070. doi: 10.3390/w13213070

Trimble, S. (2020). *Irrigating With Saline or Seawater – CID Bio-science*. Available online at: https://cid-inc.com/blog/irrigating-with-saline-or-seawater/ (accessed July 11, 2022).

Utz, H. F. (2011). *PLABSTAT: A Computer Program for the Statistical Analysis of Plant Breeding Experiments*. Hohenheim: Institute of Plant Breeding, Seed Science, and Population Genetics, University of Hohenheim.

Yildirim, Ö., Aras, S., and Ergül, A. (2004). Acta biologica cracoviensia series botanica response of antioxidant systems to short-term nacl stress in grapevine rootstock-1616c and *Vitis vinifera* l. cv. razaki. *Acta Biol. Cracoviensi A. Series Bot.* 46, 151–158. Available online at: https://citeseerx.ist.psu.edu/viewdoc/download?doi=10.1.1.333.6572&rep=rep1&type=pdf

frontiers | Frontiers in Plant Science

TYPE Original Research
PUBLISHED 24 October 2022
DOI 10.3389/fpls.2022.1035016



OPEN ACCESS

EDITED BY
Nabin Bhusal,
Agriculture and Forestry University, Nepal

REVIEWED BY
Parvaze Sofi,
Sher-e-Kashmir University of Agricultural Sciences and Technology of Kashmir, India
Manish Kumar Vishwakarma,
Borlaug Institute for South Asia (BISA), India

*CORRESPONDENCE
Hari Krishna
harikrishna.agri@gmail.com
P. K. Singh
pksinghiari@gmail.com

SPECIALTY SECTION
This article was submitted to Plant Abiotic Stress, a section of the journal Frontiers in Plant Science

RECEIVED 02 September 2022
ACCEPTED 03 October 2022
PUBLISHED 24 October 2022

CITATION
Sunilkumar VP, Krishna H, Devate NB, Manjunath KK, Chauhan D, Singh S, Sinha N, Singh JB, Prakasha TL, Pal D, Sivasamy M, Jain N, Singh GP and Singh PK (2022) Marker assisted improvement for leaf rust and moisture deficit stress tolerance in wheat variety HD3086.
*Front. Plant Sci.* 13:1035016.
doi: 10.3389/fpls.2022.1035016



# Marker assisted improvement for leaf rust and moisture deficit stress tolerance in wheat variety HD3086

V.P. Sunilkumar[1], Hari Krishna[1]*, Narayana Bhat Devate[1], Karthik Kumar Manjunath[1], Divya Chauhan[1], Shweta Singh[1], Nivedita Sinha[1], Jang Bahadur Singh[1], T. L. Prakasha[1], Dharam Pal[1], M. Sivasamy[1], Neelu Jain[1], G. P. Singh[2] and P. K. Singh[1]*

[1]Division of Genetics, Icar- Indian Agricultural Research Institute, New Delhi, India, [2]ICAR-Indian Institute of Wheat and Barley Research, Karnal, India

There is a significant yield reduction in the wheat crop as a result of different biotic and abiotic stresses, and changing climate, among them moisture deficit stress and leaf rust are the major ones affecting wheat worldwide. HD3086 is a high-yielding wheat variety that has been released for commercial cultivation under timely sown irrigated conditions in the Indo-Gangetic plains of India. Variety HD3086 provides a good, stable yield, and it is the choice of millions of farmers in India. It becomes susceptible to the most prevalent pathotypes 77-5 and 77-9 of Puccinia triticina (causing leaf rust) in the production environment and its potential yield cannot be realized under moisture deficit stress. The present study demonstrates the use of a marker-assisted back cross breeding approach to the successful transfer of leaf rust resistance gene Lr24 and QTLs linked to moisture deficit stress tolerance in the background of HD3086. The genotype HI1500 was used as a donor parent that possesses leaf rust-resistant gene Lr24, which confers resistance against the major pathotypes found in the production environment. It possesses inbuilt tolerance under abiotic stresses with superior quality traits. Foreground selection for gene Lr24 and moisture deficit stress tolerance QTLs linked to Canopy temperature (CT), Normal Differential Vegetation Index (NDVI) and Thousand Kernel Weight (TKW) in different generations of the backcrossing and selection. In BC2F2, foreground selection was carried out to identify homozygous lines based on the linked markers and were advanced following pedigree based phenotypic selection. The selected lines were evaluated against P. triticina pathotypes 77-5 and 77-9 under controlled conditions. Recurrent parent recovery of the selected lines ranged from 78-94%. The identified lines were evaluated for their tolerance to moisture stress under field conditions and their resistance to rust under artificial epiphytotic conditions for two years. In BC2F5 generation, eight positive lines for marker alleles were selected which showed resistance to leaf rust and

recorded an improvement in component traits of moisture deficit stress tolerance such as CT, NDVI, TKW and yield compared to the recurrent parent HD3086. The derived line is named HD3471 and is nominated for national trials for testing and further release for commercial cultivation.

KEYWORDS

*Lr24*, leaf rust resistance, drought tolerance, QTLs, MABB

## Introduction

Wheat (*Triticum aestivum* L.), the world's most important food grain, is the staple food for over 27% of the global population in more than 40 countries (Sharma et al., 2019). It is generally known as the "King of Cereals" due to its high economic importance and is grown in a variety of agro-climatic conditions. The total wheat production in the world is 778.6 mt from an area of 220.4 mha with a productivity of 3.47 tons/ha (FAS; USDA, 2021). Indian wheat production is 107.86 mt obtained from an area of 31.45 mha with productivity of 3.37tons/ha (FAS; USDA, 2021). Various biotic and abiotic stresses affect the wheat crop, leading to significant yield reduction in annual wheat production. It is predicted that global warming will increase by 1.5°C in the next decade and annual precipitation will decrease by 4–27% in different parts of the world (IPCC, 2021). Drought and heat cause up to 86% and 69% yield losses in wheat, respectively (Prasad et al., 2011; Yang et al., 2021). Drought is the inadequacy of water availability including precipitation and soil moisture storage during the crop growth period both in duration and quantity which restrict the genetic yield potential (Sinha, 1986). It is recognized that half of the wheat cultivated in the developing world is sown under rain fed systems, which receive less than 600mm annual rainfall. In India, erratic distribution of rainfall and reduced groundwater table (Rodell et al., 2009) have adversely affected wheat production in major wheat growing zones.

Among the biotic factors that reduce wheat productivity, rusts are of prime importance. Rusts pathogens are continuously evolving and breaking the resistance of wheat cultivars. Prevailing diverse climatic conditions provide a conducive environment for epidemics of rust in one or other parts of the country. It is estimated that diseases reduce wheat yield by 15-20 percent. However, serious epidemics of leaf rust can reduce yield by up to 50%. Yield losses from leaf rust are mostly due to reductions in kernel weight. Leaf or brown rust caused by *Puccinia triticina* Eriks is probably the most important disease worldwide. There are currently 82 leaf rust resistance genes identified so far (McIntosh et al., 2017; Qureshi et al., 2018; Bariana et al., 2022) out of which *Lr1, Lr3, Lr9, Lr10, Lr13, Lr14a, Lr17, Lr19, Lr23, Lr24, Lr26, Lr28* and *Lr34* are commonly exploited in Indian wheat breeding programs (Bhardwaj et al., 2005; Bhardwaj et al., 2010, Bhardwaj et al., 2011). Among these leaf rust resistance genes, *Lr24*/*Sr24* derived from *Agropyron elongatum*, located on 3DL, confers resistance to all the currently prevalent pathotypes in the Indian sub-continent (Bhardwaj et al., 2021). Developing resistant wheat cultivars is the most efficient, economical, and environment friendly approach for the management of rusts.

Genetic variation for moisture deficit stress tolerance exists in wheat cultivars and improved adaptation response in wheat can be achieved by implementing appropriate crossing and selection strategies (Reynolds, 2001; Langridge and Reynolds, 2015). Earlier studies suggest that physiological traits associated with yield under drought have the potential to increase selection efficiency (Condon et al., 2004; Olivares-Villegas et al., 2007; Araus et al., 2008; Reynolds and Langridge, 2016). Molecular markers proved to be an important tool in improving selection efficiency and have good prospects for marker-assisted selection in improving moisture deficit stress in wheat (Kuchel et al., 2005; Quarrie et al., 2005). Physiological traits play crucial roles in determination of moisture stress tolerance hence incorporation of them using molecular marker in to the heigh yielding genotype can produce combination of high yielding and drought tolerant genotypes. SPAD meter is a portable diagnostic tool that measures leaf chlorophyll index *via* light transmittance that is differentially observed by chlorophyll and estimates leaf chlorophyll content and nitrogen content (Prasad et al., 2011), whereas a field-portable NDVI sensor enables quick ground-level measurements of crops with the resolution necessary to characterize the canopy for its biomass, nutrient content, and leaf area and green area indices (Weier and Herring, 2000; Araus et al., 2008). QTLs linked with canopy temperature govern the deeper root system to enhance the extraction of water from deeper soil horizons and also have been found to co-localize with regions affecting other drought adaption features like kernel number, grain yield, and chlorophyll content (Diab et al., 2008; Olivares-Villegas et al., 2008; Pinto et al., 2010; Pinto and Reynolds, 2015).

Indian Agricultural Research Institute (IARI) has a major contribution in developing high yielding wheat varieties in the interest of increasing the profit of farmers and wheat annual production in the country. IARI developed many high yielding wheat varieties, among them HD2967 and HD3086 together occupying 40% of the country's total wheat area over the last several years. HD3086 (Pusa Gautami) is a high-yielding wheat variety that has been released for commercial cultivation under timely sown irrigated conditions in the North Western Plains Zone (NWPZ) and North Eastern Plains Zone (NEPZ) of the country. 'HD3086' alone occupies breeder seed indent of 34% among IARI wheat varieties and 11.6% of total wheat varieties indented in the country (https://seednet.gov.in/) (Figure 1). It is the choice of millions of farmers in the major wheat growing regions of the country, providing a good, stable yield over the years. Recent AICRIP reports (http://www.aicrpwheatbarleyicar.in) showed that HD3086 is susceptible to major pathotypes of *P. triticina* and recorded yield reduction under restricted irrigation conditions (AICRP Crop Improvement Reports, 2019). This is supported by Single Race Testing (SRT), in which HD3086 showed susceptibility to the prevalent 77 groups of pathotypes 77-5 and 77-9 of *P. triticina*. Hence, the improvement of HD3086 for leaf rust resistance and moisture deficit stress tolerance helps to expand the area of cultivation in the NWPZ, and NEPZ with a reduced number of irrigations. Because of the presence of the resistance gene *Lr24/Sr24*, the wheat variety HI1500 is promising in resistance against new pathotypes of *P. triticina*, 77-5 and 77-9. It is also known to perform well under limited irrigation conditions. Hence, HI1500 is used as a donor parent to transfer leaf rust resistance gene *Lr24/Sr24* and moisture deficit stress tolerance QTLs to improve HD3086.

## Materials and methods

### Plant materials and generation of improved lines

In this marker assisted backcross breeding (MABB) program, HD3086 was used as a recurrent parent and HI1500 as a donor parent. HD3086 has a semi-erect growth habit and matures in 140-145 days, providing an average yield of 5.46 t/ha under timely sown irrigated conditions. HI1500 is a popular variety grown in the Central Zone (CZ) under restricted irrigation conditions, giving an average yield of 2.2 t/ha. It has an erect growth habit, takes 130–134 days to mature, and shows resistance to leaf and stem rusts.

$F_1$ plant was generated from the cross HD3086/HI1500, hybridity of $F_1$ was confirmed using the *Lr24* linked SSR marker *Xbarc71*. $F_1$ plant was backcrossed to the recurrent parent HD3086 to generate $BC_1F_1$. Foreground selection was carried out with SSR marker linked to leaf rust resistance gene (*Lr24*)

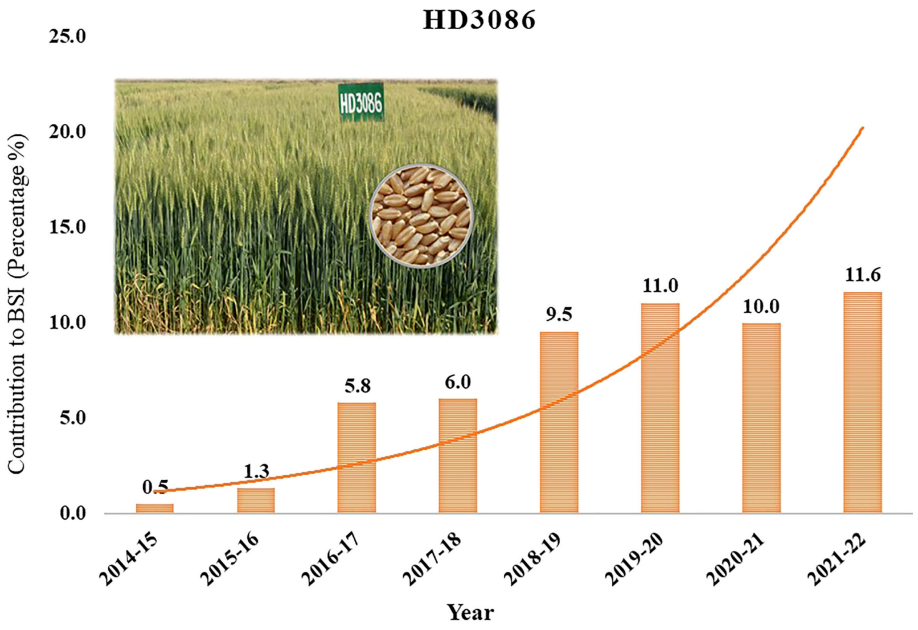


FIGURE 1
Yearly contribution of Wheat variety HD3086 to the total Breeder Seed Indent of country in percentage.

and moisture deficit stress tolerance QTLs (Table 1), followed by phenotypic selection to identify the plants with maximum recovery for recurrent parent phenome (RPP). The best $BC_1F_1$ plants having heterozygote allele for rust resistance and moisture deficit stress tolerance QTLs along with visual similarity to the recurrent parent were selected and further backcrossed with HD3086 to generate $BC_2F_1$ seeds. In a similar way, the $BC_2F_1$ plants were also subjected to screening for *Lr24* and moisture deficit stress tolerance QTLs, and the superior positive plants were advanced to $BC_2F_2$ generation and foreground selection was repeated. Further, these $BC_2F_3$ (110 lines) were advanced *via* pedigree based phenotypic selection to $BC_2F_4$ (100 lines). The identified $BC_2F_4$ (100 lines) and $BC_2F_5$ (38) lines were evaluated for their tolerance to moisture stress under field conditions and their reactions to rust in artificial epiphytotic conditions for two years. The individuals in $BC_2F_5$ with superior performance were further advanced to multiplication of seed for nominating under MABB trails of AICRP (Figure 2).

## Foreground selection

Foreground selection was done according to the methods described by Hospital and Charcosset (1997) and Rai et al. (2018). QTLs linked to SSR markers associated with component traits of moisture deficit stress tolerance such as normalized difference vegetation index (NDVI), Leaf chlorophyll index (LCI), Canopy temperature (CT), and a yield contributing trait Thousand Kernal Weight (TKW) were selected from previously validated SSR markers linked to moisture deficit stress tolerance traits in

TABLE 1 SSR and SCAR markers used in foreground selection linked to moisture deficit stress tolerant QTLs and leaf rust resistance genes *Lr24*.

| SL.NO | Traits targeted | QTLs | PVE (%) | Gene/Marker used for Foreground selection | Reference |
|---|---|---|---|---|---|
| 1 | NDVI | *Qndvi4iari-2B* | 14%, 19% (Harikrishna, 2017) | *Xcfd73* | Yang et al. (2007) |
| 2 | CT | *QCt_3A* (MQTL23) *Qct3.iari-5B* | 11% (Harikrishna, 2017) | *Xbarc12- Xgwm369, Xgwm544* | Griffiths et al. (2009); Kumar et al. (2012); Gupta et al. (2012) |
| 3 | TKW | *Qtkw_2B* | – | *Xcfd73* | Yang et al. (2007), Liu et al. (2018) |
| 4 | Leaf rust resistance | *Lr24/Sr24* | – | SCAR: SCS1302, *Xbarc71* | Gupta et al. (2006); Pallavi et al. (2015) |

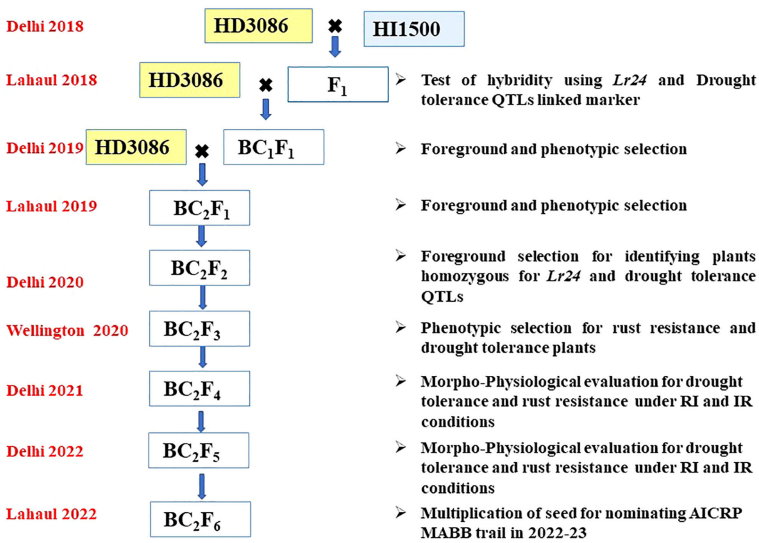


FIGURE 2
Schematic workflow of marker assisted backcross breeding of HD3086 × HI1500.

HI1500 x DBW43 cross derived RIL population from our lab (Harikrishna, 2017). A positive allele for the parent HI1500, which is associated with component traits of moisture deficit stress tolerance viz., CT, NDVI, and TKW in the HI1500 x DBW43 RIL mapping population, was used for transfer Qct.iari_3A, linked to SSR *Xbarc12*, and Qndvi4.iari-2B, linked to SSR *cfd73*, explained a phenotypic variance of 14% (R2 = 0.14) at grain filling stage; Qct3.iari-5B linked to SSR *Xgwm544* explained a phenotypic variance of 11% (R2 = 0.11) at grain filling stage (Harikrishna, 2017) (Table 1). Foreground selection for leaf rust resistance was carried out with markers, *Lr24* (Schachermayr et al., 1995) and *Xbarc71* (Mago et al., 2005; Pallavi et al., 2015).

Genomic DNA from leaf samples was extracted using the CTAB method and DNA was quantified with Nanodrop, and quality was determined using 1% agarose gel electrophoresis with λ DNA as the standard. A total reaction volume of 15 µl was used for the PCR, which contained 40 ng of genomic DNA, 1X PCR buffer with 1.5 MgCl2, 10 pmol of each PCR primer, 100 µM of each dNTP, and 0.3 µl of Taq DNA polymerase. PCR Amplification of the template DNA was carried out in a 'G-Storm thermal cycler' with SSR and SCAR markers belonging to *Xgwm*, *Xbarc*, and *Xcfd* series (Supplementary Table 1). The amplified product was resolved in gel electrophoresis using 3% Agarose SFR gel and visualized on Gel documentation systems, GelDoc-It$^{®2}$ 315 (Supplier: UVP). Primer sequences for SSR markers were obtained from the Grain Genes website (http://wheat.pw.usda.gov/GG2/index.shtml) and synthesized for the Beltsville Agricultural Research Center (BARC), Gatersleben wheat microsatellite (GWM), Wheat Microsatellite Consortium (WMC), and INRA Clermont-Ferrand (CFD).

## Background selection

The selected homozygous BC2F5 lines screened for rust and moisture deficit stress tolerance linked markers, were genotyped using 35k SNPs from Axiom wheat breeders' array along with the parents to identify plants with maximum recovery of recurrent parent genome (RPG). The recurrent parent HD3086 and donor HI1500 were analyzed for parental polymorphism and a total of 3707 polymorphic SNPs were selected. Graphical visualization of background recovery of the recurrent parent was done using software GGT 2.0 (Graphical Geno Typing 2.0) (Van Berloo, 2008). The contribution of the recurrent parent to the background of MABB derived lines was calculated by the formula:

$$G = [(B + 1/2A) \times 100]/N$$

were,

N = total number of parental polymorphic markers screened

B = number of markers showing homozygosity for recurrent parent allele

A = number of markers showing heterozygosity for parental alleles.

## Screening for leaf rust resistance at seedling stage

The uredospore inoculum of individual pathotypes of *P. triticina*, 77-5 and 77-9 was obtained from the ICAR-IIWBR, Regional Station, Flowerdale, Shimla (India) for phenotyping of NILs. The seedlings were screened for resistance to *P. triticina* races 77-5 and 77-9 in each backcrossed generation during the main season at IARI New Delhi, IARI Regional Station, Indore and Shimla. In the off season, the material was evaluated for rust resistance at National Phytotron Facility (NPF), New Delhi. Seedlings, along with their parents, were inoculated with rust spores at the first leaf stage, about 8-10 days after sowing, during evening hours. The seedlings were sprayed with water to provide a uniform layer of moisture on the leaf surface before inoculation. Inoculated seedlings were incubated for 36 h in humid glass chambers at a temperature of 23 ± 2°C and relative humidity above 85%. Seedlings were shifted to muslin cloth chambers after incubation. The disease reaction was recorded 12-14 days after inoculation, using the scoring method described by Stakman et al. (1962).

## Screening of genotypes at adult stage for leaf rust resistance

Genotypes were screened at IARI New Delhi and IARI regional station, Indore, during the main season and at IARI regional station, Wellington, Tamil Nadu, during the off season. The rust susceptible landrace 'Agra local' was used as infector and was space planted after every twenty rows of test material and around the experimental plots. The rust disease scoring was done at the adult plant stage using the modified Cobb Scale (Peterson et al., 1948), which scores, S (susceptible), MS (moderately susceptible), MR (moderately resistant) and TR (trace) (Joshi et al., 1988) in the scale of 0 to 100.

## Evaluation for moisture deficit stress tolerance traits

The back cross populations were evaluated in the experimental farm of IARI, New Delhi (280 40'N,770 13' E; MSL228m) during the year 2020-21and 2021-22. The positive BC2F4 lines having moisture deficit stress tolerance related QTLs along with the parents and 2 check varieties (GW322 and BABAX) were evaluated for agronomic and physiological traits in augmented design under restricted irrigation and irrigated condition. Lines were grown in 2 blocks containing

50 lines and four checks (2 parents and 2 checks) were replicated twice in each block. GW322 is the most common type of bread wheat in the central and peninsular zones, performs well in timely sown irrigated condition. Whereas BABAX, a drought tolerant Mexican cultivar perform well under water limited condition. Each BC2F4 line was planted in a plot containing three rows of 1m length with 23cm spacing between them, with a gross plot size of 0.63 $m^2$. Superior lines were advanced to BC2F5 and were planted in a large plot size of 7.2 $m^2$ (6m x 1.2m) Containing 6 rows. Standard agronomic management practices were followed for raising the wheat crop. The data was recorded on five plants from each of the entries for the agronomic characters such as thousand kernel weight (TKW), days to heading (DH), plant height (PH), grain yield (GY), grain weight per spike (GWPS) and grain length (GL). Physiological parameters such as NDVI (normalized difference vegetation index), CT (canopy temperature) and LCI (Leaf Chlorophyll Index), were recorded at 3 different stages such as vegetative stage (late boot stage, Z49), grain filling stage (early milk stage, Z73) and grain maturity stage (late milk stage, Z85) according to Zadoks scale (Zadoks et al., 1974).

## Statistical analysis

Calculation of descriptive statistics and analysis of variance was carried out in BC2F4 augmented RCBD, using the R program. BC2F5 derived lines sown in RBD with three replications were analyzed using data analysis add ins of MS-excel. Analysis of variance Critical Difference (CD) and Coefficient of Variation (CV) was calculated. Lines with statistical significance for moisture deficit stress tolerance with high yield under stress were identified.

# Results

## Development of backcross population following foreground selection and background analysis

The F1 plants obtained from the cross involving HI1500 (donor parent) and HD3086 (recurrent parent) were backcrossed with HD3086 to produce BC1F1 seeds. Among 120 BC1F1 plants, 16 were selected through foreground selection of QTLs associated with traits like CT, chlorophyll content, NDVI and TKW, and also for the *Lr24* gene associated with leaf rust resistance.

The selected plants for targeted traits were again backcrossed with the recurrent parent to generate BC2F1 plants. Out of 140 BC2F1 plants, 12 plants positive for a combination of moisture deficit stress tolerance QTLs and *Lr24* gene were selected and selfed to produce BC2F2 progenies (Figure 3). From these, a total of 600 BC2F2 plants were raised and subjected to stringent phenotyping of leaf rust screening for identification of homozygous plants (Table 2). Plants with rust resistance and good phenotyping background recovery were used for foreground selection using linked molecular markers to

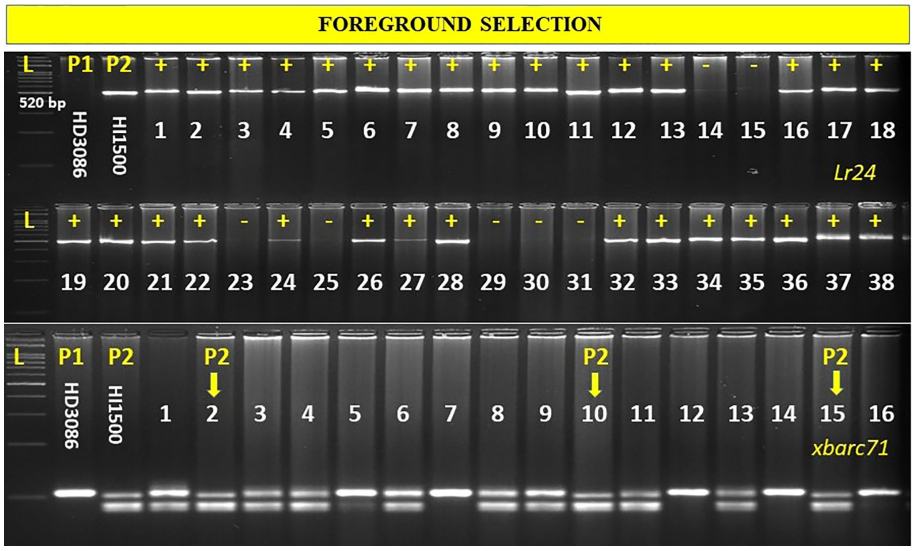


FIGURE 3
SCAR marker-assisted screening of the leaf rust resistance gene *Lr24* in selected $BC_2F_2$ lines and identity homozygous lines associated with *Lr24/Sr24* tightly linked SSR marker *Xbarc71*. In *Lr24* bands, progenies in the first row are 1-18 followed by second row from 19 to 38.

TABLE 2 Number of plants selected in each generation in HD3086*2/HI1500 derived population.

| Generation | No. of plants | Foreground Selection No. of plants selected | |
|---|---|---|---|
| $BC_1F_1$ | 120 | 16 | FS+PS |
| $BC_2F_1$ | 140 | 12 | FS+PS |
| $BC_2F_2$ | 600 | 110 | FS+PS |
| $BC_2F_3$ | 110 | 100 | PS |
| $BC_2F_4$ | 100 | 38 | BS+PS |
| $BC_2F_5$ | 38 | 14 | PS |
| $BC_2F_6$ | 10 | 1 | PS |

FS, Foreground Selection; PS, Phenotypic Selection; BS, Background Selection.

identify homozygous donor QTL combinations. From these, 110 BC2F2 plants were selected as homozygous for *Lr24*, and a combination of QTLs linked to moisture deficit stress tolerance using foreground selection. Further, these positive plants were sequentially advanced *via* pedigree based phenotypic selection until BC2F4.

## Screening for leaf rust resistance at seedling stage

The recurrent parent HD3086 showed a susceptible reaction (3 3+) for pathotypes 77-5 and 77-9 as that of susceptible check Agra local. On the other hand, donor parent HI1500 displayed an immune reaction (0) for pathotype 77-5 and resistance (; 1) for 77-9 (Table 3). In BC2F4, out of the 24 advanced lines subjected to SRT of *P. triticina* pathotypes 77-5 and 77-9, 19 lines showed resistance and 5 lines showed susceptible reaction due to the absence of *the Lr24* gene. The genotypes HD3086-E-5-17, HD3086-C-6-2 and HD3086-13-16 were identified as

TABLE 3 Screening of marker assisted derived wheat genotypes for leaf rust races at IARI regional station Indore and Shimla ($BC_2F_4$).

| Sl.no | Progenies | Rust race (77-5) | | Rust race (77-9) | | Reaction of genotypes |
|---|---|---|---|---|---|---|
| | | IARI RS, Indore | IARI RS, Shimla | IARI RS, Indore | IARI RS, Shimla | |
| 1 | HD3086 | 33+ | 3+ | 3 | 3 | Susceptible (S) |
| 2 | HI1500 | 0 | 0 | ; 1 | 0 | Immune/Resistant (R) |
| 3 | HD3086-M-1-26 | 0 | 1 | 2 | 1 | R |
| 4 | HD3086-M-1-36 | ; 1- | 1 | 2 | 1 | R |
| 5 | HD3086-M-1-49 | 0 | 2 | 2 | 0 | MR |
| 6 | HD3086-M-1-55 | 2 | 1 | 1 | ; | R |
| 7 | HD3086-E-5-3 | ; | 1 | ; | 1 | HR |
| 8 | HD3086-E-5-5 | ; | 0 | ; | 0 | HR |
| 9 | HD3086-E-5-17 | 0 | 1 | ; | 3 | R |
| 10 | HD3086-E-5-26 | 3+ | 3 | 3 | 3 | S |
| 11 | HD3086-E-5-27 | 3+ | 2 | 2 | 1 | MS |
| 12 | HD3086-E-5-33 | 0 | 1 | ; | 1 | R |
| 13 | HD3086-E-5-43 | ; | 0 | ; | 1 | HR |
| 14 | HD3086-E-5-60 | 0 | ; | ; | 0 | HR |
| 15 | HD3086-C-6-1 | 3+ | 3 | 2 3 | 3 | S |
| 16 | HD3086-C-6-2 | 0 | 1 | ; 1 | 0 | R |
| 17 | HD3086-D-7-9 | 0 | ; | 1 | ; | HR |
| 18 | HD3086-D-7-14 | ; | 0 | 1 | 2 | R |
| 19 | HD3086-D-7-56 | ; | 1 | ; | 1 | R |
| 20 | HD3086-I-3-1 | 3 | 3 | 2 3 | 2 3 | S |
| 21 | HD3086-F-13-1 | 0 | ; | 2 | 2 | R |
| 22 | HD3086-11-9 | 0 | ; | ; | 1 | HR |
| 23 | HD3086-11-10 | 3+ | 2 | 3 | 3 | S |
| 24 | HD3086-13-2 | 0 | 1 | ; | 0 | HR |
| 25 | HD3086-13-13 | 0 | 1 | 2 | 2 | MR |
| 26 | HD3086-13-16 | 0 | ; | ; | 1 | R |
| 27 | Agra Local | 3+ | 3+ | 3+ | 3+ | HS |

HR, Highly resistant; R, Resistant; MR, Moderately resistant; MS, Moderately Susceptible; S, Susceptible; HS, Highly susceptible.

resistant/immune lines for both races 77-5 and 77-9 at IARI Regional Station, Indore. Whereas genotypes evaluated for SRT at Indore such as HD3086-M-1-26, HD3086-M-1-36, HD3086-I-3-1, HD3086-F-13-1 and HD3086-13-13 were classified as resistant for 77-5 and moderately susceptible for 77-9. The genotype HD3086-M-1-49 was identified as susceptible for 77-9 and moderately resistant for 77-5 (Table 3). Finally, nineteen (7HR, 10R and 2MR) BC2F4 lines showing resistance to pathotypes 77-5 and 77-9 and also performing better under restricted irrigation conditions were selected.

## Field screening for leaf rust resistance

Rust scoring in field conditions was carried out in BC2F1 (off season nursery: Lahul-Spiti), BC2F2 (Main Season: New Delhi) and BC2F3 (off season nursery: Wellington). In all these trials the MAS-derived *Lr24* selected lines showed a very low incidence of rust infection. Whereas recurrent parent HD3086 showed a severe disease infection (60S) of leaf rust. In BC2F5, out of 10 selected lines (previously selected in BC2F4 during SRT), 8 lines *viz*., HD3086-M-1-26-410-46, HD3086-M-1-36-413-47, HD3086-M-1-55-419-49, HD3086-E-5-17-461-50, HD3086-C-6-2-481-51, HD3086-F-13-1-512-53, HD3086-13-13-562-54 and HD3086-13-16-565-55 showed resistant reaction and lines HD3086-M-1-49-417-48 and HD3086-I-3-1-507-52 showed moderately resistant reaction. One MABB derived line, HD3086-C-6-2-481-51 showed ACI '0' for leaf rust in initial plant pathological nursery data of AICRP trial 2021-22 (data available at http://www.aicrpwheatbarleyicar.in/wp-content/uploads/2022/07/PPSN-2021-22-decoded.pdf).

## Background analysis

Selected 10 best BC2F5 plants showed significant improvement over the recurrent parent HD3086, for component traits of moisture deficit stress tolerance and leaf rust resistance with maximum recovery of RPG with a range of 79%-95% and average RPG recovery, was 86%. Two superior lines HD3086-E-5-17-461-50 and HD3086-C-6-2-481-51 had maximum recovery of about 95.24% and 93.87% respectively (Figure 4; Supplementary Table 4).

## Morpho-physiological performance of the selected lines for moisture deficit stress tolerance

The phenotypic evaluation was performed in BC2F4 lines in augmented design (with 1m2 plot size) and 38 superior lines with rust resistance were advanced to BC2F5 for evaluation of yield and moisture deficit stress component traits in large plots (7.2m2) with RBD under irrigated (IR) and restricted irrigation (RI) conditions. The BC2F4 lines, HD3086-E-5-17-461-50 and HD3086-C-6-2-481-51 recorded the highest yield per plot followed by HD3086-M-1-26-410-46 and HD3086-F-13-1-512-53 during 2020-2021 under RI condition. The same lines advanced to BC2F5 showed consistent superior performance during the year 2021-22. The correlation study depicted that NDVI, LCI, TKW and GWPS were positively correlated with yield, while CT and DH were negatively correlated with yield under moisture deficit stress. MABB derived lines containing targeted QTLs were having significantly superior performance over the checks. All the 38 BC2F5 lines were evaluated under RI and IR conditions for distinctness, uniformity and stability (DUS) characterization. Eight lines are found to be consistent in performance during both the years and on par or superior to recurrent parent under moisture deficit stress with maximum phenotypic similarity to recurrent parent HD3086. All the superior 8 lines *viz*., HD3086-M-1-26-410-46, HD3086-M-1-36-413-47, HD3086-M-1-49-417-48, HD3086-M-1-55-419-49, HD3086-E-5-17-461-50, HD3086-C-6-2-481-51, HD3086-I-3-1-507-52, HD3086-F-13-1-512-53 were selected for subsequent entry and release (Table 4). The derived line HD3086-C-6-2-481-51 named HD3471, is nominated for national trials for testing and further release for commercial cultivation.

# Discussion

The wheat varieties which can grow well and produce better yields in moisture deficit/dry land areas along with resistance to biotic stresses such as leaf rust are the immediate priority of the wheat breeding program. Several severe rust epidemics have been recorded in India since the early 1800s due to cereal rust diseases (Joshi et al., 1977). An effective and desirable method would be combining conventional wheat breeding with MABB by introducing targeted genes or QTLs into superior wheat cultivars for overcoming such biotic and abiotic stresses (Collard and Mackill, 2008). MAS has been used frequently in bread wheat for introgression of traits such as disease resistance and quality improvement [(Barloy et al., 2007; Gupta et al., 2010; Kumar et al., 2010; Malik et al., 2015; Shah et al., 2017; Sharma et al., 2021)]. However, it has been used rarely to improve moisture deficit stress tolerance in wheat (Merchuk-Ovnat et al., 2016; Rai et al., 2018). In the current study, we developed improved lines with resistance to leaf rust and relatively higher grain yield under RI conditions by transferring leaf rust resistance gene *Lr24* and major QTLs linked to component traits of moisture deficit stress tolerance.

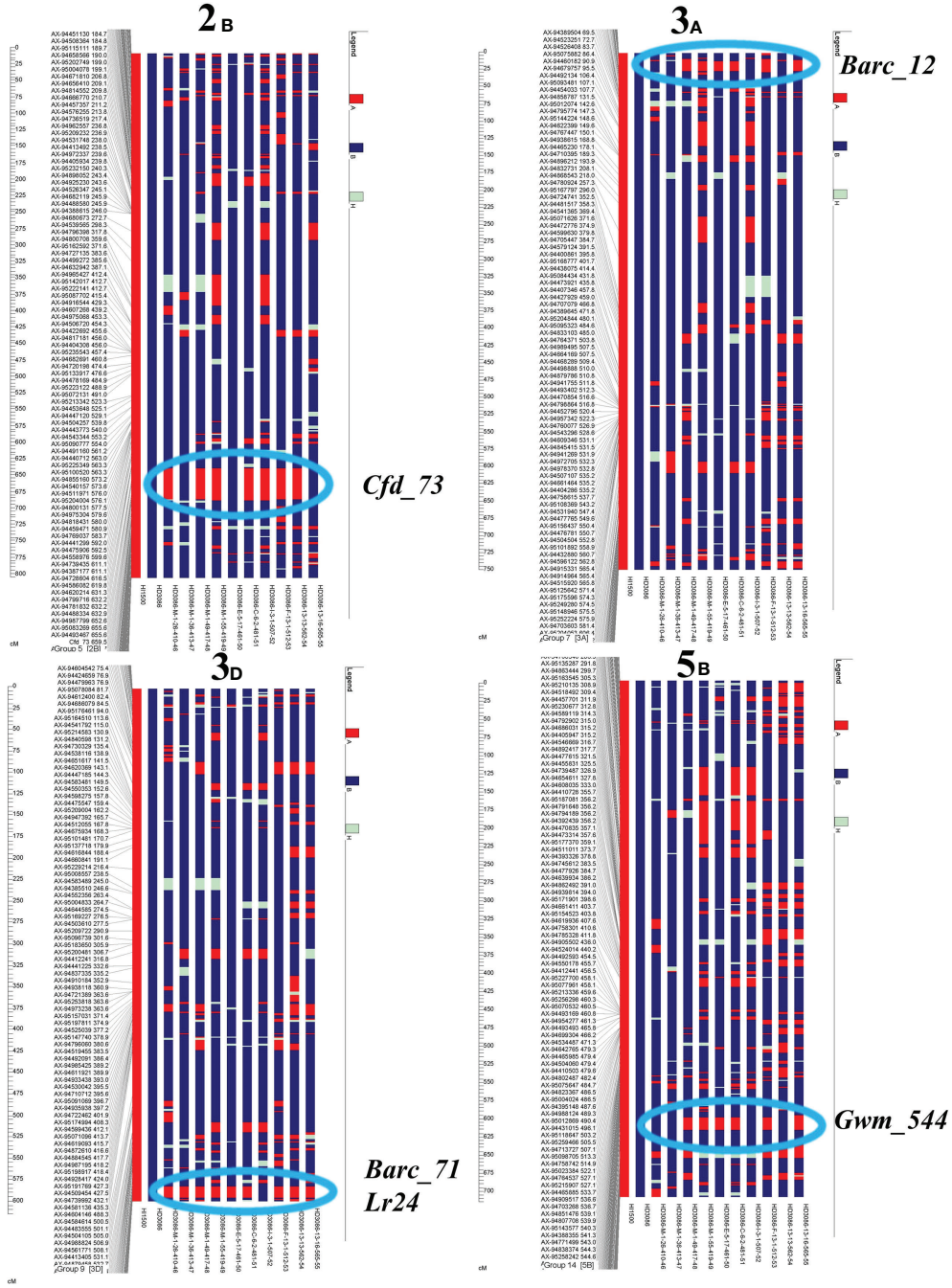


FIGURE 4
Recurrent parent recovery of chromosomes 2B, 3A, 3D and 5B.

The component traits of moisture deficit stress tolerance such as NDVI, LCI, and TKW had positive correlation and traits like CT and DH showed negative correlation with grain yield under the current investigation as previously reported (Lopes and Reynolds, 2012; Harikrishna et al., 2016; Ramya et al., 2016). Therefore, component traits of moisture deficit stress tolerance such as NDVI, leaf chlorophyll index, and canopy temperature strategically coupled with yield had a complementing influence on productivity under moisture deficit stress.

TABLE 4 Morpho-physiological characteristics of HD3086*2/HI1500 selected $BC_2F_5$ lines for component traits of moisture deficit stress tolerance under moisture deficit stress condition.

| S.no | Selected progeny | QTLs linked trait | Leaf chlorophyll index (LCI) | | Canopy temperature (°C) | | | NDVI | | | GL (mm) | DH (days) | GWPS (g) | TKW (g) | YLD (q/ha) | APR | Total % RPG % |
|---|---|---|---|---|---|---|---|---|---|---|---|---|---|---|---|---|---|
| | | | VS | GFS | VS | GFS | GMS | VS | GFS | GFS | | | | | | | |
| 1 | HD3086-M-1-26-410-46 | NDVI +*Lr24* | 44.5 | 51.8 | 28.3 | 31 | 35.3 | 0.78 | 0.66 | 0.42 | 6.84 | 88 | 1.22 | 34 | 45.01 | R | 88.31 |
| 2 | HD3086-M-1-36-413-47 | DH +*Lr24* | 51.2 | 48.4 | 25.8 | 31.6 | 35.3 | 0.77 | 0.65 | 0.41 | 6.79 | 83 | 1.71 | 41.3 | 40.16 | R | 90.46 |
| 3 | HD3086-M-1-49-417-48 | TKW +CT +*Lr24* | 49.2 | 54.2 | 27.5 | 32.1 | 35.5 | 0.76 | 0.65 | 0.4 | 7.11 | 92 | 1.41 | 39.4 | 42.24 | MR | 87.37 |
| 4 | HD3086-M-1-55-419-49 | CT +TKW +*Lr24* | 50.5 | 51.6 | 26.4 | 32.5 | 35.4 | 0.78 | 0.64 | 0.42 | 7.27 | 91 | 1.39 | 43.2 | 36.7 | R | 82.74 |
| 5 | HD3086-E-5-17-461-50 | CT+Chl +*Lr24* | 50.2 | 52.7 | 21.1 | 30.3 | 33.9 | 0.78 | 0.68 | 0.46 | 7.11 | 96 | 1.83 | 42.5 | 47.53 | R | 95.24 |
| 6 | HD3086-C-6-2-481-51 | CT +NDVI +TKW +*Lr24* | 48.4 | 54.6 | 28 | 32.7 | 34.4 | 0.72 | 0.61 | 0.32 | 6.61 | 90 | 1.74 | 41 | 48.11 | R | 93.87 |
| 7 | HD3086-I-3-1-507-52 | NDVI +TKW | 52.2 | 55.2 | 27 | 31.5 | 35.8 | 0.77 | 0.62 | 0.35 | 6.95 | 88 | 1.29 | 40.1 | 36.7 | MR | 81.71 |
| 8 | HD3086-F-13-1-512-53 | CT+ TKW +*Lr24* | 45.5 | 47.9 | 26.9 | 30.6 | 36 | 0.75 | 0.6 | 0.37 | 6.65 | 88 | 1.95 | 33.2 | 44.87 | R | 83.97 |
| 9 | HD3086-13-13-562-54 | NDVI +*Lr24* | 51.2 | 51.4 | 26.6 | 32 | 35.3 | 0.79 | 0.64 | 0.5 | 6.44 | 93 | 1.13 | 34.6 | 38.36 | R | 79.13 |
| 10 | HD3086-13-16-565-55 | CT+*Lr24* | 52 | 54.2 | 28.8 | 32.4 | 34.8 | 0.79 | 0.63 | 0.49 | 7.09 | 100 | 1.22 | 33.9 | 42.93 | R | 82.33 |
| | HD3086(RI) | | 46.3 | 51.4 | 29.1 | 31.3 | 36.8 | 0.78 | 0.61 | 0.32 | 7.01 | 92 | 0.9 | 33.3 | 34.34 | S | |
| | HD3086(IR) | | 49.4 | 52.6 | 22 | 31.3 | 32 | 0.79 | 0.72 | 0.54 | 7.1 | 93 | 1.65 | 45.6 | 63.57 | S | |
| | HI1500(RI) | | 50.2 | 50.4 | 27.9 | 30.5 | 35.7 | 0.77 | 0.65 | 0.4 | 7.18 | 86 | 1.5 | 36.1 | 37.82 | R | |
| | HI1500(IR) | | 49.2 | 51.6 | 24.5 | 29 | 31.5 | 0.75 | 0.63 | 0.4 | 7.19 | 89 | 1.69 | 43.5 | 39.84 | R | |
| | Mean | | 49.1 | 51.9 | 26.95 | 31.54 | 35.35 | 0.77 | 0.64 | 0.41 | 6.92 | 90.5 | 1.44 | 37.63 | 41.23 | | |
| | CD at 5% | | 2.42 | 2.49 | 0.97 | 1.65 | 1.56 | 0.04 | 0.02 | 0.02 | 0.31 | 4.35 | 0.06 | 1.64 | 2.25 | | |

CD, Critical Difference; LCI, Leaf Chlorophyll Index; NDVI, Normalized Difference Vegetation Index; GL, Grain Length; GWPS, Grain Weight Per Spike; TKW, Thousand Kernel Weight LR, Leaf rust; YLD, Yield; APR, Adult Plant Resistance; R, Resistant; MR, Moderately resistant; S, Susceptible; RPG, Recurrent Parent Genome; RI, Rainfed; IR, Irrigated; VS, Vegetative stage; GFS, Grain Filling Stage; GMS, Grain Maturity Stage.

## Marker-assisted selection for leaf rust resistance gene *Lr24*

Leaf rust resistance gene *Lr24*, derived from *Thinopyrum elongatum*, confers resistance right from the seedling stage and is associated with the stem rust resistance gene *Sr24* (McIntosh et al., 1976; Singh et al., 2006). Therefore, the *Lr24*/*Sr24* confers resistance to the most prevalent leaf and stem rust races in India (Singh et al., 2017). Although virulence on *Lr24* has been reported in South Africa, North America, and South America, it still provides effective resistance in India. The first wheat variety containing *Lr24* was released in 1993 and since then, a number of varieties were released with *the Lr24* gene (Tomar et al., 2014). Hence, the presence of *Lr24* in Indian wheat varieties is extremely useful for resistance against leaf rust (Pal et al., 2022). In recent years, new virulent races have appeared against some leaf rust

resistance genes (Prasad et al., 2019) among which 77-9 and 77-5 are most prevalent and virulent. The pathotype, 77-9 was found in 149 rust samples (51.1%), followed by pathotype 77-5 in 15.1% of the wheat leaf rust (Pt) samples collected from India and Nepal. The pathotype 77-9, which is virulent to *Lr37*, was unable to overcome the resistance of many varieties due to the presence of *Lr24* (Tinku Gautam et al., 2020b).

The traditional backcross strategy for transferring rust resistance genes needs discriminating races to be screened at the seedling or adult stage under epiphytotic circumstances. With the advent of genetic markers linked to resistance genes, it is possible to precisely identify the targeted rust resistance gene (s) in segregating populations (Sivasamy et al., 2009; Revathi et al., 2010; Bhawar et al., 2011). The polymorphic SCAR markers were developed for *Agropyron elongatum* derived leaf rust resistance gene *Lr24* and utilized in marker assisted selection (Gupta et al., 2006). Due to the dominant nature of the SCAR marker, identification of homozygous plants with *Lr24* in BC2F2 is not possible. Hence, it needs progeny testing in the BC2F3 generation to identify homozygous plants. In addition to this, specific microsatellite markers, *Xgwm114* and *Xbarc71*, were developed for *the Lr24* locus to select homozygous plants for leaf rust resistance at early generations (Pallavi et al., 2015) such as BC1F1, BC2F1, and BC2F2 generations. Therefore, we used codominant SSR marker *Xbarc71* in addition to *Lr24/Sr24* SCAR marker to select homozygous plants for *Lr24* in BC2F2. Homozygous lines for *Lr24* were selected in BC2F2 generation along with the phenotypic selection at each backcross generation for leaf rust in the seedling stage (SRT) and in the adult plant stage. Along with MAS, the phenotypic section for targeted traits increases the efficiency of selection (Davies et al., 2006). We developed 19 resistant (7 HR+ 10 R+2 MR) lines in BC2F4 generation against 77-5 and 77-9 races of leaf rust at two different locations. Similarly, leaf rust resistance genes *Lr19* and *Lr24* derived from *Thinopyrum* (syn. *Agropyron*) were transferred into superior wheat cultivar HD2733 through marker-assisted selection (Singh et al., 2017). The genomic segment carrying the *Lr24/Sr24* genes also resulted in improved grain quality without any yield penalty in HD2733 suggesting the added gains of utilizing this region for improving grain quality besides leaf rust resistance (Rai et al., 2021). In another study, major QTL for post-harvest sprouting tolerance and *Lr* genes such as *Lr24* + *Lr28* were transferred into a cultivar HD2329 using MAS against virulent pathotype 77-5 (Kumar et al., 2010).

## Marker-assisted selection for component traits of moisture deficit stress tolerance

tBreeding for complex traits like moisture deficit stress tolerance is a challenging task with conventional breeding methods due to the inheritance of polygenes and with relatively low heritability and high environmental influence (Talukdar et al., 2014; Ramya et al., 2016). Therefore, molecular markers assisted breeding is a better option to develop moisture deficit stress tolerance along with disease resistance. Numerous studies have revealed QTLs for grain yield and component traits of moisture deficit stress tolerance (Pinto et al., 2010; Gupta et al., 2012; Gupta et al., 2017; Shashikumara et al., 2020), which can be used in practical breeding with MABB for an effective and desirable way to introduce them into superior wheat cultivars (Collard and Mackill, 2008). CT, NDVI, LCI, and TKW are thought to be complementary traits to yield because they enhance wheat yield under moisture deficit through stress tolerance mechanisms (Lopes and Reynolds, 2012). Therefore, in this study 3 QTLs linked to component traits of moisture deficit stress tolerance (NDVI and TKW: *Xcfd73*, CT and Leaf chlorophyll index: *Xbarc12*, CT: *Xgwm544)* have been successfully transferred in the genetic background of HD3086 through MABB along with phenotypic selection. These three QTLs under transfer were validated in RIL population HI1500 x DBW43 by Harikrishna (2017). In past, a few studies have introduced QTLs into wheat to enhance drought tolerance and yield under moisture deficit conditions (Merchuk-Ovnat et al., 2016; Rai et al., 2018; Gautam et al., 2020a; Todkar et al., 2020).

Foreground selection was undertaken in BC1F1, BC2F1 and BC2F2 for the successful transfer of three QTLs in combination linked to component traits of moisture deficit stress tolerance in the present study. The four lines having better grain yield of 30-40% and best yield improvement observed in line having QTLs combination linked to traits NDVI, CT and TKW along with leaf rust resistance over recurrent parent HD3086 were developed and proposed to the varietal trial evaluation program (Figure 5). In a similar previous study by Rai et al. (2018) five potential varieties performing well under rain fed conditions were developed in the background of HD2733 lines by transferring NDVI, CT and chlorophyll content linked QTLs through MABB. Similarly, variety GW322 was improved for traits NDVI, stay green, chlorophyll content and yield through MABB and 18 superior BC2F3 moisture deficit stress tolerant progenies were identified (Todkar et al., 2020).

It is challenging to cover entire genomic regions with evenly dispersed polymorphic markers due to the large genome size of wheat (~16GB; Somers et al., 2004). To speed up the RPG recovery in MABB, background selection utilizing polymorphic markers with genome-wide coverage has been widely adopted (Chen et al., 2008; Basavaraj et al., 2010). SNPs would be a preferable option for the background selection in MABB because the background analysis using SNP assay was over 300 times more cost-effective than SSR markers (Khanna et al., 2015). We performed background analysis of selected BC2F4 lines using 35k SNPs to identify the plant with maximum recurrent parent

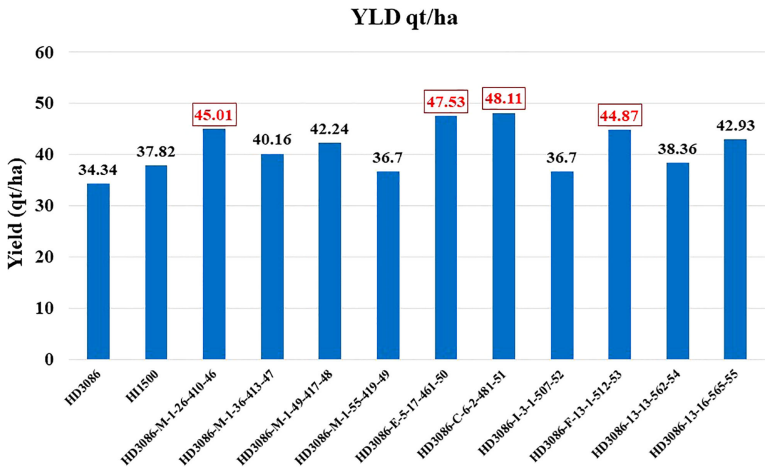


FIGURE 5
Improvement in grain yield of selected lines of HD3086*2/HI1500 derived $BC_2F_5$ population under moisture deficit stress.

genome and obtained a recovery range of selected lines from 79 to 95% with an average recovery of 86%. Two selected lines with positive *Lr24* allele *viz*., HD3086-C-6-2-481-51and HD3086-E-5-17-461-50 were having a recovery of about 95.24% and 93.87% respectively. Similarly, 94.55% genome recovery in BC2 generations was observed during pyramiding of leaf rust resistance genes into an elite cultivar HD2687 (Bhawar et al., 2011) and genome recovery of 89.2%–95.4% for drought tolerance QTLs into HD2733 by Rai et al. (2018) in MABB studies.

## Conclusion

The current study is on the improvement of wheat cultivar for both biotic and abiotic stresses in combination using MABB and phenotypic selection in wheat. We have transferred *Lr24*, and 3 QTLs linked to component traits of moisture deficit stress tolerance using MABB to develop improved lines for resistance to leaf rust and moisture deficit stress. The improved lines had comparable grain yield production to the original parent, HD3086 along with high chlorophyll content, low canopy temperature, high normalized difference vegetation index, and other favorable morpho-physiological characteristics under moisture deficit stress. Wheat variety HD3086 is a choice of millions of farmers in major wheat growing regions because of its high adaptability and quality. Improvement of other traits of this variety such as disease resistance and moisture deficit stress tolerance help in expanding the area of cultivation with a limited number of irrigations.

## Data availability statement

The raw data supporting the conclusions of this article will be made available by the authors, without undue reservation.

## Author contributions

PS, GS, and NJ designed and supervised the conduct of experiments and provided critical inputs. SP performed experiments. SP, SS, DC, ND, and JS collected phenotypic data. SP, HK, PL, DP, and SM evaluated lines for rust resistance. SP, PS, HK, SS, DC, NS, and KM contributed in the generation of genotyping data. SP, ND, and HK did the statistical analysis. SP, HK, and NJ prepared the manuscript. All authors contributed to the article and approved the submitted version.

## Funding

The part of this research supported by the grant from Bill and Melinda Gates Foundation (OPP1194767) for SNP genotyping and funding from ICAR-NICRA project.

## Acknowledgments

SP acknowledges the ICAR-Indian agriculture research institute (IARI), New Delhi for provided scholarships to complete this work as part of Ph.D. thesis.

## Conflict of interest

The authors declare that the research was conducted in the absence of any commercial or financial relationships that could be construed as a potential conflict of interest.

## Publisher's Note

All claims expressed in this article are solely those of the authors and do not necessarily represent those of their affiliated organizations, or those of the publisher, the editors and the reviewers. Any product that may be evaluated in this article, or claim that may be made by its manufacturer, is not guaranteed or endorsed by the publisher.

## Supplementary Material

The Supplementary Material for this article can be found online at: https://www.frontiersin.org/articles/10.3389/fpls.2022.1035016/full#supplementary-material

## References


Araus, J. L., Slafer, G. A., Royo, C., and Serret, M. D. (2008). Breeding for yield potential and stress adaptation in cereals. *Crit. Rev. Plant Sci.* 27, 377–412. doi: 10.1080/07352680802467736

Bariana, H. S., Babu, P., Forrest, K. L., Park, R. F., and Bansal, U. K. (2022). Discovery of the New Leaf Rust Resistance Gene Lr82 in Wheat: Molecular Mapping and Marker Development. *Genes* 13 (6), 964. doi: 10.3390/genes13060964

Barloy, D., Lemoine, J., Abelard, P., Tanguy, A. M., Rivoal, R., and Jahier, J. (2007). Marker assisted pyramiding of two cereal cyst nematode resistance genes from Aegilops variables in wheat. *Mol. Breed* 20, 31–40. doi: 10.1007/s11032-006-9070-x

Basavaraj, S. H., Singh, V. K., Singh, A., Singh, A., Singh, A., Anand, D., et al. (2010). Marker-assisted improvement of bacterial blight resistance in parental lines of pusa RH10, a superfine grain aromatic rice hybrid. *Mol. Breed* 26 (2), 293–305. doi: 10.1007/s11032-010-9407-3

Bhardwaj, S. C., Kumar, S., Gangwar, O. P., Prasad, P., Kashyap, P. L., Khan, H., et al. (2021). Physiologic specialization and genetic differentiation of puccinia triticina causing leaf rust of wheat in the Indian subcontinent during 2016-2019. *Plant Dis* 105 (7), 1992–2000. doi: 10.1094/PDIS-06-20-1382-RE

Bhardwaj, S. C., Prashar, M., Jain, S. K., Kumar, S., Sharma, Y. P., Sivasamy, M., et al. (2010). Virulence on Lr28 in wheat and its relation to prevalent pathotypes in India. *Cereal Res. Commun.* 38, 83–89. doi: 10.1556/crc.38.2010.1.9

Bhardwaj, S. C., Prashar, M., Kumar, S., Jain, S. K., and Datta, D. (2005). Lr19 resistance in wheat becomes susceptible to puccinia triticina in India. *Plant Dis.* 89, 1360. doi: 10.1094/PD-89-1360A

Bhardwaj, S. C., Prashar, M., Kumar, S., Jain, S. K., Sharma, Y. P., and Kalappanavar, I. K. (2011). Two new pathotypes 125R28 and 93R37 of puccinia triticina on wheat from India and sources of resistance. *Indian Phytopathol.* 64 (3), 240–242.

Bhawar, K. B., Vinod,, Sharma, J. B., Singh, A. K., Sivasamy, M., Singh, M., et al. (2011). Molecular marker assisted pyramiding of leaf rust resistance genes Lr19 and Lr28 in bread wheat wheat (Triticum aestivum l.) variety HD2687. *Indian J. Genet.* 71 (4), 304–311.

Chen, S., Xu, C. G., Lin, X. H., and Zhang, Q. (2008). Improving bacterial blight resistance of '6078', an elite restorer line of hybrid rice, by molecular marker-assisted selection. *Plant Breed* 120 (2), 133–137. doi: 10.1046/j.1439-0523.2001.00559.x

Collard, B. C., and Mackill, D. J. (2008). Marker-assisted selection: an approach for precision plant breeding in the twenty-first century. *Philos. Trans. R. Soc Lond. B. Biol. Sci.* 363, 557–572. doi: 10.1098/rstb.2007.2170

Condon, A. G., Richards, R. A., Rebeteke, G. J., and Farquhar, G. D. (2004). Breeding for high water use efficiency. *J. of Experimental Botany* 55, 2247–2480. doi: 10.1093/jxb/erh277

Davies, J., Berzonsky, W. A., and Leach, G. D. (2006). A comparison of marker-assisted and phenotypic selection for high grain protein content in spring wheat. *Euphytica* 152, 117–134. doi: 10.1007/s10681-006-9185-5

Diab, A. A., Kantety, R. V., Ozturk, N. Z., Benscher, D., Nachit, M. M., and Sorrells, M. E. (2008). Drought-inducible genes and differentially expressed sequence tags associated with components of drought tolerance in durum wheat. *Sci. Res. Essay* 3 (1):009–026

Gautam, T., Dhillon, G. S., Saripalli, G., Singh, V. P., Prasad, P., Kaur, S., et al. (2020b). Marker-assisted pyramiding of genes/QTL for grain quality and rust resistance in wheat (Triticum aestivum l.). *Mol. Breed.* 40 (5), 1–14. doi: 10.1007/s11032-020-01125-9

Gautam, T., Saripalli, G., Kumar, A., Gahlaut, V., Gadekar, D. A., Oak, M., et al. (2020a). Introgression of a drought insensitive grain yield QTL for improvement of four Indian bread wheat cultivars using marker assisted breeding without background selection. *J. Plant Biochem. Biotechnol.* 30 (1), 172–183. doi: 10.1007/s13562-020-00553-0

Griffiths, S., Simmonds, J., Leverington, M., Wang, Y., Fish, L., Sayers, L., et al. (2009). Meta-QTL analysis of the genetic control of ear emergence in elite European winter wheat germplasm. *Theor. Appl. Genet.* 119 (3), 383–395. doi: 10.1007/s00122-009-1046-x

Gupta, P. K., Balyan, H. S., and Gahlaut, V. (2017). QTL analysis for drought tolerance in wheat: present status and future possibilities. *Agronomy* 7, 1–21. doi: 10.3390/agronomy7010005

Gupta, P. K., Balyan, H. S., Gahlaut, V., and Kulwal, P. L. (2012). Phenotyping, genetic dissection, and breeding for drought and heat tolerance in common wheat: Status and prospects. *Plant Breed. Rev.* 36, 85–168. doi: 10.1002/9781118358566

Gupta, P. K., Langridge, P., and Mir, R. R. (2010). Marker-assisted wheat breeding: present status and future possibilities. *Mol. Breeding* 26 (2), 145–61. doi: 10.1007/s11032-009-9359-7

Gupta, S. K., Charpe, A., Koul, S., Haque, Q. M. R., and Prabhu, K. V. (2006). Development and validation of SCAR markers co-segregating with an agropyron elongatum derived leaf rust resistance gene Lr24 in wheat. *Euphytica* 150 (1), 233–240. doi: 10.1007/s10681-006-9113-8

Harikrishna, (2017). *Marker assisted recurrent selection (MARS) for drought tolerance in wheat* (New Delhi: Indian Agricultural Research Institute).

Harikrishna,, Singh, G. P., Neelu, J., Singh, P. K., Sai Prasad, S. V., Ambati, D., et al. (2016). Physiological characterization and grain yield stability analysis of RILs under different moisture stress conditions in wheat (Triticum aestivum l.). *Ind. J. Plant Physiol.* 21, 576–582. doi: 10.1007/s40502-016-0257-9

Hospital, F., and Charcosset, A. (1997). Marker assisted introgression of quantitative trait loci. *Genetics* 147, 1469–1485. doi: 10.1093/genetics/147.3.1469

Joshi, L. M., Nagarajan, S., and Srivastava, K. D. (1977). Epidemiology of brown and yellow rusts of wheat in North India I. Place and time of appearance and spread. Phytopathologische Zeitschrift, 90 (2), 116–122.

Joshi, L. M., and Singh, D. V. (1988). *Manual of wheat diseases*, Malhotra Publishing House New Delhi.

Khanna, A., Sharma, V., Ellur, R. K., Shikari, A. B., Gopala Krishnan, S., Singh, U. D., et al. (2015). Development and evaluation of near-isogenic lines for major blast resistance gene (s) in basmati rice. *Theor. Appl. Genet.* 128 (7), 1243–1259. doi: 10.1007/s00122-015-2502-4

Kuchel, H., Ye, G., Fox, R., and Jefferies, S. (2005). Genetic and economic analysis of a targeted marker-assisted wheat breeding strategy. *Molecular Breeding* 16, 67–78. doi: 10.1007/s11032-005-4785-7

Kumar, J., Mir, R. R., Kumar, N., Kumar, A., Mohan, A., Prabhu, K. V., et al. (2010). Marker-assisted selection for pre-harvest sprouting tolerance and leaf rust

resistance in bread wheat. *Plant Breed* 129, 617–621. doi: 10.1111/j.1439-0523.2009.01758.x

Kumar, S., Sehgal, S. K., Kumar, U., Vara Prasad, P. V., Joshi, A. K., and Gill, B. S. (2012). Genomic characterization of drought tolerance related traits in spring wheat. *Euphytica* 186, 265–276. doi: 10.1007/s10681-012-0675-3

Langridge, P., and Reynolds, M. P. (2015). Genomic tools to assist breeding for drought tolerance. *Curr. Opin. Biotechnol.* 32, 130–135. doi: 10.1016/j.copbio.2014.11.027

Liu, Y., Wang, R., Hu, Y. G., and Chen, J. (2018). Genome-wide linkage mapping of quantitative trait loci for late-season physiological and agronomic traits in spring wheat under irrigated conditions. *Agronomy* 8, 60. doi: 10.3390/agronomy8050060

Lopes, M. S., and Reynolds, M. P. (2012). Stay-green in spring wheat can be determined by spectral reflectance measurements (normalized difference vegetation index) independently from phenology. *J. Exp. Bot.* 63, 3789–3798. doi: 10.1093/jxb/ers071

Mago, R., Bariana, H. S., Dundas, I. S., Spielmeyer, W., Lawrence, G. J., Pryor, A. J., et al. (2005). Development of PCR markers for the selection of wheat stem rust resistance genes Sr24 and Sr26 in diverse wheat germplasm. *Theor. Appl. Genet.* 111 (3), 496–504. doi: 10.1007/s00122-005-2039-z

Malik, N., Vinod, S. J. B., Tomar, R. S., Sivasamy, M., and Prabhu, K. V. (2015). Marker-assisted backcross breeding to combine multiple rust resistance in wheat. *Plant Breed* 134 (2), 172–177. doi: 10.1111/pbr.12242

McIntosh, R. A., Dubcovsky, J., Rogers, W. J., Morris, C., and Xia, X. C. (2017) *Catalogue of gene symbols for wheat: 2017 supplement*. Available at: https://shigen.nig.ac.jp/wheat/komugi/genes/macgene/supplement2017.pdf.

McIntosh, R. A., Dyck, P. L., and Green, G. J. (1976). Inheritance of leaf rust and stem rust resistances in wheat varieties Agent and Agatha. *Aust. J. Agric. Res.* 28, 37–45.

Merchuk-Ovnat, L., Barak, V., Fahima, T., Ordon, F., Lidzbarsky, G. A., Krugman, T., et al. (2016). Ancestral QTL alleles from wild emmer wheat improve drought resistance and productivity in modern wheat cultivars. *Front. Plant Sci.* 7, 452. doi: 10.3389/fpls.2016.00452

Olivares-Villegas, J. J., Reynolds, M. P., and McDonald, G. K. (2007). Drought-adaptive attributes in the Seri/Babax hexaploid wheat population. *Funct. Plant Biol.* 34, 189–203. doi: 10.1071/FP06148

Olivares-Villegas, J. J., Reynolds, M. P., William, H. M., McDonald, G. K., and Ribaut, J. M. (2008). Drought adaptation attributes and associated molecular markers via BSA in the Seri/Babax hexaploid wheat (*Triticum aestivum* L.) population. In: *Proceedings of the 11th international wheat genetics symposium*. (Australia: Brisbane), pp. 24–29.

Pal, D., Kumar, S., Bhardwaj, S. C., Devate, N. B., Patial, M., and Parmeshwarappa, S. K. V. (2022). Molecular marker aided characterization of race specific and non-race specific rust resistance genes in elite wheat (Triticum spp.) germplasm. *Australas. Plant Pathol.* 51 (2), 261–272. doi: 10.1007/s13313-022-00850-3

Pallavi, J. K., Singh, A., Rao, U. I., and Prabhu, K. V. (2015). Identification and validation of a microsatellite marker for the seedling resistance gene Lr24 in bread wheat. *J. Plant Pathol. Microbiol.* 6 (6), 1. doi: 10.4172/2157-7471.1000276

Peterson, R. F., Campbell, A. B., and Hannah, A. E. (1948). A diagrammatic scale for estimating rust intensity on leaves and stems of cereals. *Can. J. Res.* 26 (5), 496–500. doi: 10.1139/cjr48c-033

Pinto, R. S., and Reynolds, M. P. (2015). Common genetic basis for canopy temperature depression under heat and drought stress associated with optimized root distribution in bread wheat. *Theor. Appl. Genet.* 128 (4), 575–585. doi: 10.1007/s00122-015-2453-9

Pinto, R. S., Reynolds, M. P., Mathews, K. L., McIntyre, C. L., Olivares-Villegas, J. J., and Chapman, S. C. (2010). Heat and drought adaptive QTL in a wheat population designed to minimize confounding agronomic effects. *Theor. Appl. Genet.* 121, 1001–1021. doi: 10.1007/s00122-010-1351-4

Prasad, P., Gangwar, O. P., Bharadwaj, S. C., and Kumar, S. (2019). Monitoring pathotype distribution of puccinia species on wheat and barley. *Mehtaensis* 39, 5–9. doi: 10.13140/RG.2.2.13233.53600

Prasad, P. V. V., Pisipati, S. R., Momčilović, I., and Ristic, Z. (2011). Independent and combined effects of high temperature and drought stress during grain filling on plant yield and chloroplast EF-tu expression in spring wheat. *J. Agron. Crop Sci.* 197 (6), 430–441. doi: 10.1111/j.1439-037X.2011.00477.x

Quarrie, S. A., Steed, A., Calestani, C., Semikhodskii, A., Lebreton, C., Chinoy, C., et al. (2005). A high-density genetic map of hexaploid wheat (Triticum aestivum l.) from the cross Chinese spring× SQ1 and its use to compare QTLs for grain yield across a range of environments. *Theor. Appl. Genet.* 110, 865–880. doi: 10.1007/s00122-004-1902-7

Qureshi, N., Bariana, H., Kumran, V. V., Muruga, S., Forrest, K. L., Hayden, M. J., et al. (2018). A new leaf rust resistance gene Lr79 mapped in chromosome 3BL from the durum wheat landrace Aus26582. *Theor. Appl. Genet.* 131 (5), 1091–1098. doi: 10.1007/s00122-018-3060-3

Rai, A., Ahlawat, A. K., Shukla, R. B., Jain, N., Kumar, R. R., and Mahendru-Singh, A. (2021). Quality evaluation of near-isogenic line of the wheat variety HD2733 carrying the Lr24/Sr24 genomic region. *3 Biotech.* 11 (3), 1–10. doi: 10.1007/s13205-021-02679-x

Rai, N., Bellundagi, A., Kumar, P. K., Kalasapura Thimmappa, R., Rani, S., Sinha, N., et al. (2018). Marker-assisted backcross breeding for improvement of drought tolerance in bread wheat (Triticum aestivum l. em thell). *Plant Breed.* 137 (4), 514–526. doi: 10.1111/pbr.12605

Ramya, P., Singh, G. P., Neelu, J., Singh, P. K., Manoj, K. P., Kavita, S., et al. (2016). Effect of recurrent selection on drought tolerance and related morpho-physiological traits in bread wheat. *PloS One* 11 (6), e0156869. doi: 10.1371/journal.pone.0156869

Revathi, P., Tomar, S. M. S., Vinod,, and Singh, N. K. (2010). Marker assisted gene pyramiding of leaf rust resistance genes *Lr24*, *Lr28* along with stripe rust resistance gene *Yr15* in wheat (*Triticum aestivum* l.). *Indian J. Genet. Plant Breed* 70, 349–354.

Reynolds, M. P. (2001). *Application of physiology in wheat breeding*. Eds. J. I. Ortiz-Monasterio and A. McNab (Mexico, D.F: CIMMYT), 88–100.

Reynolds, M. P., and Langridge, P. (2016). Physiological breeding. *Current Opinion in Plant Biology* 31, 162–171. doi: 10.1016/j.pbi.2016.04.005

Rodell, M., Velicogna, I., and Famiglietti, J. S. (2009). Satellite-based estimates of groundwater depletion in India. *Nature* 460, 999–1002. doi: 10.1038/nature08238

Schachermayr, G. M., Messmer, M. M., Feuillet, C., Winzeler, H., Winzeler, M., and Keller, B. (1995). Identification of molecular markers linked to the agropyron elongatum-derived leaf rust resistance gene Lr24 in wheat. *Theor. Appl. Genet.* 90 (7), 982–990. doi: 10.1007/BF00222911

Shah, L., Ali, A., Zhu, Y., Wang, S., Si, H., and Ma, C. (2017). Wheat resistance to fusarium head blight and possibilities of its improvement using molecular marker-assisted selection. *Czech J. Genet. Plant Breed* 53, 47–54. doi: 10.17221/139/2016-CJGPB

Sharma, V., Dubey, R. B., and Khan, R. (2019). Genotype-environment interaction on stability of grain yield and physio-biochemical traits in bread wheat (Triticum aestivum l.). *Bangladesh J. Bot.* 48 (4), 1143–1151. doi: 10.3329/bjb.v48i4.49070

Sharma, A., Srivastava, P., Mavi, G. S., Kaur, S., Kaur, J., Bala, R., et al. (2021). Resurrection of wheat cultivar PBW343 using marker-assisted gene pyramiding for rust resistance. *Front. Plant Sci.* 12. doi: 10.3389/fpls.2021.570408

Shashikumara, P., Harikrishna.,, Manu, B., Sunil, B., Sunilkumar, V. P., Nivedita., S., et al. (2020). Mapping genomic regions of moisture deficit stress tolerance using backcross inbred lines in wheat (Triticum aestivum l.). *Sci. Rep.* 10, 21646. doi: 10.1038/s41598-020-78671-x

Singh, M., Mallick, N., Chand, S., Kumari, P., Sharma, J. B., Sivasamy, M., et al. (2017). Marker-assisted pyramiding of thinopyrum-derived leaf rust resistance genes Lr19 and Lr24 in bread wheat variety HD2733. *J. Genet.* 96 (6), 951–957. doi: 10.1007/s12041-017-0859-7

Singh, R. P., Hodson, D. P., Jin, Y., Huerta-Espino, J., Kinyua, M. G., Wanyera, R., et al. (2006). Current status, likely migration and strategies to mitigate the threat to wheat production from race Ug99 (TTKS) of stem rust pathogen. *CAB Reviews* 1, 54. doi: 10.1079/PAVSNNR20061054"10.1079/PAVSNNR20061054

Sinha, S. K. (1986). *Approaches for incorporating drought and salinity resistance in crop plants*. Eds. V. L. Chopra and R. S. Paroda (New Delhi: Oxford and IBH), 58–78.

Sivasamy, M., Tiwari, S., Tomar, R. S., Singh, B., Sharma, J. B., Tomar, S. M. S., et al. (2009). Introgression of useful linked genes for resistance to stem rust, leaf rust and powdery mildew and their molecular validation in wheat (Triticum aestivum l.). *Indian J. Genet. Plant Breed.* 69 (1), 17.

Somers, D. J., Isaac, P., and Edwards, K. (2004). A high-density microsatellite consensus map for bread wheat (Triticum aestivum l.). *Theor. Appl. Genet.* 109, 1105–1114. doi: 10.1007/s00122-004-1740-7

Stakman, E. C., Stewart, D. M., and Loegering, W. Q. (1962). *Identification of physiologic races of puccinia graminis var. tritici*. US Dep. Agric. Res. Serv. (Washington: USDA). pp. 53.

Talukdar, A., Shivakumar, M., Verma, K., Kumar, A., Mukherjee, K., and Lal, S. K. (2014). Genetic elimination of kunitz trypsin inhibitor (KTI) from DS9712, an Indian soybean variety. *Indian J. Genet.* 74 (4 Suppl), 608–611. doi: 10.5958/0975-6906.2014.00898.0

Todkar, L., Singh, G. P., Jain, N., Singh, P. K., and Prabhu, K. V. (2020). Introgression of drought tolerance QTLs through marker assisted backcross breeding in wheat (Triticum aestivum l.). *Indian J. Genet. Plant Breed.* 80 (02), 209–212. doi: 10.31742/IJGPB.80.2.12

Tomar, S. M. S., Sanjay, K., Singh, M., Sivasamy,, and Vinod, (2014). Wheat rusts in India: Resistance breeding and gene deployment – a review. *Indian J. Genet.* 74 (2), 129–156. doi: 10.5958/0975-6906.2014.00150.3

Van Berloo, R. (2008). GGT 2.0: versatile software for visualization and analysis of genetic data. *J. Heredity* 99 (2), 232–236. doi: 10.1093/jhered/esm109

Weier, J., and Herring, D. (2000). Measuring vegetation (ndvi & evi). *NASA Earth Observatory* 20, 2.

Yang, H., Hu, W., Zhao, J., Huang, X., Zheng, T., and Fan, G. (2021). Genetic improvement combined with seed ethephon priming improved grain yield and drought resistance of wheat exposed to soil water defcit at tillering stage. *Plant Growth Regul.* 95 (3), 399–419. doi: 10.1007/s10725-021-00749-x

Yang, D. L., Jing, R. L., Chang, X. P., and Li, W. (2007). Quantitative trait loci mapping for chlorophyll fluorescence and associated traits in wheat (Triticumaestivum). *J. Integr. Plant Biol.* 49(4), 646–654. doi: 10.1111/j.1744-7909.2007.00443.x

Zadoks, J. C., Chang, T. T., and Cal Konzak, C. F. (1974). A decimal code for the growth stages of cereals. *Weed Res.* 14 (6), 415–421. doi: 10.1111/j.1365-3180.1974.tb01084

frontiers | Frontiers in Plant Science

TYPE Systematic Review
PUBLISHED 31 October 2022
DOI 10.3389/fpls.2022.1037206



OPEN ACCESS

EDITED BY
Pradeep Sharma,
Indian Institute of Wheat and Barley Research (ICAR), India

REVIEWED BY
Amit Kumar,
Central Sericultural Research & Training Institute (CSRTI), India
Mansi Sharma,
Dalhousie University, Canada

*CORRESPONDENCE
Upendra Kumar
baliyan.upendra@gmail.com
Vijai Malik
gathwalajai@gmail.com

SPECIALTY SECTION
This article was submitted to Plant Abiotic Stress, a section of the journal Frontiers in Plant Science

RECEIVED 05 September 2022
ACCEPTED 07 October 2022
PUBLISHED 31 October 2022

CITATION
Kumar V, Sharma H, Saini L, Tyagi A, Jain P, Singh Y, Balyan P, Kumar S, Jan S, Mir RR, Djalovic I, Singh KP, Kumar U and Malik V (2022) Phylogenomic analysis of 20S proteasome gene family reveals stress-responsive patterns in rapeseed (*Brassica napus* L.). *Front. Plant Sci.* 13:1037206. doi: 10.3389/fpls.2022.1037206



# Phylogenomic analysis of 20S proteasome gene family reveals stress-responsive patterns in rapeseed (*Brassica napus* L.)

Vivek Kumar[1], Hemant Sharma[2], Lalita Saini[1], Archasvi Tyagi[1], Pooja Jain[1], Yogita Singh[3], Priyanka Balyan[4], Sachin Kumar[2], Sofora Jan[5], Reyazul Rouf Mir[5], Ivica Djalovic[6], Krishna Pal Singh[7,8], Upendra Kumar[3]* and Vijai Malik[1]*

[1]Department of Botany, Chaudhary Charan Singh University, Meerut, UP, India, [2]Department of Genetics and Plant Breeding, Chaudhary Charan Singh University, Meerut, UP, India, [3]Department of Molecular Biology & Biotechnology, College of Biotechnology, Chaudhary Charan Singh (CCS) Haryana Agricultural University, Hisar, India, [4]Department of Botany, Deva Nagri Post Graduate (PG) College, Chaudhary Charan Singh (CCS) University, Meerut, India, [5]Division of Genetics and Plant Breeding, Faculty of Agriculture, Sher-e-Kashmir University of Agricultural Sciences & Technology (SKUAST)-Kashmir, Wadura, India, [6]Institute of Field and Vegetable Crops, National Institute of the Republic of Serbia, Maxim Gorki, Novi Sad, Serbia, [7]Biophysics Unit, College of Basic Sciences & Humanities, Govind Ballabh (GB) Pant University of Agriculture & Technology, Pantnagar, India, [8]Vice-Chancellor's Secretariat, Mahatma Jyotiba Phule Rohilkhand University, Bareilly, India

The core particle represents the catalytic portions of the 26S proteasomal complex. The genes encoding α- and β-subunits play a crucial role in protecting plants against various environmental stresses by controlling the quality of newly produced proteins. The 20S proteasome gene family has already been reported in model plants such as Arabidopsis and rice; however, they have not been studied in oilseed crops such as rapeseed (*Brassica napus* L.). In the present study, we identified 20S proteasome genes for α- (PA) and β-subunits (PB) in *B. napus* through systematically performed gene structure analysis, chromosomal location, conserved motif, phylogenetic relationship, and expression patterns. A total of 82 genes, comprising 35 *BnPA* and 47 *BnPB* of the 20S proteasome, were revealed in the *B. napus* genome. These genes were distributed on all 20 chromosomes of *B. napus* and most of these genes were duplicated on homoeologous chromosomes. The *BnPA* (α1-7) and *BnPB* (β1-7) genes were phylogenetically placed into seven clades. The pattern of expression of all the *BnPA* and *BnPB* genes was also studied using RNA-seq datasets under biotic and abiotic stress conditions. Out of 82 *BnPA/PB* genes, three exhibited high expression under abiotic stresses, whereas two genes were overexpressed in response to biotic stresses at both the seedling and flowering stages. Moreover, an additional eighteen genes were expressed under normal conditions. Overall, the current findings developed our understanding of the organization of the 20S proteasome genes in *B. napus*,

and provided specific *BnPA/PB* genes for further functional research in response to abiotic and biotic stresses.

KEYWORDS

*Brassica napus*, 20S proteasome, phylogenomics, digital expression, environmental stress

## 1 Introduction

Rapeseed (*Brassica napus* L.; 2n=38; AACC genome) is an allotetraploid species that is derived through interspecific hybridization of turnip rape (*B. rapa*; 2n=20; AA) with cabbage (*B. oleracea*; 2n=18; CC) (Peng et al., 1999; Chalhoub et al., 2014). Globally, *B. napus* is one of the major oil crops and ranks third in vegetable oil production. It is commonly used as edible oil (Maršalkienė et al., 2009; Lozano-Baena et al., 2015), condiments (Gilbert et al., 2012, Wiersema and Leon, 2016) and fodder (Cartea et al., 2005) in many parts of the world. In addition, canola oil has medicinal properties including a diuretic (Lust, 1983; Grieve, 1984), analgesic and anticancer activities (Duke, 1983). The crop is adapted to the temperate regions of the world and is therefore, very sensitive to a series of environmental threats such as fungal/bacterial diseases, and cold, heat, and drought stresses. These stresses limit the growth and development at different stages during the crop cycle (Kutcher et al., 2010). The presence of high-quality genome sequences and bioinformatics toolkits may help to identify various genes or gene families to elucidate their functional relevance to environmental stress factors to breed climate-smart cultivars.

The ubiquitin-mediated proteolysis system (UPS) also known as the ubiquitin-proteasome pathway (UPP), regulates the degradation of many proteins in eukaryotic cells (Vierstra, 2009). The UPS consists of two distinct, consecutive steps: ubiquitylation (identification of a substrate) and proteasomal degradation (elimination of the ubiquitinated protein) (Kleiger and Mayor, 2014; Sharma et al., 2016). Briefly, ubiquitination is a complicated process that usually necessitates the use of three enzymes: E1, E2, and E3. Ubiquitin is covalently attached to substrate proteins catalyzed by a cascade of enzymes consisting of ubiquitin activator (E1), conjugase (E2), and ligase (E3). Ubiquitin is commonly conjugated to an internal lysine (Lys) residue but can also be conjugated to the free amino terminus of the substrate *via* its carboxy-terminal glycine. A polyubiquitin chain generated by multiple rounds of ubiquitylation can serve as a signal for degradation by the 26S proteasome machinery, a multiprotein complex consisting of a 20S core particle and 19S regulatory particles (Kleiger and Mayor, 2014). The proteasome has two main origins: the primitive form seen in *Thermoplasma acidophilum* (Archaea bacteria) and the evolutionarily improved form found in yeast, plants, and mammals. Numerous investigations in eukaryotes have been conducted to understand the dynamics of the proteasomal complex during the last decade (Dantuma and Bott, 2014; Stone, 2019).

The genetics of 20S proteasome core particles in plant species, including Arabidopsis (Yang et al., 2004), rice (Fu et al., 1998) and wheat (Sharma et al., 2022), have been well studied. Morphologically, the 20S core particle is barrel-shaped, and is composed of 28 nonidentical subunits arranged in 4 axially stacked rings. The rings at the two ends are identically formed by 7α subunits, and the rings in the middle are identically formed by 7β subunits. This gives rise to the 20S core particle having a symmetric configuration of α1-7/β1-7/β1-7/α1-7 (Chen and Hochstrasser, 1996; Wolf and Hilt, 2004). The β-subunits β1, β2, and β5 have proteolytic properties for different substrates. The protein enters the 20S core particle through α-subunits present at the top, and after processing this protein comes out through the α-subunits located at the bottom of the core particle (Chen and Hochstrasser, 1996). In Arabidopsis and many eukaryotes, there are 7α- (α1-7) and 7β-subunits (β1-7). Based on nomenclature, these 7 α- and 7 β-subunits can be represented as proteasome alpha A-G and proteasome beta A-G (i.e., PAA-PAG and PBA-PBG) respectively. There are 23 genes encoding 12 α- and 11 β-subunits in Arabidopsis (Fu et al., 1998). Of these subunits, one gene encodes four subunits (1α and 3β) whereas two genes encode the rest of the subunits. In common wheat (*Triticum aestivum*), 67 members of the 20S proteasome α (*TaPA*) and β (*TaPB*) gene family have recently been discovered (Sharma et al., 2022). These 67 *TaPA* and *TaPB* genes were distributed in all 21 chromosomes of wheat and some of them were found to be involved in heat/drought stress tolerance.

Phylogenomics uses genome-wide data to infer the evolution of genes, genomes, and the tree of life. (Eisen, 1998). The term conventional phylogenetics is based upon the study of a few genes or morphology whereas phylogenomics is an update of the term phylogenetics and concentrates on genome-level analysis (DeSalle et al., 2020). According to the principle of phylogenomics, orthologous sequences conserve more protein function than paralogous sequences. The most commonly used data in phylogenomics are sequence data including whole

genome nucleotide sequences, orthologous genomic blocks, core genomes, core coding genomes, exons, introns, and other conserved biological molecules. The present study involves a phylogenomic analysis of the *B. napus* 20S proteasome gene family and its putative role in biotic and abiotic stresses.

# 2 Materials and methods

## 2.1 Analysis of gene sequence

### 2.1.1 Identification and retrieval of 20S proteasome gene sequences

Since 20S proteasome family genes have already been characterized in *Arabidopsis thaliana* and rice (*Oryza sativa*), the DNA and protein sequences of *AtPA/PB* and *OsPA/PB* were used as a reference to detect the true orthologs in the *B. napus* genome. Criteria for the identification of true orthologs that were developed (Dhaliwal et al., 2014) were strictly followed in the present analysis. The coding DNA sequences of 20S proteasome family genes related to *A. thaliana* and rice were retrieved from the Ensembl Plants database (https://plants.ensembl.org/index.html). Consequently, coding sequences of 24 genes of *A. thaliana* and 23 genes of rice were subjected to tBLASTx and BlastP searches against the *B. napus* genome assembly available at the Ensembl Plants database (https://plants.ensembl.org/Brassica_napus/Info/Index?db=core).

### 2.1.2 Structural features of the 20S proteasome gene family

The tools of Ensembl Plants (https://plants.ensembl.org/index.html), Multiple Em for Motif Elicitation Suite Version 5.4.1 (MEME v5.4.1; https://meme-suite.org/meme/tools/meme) and TB tools (https://github.com/CJ-Chen/TBtools/releases) were employed for gene structure analysis. RepeatMaskerv4.0.9 (https://www.repeatmasker.org/cgi-bin/WEBRepeatMasker) and BatchPrimer3 v1.0 (http://probes.pw.usda.gov/batchprimer3) were used to identify transposable elements (TEs) and microsatellites or simple sequence repeats (SSRs) in gene sequences, respectively. The Plant Care database was used to search for the presence of cis-acting regulatory elements in gene sequences, 1500 base pairs (bp) upstream of the promoter region (http://bioinformatics.psb.ugent.be/webtools/plantcare/html/). The plant small RNA target analysis server psRNATarget (https://www.zhaolab.org/psRNATarget/) was used to search for putative microRNAs and their targets in the BnPA/BnPB genes of *B. napus*. Here, 0-3 e-value was used (Dai and Zhao, 2011; Dai et al., 2018). All the abovementioned analyses were performed with default parameters.

### 2.1.3 Gene duplication and synteny analysis

The gene tree pipeline available in the Ensembl Plants database (Vilella et al., 2009; Bolser et al., 2015) was utilized to infer evolutionary relationships among proteasome genes (*BnPA* and *BnPB*) with the help of a gene identifier. A phylogenetic tree of homologous genes across the genome of *B. napus* and Arabidopsis was constructed using the Plant Compara option. This gene tree was further utilized to identify duplication and speciation events. Synteny and collinearity between chromosomes of *B. napus* and Arabidopsis were determined covering the stretch of 25 genes. For this purpose, the genome browser biotool GENOMICUSv49.01 (https://www.genomicus.bio.ens.psl.eu/genomicus-plants-49.01/cgi-bin/search.pl) was used.

## 2.2 Analysis of protein sequence

### 2.2.1 Structure, conserved motifs and physio-chemical properties of protein sequences

The CD-search program of the conserved domain database (CDD) at NCBI was used to identify domain features in BnPA/BnPB protein sequences. The physiochemical properties, including amino acid composition, molecular weight, theoretical PI, number of positively/negatively charged residues, instability index, aliphatic index, and grand average of hydropathy (GRAVY) were computed using ExPASy's ProtParam tool (https://web.expasy.org/protparam/). The network protein sequence (NPS) analysis was performed using a self-optimized prediction method with an alignment (SOPMA) tool (https://npsa-prabi.ibcp.fr/cgi-bin/npsa_automat.pl?page=/NPSA/npsa_sopma.html). Motifs in protein sequences were searched using the MEME suite (https://meme-suite.org/meme/tools/meme). Annotation and visualization of identified motifs were performed using InterPro Scan (https://www.ebi.ac.uk/interpro/search/sequence/) and TB tool, respectively.

### 2.2.2 Computational analysis, structure and validation of predicted proteins

Homology modeling (HM) was applied to deduce the 3D structure of the predicted proteins. For HM, PSI-BLAST was performed against two databases, the Swiss Model template library (https://swissmodel.expasy.org/), and the protein data bank (http://www.rcsb.org/pdb/home/home) with 100 iterations. A structure analysis and validation server (SAVES; https://saves.mbi.ucla.edu/) was used to verify the predicted 3D structures of *BnPA* and *BnPB* proteins. The relative proportion of amino acids that appear in the favored region was found with the help of the PROCHECK option of SAVES v6.0 (Laskowski et al., 1993). VERIFY 3D was utilized to determine the compatibility of the atomic model (3D) with its amino acid sequence (1D) (Eisenberg et al., 1997). The ERRAT program was used to verify the protein structures through patterns of nonbonded interactions among C, N, and O atoms (Colovos and Yeates, 1993).

### 2.2.3 Functional annotation and superimposition of 3D structures

The Flexible structure AlignmenT by Chaining Aligned Fragment pairs allowing Twists (FATCAT) server (https://fatcat.godziklab.org/fatcat/fatcat_pair.html) was used to compare the 3D structure of the proteins encoded by various genes belonging to *A. thaliana* with that of predicted *B. napus* proteins by aligning the representative structure. The similarity of 3D structures was measured by the root mean square deviation (RMSD) value of the Cα atoms.

## 2.3 Phylogenetic analysis

The MultAlin program (http://multalin.toulouse.inra.fr/multalin/) was used for multiple sequence alignments to determine conserved amino acid residues in *B. napus*, Arabidopsis and rice. A mutual information server to infer coevolution (MISTIC; http://mistic.leloir.org.ar/results.php?jobid=20211202121102296) was employed to determine the mutual information (MI) between two amino acid positions in multiple sequence alignment (MSA). The identical amino acid between two positions (homologous protein), called mutual information (MI), was predicted to correlate and compensate for mutations, and was used to identify coevolving residues (Sharma et al., 2022). The amino acid sequences of proteins were utilized for phylogenetic analysis by molecular evolutionary genetics analysis version 6.0 (MEGA v6.0) software using the neighbor-joining method (Tamura et al., 2011). The Newick format tree prepared in MEGA was visualized in iTOL (https://itol.embl.de/).

## 2.4 *In silico* expression profile of 20S proteasome genes

Digital expression of *BnPA* and *BnPB* genes was analyzed using transcriptomic data available at *the Brassica expression database* (https://brassica.biodb.org/). Expression was studied in FPKM values using six different tissues (seed, cotyledon, hypocotyls, radical, root, & leaf) belonging to the germination and seedling stages under normal conditions. Under both biotic and abiotic stress conditions, expression was observed at the seedling and flowering stages. Under both normal and stress conditions, the expression pattern of the selected genes was studied.

# 3 Result

## 3.1 Analysis of gene sequence

### 3.1.1 Identification of genes for the 20S proteasome in *B. napus*

Out of 92 20S proteasome genes initially identified in the *B. napus* genome, 10 genes were incomplete; therefore, these genes were removed from further analysis. The remaining 82 full-length genes involving 35 *BnPA* and 47 *BnPB* of the 20S proteasome family were further characterized in the present study. Comprehensive information on the full-length gene and coding sequences of *B. napus* α-subunits (*BnPAA-BnPAG*) and β-subunits (*BnPBA-BnPBG*) and their comparison with corresponding *A. thaliana* and rice genes are provided in Supplementary Table S1. The name of all 82 *B. napus* genes of the 20S proteasome family was designated according to the corresponding genes reported earlier for Arabidopsis, rice and wheat (Fu et al., 1998; Sassa et al., 2000; Sharma et al., 2022). The sizes of the *BnPA* and *BnPB* genes varied from 1039-5449 bp and 618-5132 bp, respectively. The cDNA sequence of *BnPA* genes ranged from 852 to 2355 bp and that of *BnPB* genes ranged from 249 to 1818 bp. Furthermore, variations in coding DNA sequence (CDS) were also observed individually in *BnPA* (606-2199 bp) and *BnPB* (249-1578 bp) genes (Supplementary Table S1). The intron-exon features of *B. napus* 20S proteasome genes were studied to gain an improved understanding of their structural patterns. The number of exons and introns in *BnPA* genes varied from 2-17 and 1-16, respectively. All 35 *BnPA* genes had introns. The number of exons and introns in *BnPB* genes varied from 3-12 and 2-11, respectively (Supplementary Table S2). The intron phases were phase 0 (56.75%), phase 1 (30.45%) and phase 2 (12.79%) (Figure 1).

### 3.1.2 Assignment of chromosome and gene duplication

All 82 *BnPA* and *BnPB* genes were physically mapped to 18 individual chromosomes of *B. napus* along with two additional Cnn and Ann chromosomes. The maximum number of six genes were located on each A07, A09, and C07, while the minimum number of two genes each was located on A04, A02, and C09. All the genes were located in the terminal and subterminal positions (Figure 2). The tree involving *B. napus* genes along with genes from other taxa was developed using the Ensembl Plants Compara pipeline (Supplementary Figure S1). This was done to examine orthology and paralogy among 35 *BnPA* and 47 *BnPB* genes.

Detailed information on the orthologous and paralogous relationships of the *BnPA* and *BnPB* genes with different species is given in Supplementary Table S1. Orthologs and paralogs among Brassica, Arabidopsis and rice 20S proteasome genes have been investigated using the order of genes of 14 subunits (7-α and 7-β). Out of the 24 genes in Arabidopsis (13- α and 11- β), the number of duplicated genes was 10 and those that remained single were 4. Out of the 23 rice genes (13-α and 10-β), duplication was observed in seven genes, triplication in 1, and the rest 6 genes remained single (Supplementary Table S1). The observed pattern of duplicated genes in *B. napus* was similar to that in Arabidopsis and rice for the corresponding *PA/PB* genes. The orthologs were distinguished from paralogs using Ensembl Plant Compara.

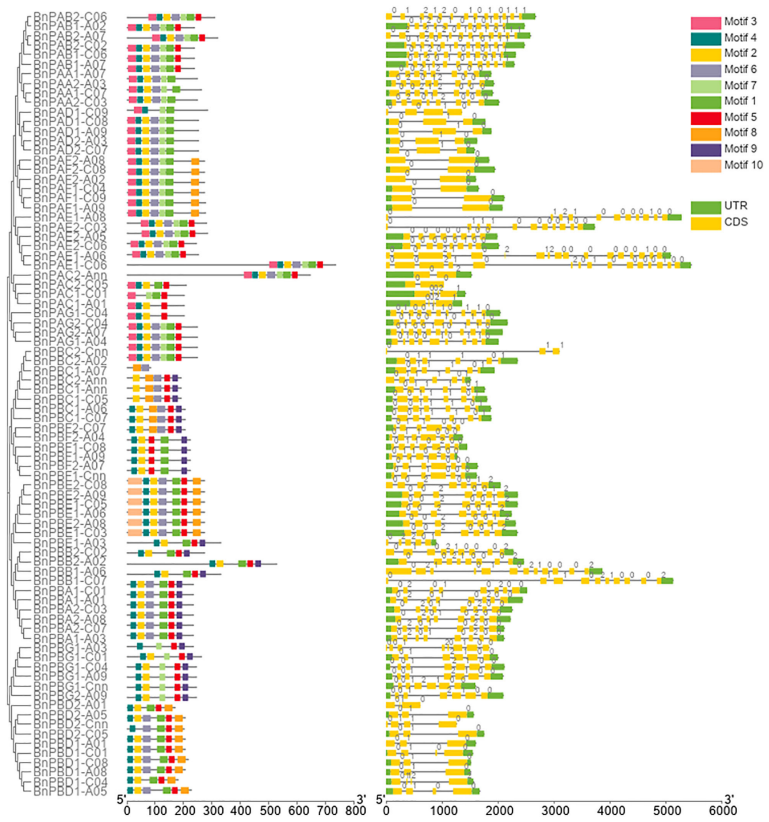


FIGURE 1
Structure of *BnPA* and *BnPB* genes of *Brassica napus* showing the distribution of exons (yellow solid bars), introns (black lines), upstream/downstream regions (solid green bars), and intron phases marked as 0, 1 and 2. The figure also represents the conserved motifs identified in BnPA and BnPB proteins.

### 3.1.3 Synteny between *B. napus*, *A. thaliana*, and rice

Synteny analysis of 82 *BnPA* and *BnPB* genes with the corresponding Arabidopsis genes was highly conserved (Figure 3). The collinearity of *BnPA* and *BnPB* genes with Rice was negligible; however, collinearity with *A. thaliana* was found with only one gene, i.e., *BnPBC2*-Cnn with *At1*.

### 3.1.4 SSRs in *BnPA* and *BnPB* genes

A total of 66 SSRs were identified in 45 (54.87%) of the 82 genes. Of these, 28 SSRs were identified in 16 *BnPA* genes and 38 SSRs were identified in 29 *BnPB* genes. The SSR numbers vary per gene. There were only six SSRs in *BnPAE1-A08*, only four SSRs in *BnPBB1-C07*, three SSRs in two genes (*BnPAE2-C03*, *BnPBD2-C05*), and two SSRs each in nine genes (*BnPAA2-A03, BnPAE1-C06, BnPAE2-A05, BnPAF1-C09, BnPAG2-C04, BnPBA1-A01, BnPBC1-A06*, *BnPBD2-Cnn* and *BnPBF2-A07*), whereas single SSRs were present in the remaining 32 genes (Supplementary Table S3). SSRs with dinucleotide motifs (20) are more frequent followed by tetranucleotide (10) and hexanucleotide (10), trinucleotide and mononucleotide (9), pentanucleotide (5) and heptanucleotide (3) motifs.

### 3.1.5 Analysis of promoter and cis-acting regulatory elements

Cis-acting regulatory elements present 1500 bp upstream of the 5' promoter sequence were studied in each of 82 *BnPA/BnPB* genes. It was observed that the promoter region of all the genes contains many light-responsive elements along with phytochrome and other cis-acting elements. The maximum number of genes was for light, methyl jasmonate (MeJA), and endosperm elements (Supplementary Figure S2).

### 3.1.6 MicroRNAs and their targets in *BnPA* and *BnPB* genes

A total of 44 microRNAs (miRNAs) were found. These miRNAs had their targets in 21 genes (8 *BnPA* and 13 *BnPB*). The maximum number of target sites i.e., six microRNAs were available for each of two genes (*BnPAC1-A01* and *BnPBD2-A01*). The targets for *BnPBD1-C08, BnPBD1-A08* and *BnPBD2-Cnn* were available

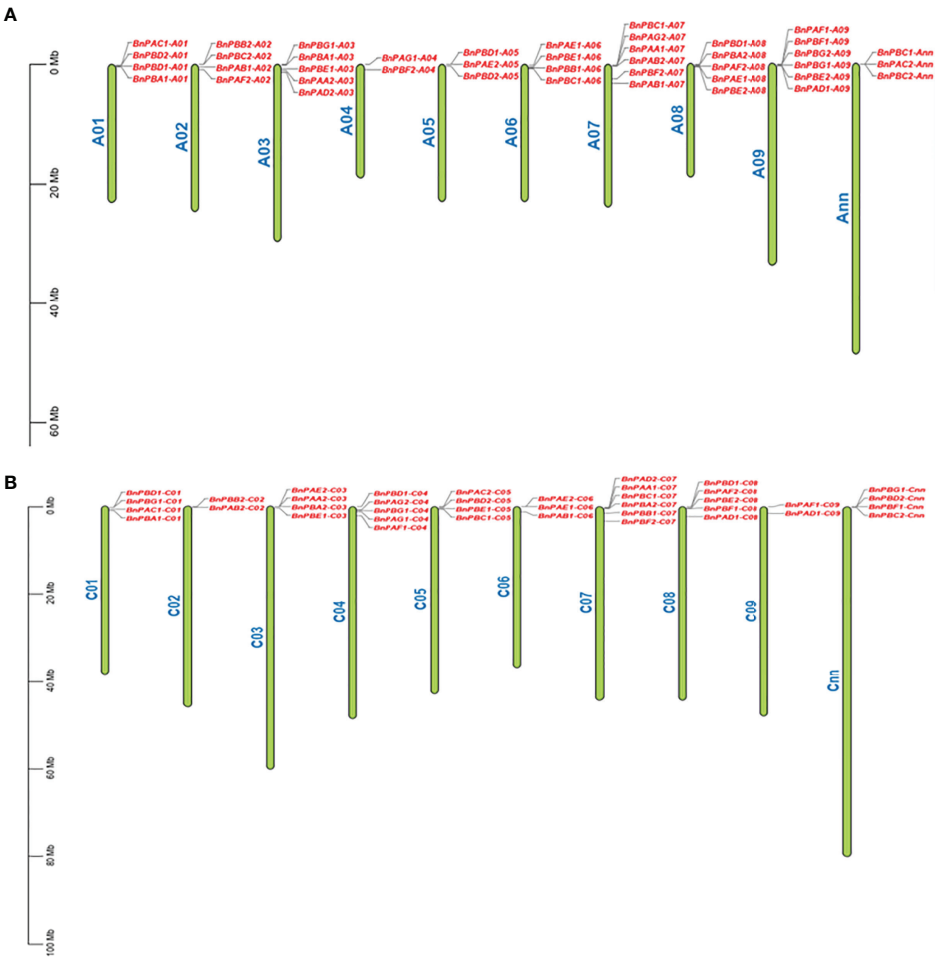


FIGURE 2
Distribution of 82 *BnPA* and *BnPB* genes on 20 chromosomes of *B. napus* belonging to the A **(A)** and C **(B)** subgenomes. On each chromosome, gene names are given on the right side. A scale of physical positions in megabases (Mb) is shown on the far left.

for four miRNAs. The target for *BnPAF2-C08* was available for three miRNAs. Similarly, the targets for *BnPBA1-A01* and *BnPBA2-C07* were available for two miRNA each. The target for the remaining 13 miRNAs was available in different *BnPA* and *BnPB* genes distributed on several Brassica chromosomes (Supplementary Table S4).

## 3.2 *In silico* expression analysis of *BnPA* and *BnPB* genes

The expression pattern of genes was studied under normal and stress conditions. Under normal conditions, two different developmental stages (germination and seedling) for six different organs (seed, cotyledon, hypocotyl, radicle, leaf, and root) were examined. Under both abiotic and biotic stress conditions, two different developmental stages (seedling both flowering) were examined.

### 3.2.1 Tissue-specific expression under normal conditions

Under two different developmental stages (germination and seedling), the six different organs (seed, cotyledons, hypocotyl, radical, leaf, and root) showed variation in expression (Figure 4). Out of 82, 18 genes showed higher expression in the two stages and the expression data are provided in the form of FPKM values.

### 3.2.2 Abiotic stresses

Cold stress. We observed two genes under 24 h cold stress (seedling and flowering stages) whose expression was upregulated i.e., >1.70-fold change (FC). During this same duration, the expression of 33 genes ranged from 0.00 to 0.99 FC i.e., the expression of these genes in response to cold stress was very poor (Figure 5A).

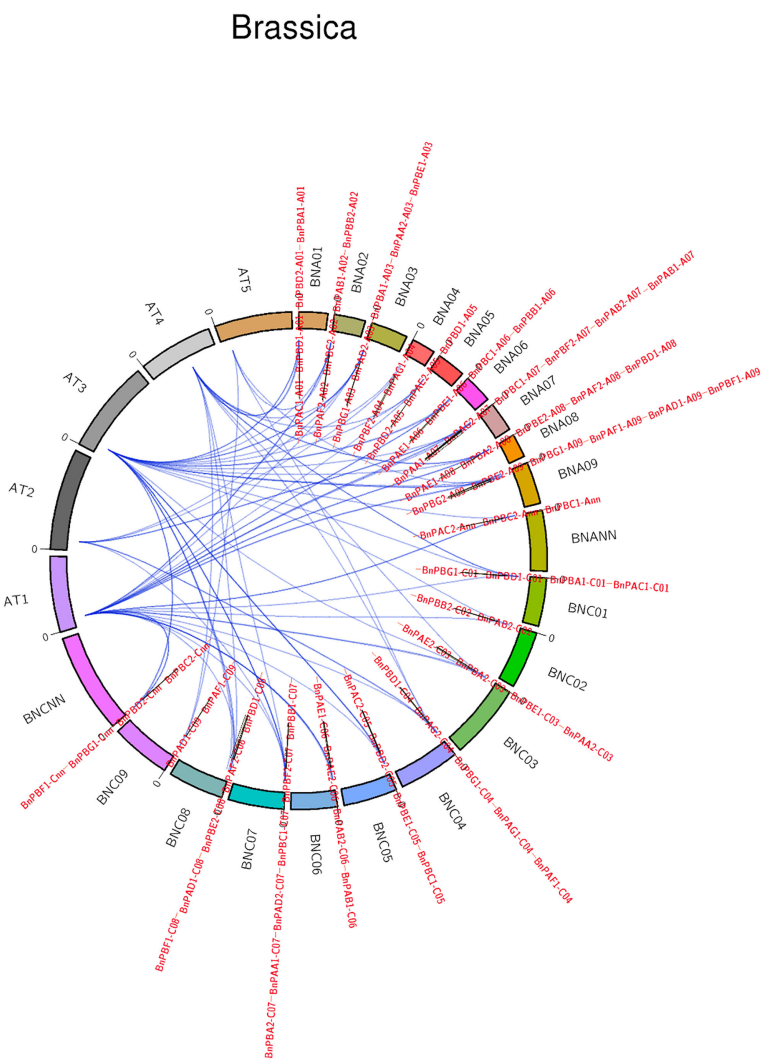


FIGURE 3
A circular map showing synteny among PA and PB genes of *B. napus*, *A. thaliana* and rice (name of chromosomes given outside the circle, name of genes given outside and inside the circle).

Drought stress. Only one gene showed high expression (FC>1.70) under 24 h drought stress (seedling and flowering stages), whereas 62 genes showed their expression from 0.00 to 0.99 FC (Figure 5B).

Heat Stress. Under 24 h of heat stress, all genes (seedling and flowering stages) showed expression FC<1.70. However, the expression of 57 genes ranged from 0.00 to 0.80.

As a result, we concluded that in *B. napus*, there are only five genes that can tolerate cold stress and there is only one gene that is expressed under drought conditions. Moderate to poor expression of genes was observed under heat stress conditions.

### 3.2.3 Biotic stresses

Under biotic stress in *B. napus*, 20S proteasome genes were expressed against two fungal pathogens *Leptosphaeria maculans* (blackleg) and *Sclerotinia sclerotiorum* (white mold), at the seedling and flowering stages, respectively. After 264 h of *L. maculans* infection at the seedling stage, one gene with FC>0.99 was expressed against fungal infection (Figure 5C). Relative to the control, 1 gene was stimulated (FC>1.70) after 72 h of infection at the seedling stage. At the flowering stage, BnPAB1-A07 and BnPBA2-A08 genes were expressed with FC>0.99 after 48 h and 96 h of *S. sclerotiorum* inoculation, respectively (Figure 5D).

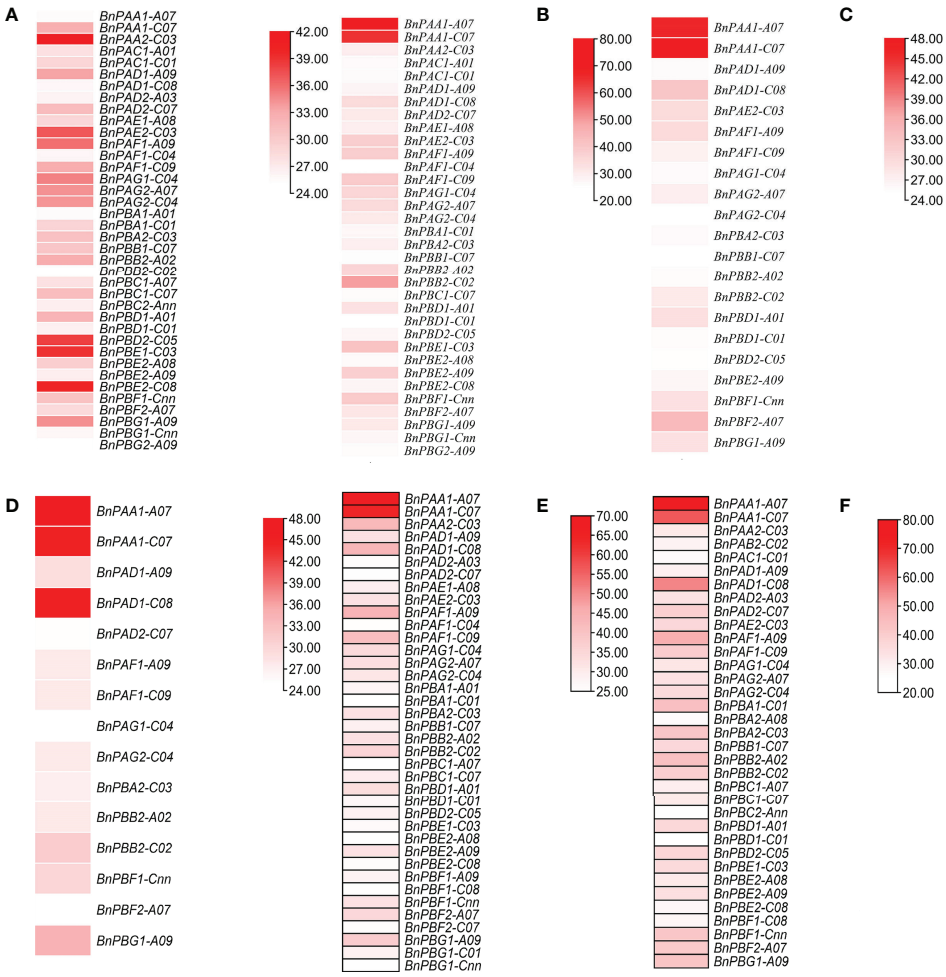


FIGURE 4
Expression profile of *BnPA* and *BnPB* genes at two developmental stages in six different tissues, **(A)** germination (cotyledon), **(B)** germination (seed), **(C)** germination (hypocotyl), **(D)** seedling (leaf), **(E)** germination (radicle) and **(F)** seedling (root), under normal conditions in *B. napus*. The expression data are represented in the form of FPKM values.

## 3.3 Analysis of Proteins

### 3.3.1 Characterization of BnPA and BnPB proteins

The molecular weight of BnPA and BnPB proteins ranged from 9510.19 to 82935.95. the isoelectric point (PI) ranged from 4.65 to 9.93. The total acidic and alkaline proteins were 71 and 11 respectively. The proteins (41) with a lower aliphatic index i.e., 67.30 to 98.52 were unstable, whereas the remaining proteins (41) had a higher aliphatic index of 79.60 to 100.36 and were stable. The grand average of hydropathy (GRAVY) ranged from -0.669 to 0.093 (Supplementary Table S5).

### 3.3.2 Functional domains and motifs of BnPA and BnPB proteins

The number of amino acids in 82 BnPA/BnPB proteins varied from 82 amino acids (aa) (BnPBC2-Cnn) to 732 aa (BnPAE1-A06), the mean of which was 251.85 aa (Supplementary Table 2). The length of α-subunits ranged from 201 to 732 aa, and the β-subunits ranged from 82 to 525 aa (Supplementary Table 2). A total of 10 separate motifs are given in Figure 1. The logo of 10 separate motifs and the associated amino acids identified in the BnPA and BnPB proteins are provided in Supplementary Figure S3. The list of identified motifs along with their sequence and e-value are given in Supplementary Table S7.

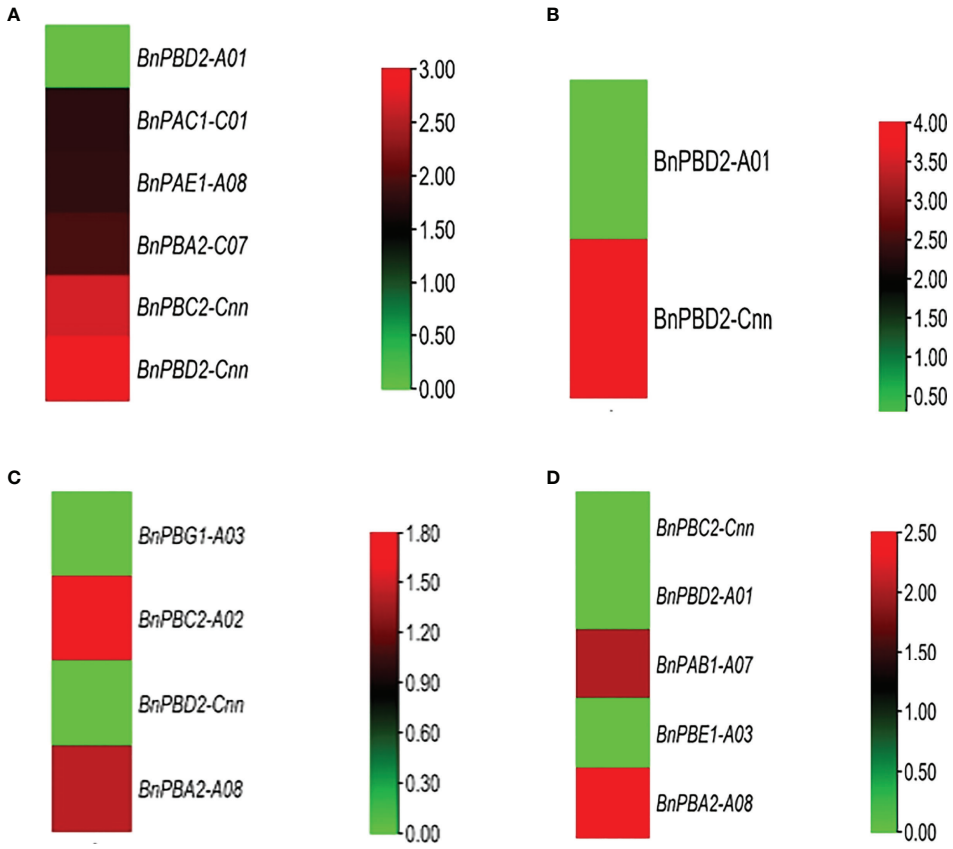


FIGURE 5
*In silico* expression profiling of *BnPA* and *BnPB* genes at seedling and flowering stages under abiotic stresses **(A)** cold and **(B)** drought and biotic stresses **(C)** *Leptosphaeria maculans* and **(D)** *Sclerotinia sclerotiorum*. The expression data of control and stress conditions are shown in the form of relative fold change (FC).

### 3.3.3 Sequence alignment and assessment of conserved amino acids

The percent similarity among the α-subunit of *B. napus* was 30 (Supplementary Table S8) whereas in the β-subunit it was 20.72 (Supplementary Table S9). The similarity percentage between the α and β- subunits of *B. napus* was 21.33. The percentsimilarity among *B. napus* and Arabidopsis *BnPA* proteins was 91.06 (Supplementary Table S8) and for BnPB protein was 99.14 (Supplementary Table S9). High amino acid similarity was observed among the α and β-subunits of *B. napus*, Rice, and Arabidopsis (Supplementary Figures 4a, b). A high conservation pattern of 31 amino acids (aa) of α-subunits and 15 β-subunits was found among *B. napus*, rice, and Arabidopsis. These 31 (α-subunits) and 15 (β-subunits) residues also had the highest MI (Supplementary Figures S5, S6).

### 3.3.4 Localization of subcellular proteins and their functions

Gene ontology analysis and functional annotation suggested that *BnPA and BnPB* proteins have proteolytic functions and other molecular functions such as threonine type endopeptidase activity, threonine type peptidase activity, peptidase activity and endopeptidase activity (Figure 6).

### 3.3.5 Protein structures

The secondary structure of all the proteins was compared. It has been found that the secondary structure is dominated by α-helices followed by random coils (Supplementary Table S10). The latter form irregular structures that permit polypeptide chains to fold uniquely. Proteins such as *BnPA and BnPB* tend to form a highly stable structure. *In-silico* 3D structures were determined for 20 (24.39%) BnPA and BnPB proteins with similarity ranges of 10.85-100% with the corresponding template of Arabidopsis (Supplementary Figure S7). The GMQE for these 20 proteins ranged from 0.59 to 0.82. A high-quality protein model was suggested by it. Q-mean value ranged from 0.73 ± 0.06 to 0.82 ± 0.06. The similarity between the protein model and reference (Arabidopsis) proteins ranged from 42 to 69%. The quality factor was determined with the help of ERRAT and ranged from 88.2096 to 100%. The 3D-1D score was

determined with the help of VERIFY 3D and ranged from 77.95 to 99.58% (Supplementary Table S11)

### 3.3.6 Alignment and functional annotation of 3D-structure

The 3D protein structures (with minimum energy) of *B. napus* were superimposed with the reference protein (3D) of Arabidopsis (Figure 7 and Supplementary Table S12). The 3D structure of five (BnPAA1-A07, BnPAA1-C07, BnPAF1-A09, BnPBE1-C03, and BnPBF1-Cnn) proteins showed a similarity of 33 to 98% with the corresponding 3D structure of the AtPAF2 protein with RMSD values in the range of 0.04 to 2.66 Å.

## 3.4 Phylogenetic analysis

The amino acid sequences of *B. napus*, *A. thaliana* and *O. sativa* for α- (PA) and β-subunits (PB) were utilized separately to construct a phylogenetic tree. Seven clades that belong to 1 to 7 subunits were observed in each phylogenetic tree. These clades showed similarities with the conserved motifs (Figure 1). It was interesting to note that the orthologs of all three taxa belong to each of the α and β-subunits and formed seven clades in both phylogenetic trees. In the α-subunit tree, 7-10 orthologs formed clades (Figure 8A) whereas, in the β-subunit tree, 7-13 orthologs formed clades (Figure 8B).

# 4 Discussion

Plant genome sequencing has been utilized to study genes related to various developmental stages and stress tolerance in many crops (Lu et al., 2019; Mehla et al., 2022). Crops whose genomes have not been sequenced are receiving benefits from those crops whose genomes have been sequenced. *A. thaliana* and *O. sativa* (Rensink and Buell, 2004) have been utilized for such studies.

## 4.1 Identification of *BnPA* and *BnPB* genes

The present study is the first report in *B. napus* on phylogenomic analysis for identifying and describing genes that encode for various subunits (α1-7 and β1-7) of the 20S proteasome. In this study, 82 *BnPA* and *BnPB* genes of *B. napus* were arranged into seven different α and β types of 20S proteasome. The sub-genomes A and C contain 42 and 40 genes, respectively. When compared to previously identified *A. thaliana* (*AtPAA-AtPAG and AtPBA-AtPBG*) and rice genes (*OsPAA-OsPAG and OsPBA-OsPBG*) (Fu et al., 1998; Sharma et al., 2022), a fairly large number of these genes were detected in *B. napus*. These findings may justify the fact that *B. napus* has a large genome and evolved with a higher ploidy level. The presence of two more genes in genome A of *B. napus* may be due to duplication, and a lower number of genes in genome C than genome A may be due to the loss of the gene. In the majority of the *BnPA* and *BnPB* genes, the structural pattern of exons and introns was found to be similar; however, in some cases, this similar pattern deviates. This deviation in gene structure may be due to the loss/gain of introns during the course of evolution (Rogozin et al., 2003; Yu et al., 2019). In cDNA sequences, this may be due to differences in intron number and size located in *BnPA* and *BnPB* genes. In addition, the variation in the length of UTRs present on the borders of cDNA may be due to differences in the length of cDNA sequences. The phylogenomic analysis of 82 genes revealed seven clades of each α (BnPAA-BnPAG) and β (BnPBA-BnPBG) subunit. The different α and β subunits of *B. napus* varied from each other but they showed similarities with Arabidopsis, a close relative of *B. napus*. This means that the 20S proteasome might have not changed after the divergence of these two taxa due to common ancestry. The distribution pattern of *BnPA* and *BnPB* genes on A-09, C-09, Ann and Cnn differed. In our findings, we found an uneven distribution of genes in genomes A and C. The general pattern is four genes per chromosome but in some cases, there is a deviation from this pattern. This deviation may be due to gene duplication or

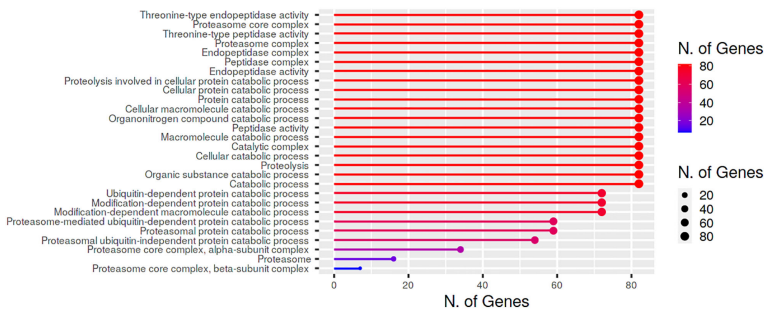


FIGURE 6
Cellular location and biological/molecular functions of BnPA/BnPB proteins in *Brassica napus*.

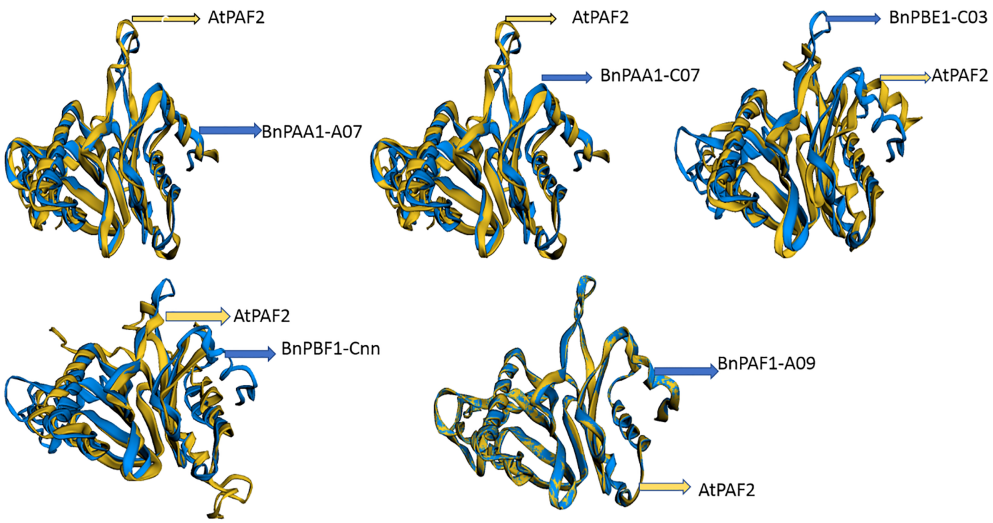


FIGURE 7
Representative figure showing the superimposed structure of the predicted 3D structure of BnPAA1-A07, BnPAA1-C07, BnPAF1-A09, BnPBE1-C03 and BnPBF1-Cnn proteins over the 3D structure of *Arabidopsis* PAA (AtPAF2) proteins.

gene loss (Clavijo et al., 2017; Yu et al., 2019). The difference in the distribution of orthologous genes in the A and C genomes may be due to inversion and translocation.

## 4.2 Number of genes in Arabidopsis, rice and *B. napus*

In *B. napus*, 82 *BnPA* and *BnPB* genes of 20S PA and PB have been reported so far which represent the highest numbers in the plant kingdom. This number is thrice the number reported in Arabidopsis and rice (Figure 9). The number of genes in A and C suggests that different genes have undergone duplication (paralogy) and speciation events (orthology). In Arabidopsis, out of 24 genes (Supplementary Table S2), instead of 14 genes as published in earlier studies (Fu et al., 1998), 13 genes with duplications for all α-subunits except *AtPAG* (α-7), whereas 11 genes with duplications in only 4 β-subunits, *AtPBB* (β-2), *AtPBC* (β-3), *AtPBD*(β-4), and *AtPBE* (β-5), have been reported (Parmentier et al., 1997; Fu et al., 1998).

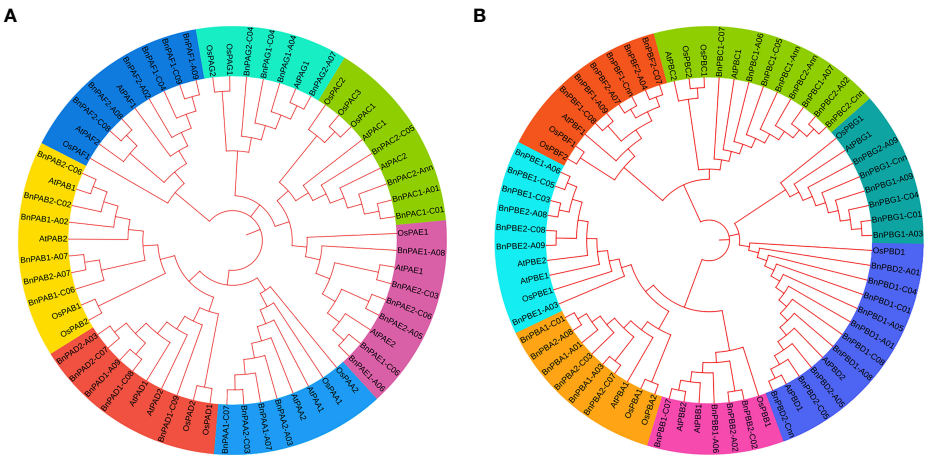


FIGURE 8
Phylogenetic tree constructed using protein sequences of **(A)** α-subunits and **(B)** β-subunits belonging to three plant species (*A. thaliana*, *O. sativa* and *B. napus*). Seven different colors in the tree represent seven different clades.

Similarly, a phylogenomic survey of rice determined 23 genes instead of 14, as published in previous studies (Sassa et al., 2000). The duplications and heterogeneity have also been resolved in other organisms by phylogenomic surveys. A phylogenomic survey in *B. napus* revealed that the α-subunit included 35 genes with duplications except for *BnPAC1, BnPAA2, BnPAD2, BnPAG1, BnPAG2, BnPAA1*, and *BnPAC2*, and the β-subunit include 47 genes with duplication except for *BnPBB2, BnPBB1*, and *BnPBG2* (Supplementary Table S2). The α-genes found with maximum duplication are *BnPAB1, BnPAF2, BnPAE2, BnPAE1, BnPAB2, BnPAF1*, and *BnPAD1*. Similarly, the β-genes found with maximum duplication are *BnPBD1, BnPBG1*, and *BnPBC1*.

## 4.3 Duplication and analysis of synteny in *BnPA* and *BnPB* genes

The present results on the 20S proteasome gene family of *B. napus* showed that in most cases duplication events have occurred in both the A and C genomes. The duplication events are from 1 (*BnPBG2-A09*) to 6 (*BnPBD1*). *BnPBD1* was reported on A01, A05, A08, C01, C04, and C08 suggesting maximum duplication (paralogy). These duplications may be due to translocation during the course of evolution. The absence of any duplication in *BnPBG2-A09* may be due to deletion. We have checked the synteny of all five chromosomes of Arabidopsis with all proteasome genes of *B. napus*. It was found that 81 genes of *B. napus* were syntenic with the genes on the chromosomes of *A. thaliana*. One gene of *B. napus* (*BnPAD1-C09*) was found to be nonsyntenic with *A. thaliana*. This could be due to deletion. Chromosome 1 and chromosome 3 of *A. thaliana* showed synteny with 29 genes of *B. napus*, whereas the least synteny was observed with chromosome 5, i.e., only with 4 genes of *B. napus*. All the genes on the chromosome of *O. sativa* were nonsyntenic.

## 4.4 Analysis of promoter sequences in *BnPA* and *BnPB* genes

The cis regulatory elements, present mostly near the start codon, are noncoding in nature and under different environmental conditions, they modulate gene expression in response to different transcription factors. Gene regulation is determined by cis regulatory elements at the basic level (Mondal and Das, 2020). The identified cis regulatory elements that spanned the promoter of 82 proteasomal genes were found to be associated with development and stress responses (light responsive, endosperm, and MeJA signaling) in Brassica (Supplementary Figure S2). Thus, it is evident that MeJA regulates plant growth and environmental stress (Wang et al., 2020) and defense against pathogens and herbivores (Fürstenberg-Hägg et al., 2013). There is a large number of evidence suggesting that hormonal signals affect the expression of the 20S proteasome gene. This expression leads to biotic and abiotic stresses (Kurepa et al., 2009). The presence of light-responsive elements indicates that they are required for light-dependent transcriptional regulation (Hiratsuka and Chua, 1997; Mondal et al., 2022). Similarly, the presence of endosperm elements is expressed during developmental stages. A large number of GBREs along with other cis-elements respond to phytohormones such as MeJA, and ABA available in *BnPA* and *BnPB* genes may control the expression of genes (*BnPA* and *BnPB*) under heat stress (Cao et al., 2015).

## 4.5 SSR with SSRs and miRNA with miRNAs

In this study, out of 82 genes, we found 66 SSRs in only 45 genes. This suggests that a fraction of genes in a gene family contain SSRs. The structural and functional aspects of SSR have been reported in a large number of genes (Li et al., 2004; Gupta

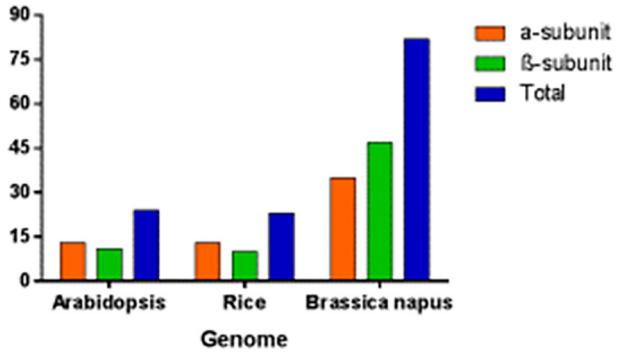


FIGURE 9
Genes encoding seven α and seven β subunit proteins of the 20S proteasome in Arabidopsis, rice and *B. napus*.

and Rustgi, 2004; Varshney et al., 2005). The frequency of dinucleotide was highest (20). It was followed by tetranucleotide and hexanucleotide. Such occurrence is unusual because trinucleotide repeats are generally found most frequently in comparison to other SSRs (Gupta and Varshney, 2000). The SSR reported in the gene that encodes the α and β-subunits of proteasome core particles, shows polymorphism which can be helpful to develop functional molecular markers. Such a marker can be used to improve tolerance against different physiological stresses in the plant. The absence of transposable and retroelements in the genes studied indicates the nonexpression of the 20S proteasome family in *B. napus*.

The mi-RNAs are small noncoding RNAs that have a regulatory function inside the cells at the post-transcriptional and translocation levels. These cause the degradation of targets of the gene (Budak & Zhang, 2017; Liu et al., 2017). In this study, 44 miRNAs involving sequences of *BnPA* and *BnPB* genes were identified. The target sites for these miRNAswere found only in 21 genes (8 *BnPA* and 13 *BnPB*). Among the predicted miRNAs, candidates of bna-miR166 (miR166 a-f; each 21 nucleotides long) were detected in *BnPAC1-A01* and those of miR160 (miR160 a-d) were detected in *BnPBD-C08, BnPBD1-A08, BnPBD2-A01*, and *BnPBD2-Cnn* (Supplementary Table S4). Micro-RNA166 (miR166), a highly conserved family of miRNAsis involved in several cellular and physiological processes in plants (Li et al., 2017), such as drought stress (Kantar et al., 2011), cold stress (Liu et al., 2008) and heat stress (Khraiwesh et al., 2012). F-box/SCF is encoded by miR2111, which is involved in ubiquitin-mediated proteolysis and then in the adaptive response of Pi-deficiency (Kumar et al., 2017). miR160 has a role in both abiotic and biotic stress responses in Arabidopsis and maize (Zhang et al., 2009; Moldovan et al., 2010). miR160a is involved in regulating auxin response genes, club root development, and disease modulation (Verma et al., 2014). In this way, the function of miR166 and miR160 is understood in plants. The presence of miR166 and miR160 in *B. napus* may be significant for future studies on the biological role of these miRNAs.

## 4.6 Structural and functional features of *BnPA and BnPB* proteins

The predicted proteins of *BnPA* and *BnPB* genes were found to be variable and, differed in theprotein length of similar genes from *A. thaliana* and *O. sativa*. The number of amino acids in BnPA and BnPB varies from 82 aa (*BnPBC2-Cnn*) to 732 aa (*BnPAE1-A06*). This length is more variable than those of rice proteins (237 to 256 aa). Similarly, the length of proteins (199 to 298 aa) of *A. thaliana* is the least variable (Town et al., 2006). The GRAVY ranged from -0.669 to 0.093. This suggests the hydrophobic nature of these proteins. Due to this property, there will be proper folding of proteins to keep them stable and biologically active.

The *BnPA* and *BnPB* genes encode proteins that contain 10 different motifs. Similarly, 10 motifs are present in the database for Arabidopsis and rice (Parmentier et al., 1997; Fu et al., 1998; Sassa et al., 2000). The length of the individual motif varied from 15 aa (motif 3) to 41 aa (motif 10). Motifs 1, 4, 5, and 6 are concerned with catabolic processes at the cellular level (https://www.ebi.ac.uk/interpro/result/InterProScan/iprscan5-R20211209-091508-0331-1308065-p2m/). The remaining 6 motifs were found to be novel and need to be characterized at the molecular level. Earlier studies reported that in eukaryotes, proteins of the 20S proteasome could be in the nucleus and cytoplasm, and the same case may be true for BnPA and BnPB proteins (Fu et al., 1998). A single specific domain of α-type (α 1-7) or β-type (β 1-7) is present in all 82 BnPA and BnPB proteins. Of these, 35 BnPA proteins contain a single α-type domain and 47 BnPB proteins contain a single β-type domain (Supplementary Table 2). Similar findings have been observed in yeast, Arabidopsis and rice (Parmentier et al., 1997; Groll et al., 1997; Fu et al., 1998; Arias and Pires, 2012). A majority of aa residues (>90%) that fall in the most favored region were shown by modeled 3D structures of 20 BnPA/BnPB proteins. This suggested that the predicted models are reliable (Laskowski et al., 1993; Kumar et al., 2018; Batra et al., 2019). The predicted 3D structures of BnPA and BnPB proteins may be helpful for the initial understanding of molecular functions.

## 4.7 Phylogenetic analysis of BnPA and BnPB protein sequences

The different orthologs of the α and β-subunits of 20S proteasome were examined, and phylogenetic trees were constructed. The orthologs of Brassica, Rice and Arabidopsis that belong to different α and β-subunits were depicted into seven clades for the α and β subfamilies. Similar findings have been reported for yeast, Arabidopsis and rice proteins (Fu et al., 1998; Sassa et al., 2000). These findings suggest that the α and β-subunits of *B. napus* have a higher level of similarity with those of Arabidopsis and rice.

## 4.8 Digital expression analysis of *BnPA* and *BnPB* genes

All 20S proteasome genes and core particles are involved in plant responses to different biotic and abiotic stresses (Xu and Xue, 2019). This is due to different signaling molecules that control the development of plants under different stress conditions (Livneh et al., 2016). Earlier a few studies (Fu et al., 1998; Li et al., 2015) examined digital expression analysis of the

20S proteasome gene in a plant system. The present study is the first report in *B. napus* on phylogenomic analysis and digital expression of the 20S proteasome gene under normal tissue-specific and stress conditions in the germination and seedling stages. This was done using a transcriptome database in which approximately 18/82 genes showed higher expression at different germination and seedling stages of *B. napus* in root, seed, leaf, cotyledon, hypocotyls, and radicle (Figure 4). A greater mRNA level expression for six 20S proteasome subunit genes compared to β-tubulin in flower and fruit tissues of Arabidopsis has been observed *via* RNA blot analysis (Fu et al., 1998). Under 24 h of abiotic stress (cold, drought, and heat), two genes for cold and one gene for drought exhibited high expression at the seedling and flowering stage. No gene was reported for heat. However, in wild rice, the *OgTT1* gene was reported under heat stress conditions (Li et al., 2015). Under 264 h and 72 h of biotic stress (*L. maculans)* as many as one gene exhibited higher expression at the seedling stage. Under 96 h, 48 h and 24 h of biotic stress (*S. sclerotiorum)* as many as 1, 1 and 0 genes respectively, showed high expression in the flowering stage. In this way, the 20S proteasome gene plays a significant role in the development of different plant organs such as roots, seeds, leaves, cotyledons, hypocotyls, and radicles, as well as in abiotic stresses (Xu and Xue, 2019). The functions of the aforementioned genes that showed differential expression under biotic and abiotic stresses may be investigated in future studies.

## 5 Conclusion

The present study is the first report in *B. napus* on phylogenomic analysis for identifying and describing genes that encode 35 *BnPA* and 47 *BnPB* genes of the 20S proteasome. The orthology and paralogy of *BnPA* and *BnPB* genes were inferred and identified on the basis of the pattern of speciation and duplication of genes in Arabidopsis and rice. A full-length 3D model was predicted for the proteins encoded by *BnPA* and *BnPB* genes. A number of *BnPA* and *BnPB* genes were found to be expressed in many organs of *B. napus* under normal as well as abiotic and biotic stress conditions. In this way, the present study provides much information that can be utilized for the development of climate resilient cultivars of *B. napus*.

## Author contributions

VM, SK and UK planned and guided the design of this study. VK, HS, LS, AT, PJ, PB, SJ and ID retrieved sequence data, conducted computational analysis. VK, HS, LS, AT, PJ and PB performed data visualization, and wrote the first draft of the manuscript. VM, RM, KS, SK, YS, SJ, ID and UK critically revised and edited the manuscript. All authors have read and agree to the final version of the manuscript.

## Acknowledgments

The authors thank the Head, Department of Botany, Chaudhary Charan Singh University, Meerut, India for providing the necessary facilities to carry out this study and Head of Department of Molecular Biology & Biotechnology, College of Biotechnology, Chaudhary Charan Singh Haryana Agricultural University, Hisar, India for providing the necessary facilities to carry out this study.

## Conflict of interest

The authors declare that the research was conducted in the absence of any commercial or financial relationships that could be construed as a potential conflict of interest.

## Publisher's note



## Supplementary material

The Supplementary Material for this article can be found online at: https://www.frontiersin.org/articles/10.3389/fpls.2022.1037206/full#supplementary-material

## References

Arias, T., and Pires, J. C. (2012). A fully resolved chloroplast phylogeny of the brassica crops and wild relatives (Brassicaceae: Brassiceae): Novel clades and potential taxonomic implications. *Taxon* 61 (5), 980–988. doi: 10.1002/tax.615005

Batra, R., Agarwal, P., Tyagi, S., Saini, D. K., Kumar, V., Kumar, A., et al. (2019). A study of CCD8 genes/proteins in seven monocots and eight dicots. *PloS One* 14 (3), e0213531. doi: 10.1371/journal.pone.0213531

Bolser, D. M., Kerhornou, A., Walts, B., and Kersey, P. (2015). Triticeae resources in ensembl plants. *Plant Cell Physiol.* 56 (1), e3. doi: 10.1093/pcp/pcu183

Budak, H., and Zhang, B. (2017). MicroRNAs in model and complex organisms. *Funct. Integr. Genomics* 17 (2), 121–124. doi: 10.1007/s10142-017-0544-1

Cao, Y., Jiang, Y., Ding, M., He, S., Zhang, H., Lin, L., et al. (2015). Molecular characterization of a transcriptionally active Ty1/copia-like retrotransposon in gossypium. *Plant Cell Rep.* 34 (6), 1037–1047. doi: 10.1007/s00299-015-1763-3

Cartea, M. E., Soengas, P., Picoaga, A., and Ordas, A. (2005). Relationships among brassica napus (L.) germplasm from Spain and great Britain as determined by RAPD markers. *Genet. Resour. Crop Evol.* 52 (6), 655–662. doi: 10.1007/s10722-003-6014-8

Chalhoub, B., Denoeud, F., Liu, S., Parkin, I. A., Tang, H., Wang, X., et al. (2014). Early allopolyploid evolution in the post-neolithic brassica napus oilseed genome. *Science* 345, 950–953. doi: 10.1126/science.1253435

Chen, P., and Hochstrasser, M. (1996). Autocatalytic subunit processing couples active site formation in the 20S proteasome to completion of assembly. *Cell* 86 (6), 961–972. doi: 10.1016/S0092-8674(00)80171-3

Clavijo, B. J., Venturini, L., Schudoma, C., Accinelli, G. G., Kaithakottil, G., Wright, J., et al. (2017). An improved assembly and annotation of the allohexaploid wheat genome identifies complete families of agronomic genes and provides genomic evidence for chromosomal translocations. *Genome Res.* 27 (5), 885–896. doi: 10.1101/gr.217117.116

Colovos, C., and Yeates, T. (1993). ERRAT: an empirical atom-based method for validating protein structures. *Protein Sci.* 2 (9), 1511–1519. doi: 10.1002/pro.5560020916

Dai, X., and Zhao, P. X. (2011). psRNATarget: a plant small RNA target analysis server. *Nucleic Acids Res.* 39, W155–W159. doi: 10.1093/nar/gkr319

Dai, X., Zhuang, Z., and Zhao, P. X. (2018). psRNATarget: a plant small RNA target analysis server, (2017 Release). *Nucleic Acids Res.* 46, W49–W54. doi: 10.1093/nar/gky316

Dantuma, N. P., and Bott, L. C. (2014). The ubiquitin-proteasome system in neurodegenerative diseases: precipitating factor, yet part of the solution. *Front. Mol. Neurosci.* 7. doi: 10.3389/fnmol.2014.00070

DeSalle, R., Tessler, M., and Rosenfeld, J. (2020). *Phylogenomics: a primer* (Boca Raton, London, New York: CRC Press) Boca Raton, London, New york.

Dhaliwal, A. K., Mohan, A., and Gill, K. S. (2014). Comparative analysis of ABCB1 reveals novel structural and functional conservation between monocots and dicots. *Front. Plant Sci.* 5. doi: 10.3389/fpls.2014.00657

Duke, J. A. (1983). *Handbook of energy crops* (Sydney, Australia: Center for New Crops & Plants Products).

Eisen, J. A. (1998). Phylogenomics: improving functional predictions for uncharacterized genes by evolutionary analysis. *Genome Res.* 8 (3), 163–167. doi: 10.1101/gr.8.3.163

Eisenberg, D., Lüthy, R., and Bowie, J. U. (1997). [20] VERIFY3D: assessment of protein models with three-dimensional profiles. *Methods Enzymol.* 277, 396–404. doi: 10.1016/S0076-6879(97)77022-8

Fu, H., Doelling, J. H., Arendt, C. S., Hochstrasser, M., and Vierstra, R. D. (1998). Molecular organization of the 20S proteasome gene family from arabidopsis thaliana. *Genetics* 149 (2), 677–692. doi: 10.1093/genetics/149.2.677

Fürstenberg-Hägg, J., Zagrobelny, M., and Bak, S. (2013). Plant defense against insect herbivores. *Int. J. Mol. Sci.* 14 (5), 10242–10297. doi: 10.3390/ijms140510242

Gilbert, A., Cosgrove, L., and Wilkinson, J. (2012). *"The royal horticultural society VegeTable and fruit gardening in australia,"* (Melbourne, Australia: Dorling Kindersly Australia Pty Ltd.).

Grieve, M. A. (1984). *"Modern herbal,"* (Melbourne, Australia: Penguin Books Australia).

Groll, M., Ditzel, L., Löwe, J., Stock, D., Bochtler, M., Bartunik, H. D., et al. (1997). Structure of 20S proteasome from yeast at 2.4 Å resolution. *Nature* 386 (6624), 463–471. doi: 10.1038/386463a0

Gupta, P. K., and Rustgi, S. (2004). Molecular markers from the transcribed/expressed region of the genome in higher plants. *Funct. Integr. Genomics* 4 (3), 139–162. doi: 10.1007/s10142-004-0107-0

Gupta, P. K., and Varshney, R. K. (2000). The development and use of microsatellite markers for genetic analysis and plant breeding with emphasis on bread wheat. *Euphytica* 113 (3), 163–185. doi: 10.1023/A:1003910819967

Hiratsuka, K., and Chua, N. H. (1997). Light-regulated transcription in higher plants. *J. Plant Res.* 110 (1), 131–139. doi: 10.1007/BF02506852

Kantar, M., Lucas, S. J., and Budak, H. (2011). miRNA expression patterns of *Triticum dicoccoides* in response to shock drought stress. *Planta* 233, 471–484. doi: 10.1007/s00425-010-1309-4

Khraiwesh, B., Zhu, J. K., and Zhu, J. (2012). Role of miRNAs and siRNAs in biotic and abiotic stress responses of plants. *Biochim. Biophys. Acta (BBA) Gene Regul. Mech.* 1819 (2), 137–148. doi: 10.1016/j.bbagrm.2011.05.001

Kleiger, G., and Mayor, T. (2014). Perilous journey: a tour of the ubiquitin-proteasome system. *Trends Cell Biol.* 24 (6), 352–359. doi: 10.1016/j.tcb.2013.12.003

Kumar, A., Sharma, P., Gomar-Alba, M., Shcheprova, Z., Daulny, A., Sanmartín, T., et al. (2018). Daughter-cell-specific modulation of nuclear pore complexes controls cell cycle entry during asymmetric division. *Nat. Cell Biol.* 20 (4), 432–442. doi: 10.1038/s41556-018-0056-9

Kumar, S., Verma, S., and Trivedi, P. K. (2017). Involvement of small RNAs in phosphorus and sulfur sensing, signaling and stress: Current update. *Front. Plant Sci.* 8. doi: 10.3389/fpls.2017.00285

Kurepa, J., Wang, S., Li, Y., and Smalle, J. (2009). Proteasome regulation, plant growth and stress tolerance. *Plant Signaling Behav.* 4 (10), 924–927. doi: 10.4161/psb.4.10.9469

Kutcher, H. R., Warland, J. S., and Brandt, S. A. (2010). Temperature and precipitation effects on canola yields in Saskatchewan, Canada. *Agric. For. Meteorol.* 150 (2), 161–165. doi: 10.1016/j.agrformet.2009.09.011

Laskowski, R. A., MacArthur, M. W., Moss, D. S., and Thornton, J. M. (1993). PROCHECK: a program to check the stereochemical quality of protein structures. *J. Appl. Crystallogr.* 26 (2), 283–291. doi: 10.1107/S0021889892009944

Li, X. M., Chao, D. Y., Wu, Y., Huang, X., Chen, K., Cui, L. G., et al. (2015). Natural alleles of a proteasome α2 subunit gene contribute to thermotolerance and adaptation of African rice. *Nat. Genet.* 47 (7), 827–833. doi: 10.1038/ng.3305

Li, Y. C., Korol, A. B., Fahima, T., and Nevo, E. (2004). Microsatellites within genes: structure, function, and evolution. *Mol. Biol. Evol.* 21 (6), 991–1007. doi: 10.1093/molbev/msh073

Liu, W., Ma, R., and Yuan, Y. (2017). Post-transcriptional regulation of genes related to biological behaviors of gastric cancer by long noncoding RNAs and microRNAs. *J. Cancer* 8 (19), 4141–4154. doi: 10.7150/jca.22076

Liu, H.-H., Tian, X., Li, Y.-J., Wu, C.-A., and Zheng, C.-C. (2008). Microarray-based analysis of stress-regulated microRNAs in *Arabidopsis thaliana*. *RNA* 14, 836–843. doi: 10.1261/rna.895308

Livneh, I., Cohen-Kaplan, V., Cohen-Rosenzweig, C., Avni, N., and Ciechanover, A. (2016). The life cycle of the 26S proteasome: from birth, through regulation and function, and onto its death. *Cell Res.* 26 (8), 869–885. doi: 10.1038/cr.2016.86

Li, X., Xie, X., Li, J., Cui, Y., Hou, Y., Zhai, L., et al. (2017). "Conservation and diversification of the miR166 family in soybean and potential roles of newly identified miR166s,". *BMC Plant Biol.* 17 (1), 1–18. doi: 10.1186/s12870-017-0983-9

Lozano-Baena, M. D., Tasset, I., Obregón-Cano, S., de Haro-Bailon, A., Muñoz-Serrano, A., and Alonso-Moraga, Á. (2015). Antigenotoxicity and tumor growing inhibition by leafy *Brassica carinata* and sinigrin. *Molecules* 20 (9), 15748–15765. doi: 10.3390/molecules200915748

Lust, J. (1983). *The herb book* (Melbourne, Australia: Penguin Books Australia).

Lu, K., Wei, L., Li, X., Wang, Y., Wu, J., Liu, M., et al. (2019). Whole-genome resequencing reveals *Brassica napus* origin and genetic loci involved in its improvement. *Nat. Commun.* 10 (1), 1–12. doi: 10.1038/s41467-019-09134-9

Maršalkienė, N., Sliesaravičius, A., Karpavičienė, B., and Dastikaitė, A. (2009). Oil content and fatty acid composition of seeds of some Lithuanian wild crucifer species. *Agron. Res.* 7, 654–661.

Mehla, S., Kumar, U., Kapoor, P., Singh, Y., Sihag, P., Sagwal, V., et al. (2022). Structural and functional insights into the candidate genes associated with different developmental stages of flag leaf in bread wheat (Triticum aestivum l.). *Front. Genet.* 13. doi: 10.3389/fgene.2022.933560

Moldovan, D., Spriggs, A., Yang, J., Pogson, B. J., Dennis, E. S., and Wilson, I. W. (2010). Hypoxia-responsive microRNAs and trans-acting small interfering RNAs in arabidopsis. *J. Exp. Bot.* 61 (1), 165–177. doi: 10.1093/jxb/erp296

Mondal, R., and Das, P. (2020). Data-mining bioinformatics: suggesting arabidopsis thaliana l-type lectin receptor kinase IX. 2 (LecRK-IX. 2) modulate metabolites and abiotic stress responses. *Plant Signaling Behav.* 15, 1818031. doi: 10.1080/15592324.2020.1818031

Mondal, R., Madhurya, K., Saha, P., Chattopadhyay, S. K., Antony, S., Kumar, A., et al. (2022). Expression profile, transcriptional and post-transcriptional regulation of genes involved in hydrogen sulphide metabolism connecting the balance between development and stress adaptation in plants: a data-mining bioinformatics approach. *Plant Biol.* 24, 602–617 doi: 10.1111/plb.13378

Parmentier, Y., Bouchez, D., Fleck, J., and Genschik, P. (1997). The 20S proteasome gene family in *Arabidopsis thaliana*. *FEBS Lett.* 416 (3), 281–285. doi: 10.1016/S0014-5793(97)01228-3

Peng, J., Richards, D. E., Hartley, N. M., Murphy, G. P., Devos, K. M., Flintham, J. E., et al. (1999). 'Green revolution' genes encode mutant gibberellin response modulators. *Nature* 400, 256–261. doi: 10.1038/22307

Rensink, W. A., and Buell, C. R. (2004). Arabidopsis to rice. applying knowledge from a weed to enhance our understanding of a crop species. *Plant Physiol.* 135 (2), 622–629. doi: 10.1104/pp.104.040170

Rogozin, I. B., Wolf, Y. I., Sorokin, A. V., Mirkin, B. G., and Koonin, E. V. (2003). Remarkable interkingdom conservation of intron positions and massive, lineage-specific intron loss and gain in eukaryotic evolution. *Curr. Biol.* 13 (17), 1512–1517. doi: 10.1016/S0960-9822(03)00558-X

Sassa, H., Oguchi, S., Inoue, T., and Hirano, H. (2000). Primary structural features of the 20S proteasome subunits of rice (*Oryza sativa*). *Gene* 250 (1-2), 61–66. doi: 10.1016/S0378-1119(00)00190-6

Sharma, H., Batra, R., Kumar, S., Kumar, M., Kumar, S., Balyan, H. S., et al. (2022). Identification and characterization of 20S proteasome genes and their relevance to heat/drought tolerance in bread wheat. *Gene Rep.* 27, 101552. doi: 10.1016/j.genrep.2022.101552

Sharma, B., Joshi, D., Yadav, P. K., Gupta, A. K., and Bhatt, T. K. (2016). Role of ubiquitin-mediated degradation system in plant biology. *Front. Plant Sci.* 7. doi: 10.3389/fpls.2016.00806

Stone, S. L. (2019). Role of the ubiquitin-proteasome system in plant response to abiotic stress. *Int. Rev. Cell Mol. Biol.* 343, 65–110. doi: 10.1016/bs.ircmb.2018.05.012

Tamura, K., Peterson, D., Peterson, N., Stecher, G., Nei, M., and Kumar, S. (2011). MEGA5: molecular evolutionary genetics analysis using maximum likelihood, evolutionary distance, and maximum parsimony methods. *Mol. Biol. Evol.* 28 (10), 2731–2739. doi: 10.1093/molbev/msr121

Town, C. D., Cheung, F., Maiti, R., Crabtree, J., Haas, B. J., Wortman, J. R., et al. (2006). Comparative genomics of *Brassica oleracea* and *Arabidopsis thaliana* reveal gene loss, fragmentation, and dispersal after polyploidy. *Plant Cell* 18 (6), 1348–1359. doi: 10.1105/tpc.106.041665

Varshney, R. K., Graner, A., and Sorrells, M. E. (2005). Genic microsatellite markers in plants: features and applications. *Trends Biotechnol.* 23 (1), 48–55. doi: 10.1016/j.tibtech.2004.11.005

Verma, S. S., Rahman, M. H., Deyholos, M. K., Basu, U., and Kav, N. N. (2014). Differential expression of miRNAs in *Brassica napus* root the following infection with *Plasmodiophora brassicae*. *PloS One* 9 (1), e86648. doi: 10.1371/journal.pone.0086648

Vierstra, R. D. (2009). The ubiquitin–26S proteasome system at the nexus of plant biology. *Nat. Rev. Mol. Cell Biol.* 10 (6), 385–397. doi: 10.1038/nrm2688

Vilella, A. J., Severin, J., Ureta-Vidal, A., Heng, L., Durbin, R., and Birney, E. (2009). EnsemblCompara gene trees: Complete, duplication-aware phylogenetictrees in vertebrates. *Genome Res.* 19 (2), 327–335. doi: 10.1101/gr.073585.107

Wang, J., Song, L., Gong, X., Xu, J., and Li, M. (2020). Functions of jasmonic acid in plant regulation and response to abiotic stress. *Int. J. Mol. Sci.* 21 (4), 1446. doi: 10.3390/ijms21041446

Wiersema, J. H., and Leon, B. (2016). *"World economic plants: A standard reference,"* (Melbourne, Australia: CRC press).

Wolf, D. H., and Hilt, W. (2004). The proteasome: a proteolytic nanomachine of cell regulation and waste disposal. *Biochim. Biophys. Acta (BBA) Mol. Cell Res.* 1695 (1-3), 19–31. doi: 10.1016/j.bbamcr.2004.10.007

Xu, F. Q., and Xue, H. W. (2019). The ubiquitin-proteasome system in plant responses to environments. *Plant Cell Environ.* 42 (10), 2931–2944. doi: 10.1111/pce.13633

Yang, P., Fu, H., Walker, J., Papa, C. M., Smalle, J., Ju, Y. M., et al. (2004). Purification of the arabidopsis 26 s proteasome: biochemical and molecular analyses revealed the presence of multiple isoforms. *J. Biol. Chem.* 279 (8), 6401–6413. doi: 10.1074/jbc.M311977200

Yu, X., Han, J., Wang, E., Xiao, J., Hu, R., Yang, G., et al. (2019). Genome-wide identification and homoeologous expression analysis of *PP2C* genes in wheat (*Triticum aestivum* l.). *Front. Genet.* 10. doi: 10.3389/fgene.2019.00561

Zhang, L., Chia, J. M., Kumari, S., Stein, J. C., Liu, Z., Narechania, A., et al. (2009). A genome-wide characterization of microRNA genes in maize. *PloS Genet.* 5 (11), e1000716. doi: 10.1371/journal.pgen.1000716

frontiers | Frontiers in Plant Science

TYPE Review
PUBLISHED 29 November 2022
DOI 10.3389/fpls.2022.1008993



OPEN ACCESS

EDITED BY
Sindhu Sareen,
Indian Institute of Wheat and Barley Research (ICAR), India

REVIEWED BY
Mostafa Aalifar,
University of Tehran, Iran
Guihong Bi,
Mississippi State University, United States
Rohit Joshi,
Institute of Himalayan Bioresource Technology (CSIR), India

*CORRESPONDENCE
Aruna Tyagi
arunatyagibiochem@gmail.com

†These authors have contributed equally to this work

SPECIALTY SECTION
This article was submitted to Plant Abiotic Stress, a section of the journal Frontiers in Plant Science

RECEIVED 01 August 2022
ACCEPTED 07 November 2022
PUBLISHED 29 November 2022

CITATION
Maheshwari C, Garg NK, Hasan M, V P, Meena NL, Singh A and Tyagi A (2022) Insight of PBZ mediated drought amelioration in crop plants. *Front. Plant Sci.* 13:1008993. doi: 10.3389/fpls.2022.1008993



# Insight of PBZ mediated drought amelioration in crop plants

Chirag Maheshwari[1†], Nitin Kumar Garg[1,2†], Muzaffar Hasan[1,3], Prathap V[1], Nand Lal Meena[1], Archana Singh[1] and Aruna Tyagi[1*]

[1]Division of Biochemistry, ICAR-Indian Agricultural Research Institute, New Delhi, India, [2]Sri Karan Narendra Agriculture University, Jobner, India, [3]Agro Produce Processing Department, Indian Council of Agricultural Research (ICAR)-Central Institute of Agricultural Engineering, Bhopal, India

Water scarcity is a significant environmental limitation to plant productivity as drought-induced crop output losses are likely to outnumber losses from all other factors. In this context, triazole compounds have recently been discovered to act as plant growth regulators and multi-stress protectants such as heat, chilling, drought, waterlogging, heavy metals, etc. Paclobutrazol (PBZ) [(2RS, 3RS)-1-(4-chlorophenyl)- 4, 4-dimethyl-2-(1H-1, 2, 4-trizol-1-yl)-pentan-3-ol)] disrupts the isoprenoid pathway by blocking ent-kaurene synthesis, affecting gibberellic acid (GA) and abscisic acid (ABA) hormone levels. PBZ affects the level of ethylene and cytokinin by interfering with their biosynthesis pathways. Through a variety of physiological responses, PBZ improves plant survival under drought. Some of the documented responses include a decrease in transpiration rate (due to reduced leaf area), higher diffusive resistance, relieving reduction in water potential, greater relative water content, less water use, and increased antioxidant activity. We examined and discussed current findings as well as the prospective application of PBZ in regulating crop growth and ameliorating abiotic stresses in this review. Furthermore, the influence of PBZ on numerous biochemical, physiological, and molecular processes is thoroughly investigated, resulting in increased crop yield.

KEYWORDS

**PBZ, drought, gibberellic acid, abscisic acid, physiological and biochemical response**

## Introduction

Climate change has posed a severe danger to crop productivity and output. Numerous types of abiotic stressors, such as heat, drought, and salt, cause morphological, physiological, and biochemical alterations that eventually hamper crop growth (Yadav et al., 2020). Drought is a big worry since numerous variables such as high

and low temperatures, limited water availability, erratic rain patterns, low rainfall, salt, high light intensity, etc. led to drought (Salehi-Lisar and Bakhshayeshan-Agdam, 2016). Drought in plants is characterized by decreased leaf water potential, turgor pressure, stomatal closure, and impaired cell growth. Drought impacts photosynthesis, chlorophyll production, nutrient metabolism, ion uptake and translocation, respiration, carbohydrate metabolism, etc. in plants (Farooq et al., 2009).

When it comes to drought-induced plant damage, oxidative stress is critical. Drought raises reactive oxygen species (ROS) levels in plant cells (Smirnoff, 1993). Excessive ROS generation and accumulation induce cellular oxidative damage, disrupt cellular membranes, and result in enzyme inactivation, protein breakdown, and ionic imbalance in plants (Hasanuzzaman et al., 2020). ROS disrupts cellular macromolecules, including DNA, and may result in base deletion owing to alkylation and oxidation, both of which have been associated with a variety of physiological and biochemical ailments in plants (Apel and Hirt, 2004). Plants have a sophisticated antioxidative defense system that controls the overproduction of ROS. The ROS-induced damages and disruption of cellular homeostasis are alleviated by the action of different enzymatic (e.g., catalase, CAT; superoxide dismutase, SOD; peroxidase, POD; glutathione reductase, GR; glutathione peroxidase, GPX) and non-enzymatic (e.g., ascorbic acid, carotenoids, tocopherols, and glutathione content) antioxidants (Prochazkova et al., 2001; Rady and Gaballah, 2012). This plant defense system is only active up to a specific threshold of tolerance. Under severe and persistent stress, the natural defense system is hampered, resulting in physiological anomalies (Smirnoff, 1993). The mechanism of ROS generation and scavenging by plants with high antioxidative capacity has been linked to plant tolerance to abiotic stressors (Wahid et al., 2014). As a result, various studies have been conducted to improve plant resilience and drought adaptations, as well as to mitigate the negative effects of drought. These studies mostly involve the use of phytoprotectants (such as growth promoters, antioxidant compounds, and osmoprotectants), which are highly effective measures of promoting drought responses in agricultural plants (Garg et al., 2019; Desta and Amare, 2021).

Plant growth regulators (PGRs) are commonly utilized in agriculture to augment overall plant growth. Plant growth regulators have both beneficial and negative effects on growth, development, and plant metabolism (Ashraf et al., 2011; Desta and Amare, 2021). There are several classes of PGR including auxin, abscisic acid, cytokinins, gibberellin, salicylic, jasmonic acid, and ethylene, as well as more recently investigated brassinosteroids, strigolactones, polyamine, and triazole, etc. Due to their intrinsic abiotic stress tolerance inducement through augmenting plant self-defense systems such as antioxidant enzymes and molecules in stress-affected plants, triazole compounds, a class of systemic fungicides, have been investigated to have plant growth promoting properties and are sometimes used as stress-safeguards (Jaleel et al., 2007). Various triazole compounds are used as PGRs such as PBZ, uniconazole, triapenthenol and BAS 111, etc. Triazoles regulate plant growth by changing the balance of key plant hormones i.e., cytokinins, gibberellic, and abscisic acid (Hajihashemi, 2018). Triazoles induce morphological (root growth stimulated and shoot elongation inhibition) and biochemical (enhanced cytokinin synthesis and temporary increase in ABA) changes (Fletcher et al., 2000; Gopi et al., 2007).

PBZ is a triazole compound that plays an important function in reducing water deficit stress by lowering glutathione levels and reducing the peroxidation of lipids (Aly and Latif, 2011). Many plants, including tomato, sesame seeds, and mango have been shown to use PBZ to reduce the negative effects of drought by enhancing the activity of anti-oxidative enzymes (Somasundaram et al., 2009; Srivastav et al., 2010). PBZ has been known to be used in horticultural crops for a long time to increase yield. (Assuero et al., 2012; Kamran et al., 2020). PBZ prevents the biosynthesis of sterol and gibberellins (Khan et al., 2009). By modifying the photosynthetic rate and phytohormone levels, PBZ can significantly affect plant growth and development (Kim et al., 2012) (Table 1). The application of PBZ improved leaf number, stem diameter, modified root architecture, decreased plant height, and contributed to enhanced yield and tolerance to lodging (Syahputra et al., 2016; Pal et al., 2016). An enzyme ent-kaurene oxidase in GA biosynthetic pathway which catalyzes ent-kaurene oxidation into ent-kaurene acid is inhibited by PBZ (Rady and Gaballah, 2012; Kondhare et al., 2014). Sankar et al. (2013), reported that PBZ retains endogenous cytokinin levels, stabilizes leaf water capacity, and induces increased leaf and epidermal thickness. Besides discussing possible theories on the regulation of water deficit stress tolerance, this article aims to investigate the impact of PBZ on morphological, biochemical, and molecular responses to drought.

## Chemical structure and modes of application

### Chemical structure and translocation of PBZ in plant

PBZ is a synthetic compound having the empirical formula (1-(4-chloro-phenyl) 4,4-dimethyl-2-(1,2,4-triazol-1-yl)-pentan-3-ol) with two asymmetric carbon (Figure 1B). Therefore, two pairs of enantiomers may exist, (2R, 3R) - and (2S, 3S) -PBZ, and (2S, 3R) - and (2R, 3S) -PBZ. However, due to steric hindrance production of only the first pair of enantiomers is possible (Wu et al., 2013). While in the case of wheat (2S, 3S) -PBZ was a more effective regulator of plant growth inhibition than (2R, 3R) -PBZ (Lenton et al., 1994).

Triazoles were previously thought to be transported mainly acropetally in the xylem, (Davis et al., 1988). Later research on

TABLE 1 Summary of effect of PBZ on different parameters under the drought stress in various crops species.

**Effect of PBZ on RWC**

| S.No. | Crop | Effective dose | Key findings | References |
|---|---|---|---|---|
| 1. | *Triticum aestivum* | 30 mg/l | RWC was increased by 5% in control and 11% in drought plants treated with PBZ | Dwivedi et al., 2017 |
| 2. | *Oryza sativa* | 90 mg/l | 15% increase in RWC under drought compared to control | Garg et al., 2019 |
| 3. | *Curcuma alismatifolia* | 1500 mg/l | RWC increased by 5% under drought | Jungklang et al., 2017 |
| 4. | *Abelmoschus esculentus* | 80 mg/l | RWC increased by 60.1% under drought | Iqbal et al., 2020 |
| ***Effect of PBZ on MSI*** | | | | |
| | *Oryza sativa* | 90 mg/l | 15% increase in mean MSI under drought | Garg et al., 2019 |
| | *Triticum aestivum* | 30 mg/l | 4-5% increase in mean MSI under drought | Dwivedi et al., 2017 |
| ***Effect of PBZ on plant growth*** | | | | |
| | *Curcuma alismatifolia* | 1500 mg/l | The plant height was 1.2 times lower under drought | Jungklang and Saengnil, 2012 |
| | *Curcuma alismatifolia* | 3.75 g/l | Shoot height was reduced by 48.93% under drought | Jungklang and Saengnil, 2012 |
| | *Helianthus annuus* and *zinnia* | 2.0 mg/pot | Shoot height was reduced by 26.3 and 42.1%, respectively | Ahmad et al., 2014 |
| | *Syzygium myrtifolium* | 3.75 g/l | Plant height was reduced by 19.93% | Roseli et al., 2012 |
| | *Curcuma alismatifolia* | 1500 mg/l | Plant height was reduced by 50% under drought | Jungklang et al., 2017 |
| | *Odontonema strictum* | 0.24 mg/pot | Plants were 11 cm taller under drought | Rezazadeh et al., 2016 |
| | *Amorpha fruticosa* | 150 mg/l | 61% increase in the plant height | Fan et al., 2020 |
| | *Zea mays* L | 300 mg/l | Increased root dry weight by 102.1% at the seventh leaf stage, 65.1% at the ninth leaf stage, 47.9% at the twelfth leaf stage | Kamran et al., 2018 |
| | *Arachis hypogaea* | 10 mg/l | Increased root length from 18.17 to 28.15 cm/plant, total leaf area from 96.38 to 117.31 $cm^2$/plant, whole plant fresh weight from 33.72 to 39.16 gm/plant, whole plant dry weight from 3.49 to 4.12 g/plant | Sankar et al., 2014 |
| | *Sesamum indicum* | 5 mg/l | | Abraham et al., 2008 |
| | *Ipomoea batatas* | 34 μm | Increased vine fresh weight, root fresh weight, vine dry weight, and root dry weight by 40.10, 65.47, 66.91, and 67.86% respectively | Yooyongwech et al., 2017 |
| ***Effect of PBZ on photosynthetic pigments*** | | | | |
| | *Anacardium occidentale* | 3 g a.i./tree | Increased Chlorophyll a (27.35%), Chlorophyll b (54.54%), total chlorophyll (30.98%) and Carotenoids (13.55%) under control conditions | Mog et al., 2019 |
| | *Triticum aestivum* | 30 mg/l | 25.7% increase in chlorophyll content under drought | Dwivedi et al., 2018 |
| | *Zea mays* L | 300 mg/l | Increased the chlorophyll content by 48.2%, 54.3%, 51.2% and 79.0%, at 0, 15, 30 and 45 DAS respectively.<br>Carotenoid contents increased by 15.7%, 17.3%, 27.9% and 36.7% at 0, 15, 30 and 45 DAS respectively | Kamran et al., 2020 |
| | *Arachis hypogaea* | 10 mg/l | Increased total chlorophyll, carotenoid, xanthophyll and anthocyanin content by 120.22%, 112.66%, 116.48%, 111.26%, 114.44% and 112.24% respectively | Sankar et al., 2013 |
| | *Zea mays* L | 2 mg/l | Increased chlorophyll content by 62% | |
| | *Oryza sativa L. indica* | 25 or 50 mg/l | Plants had greener leaves and delayed late senescence | Dewi, 2018 |
| | *Odontonema strictum* | 0.24 mg/pot | Net photosynthesis was 51% higher under drought | Rezazadeh et al., 2016 |

*(Continued)*

TABLE 1 Continued

**Effect of PBZ on RWC**

| S.No. | Crop | Effective dose | Key findings | References |
|---|---|---|---|---|
| | *Zoysia japonica* | 50 mg/l | Increased leaf chlorophyll content by 0.6 mg $g^{-1}$ FW | Cohen et al., 2019 |
| | *Festuca arundinacea* and *Lolium perenne* | | Increased the photosynthetic pigment content | Shahrokhi et al., 2011 |
| | *Vigna radiata* | 150 mg/l | Increased SPAD value from 34 to 37.7 | Babarashi et al., 2021 |
| ***Effect of PBZ on grain yield and dry matter partitioning*** | | | | |
| | *Zea mays* L | 50 mg/l | Increased the average weight of 1,000 seeds and yield | Bayat and Sepehri 2012 |
| | *Zea mays* L | 300 mg/l | Kamran et al. (2018), average maize grain yields increased by 61.3% after seed soaking with 300 mg/l PBZ, while seed dressing with PBZ at 2.5 g $kg^{-1}$ increased yield by 33.3% | Kamran et al., 2018 |
| | *Triticum aestivum* | | Increased grain yield per plant by 6-7%, grain numbers per panicle by 24-33%, 1,000-grain mass by 3-6%, and harvest index by 2-4% | Dwivedi et al., 2017 |
| | *Vigna radiata* | 150 mg/l | Increased seed yield from 622 to 1921 kg/ha | Babarashi et al., 2021 |
| | *Odontonema strictum* | 0.24 mg/ plant | Promoted flowering and maintained the same numbers of flower (6 flowers/plant) | Rezazadeh et al., 2016 |
| | *Solanum lycopersicum* | 50 mg/l | Yield increased by 1.37 times more | Rezazadeh et al., 2016 |
| | *Solanum lycopersicum* | 30 mg/l | Pretreated tomato plants retained their fruit yield (3.89 kg/plant) and number of fruits (31 fruits/plant) when exposed to drought | Latimer, 1992 |

castor bean (Witchard, 1997) and pear (Browning et al., 1992) found their presence in both xylem and phloem sap, suggesting that these can be transported both acropetally and basipetally. PBZ was also held by roots, translocated through the xylem mainly in the stems, and collected in leaves (Wang et al., 1985). Early and Martin (1988) found that PBZ was metabolized more quickly in apple leaves than in other plant sections.

## Mode of action and methods of application

PBZ is a growth retardant and stress protectant that works by inhibiting GA biosynthesis (Gopi et al. 2009). PBZ suppressed the GA biosynthesis by inactivating ent-kaurene oxidase or cytochrome P450-dependent oxygenase, preventing ent-kaurene to ent-kauronoic acid oxidation (Zhu et al., 2004; Rady and Gaballah, 2012). Since both abscisic acid and chlorophyll are synthesized through the terpenoid pathway, PBZ has been shown to influence their synthesis too (Figure 1A). As PBZ inhibits GA synthesis, common terpenoid pathway precursors accumulate and are redirected to promote ABA biosynthesis (Rademacher, 2018). Kitahata et al. (2005) found that PBZ inhibited natural ABA catabolism by inhibiting the ABA 8' hydroxylase enzyme (Fig 1a).PBZ is more effective even at lower dose of application compared to other PGRs (Rady and Gaballah, 2012).

Foliar sprays, drenching, and seed priming are the most popular methods of PBZ application. All methods yield good results (Rademacher, 2015) but drenching works for a longer duration and provide uniform regulation at lower doses (10 μM) in *Capsicum chinense* (Franca et al., 2017). As PBZ is poorly soluble (0.12 mM) in water when applied as a foliar spray, it is only partially translocated in the phloem (Ribeiro et al., 2011). In contrast to foliar spray, PBZ application by drenching is more uniform as PBZ is transported *via* xylem vessels. Further, PBZ application by drenching inhibits GA more effectively as roots synthesize a significant amount of GA (Sopher et al., 1999). Ruter (1996), demonstrated that drench application was more effective than foliar spray at the lower dose of PBZ (0.5 mg a.i./pot) in shrub lantana. Seed priming treatment using PBZ (100μM) under drought in rice genotypes leads to better growth of the plants compared to unprimed seed plants (Samota et al., 2017a).

# Morphological and physio-biochemical responses of plants to PBZ

## Effect of PBZ on relative water content

Relative water content (RWC), directly related to the content of soil water (Sarker et al., 1999) is a significant indicator of water stress in leaves (Merah, 2001). Plant exposure to water

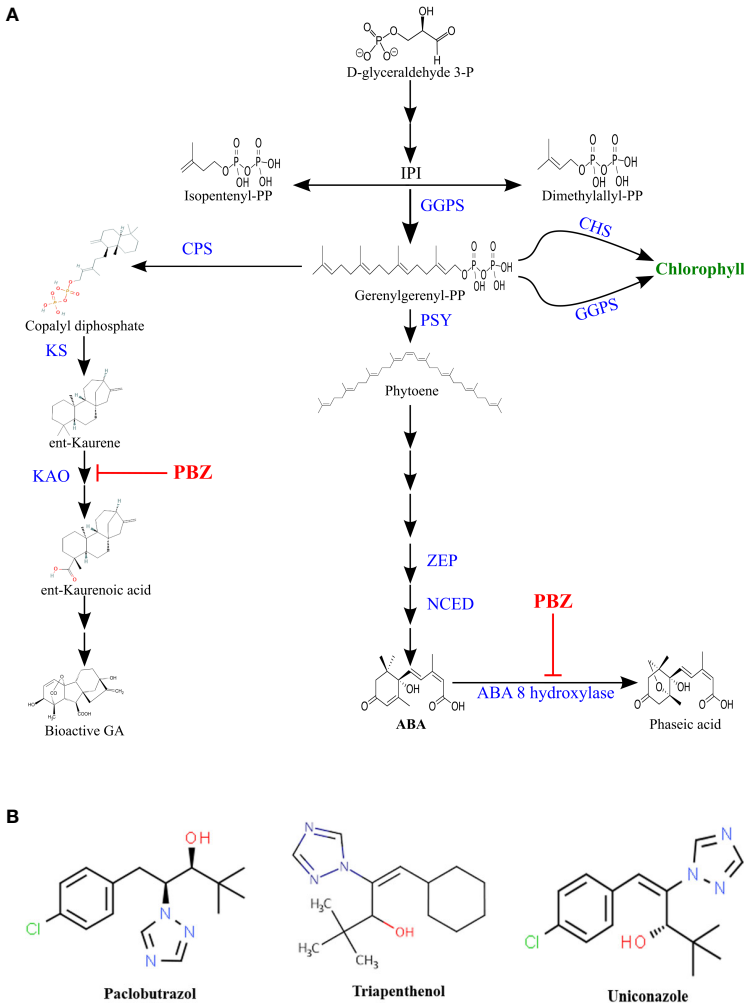


FIGURE 1

**(A)**Terpenoid pathway. Paclobutrazol inhibition is indicated by ⊣. (*CPS*), Copalyl diphosphate synthase; (*KAO*), ent-kaurenoic acid oxidase; (*KS*), ent-kaurene synthase; (*GGPPS*), geranylgeranyl pyrophosphate synthase; (*PSY*), phytoene synthase; (*ZEP*), zeaxanthin epoxidase; (*NCED*), 9-*cis*epoxycarotenoid dioxygenase; (*CHS*), chlorophyll Synthase; (*GGRS*), geranylgeranyl reductase. **(B)** Chemical structure of some triazoles.

stress results in an immediate reduction of RWC (Mawlong et al., 2014; Kumar et al., 2015). PBZ accelerated the stomatal closure, improved water retention, and increased drought tolerance in jack pine and oak ( (Marshall et al., 2000; Percival and Salim AlBalushi., 2007). PBZ-treated plants maintained higher RWC than the non-treated ones' (Jungklang and Saengnil, 2012; Dwivedi et al., 2017; Jungklang et al., 2017). Dwivedi et al. (2017), stated that the application of PBZ (30 mg/l) in wheat under control and water-stressed plants resulted in an increase of 5% and 11% respectively in the mean RWC. The reduced rate of evapotranspiration helps plants maintain a higher RWC, and overcome stress, and developed tolerance to various environmental stresses (Yadav et al., 2005). RWC increased in PBZ-treated triticale (*Triticale hexaploide*) plants during water stress (Berova and Zlatev, 2003)., Under water stress, PBZ treatment assists plants in retaining water for 30-40 days (Jungklang and Saengnil, 2012). Garg et al. (2019), observed that application of PBZ (90 mg/l) under drought in rice genotypes was responsible for about a 15% increase in RWC as compared to drought without PBZ treatment. Jungklang et al. (2017), found that in *Curcuma alismatifolia* leaves, PBZ (1500 mg/l) increased RWC by 5% under drought. Iqbal et al. (2020), reported that in okra (*Abelmoschus esculentu*) cultivar Nutec, application of PBZ (80 mg/l) along with drought increased RWC (60.1%) compared to drought without PBZ treatment (57.2%) although the result was not statistically significant. Similarly, in Safflower (*Carthamus tinctorius L.*) application of PBZ under drought enhances the RWC (Davari et al., 2022). Overall PBZ enhances the RWC of plants under drought conditions by a reduction in evapotranspiration.

## Effect of PBZ on membrane stability index

Membrane stability is a common criterion for determining drought tolerance because water deficit induces water loss from plant tissues, which severely impairs membrane structure and function. The stability of the cell membrane was used as a drought tolerance indicator and leakage of electrolytes showed an increase in water deficit (Agarie et al., 1995). Garg et al. (2019), reported that PBZ (90 mg/l) in rice genotypes led to an 11% increase in mean MSI as compared to drought-stressed plants without PBZ treatment. PBZ (20 mg/l) minimized the leakage of electrolytes in carrots (Gopi et al., 2007). Dwivedi et al. (2017) reported that the application of PBZ (30 mg/l) in wheat under control and water-stressed plants resulted in an increase of 1-2% and 4-5% respectively in the mean MSI. Similarly, Jungklang et al. (2017), reported that PBZ (1500 mg/l) decreased electrolyte leakage by 60% under water deficit stress in *Curcuma alismatifolia*. Babarashi et al. (2021), observed that the application of PBZ (150 mg/l) in mungbean under drought decreased electrolyte leakage from 52.6% (drought without PBZ) to 47.1%. Similarly, in Safflower (*Carthamus tinctorius L.*) application of PBZ under drought enhances the cell membrane stability (Davari et al., 2022). Collectively, these findings suggest that PBZ improves MSI by minimizing electrolyte and ion leakage under stress conditions.

## Effect of PBZ on plant growth

The most striking growth response observed in PBZ-treated plants is a reduction in shoot growth (Pinto et al., 2005). This response is mainly attributed to internode length reduction. Hua et al. (2014), reported that canola plant height was reduced by 27% when PBZ was applied at 10 cm stalk height as compared to without PBZ. Rezazadeh et al. (2016), reported that red firespike plants treated with PBZ (.24 mg/pot) under drought were 11 cm taller than untreated plants. Under water deficit stress, Jungklang et al. (2017) found that applying PBZ (1500 mg/l) decreased the plant height of *Curcuma alismatifolia* by 50% relative to non-treated plants. In *Amorpha fruticosa*, Fan et al. (2020) found that PBZ treatment (150 mg/l) under extreme drought (RWC 35-40%) resulted in a 61% increase in height relative growth rate compared to drought without PBZ. Jungklang and Saengnil (2012), observed that in Patumma after 40 days of withholding water, the plant height was 1.2 times lower in PBZ (1500 mg/l) treated plants compared to water-stressed without PBZ. When PBZ (3750 mg/L) was applied to Patumma, shoot height was reduced by 48.93% relative to untreated plants. In comparison to non-treated plants, soil drenching with PBZ (1500 mg/l) under water stress for 20- and 30-days periods-maintained shoot length (Jungklang et al., 2017). However, in sunflower and zinnia shoot height was reduced by 26.3 and 42.1%, respectively, after soil drenching with PBZ (2.0 mg/pot) (Ahmad et al., 2014). According to Roseli et al. (2012), *Syzygium myrtifolium* (Roxb.) Walp. plant height was reduced by 19.93% when treated with PBZ (3750 mg/L). According to Azarcon et al. (2022), PBZ (500ppm) increased panicle number, resulting in higher grain yield while reducing water demand, hence increasing rice water use efficiency under drought conditions.

Berova et al. (2002) reported that PBZ (50 mg/l) increased wheat seedling length, fresh and dry weight of shoots, under low-temperature stress as compared to control (low-temperature stress without PBZ). PBZ has been shown to increase both the fresh and dry weight of shoots and roots in cucumber seedlings that have been exposed to high temperatures (Baninasab and Ghobadi, 2011). Kamran et al. (2018), reported that seed soaking of maize with PBZ (300 mg/l) under a semi-arid region increased root dry weight by 102.1% at the seventh leaf stage, 65.1% at the ninth leaf stage, 47.9% at the twelfth leaf stage, compared to drought without PBZ treatment. Sankar et al. (2014), reported that in peanut plants at 80 days after sowing (DAS) application of PBZ (10 mg/l) under drought increased root length from 18.17 to 28.15 cm/plant, total leaf area from 96.38 to 117.31 $cm^2$/plant, whole plant fresh weight from 33.72 to 39.16 g/plant, whole plant dry weight from 3.49 to 4.12 g/plant as compared to drought-stressed plants without PBZ treatment. A similar pattern of results was also obtained by Abraham et al. (2008) in *Sesamum indicum* by application of PBZ (5 mg/l) during drought. Yooyongwech et al. (2017) observed that in sweet potatoes, PBZ (34 μM) under drought increased vine fresh weight, root fresh weight, vine dry weight, and root dry weight by 40.10, 65.47, 66.91, and 67.86% respectively, compared to water-stressed plants.

After PBZ (500 mg/l) application, the root dry weight of *Aesculus hippocastanum* was improved (18.4% reduction) after water deficit stress (Percival and Noviss, 2008). Under drought conditions, the dry weight of PBZ (60 mg/l) treated tomato shoots (37.17% reduction) and root dry weight (13.04% reduction) were higher (Latimer, 1992) as compared to the control. Similarly, the dry weight of PBZ (50 mg/l) treated plants decreased by 20.45%, compared to 36.77% for non-treated plants (Bayat and Sepehri, 2012). In turf grass, shoot dry weight was extremely responsive to water deficit conditions (25% FC), resulting in 95 to 97% reduction, respectively, while treatment with PBZ (30 mg/l) reduced the shoot dry weight by 3.14% only (Shahrokhi et al., 2011).

The leaf area of *P. angustifolia* plants treated with PBZ (30 mg/l) and grown under well-watered conditions was reduced by 83.25%. However, when exposed to mild water deficit conditions, the growth of PBZ-treated plants improved but declined when exposed to severe water deficit stress (Fernández et al., 2006). When exposed to drought,

shoot height, leaf area, and root length of PBZ (10 mg/l) pre-treated peanut plants improved compared to the control (Sankar et al., 2014a). Farooqi et al. (2010), reported that the diameter of *Vetiveria Zizanioides* increased in stressed plants due to 12% PBZ application. According to Pal et al. (2016), PBZ (1.6 mg/l) reduced leaf area (LA) in tomato plants by 24% under water deficit conditions. Overall, PBZ enhanced plant development under stressful circumstances by increasing shoot and root biomass. Although some research implies that PBZ reduces plant height, others report that PBZ increases plant height, hence a greater knowledge of the influence of PBZ application on plant development is required before future application.

## Effect of PBZ on photosynthetic pigments

Water stress alters the total chlorophyll content and stability within thylakoid membrane protein-pigment complexes which are the first structures to be weakened under stress conditions (Pospíšilová et al. 2000). Chlorophyll reduction under water deficit stress is mainly due to chloroplast damage caused by ROS (Smirnoff, 1995). PBZ (3 g a.i./tree) increased Chlorophyll a (27.35%), Chlorophyll b (54.54%), total chlorophyll (30.98%) and carotenoids (13.55%) compared to control without PBZ in cashew (Mog et al., 2019). According to Dwivedi et al. (2018), applying PBZ (30 mg/l) to wheat plants under water deficit stress resulted in a 25.7% increase in chlorophyll content as compared to stressed plants without PBZ. Kamran et al. (2020), reported that in maize PBZ (300 mg/l) increased the chlorophyll content by 48.2%, 54.3%, 51.2%, and 79.0%, at 0, 15, 30, and 45 DAS respectively Similarly carotenoid contents increased by 15.7%, 17.3%, 27.9% and 36.7% at 0, 15, 30 and 45 DAS in water deficit stress as compared to control (drought without PBZ application). Berova et al. (2002) observed that PBZ treatment was 15–18% more effective than the control at preventing chlorophyll loss in wheat during low-temperature stress. PBZ (10 mg/l) increased total chlorophyll, carotenoid, xanthophyll, and anthocyanin content in 80 days old *Arachis hypogaea* by 120.22%, 112.66%, 116.48%, 111.26%, 114.44%, and 112.24% respectively over control under drought (Sankar et al., 2013) reported that PBZ (2 mg/l) increased chlorophyll content by 62% as compared to control in maize. Dewi et al. (2018), observed that treatment with 25 or 50 mg/l PBZ in black rice plants had greener leaves and encountered late senescence than control plants. Similarly, in Safflower (*Carthamus tinctorius L.*) application of PBZ under drought enhances the photosynthetic pigments (Davari et al., 2022).

Rezazadeh et al. (2016), reported that net photosynthesis was 51% higher in red firespike plants treated with PBZ (0.24 mg/pot) under drought than in those without PBZ. In *Zoysia japonica*, PBZ (50 mg/l) during water deficit stress increased leaf chlorophyll content by 0.6 mg/g FW compared to water-stressed without PBZ (Cohen et al., 2019). Similarly, Pal et al. (2016), recorded that PBZ in both irrigated and deficit-irrigated plants increased chlorophyll content as compared to control plants (without PBZ). PBZ increased the photosynthetic pigment content in *Festuca arundinacea* and *Lolium perenne* under water stress (Shahrokhi et al., 2011). Under water deficit stress, PBZ significantly increased chlorophyll a, chlorophyll b, and carotenoids in wheat cultivars (Aly and Latif, 2011). Babarashi et al. (2021), reported that PBZ (150 mg/l) treatment in mungbean under drought increased SPAD value from 34 (drought without PBZ) to 37.7. All prior investigations have concluded that PBZ improves photosynthesis by increasing chlorophyll and other photosynthetic pigments under stressful circumstances.

## Effect of PBZ on grain yield and dry matter partitioning

Drought primarily affects production by reducing the number of seeds by either influencing the quantity of dry matter produced at the time of flowering or by directly affecting pollen or ovules, leading to a decrease in seed collection. PBZ has been shown to modify sink efficiency, prompting assimilates to be redistributed to meristematic regions other than shoot apices and improving assimilate flow to reproductive structures in plants (Setia et al., 1996). Under drought, the use of PBZ (50 mg/l) increased the average weight of 1,000 seeds and yield in maize (*Zea mays* L.) (Bayat and Sepehri, 2012). According to Kamran et al. (2018), average maize grain yields increased by 61.3% after seed soaking with 300 mg/l PBZ, while seed dressing with PBZ at 2.5 g/kg increased yield by 33.3% compared to control without PBZ in semi-arid regions. Under water stress, wheat genotypes treated with PBZ increased grain yield per plant by 6-7%, grain numbers per panicle by 24-33%, 1,000-grain mass by 3-6%, and harvest index by 2-4% (Dwivedi et al., 2017). According to Iqbal et al. (2020), under water stress, yield per plant was reduced. Stress effects, on the other hand, were found to be reduced when PBZ was applied (40 mg/l). Babarashi et al. (2021) reported that the application of PBZ (150 mg/l) in mungbean under drought increased seed yield from 622 (drought without PBZ) to 1921 kg/ha. Drought impaired flowering in red firespike plants, but PBZ treatment (0.24 mg/plant) promoted flowering and maintained the same number of flowers (6 flowers/plant) as the control (Rezazadeh et al., 2016). Tomato plants treated with PBZ (50 mg/l) produced 1.37 times more fruit than non-treated plants. The yield of pre-treated plants was reduced by 4.79% when they were subjected to drought at 60% field capacity (Mohamed et al., 2011). (Latimer 1992) observed that PBZ (30 mg/l) pre-treated tomato plants retained their fruit yield (3.89 kg/plant) and fruits per plant (31 fruits/plant) when exposed to water deficit stress. Overall, past

research indicates that the use of PBZ boosted grain yield/fruit set under drought by improving sink efficiency.

## PBZ hampered the gibberellin biosynthesis

GAs are growth regulators which fall under a large family of tetracyclic diterpenoids. GAs are plant hormones that are required for a variety of developmental activities in plants such as pollen maturation, stem elongation, leaf expansion, trichome creation, seed germination, and flowering induction (Achard et al., 2009). Furthermore, the exogenous application of gibberellins can reverse PBZ-induced growth inhibition (Lever, 1986). These findings support the theory that PBZ-induced growth inhibition is due to a reduction in gibberellin biosynthesis. Wu et al. (2019), studied the effect of PBZ (200 mg/l) in rice varieties under submergence stress and found that gibberellic acid content was decreased by the application of PBZ compared to submergence stress without PBZ. Fan et al. (2020) found that PBZ (150 mg/l) under severe drought (RWC 35-40%) decreased GA content more than drought without PBZ in *Amorpha fruticosa*.

PBZ-induced abscisic acid biosynthesiAbscisic acid (ABA) is classified as a stress phytohormone because it accumulates quickly in response to stress and mediates many stress responses that help plants survive (Zhang et al., 2006). The effect of PBZ on ABA is of significant importance because ABA is synthesized through the isoprenoid pathway. Fan et al. (2020), reported that PBZ (150 mg/l) under severe drought (RWC 35-40%) increased ABA (27.1%) than without PBZ in *Amorpha fruticosa*. Similarly, Dwivedi et al. (2018), recorded that treatment with PBZ in wheat cultivars did not significantly affect ABA content, however, mean ABA content was significantly enhanced by 25% under water deficit stress. Pal et al. (2016), showed that DI (Deficit irrigated) + PBZ treated plants significantly increased ABA accumulation compared to DI control plants. PBZ application increased ABA and decreased gibberellins during the reproductive stage in the shoot of mango plants (Burondkar et al., 2016). Compared to untreated seedlings, PBZ treatment has been shown to minimize endogenous ABA by about one-third caused by water stress in apples and wheat (Buta and Spaulding, 1991; Wang et al., 2016). Mackay et al. (1990), found that PBZ-induced stress tolerance in snap beans was due to increased endogenous ABA content. PBZ substantially enhanced endogenous ABA levels in hydroponically grown seedlings and detached leaves of oilseed rape, according to Häuser et al. (1990). According to Aly and Latif (2011), PBZ enhanced the endogenous level of ABA in wheat under water deficit stress. Wu et al. (2019), observed that PBZ (200 mg/l) increased ABA content in rice varieties under submergence stress compared to submergence stress without PBZ application. The effect of PBZ on ABA may be the source of stress defense (Fletcher and Hofstra 1988).

## PBZ elevated antioxidant enzymes activity

PBZ enhances the detoxification of ROS, antioxidant, and chlorophyll (Chl) content (Rady and Gaballah, 2012). As photosystem II (PSII) operation is reduced, an imbalance between electron generation and usage occurs, causing quantum yield shifts. These changes in chloroplastic photochemistry cause excess light energy to be dissipated in the PSII core and antenna under drought, resulting in the development of potentially harmful active oxygen species ($O_2^-$, $^1O_2$, $H_2O_2$, OH) (Peltzer et al., 2002). ROS detoxification pathways can be found in all plant species and are classified as enzymatic which include ascorbate peroxidase (APX), superoxide dismutase (SOD), catalase (CAT), peroxidase (POX), and non-enzymatic which include reduced glutathione (GSH), ascorbic acid and tocopherol (Prochazkova et al., 2001).

Somasundaram et al. (2009) showed that PBZ (5 mg/l) application to *Sesamum indicum* resulted in 464.74%, 267.49%, and 359.08% increase in SOD, APX, and POX activity respectively in leaf tissue under drought conditions as compared to without PBZ. Different PBZ treatments increased SOD activity in maize grown in the semi-arid environment to varying degrees. From 0 to 15 days after silking (DAS), SOD activity increased, then decreased until it reached 45 DAS (Kamran et al., 2020). The APX activity of PBZ-treated ryegrasses was found to be 25% higher than that of untreated under drought. No considerable difference in CAT activity was observed in PBZ-treated plants under drought. PBZ increased POX activity considerably under drought (Sheikh Mohammadi et al., 2017). Under salt stress, a higher dose of PBZ (1500 mg/l) increased the activity of antioxidant enzymes in mango leaves. Under salt stress, mango plants treated with PBZ had higher SOD (24%), POX (163%), and CAT (46%) activity than control plants without PBZ treatment (Srivastav et al., 2010). Application of PBZ increased SOD by 19.09% and 33.07% in roots and leaves, respectively, and CAT activity by 33.17% in quinoa leaves under salinity. Similarly, PBZ improved POD activity in quinoa by 78.18% in roots and 55.56% in leaves under salinity stress (Waqas et al., 2017). Kamran et al. (2020), reported that PBZ (300 mg/l) in semi-arid region increased the mean SOD activity by 12.4%, 22.9%, 29.1%, and 38.6%, POD activity by 21.0%, 33.0%, 32.2% and 59.2%, CAT activity by 29.7, 25.6%, 45.0%, and 70.6%, APX activity by 40.9%, 28.7%, 56.2%, and 53.8% at 0, 15, 30, and 45 DAS, respectively in maize compared with the drought-stressed plants without PBZ treatment. PBZ decreased $H_2O_2$ and $O_2^-$ contents by 51.0% and 40.1% at 0 DAS, 45.0% and 42.0% at 15 DAS, 63.4% and 51.8% at 30 DAS, and 58.2% and 50.4% at 45 DAS, respectively,

compared with the water-stressed plants without PBZ treatment. Similarly, Forghani et al. (2020), reported an increase in antioxidant enzymes under salt stress with PBZ in sweet sorghum.

Under water deficit stress, PBZ application resulted in a 2-fold increase in GSH/GSSG ratio compared to control allowing for precise regulation of the ascorbate-peroxidase pathway and, as a result, preventing oxidative damage in tomato plants (Pal et al., 2016). Sankar et al. (2007), reported that in *Arachis hypogaea L.* (ICG221) application of PBZ (10mg/l) under water deficit stress increased ascorbic acid content in leaf from 9.08 to 9.52 mg/g dry weight basis, ά tocopherol from 0.52 to 0.70 mg/g fresh weight basis, reduced glutathione from 33.06 to 47.48 µg/g fresh weight basis as compared to drought-stressed plants without PBZ.

## PBZ enhanced proline content

Proline is a key amino acid in protein and membrane structures, as well as a ROS scavenger under drought (Ashraf and Foolad, 2007). PBZ treatment enhanced proline content and improved drought tolerance. However, further research is needed to determine the actual molecular mechanism underlying the effect of PBZ on mobile proline concentration in plants (Chandra and Roychoudhury, 2020). PBZ treatment (75 mg/L) significantly reduced proline content (0.030 µmol/g FW) in pomegranate leaves by 59.22% to control (0.067 µmol/g FW) (Moradi et al., 2017). Mohamed et al. (2011) found that free proline concentration increased by 54.56 mg $g^{-1}$ in PBZ (50 mg/l) treated tomato plants grown at 60% field capacity, which was 1.52-fold greater than the control. However, in water-stressed conditions, the free proline level in PBZ (10 mg/l) in pre-treated peanuts was lower (1.04-fold over control) than in untreated plants (1.49-fold over control) (Sankar et al., 2014). Dwivedi et al. (2017), showed that the wheat plants treated with PBZ under water stress had a 40% decrease in proline content as compared to the stressed plants without PBZ. These findings suggested that the wheat genotypes experienced less stress (as indicated by the proline content) and improved drought tolerance as a result of PBZ application. Another study showed a considerable increase in free proline content after Mannitol+PBZ treatment in wheat cultivar Sakha 8 (3.342 mg $g^{-1}$ f.w) as compared to control (without PBZ+Mannitol) and the same pattern was observed in all the wheat cultivars (Aly and Latif, 2011). Endogenous proline level increased by 17% in mango leaves treated with PBZ (1500 mg/L) under salt stress when compared to salinized plants without PBZ treatment (Srivastav et al., 2010). Samota et al. (2017a), showed a significant increase in proline content in drought-sensitive and drought tolerant rice genotypes after priming with PBZ under drought as compared to their unprimed samples. Babarashi et al. (2021) reported that the application of PBZ (150 mg/l) in mungbean under drought increased proline content from 7.28 (drought without PBZ) to 7.87 µmol/g f.wt. Similarly, in Safflower (*Carthamus tinctorius L.*) application of PBZ under drought enhances the proline content (Davari et al., 2022).

## PBZ reduced malondialdehyde content

Usually, membrane lipid peroxidation in plants is detected by measuring malondialdehyde (MDA). MDA is a widely used marker of oxidative lipid injury caused by environmental stress. Kamran et al. (2020), showed that the MDA content was significantly lower in the PBZ-treated maize plants over the control under drought. PBZ treatment under drought considerably reduced the MDA content in maize leaf by 31.5% at 0 DAS, 31.4% at 15 DAS, 32.2% at 30 DAS, and 20.2% at 45 DAS compared with drought without PBZ. Other studies carried out on PBZ-primed rice samples indicated that PBZ showed insignificant change in MDA content in the sensitive genotype under drought while a 55% decrease in MDA content was found in the tolerant genotype as compared to PBZ treated under control conditions (Sasi et al., 2021). Similar findings were documented by Samota et al. (2017b), who observed that plants raised from PBZ-primed seeds had lower MDA levels under control and drought conditions than plants raised from unprimed seeds. The amount of MDA decreased as the amount of PBZ increased. PBZ (80 mg/l) decreased MDA content (51.15 mol/g f.wt.) under water deficit stress relative to drought alone (61.92 mol/g f.wt.) (Samota et al. (2017b). Kamran et al. (2020), reported that PBZ (300 mg/l) in the semi-arid region reduced MDA content by 44.1%, 50.4%, 66.3%, 40.5%, at 0, 15, 30, and 45 DAS respectively compared with the water-stressed plants without PBZ treatment.

## PBZ influence on protein content

The protein content in plants decreases with the onset of water deficiency. PBZ treatment increased the protein content of the leaves and tubers in carrots (Gopi et al., 2007). From 0 to 15 DAS, the soluble protein content of maize increased slightly, then steadily decreased from 15 to 45 DAS. Plants treated with a high concentration of PBZ under drought retained higher protein content from 0 to 15 DAS, but protein content was significantly inhibited from 30 to 45 DAS (Kamran et al., 2020). Wheat seeds primed with PBZ had increased protein content (Nouriyani et al., 2012). Also, there are other similar reports which showed that PBZ priming increased the protein content under abiotic stress and non-stress conditions (Razavizadeh and Amu, 2013). According to Iqbal et al. (2020) when PBZ was applied under drought to the okra cultivar Nutec, total soluble proteins increased as the amount of PBZ was increased. Total soluble proteins were 11.04, 11.29, 10.75, and 11.76 mg/g f.wt. at

four different PBZ treatments of 0, 20, 40, and 80 mg/l, respectively under water stress conditions.

## PBZ influence on sugar content

During drought, the accumulation of compatible solutes such as carbohydrates is claimed to be an effective stress tolerance mechanism (McKersie and Leshem, 1994). Sugar resulting from transitory starch degradation was noticed in PBZ-pretreated plants (Kaur and Gupta, 1991), which retains the leaf water potential under water deficit stress conditions (Zhu et al., 2004). PBZ treatment in mango increased total sugar, sugar: acid ratio, reducing sugar, and titratable acidity reduction (Vijayalakshmi and Srinivasan, 1999; Yeshitela et al., 2004). In drought-stressed ryegrass, PBZ application significantly increased soluble sugar content compared to untreated plants. The impact of PBZ was mainly pronounced on 30 and 45 days of drought treatment in Iranian perennial ryegrass (Sheikh Mohammadi et al., 2017). According to Fan et al. (2020), PBZ (150 mg/l) under extreme drought (RWC 35-40%) had 119% higher soluble sugar content than drought without PBZ in *Amorpha fruticosa*. In untreated and PBZ-treated (50 mg/l) tomato plants total soluble sugars increased by 1.16 and 1.52 times under water deficit (60% FC), respectively (Mohamed et al., 2011). Sugar content increased by 2 mg/l after foliar application of PBZ under 6% PEG-induced water deficit stress in *S. rebaudiana Bertoni* as compared to stressed plants (Hajihashemi and Ehsanpour, 2014). Total soluble sugar enrichment in PBZ-treated sweet potatoes may be required for cellular osmotic adjustment under water deficit stress situations.

# Molecular responses of plants to PBZ

PBZ inhibits GA biosynthesis by inactivating cytochrome P 450-dependent oxygenase, which inhibits the oxidation of ent-kaurene to ent-kauronoic acid (Zhu et al., 2004; Rady and Gaballah, 2012). PBZ inhibits ABA degradation into phaseic acid, resulting in ABA accumulation. In drought-stressed tomato plants, PBZ increased the expression of ABA biosynthesis genes (SlZEP, SlNCED, and SlAAO1) (Pal et al., 2016). To gain a better understanding of the dwarfism mechanism, Zhu et al. (2016), analyzed gene transcripts of Lily leaves after PBZ treatment. 2704 genes were found to be differentially expressed by comparing PBZ-treated samples to untreated samples. PBZ increased the expression of nine genes encoding GA biosynthesis enzymes (one KAO and eight GA20ox genes) while decreasing the expression of a gene involved in GA deactivation (GA2ox gene). Song et al. (2011) reported that the expression of ent-kaurene oxidase (ZmKO1-2), ent-kaurene synthase (ZmKS1,2,4), and ent-copalyl diphosphate synthase (ZmCPS) decreased, whereas the expression of GA 3-oxidase (*ZmGA3ox1*), GA20-oxidase (*ZmGA20ox1,5*) and ent-kaurenoic acid oxidase (ZmKAO) increased in maize seedlings treated with PBZ. PBZ has been shown to increase SLGA20ox-3 and SLGA3ox2 expression in tomato plants through feedback regulation. Upregulation of SLGA20ox-3 and SLGA3ox2 transcript accumulation was observed in response to PBZ-induced ent-kaurene oxidase inhibition, which was thought to be a feedback upregulation of GA biosynthesis in response to lower GA content (Hedden and Thomas, 2012).

Another study examined the expression profiles of GA biosynthesis genes (ent-kaurene oxidase; *KO*, gibberellin 20-oxidase1; *GA20ox1* and *gibberellin 3-oxidase*; *GA3ox*) and floral transcription factor genes (*UFO*, *WUSCHEL*; *WUS*, and *LFY*) in response to 1,250 mg/l of PBZ treatment of *Jatropha* floral buds. Then, samples were selected at the different time points of 14 days (no sex organs observed), and 20 days after treatment (blooming and sex organs observed). The results showed that PBZ significantly reduced the expression level of *GA20ox1*, *GA3ox*, and *LFY* as compared to the control ($P<0.05$) at 14 days. On the other hand, the expression level of *UFO* and *WUS1* were significantly higher than the control. At 20 days, there was no difference in the expression level of GA biosynthesis genes between the control and treatment. At the same time blooming time of PBZ-treated flowers was delayed which might be due to low expression levels of *GA20ox1*, *GA3ox*, and *LFY* in treated floral buds (Seesangboon et al., 2018).

PBZ (200 mg/l) inhibited the GAs content in rice varieties under submergence stress compared to submergence stress without PBZ (Wu et al., 2019). qRT-PCR was used to analyze the expression of GAs biosynthetic genes such as OsCPS1, OsKS1, and OsGA2ox1. *OsCPS1* mRNA was repressed in PBZ treatment, which was consistent with the GA content in leaves. PBZ application increased ABA content regardless of rice genotypes due to the upregulation of 9-cis-epoxycarotenoid dioxygenase (NCED), the main enzyme in ABA biosynthesis, encoded by OsNCED3 (Barrero et al., 2006).

In contrast to plants not treated with PBZ, Rubisco-small subunit expression was higher at the anthesis and post-anthesis stages in all wheat cultivars with PBZ (Dwivedi et al., 2017). At the anthesis and post-anthesis stages of wheat growth, the PBZ-treated water-stressed plants showed downregulation of the stress marker pyrroline-5-carboxylate synthase (P5CS) expression in all genotypes studied (Dwivedi et al., 2017). At various growth stages after the formation of the basal second internode of wheat, the complex changes in the activities of enzymes involved in lignin biosynthesis, such as phenylalanine ammonia-lyase (PAL) and 4-coumarate: CoA ligase (4CL), were assessed in response to PBZ (200 mg/l) application. The activity of PAL and *4CL* were higher by 42% and 35.6% respectively as compared to the control (Peng et al., 2014; Wang et al., 2016; Kamran et al., 2018).

PBZ (PBZ) at 0.8 and 1.6 mg/l significantly increased aquaporin (gene and protein) expression in tomato plants

compared to controls, implying a coordinated increase in ABA and aquaporin levels in response to water stress. Treatment with PBZ during deficit irrigation increased SlTIP2 expression by 5.3-fold above the control and resulted in greater PIP2-7 protein levels (compared to PBZ-irrigated). The increased expression of PIP2-7 in response to PBZ treatment during deficit irrigation shows that it enhances water intake and management by encouraging *de novo* synthesis of aquaporin (AP) channels. Under deficit irrigation, PBZ (0.8 and 1.6 mg/l) administration raised citrate content 2.18 and 1.64-fold, respectively, compared to PBZ-treated irrigated plants (control). This was due to the up-regulation of Sl Citrate synthase (SlCS) by 1.28 and 1.73-folds, respectively. Application of PBZ under irrigated conditions and PBZ-treated deficit irrigated plants increased Sl Succinyl-CoA ligase, SlSCoAL1, and SCoAL2 expression by 1.66 and 2.01-fold, 1.21, and 3.66-fold, respectively, resulting in substantially increased succinate abundance (1.63-fold). PBZ-treated irrigated and deficit irrigated plants produced more GABA than control plants. When PBZ-treated irrigated and

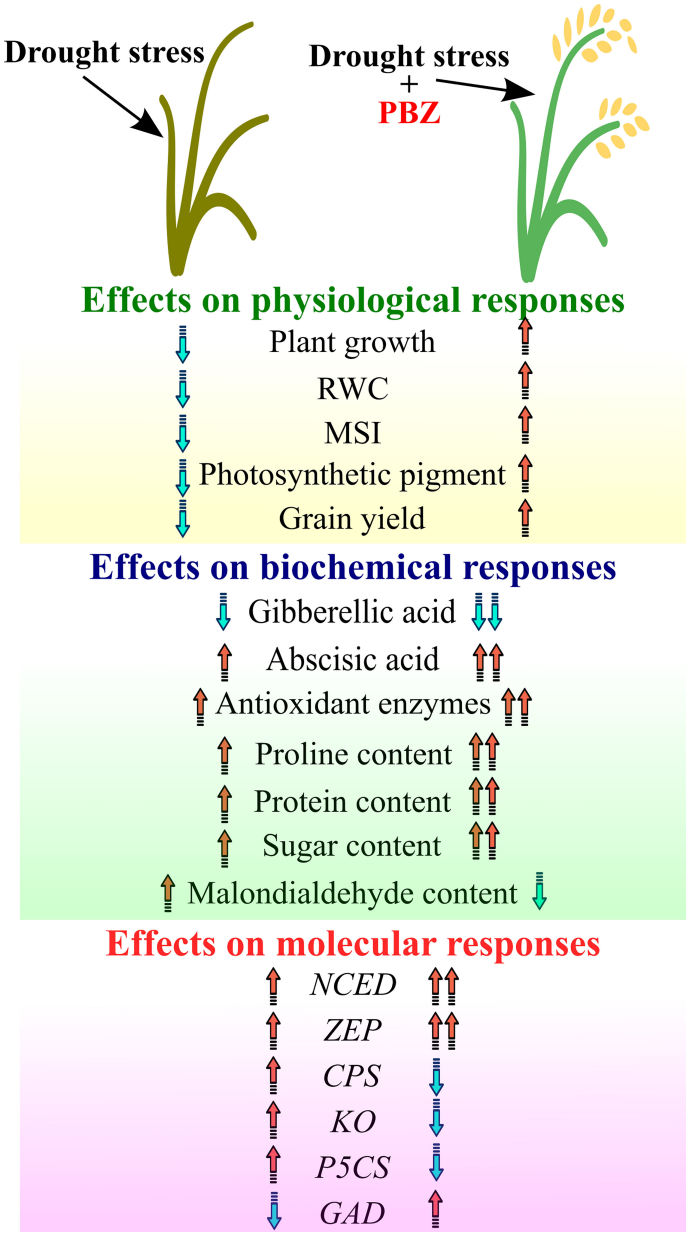


FIGURE 2
Depiction of overall impact of paclobutrazol under drought on physiological, biochemical, and molecular responses. Arrow showing the trend (Upward-Increase; Downward- Decrease).

deficit irrigated plants were compared to their respective control plants, increased expression of glutamate decarboxylase, SlGAD, was connected to better GABA buildup. GABA production was boosted by increasing the expression of SlGAD, an enzyme necessary for glutamate to GABA conversion.

DNA methylation plays an important role in plant growth and development. Recent research findings have shown that the imposition of various biotic and abiotic stresses on the plant contributes to increased methylation of the genome and thus leads to genome activity degeneration. Garg et al. (2019), found that the application of PBZ under water deficit stress leads to hypermethylation which was predominant in the drought susceptible genotype as compared to drought tolerant genotypes.

## Conclusion

By suppressing GA biosynthesis, PBZ increases ABA and chlorophyll. By reducing stomatal conductance and transpiration rates, the increased ABA level increases the RWC and WUE of crop plants. By increasing antioxidant activity and limiting lipid peroxidation, PBZ improved membrane stability and maintained photosynthetic machinery integrity under stress conditions. It also increased the photosynthetic pigment profile, suggesting that the application of PBZ triggers the xanthophyll cycle pigments and thus contributes to the defense of the photosynthetic machinery. As a result, PBZ application increases grain yield by facilitating greater photo assimilation by increasing the exchange of photosynthetic gases, higher chlorophyll content, and photosynthetic activity for longer periods. As a result, PBZ-induced physiological activities boost crop yield under water stress, salinity, temperature stress, and climate change conditions (Figure 2), resulting in more sustainable agricultural practices. This, however, is contingent on attracting agricultural scientists' attention and farmers' trust in this novel compound in the future. Furthermore, further research is needed to uncover the PBZ-induced multi-stress defense mechanism, especially in terms of its association, interrelation, and crosstalk with other phytohormones and stress-sensitive genes. As PBZ causes many physiological changes as a drought defence mechanism, these changes are not the same in all plant species, so more research is needed to determine the impact of PBZ and its application in crop fields along with its residual impact on soil.

## Author contributions

CM and NKG wrote the manuscript. MH and PV drew figures and tables. CM, NKG, and NLM contributed to collecting the data. CM, NKG, MH, and PV performed editing and helped with tables and figures. AT and AS conceptualized the manuscript. All authors contributed to the article and approved the submitted version.

## Conflict of interest

The authors declare that the research was conducted in the absence of any commercial or financial relationships that could be construed as a potential conflict of interest.

## Publisher's note

All claims expressed in this article are solely those of the authors and do not necessarily represent those of their affiliated organizations, or those of the publisher, the editors and the reviewers. Any product that may be evaluated in this article, or claim that may be made by its manufacturer, is not guaranteed or endorsed by the publisher.

## References


Abraham, S. S., Jaleel, C. A., Chang-Xing, Z., Somasundaram, R., Azooz, M. M., Manivannan, P., et al. (2008). Regulation of growth and metabolism by PBZ and ABA in sesamum indicum l. under drought condition. *Glob J. Mol. Sci.* 3 (2), 57–66.

Achard, P., Gusti, A., Cheminant, S., Alioua, M., Dhondt, S., Coppens, F., et al. (2009). Gibberellin signaling controls cell proliferation rate in arabidopsis. *Curr. Biol.* 19 (14), 1188–1193. doi: 10.1016/j.cub.2009.05.059

Agarie, S., Hanaoka, N., Kubota, F., Agata, W., and Kaufman, P. B. (1995). Measurement of cell membrane stability evaluated by electrolyte leakage as a drought and heat tolerance test in rice (*Oryza sativa* l.). *J. Fac Agric. Kyushu Univ* 40 (1/2), 233–240. doi: 10.5109/24109

Ahmad, I., Whipker, B. E., Dole, J. M., and McCall, I. (2014). PBZ and ancymidol lower water use of potted ornamental plants and plugs. *Eur. J. Hortic. Sci.* 79 (6), 318–326.

Aly, A. A., and Latif, H. H. (2011). Differential effects of PBZ on water stress alleviation through electrolyte leakage, phytohormones, reduced glutathione and lipid peroxidation in some wheat genotypes (Triticum aestivum l.) grown in-vitro. *Rom Biotechnol. Lett.* 6, 6710–6721.

Apel, K., and Hirt, H. (2004). Reactive oxygen species: metabolism, oxidative stress, and signal transduction. *Annu. Rev. Plant Biol.* 55, 373–399. doi: 10.1146/annurev.arplant.55.031903.141701

Ashraf, M., Akram, N. A., Al-Qurainy, F., and Foolad, M. R. (2011). Drought tolerance. *Adv. Agron.* 111, 249–296. doi: 10.1016/B978-0-12-387689-8.00002-3

Ashraf, M. F. M. R., and Foolad, M. R. (2007). Roles of glycine betaine and proline in improving plant abiotic stress resistance. *Environ. Exp. Bot.* 59 (2), 206–16. doi: 10.1016/j.envexpbot.2005.12.006

Assuero, S. G., Lorenzo, M., Pérez Ramírez, N. M., Velázquez, L. M., and Tognetti, J. A. (2012). Tillering promotion by paclobutrazol in wheat and its relationship with plant carbohydrate status. *New Zealand J. Agric. Res.* 554 (4), 347–58. doi: 10.1080/00288233.2012.706223

Azarcon, R. P., Vizmonte, P. T. Jr., and Agustin, AML Jr. (2022). effects of paclobutrazol on growth, yield and water use efficiency of rice (Oryza sativa l.) under drought stress condition. *Mindanao J. Sci. Technol.* 20 (1), 38–60.

Babarashi, E., Rokhzadi, A., Pasari, B., and Mohammadi, K. (2021). Ameliorating effects of exogenous PBZ and putrescine on mung bean (Vigna

radiata (L.) wilczek) under water deficit stress. *Plant Soil Environ.* 67 (1), 40–45. doi: 10.17221/437/2020-PSE

Baninasab, B., and Ghobadi, C. (2011). Influence of PBZ and application methods on high-temperature stress injury in cucumber seedlings. *J. Plant Growth Regul.* 30 (2), 213–219. doi: 10.1007/s00344-010-9188-2

Barrero, J. M., Rodríguez, P. L., Quesada, V., Piqueras, P., Ponce, M. R., and Micol, J. L. (2006). Both abscisic acid (ABA)-dependent and ABA-independent pathways govern the induction of NCED3, AAO3 and ABA1 in response to salt stress. *Plant Cell Environ.* 29 (10), 2000–2008. doi: 10.1111/j.1365-3040.2006.01576.x

Bayat, S., and Sepehri, A. (2012). PBZ and salicylic acid application ameliorates the negative effect of water stress on growth and yield of maize plants. *J. Res. Agric. Sci.* 8 (2), 127–139.

Berova, M., and Zlatev, Z. (2003). Physiological response of PBZ treated triticale plants to water stress. *Biol. Plant* 46 (1), 133–136. doi: 10.1023/A:1022360809008

Berova, M., Zlatev, Z., and Stoeva, N. (2002). Effect of PBZ on wheat seedlings under low temperature stress. *Bulg J. Plant Physiol.* 28 (1-2), 75–84.

Browning, G., Kuden, A., and Blake, P. (1992). PBZ promotion of axillary flower initiation in pear cv. *J. Hortic. Sci.* 67 (1), 121–128. doi: 10.1080/00221589.1992.11516228

Burondkar, M. M., Upreti, K. K., Ambavane, A. R., Rajan, S., Mahadik, S. G., and Bhave, S. G. (2016). Hormonal changes during flowering in response to PBZ application in mango cv. alphonso under konkan conditions. *Ind. J. Plant Physiol.* 21 (3), 306–311. doi: 10.1007/s40502-016-0236-1

Buta, J. G., and Spaulding, D. W. (1991). Effect of PBZ on abscisic acid levels in wheat seedlings. *J. Plant Growth Regul.* 10 (1-4), 59–61. doi: 10.1007/BF02279312

Chandra, S., and Roychoudhury, A. (2020). Penconazole, paclobutrazol, and triacontanol in overcoming environmental stress in plants. Protective Chemical Agents in the Amelioration of Plant Abiotic Stress: Biochemical and Molecular Perspectives. 510–534. doi: 10.1002/9781119552154.ch26

Cohen, I., Netzer, Y., Sthein, I., Gilichinsky, M., and Tel-Or, E. (2019). Plant growth regulators improve drought tolerance, reduce growth and evapotranspiration in deficit irrigated zoysia japonica under field conditions. *Plant Growth Regul.* 88 (1), 9–17. doi: 10.1007/s10725-019-00484-4

Davari, K., Rokhzadi, A., Mohammadi, K., and Pasari, B. (2022). Paclobutrazol and amino acid-based biostimulant as beneficial compounds in alleviating the drought stress effects on safflower (Carthamus tinctorius l.). *J. Soil Sci. Plant Nutr.* 22 (1), 674–690. doi: 10.1007/s42729-021-00677-9

Davis, T. D., Steffens, G. L., and Sankhla, N. (1988). Triazole plant growth regulators. *Hortic. Res.* 10, 63–105. doi: 10.1002/9781118060834.ch3

Desta, B., and Amare, G. (2021). PBZ as a plant growth regulator. *Chem. Biol. Technol. Agric.* 8 (1), 1–15. doi: 10.1186/s40538-020-00199-z

Dewi, K., and Amare, G. (2021). Effect of paclobutrazol and cytokinin on growth and source–sink relationship during grain filling of black rice (Oryza sativa L."Cempo Ireng"). *Indian J. Plant Physiol.* 23 (3), 507–515. doi: 10.1007/s40502-018-0397-1

Dwivedi, S. K., Arora, A., and Kumar, S. (2017). PBZ-induced alleviation of water-deficit damage in relation to photosynthetic characteristics and expression of stress markers in contrasting wheat genotypes. *Photosynthetica* 55 (2), 351–359. doi: 10.1007/s11099-016-0652-5

Dwivedi, S. K., Arora, A., Singh, V. P., and Singh, G. P. (2018). Induction of water deficit tolerance in wheat due to exogenous application of plant growth regulators: membrane stability, water relations and photosynthesis. *Photosynthetica* 56 (2), 478–486. doi: 10.1007/s11099-017-0695-2

Early, J. D., and Martin, G. C. (1988). Translocation and breakdown of 14C-labeled PBZ in 'Nemaguard' peach seedling. *Hortic. Sci.* 23 (1), 197–199. doi: 10.17660/ActaHortic.1989.239.6

Fan, Z. X., Li, S. C., and Sun, H. L. (2020). PBZ modulates physiological and hormonal changes in amorpha fruticosa under drought. *Stress Russ J. Plant Physiol.* 67 (1), 122–130. doi: 10.1134/S1021443720010069

Farooqi, A. H. A., Khan, A., and Srivastava, A. K. (2010). Ameliorative effect of PBZ and chlormequat on drought stress plants of vetiveria zizanioides. *Indian J. Plant Physiol.* 15 (1), 19.

Farooq, M., Wahid, A., Kobayashi, N., Fujita, D., and Basra, S. M. A. (2009). Plant drought stress: effects, mechanisms and management. *Agron. Sustain Dev.* 29 (1), 185–212. doi: 10.1051/agro:2008021

Fernández, J. A., Balenzategui, L., Bañón, S., and Franco, J. A. (2006). Induction of drought tolerance by PBZ and irrigation deficit in phillyrea angustifolia during the nursery period. *Sci. Hortic.* 107 (3), 277–283. doi: 10.1016/j.scienta.2005.07.008

Fletcher, R. A., Gilley, A., Davis, T. D., and Sankhla, N. (2000). Triazoles as plant growth regulators and stress protectants. *Hortic. Rev.* 24, 55–138. doi: 10.1002/9780470650776.ch3

Fletcher, R. A., and Hofstra, G. (1988). Triazoles as potential plant protectants. *Sterol biosynthesis inhibitors: pharmaceutical and agrochemical aspects/* D. Berg and M. Plempel.

Forghani, A. H., Almodares, A., and Ehsanpour, A. A. (2020). The role of gibberellic acid and PBZ on oxidative stress responses induced by *in vitro* salt stress in sweet sorghum. *Russ J. Plant Physiol.* 67 (3), 555–563. doi: 10.1134/S1021443720030073

Franca, C. F. M., Costa, L. C., Ribeiro, W. S., Mendes, T. D. C., Santos, M. N. S., and Finger, F. L. (2017). Evaluation of PBZ application method on quality characteristics of ornamental pepper. *Ornam Hortic.* 23 (3), 821–829. doi: 10.14295/oh.v23i3.1074

Garg, N. K., Maheshwari, C., Changan, S. S., Kumar, V., Kumar, A., Singh, A., et al. (2019). PBZ induced physio-biochemical manifestations to ameliorate water deficit stress in rice (Oryza sativa). *Indian J. Agric. Sci.* 89 (11), 80–84.

Gopi, R., Jaleel, C., Azooz, M. M., and Panneerselvam, R. (2009). Photosynthetic alterations in *Amorphophallus campanulatus* with triazoles drenching. *Glob J. Mol. Sci.* 4 (1), 15–18.

Gopi, R., Jaleel, C. A., Sairam, R., Lakshmanan, G. M. A., Gomathinayagam, M., and Panneerselvam, R. (2007). Differential effects of hexaconazole and PBZ on biomass, electrolyte leakage, lipid peroxidation and antioxidant potential of *Daucus carota* l. *Colloids Surf B Biointerfaces* 60 (2), 180–186. doi: 10.1016/j.colsurfb.2007.06.003

Gopi, R., Jaleel, C. A., Azooz, M. M., and Panneerselvam, R. (2009). Photosynthetic alterations in Amorphophallus campanulatus with triazoles drenching. *Global J. Mol. Sci.* 4, 15–18.

Hajihashemi, S. (2018). Physiological, biochemical, antioxidant and growth characterizations of gibberellin and PBZ-treated sweet leaf (stevia rebaudiana b.) herb. *J. Plant Biochem. Biotechnol.* 27 (2), 237–240. doi: 10.1007/s13562-017-0428-4

Hajihashemi, S., and Ehsanpour, A. A. (2014). Antioxidant response of steviarebaudiana b. @ to polyethylene glycol and PBZ treatments under*in vitro* culture. *Appl. Biochem. Biotechnol.* 172 (8), 4038–4052. doi: 10.1007/s12010-014-0791-8

Hasanuzzaman, M., Bhuyan, M. H., Zulfiqar, F., Raza, A., Mohsin, S. M., Mahmud, J. A., et al. (2020). Reactive oxygen species and antioxidant defense in plants under abiotic stress: Revisiting the crucial role of a universal defense regulator. *Antioxidants* 9 (8), 681. doi: 10.3390/antiox9080681

Häuser, C., Kwiatkowski, J., Rademacher, W., and Grossmann, K. (1990). Regulation of endogenous abscisic acid levels and transpiration in oilseed rape by plant growth retardants. *J. Plant Physiol.* 137 (2), 201–207. doi: 10.1016/S0176-1617(11)80082-9

Hedden, P., and Thomas, S. G. (2012). Gibberellin biosynthesis and its regulation. *Biochem. J.* 444 (1), 11–25. doi: 10.1042/BJ20120245

Hua, S., Zhang, Y., Yu, H., Lin, B., Ding, H., Zhang, D., et al. (2014). PBZ application effects on plant height seed yield and carbohydrate metabolism in canola. *Int. J. Agric. Biol.* 16 (3), 471–479.

Hussain, S., Khan, F., Cao, W., Wu, L., and Geng, M. (2016). Seed priming alters the production and detoxification of reactive oxygen intermediates in rice seedlings grown under sub-optimal temperature and nutrient supply. *Front. Plant Sci.* 7. doi: 10.3389/fpls.2016.00439

Iqbal, S., Parveen, N., Bahadur, S., Ahmad, T., Shuaib, M., Nizamani, M. M., et al. (2020). PBZ mediated changes in growth and physio-biochemical traits of okra (Abelmoschus esculentus l.) grown under drought stress. *Gene Rep.* 21, 100908. doi: 10.1016/j.genrep.2020.100908

Jaleel, C. A., Gopi, R., Manivannan, P., and Panneerselvam, R. (2007). Responses of antioxidant defense system of catharanthus roseus (L.) g. don. to PBZ treatment under salinity. *Acta Physiol. Plant* 29 (3), 205–209. doi: 10.1007/s11738-007-0025-6

Jungklang, J., and Saengnil, K. (2012). Effect of PBZ on patumma cv. Chiang mai pink under water stress. *Songklanakarin J. Sci. Technol.* 34 (4), 361–366.

Jungklang, J., Saengnil, K., and Uthaibutra, J. (2017). Effects of water-deficit stress and PBZ on growth, relative water content, electrolyte leakage, proline content and some antioxidant changes in curcuma alismatifolia gagnep. cv. Chiang mai pink. *Saudi J. Biol. Sci.* 24 (7), 1505–1512. doi: 10.1016/j.sjbs.2015.09.017

Kamran, M., Ahmad, S., Ahmad, I., Hussain, I., Meng, X., Zhang, X., et al. (2020). PBZ application favors yield improvement of maize under semiarid regions by delaying leaf senescence and regulating photosynthetic capacity and antioxidant system during grain-filling stage. *Agronomy* 10 (2), 187. doi: 10.3390/agronomy10020187

Kamran, M., Wennan, S., Ahmad, I., Xiangping, M., Wenwen, C., Xudong, Z., et al. (2018). Application of PBZ affect maize grain yield by regulating root morphological and physiological characteristics under a semi-arid region. *Sci. Rep.* 8 (1), 4818. doi: 10.1038/s41598-018-23166-z

Kaur, C., and Gupta, K. (1991). Effect of triazole-type plant growth regulators on sunflower and safflower seed viability. *Canadian journal of botany* 69 (6), 1344–48. doi: 10.1139/b91-174

Khan, M. S. H., Wagatsuma, T., Akhter, A., and Tawaraya, K. (2009). Sterol biosynthesis inhibition by paclobutrazol induces greater aluminum (Al) sensitivity in Al-tolerant rice. *Am. J. Plant Physiol* 4, 89–99. doi: 10.3923/ajpp.2009.89.99

Kim, J., Wilson, R. L., Case, J. B., and Binder, B. M. (2012). A comparative study of ethylene growth response kinetics in eudicots and monocots reveals a role for gibberellin in growth inhibition and recovery. *Plant Physiology* 160 (3), 1567–80. doi: 10.1104/pp.112.205799

Kitahata, N., Saito, S., Miyazawa, Y., Umezawa, T., Shimada, Y., Min, Y. K., et al. (2005). Chemical regulation of abscisic acid catabolism in plants by cytochrome P450 inhibitors. *Bioorg Med. Chem.* 13 (14), 4491–4498. doi: 10.1016/j.bmc.2005.04.036

Kondhare, K. R., Hedden, P., Kettlewell, P. S., Farrell, A. D., and Monaghan, J. M. (2014). Use of the hormone-biosynthesisinhibitors fluridone and PBZ to determine the effects of altered abscisic acid and gibberellin levelson prematurity amylase formation in wheat grains. *J. Cereal Sci.* 60 (1), 210–216. doi: 10.1016/j.jcs.2014.03.001

Kumar, M. S., Ali, K., Dahuja, A., and Tyagi, A. (2015). Role of phytosterols in drought stress tolerance in rice. *Plant Physiol. Biochem.* 96, 83–89. doi: 10.1016/j.plaphy.2015.07.014

Latimer, J. G. (1992). Drought, paclobutrazol, abscisic acid, and gibberellic acid as alternatives to daminozide in tomato transplant production. *J. Am. Soc. Hortic. Sci.* 117 (2), 243–247. doi: 10.21273/JASHS.117.2.243

Lenton, J. R., Appleford, N. E. J., and Croker, S. J. (1994). Gibberellins and α-amylase gene expression in germinating wheat grains. *Plant Growth Regul.* 15 (3), 261–270. doi: 10.1007/BF00029899

Lever, B. G. (1986). "Cultar"–a technical overview. *Acta Hortic.* 179 (179), 459–466. doi: 10.17660/ActaHortic.1986.179.71

Mackay, C. E., Christopher Hall, J., Hofstra, G., and Fletcher, R. A. (1990). Uniconazole-induced changes in abscisic acid, total amino acids and proline in phaseolus vulgaris. *Pesti Biochem. Physiol.* 37 (1), 74–82. doi: 10.1016/0048-3575(90)90110-N

Marshall, J. G., Rutledge, R. G., Blumwald, E., and Dumbroff, E. B. (2000). Reduction in turgid water volume in jack pine, white spruce and black spruce in response to drought and PBZ. *Tree Physiol.* 20 (10), 701–707. doi: 10.1093/treephys/20.10.701

Mawlong, I., Ali, K., Kurup, D., Yadav, S., and Tyagi, A. (2014). Isolation and characterization of an AP2/ERF-type drought stress inducible transcription factor encoding gene from rice. *J. Plant Biochem. Biotechnol.* 23 (1), 42–51. doi: 10.1007/s13562-012-0185-3

McKersie, B. D., and Leshem, Y. Y. (1994). *Stress and Stress Coping in Cultivated Plants.* Dordrecht-Boston-London: Kluwer Academic Publishers. 256 pp.

Merah, O. (2001). Potential importance of water status traits for durum wheat improvement under Mediterranean conditions. *J. Agric. Sci.* 137 (2), 139–145. doi: 10.1017/S0021859601001253

Mog, B., Janani, P., Nayak, M. G., Adiga, J. D., and Meena, R. (2019). Manipulation of vegetative growth and improvement of yield potential of cashew (Anacardium occidentale l.) by PBZPBZ. *Sci. Hortic.* 257, 108748. doi: 10.1016/j.scienta.2019.108748

Mohamed, G. F., Agamy, R. A., and Rady, M. M. (2011). Ameliorative effects of some antioxidants on water-stressed tomato (*Lycopersicon esculentum* mill.) plants. *J. Appl. Sci. Res.* 7, 2470–2478.

Moradi, S., Baninasab, B., Gholami, M., and Ghobadi, C. (2017). PBZ application enhances antioxidant enzyme activities in pomegranate plants affected by cold stress. *J. Hortic. Sci. Biotechnol.* 92 (1), 65–71. doi: 10.1080/14620316.2016.1224605

Nouriyani, H., Majidi, E., Seyyednejad, S. M., Siadat, S. A., and Naderi, A. (2012). Effect of PBZ under different levels of nitrogen on some physiological traits of two wheat cultivars (*Triticum aestivum* l.). *World Appl. Sci. J.* 16, 1–6.

Pal, S., Zhao, J., Khan, A., Yadav, N. S., Batushansky, A., Barak, S., et al. (2016). PBZ induces tolerance in tomato to deficit irrigation through diversified effects on plant morphology, physiology and metabolism. *Sci. Rep.* 6, 39321. doi: 10.1038/srep39321

Peltzer, D., Dreyer, E., and Polle, A. (2002). Temperature dependencies of antioxidative enzymes in two contrasting species. *Plant Physiol. Biochem.* 40 (2), 141–150. doi: 10.1016/S0981-9428(01)01352-3

Peng, D., Chen, X., Yin, Y., Lu, K., Yang, W., Tang, Y., et al. (2014). Lodging resistance of winter wheat (Triticum aestivum l.): lignin accumulation and its related enzymes activities due to the application of PBZ or gibberellin acid. *Field Crops Res.* 157, 1–7. doi: 10.1016/j.fcr.2013.11.015

Percival, G. C., and Noviss, K. (2008). Triazole induced drought tolerance in horse chestnut (*Aesculus hippocastanum*). *Tree Physiol.* 28 (11), 1685–1692. doi: 10.1093/treephys/28.11.1685

Percival, G., and Salim AlBalushi, A. M. (2007). PBZ-induced drought tolerance in containerized English and evergreen oak. *Arboric Urban For* 33 (6), 397–409. doi: 10.48044/jauf.2007.046

Pinto, A. C. R., Rodrigues, T., Leite, I. C., and Barbosa, J. C. (2005). Growth retardants on development and ornamental quality of potted 'lilliput' *Zinnia elegans* jacq. *Sci. Agric.* 62 (4), 337–345. doi: 10.1590/S0103-90162005000400006

Pospíšilová, J., Synková, H., and Rulcová, J. (2000). Cytokinkins and water stress. *Biol. Plant* 43 (3), 321–328. doi: 10.1023/A:1026754404857

Prochazkova, D., Sairam, R. K., Srivastava, G. C., and Singh, D. V. (2001). Oxidative stress and antioxidant activity as the basis of senescence in maize leaves. *Plant Sci.* 161 (4), 765–771. doi: 10.1016/S0168-9452(01)00462-9

Rademacher, W. (2015). Plant growth regulators: backgrounds and uses in plant production. *J. Plant Growth Regul.* 34 (4), 845–872. doi: 10.1007/s00344-015-9541-6

Rademacher, W. (2018). Chemical regulators of gibberellin status and their application in plant production. *Annu. Plant Rev. Online* 49, 359–403. doi: 10.1002/9781119312994.apr0541

Rady, M., and Gaballah, S. (2012). Improving barley yield grown under water stress conditions. *Res. J. Recent Sci.* 1 (6), 1–6.

Razavizadeh, R., and Amu, B. M. (2013). Effect of PBZ on improving drought tolerance in seedlings of (*Brassica napus* l.) *in vitro*. *Plant Process Funct.* 2 (1), 21–34.

Rezazadeh, A., Harkess, R. L., and Bi, G. (2016). Effects of PBZ and flurprimidol on water stress amelioration in potted red firespike. *Hortic. Technol.* 26 (1), 26–29. doi: 10.21273/HORTTECH.26.1.26

Ribeiro, D. M., Müller, C., Bedin, J., Rocha, G. B., and Barros, R. S. (2011). Effects of autoclaving on the physiological action of PBZ. *Agric. Sci.* 02 (3), 191–197. doi: 10.4236/as.2011.23026

Roseli, A. N. M., Ying, T. F., and Ramlan, M. F. (2012). Morphological and physiological response of syzygium myrtifolium (Roxb.) walp. to PBZ. *Sains Malays* 41 (10), 1187–1192.

Ruter, J. M. (1996). PBZ application method influences growth and flowering of new gold'lantana. *Hortic. Technol.* 6 (1), 19–20. doi: 10.21273/HORTTECH.6.1.19

Salehi-Lisar, S. Y., and Bakhshayeshan-Agdam, H. (2016). "Drought stress in plants: causes, consequences, and tolerance," in *Drought stress tolerance in plants*, vol. . p. (Cham: Springer), 1–16.

Samota, M. K., Sasi, M., Awana, M., Yadav, O. P., Amitha Mithra, S. V., Tyagi, A., et al. (2017b). Elicitor induced biochemical and molecular manifestations to improve drought tolerance in rice (*Oryza sativa* l.) through seed-priming. *Front. Plant Sci.* 8. doi: 10.3389/fpls.2017.00934

Samota, M. K., Sasi, M., and Singh, A. (2017a). Impact of seed priming on proline content and antioxidant enzymes to mitigate drought stress in rice genotype. *Int. J. Curr. Microbiol. Appl. Sci.* 6 (5), 2459–2466. doi: 10.20546/ijcmas.2017.605.275

Sankar, B., Gopinathan, P., Karthishwaran, K., and Somasundaram, R. (2014). Biochemical content variation in arachis hypogaea under drought stress with or without PBZ and abscisic acid. *J. Ecobiotechnol* 6, 9–14.

Sankar, B., Jaleel, C. A., Manivannan, P., Kishorekumar, A., Somasundaram, R., and Panneerselvam, R. (2007). Effect of PBZ on water stress amelioration through antioxidants and free radical scavenging enzymes in *Arachis hypogaea* l. *Colloids Surf B Biointerfaces* 60 (2), 229–235. doi: 10.1016/j.colsurfb.2007.06.016

Sankar, B., Karthishwaran, K., and Somasundaram, R. (2013). Leaf anatomy changes in peanut plants in relation to drought stress with or without PBZ and abscisic acid. *J. Phytol.* 5, 25–29.

Sarker, A. M., Rahman, M. S., and Paul, N. K. (1999). Effect of soil moisture on relative leaf water content, chlorophyll, proline and sugar accumulation in wheat. *J. Agron. Crop Sci.* 183 (4), 225–229. doi: 10.1046/j.1439-037x.1999.00339.x

Sasi, M., Awana, M., Samota, M. K., Tyagi, A., Kumar, S., Sathee, L., et al. (2021). Plant growth regulator induced mitigation of oxidative burst helps in the management of drought stress in rice (*Oryza sativa* l.). *Environ. Exp. Bot.* 185, 104413. doi: 10.1016/j.envexpbot.2021.104413

Seesangboon, A., Gruneck, L., Pokawattana, T., Eungwanichayapant, P. D., Tovaranonte, J., and Popluechai, S. (2018). Transcriptome analysis of jatropha curcas l. flower buds responded to the PBZ treatment. *Plant Physiol. Biochem.* 127, 276–286. doi: 10.1016/j.plaphy.2018.03.035

Sestak, Z., and Pospisilova, J. (1986). Water-stress induced changes in photosynthetic characteristics of chloroplasts and their dependence on leaf development. *Photobiochem Photobiophysics* 12, 163–172.

Setia, R. C., Kaur, P., and Setia, N. (1996). Anuradha. influence of PBZ on growth and development of fruit in *Brassica juncea* (L.) czern and coss. *Plant Growth Regul.* 20 (3), 307–316. doi: 10.1007/BF00043323

Shahrokhi, M., Tehranifar, A., Hadizadeh, H., and Selahvarzi, Y. (2011). Effect of drought stress and PBZ-treated seeds on physiological response of festuca arundinacea l. master and lolium perenne l. *Barrage J. Biol. Environ. Sci.* 5 (14), 77–85.

Sheikh Mohammadi, M. H. S., Etemadi, N., Arab, M. M., Aalifar, M., Arab, M., and Pessarakli, M. (2017). Molecular and physiological responses of Iranian perennial ryegrass as affected by trinexapac ethyl, PBZPBZ and abscisic acid under drought stress. *Plant Physiol. Biochem.* 111, 129–143. doi: 10.1016/j.plaphy.2016.11.014

Smirnoff, N. (1993). The role of active oxygen in the response of plants to water deficit and desiccation. *New Phytol.* 125, 27–58. doi: 10.1111/j.1469-8137.1993.tb03863.x

Smirnoff, N. (1995). "Antioxidant systems and plant responses to the environment," in *Environment and plant metabolism: Flexibility and acclimation*. Ed. V. Smirnoff (Oxford, UK: Bios Scientific Publishers).

Somasundaram, R., Abdul Jaleel, C., Sindhu, S. A., Azooz, M. M., and Panneerselvam, R. (2009). Role of PBZPBZ and ABA in drought stress amelioration in *Sesamum indicum* l. *Glob J. Mol. Sci.* 4 (2), 56–62.

Song, J., Guo, B., Song, F., Peng, H., Yao, Y., Zhang, Y., et al. (2011). Genome-wide identification of gibberellins metabolic enzyme genes and expression profiling analysis during seed germination in maize. *Gene* 482 (1-2), 34–42. doi: 10.1016/j.gene.2011.05.008

Sopher, C. R., Król, M., Huner, N. P. A., Moore, A. E., and Fletcher, R. A. (1999). Chloroplastic changes associated with PBZ-induced stress protection in maize seedlings. *Can. J. Bot.* 77 (2), 279–290. doi: 10.1139/b98-236

Srivastav, M., Kishor, A., Dahuja, A., and Sharma, R. R. (2010). Effect of PBZ and salinity on ion leakage, proline content and activities of antioxidant enzymes in mango (*Mangifera indica* l.). *Sci. Hortic.* 125 (4), 785–788. doi: 10.1016/j.scienta.2010.05.023

Syahputra, B. S. A., Sinniah, U. R., Ismail, M. R., and Swamy, M. K. (2016). Optimization of paclobutrazol concentration and application time for increased lodging resistance and yield in field-grown rice. *Philipp. Agric. Sci.* 99 (3), 221–228.

Vijayalakshmi, D., and Srinivasan, P. S. (1999). Morphophysiological changes as influenced by chemicals and growth regulators in alternate bearing mango cv. 'Alphonso'. *Madaras Agric. J.* 86, 485–487.

Wahid, A., Farooq, M., and Siddique, K. H. M. (2014). "Implications of oxidative stress for plant growth and productivity," in *Handbook of plant and crop physiology*, *3rd edn*. Ed. M. Pessarakli (Broken Sound Parkway, Suite 300, Boca Raton, FL 33487 USA: Taylor & Francis Group), 549–556.

Wang, S. Y., Byun, J. K., and Steffens, G. L. (1985). Controlling plant growth *via* the gibberellin biosynthesis system. II. biochemical and physiological alterations in apple seedlings. *Physiol. Plant* 63 (2), 169–175. doi: 10.1111/j.1399-3054.1985.tb01898.x

Wang, W., Xin, H., Wang, M., Ma, Q., Wang, L., Kaleri, N. A., et al. (2016). Transcriptomic analysis reveals the molecular mechanisms of drought-stress-induced decreases in camellia sinensis leaf quality. *Front. Plant Sci.* 7. doi: 10.3389/fpls.2016.00385

Waqas, M., Yaning, C., Iqbal, H., Shareef, M., Rehman, H., and Yang, Y. (2017). PBZ improves salt tolerance in quinoa: beyond the stomatal and biochemical interventions. *J. Agron. Crop Sci.* 203 (4), 315–322. doi: 10.1111/jac.12217

Witchard, M. (1997). PBZ is phloem mobile in castor oil plants (*Ricinus communis* l.). *J. Plant Growth Regul.* 16 (4), 215–217. doi: 10.1007/PL00006999

Wu, H., Chen, H., Zhang, Y., Zhang, Y., Zhu, D., and Xiang, J. (2019). Effects of 1-aminocyclopropane-1-carboxylate and PBZ on the endogenous hormones of two contrasting rice varieties under submergence stress. *Plant Growth Regul.* 87 (1), 109–121. doi: 10.1007/s10725-018-0457-6

Wu, C., Sun, J., Zhang, A., and Liu, W. (2013). Dissipation and enantioselective degradation of plant growth retardants paclobutrazol and uniconazole in open field, greenhouse, and laboratory soils. *Environ. Sci. Technol.* 47 (2), 843–49. doi: 10.1021/es3041972

Yadav, S., Modi, P., Dave, A., Vijapura, A., Patel, D., and Patel, M. (2020). Effect of abiotic stress on crops. *Sustain. Crop Production*, 1–21. doi: 10.5772/intechopen.88434

Yadav, R. K., Rai, N., Yadav, D. S., and Asati, B. S. (2005). Use of PBZ in horticultural crops-a review. *Agric. Rev. (Karnal)* 26, 124–132.

Yeshitela, T., Robbertse, P. J., and Stassen, P. J. C. (2004). Effects of various inductive periods and chemicals on flowering and vegetative growth of 'Tommy atkins' and 'Keitt' mango (*Mangifera indica*) cultivars. *N Z J. Crop Hortic. Sci.* 32 (2), 209–215. doi: 10.1080/01140671.2004.9514298

Yooyongwech, S., Samphumphuang, T., Tisarum, R., Theerawitaya, C., and Cha-Um, S. (2017). Water-deficit tolerance in sweet potato [Ipomoea batatas (L.) lam.] by foliar application of PBZ: role of soluble sugar and free proline. *Front. Plant Sci.* 8. doi: 10.3389/fpls.2017.01400

Zhang, J., Jia, W., Yang, J., and Ismail, A. M. (2006). Role of ABA in integrating plant responses to drought and salt stresses. *Field Crops Res.* 97 (1), 111–119. doi: 10.1016/j.fcr.2005.08.018

Zhu, X., Chai, M., Li, Y., Sun, M., Zhang, J., Sun, G., et al. (2016). Global transcriptome profiling analysis of inhibitory effects of PBZ on leaf growth in lily (Lilium longiflorum-Asiatic hybrid). *Front. Plant Sci.* 7. doi: 10.3389/fpls.2016.00491

Zhu, L., van de Peppel, A., Li, X., and Welander, M. (2004). Changes of leaf water potential and endogenous cytokinins in young apple trees treated with or without PBZ under drought conditions. *Sci. Hortic.* 99 (2), 133–141. doi: 10.1016/S0304-4238(03)00089-X

frontiers | Frontiers in Plant Science

TYPE Review
PUBLISHED 11 January 2023
DOI 10.3389/fpls.2022.996514



OPEN ACCESS

EDITED BY
Pradeep Sharma,
Indian Institute of Wheat and Barley Research (ICAR), India

REVIEWED BY
Reetika Mahajan,
Sher-e-Kashmir University of Agricultural Sciences and Technology, India
Ruchi Bansal,
National Bureau of Plant Genetic Resources (ICAR), India

*CORRESPONDENCE
Beena Radha
beena.r@kau.in

SPECIALTY SECTION
This article was submitted to Plant Abiotic Stress, a section of the journal Frontiers in Plant Science

RECEIVED 17 July 2022
ACCEPTED 05 December 2022
PUBLISHED 11 January 2023

CITATION
Radha B, Sunitha NC, Sah RP, T. P. MA, Krishna GK, Umesh DK, Thomas S, Anilkumar C, Upadhyay S, Kumar A, Ch L. N. M, S. B, Marndi BC and Siddique KHM (2023) Physiological and molecular implications of multiple abiotic stresses on yield and quality of rice.
*Front. Plant Sci.* 13:996514.
doi: 10.3389/fpls.2022.996514



# Physiological and molecular implications of multiple abiotic stresses on yield and quality of rice

Beena Radha[1]*, Nagenahalli Chandrappa Sunitha[2], Rameswar P. Sah[3], Md Azharudheen T. P.[3], G. K. Krishna[4], Deepika Kumar Umesh[5], Sini Thomas[6], Chandrappa Anilkumar[3], Sameer Upadhyay[3], Awadhesh Kumar[3], Manikanta Ch L. N.[7], Behera S.[3], Bishnu Charan Marndi[3] and Kadambot H. M. Siddique[8]

[1]Department of Plant Physiology, Kerala Agricultural University-College of Agriculture, Vellayani, Thiruvananthapuram, Kerala, India, [2]Department of Genetics and Plant Breeding, University of Agricultural Sciences, Bangalore, Karnataka, India, [3]Division of Crop Production, Indian Council of Agricultural Research-National Rice Research Institute, Cuttack, Odisha, India, [4]Department of Plant Physiology, Kerala Agricultural University-College of Agriculture, Thrissur, Kerala, India, [5]Mulberry Breeding & Genetics Section, Central Sericultural Research and Training Institute-Berhampore, Central Silk Board, Murshidabad, West Bengal, India, [6]Department of Plant Physiology, Kerala Agricultural University-Regional Agricultural Research Station, Kumarakom, Kerala, India, [7]Department of Plant Physiology, Indira Gandhi Krishi Vishwavidyalaya, Raipur, India, [8]The University of Western Australia Institute of Agriculture, The University of Western Australia, Perth, WA, Australia

Abiotic stresses adversely affect rice yield and productivity, especially under the changing climatic scenario. Exposure to multiple abiotic stresses acting together aggravates these effects. The projected increase in global temperatures, rainfall variability, and salinity will increase the frequency and intensity of multiple abiotic stresses. These abiotic stresses affect paddy physiology and deteriorate grain quality, especially milling quality and cooking characteristics. Understanding the molecular and physiological mechanisms behind grain quality reduction under multiple abiotic stresses is needed to breed cultivars that can tolerate multiple abiotic stresses. This review summarizes the combined effect of various stresses on rice physiology, focusing on grain quality parameters and yield traits, and discusses strategies for improving grain quality parameters using high-throughput phenotyping with *omics* approaches.

KEYWORDS

**multiple abiotic stresses, physiology, high temperature, salinity, drought, eCO2, sensitivity, tolerance**

# 1 Introduction

Global warming and accompanying climate variabilities adversely impact global agricultural output, dwindling the production of food grains such as rice (Ramegowda and Senthil-Kumar, 2015). Abiotic stresses such as heat or temperature stress, submergence, drought, or nutritional deficiency create suboptimal environments (Jeyasri et al., 2021) that impair germination, seedling establishment, vegetative growth, flower initiation, panicle growth, grain filling, and productivity (Banerjee and Roychoudhury, 2020; Beena et al., 2021a). In rice, these attributes severely compromise crop establishment, growth (Beena et al., 2021b; Anie et al., 2022; Stephen et al., 2022), grain quality, and productivity (Pravallika et al., 2020; Pathak et al., 2021). Some abiotic pressures in rice-growing environments spur the development and infection of biotic causal agents, aggravating the losses in productivity (Narsai and Whelan, 2013) and grain quality.

As the major staple food crop in the world, reductions in rice production due to climate change will have serious socioeconomic impacts. Many paddy growers experience frequent crop failure, resulting in unprecedented hardships such as starvation and financial pressure (Rejeth et al., 2020). Exposure to multiple abiotic stresses leads to physical and biochemical alterations in crop produce (Manikanta et al., 2020; Ali et al., 2022; Manikanta et al., 2022). Concurrent abiotic stresses damage rice crops more than individual stresses (Pandey et al., 2017), posing various physiological effects that trigger cross-talk reactions that affect rice phenology (Ramu et al., 2016; Ali et al., 2022). While not an abiotic stress component, elevated $CO_2$ ($eCO_2$) can alleviate or aggravate the stress effects.

Rice grain quality is measured primarily on the physical appearance of the grain, mineral content, proportion of amylose and amylopectin starch, aroma, and cooking quality (Chakraborti et al., 2021). Abiotic stresses during grain filling affect milling quality, grain chalkiness, starch composition, and cooking quality (Lanning and Siebenmorgen, 2013). According to ; Liu et al. (2021), high-temperature stress has the greatest impact on grain quality attributes, including reducing the sensory qualities of milled rice. Numerous studies have investigated the fundamentals of rice grain biochemistry, but few have examined how multiple abiotic stresses affect grain quality (Liu et al., 2013; Kadam et al., 2014).

Among abiotic stresses, high temperatures are particularly devastating, decreasing productivity and grain biochemical components. High temperatures decrease photosynthesis and photorespiration, decreasing total biomass production (Moore et al., 2021). High temperatures post-anthesis affect grain quality and appearance and decrease grain production (Dong et al., 2014). Similarly, high temperatures reduce pollen viability and increase spikelet sterility, decreasing grain production and quality (Rang et al., 2011). Extreme temperature stress at the maturity stage abates grain chalkiness, physical appearance, and biochemical properties such as amylose content and protein composition (Ahmed et al., 2015).

Excessive water stresses such as waterlogging and submergence adversely affect rice growth and grain yield. While some historical rice cultivars exhibit notable resilience to submergence, their total yield suffers (Singh et al., 2014). In contrast, modern rice cultivars are sensitive to flooding, often resulting in farmers losing their whole crop. Rice plants can perish soon after flooding due to high energy expenditure and protein hydrolysis during submergence. Flooding degrades the quality of endosperm reserves, adversely affecting the nutritional value and milling and cooking properties of rice grain (Zhou et al., 2020). Flooding at harvest-ready stages results in pre-harvest sprouting, compromising the marketable grain quality (Nonogaki et al., 2018) and reducing the grain's eating and cooking quality (Zhou et al., 2020).

In recent decades, rice researchers have been working to improve crop yield and quality under stressful situations (Patra et al., 2020). Genomic techniques have been used to investigate how abiotic stresses affect grain development (Verma et al., 2021), with several genetic regulators of tolerance identified and successfully used to improve rice cultivars. For example, genetic loci controlling salinity stress have been discovered and pyramided to develop green super rice types (Pang et al., 2017). Using marker-assisted breeding, Kumar et al. (2018) combined quantitative trait loci (QTL) for submergence and drought tolerance to identify varieties with high yield potential, validating their performance by exposing them to various stresses. However, little information is available on combining stress tolerance and grain quality traits to fulfill food security (Ali et al., 2021).

Another major concern affecting plant growth is $eCO_2$, with carbon dioxide levels expected to reach 685 ppm by 2050, raising the global mean temperature by 3–6°C relative to the pre-industrial era (Kilkis and Caglar, 2022). At the global level, crop models suggest that $eCO_2$ levels could increase precipitation, but large spatial and temporal variabilities exist at the regional scale. Rainfall occurrence and intensity can be unpredictable, creating patches of drought and waterlogging (Walter, 2018). Various experiments have indicated that optimum levels of $eCO_2$ can mitigate the effects of drought stress.

Candidate gene markers can be used to identify genes or QTL for grain production (Azharudheen et al., 2022). Anabolic gene expression requires favorable environmental conditions. Increased temperature impairs starch production, slowing sugar and starch metabolism and thus reducing grain filling and the number of filled grains per panicle (Fahad et al., 2019); a similar response occurs under salt stress (Hussain et al., 2017). Furthermore, significant QTL identified for drought tolerance are crucial for normal reproduction in paddy under drought (Catolos et al., 2017; Feng et al., 2018). The effects of combined

mild salinity stress (75 mM NaCl) and moderately high temperatures (30/26°C day/night) were not additive when compared to the individual stresses. The combined stress had longer seedling roots and higher relative water content and Chl b than the salinity treatment alone. He et al. (2018) reported that ABA treatment mimicked protein perturbations in rice subjected to combined salinity stress and desiccation. In another study, Wytynck et al., 2021 reported similar ultrastructural changes in young leaf cells of rice seedlings subjected to salinity or high temperature stress, including the enhanced formation of rough endoplasmic reticulum assembly, reduced cristae formation in mitochondria, and disorganized cell wall fibrils.

QTL conferring tolerance to drought (*qDTY1.1, qDTY2.1*), salinity (Saltol), and submergence (Sub1) were introgressed by marker-assisted breeding, resulting in a climate-ready rice genotype, Improved White Ponni, a classic example of how information from multiple studies can assist in pyramiding traits for crop improvement (Muthu et al., 2020). The basal methylation patterns in the genomes of Pokkali (salinity tolerant), Nagina 22 (drought tolerant), and IR64 (susceptible) revealed that various stress-associated transcription factors (TFs) and signaling intermediates hypermethylated and thus downregulated to impart stress tolerance relative to IR64 (Garg et al., 2015). In addition, submergence-tolerant rice (FR13A) could withstand the compromise in photosynthetic traits despite lacking innate salinity tolerance (Sarkar et al., 2016). Several combined salinity and submergence stress experiments have revealed various physiological responses in rice. In one study, one week of this combined stress had little impact, while two weeks had detrimental effects on paddy rice, decreasing the relative growth rate, increasing the time to flowering, and decreasing yield (Kurniasih et al., 2021).

This review investigates the individual and interactive effects of various abiotic stresses (e.g., drought, salinity, high temperature, $eCO_2$, submergence, nutrient deficiency) on rice growth, agronomy, and physiological traits, including grain quality and production, and the benefits of genomics for improving rice productivity and grain quality.

# 2 Physiological and molecular implications of individual stresses in rice yield and quality

## 2.1 Impact of drought stress on paddy

Climate change disrupts the regularity and magnitude of hydrological events, threatening crop production and affecting food security. The major regions affected include South and Southeast Asia, Sub-Saharan Africa, and Latin America, with unbunded and bunded uplands and shallow rainfed lowlands. Globally, drought stress events account for up to 40% of overall crop and livestock output losses, totaling nearly USD 28 billion (FAO, 2017). In Asia, frequent drought stress affects about 34 million ha of rainfed lowland rice and 8 million ha of upland rice (Barik et al., 2019). Drought stress frequently affects an area of 27 million ha of rainfed rice area (Shamsudin et al., 2016). In 2002, severe drought and depleted soil moisture affected over 65% of South Asia, resulting in considerable rice yield losses (~400 kg $ha^{-1}$).

Water deficit causes numerous unfavorable changes in rice (Nithya et al., 2020). For example, 15 days of drought stress during reproductive stage reduced rice yields by up to 70%, increasing to up to 88% during flowering and 52% during grain filling. Drought stress at the flowering stage resulted in incomplete panicle exertion, 30% spikelet sterility, and a 20–46% reduction in seed set in a set of rice cultivars (Bahuguna et al., 2018). Drought stress during grain filling stage increases the proportion of chalky grains (Yang et al., 2018). The imposition of drought stress at the onset of anthesis for 30 days reduced the grain yield and harvest index of 25 rice genotypes, with reduced pollen fertility and test weight of grains for most genotypes, compared to irrigated conditions (Ahmad et al., 2022). While leaf rolling is considered a defense mechanism against drought stress, its promptness correlated with anatomical traits rather than water deficit (Nithya et al., 2021. While more leaf rolling occurred in genotypes such as Dangar, water deficit did not affect transpiration (Cal et al., 2019). Drought stress also affects the root system, with the ill-effects on root architecture and yield genotype-dependent (Prince et al., 2015; Beena et al., 2017; Beena et al., 2018c).

Plants have developed numerous adaptive responses to drought stress that aid their survival, including deeper roots, reduced water loss from shoots due to thick cuticle deposition, reduced leaf area, and osmotic adjustment, primarily by maintaining a high internal water status (Beena et al., 2018b; Manikanta et al., 2020; Rejeth et al., 2020). Beena et al. (2012) reported that root architecture, water uptake, and osmotic adjustment are important traits for drought tolerance screening. Physiological and biochemical changes in rice under drought are given in Supplementary Table 1. In rice, QTL mapping has revealed regions responsible for physiological traits, yield, and yield components. Table 1 lists QTL/genes introgressed into rice for drought stress tolerance.

## 2.2 Impacts of submergence on paddy

Rice is adapted to stagnant conditions because its well-developed aerenchyma promotes oxygen transport through roots. However, submergence caused by recurrent flooding can adversely affect plant growth and productivity. In lowland and deep-water rice areas, flooding occurs on more than 16 million ha, with annual economic losses estimated to exceed $600 USD million (www.knowledgebank.irri.org). In addition, unpredictable flash floods can occur at any stage of paddy development.

TABLE 1 Major QTLs reported for physio-morphological traits under various abiotic stress conditions in rice.

| Trait | QTLs/Genes | Chromosome | Flanking markers | References |
|---|---|---|---|---|
| High yield under drought deployed for introgression using MAS in rice | | | | |
| High yield under drought condition | *qDTY1.1* | 1 | RM431–RM104 | Ghimire et al. (2012) |
| | | 1 | RM104–RM12091 | |
| | | 1 | RM11943–RM12091 | Vikram et al. (2011) |
| | | 1 | RM486–RM472 | Venuprasad et al. (2012) |
| | | 1 | RM472 | Muthu et al. (2020) |
| | *qDTY1.3* | 1 | RM488–RM315 | Sandhu et al. (2014) |
| | *qDTY1.2* | 1 | RM259–RM315 | |
| | *qDTY2.1* | 2 | RM2634 | Muthu et al. (2020) |
| | *qDTY2.2* | 2 | RM236–RM279 | Swamy BP. et al. (2013) |
| | | 2 | RM211–RM263 | Sandhu et al. (2014) |
| | | 2 | RM211–233A | Palanog et al. (2014) |
| | *qDTY2.3* | 2 | RM263–RM573 | Sandhu et al. (2014) |
| | | 2 | RM573–RM250 | Palanog et al. (2014) |
| | | 3 | RM168–RM468 | Dixit et al. (2014) |
| | *qDTY3.2* | 3 | RM569–RM517 | Yadaw et al. (2013) |
| | | 3 | RM60–RM22 | Vikram et al. (2011) |
| | *qDTY4.1* | 4 | RM551–RM16368 | Swamy BP. et al. (2013) |
| | *qDTY6.1* | 6 | RM589–RM204 | Venuprasad et al. (2012) |
| | | 6 | RM589-RM204 | |
| | | 6 | RM586-RM217 | Dixit et al. (2014) |
| | *qDTY6.2* | 6 | RM121-RM541 | Dixit et al. (2014) |
| | *qDTY9.1.* | 9 | RM105-RN434 | Swamy BP. et al. (2013) |
| | *qDTY10.1* | 10 | RM216–RM304 | Vikram et al. (2011) |
| | *qDTY10.2* | 10 | RM269–G2155 | Swamy BP. et al. (2013) |
| | *qDTY12.1* | 12 | RM28166–RM28199 | Mishra et al. (2013) |
| Submergence | | | | |
| High survival | qSUB1.1 | 1 | id1000556-id1003559 | Gonzaga et al. (2016) |
| High survival | qSUB4.1 | 4 | id4010621-id4012434 | Gonzaga et al. (2016) |
| High survival | qSUB8.1 | 8 | id08005815-id8007472 | Gonzaga et al. (2016) |
| High survival | qSUB10.1 | 10 | id10005538-RM25835 | Gonzaga et al. (2016) |
| Anaerobic germination | qAG-5 | 5 | RM405–RM249 | Jiang et al. (2006) |
| Anaerobic germination | qAG-7-2 | 7 | RM21868-RM172, seq- rs3583 | Angaji et al. (2010); Zhang et al. (2017) |
| Anaerobic germination | qAG-7-1, AG2 | 7 | RM3583–RM21427 | Septiningsih et al. (2013) |
| Anaerobic germination | qAG-9-2, AG1 | 9 | RM3769-RM105, seq- rs4216 | Angaji et al. (2010); Zhang et al. (2017) |

*(Continued)*

TABLE 1 Continued

| Trait | QTLs/Genes | Chromosome | Flanking markers | References |
|---|---|---|---|---|
| Anaerobic germination | qAG-11 | 11 | RM21–RM22, seq-rs5125 | Angaji et al. (2010); Zhang et al. (2017) |
| Anaerobic germination | qAG-1-2 | 1 | RM11125-RM104; id29187939id32847451 | Angaji et al. (2010); Hsu and Tung (2015) |
| Anaerobic germination | | 3 | RM7097-RM520 | Angaji et al. (2010) |
| Anaerobic germination | qAG-9-1 | 9 | RM8303-RM5526 | Angaji et al. (2010) |
| High survival | *qSUB8.1* | 8 | 8,608,433–8,686,009 | Gonzaga et al. (2017) |
| High survival | *qSUB2.1* | 2 | 2,430,179–2,470,790 | Gonzaga et al. (2017) |
| Salinity | | | | |
| $Na^+$ absorption/$Na^+$ uptake | *qSNK1* | 1 | RM1287-RM10825 | Thomson et al., 2010 |
| | *qSNK2* | 2 | 2422788 – 2437583* | Gimhani et al., 2016 |
| | *qSNK4.1* | 4 | 4355198 – 4384860* | |
| | *qNaK3.1* | 3 | RM282-RM156 | Puram et al., 2018 |
| | snkr1.1 | 1 | RM1287-AP3206d | de Ocampo et al., 2022 |
| | *qNaK-R1.1* | 1 | RM472-RM14 | Rahman et al., 2019 |
| | *qNaK-R3.3* | 3 | RM5626- R3M53 | |
| | *qNaK-R5.4* | 5 | RM163-RM19199 | |
| Relative shoot potassium conc. compared to control | *qSRI-K9.1* | 9 | RM296-RM105 | Puram et al., 2018 |
| | *qSRI-NaK9.1* | 9 | RM296-RM105 | |
| $Na^+/K^+$ ratio in root | *qNa/KR-9* | 9 | HvSSR09-11-HvSSR09-39 | Pundir et al., 2021 |
| | *qRNK1* | 1 | RM1287-RM10825 | Thomson et al., 2010 |
| $Na^+/K^+$ ratio in leaf | *qNa/KL-1.3* | 1 | HvSSR01-56HvSSR01-70 | Pundir et al., 2021 |
| $Na^+/K^+$ ratio in leaf at reproductive stage | *qNa+/K+LR-3.1* | 3 | RM563-RM186 | |
| Root $Na^+/K^+$ ratio | *qRNK1* | 1 | RM1287-RM10825 | Thomson et al., 2010 |
| | *qSNC1* | 1 | RM1287-RM10793 | Thomson et al., 2010 |
| | *qSNC-12* | 12 | RM1285-RM423 | Zheng et al., 2015 |
| | *qSNC3* | 3 | 3528886– id3017899* | Gimhani et al., 2016 |
| | *qSNC10* | 10 | 9898598 – id10000153* | |
| | *qNa3.3* | 3 | RM5626-R3M53 | Rahman et al., 2019 |
| $Na^+$ in leaves at vegetative stage | *qNa+LV-8.2* | 8 | RM3395-RM281 | |
| $Na^+$ in leaves at reproductive stage | *qNa+LR-8.1* | 8 | RM3395-RM281 | |
| $Na^+$ conc.in leaf | *qNaL-1.2* | 1 | HvSSR01-56HvSSR01-70 | Pundir et al., 2021 |
| Shoot $K^+$ Conc | *Trait based QTL* | 12 | G24-R1684 | Lang et al., 2001 |
| | *Trait based QTL* | 1 | G24-R1684 | Koyama et al., 2001 |
| | *qSKC1* | 1 | RM8094-RM10825 | Thomson et al., 2010 |
| | *qSKC-2* | 2 | RM1285-RM423 | Zheng et al., 2015 |
| | *qSKC10* | 10 | 13069784 – 9922981* | Gimhani et al., 2016 |

*(Continued)*

TABLE 1 Continued

| Trait | QTLs/Genes | Chromosome | Flanking markers | References |
|---|---|---|---|---|
| | *qK-6* | 6 | RM3827-RM340 | Sabouri et al., 2009 |
| | *qK3.2* | 3 | RM5626-R3M53 | Rahman et al., 2019 |
| | *qK12.3* | 12 | RM27615-RM27877 | |
| | *qK3.1* | 3 | RM282-RM156 | Puram et al., 2018 |
| Root $Na^+$ content | *qRNC-9* | 9 | RM201-RM215 | Zheng et al., 2015 |
| | *qNaR-9* | 9 | HvSSR09-11-HvSSR09-39 | Pundir et al., 2021 |
| | rnc3.1 | 3 | SO3072-SO3099 | de Ocampo et al., 2022 |
| Root $K^+$ Conc | *qRKC-4* | 4 | C891-C513 | Lin et al., 2004 |
| | *qRKC1* | 1 | RM1287-RM11330 | Thomson et al., 2010 |
| | *qRKC6* | 6 | RM19840-RM20350 | |
| | *qKR-1* | 1 | HvSSR01-11-HvSSR01-34 | Pundir et al., 2021 |
| | *qKR-12* | 12 | HvSSR12-11-HvSSR12-28 | |
| | *qKR-7.1* | 7 | HvSSR07-25-HvSSR07-37 | |
| | *rkc3.1* | 3 | SO3072-SO3099 | de Ocampo et al., 2022 |
| | *qSGEM-7* | 7 | CDO59-RG477 | |
| Seedling dry matter | *qSDM-5* | 5 | RZ70-RZ225 | |
| | *qSDM-6* | 6 | CDO544-Amy2A | |
| | *qSDM-10* | 10 | RZ625-RZ500 | |
| Seedling root length | qSRTL-6 | 6 | RG162-RG653 | |
| Seedling height | *qSH1.2* | 1 | RM5389-RM5759 | Wang et al., 2012 |
| | *qSH1.3* | 1 | RM3482-RM3362 | |
| | *Trait based QTL* | 7 | C1057-R565 | |
| | *qSL1.3* | 1 | id1023892–id1017885* | Rahman et al., 2017 |
| | *qSL5.3* | 5 | RM163-RM19199 | |
| | *qSHL4.2* | 4 | RM3866-RM3288 | Puram et al., 2018 |
| | *qSHL-5* | 5 | RM13-RM164 | Ghomi et al., 2013 |
| Shoot Fresh weight | *qFWsht1.2* | 1 | id1023892 –id1017885* | Rahman et al., 2017 |
| | *qFWsht6.1* | 6 | id6016941–id6001397* | |
| | *qSFW-5b* | 5 | RM459-RM3800 | Ghomi et al., 2013 |
| | *qDSW6.1* | 6 | RM6818-RM6811 | Wang et al., 2012 |
| | *qDSW6.2* | 6 | RM340-RM3509 | |
| | *qDWsht5.1* | 5 | id5007714–id5014589* | |
| | *qDWT8.1* | 8 | RM44-RM515 | Puram et al., 2018 |
| | *qSDW-2* | 2 | RM279-RM5911 | Ghomi et al., 2013 |
| Root fresh weight | *qRFW-4b* | 4 | E36-M59-5E37-M60-3 | Ghomi et al., 2013 |
| | *rdw1.2* | 1 | RM11570-S01132A | de Ocampo et al., 2022 |
| | *qRL-9* | 9 | RM219-RM7038 | Zheng et al., 2015 |

*(Continued)*

TABLE 1 Continued

| Trait | QTLs/Genes | Chromosome | Flanking markers | References |
|---|---|---|---|---|
| | *rl2.1* | 2 | RM13332-RM5404 | de Ocampo et al., 2022 |
| Plant height | *qPH2* | 2 | RM13197-RM6318 | Thomson et al., 2010 |
| | *qSTR-3a* | 3 | RM1022-RM6283 | |
| Visual tolerance score | *qSES-2* | 2 | RM1285-RM423 | Zheng et al., 2015 |
| Standard Evaluation | *qSES1.1* | 1 | ud1000711– Id1004348* | Rahman et al., 2017 |
| | *qSES1.3* | 1 | id1024972– id1023892* | Gimhani et al., 2016 |
| Overall Phenotypic performance | *qSES3.1* | 3 | RM5626- R3M53 | Rahman et al., 2017 |
| | *qSES5.2* | 5 | RM163-RM19199 | Rahman et al., 2019 |
| Survival % | *qSur1.1* | 1 | RM472-RM14 | Puram et al., 2018 |
| | *qSTR-3a* | 3 | RM1022-RM6283 | |
| Salt survival index | *qSSI4.2* | 4 | 454365 – 24572241* | Zheng et al., 2015<br>* SNPs were used |
| | *qSSI10* | 10 | 9898598 – id10000153* | |
| Panicle length | *qPL-2* | 2 | HvSSR02-66-HvSSR02-68 | Rahman et al., 2019 |
| Biomass | *qBM-8* | 8 | HvSSR08-11-HvSSR08-15 | |
| | *qBM-5a* | 5 | E36-M59-10-RM440 | Ghomi et al., 2013 |
| **High temperature** | | | | |
| 1. Spikelet fertility<br>2. Daily flowering time<br>3. Spikelet fertility and pollen shedding | *qSF$^{ht}$2, qSF$^{ht}$4.2*<br>*qDFT3, qDFT8,*<br>*qDFT10.1,*<br>*qDFT11*<br>*qPSL$^{ht}$1,*<br>*qPSL$^{ht}$4.1,*<br>*qPSL$^{ht}$5,*<br>*qPSL$^{ht}$7,*<br>*qPSL$^{ht}$10.2* | 2.4<br>3,8,10, 11<br>1,4,5,7,10 | RM1234–RM3850,<br>RM3916–RM2431<br>RM3766–RM3513<br>RM5891–RM4997<br>RM6737–RM6673<br>RM1355–RM2191<br>RM1196–RM6581<br>RM7585–Bb38P21<br>RM1248–RM4915<br>RM6394–RM1364<br>RM7492–RM1859 | Zhao et al., 2016 |
| Flowering time HT QTL | *qHTT8* | 8 | *LOC_Os08g07010*<br>*LOC_Os08g07440* | Chen et al., 2021 |
| 1. Vegetative stage root length QTL<br>2. Vegetative stage root length QTL | *rlc1.1*<br>*rlc1.2*<br>*rlc4.1*<br>*rlc4.2*<br>*rlc4.3*<br>*rlc7.1*<br>*slc6.1*<br>*slc6.2* | 1,2,.3<br>1,2 | S1_10221082<br>S1_30191377<br>S4_100099<br>S4_1911293<br>S4_13167045<br>S7_24934857<br>S6_9368784<br>S6_32050861 | Kilasi et al., 2018 |
| 1. Filled grain number per panicle<br>2. Grain yield<br>3. HT Score | | | RM468 - RM7076<br>RM241 - RM26212<br>RM16686 - RM564<br>RM241 - RM26212<br>RM26212 - RM127<br>RM3586 - RM160 | Buu et al., 2014 |
| 1. Spikelet sterility %<br>2. Yield per plant | *qSTIPSS9.1*<br>*qSTIY5.1* | 1,5 | | Shanmugavadivel et al., 2017 |
| 1. Spikelet fertility % | *qHTSF4.1* | 4 | | Ye et al., 2015 |

*(Continued)*

TABLE 1 Continued

| Trait | QTLs/Genes | Chromosome | Flanking markers | References |
|---|---|---|---|---|
| 1. Spikelet fertility % | *qHTSF1.2*<br>*qHTSF2.1*<br>*qHTSF3.1* | 2,1,3 | | Ye et al., 2015 |
| 1. Spikelet fertility % | *qHTSF6.1*<br>*qHTSF11.2* | 6,11 | | Ye et al., 2015 |
| * represents Single NucleotidePolymorphisms (SNPs). | | | | |

Submergence reduces the quality and quantity of rice, especially when it occurs during the reproductive and maturity stages. Submergence significantly delays flowering and maturity, reducing grain yield, shoot biomass, harvest index, and yield components (Marndi et al., 2022). Reductions in grain filling, grain number per panicle, and grain weight are primarily responsible for decreased grain production due to submergence (Kato et al., 2014). Submergence during the vegetative stage affects critical grain quality parameters, with a higher proportion of hull, brown rice, and bran in rough rice compared to non-stressed counterparts, as well as chalky grains, breakage during hulling, and reduced proportion of amylose, but increased in crude protein content. Starch accumulation negatively correlated with ADP-glucose pyrophosphorylase activity in submerged rice. ADP-glucose pyrophosphorylase (AGPase) catalyzes the first committed reaction in the pathway of starch synthesis. ADP-glucose pyrophosphorylase is activated by posttranslational redox-modification in response to light and to sugars in leaves of wheat and other plant species (Ferrero et al., 2020).

Yield losses due to submergence are attributable to a smaller sink size/capacity and reduced carbohydrate metabolism and thus reduced partitioning into grain. Djali et al. (2012) reported that submerged rice had higher protein, moisture, and amylase contents than the control plants but lower yield, hardness, stickiness, and brightness. Physiological and biochemical changes in rice under submergence/flash flooding is given in Supplementary Table 1. Further, increased starch and non-structural carbohydrate accumulation positively correlated with survival percentage under submerged conditions (Panda and Sarkar, 2014). Table 1 lists QTL/genes identified in rice for submergence tolerance.

## 2.3 Impact of salt stress on paddy

Rice is sensitive to soil salinity, which occurs in 25–30% of irrigated regions of rice, equating to more than 1 billion ha of saline or sodic land (Shahid et al., 2018). Rice is more resistant to salt during the germination and vegetative stages than the seedling and reproductive stages. High-yielding rice cultivars at salinity levels >3 dS $m^{-1}$ suffered yield losses of ~12%, which increased to ~50% at 6 dS $m^{-1}$ (Kumar and Sharma, 2020). Plants subjected to salt stress have delayed seed germination and seed set, sterile spikelets, and reduced leaf dry matter, leaf area, tiller number, grains per panicle, pollen viability (Reshma et al., 2021).

Salt-stressed rice plants suffer from a reduced water potential, poor nutrient uptake, and increased sodium ($Na^+$) and chlorine ($Cl^-$) uptake. Salinity stress also affects proline and anthocyanin contents, peroxidase activity, and $Ca^{2+}$, $Na^+$, $K^+$, chlorophyll, and $H_2O_2$ concentrations (Negrão et al., 2017). Salt stress significantly reduced amylose concentration in a salt-tolerant rice genotype but not a semi-tolerant genotype, even at low EC (4 mS $cm^{-1}$) and alkalinity (pH 9.5), while high EC (8 dS $m^{-1}$) and alkalinity (pH 9.8) significantly reduced starch content in both genotypes, but not the susceptible genotype (Rao et al., 2013). Details of physiological and biochemical changes in rice under salinity is listed in Supplementary Table 1. In addition, salinity (EC 4 and 8 mS/cm) and high alkalinity (pH 9.8) affected gel consistency in the salt-susceptible genotype (Rao et al., 2013). Table 1 lists QTL/genes identified in rice for salinity-related traits.

## 2.4 Impact of high temperature on paddy

Heat stress in rice is related to specific morphological, physiological, biochemical, and molecular changes. Morphological aspects include genotypes that shield the panicles with their foliage to maintain a lower spikelet temperature for increased spikelet fertility (Beena et al., 2018a). An early morning flowering habit also plays a vital role in plants avoiding high temperatures later in the day (Hirabayashi et al., 2015; Raghunath and Beena, 2021).

Physiological mechanisms that provide heat stress tolerance in rice include an increased membrane stability index, which reduces reactive oxygen species (ROS) damage to biological membranes (Kumar et al., 2016). Increased pollen viability ensures increased fertilization success, maintaining a higher photosynthetic rate to offset yield losses due to excess transpiration rate under heat stress (Sinha et al., 2022). An increased transpiration rate ensures transpirational cooling to prevent ROS increases (Xiong et al., 2014). Physiological adaptations play a critical role in protecting membrane integrity and the biological compounds required to maintain cellular homeostasis. Heat shock proteins (HSPs), which maintain the tertiary structure of proteins, are also critical players in cellular tolerance (Khan and Shahwar, 2020). In addition, enzymatic and non-enzymatic antioxidants such as superoxide dismutase (SOD), peroxidase (POD), glutathione peroxidase (GPX), catalase (CAT), ascorbic acid, phenolic compounds, and carotenoids are crucial for negating the toxic effects of ROS (Irato and Santovito, 2021). Physiological and biochemical changes in rice under high temperature stress is given in Supplementary Table 1.

Marker-assisted introgression of QTL controlling spikelet fertility (Vivitha et al., 2018) and early morning anthesis traits (Ishimaru et al., 2022) under high-temperature conditions have contributed greatly to crop improvement. Table 1 lists QTL/genes identified for physiological and yield traits in rice under high-temperature stress.

## 2.5 Impact of elevated $CO_2$ on paddy

$CO_2$ levels have risen from 270 ppm during the pre-industrial era (1850s) to 400 ppm. At this rate, atmospheric $CO_2$ ($aCO_2$) will reach $eCO_2$ levels by 2050, estimated at 550 ppm, affecting the morphology, physiology and biochemistry of rice (Abdelhakim et al., 2022). A meta-analysis involving 125 studies on the effect of $eCO_2$ in rice showed that hybrid cultivars respond with higher biomass and yield over popular *indica* and japonica types, primarily due to increased panicle and spikelet numbers, followed by tiller number. $eCO_2$ levels increase the accumulation of root biomass more than shoot biomass (Wang et al., 2018). A three-year experiment in a free-air $CO_2$ enrichment (FACE) facility revealed a declining proportion of brown, milled, and head rice under $eCO_2$ (200 ppm above ambient) relative to $aCO_2$ (Gao et al., 2021). In addition, the $eCO_2$ increased grain chalkiness, viscosity, and stickiness but, improving palatability; however, the $eCO_2$ compromised the processing quality and nutritional attributes such as protein and mineral contents (Ca, Cu and S; except for K) (Gao et al., 2021). A comparative study at $eCO_2$ (700 ppm) improved seedling emergence, C/N ratio, and biomass in two rice genotypes (IR20 and ADT46). Changes in physiological traits under elevated $CO_2$ is given in Supplementary Table 1. When subjected to brown plant hopper infestation, the $eCO_2$-grown plants had greater insect attack, but insect survival decreased by several days, relative to the control plants (SenthilNathan, 2021). Thus $eCO_2$ poses several ecological effects on rice-based agri-ecosystem.

## 2.6 Impact of soil nutrient deficit on paddy

Since the green revolution, fertilizer application is essential due to the unintentional emergence of fertilizer-responsive, high-yielding semi-dwarf rice cultivars (Neeraja et al., 2021). Reported poor nutrient use efficiencies in rice, with 30–50% for nitrogen, 30% for phosphorous, and 26% for potassium. In addition to macronutrients, breeders are now paying close attention to micronutrient deficits ('hidden hunger') due to human health concerns. The most common micronutrient disorders are Fe insufficiency, Zn deficiency, and B toxicity for wetland rice and Fe and B deficiency and Mn toxicity for upland rice (Shrestha et al., 2020).

Rice is the primary source of nutrition for much of the world's population. However, rice is deficient in essential fatty acids, vitamins, minerals, phytochemicals, and amino acids (Sultana et al., 2022). Zhou et al. (2018) reported positive effects of nitrogen on the milling and nutritional quality of rice. Increased nitrogen application increased protein content but decreased milling quality, appearance, amylose content, gel consistency, cooking/eating quality, and rice flour viscosity (Zhu et al., 2017). The nitrogen-efficient line (*OsNRT2*.3b-overexpressing (O8) and wild type (WT) were treated with different levels of nitrogen and carbon fertilizers under field conditions to study the effects of different fertilization treatments on rice quality. The results showed that the appearance, nutrition, and taste qualities of O8 were generally high compared with WT under various fertilization treatment conditions (Zhang et al., 2022).

Rice is particularly vulnerable to nutrient deficit stress at the seedling emergence, tillering, panicle initiation, booting, heading, and maturity stages (Shrestha et al., 2020). During the early and mid-phases of grain filling, K and Ca control root exudation, which affects grain quality characteristics such as the proportion of chalky kernels, chalkiness, and amylose content (Lijun et al., 2011). N fertilization can affect micronutrient concentrations.

# 3 Physiological and molecular implications of combined abiotic stresses on rice yield and quality

## 3.1 Effect of combined drought and temperature

Drought and high-temperature stress often occur simultaneously in the field, drastically affecting plant growth,

development, and yield by inducing physiological, biochemical, and molecular changes and responses that impact various cellular and whole plant functions (Figure 1). Combined effect of drought and high temperature is more severe than individual effects (Dreesen et al., 2012).

### 3.1.1 Physiological and genetic components of sensitivity

Drought and heat stress combined affect rice crops at the cell, organ, plant, and canopy level, ultimately reducing growth and yield. The combined stress often has conflicting or antagonistic responses dissimilar to their individual effects. Vapor pressure deficit (VPD) naturally increases during heat waves and droughts, impacting rice physiology (Williams et al., 2014). During heat stress, plants open stomata to cool their leaves by transpiration but cannot open them when faced with combined heat and drought stress (Sinha et al., 2022). In perennial grasses, combined heat and drought stress reduces PSII function, weakens N anabolism, strengthens protein catabolism, and increases lipid peroxidation. Long-term combined heat and drought stress affects growth, leaf gas exchange, and water use efficiency (WUE) in rice, severely reducing total biomass relative to individual stresses (Perdomo et al., 2015; Perdomo et al., 2016).

Rice is more sensitive to drought, heat, and combined stress during the reproductive stage, specifically flowering, than the vegetative stage. Combined heat and drought stress at the seedling and tillering stages resulted in the absence of panicles for seven African rice cultivars (Mukamuhirwa et al., 2019). The number of germinated pollens on the stigma decreased when exposed to heat (81%), drought (59%) and concomitant stress (Rang et al., 2011). Combined heat and drought stress at flowering significantly affected peduncle length, anther dehiscence, pollen number, pollen germination, spikelet fertility, and thus yield in rice (Li et al., 2015; Rang et al., 2010). Heat and drought stress hinder the accumulation of various seed constituents in rice by inhibiting starch processes and protein synthesis. Grain quality is more susceptible to combined stress than yield. High temperature (30°C) inhibited starch metabolism by decreasing starch synthase activity due to thermal denaturation (Pravallika et al., 2020). Reduced grain endosperm starch content is a leading cause of reduced quality and yield in crops subjected to drought and heat (Worch et al., 2011). Similar to drought, heat stress decreases starch content but increases grain protein and mineral concentrations (Mariem et al., 2021). Heat stress reduced amylose content and partially altered the fine structure of amylopectin, indicating that the abnormal expression of the starch synthesizing enzymes is a key factor causing chalkiness (Nakata et al., 2017).

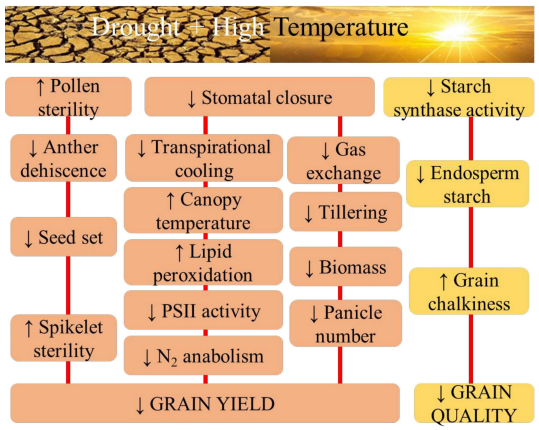


FIGURE 1
The physiological aspects of sensitivity to combined drought and high temperature stress in rice with respect to grain yield, and quality.

The changing climate is adversely affecting the nutritional quality in terms of mineral content and protein, which will impact human health (Mariem et al., 2021). Higher temperatures also decrease aroma quality in rice. Basmati rice had excellent aroma when grown under relatively cool temperatures in the afternoon (25–32°C) and night (20–25°C) and 70–80% humidity during the primordial and grain-filling stages (Singh et al., 2000). It is important to understand the physiological, biochemical and genetic mechanisms governing the response to combined heat and drought stress to develop strategies to improve stress tolerance.

### 3.1.2 Physiological and genetic components of tolerance

Plants cope with drought and heat stress through cellular tolerance *via* metabolic homeostasis, osmotic adjustment, cellular membrane stability, oxidative stress management, production of stress proteins (e.g., late embryogenesis abundant proteins and HSPs) and secondary metabolites, and reducing fatty acid desaturation. Sucrose accumulated in the anthers of rice genotype Nagina 22 under combined drought and high-temperature stress (Li et al., 2015). Heat shock factors (HSFs) and HSPs showed differential upregulation in rice, with HSF7A upregulated under drought stress, *HSF2a* upregulated under heat stress, and HSP74.8, HSP80.2, and HSP24.1 upregulated under the combined stress (Piveta et al., 2020).

He et al. (2018) noted that a complex regulatory network mobilizes these defenses by involving upstream signaling molecules that transmit the stress signal *via* hormones, ROS, and nitric oxide (NO). Under drought and heat stress condition, overexpression of the gene Rab7 (*OsRab7*) improved tolerance in rice by high survival rate, relative water content, chlorophyll content, gas-exchange characteristics, soluble protein content, soluble sugar content, proline content, and activities of antioxidant enzymes (CAT, SOD, APX, POD) than that of the wild-type. In contrast, the levels of hydrogen peroxide, electrolyte

leakage, and malondialdehyde of the transgenic lines were significantly reduced when compared to wild-type. Furthermore, the expression of four genes encoding reactive oxygen species (ROS)-scavenging enzymes (*OsCATA, OsCATB, OsAPX2, OsSOD-Cu/Zn*) and eight genes conferring abiotic stress tolerance (*OsLEA3, OsRD29A, OsSNAC1, OsSNAC2, OsDREB2A, OsDREB2B, OsRAB16A, OsRAB16C*) was significantly up-regulated in the transformed rice lines as compared to their expression in wild-type (El- Esawi and Alayafi, 2019).

Combined heat and drought stress studies have been undertaken on a few cultivars in rice, with one study identifying Nagina 22 as the only tolerant cultivar (Reshma et al., 2021). Therefore, systematic screening of rice germplasm and mapping populations are needed to identify and introgress QTL into elite cultivars. Genome-wide association studies can identify QTL/genes for dissecting the genetic basis of combined stress tolerance. The grain-filling stage is one of the most important phases that determine yield. Stay green traits can be used as an indicator of sustainable assimilate supply and stem reserve utilization to promote seed filling under stressful conditions (Abdelrahman et al., 2017). There is an immense need to identify plant species and genotypes tolerant to combined stresses (Zandalinas et al., 2018) and tailor genotypes with acceptable performance under combined drought and high-temperature stress for sustainable crop production.

## 3.2 Effect of combined drought and elevated $CO_2$

### 3.2.1 Physiological and genetic components of sensitivity

Rice requires 5000 L of water to produce 1 kg biomass and 3,000–5,000 L for 1 kilo grain (Mainuddin et al., 2020). Studies in controlled environment chambers showed that $eCO_2$ reduced evapotranspiration, allowing photosynthesis to continue for 1–2 days longer than $aCO_2$ under drought stress (Supplementary Figure 1). While the saturation point for $CO_2$ is 500 ppm in rice, the down regulation of photosynthesis occurred beyond 900 ppm. In addition, $eCO_2$ attenuated the canopy dark respiration. Dark respiration has physiological relevance, as the energy derived is used for plant growth and metabolism (Zou and Xu, 2021). The reduced stomatal aperture increased the canopy temperature due to the suppression of transpiration. Prolonged exposure to $eCO_2$ also reduced the net photosynthetic rate. The resultant decrease or increase in yield will be location specific, influenced by regional temperatures. Drought stress increases ABA content, which affects $CO_2$ intake. Drought stress also reduces the levels of RuBisCo large and small subunits at the proteomic level. Thus plants cannot harness all of the benefits of $CO_2$ fertilization under drought stress (Perdomo et al., 2017).

Prolonged drought stress significantly decreases some core physiological traits. The $eCO_2$ treatment increased RuBisCo activity by 17.5% compared to the $aCO_2$ treatment. One study showed that $eCO_2$ (700 ppm) treated plants under drought stress had a 40% lower $CO_2$ exchange rate than drought-stressed plants under $aCO_2$ (350 ppm). The Km of RuBisCo also decreased compared to irrigated and drought-stressed plants under $aCO_2$. Plants raised in a $CO_2$-enriched atmosphere had higher RuBisCo content and activity after ~20 days of drought stress, but this comparative advantage did not occur after ~30 days of stress. In this situation, $eCO_2$ plants had inferior physiological traits. Prabnakorn et al. (2018) reported that rice production would suffer more under climate change events, where increases in $CO_2$ cannot mitigate the adverse effects on rice productivity.

### 3.2.2 Physiological and genetic components of tolerance

Rice grown under $eCO_2$ has more tillers and higher grain yield (Cho and Oki, 2012). $eCO_2$ increased biomass by 5.7% due to an increased leaf area index and leaf water potential in rice (Kumar et al., 2017). Certain simulation models have highlighted the significance of $CO_2$ fertilization in assisting crops to withstand water deficits (Kang et al., 2021). A meta-analysis study on rice, wheat, and maize under increased $CO_2$ levels and drought stress revealed that the $CO_2$ component alone increased grain yield and starch content but decreased protein and mineral contents. The inevitable consequence of stomatal conductance for $CO_2$ leads to loss of water, affecting the proportion of net photosynthesis to transpiration rate (i.e., transpiration efficiency), as a function of leaf anatomical features that determine the utilization of $CO_2$ levels in the atmosphere (Ouyang et al., 2017). Under $eCO_2$ (700 ppm), the imposition of drought stress had less effect on yield attributes than $aCO_2$ and reduced water use by 10% (Shanker et al., 2022) Similarly, combined $eCO_2$ and drought stress maintained canopy net photosynthesis by 6–12%. $CO_2$ supply extended the maintenance of mid-day photosynthesis for a few days, which had an ameliorative effect on rice.

In rice, a soil matric potential of –40 kPa (~43% moisture) or below results in water deficit stress (Kumar et al., 2019). An $eCO_2$ (550 ppm) treatment at a 2°C elevated temperature imparted intrinsic drought (–40 kPa) stress tolerance traits in aerobic rice genotypes (CR-143-2-2, APO, and CR Dhan 201), reducing antioxidant enzyme (SOD, POX, CAT) activities in leaves (Padhy et al., 2018). Drought stress also decreased the aboveground biomass and yield in IR72. However, an $eCO_2$ (700 ppm) treatment maintained higher rice biomass and yield than $aCO_2$ (350 ppm), with both $CO_2$ regimes maintaining a comparable harvest index in corresponding treatments. Both $CO_2$ regimes increased sucrose and reduced starch content in drought-stressed IR72, reducing grain quality. Plants raised under $aCO_2$ conditions exposed to drought stress had more pronounced reductions (45%) in sucrose phosphate synthase

activity (sucrose biosynthesis enzyme) than those raised under $eCO_2$ (Wang et al., 2022).

Under drought stress, ABA acts as the primary regulator of stomatal closure, $eCO_2$ delays the sunthesis of ABA. Crosstalk also occurs between these two components at the aquaporin level (Li et al., 2020). A brassinosteroid (BR) treatment ameliorated the ill-effects of drought stress by improving $CO_2$ assimilation (Raghunath et al., 2021; Lakshmi et al., 2022). The induction of endogenous BR under drought stress might help accumulate carbon. A study on *d1* mutants for the Gα subunit (of heterotrimeric G protein complex) gene RGA1 (Rice Gα subunit 1) reported that Nipponbare and Taichung 65 had higher mesophyll conductance for $CO_2$ than the wild type and likely had higher WUE and productivity under drought stress (Zait et al., 2021). Overexpression of the *OsEPF1* (Epidermal Patterning Factor 1) gene reduced stomatal density in rice, enhancing drought tolerance but compromising yield, which improved with 450–480 ppm $CO_2$ supply. Such a plant type will benefit future climate scenarios with scant rainfall and elevated $CO_2$ (Caine et al., 2019).

## 3.3 Effect of combined high temperature and $eCO_2$

### 3.3.1 Physiological and genetic components of sensitivity

Periods of high temperature and $eCO_2$ concentration due to anthropogenic activities threaten rice production (Supplementary Table 2). $eCO_2$ should enhance the photosynthetic rate, increasing total yield and productivity (Kant et al., 2012; Hasegawa et al., 2013) because $CO_2$ is directly involved in major physiological processes such as photosynthesis and stomatal conductance. Rising temperatures reduce rice yield alone or in combination with $eCO_2$ (Wang et al., 2020). A higher respiration rate and declining membrane thermostability reduce rice yield under high night temperature (HNT) conditions (Mohammed and Tarpley, 2010). The decreased membrane stability index in susceptible rice varieties under elevated temperature was related to the extent of lipid peroxidation by ROS (Das et al., 2014; Kumar et al., 2016).

The most sensitive stages to high-temperature stress in rice are booting, anthesis, and fertilization. Several studies have investigated the effect of high temperature and $eCO_2$ concentrations in rice in growth or open-top chambers. The closed chamber experiments revealed that rice is highly susceptible to heat stress and heat-induced spikelet sterility (HISS) at flowering, resulting in yield losses. $eCO_2$ cannot ameliorate yield losses due to the high temperature (Wang et al., 2018). Cai et al. (2016) and Wang et al., (2018, 2020) reported that rising temperatures decreased panicle number per unit area and spikelet number per panicle, decreasing rice yields; these effects escalated under $eCO_2$. $eCO_2$ alone exacerbates HISS as stomatal closure increases the canopy temperature, with a stimulatory effect on biomass production, but an increase in night temperatures counteracts this effect. Significant compromises in yield occur due to the higher respiratory cost of the increased biomass. Night respiration increased by 4–18 mg C $hill^{-1}$ $h^{-1}$ in rice genotypes under $eCO_2$ and HNT at various crop stages before heading (Shanker et al., 2022).

The interactive effect of heat stress and $eCO_2$ adversely impacts rice growth, development, and pollen viability (Mittler et al., 2012). Decreased anther dehiscence, poor pollen shedding, poor pollen grain germination on stigmas, and decreased pollen tube elongation led to spikelet sterility under heat stress. Raised night temperatures have more adverse effects than raised day temperatures due to deprived anther dehiscence, impaired pollination, abnormal pollen germination, and floret sterility (Das et al., 2014; Fahad et al., 2018). Floral sterility under high temperatures reduces sink demand due to the reduction in carbohydrate transfer from shoots to grain (Madan et al., 2012). Active selection and breeding for the $eCO_2$ response and HNT-resilient rice are needed to compensate for yield losses.

Heat stress during the reproductive and grain-filling stage reduces rice yield by diminishing the proportion of fertile spikelets (Beena et al., 2018a), shortening the grain-filling period (Ahmed et al., 2015), and reduction in sink activity (Kim et al., 2011). Thus, elevated $CO_2$ and high-temperature stress during flowering and early grain filling significantly reduce rice seed set and thousand-grain weight (Chaturvedi et al., 2017). $eCO_2$ and high temperature also shorten the phenology of rice. Rice grain quality is reflected in parameters such as head and chalky rice rate, amylose and protein contents, and edible quality, as indicated by gel consistency. As $CO_2$ and temperature increased, rice grain appearance initially declined but then improved (Liu et al., 2017). Exposure to high temperature during ripening causes abnormal morphology and grain discoloration in rice, probably due to reduced enzymatic activity related to grain filling, respiratory consumption of assimilation products, and decreased sink activity. Combined $eCO_2$ and high-temperature stress significantly affects amylose content and gel consistency (Supplementary Figure 2). Madan et al. (2012) reported a slight decrease in amylose content and gel consistency in the sensitive genotype IR64, which carries one of two heat-sensitive alleles responsible for amylose accumulation during grain filling.

Soluble protein is the principal holder of plant nitrogen and an important index for measuring leaf aging. Liu et al. (2017) documented that soluble protein content did not vary widely across rice growth stages under $eCO_2$ and high-temperature conditions. In another study, $eCO_2$ stimulated grain production and starch accumulation but negatively affected nutritional traits such as protein and mineral contents (Mariem et al., 2021). The severity of $eCO_2$ and high-temperature stress increases when the stress period coincides with flowering and grain filling and further intensified by high canopy temperatures associated

with stomatal opening. Elevated $CO_2$ combined with canopy warming affects plant C, N, and P ratios due to insufficient N uptake and allocation (Wang et al., 2019). The whole plant C/N ratio will remain unaffected if C assimilation and N absorption both increase under $eCO_2$ and HNT conditions (Cheng et al., 2010).

### 3.3.2 Physiological and genetic components of tolerance

Being a C3 crop, rice theoretically will benefit from the $eCO_2$ fertilization effect, whereas the concomittent increase in temperature will negate the positive benefit of $eCO_2$ (Chaturvedi et al., 2017). At the cellular level, the photosynthetic response to $eCO_2$ will be greater at higher temperatures due to the reduction in RuBisCo activity. In addition, canopy photosynthesis will significantly increase with $eCO_2$, which could negate the adverse effects of high-temperature stress on the C3 pathway (Kadam et al., 2014).

In contrast to high day temperature (HDT) stress, rice lacks an escape or avoidance mechanism under HNT stress (Bahuguna et al., 2014; Bahuguna et al., 2015; Hirabayashi et al., 2015). However, rice may have an enhanced ability to meet the increased carbon demand under increased night respiration, minimizing the negative impact of HNT on grain yield and quality (Impa et al., 2020). The usefulness of increased crop responsiveness to $eCO_2$ under warmer nights has not been investigated. Bahuguna et al. (2022) reported that rice cultivars with significantly higher $CO_2$ responsiveness could fix the additional carbon available under future scenarios.

FACE experiments revealed that $eCO_2$ significantly reduced rice grain quality. However, newly developed heat-tolerant rice cultivars retained high grain quality under $eCO_2$ (Usui et al., 2014), suggesting that current breeding efforts for heat tolerance will be useful for the projected climate change scenarios. Under climate change, the photosynthetic apparatus should be improved and some physiological responses such as stomatal conductance and transpiration rate should be maintained. The sensitivity of rice to HNT could be overcome by surveying germplasm to develop climate-resilient varieties for $eCO_2$ responsiveness through marker development and genomic mapping (Silva et al., 2020; Bahuguna et al., 2022). Supplementary Figure 2 shows the interactive effect of high temperature, and $eCO_2$.

## 3.4 Effect of combined salinity and drought stress

### 3.4.1 Physiological and genetic components of sensitivity

Salinity and drought stress disrupt morphological features and physiological and biochemical processes in rice. While these stresses have their respective domains and scopes, drought and salinity stress often co-occur in natural field environments (Fan et al., 2015; Paul et al., 2019; Yadav et al., 2022). The severity and occurrence of combined drought and salinity stress are expected to increase with global environmental changes, which could have profound implications on the food supply. This combined stress is a major limiting factor for rice cultivation and productivity (Landi et al., 2017), triggering oxidative, osmotic, and temperature stresses leading to cellular dehydration and reduced cytosolic and vacuolar volume (Fan et al., 2015). ROS production under combined salinity and drought stress amplifies the damage to proteins, DNA, and membranes (Landi et al., 2017), reducing the photosynthetic rate and efficiency and inducing programmed cell death; thus reducing yields by more than 30% each year (Bhar, 2020).

Several studies have shown that drought and salt stress share similar initial plant responses, resulting in ion toxicity in the long term. Salinity and drought stress both cause physiological water deficits that affect all plant organs to varying degrees. However, plants react to hyper-ionic and hyper-osmotic stress under extended salt stress. Concomitantly large VPD also increases under drought stress. The effect of drought and salinity on photosynthesis ranges from restricted $CO_2$ diffusion into chloroplasts, limited stomatal opening mediated by shoot and root-generated hormones and $CO_2$ transport through the mesophyll, and changes in leaf photochemistry and carbon metabolism (Ma et al., 2020). The combined effect of drought and salinity at early stages (germination, seedling establishment, and tillering) delays transplantation (in rainfed lowlands) or crop establishment (in uplands) and stunts growth, resulting in poor stand establishment and ultimately reducing the number of panicles per unit area and panicle size. The combined stresses at the reproductive stage (panicle initiation, flowering, and grain filling) cause varying degrees of spikelet sterility and poor grain filling, with greater detrimental effects on grain yield (Ali et al., 2022).

### 3.4.2 Physiological and genetic components of tolerance

Most drought and salt stress studies focus on roots and shoots, with measurements of physiological and genetic parameters (Qin et al., 2020; Hao et al., 2022). Among them, ABA plays an important role in plant responses to abiotic stresses (Zhao et al., 2021). The overexpression of *OsPYL5* can improve drought and salt tolerance through ABA-mediated processes (Ruiz et al., 2021). Secondary messengers such as $Ca^{2+}$ and ROS can alleviate osmotic stress damage and improve drought and salt tolerance through ABA-dependent/independent pathways. In addition, $H_2O_2$ plays a vital role in stomatal closure through ABA-dependent and ABA-independent pathways (Chen et al., 2021). Under drought and salt stress, stress-response genes increase plant resistance by activating the associated proteins and accumulating protective metabolites. Downregulating the expression of *DST1* (*DROUGHT AND SALT TOLERANT 1*), *ABIL2* (ABL INTERACTOR-LIKE PROTEIN 2), and *HDA704* (histone deacetylase) positively regulates drought

and stress tolerance in rice. *hda704* knockdown mutants exhibited susceptibility to drought and salinity stress. HDA704 imparts drought tolerance by promoting stomatal closure (Zhao et al., 2021). Shikimate pathway is known to be activated under abiotic stress conditions, such as drought and salinity, resulting in the accumulation of high levels of aromatic amino acids and related secondary metabolites (Francini et al., 2019). Overexpression of *OsSKL2* in rice increased tolerance to salinity, drought and oxidative stress by increasing antioxidant enzyme activity, and reducing levels of $H_2O_2$, malondialdehyde, and relative electrolyte leakage (Jiang et al., 2022).

## 3.5 Effect of combined salinity and submergence stress

The changing climate and resultant rise in sea water levels lead to unexpected spells of multiple abiotic stresses at different stages of paddy production. In coastal areas, increasing temperatures, erratic rainfall, and inundation of saline water due to sea-level rises can change the micro-environment in fields. Studies are limited in this arena for rice. Tolerant rice genotypes adapt to combined salinity and submergence due to the presence of well-developed constitutive aerenchyma and increased ethylene production and respiratory burst oxidase homolog (RBOH) signaling. RBOH-mediated ROS production resulted in the development of constitutive aerenchyma in a saline and flooding tolerant rice variety, Rashpanjor (Chakraborty et al., 2021). Chlorophyll fluorescence imaging identified tolerant varieties under combined salinity and partial submergence (Pradhan et al., 2018).

## 3.6 Effect of combined salinity and high temperature

High temperature and salinity in tropical coastal belts derail rice productivity. Exposure to salinity and high temperature, in combination or in tandem, changes rice growth patterns, defense mechanisms, reproduction, and survival functions, reducing shoot fresh weight, relative water content, photosynthetic pigments, and protein content and increasing proline and SOD activities. A saline-tolerant rice variety, YNU31-2-4, under combined high temperature and salinity stress, downregulated $K^+$ transporter *OsHKT1;5* and upregulated *OsHSP18*, *OsP5CS*, and $Na^+/H^+$ antiporter *OsNHX* (Nahar et al., 2022). However, under combined stress condition Nagina-22 performed well than other genotypes in terms of proline content, cell membrane stability index, SOD activity, pollen viability, spikelet fertility, and yield per plant and lower lipid peroxidation and $Na^+/K^+$ ratio than susceptible genotypes (Ali et al., 2021). Combined effects of various abiotic stresses on physio-biochemical traits in rice is given in Supplementary Table 2. Figure 2 shows the interactive effect of high temperature, $eCO_2$, and drought.

# 4 Conclusion

Rice (*Oryza sativa* L.) is the staple food crop consumed by much of the world's population. Projected rice statistics for 2021–22 estimated global production of 505.4 million tons, an increase of 1.9 million tons than previous year, mainly attributed to China, Bangladesh, South Korea, and Taiwan. Paddy is cultivated primarily in tropical climates, where water scarcity, high temperatures, salinity, and nutrient deficits can significantly reduce yields. Rapid fluctuations in environmental conditions can impact the adaptive ability of rice, further impairing its productivity. Various abiotic stresses affect seed germination, seedling establishment, shoot and root lengths, plant height, days to flowering, grain filling, maturity, and grain quality. Abiotic stresses during both vegetative and reproductive stage compromise panicle development and grain filling, impacting overall grain production and jeopardizing global food security. Genomics and QTL-based approaches have helped identify genes and loci responsible for abiotic stress tolerance in rice. Introgressing these newly identified molecular candidates can improve rice physiological growth under suboptimal conditions and stimulate reproductive development and grain production. However, further studies involving next-generation sequencing platforms and high-throughput phenotyping will help identify novel candidate genes responsible for regulating grain development in combined stress situations and pave the way for developing climate-ready crops.

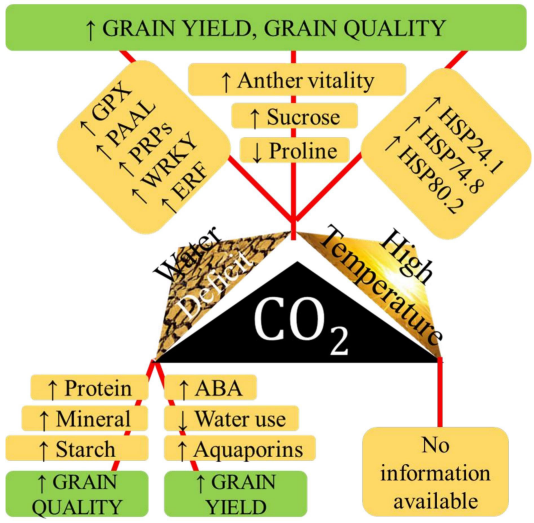


FIGURE 2
The physiological aspects of tolerance to various paired combinations of high temperature, water deficit stress and elevated CO2 with respect to grain yiled, and quality in rice.

## Author contributions

BR, RS and GK conceived and designed the study; GK prepared the figures; All authors review the literature, synthesize the data/material and draft the review; KS critically edited the manuscript; RS, MT, GK, DU, ST, CA, BS, BM and BR, helped in developing main andsupplementary tables. All authors have read and agreed to the published version of the manuscript.

## Conflict of interest

The authors declare that the research was conducted in the absence of any commercial or financial relationships that could be construed as a potential conflict of interest.

## Publisher's note



## Supplementary material

The Supplementary Material for this article can be found online at: https://www.frontiersin.org/articles/10.3389/fpls.2022.996514/full#supplementary-material

## References

Abdelrahman, M., El-Sayed, M., Jogaiah, S., Burritt, D. J., and Tran, L. S. P. (2017). The "Stay-green" trait and phytohormone signaling networks in plants under heat stress. *Plant Cell Rep.* 36, 1009–1025. doi: 10.1007/s00299-017-2119-y

Abdelrahman, L. O. A., Zhou, R., and Ottosen, C.O. (2022). Physiological Responses of Plants to Combined Drought and Heat under Elevated $CO_2$. *Agronomy* 12, 2526. doi: 10.3390/agronomy12102526

Abdelhakim, L. O. A. , Zhou, R. , and Ottosen, C.-O. . (2022). Physiological Responses of Plants to Combined Drought and Heat under Elevated CO2. *Agronomy* 12, 2526. doi: 10.3390/agronomy12102526

Ahmad, H., Zafar, S. A., Naeem, M. K., Shokat, S., Inam, S., Rehman, M. A., et al. (2022). Impact of preanthesis drought stress on physiology, yield-related traits, and drought-responsive genes in green super rice. *Front. Genet.* 13. doi: 10.3389/fgene.2022.832542

Ahmed, N., Tetlow, I. J., Nawaz, S., Iqbal, A., Mubin, M., Nawaz ul Rehman, M. S., et al. (2015). Effect of high temperature on grain filling period, yield, amylose content and activity of starch biosynthesis enzymes in endosperm of basmati rice. *J. Sci. Food Agric.* 95 (11), 2237–2243. doi: 10.1002/jsfa.6941

Ali, A., Beena, R., Manikanta, Ch L. N., Swapna, A., Soni, K. B., and Viji, M. M. (2022). Molecular characterization and varietal identification for multiple abiotic stress tolerance in rice (*Oryza sativa* l.). *Oryza -An Int. J. rice.* 59 (1), 140–15). doi: 10.35709/ory.2022.59.1.7

Ali, B. S. A., Beena, R., and Stephen, K. (2021). Combined effect of high temperature and salinity on growth and physiology of rice (*Oryza sativa* l.). *Agric. Res. J.* 58 (5), 783–788. doi: 10.5958/2395-146X.2021.00111.3

Angaji, S. A., Septiningsih, E. M., Mackill, D. J., and Ismail, A. M. (2010). QTLs associated with tolerance of flooding during germination in rice (*Oryza sativa* l.).". *Euphytica* 172 (2), 159–168. doi: 10.1007/s10681-009-0014-5

Anie, T., Beena, R., Lakshmi, G., Soni, K. B., Swapna, A., and Viji, M. M. (2022). Changes in sucrose metabolic enzymes to water stress in contrasting rice genotypes. *Plant Stress* 5. doi: 10.1016/j.stress.2022.100088

Azharudheen, M. T. P., Nayak, A. K., Behera, S., Anilkumar, C., Marndi, B. C., Moharana, D., et al. (2022). Genome-wide association analysis for plant type characters and yield using cgSSR markers in rice (*Oryza sativa* l.). *Euphytica* 218 (69). doi: 10.1007/s10681-022-03021-z

Bahuguna, R. N., Chaturvedi, A. K., Pal, M., Viswanathan, C., Jagadish, S. K., and Pareek, A. (2022). Carbon dioxide responsiveness mitigates rice yield loss under high night temperature. *Plant Physiol.* 188 (1), 285–300. doi: 10.1093/plphys/kiab470

Bahuguna, R. N., Jagadish, K. S. V., Coast, O., and Wassmann, R. (2014). Plant abiotic stress: Temperature extremes. *Encyclopedia Agric. Food Syst.*, 330–334. doi: 10.1016/B978-0-444-52512-3.00172-8

Bahuguna, R. N., Jha, J., Pal, M., Shah, D., Lawas, L. M., Khetarpal, S., et al. (2015). Physiological and biochemical characterization of NERICA-L-44: a novel source of heat tolerance at the vegetative and reproductive stages in rice. *Physiologia plantarum.* 154 (4), 543–559. doi: 10.1111/ppl.12299

Bahuguna, R. N., Tamilselvan, A., Muthurajan, R., Solis, C. A., and Jagadish, S. V. K. (2018). Mild preflowering drought priming improves stress defences, assimilation and sink strength in rice under severe terminal drought. *Funct. Plant Biol.* 45, 827–839. doi: 10.1071/FP17248

Banerjee, A., and Roychoudhury, A. (2020). "Rice grain quality and abiotic stress: Genomics and biotechnological perspectives," in *Rice research for quality improvement: Genomics and genetic engineering: Volume 1: Breeding techniques and abiotic stress tolerance*. Ed. A. Roychoudhury (Singapore: Springer), 747–752. doi: 10.1007/978-https://doi.org/10.1007/978-981-15-4120-9_30

Barik, S. R., Pandit, E., Pradhan, S. K., Mohanty, S. P., and Mohapatra, T. (2019). Genetic mapping of morpho-physiological traits involved during reproductive stage drought tolerance in rice. *PloS One* 14, e0214979. doi: 10.1371/journal.pone.0214979

Beena, R., Praveenkumar, V. P., Vighneswaran, V., and Narayankutty, M. C. (2018c). Bulked line analysis: A useful tool to identify microsatellite markers linked to drought tolerance in rice. *Indian J. Plant Physiol.* 23 (1), 7–15. doi: 10.1007/s40502-017-0321-0

Beena, R., Praveenkumar, V. P., Vighneswaran, V., Sindhumol, P., and Narayankutty, M. C. (2017). Phenotyping for root traits and carbon isotope in rice genotypes of kerala. *Oryza Int. J. Rice.* 54 (3), 282–289. doi: 10.5958/2249-5266.2017.00039.X

Beena, R., Silvas, K., Nithya, N., Manickavelu, A., Sah, R. P., Abida, P. S., et al. (2021a). Association mapping of drought tolerance and agronomic traits in rice (*Oryza sativa* l.) landraces. *BMC Plant Biol.* 21 (1), 1–21. doi: 10.1186/s12870-021-03272-3

Beena, R., Thandapani, V., and Chandrababu, R. (2012). Physio-morphological and biochemical characterization of selected recombinant inbred lines of rice for drought resistance. *Indian J. Plant Physiol.* 17 (2), 189–193.

Beena, R., Veena, V., Jaslam, M. P. K., Nithya, N., and Adarsh, V. S. (2021b). Germplasm innovation for high temperature tolerance from traditional rice accessions of kerala using genetic variability, genetic advance, path coefficient analysis and principal component analysis. *J. Crop Sci. Biotechnol.* 24 (5), 555–566. doi: 10.1007/s12892-021-00103-7

Beena, R., Veena, V., and Narayankutty, M. C. (2018b). Evaluation of rice genotypes for acquired thermo-tolerance using temperature induction response technique. *Oryza-An Int. J. Rice.* 55 (2), 285–291. doi: 10.5958/2249-5266.2018.00035.8

Beena, R., Vighneswaran, V., Sindumole, P., Narayankutty, M. C., and Voleti, S. R. (2018a). Impact of high temperature stress during reproductive and grain filling stage in rice. *Oryza Int. J. Rice.* 55 (1), 126–133. doi: 10.5958/2249-5266.2018.00015.2

Bhar, A. (2020). "Rice tolerance to multiple abiotic stress: Genomics and genetic engineering," in *Rice research for quality improvement: Genomics and genetic engineering* (Singapore: Springer), 591–615.

Buu, B. C., Ha, P. T. T., Tam, B. P., Nhien, T. T., Hieu, N. V., Phuoc, N. T., et al. (2014). Quantitative trait loci associated with heat tolerance in rice (*Oryza sativa* l.). *Plant Breed. Biotech.* 2 (1), 14~24. doi: 10.9787/PBB.2014.2.1.014

Caine, R. S., Yin, X., Sloan, J., Harrison, E. L., Mohammed, U., Fulton, T., et al. (2019). Rice with reduced stomatal density conserves water and has improved drought tolerance under future climate conditions. *New Phytol.* 221, 371–384. doi: 10.1111/nph.15344

Cai, C., Yin, X., He, S., Jiang, W., Si, C., Struik, P. C., et al. (2016). Responses of wheat and rice to factorial combinations of ambient and elevated CO2 and temperature in FACE experiments. *Global Change Biol.* 22 (2), 856–874. doi: 10.1111/gcb.13065

Cal, A. J., Sanciangco, M., Rebolledo, M. C., Luquet, D., Torres, R. O., McNally, K. L., et al. (2019). Leaf morphology, rather than plant water status, underlies genetic variation of rice leaf rolling under drought. *Plant Cell Environ.* 42 (5), 1532–1544. doi: 10.1111/pce.13514

Catolos, M., Sandhu, N., Dixit, S., Shamsudin, N. A. A., Naredo, M. E. B., McNally, K. L., et al. (2017). Genetic loci governing grain yield and root development under variable rice cultivation conditions. *Front. Plant Sci.* 8. doi: 10.3389/fpls.2017.01763

Chakraborti, M., Anilkumar, C., Verma, R. L., Abdul Fiyaz, R., Raj, K. R., Patra, B. C., et al. (2021). Rice breeding in India: eight decades of journey towards enhancing the genetic gain for yield, nutritional quality, and commodity value. *Oryza* 58, 69–88. doi: 10.35709/ory.2021.58.spl.2

Chakraborty, K., Ray, S., Vijayan, J., Molla, K., Nagar, R., Jene, P., et al. (2021). Preformed aerenchyma determines the differential tolerance response under partial submergence imposed by fresh and saline water flooding in rice. *Physiologia Plantarum* 173 (4). doi: 10.1111/ppl.13536

Chaturvedi, A. K., Bahuguna, R. N., Shah, D., Pal, M., and Jagadish, S. V. (2017). High temperature stress during flowering and grain filling offsets beneficial impact of elevated $CO_2$ on assimilate partitioning and sink-strength in rice. *Sci. Rep.* 7 (1), 1–13. doi: 10.1038/s41598-017-07464-6

Cheng, W., Sakai, H., Yagi, K., and Hasegawa, T. (2010). Combined effects of elevated CO2 and high night temperature on carbon assimilation, nitrogen absorption and the allocations of c and n by rice (*Oryza sativa* l.). *Agri For. meteorology* 150 (9), 1174–1181. doi: 10.1016/j.agrformet.2010.05.001

Chen, L., Wang, Q., Tang, M., Zhang, X., Pan, Y., Yang, X., et al. (2021). QTL mapping and identification of candidate genes for heat tolerance at the flowering stage in rice. *Front. Plant Sci.* 11:621871. doi: 10.3389/fgene.2020.621871

Cho, J., and Oki, T. (2012). Application of temperature, water stress, CO2 in rice growth models. *Rice.* 5 (1), 10. doi: 10.1186/1939-8433-5-10

Das, S., Krishnan, P., Nayak, M., and Ramakrishnan, B. (2014). High temperature stress effects on pollens of rice (*Oryza sativa* l.) genotypes. *Environ. Exp. Bot.* 101, 36–46. doi: 10.1016/j.envexpbot.2014.01.004

de Ocampo, M. P., Thomson, M. J., Mitsuya, S., Yamauchi, A., and Ismail, A. M. (2022). QTL mapping under salt stress in rice using a kalarata–azucena population. *Euphytica* 218 (6), 1–15. doi: 10.1007/s10681-022-03026-8

Dixit, S., Singh, A., Sta Cruz, M. T., Maturan, P. T., Amante, M., and Kumar, A. (2014). Multiple major QTL lead to stable yield performance of rice cultivars across varying drought intensities. *BMC Genet.* 15, 1–13. doi: 10.1186/1471-2156-15-16

Djali, M., Nurhasanah, S., Lembong, E., and Rahmat, R. (2012). The effect of flooding on rice characteristics of Cilamaya muncul'on various days after planting during the last reproductive and maturation phase. *II Asia Pacific Symposium Postharvest Res. Educ. Extension: APS2012* 1011, 285–291. doi: 10.17660/ActaHortic .2013.1011.35

Dong, W., Chen, J., Wang, L., Tian, Y., Zhang, B., Lai, Y., et al. (2014). Impacts of nighttime post-anthesis warming on rice productivity and grain quality in East China. *Crop J.* 2, 63–69. doi: 10.1016/j.cj.2013.11.002

Dreesen, F. E., De Boeck, H. J., Janssens, I. A., and Nijs, I. (2012). Summer heat and drought extremes trigger unexpected changes in productivity of a temperate annual/biannual plant community. *Environ. Exp. Bot.* 79, 21–30. doi: 10.1016/j.envexpbot.2012.01.005

El- Esawi, M. A., and Alayafi, A. A. (2019). Overexpression of rice Rab7 gene improves drought and heat tolerance and increases grain yield in rice (Oryza sativa l.). *Genes* 10, 56. doi: 10.3390/genes10010056

Fahad, S., Ihsan, M. Z., Khaliq, A., Daur, I., Saud, S., Alzamanan, S., et al. (2018). Consequences of high temperature under changing climate optima for rice pollen characteristics-concepts and perspectives. *Arch. Agron. Soil Sci.* (Singapore: Springer) 64 (11), 1473–1488. doi: 10.1080/03650340.2018.1443213

Fahad, S., Noor, M., Adnan, M., Khan, M. A., Rahman, I. U., Alam, M., et al. (2019). "Abiotic stress and rice grain quality," in *In advances in rice research for abiotic stress tolerance* (Woodhead Publishing), 571–583. doi: 10.1016/B978-0-12-814332-2.00028-9

Fan, Y., Shabala, S., Ma, Y., Xu, R., and Zhou, M. (2015). Using QTL mapping to investigate the relationships between abiotic stress tolerance (drought and salinity) and agronomic and physiological traits. *BMC Genomics* 16 (1), 1–11. doi: 10.1186/s12864-015-1243-8

FAO (2017). *The impact of natural hazards and disasters on agriculture and food and nutrition security: A call for action to build resilient livelihoods.*

Feng, B., Chen, K., Cui, Y., Wu, Z., Zheng, T., Zhu, Y., et al. (2018). Genetic dissection and simultaneous improvement of drought and low nitrogen tolerances by designed QTL pyramiding in rice. *Front. Plant Sci.* 9. doi: 10.3389/fpls.2018.00306

Ferrero, D. M. L., Piattoni, C. V., Asencion Diez, M. D., Rojas, B. E., Hartman, M. D., Ballicora, M. A., et al. (2020). Phosphorylation of ADP-glucose pyrophosphorylase during wheat seeds development. *Front. Plant Sci.* 11. doi: 10.3389/fpls.2020.01058

Francini, A., Giro, A., and Ferrante, A. (2019). Biochemical and molecular regulation of phenylpropanoids pathway under abiotic stresses. *Plant Sign Mole* 2019, 183–192. doi: 10.1016/B978-0-12-816451-8.00011-3

Gao, B., Hu, S., Jing, L., Wang, Y., Zhu, J., Wang, K., et al. (2021). Impact of elevated CO2 and reducing the source- sink ratio by partial defoliation on rice grain quality - a 3-year free-air CO2 enrichment study. *Front. Plant Sci.* 12. doi: 10.3389/fpls.2021.788104

Garg, R., Chevala, V. V. S. N., Shankar, R., and Mukesh Jain, M. (2015). Divergent DNA methylation patterns associated with gene expression in rice cultivars with contrasting drought and salinity stress response. *Sci. Rep.* 5, 14922. doi: 10.1038/srep14922

Ghimire, K. H., Quiatchon, L. A., Vikram, P., Swamy, B. M., Dixit, S., Ahmed, H., et al. (2012). Identification and mapping of a QTL (qDTY1. 1) with a consistent effect on grain yield under drought. *Field Crops Res.* 131, 88–96. doi: 10.1016/j.fcr.2012.02.028

Ghomi, K., Rabiei, B., Sabouri, H., and Sabouri, A. (2013). Mapping QTLs for traits related to salinity tolerance at seedling stage of rice (Oryza sativa l.): an agrigenomics study of an Iranian rice population. *Omics: J. Integr. Biol.* 17 (5), 242–251. doi: 10.1089/omi.2012.0097

Gimhani, D. R., Gregorio, G. B., Kottearachchi, N. S., and Samarasinghe, W. L. G. (2016). SNP-based discovery of salinity-tolerant QTLs in a bi-parental population of rice (Oryza sativa). *Mol. Genet. Genomics* 291 (6), 2081–2099. doi: 10.1007/s00438-016-1241-9

Gonzaga, Z. J. C., Carandang, J., Sanchez, D. L., Mackill, D. J., and Septiningsih, E. M. (2016). Mapping additional QTLs from FR13A to increase submergence tolerance in rice beyond SUB1. *Euphytica* 209 (3), 627–636. doi: 10.1007/s10681-016-1636-z

Gonzaga, Z. J. C., Carandang, J., Singh, A., Collard, B. C. Y., Thomson, M. J., and Septiningsih, E. M. (2017). Mapping QTLs for submergence tolerance in rice using a population fixed for SUB1A tolerant allele. *Mol. breeding.* 37 (4), 1–10. doi: 10.1007/s11032-017-0637-5

Hao, Z., Ma, S., Liang, L., Feng, T., Xiong, M., Lian, S., et al. (2022). Candidate genes and pathways in rice co-responding to drought and salt identified by gcHap network. *Int. J. Mol. Sci.* 23 (7), 4016. doi: 10.3390/ijms23074016

Hasegawa, T., Sakai, H., Tokida, T., Nakamura, H., Zhu, C., Usui, Y., et al. (2013). Rice cultivar responses to elevated CO2 at two free-air CO2 enrichment (FACE). *Japan. Funct. Plant Biol.* 40, 148–159. doi: 10.1071/FP12357

He, M., He, C. Q., and Ding, N. Z. (2018). Abiotic stresses: General defenses of land plants and chances for engineering multistress tolerance. *Front. Plant Sci.* 9. doi: 10.3389/fpls.2018.01771

Hirabayashi, H., Sasaki, K., Kambe, T., Gannaban, R. B., Miras, M. A., Mendioro, M. S., et al. (2015). qEMF3, a novel QTL for the early-morning flowering trait from wild rice, oryza officinalis, to mitigate heat stress damage at flowering in rice, o. sativa. *J. Exp. Bot.* 66 (5), 1227–1236. doi: 10.1093/jxb/eru474

Hussain, S., Jun-hua, Z., Chu, Z., Lian-feng, H., Xiao-chuang, C., Sheng-miao, Y., et al. (2017). Effects of salt stress on rice growth, development characteristics, and the regulating ways: A review. *J. Integr. Agric.* 16 (11), 2357–2374. doi: 10.1016/S2095-3119(16)61608-8

Hsu, S.-K., and Chih-Wei, T. (2015). "Genetic mapping of anaerobic germination-associated QTLs controlling coleoptile elongation in rice.". *Rice* 8 (1), 1–12. doi: 10.1186/s12284-015-0072-3

Impa, S. M., Vennapusa, A. R., Bheemanahalli, R., Sabela, D., Boyle, D., Walia, H., et al. (2020). High night temperature induced changes in grain starch metabolism alters starch, protein, and lipid accumulation in winter wheat. *Plant Cell Environ.* 43 (2), 431–447. doi: 10.1111/pce.13671

Irato, P., and Santovito, G. (2021). Enzymatic and non-enzymatic molecules with antioxidant function. *Antioxidants* 10, 579. doi: 10.3390/antiox10040579

Ishimaru, T., Hlaing, K. T., Oo, Y. M., Lwin, T. M., Sasaki, K., Lumanglas, P. D., et al. (2022). An early-morning flowering trait in rice can enhance grain yield under heat stress field conditions at flowering stage. *Field Crops Res.* doi: 10.1016/j.fcr.2021.108400

Jeyasri, R., Muthuramalingam, P., Satish, L., Pandian, S. K., Chen, J.-T., Ahmar, S., et al. (2021). An overview of abiotic stress in cereal crops: Negative impacts, regulation, biotechnology and integrated omics. *Plants.* 10, 1472. doi: 10.3390/plants10071472.https://doi.org/10.3390/plants10071472

Jiang, L., Shijia, L., Mingyu, H., Jiuyou, T., Liangmin, C., Huqu, Z., et al. (2006). Analysis of QTLs for seed low temperature germinability and anoxia germinability

in rice (Oryza sativa l.). *Field Crops Res.* 98 (1), 68–75. doi: 10.1016/j.fcr.2005.12.015

Jiang, Y., Peng, X., Zhang, Q., Liu, Y., Li, A., Cheng,, et al. (2022). Regulation of drought and salt tolerance by OsSKL2 and OsASR1 in rice. l. *Rice* 15, 46. doi: 10.1186/s12284-022-00592-2

Kadam, N. N., Xiao, G., Melgar, R. J., Bahuguna, R. N., Quinones, C., Tamilselvan, A., et al. (2014). Agronomic and physiological responses to high temperature, drought and elevated CO2 interactions in cereals. *Adv. Agron.* 127, 111–156. doi: 10.1016/B978-0-12-800131-8.00003-0

Kang, H., Sridhar, V., Mainuddin, M., and Trung, L. D. (2021). Future rice farming threatened by drought in the lower Mekong basin. *Sci. Rep.* 11 (1), 1–15. doi: 10.1038/s41598-021-88405-2

Kant, S., Seneweera, S., Rodin, J., Materne, M., Burch, D., Rothstein, S. J., et al. (2012). Improving yield potential in crops under elevated CO2: integrating the photosynthetic and nitrogen utilization efficiencies. *Front. Plant Sci.* 3. doi: 10.3389/fpls.2012.00162

Kato, Y., Collard, B. C., Septiningsih, E. M., and Ismail, A. M. (2014). Physiological analyses of traits associated with tolerance of long-term partial submergence in rice. *AoB Plants* 6, plu058. doi: 10.1093/aobpla/plu058

Kilasi, N. L., Singh, J., Vallejos, C. E., Ye, C., Jagadish S.V, K., Paul Kusolwa, P., et al. (2018). Heat stress tolerance in rice (Oryza sativa l.): Identification of quantitative trait loci and candidate genes for seedling growth under heat stress. *Front. Plant Sci* 9:1578. doi: 10.3389/fpls.2018.01578

Kilkis, B., and Caglar, M. (2022). "May. exergy guided optimization model for decarbonized solar districts," in *CLIMA 2022 conference*.

Kim, J., Shon, J., Lee, C. K., Yang, W., Yoon, Y., Yang, W. H., et al. (2011). Relationship between grain filling duration and leaf senescence of temperate rice under high temperature. *Field Crops Res.* 122 (3), 207–213. doi: 10.1016/j.fcr.2011.03.014

Koyama, M. L., Levesley, A., Koebner, R. M., Flowers, T. J., and Yeo, A. R. (2001). Quantitative trait loci for component physiological traits determining salt tolerance in rice. *Plant Physiol.* 125 (1), 406–422. doi: 10.1104/pp.125.1.406

Kumar, A., Nayak, A. K., Das, B. S., Panigrahi, N., Dasgupta, P., Mohanty, S., et al. (2019). Effects of water deficit stress on agronomic and physiological responses of rice and greenhouse gas emission from rice soil under elevated atmospheric CO2. *Sci. Total Environ.* 650, .2032–.2050. doi: 10.1016/j.scitotenv.2018.09.332

Kumar, A., Sandhu, N., Dixit, S., Yadav, S., Swamy, B. P. M., and Shamsudin, N. A. A. (2018). Marker-assisted selection strategy to pyramid two or more QTLs for quantitative trait-grain yield under drought. *Rice* 11, 35. doi: 10.1186/s12284-018-0227-0

Kumar, N., Shankhdhar, S. C., and Shankhdhar, D. (2016). Impact of elevated temperature on antioxidant activity and membrane stability in different genotypes of rice (Oryza sativa l.). *Indian J. Plant Physiol.* 21 (1), 37–43. doi: 10.1007/s40502-015-0194-z

Kumar, P., and Sharma, P. K. (2020). Soil salinity and food security in India. *Front. Sustain. Food Syst.* 4, 533781. doi: 10.3389/fsufs.2020.533781

Kurniasih, B., Tarigan, I., Firmansyah, E., and Indradewa, D. (2021). "Rice growth in a combined submergence and salinity stresses," in *IOP Conference Series: Earth and Environmental Science*, Vol. 012012 (Indonesia: IOP Publishing).

Kumar, A., Nayak, A. K., Sah, R. P., and Das, B. S. (2017). Effects of elevated CO 2 concentration on water productivity and antioxidant enzyme activities of rice (Oryza sativa l.) under water deficit stress. *Field Crops Res.* 212 (2), 61–72. doi: 10.1016/j.fcr.2017.06.020

Lang, N. T., Yanagihara, S., and Buu, B. C. (2001). A microsatellite marker for a gene conferring salt tolerance on rice at the vegetative and reproductive stages. *SABRAO J. Breed. Genet.* 33, 1–10.

Lakshmi, G., Beena, R., Soni, K. B., Viji, M. M., and Uday, C. J. (2022). Exogenously applied plant growth regulator protects rice from heat induced damage by modulating plant defense mechanism. *J. Crop Sci. Biotechnol.* doi: 10.1007/s12892-022-00162-4

Landi, S., Hausman, J. F., Guerriero, G., and Esposito, S. (2017). Poaceae vs. abiotic stress: focus on drought and salt stress, recent insights and perspectives. *Front. Plant Sci.* 8, 1–9. doi: 10.3389/fpls.2017.01214

Lanning, S., and Siebenmorgen, T. (2013). Effects of preharvest nighttime air temperatures on whiteness of head rice. *Cereal Chem.* 90, 218–222. doi: 10.1094/cchem-07-12-0082-r

Li, X., Lawas, L. M., Malo, R., Glaubitz, U., Erban, A., Mauleon, R., et al. (2015). Metabolic and transcriptomic signatures of rice floral organs reveal sugar starvation as a factor in reproductive failure under heat and drought stress. *Plant Cell Environ.* 38, 2171–2192. doi: 10.1111/pce.12545

Li, S., Li, X., Wei, Z., and Liu, F. (2020). ABA-mediated modulation of elevated CO2 on stomatal response to drought. *Curr. Opin. Plant Biol.* 56, 174–180. doi: 10.1016/j.pbi.2019.12.002

Lijun, L., Chang, E. H., Fan, M. M., and Zhang, J. (2011). Effects of potassium and calcium on root exudates and grain quality during grain filling. *Acta agronomica Sin.* 37 (4), 661–669. doi: 10.1016/S1875-2780(11)60018-7

Lin, H. X., Zhu, M. Z., Yano, M., Gao, J. P., Liang, Z. W., Su, W. A., et al. (2004). QTLs for na+ and k+ uptake of the shoots and roots controlling rice salt tolerance. *Theor. Appl. Genet.* 108 (2), 253–260. doi: 10.1007/s00122-003-1421-y

Liu, S., Waqas, M. A., Wang, S. H., Xiong, X. Y., and Wan, Y. F. (2017). Effects increased levels atmospheric $CO_2$ High temperatures Rice Growth quality. *PloS One* 12 (11), e0187724. doi: 10.1371/journal.pone.0187724

Liu, W., Yin, T., Zhao, Y., Wang, X., Wang, K., Shen, Y., et al. (2021). Effects of high temperature on rice grain development and quality formation based on proteomics comparative analysis under field warming. *Front. Plant Sci.* 12. doi: 10.3389/fpls.2021.746180

Liu, L., Waters, D. L., Rose, T. J., Bao, J., and King, G. J. (2013). Phospholipids in rice: Significance in grain quality and health benefits: A review. *Food Chem.* 139, 1133–1145. doi: 10.1016/j.foodchem.2012.12.046

Ma, Y., Dias, M. C., and Freitas, H. (2020). Drought and salinity stress responses and microbe-induced tolerance in plants. *Front. Plant Sci.* 11. doi: 10.3389/fpls.2020.591911

Madan, P., Jagadish, S. V. K., Craufurd, P. Q., Fitzgerald, M., Lafarge, T., and Wheeler, T. R. (2012). Effect of elevated CO2 and high temperature on seedset and grain quality of rice. *J. Exp. Bot.* 63 (10), 3843– 3852. doi: 10.1093/jxb/ers077

Mainuddin, M., Maniruzzaman, M. D., Alam, M. M., Mojid, M. A., Schmidt, E. J., Islam, M. T., et al. (2020). Water usage and productivity of boro rice at the field level and their impacts on the sustainable groundwater irrigation in the north-West Bangladesh. *Agric. Water Manage.* 240, 106294. doi: 10.1016/j.agwat.2020.106294

Manikanta, C. L. N., Beena, R., and Rejeth, R. (2022). Root anatomical traits influence water stress tolerance in rice (Oryza sativa l.). *J. Crop Sci. Biotechnol.* doi: 10.1007/s12892-022-00142-8

Manikanta, C., Beena, R., Roy, S., Manju, R. V., Viji, M. M., and Swapna, A. (2020). Physio-morphological plasticity of rice (Oryza sativa l.) genotypes exposed to water stress. *J. Trop. Agriculture.* 58 (1), 139–145.

Mariem, S. B., Soba, D., Zhou, B., Loladze, I., Morales, F., and Aranjuelo, I. (2021). Climate change, crop yields, and grain quality of C3 cereals: A meta-analysis of CO2, temperature and drought effects. *Plants* 10, 6–1052. doi: 10.3390/plants10061052`

Marndi, B. C., Anilkumar, C., Muhammed, Azharudheen, T. P., Sah, R. P., Moharana, D., et al. (2022). "Cataloguing of rice varieties of NRRI suitable for different abiotic stress-prone ecologies. *Climate resilient technologies for rice based production systems in Eastern india. ICARNational rice research institute*,". P. Bhattacharyya, K. Chakraborty, K. A. Molla, A. Poonam, D. Bhaduri, R. P. Sah, et al (Eds.) (India: Cuttack, Odisha), 408.

Mishra, K. K., Vikram, P., Yadaw, R. B., Swamy, B. P., Dixit, S., Cruz, M. T. S., et al. (2013). qDTY12. 1: a locus with a consistent effect on grain yield under drought in rice. *BMC Genet.* 14, 1–10. doi: 10.1186/1471-2156-14-1

Mittler, R., Finka, A., and Goloubinoff, P. (2012). How do plants feel the heat? *Trends Biochem. Sci.* 37 (3), 118–125. doi: 10.1016/j.tibs.2011.11.007

Mohammed, A. R., and Tarpley, L. (2010). Effects of high night temperature and spikelet position on yield-related parameters of rice (*Oryza sativa* l.) plants. *Eur. J. Agron.* 33, 117–123. doi: 10.1016/j.eja.2009.11.006

Moore, C. E., Hensold, K. M., Lemonnier, P., Slattery, R. A., Benjamin, C., Bernacchi, C. J., et al. (2021). The effect of increasing temperature on crop photosynthesis: From enzymes to ecosystems. *J. Exp. Bot.* 72 (8), 2822–2844. doi: 10.1093/jxb/erab090

Muthu, V., Abbai, R., Nallathambi, J., Rahman, H., Ramasamy, S., Kambale, R., et al. (2020). Pyramiding QTLs controlling tolerance against drought, salinity, and submergence in rice through marker assisted breeding. *PloS One* 15, e0227421. doi: 10.1371/journal.pone.0227421

Mukamuhirwa, A., Hovmalm, H. P., Bolinsson, H., Ortiz, R., Nyamangyoku, O., and Johansson, E. (2019). Concurrent drought and temperature stress in rice–a possible result of the predicted climate change: Effects on yield attributes, eating characteristics, and health promoting compounds. *Int. J. Environ. Res. Public Health* 16, 1043. doi: 10.3390/ijerph16061043

Nahar, L., Aycan, M., Hanamata, S., Marouane Baslam, M., and Mitsui, T. (2022). Impact of single and combined salinity and high-temperature stresses on agro-physiological, biochemical, and transcriptional responses in rice and stress-release. *Plants.* 11 (501), 1–23. doi: 10.3390/plants11040501

Nakata, M., Fukamatsu, Y., Miyashita, T., Hakata, M., Kimura, R., Nakata, Y., et al. (2017). High temperature-induced expression of rice α-amylases in developing endosperm produces chalky grains. *Front. Plant Sci.* 8. doi: 10.3389/fpls.2017.02089

Narsai, R., and Whelan, J. (2013). How unique is the low oxygen response? Ananalysis of the an aerobic response during germination and comparison with abiotic stress in rice and Arabidopsis. *Front. Plant science.* 4 (349). doi: 10.3389/fpls.2013.00349

Neeraja, C. N., Voleti, S. R., Desiraju, S., Kuchi, S., Bej, S., Talapanti, K., et al. (2021). "Molecular breeding for improving nitrogen use efficiency in rice: Progress and perspectives," in *Molecular breeding for rice abiotic stress tolerance and nutritional quality* (USA: John Wiley & Sons, Ltd), 234–248. doi: 10.1002/9781119633174.ch12

Negrão, S., Schmöckel, S. M., and Tester, M. (2017). Evaluating physiological responses of plants to salinity stress. *Ann. Bot.* 119, 1–11. doi: 10.1093/aob/mcw191

Nithya, N., Beena, R., Abida, P. S., Sreekumar, J., Roy, S., Jayalekshmi, V. G., et al. (2021). Genetic diversity and population structure analysis of bold type rice collection from southern India. *Cereal Res. Commun.* 49 (2), 311–328. doi: 10.1007/s42976-020-00099-w

Nithya, N., Beena, R., Stephen, R., Abida, P. S., Jayalekshmi, V. G., Viji, M. M., et al. (2020). Genetic variability, heritability, correlation coefficient and path analysis of morpho-physiological and yield related traits of rice under drought stress. *Chem. Sci. Rev. Lett.* 9 (33), 48–54. doi: 10.37273/chesci.cs142050122

Nonogaki, H., Barrero, J. M., and Li, C. (2018). Editorial: Seed dormancy, germination, and pre-harvest sprouting. *Front. Plant Sci.* 9. doi: 10.3389/fpls.2018.01783

Ouyang, W., Struik, P. C., Yin, X., and Yang, J. (2017). Stomatal conductance, mesophyll conductance, and transpiration efficiency in relation to leaf anatomy in rice and wheat genotypes under drought. *J. Exp. Bot.* 68 (18). doi: 10.1093/jxb/erx314

Padhy, S. R., Nayak, S., Dash, P. K., Das, M., Roy, K. S., Nayak, A. K., et al. (2018). Elevated carbon dioxide and temperature imparted intrinsic drought tolerance in aerobic rice system through enhanced exopolysaccharide production and rhizospheric activation. *Agriculture Ecosyst. Environ.* 268, 52–60. doi: 10.1016/j.agee.2018.08.009

Palanog, A. D., Swamy, B. M., Shamsudin, N. A. A., Dixit, S., Hernandez, J. E., Boromeo, T. H., et al. (2014). Grain yield QTLs with consistent-effect under reproductive-stage drought stress in rice. *Field Crops Res.* 161, 46–54. doi: 10.1016/j.fcr.2014.01.004

Panda, D., and Sarkar, R. K. (2014). Mechanism associated with nonstructural carbohydrate accumulation in submergence tolerant rice (*Oryza sativa* l.) cultivars. *J. Plant Interact.* 9, 62–68. doi: 10.1080/17429145.2012.763000

Pandey, P., Irulappan, V., Bagavathiannan, M. V., and Senthil-Kumar, M. (2017). Impact of combined abiotic and biotic stresses on plant growth and avenues for crop improvement by exploiting physio-morphological traits. *Front. Plant Sci.* 8. doi: 10.3389/fpls.2017.00537

Pang, Y., Chen, K., Wang, X., Wang, W., Xu, J., Ali, J., et al. (2017). Simultaneous improvement and genetic dissection of salt tolerance of rice (*Oryza sativa* l.) by designed QTL pyramiding. *Front. Plant Sci.* 8. doi: 10.3389/fpls.2017.01275

Pathak, H., Kumar, M., Molla, K. A., and Chakraborty, K. (2021). Abiotic stresses in rice production: impacts and management. *Oryza* 58, 103–125. doi: 10.35709/ory.2021.58.spl.4

Patra, B. C., Anilkumar, C., and Chakraborti, M. (2020). Rice breeding in India: A journey from phenotype-based pure-line selection to genomics assisted breeding. *Agric. Res. J.* 57, 816–825. doi: 10.5958/2395-146X.2020.00120.9

Paul, K., Pauk, J., Kondic-Spika, A., Grausgruber, H., Allahverdiyev, T., Sass, L., et al. (2019). Co-Occurrence of mild salinity and drought synergistically enhances biomass and grain retardation in wheat. *Front. Plant Sci.* 10, 501. doi: 10.3389/fpls.2019.00501

Perdomo, J. A., Capó-Bauçà, S., Carmo-Silva, E., and Galmés, J. (2017). Rubisco and rubisco activase play an important role in the biochemical limitations of photosynthesis in rice, wheat, and maize under high temperature and water deficit. *Front. Plant Sci.* 8. doi: 10.3389/fpls.2017.00490

Perdomo, J. A., Carmo-Silva, E., Hermida-Carrera, C., Flexas, J., and Galmés, J. (2016). Acclimation of biochemical and diffusive components of photosynthesis in rice, wheat, and maize to heat and water deficit: Implications for modeling photosynthesis. *Front. Plant Sci.* 7, 1719. doi: 10.3389/fpls.2016.01719

Perdomo, J. A., Conesa, M.À, Medrano, H., Ribas-Carbó, M., and Galmés, J. (2015). Effects of long-term individual and combined water and temperature stress on the growth of rice, wheat and maize: Relationship with morphological and physiological acclimation. *Physiol. Plant* 155 (2), 149–165. doi: 10.1111/ppl.12303

Piveta, L. B., Roma-Burgos, N., Noldin, J. A., Viana, V. E., Oliveira, C., Lamego, F. P., et al. (2020). Molecular and physiological responses of rice and weedy rice to heat and drought stress. *Agriculture* 11, 9. doi: 10.3390/agriculture11010009

Prabnakorn, S., Maskey, S., Suryadi, F., and de Fraiture, C. (2018). Rice yield in response to climate trends and drought index in the mun river basin, Thailand. *Sci. Total Environ.* 621, 108–119. doi: 10.1016/j.scitotenv.2017.11.136

Pradhan, B., Chakraborty, K., Prusty, N., Deepa, M. A. K., Chattopadhyay, K., et al. (2019). Distinction and characterisation of rice genotypes tolerant to combined stresses of salinity and partial submergence, proved by a high-resolution chlorophyll fluorescence imaging system. *Funct. Plant Biol.* 46, 248–261. doi: 10.1071/FP18157

Pravallika, K., Arunkumar, C., Vijayakumar, A., Beena, R., and Jayalekshmi, V. G. (2020). Effect of high temperature stress on seed filling and nutritional quality of rice (*Oryza sativa* l.). *J. Crop Weed* 16 (2), 18–23. doi: 10.22271/09746315.2020.v16.i2.1310

Prince, S. J., Beena, R., Michael Gomez, S., Senthivel, S., and Chandra Babu, R. (2015). Mapping consistent yield QTLs under drought stress in target rainfed environments. *Rice.* 8 (1), 53. doi: 10.1186/s12284-015-0053-6

Pundir, P., Devi, A., Krishnamurthy, S. L., Sharma, P. C., and Vinaykumar, N. M. (2021). QTLs in salt rice variety CSR10 reveals salinity tolerance at reproductive stage. *Acta Physiologiae Plantarum* 43 (2), 1–15. doi: 10.1007/s11738-020-03183-0

Puram, V. R. R., Ontoy, J., and Subudhi, P. K. (2018). Identification of QTLs for salt tolerance traits and prebreeding lines with enhanced salt tolerance in an introgression line population of rice. *Plant Mol. Biol. Rep.* 36 (5), 695–709. doi: 10.1007/s11105-018-1110-2

Qin, H., Li, Y., and Huang, R. (2020). Advances and challenges in the breeding of salt-tolerant rice. *Int. J. Mol. Sci.* 21 (21), 8385. doi: 10.3390/ijms21218385

Raghunath, M. P., and Beena, R. (2021). Manipulation of flowering time to mitigate high temperature stress in rice (*Oryza sativa* l.). *Indian J. Agric. Res.* doi: 10.18805/IJARe.A-5707

Raghunath, M. P., Beena, R., Vipin, M., Viji, M. M., Manju, R. V., and Roy, S. (2021). High temperature stress mitigation in rice: foliar application of plant growth regulators and nutrients. *J. Crop Weed.* 17 (1), 34–47. doi: 10.22271/09746315.2021.v17.i1.1404

Rahman, M. A., Bimpong, I. K., Bizimana, J. B., Pascual, E. D., Arceta, M., Swamy, B. P., et al. (2017). Mapping QTLs using a novel source of salinity tolerance from hasawi and their interaction with environments in rice. *Rice.* 10 (1), 1–17. doi: 10.1186/s12284-017-0186-x

Rahman, M. A., Thomson, M. J., De Ocampo, M., Egdane, J. A., Salam, M. A., and Ismail, A. M. (2019). Assessing trait contribution and mapping novel QTL for salinity tolerance using the Bangladeshi rice landrace capsule. *Rice.* 12 (1), 1–18. doi: 10.1186/s12284-019-0319-5

Ramegowda, V., and Senthil-Kumar, M. (2015). The interactive effects of simultaneous biotic and abiotic stresses on plants: Mechanistic understanding from drought and pathogen combination. *J. Plant Physiol.* 176, 47–54. doi: 10.1016/j.jplph.2014.11.008

Ramu, V. S., Paramanantham, A., Ramegowda, V., Mohan-Raju, B., Udayakumar, M., and Senthil-Kumar, M. (2016). Transcriptome analysis of sunflower genotypes with contrasting oxidative stress tolerance reveals individual- and combined- biotic and abiotic stress tolerance mechanisms. *PloS One* 11, e0157522. doi: 10.1371/journal.pone.0157522

Rang, Z. W., Jagadish, S. V. K., Zhoua, Q. M., Craufurd, P. Q., and Heuer, S. (2010). Effect of high temperature and water stress on pollen germination and spikelet fertility in rice. *Environ. Exp. Botany.* 70 (1), 58–65. doi: 10.1016/j.envexpbot.2010.08.009

Rejeth, R., Manikanta, C., Beena, R., Roy, S., Manju, R. V., and Viji, M. M. (2020). Water stress mediated root trait dynamics and identification of microsatellite markers associated with root traits in rice (Oryza sativa l.). *Physiol. Mol. Biol. Plants.* 26 (6), 1225–1236. doi: 10.1007/s12298-020-00809

Reshma, M., Beena, R., Viji, M. M., Manju, R. V., and Roy, S. (2021). Validation of temperature induction response technique on combined effect of drought and heat stress in rice (Oryza sativa l.). *J. Crop Weed.* 17 (2), 119–128. doi: 10.22271/09746315.2021.v17.i2.1461

Ruiz, P. R., Rosario, S. M., and Lozano-Juste, J. (2021). An update on crop ABA receptors. *Plants* 10 (6), 1087. doi: 10.3390/plants10061087

Sabouri, H., Rezai, A. M., Moumeni, A., Kavousi, A., Katouzi, M., and Sabouri, A. (2009). QTLs mapping of physiological traits related to salt tolerance in young rice seedlings. *Biol. Plantarum* 53 (4), 657–662. doi: 10.1007/s10535-009-0119-7

Sandhu, N., Singh, A., Dixit, S., Sta Cruz, M. T., Maturan, P. C., Jain, R. K., et al. (2014). Identification and mapping of stable QTL with main and epistasis effect on rice grain yield under upland drought stress. *BMC Genet.* 15, 1–15. doi: 10.1186/1471-2156-15-63

Sarkar, R. K., and Ray, A. (2016). Submergence-tolerant rice withstands complete submergence even in saline water: Probing through chlorophyll a fluorescence induction O-J-I-P transients. *Photosynthetica* 54 (2), 275–287. doi: 10.1007/s11099-016-0082-4

SenthilNathan, S. (2021). Effects of elevated $CO_2$ on resistant and susceptible rice cultivar and its primary host, brown planthopper (BPH), *Nilaparvata lugens* (Stål). *Sci. Rep.* 11, 8905. doi: 10.1038/s41598-021-87992-4

Septiningsih, E. M., Ignacio, J. C. I., Sendon, P., Sanchez, D. L., Ismail, A. M., and Mackill, D. J. (2013). QTL mapping and confirmation for tolerance of anaerobic conditions during germination derived from the rice landrace ma-zhan red. *Theor. Appl. Genet.* 12 (6), 1357–1366. doi: 10.1007/s00122-013-2057-1

Shahid, S. A., Zaman, M., and Heng, L. (2018). "Soil salinity: Historical perspectives and a world overview of the problem," in *In guideline for salinity*

*assessment, mitigation and adaptation using nuclear and related techniques* (Cham, Switzerland: Springer International Publishing), 43–53.

Shamsudin, N. A. A., Swamy, B. P. M., Ratnam, W., Cruz, M. T. S., Sandhu, N., Raman, A. K., et al. (2016). Pyramiding of drought yield QTLs into a high quality Malaysian rice cultivar MRQ74 improves yield under reproductive stage drought. *Rice.* 9, 21. doi: 10.1186/s12284-016-0093-6

Shanker, A. K., Gunnapaneni, D., Bhanu, D., Vanaja, M., Lakshmi, N. J., Yadav, S. K., et al. (2022). Elevated $CO_2$ and water stress in combination in plants: Brothers in arms or partners in crime? *Biology* 11, 1330. doi: 10.3390/biology11091330

Shanmugavadivel, P. S., Mithra, S. V. A., Prakash, C., Ramkumar, M. K., Tiwari, R., Mohapatra, T., et al. (2017). High resolution mapping of QTLs for heat tolerance in rice using a 5K SNP array. *Rice* 10 (28). doi: 10.1186/s12284-017-0167-0

Shrestha, J., Kandel, M., Subedi, S., and Shah, K. K. (2020). Role of nutrients in rice (*Oryza sativa* l.): A review. *Agrica* 9, 53–62. doi: 10.5958/2394-448X.2020.00008.5

Singh, R. K., Singh, U. S., Khush, G. S., and Rohilla, R. (2000). Genetics and biotechnology of quality traits in aromatic rices. *Aromatic Rices* (Manila, the Philippines), 47–70.

Silva, R. G. D., Alves, R. D. C., and Zingaretti, S. M. (2020). Increased [CO2] causes changes in physiological and genetic responses in C4 crops: A brief review. *Plants* 9 (11), 1567. doi: 10.3390/plants9111567

Singh, S., Mackill, D. J., and Ismail, A. M. (2014). Physiological basis of tolerance to complete submergence in rice involves genetic factors in addition to the *SUB1* gene. *AoB Plants* 6. doi: 10.1093/aobpla/plu060

Sinha, R., Zandalinas, S. I., Fichman, Y., Sen, S., Zeng, S., Cadenas, A. G., et al. (2022). Differential regulation of flower transpiration during abiotic stress in annual plants. *New Phytologist.* 235, 611–629. doi: 10.1111/nph.18162

Stephen, K., Beena, R., Kiran, A. G., Shanija, S., and Saravanan, R. (2022). Changes in physiological traits and expression of key genes involved in sugar signaling pathway in rice under high temperature stress. *3 Biotech.* 12 (2), 183. doi: 10.1007/s13205-022-03242-y

Sultana, S., Faruque, M., and Islam, M. R. (2022). Rice grain quality parameters and determination tools: a review on the current developments and future prospects. *Int. J. Food Properties* 25, 1063–1078. doi: 10.1080/10942912.2022.2071295

Swamy BP, M., Ahmed, H. U., Henry, A., Mauleon, R., Dixit, S., Vikram, P., et al. (2013). Genetic, physiological, and gene expression analyses reveal that multiple QTL enhance yield of rice mega-variety IR64 under drought. *PloS One* 8. doi: 10.1371/journal.pone.0062795

Thomson, M. J., de Ocampo, M., Egdane, J., Rahman, M. A., Sajise, A. G., Adorada, D. L., et al. (2010). Characterizing the saltol quantitative trait locus for salinity tolerance in rice. *Rice.* 3 (2), 148–160. doi: 10.1007/s12284-010-9053-8

Usui, Y., Sakai, H., Tokida, T., Nakamura, H., Nakagawa, H., and Hasegawa, T. (2014). Heat-tolerant rice cultivars retain grain appearance quality under free-air CO2 enrichment. *Rice* 7 (1), 1–9. doi: 10.1186/s12284-014-0006-5

Venuprasad, R., Bool, M. E., Quiatchon, L., Sta Cruz, M. T., Amante, M., and Atlin, G. N. (2012). A large-effect QTL for rice grain yield under upland drought stress on chromosome 1. *Mol. Breed.* 30, 535–547. doi: 10.1007/s11032-011-9642-2

Verma, R., Katara, J., Anilkumar, C., Devanna, B. N., Chidambaranathan, P., Dash, B., et al. (2021). "Advanced breeding strategies for rice improvement," 263.

Vikram, P., Swamy, B. P., Dixit, S., Ahmed, H. U., Teresa Sta Cruz, M., Singh, A. K., et al. (2011). qDTY 1.1, a major QTL for rice grain yield under reproductive-stage drought stress with a consistent effect in multiple elite genetic backgrounds. *BMC Genet.* 12, p. 1-15. doi: 10.1186/1471-2156-12-89

Vivitha, P., Raveendran, M., Vijayalakshmi, C., and Vijayalakshmi, D. (2018). Genetic dissection of high temperature stress tolerance using photosynthesis parameters in QTL introgressed lines of rice cv. *Improved White Ponni. Indian J. Plant Physiol.* 23 (4), 741–747. doi: 10.1007/s40502-018-0408-2

Walter, J. (2018). Effects of changes in soil moisture and precipitation patterns on plant-mediated biotic interactions in terrestrial ecosystems. *Plant Ecol.* 219, 1449–1462. doi: 10.1007/s11258-018-0893-4

Wang, W., Cai, C., He, J., Gu, J., Zhu, G., Zhang, W., et al. (2020). Yield, dry matter distribution and photosynthetic characteristics of rice under elevated CO2 and increased temperature conditions. *Field Crops Res.* 248, 107605. doi: 10.1016/j.fcr.2019.107605

Wang, W., Cai, C., Lam, S. K., Liu, G., and Zhu, J. (2018). Elevated $CO_2$ cannot compensate for japonica grain yield losses under increasing air temperature because of the decrease in spikelet density. *Eur. J. Agron.* 99, 21–29. doi: 10.1016/j.eja.2018.06.005

Wang, Z., Cheng, J., Chen, Z., Huang, J., Bao, Y., Wang, J., et al. (2012). Identification of QTLs with main, epistatic and QTL× environment interaction effects for salt tolerance in rice seedlings under different salinity conditions. *Theor. Appl. Genet.* 125 (4), 807–815. doi: 10.1007/s00122-012-1873-z

Wang, J., Liu, X., Zhang, X., Li, L., Lam, S. K., and Pan, G. (2019). Changes in plant c, n and p ratios under elevated ($CO_2$) and canopy warming in a rice-winter wheat rotation system. *Sci. Rep.* 9 (1), 1–9. doi: 10.1038/s41598-019-41944-1

Wang, X., Liu, H., Zhang, D., Zou, D., Wang, J., Zheng, H., et al. (2022). Photosynthetic carbon fixation and sucrose metabolism supplemented by weighted gene Co-expression network analysis in response to water stress in rice with overlapping growth stages. *Front. Plant Sci.* 13. doi: 10.3389/fpls.2022.864605

Williams, A. P., Seager, R., Berkelhammer, M., Macalady, A. K., Crimmins, M. A., Swetnam, T. W., et al. (2014). Causes and implications of extreme atmospheric moisture demand during the record-breaking 2011 wildfire season in the southwestern united states. *J. Appl. Meteorology Climatology* 53, 2671–2684. doi: 10.1175/JAMC-D-14-0053.1

Worch, S., Rajesh, K., Harshavardhan, V. T., Pietsch, C., Korzun, V., Kuntze, L., et al. (2011). Haplotyping, linkage mapping and expression analysis of barley genes regulated by terminal drought stress influencing seed quality. *BMC Plant Biol.* 11, 1–14.

Wytynck, P., Lambin, J., Chen, S., Asci, S. D., Verbeke, I., De Zaeytijd, J., et al. (2021). Effect of RIP overexpression on abiotic stress tolerance and development of rice. *Int. J. Mol. Sci.* 22, 1434. doi: 10.3390/ijms22031434

Xiong, D., Yu, T., Ling, X., Fahad, S., Peng, S., Li, Y., et al. (2014). Sufficient leaf transpiration and nonstructural carbohydrates are beneficial for high-temperature tolerance in three rice (Oryza sativa) cultivars and two nitrogen treatments. *Funct. Plant Biol.* 42, 347–356. doi: 10.1071/FP14166

Yadav, C., Bahuguna, R. N., Dhankher, O. P., Singla-Pareek, S. L., and Pareek, A. (2022). Physiological and molecular signatures reveal differential response of rice genotypes to drought and drought combination with heat and salinity stress. *Physiol. Mol. Biol. Plants* 28 (4), 899–910. doi: 10.1007/s12298-022-01162-y

Yadaw, R. B., Dixit, S., Raman, A., Mishra, K. K., Vikram, P., Swamy, B. M., et al. (2013). A QTL for high grain yield under lowland drought in the background of popular rice variety sabitri from Nepal. *Field Crops Res.* 144, 281–287. doi: 10.1016/j.fcr.2013.01.019

Yang, X., Wang, B., Chen, L., Li, P., and Cao, C. (2018). The different influences of drought stress at the flowering stage on rice physiological traits, grain yield, and quality. *Sci. Rep.* 9, 3742. doi: 10.1038/s41598-019-40161-0

Ye, C., Tenorio, F. A., Argayoso, M. A., Laza, M. A., Koh, H. J., Redoña, E. D., et al. (2015). Identifying and confirming quantitative trait loci associated with heat tolerance at flowering stage in different rice populations. *BMC Genet.* 16, 41. doi: 10.1186/s12863-015-0199-7

Zait, Y., Ferrero-Serrano, ,. A., and Assmann, S. M. (2021). The α subunit of the heterotrimeric G protein regulates mesophyll $CO_2$ conductance and drought tolerance in rice. *New Phytologist.* 232, 2324–2338. doi: 10.1111/nph.17730

Zandalinas, S. I., Mittler, R., Balfagon, D., Arbona, V., and Gomez-Cadenaz, A. (2018). Plant adaptations to the combination of drought and high temperatures. *Physiolgia Plantarum* 162, 2–12. doi: 10.1111/ppl.12540

Zhang, M., Lu, Q., Wu, W., Niu, X., Wang, C., Feng, Y., et al. (2017). Association mapping reveals novel genetic loci contributing to flooding tolerance during germination in indica rice. *Front. Plant Sci.* 8. doi: 10.3389/fpls.2017.00678

Zhang, R., Wang, Y., Hussain, S., Yang, S., Li, R., Liu, S., et al. (2022). Study on the effect of salt stress on yield and grain quality among different rice varieties. *Front. Plant Sci.* 13. doi: 10.3389/fpls.2022.918460

Zhao, L., Lei, J., Huang, Y., Zhu, S., Chen, H., Renliang Huang, R., et al. (2016). Mapping quantitative trait loci for heat tolerance at anthesis in rice using chromosomal segment substitution lines. *Breed. Sci.* 66, 358–366. doi: 10.1270/jsbbs.15084.4

Zhao, J., Zhang, W., da Silva, J. A. T., Liu, X., and Duan, J. (2021). Rice histone deacetylase HDA704 positively regulates drought and salt tolerance by controlling stomatal aperture and density. *Planta* 254 (4), 1–15. doi: 10.1007/s00425-021-03729-7

Zheng, H., Zhao, H., Liu, H., Wang, J., and Zou, D. (2015). QTL analysis of na+ and k+ concentrations in shoots and roots under NaCl stress based on linkage and association analysis in japonica rice. *Euphytica.* doi: 10.1007/s10681-014-1192-3

Zhou, C., Huang, Y., Jia, B., Wang, Y., Wang, Y., Xu, Q., et al. (2018). Effects of cultivar, nitrogen rate, and planting density on rice-grain quality. *Agronomy* 8, 246. doi: 10.3390/agronomy8110246

Zhou, L., Lu, Y., Zhang, Y., Zhang, C., Zhao, L., Yao, S., et al. (2020). Characteristics of grain quality and starch fine structure of japonica rice kernels following preharvest sprouting. *J. Cereal Sci.* 95, 103023. doi: 10.1016/j.jcs.2020.103023

Zhu, D., Zhang, H., Guo, B., Xu, K., Dai, Q., Wei, H., et al. (2017). Effects of nitrogen level on yield and quality of japonica soft super rice. *J. Integr. Agric.* 16, 1018–1027. doi: 10.1016/S2095-3119(16)61577-0

Zou, D., and Xu, J. (2021). "Photorespiration and dark respiration," in *Research methods of environmental physiology in aquatic sciences* (Singapore: Springer), 149–152.

frontiers | Frontiers in Plant Science

TYPE Original Research
PUBLISHED 12 January 2023
DOI 10.3389/fpls.2022.1008756



OPEN ACCESS

EDITED BY
Nabin Bhusal,
Agriculture and Forestry University, Nepal

REVIEWED BY
Md Mehedi Hasan,
Tulane University, United States
Piyush Priya,
National Institute of Plant Genome Research (NIPGR), India

*CORRESPONDENCE
Sarika Jaiswal
sarika@icar.gov.in

SPECIALTY SECTION
This article was submitted to Plant Abiotic Stress, a section of the journal Frontiers in Plant Science

RECEIVED 01 August 2022
ACCEPTED 14 November 2022
PUBLISHED 12 January 2023

CITATION
Ahmed B, Haque MA, Iquebal MA, Jaiswal S, Angadi UB, Kumar D and Rai A (2023) DeepAProt: Deep learning based abiotic stress protein sequence classification and identification tool in cereals. *Front. Plant Sci.* 13:1008756. doi: 10.3389/fpls.2022.1008756



# DeepAProt: Deep learning based abiotic stress protein sequence classification and identification tool in cereals

Bulbul Ahmed[1], Md Ashraful Haque[2], Mir Asif Iquebal[1], Sarika Jaiswal[1]*, U. B. Angadi[1], Dinesh Kumar[1,3] and Anil Rai[1]

[1]Division of Agricultural Bioinformatics, ICAR-Indian Agricultural Statistics Research Institute, New Delhi, India, [2]Division of Computer Application, ICAR-Indian Agricultural Statistics Research Institute, New Delhi, India, [3]Department of Biotechnology, School of Interdisciplinary and Applied Sciences, Central University of Haryana, Mahendergarh, Haryana, India

The impact of climate change has been alarming for the crop growth. The extreme weather conditions can stress the crops and reduce the yield of major crops belonging to Poaceae family too, that sustains 50% of the world's food calorie and 20% of protein intake. Computational approaches, such as artificial intelligence-based techniques have become the forefront of prediction-based data interpretation and plant stress responses. In this study, we proposed a novel activation function, namely, Gaussian Error Linear Unit with Sigmoid (SIELU) which was implemented in the development of a Deep Learning (DL) model along with other hyper parameters for classification of unknown abiotic stress protein sequences from crops of Poaceae family. To develop this models, data pertaining to four different abiotic stress (namely, cold, drought, heat and salinity) responsive proteins of the crops belonging to poaceae family were retrieved from public domain. It was observed that efficiency of the DL models with our proposed novel SIELU activation function outperformed the models as compared to GeLU activation function, SVM and RF with 95.11%, 80.78%, 94.97%, and 81.69% accuracy for cold, drought, heat and salinity, respectively. Also, a web-based tool, named DeepAProt (http://login1.cabgrid.res.in:5500/) was developed using flask API, along with its mobile app. This server/App will provide researchers a convenient tool, which is rapid and economical in identification of proteins for abiotic stress management in crops Poaceae family, in endeavour of higher production for food security and combating hunger, ensuring UN SDG goal 2.0.

KEYWORDS

**abiotic stress, activation function, deep learning, web-server, mobile application**

# 1 Introduction

The drastic climatic changes due to global warming after the 1980s lead to significant yield loss in various crops (Lobell et al., 2011). The Poaceae family of crops, especially rice, wheat, and maize, which account for ~50% of the world's food calories and 20% of its protein intake (Erenstein et al., 2022), are highly susceptible to abiotic stress like heat, salinity, drought, and cold (Landi et al., 2017). On the other hand, due increasing global population, which may be around 9.5 billion by 2050, the current food availability gap requires a dramatic increase in food by 2050 (Cobb et al., 2013). It is already well known that environmental stressors negatively regulate the growth and development of plants leading to substantial yield and quality losses (Boyer, 1982; Palanog et al., 2014, Gupta et al., 2021). A recent study suggests that climate change could reduce global crop yields by 3–12% by mid-century, and by 11–25% by the century's end, under a vigorous warming scenario (Sue Wing et al., 2021).

Stresses in plants, like drought, salinity, cold, etc. are their defensive states which result from deviations from their optimal growth conditions (Jansen and Potters, 2017). These stresses lead to a loss in yield, thus affecting food security, especially in the current scenario of climate change (Rico-Chávez et al., 2022). Therefore, there is a need to conceive comprehensive strategies for trait improvement of important crops, especially of the Poaceae family, under adverse climatic conditions. Artificial intelligence (AI)- based machine learning techniques have become the forefront of prediction-based data interpretation and plant stress responses (Gill et al., 2022). Analyses of high-throughput genomic data in recent years, like, genes, transcripts, proteins, metabolites, etc., require advanced analytical methods for proper associations and interactions. The promising computational power in terms of artificial intelligence (AI) based methodologies had been a promising means for analyzing various plant stress mechanisms (Fenu and Malloci, 2021). Also, machine learning (ML) based methodologies for identifying DNA N6-methyladenine sites of plant genomes (Hasan et al., 2021), a deep-learning-based hybrid framework for identifying human RNA N5-methylcytosine sites (Hasan et al., 2022), solving classification problems in molecular data like amino acid sequence, protein sequences and structures (Cai et al., 2020; Xu et al., 2020; Gelman et al., 2021; Sridevi and Kanimozhi, 2021; Wang, 2022; Ding et al., 2022) proves the versatility of ML methodologies. The use of ML-based studies to identify, classify, and predict various stresses in plants are well reported, *namely*, in basil, coriander, parsley, baby-leaf, coffee, pea, and maize for water stress (Niu et al., 2021; Zahid et al., 2022), in *Arabidopsis thaliana* for heat, cold, salt, and drought (Kang et al., 2018), salt stress in rice (Das et al., 2020) and wheat (Moghimi et al., 2018), drought stress in *Bromus inermis* (Dao et al., 2021), and biotic stresses in soybean (Venal et al., 2019), etc.

Various studies have been done using ML/Deep Learning techniques to classify stress-responsive varieties in corn using deep convolutional neural networks (Ghosal et al., 2018; Khaki et al., 2019), neural networks (Etminan et al., 2019), linear mixed model (Chen et al, 2012) and CNN (An et al., 2019), etc. However, there are limited resources of deep-learning-based prediction models for the abiotic stress protein sequence of the Poaceae crop family. Therefore, we developed a deep learning approach for the classification of the abiotic stress protein sequence of this family. In addition, we developed a novel activation function, namely, *sielu* that has increased accuracy as compared to the existing models. The same has been applied to the stress datasets. Most of the data under study were benchmark data collected from Uniprot. Although, the DL model works well in the structure, unstructured, and complex features of the dataset, however, it requires a large dataset to train the model (Elaraby and Elmogy, 2016). It also uses different optimization techniques, weight functions, loss functions, and activation functions during model development (Wen et al., 2018; Salman and Liu, 2019). During model building, an activation function plays an important role in boosting the performance of the model as this helps in the activation or deactivation of neurons (Benvenuto and Piazza, 1992; Sarker, 2021). DL model without an activation function converges to linear regression model. Several activation functions like sigmoid, ReLU, LeakyReLU, Tanh, and Softmax have been reported in the literature (Xu et al., 2015; Hendrycks and Gimpel, 2016; Agarap, 2018; Pratiwi et al., 2020) are being used in building DL for the classification and prediction (Li et al., 2018; Armenteros et al., 2019; Bileschi et al., 2022). Some of the major limitations of these activation functions are the vanishing gradient, loss of neurons, and problems in training small datasets (Srinivasan et al., 2019).

In this study, we proposed a novel activation function, named Gaussian Error Linear Unit with Sigmoid *(SIELU)* to overcome issues related to the activation function. Further, we have built a DL model using the proposed activation function for the prediction of abiotic stresses, i.e. heat, drought, cold, and salinity responsive protein sequences from the crops of the Poaceae family. Also, a Web server has been developed, which can be extensively used by researchers/breeders for the development of abiotic stress resistance varieties of the crops of the Poaceae family for increasing agricultural production and productivity. In the future, there is a scope for developing different weight initialization techniques, activation functions, optimizers, etc. for more efficient classification using deep learning models.

# 2 Materials and methodology

## 2.1 Activation function

A series of studies have been carried out related to various activation functions and their performance in DL network

building. The extensively used activation functions in DL models are *Sigmoid*, *Tanh*, *ReLU*, *LeakyReLU*, *SoftMax*, etc. (Dunn et al., 2011).

*Sigmoid function*: For any given input of data, the sigmoid maps to 0 or 1. If a given input goes above the predetermined threshold value, it will give output as 1, otherwise, 0, *i.e.*, the neuron will remain deactivated. Scientifically, it has been proven that the human brain functions like the sigmoid function for differentiating and classifying objects (Pratiwi et al., 2020). Mathematically, it is expressed as:

$$f(x) = \frac{1}{1 + e^{-x}}$$

*Tanh function*: It is similar to the Sigmoid function with little modification for the output and expressed mathematically as (LeCun et al., 2012):

$$f(x) = \frac{2}{1 + e^{-2x}} - 1$$

*Rectified Linear Unit (ReLU):* This activation function uses stochastic gradient descent for back-propagation by adjusting the learning rate and minimizing the errors during training a model. Also, it provides a better solution without decaying the hidden layers by adjusting the learning rate and minimizing the error differentiation by removing all the negative values in back-propagation. Mathematically, *ReLU* can be expressed as (Agarap, 2018):

$$f(x) = \begin{cases} x, & for\ \ x \geq 0 \\ 0, & for\ \ x < 0 \end{cases}$$

*Leaky Rectified Linear Unit (LaekyReLU):* It is an extension of *ReLU i.e.*, by using some value, say $\sigma$=0.01 that makes the neuron active instead of deactivating for zero values. Mathematically, the *LeakyReLU* function is expressed as (Xu et al., 2015):

$$f(x) = \begin{cases} x, & for\ \ x \geq 0 \\ \sigma * x, & for\ \ x < 0 \end{cases}$$

*Softmax function:* It gives the probability of each true class and is expressed as (Kanai et al., 2018):

$$f(x_j) = \frac{e^{x_j}}{\sum_{k=1}^{k} e^{x_k}}$$

Many other activation functions have been developed which are mainly derived from the above activation functions such as Gaussian Error Linear Unit (*gelu*) (Hendrycks and Gimpel, 2016), a multi-layer perceptron model with a *sigmoid, tanh, conic section, and radial bases function (RBF)*, etc. (Karlik and Olgac, 2011; Cai et al., 2015).

## 2.2 Proposed Gaussian error linear unit with sigmoid activation function (SIELU) activation function

It may be noted that the *Tanh* activation is used in the Cumulative Distribution Function of GELU. Also, *Tanh* activation function is reported to perform better than sigmoid (Szandała, 2021; Ingole and Patil 2020; Jiang et al., 2020) but takes more time. However, in the prediction of high-dimension datasets, computational time is one of the crucial factors. It has been pointed out that the sigmoid function requires less time and is computationally inexpensive by approximating its polynomial for positive outputs (Wang et al., 2020). Further, the sigmoid function is computationally easy to perform. Therefore, a thorough investigation was done to derive a novel activation function *i.e.*, *SIELU* from the *GELU* function.

An approximation of normal distribution (q) was carried out in 1955 for the first time by (Hastings, 1955; Brophy, 1985) which was expressed as:

$$q = \frac{1}{\sqrt{2\pi}} \int_{-\infty}^{\infty} e^{-\frac{1}{2}t^2}\, \partial\, t; 0 \leq q \leq 0.5$$

Hence $X^*(q) = \eta - \{\frac{\alpha_0 + \alpha_1 \eta}{1 + b_1 \eta + b_2 \eta^2}\};\ \eta = \sqrt{ln\frac{1}{q^2}};$

where , $\alpha_0$=2.30753 , $\alpha_1$=0.27061 , $b_1$=0.99229 , $b_2$=0.04481 or $X^*(q) = \eta - \{\frac{\alpha_0 + \alpha_1 \eta + \alpha_2 \eta^2}{1 + b_1 \eta + b_2 \eta^2 + b_3 \eta^3}\}$,

were, $q \rightarrow$ *normal distribution* , $t \rightarrow$ *time*, $\alpha_0$=2.515517 , $\alpha_1$=0.802853 , $\alpha_1$=0.010328 , $b_1$=1.432788 , $b_2$=0.189269 , $b_2$=0.001308 (Hastings., 1955).

With the advancement of technology, a more accurate approximation was introduced by estimating the standard normal deviated distribution $z$ by (Zelen and Severo, 1964) followed by Emerson, 1979.

$$z = t - \left\{\frac{C_0 + C_1 t + C_2 t^2}{1 + d_1 t + d_2 t^2 + d_3 t^3}\right\} + e(p)$$

where, $t = \sqrt{ln\frac{1}{p^2}}$ and $|e(p)|<4{,}5\times10^{-4}$ , $C_0$=2.515517 , $C_1$=0.802853 , $C_2$=0.010328 , $d_1$=1.43288 , $d_2$=0.189269 , $d_3$=0.001308 .

Later, in 2008, standard normal deviated distribution to approximate the function was given by Kiani and co-workers (Kiani et al., 2008) as follows:

$\Phi(x) = \frac{1}{2}\{1 - erf(\frac{-z}{\sqrt{2}})\};\ -\infty<z<\infty$ where $erf(z) = \int_0^z \frac{2}{\sqrt{\pi}} e^{-t^2}\, \partial\, t;\ -\infty<z<\infty$ .

Moreover, the approximation of $\Phi(x)-0.5$ with absolute error< $3\times10^{-5}$ (Bagby, 1995) is estimated from:

$$\Phi(x) - 0.5 \approx 0.5\left(1 - \frac{1}{30}\right)\left[7 \times \exp\left(\frac{-z^2}{2}\right) + 16 \times exp\left\{-z^2\left(2 - \sqrt{2}\right)\right\} + \left(7 + \frac{\pi z^2}{4}\right) \times exp\left(-z^2\right)\right]^{0.5}$$

Our proposed Gaussian Error Linear Unit with Sigmoid (*SiELU*) was constructed by modifying the GELU function as follows:

$$\text{GELU}: f(x) = 0.5x\left[1 + tanh\left\{\sqrt{\frac{2}{\pi}} \times \left(x + 0.044715x^3\right)\right\}\right] \quad (1)$$

Let $tanh\{\sqrt{\frac{2}{\pi}} \times (x + 0.044715x^3)\} = \tanh(y)$ where, $y = \sqrt{\frac{2}{\pi}} \times (x + 0.044715x^3)$

On simplification of the equation (1):

$$f(x) = 0.5x[1 + tanhy]$$

Tanh and Sigmoid functions are mathematically defined as:

$$Tanh(x) = \frac{e^x - e^{-x}}{e^x + e^{-x}} \quad (2)$$

$$Sigmoid(x) = \frac{1}{1 + e^{-x}} \quad (3)$$

On further simplification of the equation (2),

$$Tanh(x) = \frac{e^x - e^{-x} + e^{-x} - e^{-x}}{e^x + e^{-x}} = 1 - \frac{2e^{-x}}{e^x + e^{-x}} \quad (4)$$

By dividing numerator and denominator by $e^{-x}$, equation (4) is changes to:

$$Tanh(x) = \frac{e^x - e^{-x} + e^{-x} - e^{-x}}{e^x + e^{-x}} = 1 - \frac{2}{e^{2x} + 1} = 1 - 2 \times Sigmoid(-2x) \quad (5)$$

From equation (1) , $f(x)=0.5x[1+tanhy]$ Now, equating sigmoid with *tanh* function and simplifying, we get:

$$sigmoid(y) = \frac{\tanh\left(\frac{y}{2}\right) + 1}{2} - 1$$

$$2 \times sigmoid(2y) - 1 = \tanh(y)$$

Finally, the *SiELU* can be expressed as:

$$SiELUf(x) = 0.5x\left[1 + 2 \times sigmoid\left\{2 \times \sqrt{\frac{2}{\pi}}\left(x + 0.044715x^3\right) - 1\right\}\right]$$

On simplification, we got the Gaussian Error Linear Unit with Sigmoid activation function, termed *SIELU* as follows:

$$\boldsymbol{SiELUf(x)} = 0.5x\left[2 \times sigmoid\left\{2 \times \sqrt{\frac{2}{\pi}}\left(x + 0.044715x^3\right)\right\}\right]$$

## 2.3 Deep learning model with proposed activation function

### 2.3.1 Data collection and pre-processing:

Abiotic stress responsive protein sequence data, *namely*, "salt stress", "drought stress", "heat stress" and "cold stress" of the *Poaceae* family were retrieved using Boolean operator from the public domain (Uniprot database: https://www.uniprot.org/). Also, the negative dataset of the corresponding stress conditions has been downloaded with the NOT operator. A total of 46 features were extracted from each of these sequences using the bio-python package, (Cock et al., 2009) (Table 1). All the redundant sequences were removed with a similarity of 80% or more using the CD-Hit suite (Huang et al., 2010). For pre-processing the dataset, StandardScaler was used to transform these datasets into Standard Normal Distribution (SND) of the data having zero mean and unit variance, which reduces the biases of the models (Ahsan et al., 2021; Karlaš et al., 2022; Cha and Bae, 2022).

This data pertains to various features that were scaled down and standardized as follows to achieve consistency in the varying range of datasets:

$$Scaling(\hat{x}) = \frac{x - \min(x)}{\max(x) - \min(x)}$$

$$\text{Standardization}(Z) = \frac{x - \mu}{\sigma};\ \mu = 0;\ \sigma^2 = 1$$

where, $Z$ is standard normalization with $x$ variables, $\mu$ mean, and $\sigma^2$ variance (Tauber and Sánchez, 2002).

For different layers and epochs, first, stratified sampling was performed, followed by random selection of the training dataset using python script, sklearn library. Different combinations of training:test sets, like, 70:30, 80:20, and 90:10 were made, and finally we proceeded with 80:20 based on the accuracy parameter (Gholamy et al., 2018; Akarsh et al., 2019; Pham et al., 2020; Nguyen et al., 2021; Gu et al., 2022). From this training data, actual training data and drop-out prediction data were retained at 80:20. Fine tuning of weight initializer, layers, epochs, and activation function was carried out in the model to assess the model performance in each epoch. For the given datasets of four stresses, different machine learning algorithms such as SVM, RF, LSTM models were applied using GeLU. For SVM models, polynomial kernel function, 0.01 coeff, and 5-fold StratifiedKFold were used in SVM models for maximum efficiency. In the case of Random Forest, we used a minimum of 0.1 leaf weight with 5-fold StratifiedKFold. For the deep learning model, 150 units, *He* normal kernel initializers, *gelu* activation function, and the proposed activation function *i.e.*, *sielu* were used for comparative analysis in input layers. In the case of the hidden layer, 50 units, 0.02 dropout, and sigmoid activation with 1 unit for binary classification (in the output layer) were employed. During the model compilation, an Adam optimizer and mean square error loss function were used with 500 epochs. The schematic diagram of the methodology is represented in Figure 1.

TABLE 1 Set of features under study.

| Sl. No. | Features | Sl. No. | Features |
|---|---|---|---|
| 1 | Composition of Alanine (A) | 24 | C- *Nitrosylation (Nito C)* |
| 2 | Composition of Arginine (R) | 25 | Total N*itrosylation (Total Nitro)* |
| 3 | Composition of Asparagine (N) | 26 | A- *Nitrotyrosine (YNO A)* |
| 4 | Composition of Aspartate (D) | 27 | B- *Nitrotyrosine (YNO B)* |
| 5 | Composition of Cysteine (C) | 28 | C- *Nitrotyrosine (YNO C)* |
| 6 | Composition of Glutamine (Q) | 29 | Total *Nitrotyrosine* (YNO Total) |
| 7 | Composition of Glutamate (E) | 30 | SUMOylation I (SUMO I) |
| 8 | Composition of Glycine (G) | 31 | SUMOylation II (SUMO II) |
| 9 | Composition of Histidine (H) | 32 | SUMOylation III (SUMO III) |
| 10 | Composition of Isoleucine (I) | 33 | Total SUMOylation (SUMO Total) |
| 11 | Composition of Leucine (L) | 34 | Amino acid number |
| 12 | Composition of Lysine (K) | 35 | Number of negative amino acids |
| 13 | Composition of Methionine (M) | 36 | Number of positive amino acids |
| 14 | Composition of Phenylalanine (F) | 37 | Molecular weight |
| 15 | Composition of Proline (P) | 38 | Theoretical PI |
| 16 | Composition of Threonine (T) | 39 | Number of carbon atoms |
| 17 | Composition of Serine (S) | 40 | Number of hydrogen atoms |
| 18 | Composition of Tryptophan (W) | 41 | Number of nitrogen atoms |
| 19 | Composition of Tyrosine (Y) | 42 | Number of oxygen atoms |
| 20 | Composition of Valine (V) | 43 | Number of sulphur atoms |
| 21 | Coiled-coil domain (CCD) | 44 | Instability index |
| 22 | A- *Nitrosylation (Nito A)* | 45 | Aliphatic index |
| 23 | B- *Nitrosylation (Nito B)* | 46 | Grand average hydropathy (GRAVY) |

## 2.4 Model evaluation indicators

For model evaluation, measures such as accuracy, precision, recall, F1 Score, specificity, and MCC were applied. These parameters were calculated for all four abiotic stresses for SVM, RF, LSTM with GeLU, and LSTM with SieLU activation functions. These are expressed as follows:

$$Sensitivity = \left(\frac{TP}{TP + FN}\right) \times 100$$

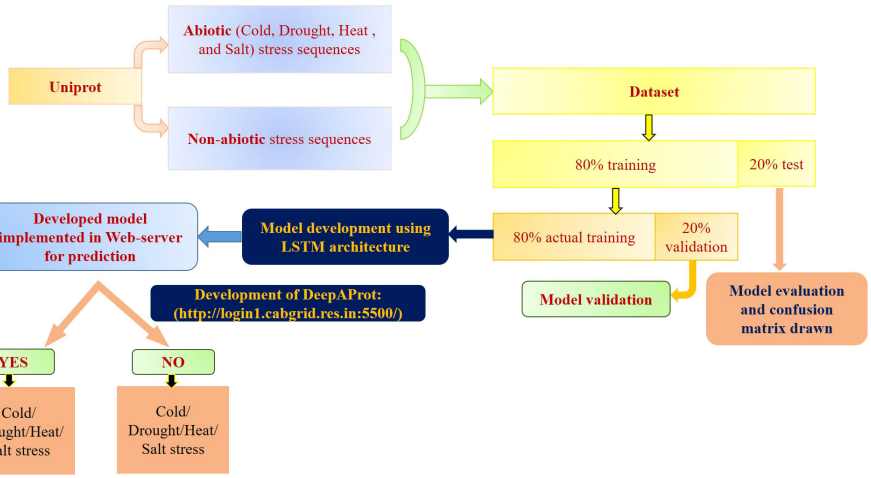


FIGURE 1
Schematic workflow for model implementation in the development of DeepAProt.

$$Precision = \left(\frac{TP}{TP + FP}\right) \times 100$$

$$F_1 = 2 \times \left(\frac{Precision \times Recall}{Precision + Recall}\right)$$

$$Recall = \left(\frac{TP}{TP + FN}\right)$$

$$Accuracy = \left(\frac{TP + TN}{TP + TN + FP + FN}\right) \times 100$$

$$MCC = \left(\frac{TP \times TN - FP \times FN}{\sqrt{(TP + FP)(TP + FN)(TN + FP)(TN + FN)}}\right) \times 100$$

where, TP = True Positive, TN = True Negative, FP = False Positive, FN = False Negative.

## 3 Results and discussion

A thorough screening of "salt stress", "drought stress", "heat stress" and "cold stress" associated protein sequences from the Poaceae family retrieved from the public domain resulted in a total of 739 positive and 1305 negative protein sequences of cold stress, 642 positive and 1284 negative protein sequences of drought stress, 977 positive and 1305 negative protein sequences of drought stress, and 473 positive and 946 negative protein sequences of salt stress. For these datasets, 46 protein sequence features were extracted (Table 1) using the bio-python package. These features were scaled down and standardized. The scaling method was used followed by the transformation of feature information into 0 to 1 to reduce the dominance of one feature over others (Beljkas et al., 2020).

The DL models were built using Sigmoid, Tanh, ReLU, LeakyReLU, SoftMax using the above data set and their performance was evaluated with respect model using the proposed SIELU activation function. Also, models were built based on these stress-associated datasets with different machine learning algorithms, namely, SVM, RF, and DL with GeLU activation function were also evaluated with the model using the proposed SEILU activation function. Off course, the proposed SIELU activation function was used in LSTM along with other fine-tuning hyper-parameters for the model development of four different abiotic stress protein sequence datasets of the Poaceae family. All these developed models were subjected to five-fold cross-validation.

The performance of these models was recorded from the test dataset in the form of a confusion matrix for calculating the various evaluation measures, *namely*, accuracy, precision, recall, F1 Score, specificity, and MCC. The following points emerged from this analysis:

It was observed that, for the cold stress dataset, accuracy and MCC were highest for LSTM with the proposed activation function, SieLU, i.e., 95.11% and 0.90, respectively for testing and 99.20% and 0.98 for the training dataset. LSTM with GeLU activation function gave an accuracy of 94.62% and MCC of 0.89 for the testing dataset and 100% accuracy and MCC of 0.89 in the training dataset. The performance of RF was lowest, i.e., 87.53% accuracy and 0.74 MCC for the testing dataset, accuracy of 88.43% and MCC of 0.75 for the training dataset (Table 2).

For the drought-responsive protein sequences, the performance of LSTM with SieLU activation function was best with accuracy and MCC as 80.78% and 0.58, respectively for the testing dataset and 97.79% accuracy and MCC 0.95 for the training dataset. This was followed by LSTM with GeLU activation function (Accuracy 78.18%, MCC 0.53 for testing dataset and Accuracy of 100% and MCC 0.53 for training dataset), SVM (Accuracy 75.06%, MCC 0.45 for testing and Accuracy 85.39% and MCC 0.67 for training dataset) and RF (Accuracy 67.53, MCC 0.26 for testing dataset and Accuracy 72.03% and MCC 0.30 for training dataset).

In the case of heat stress also, we found LSTM with a novel activation function, SieLU to perform best with 94.97% accuracy and 0.90 MCC for the testing dataset while an Accuracy of 99.12% and MCC 0.98 for the training dataset. The accuracies for LSTM (GeLU), SVM, and RF were 94.97%, 93.65%, and 87.31%, and 87.96% respectively for the testing dataset whereas for the training dataset, it was found as 99.12%, 100%, 88.71%, and 85.64% respectively, while MCCs were 0.90, 0.87, 0.74, and 0.77 respectively for testing dataset whereas for training it was 0.98, 0.87, 0.77, and 72 respectively. A similar trend was observed in performance for the salt stress dataset also. Accuracy of LSTM (SieLU), LSTM (GeLU), SVM, and RF were 81.69%, 80.63%, 75.35, and 79.93 respectively for the testing dataset, whereas for the training dataset, it was 98.06%, 100%, and 75.49%, and 84.92% respectively. Table 2 delineates the performance of models in detail.

Training accuracy vs. validation accuracy was captured for each epoch in which performance LSTM (SieLU) was found to be superior for all four abiotic stress datasets (Figure 2). For the binary classification of four different abiotic datasets, we used a precision-Recall graph (Supplementary Figure 1) for measurement of the performance of our developed models (Flach and Kull 2015; Boyd et al., 2012). Analogously, the ROC (Receiver Operating Characteristics) curve shows the comparison of the performance of the developed ML/DL models for all the abiotic stress datasets (Supplementary Figure 2) (Majnik and Bosnić, 2013). Therefore, it can be concluded that the LSTM model with the proposed *SIELU* activation function outperformed in all datasets as compared to the other competitive models used in this study for classifying protein sequences. Further, these models were also cross-validated with the benchmark heart disease dataset available in

TABLE 2 Comparison of LSTM with *sielu* and *gelu*, SVM, and RF for different abiotic stress-associated protein sequences. The figures in bold denote the evaluation parameters of the best fit model for given stress.

| Samples | Models | Accuracy (%) | | Precision (%) | | Recall (%) | | F1 Score (%) | | Specificity (%) | | MCC | |
|---|---|---|---|---|---|---|---|---|---|---|---|---|---|
| | | Training | Testing | Training | Testing | Training | Testing | Training | Testing | Training | Testing | Training | Testing |
| **Cold** | ***LSTM (sielu)*** | **99.2** | **95.11** | **98.97** | **92.95** | **98.8** | **94.16** | **98.88** | **93.55** | **99.43** | **95.69** | **0.98** | **0.9** |
| | LSTM (*gelu*) | 100 | 94.62 | 100 | 93.42 | 100 | 92.21 | 100 | 92.45 | 100 | 96.08 | 0.89 | 0.89 |
| | SVM | 97.25 | 94.38 | 100 | 96.45 | 92.29 | 88.31 | 95.99 | 92.2 | 100 | 98.04 | 0.94 | 0.88 |
| | RF | 88.43 | 87.53 | 97.14 | 96.4 | 69.69 | 69.48 | 81.15 | 80.75 | 98.86 | 98.43 | 0.75 | 0.74 |
| **Drought** | **LSTM (*sielu*)** | **97.79** | **80.78** | **97.11** | **79.31** | **95.92** | **64.79** | **96.5** | **71.32** | **98.67** | **90.12** | **0.95** | **0.58** |
| | LSTM (*gelu*) | 100 | 78.18 | 100 | 71.32 | 100 | 68.31 | 100 | 69.78 | 100 | 83.95 | 0.53 | 0.53 |
| | SVM | 85.39 | 75.06 | 96.6 | 82.86 | 56.91 | 40.85 | 71.62 | 54.71 | 99.04 | 95.06 | 0.67 | 0.45 |
| | RF | 72.08 | 67.53 | 88.76 | 84 | 15.83 | 14.79 | 26.87 | 25.14 | 99.04 | 98.35 | 0.3 | 0.26 |
| **Heat** | **LSTM (*sielu*)** | **99.12** | **94.97** | **99.1** | **95.31** | **98.85** | **92.89** | **98.97** | **94.09** | **99.33** | **96.54** | **0.98** | **0.9** |
| | LSTM (*gelu*) | 100 | 93.65 | 100 | 92.42 | 100 | 92.89 | 100 | 92.66 | 100 | 94.23 | 0.87 | 0.87 |
| | SVM | 88.71 | 87.31 | 89.3 | 87.17 | 83.57 | 82.74 | 86.33 | 84.89 | 92.54 | 90.77 | 0.77 | 0.74 |
| | RF | 85.64 | 87.96 | 95.59 | 97.97 | 69.58 | 73.6 | 80.53 | 84.05 | 97.61 | 98.85 | 0.72 | 0.77 |
| **Salt** | **LSTM (*sielu*)** | **98.06** | **81.69** | **97.28** | **72.63** | **96.76** | **72.63** | **97.01** | **72.63** | **98.69** | **86.24** | **0.96** | **0.59** |
| | LSTM (gelu) | 100 | 80.63 | 100 | 73.81 | 100 | 65.26 | 100 | 69.27 | 100 | 88.36 | 0.55 | 0.55 |
| | SVM | 75.49 | 75.35 | 63.56 | 62.63 | 61.54 | 65.26 | 62.53 | 63.91 | 82.43 | 80.42 | 0.44 | 0.45 |
| | RF | 84.92 | 79.93 | 94.4 | 88 | 58.09 | 46.32 | 71.92 | 60.68 | 98.28 | 96.83 | 0.66 | 0.53 |



10.3389/fpls.2022.1008756

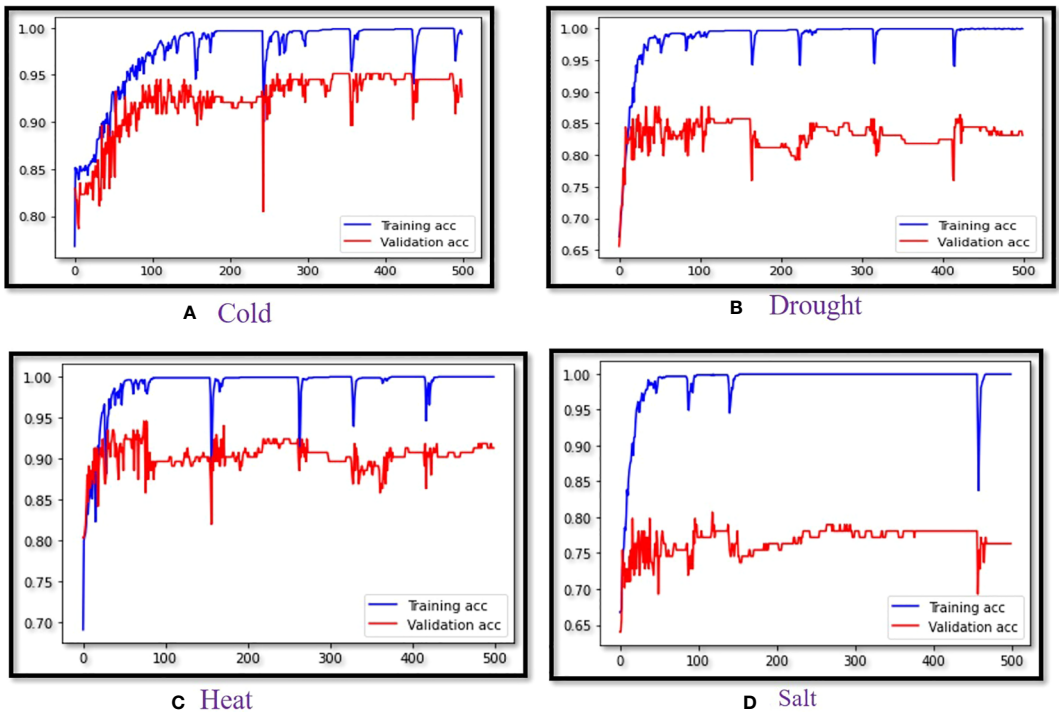


FIGURE 2
Validation curve of LSTM (SiELU) for (A) Cold stress , (B) Drought stress, (C) Heat stress and (D) Salt stress.

the UCI machine learning repository which consists of 303 samples with the 13 most significant features (Otoom et al., 2015). The results showed LSTM (SiELU) to have the highest accuracy (94.74%) and MCC (0.89) as compared to other machine learning models, namely, LSTM (GELU), SVM and RF which showed MCC of 0.86, 0.57 and 0.53, respectively.

## 3.1 DeepAProt: Web implementation

A web-based tool, named as *DeepAProt*, was developed using the Application Programming Interface (API) flask for the deployment of these DL models. In this web server, the best model for each of the stress-responsive datasets was implemented at the backend to develop a web server for the prediction of related stress-responsive proteins. The architecture of a web-based tool followed the standard three-tier architecture, *namely*, presentation, web-API, and application layer. The presentation layer is the user interface of the tool which was implemented using HTML and CSS languages. In web-API, a REST API was developed for deploying the model in the server. This layer was implemented using the Python programming language. Finally, the application layer contains the models for the end users, making it more user-friendly for easy use and access. For its application at remote locations, a mobile app "DeepAProt app" was also developed. "DeepAProt app" is developed using Java and XML as a front-end mobile app using android studio. For the interface of the web tool, the Python Flask framework has been used. The Back-end web tool is developed on a python framework using a deep learning module *i.e.*, TensorFlow. This app has the provision to upload protein sequence data in *fasta* format for analysis and the result will be presented in a tabular form regarding the given protein sequences association with abiotic stresses such as cold, drought, heat, and salt. In this app, a provision was also made to download and help document and sample data. It makes use of HTML (Peroni et al., 2017), javascript (Delcev and Draskovic, 2018), and CSS (Genevès et al., 2012) at the back-end and front-end to classify any protein sequence (in *fasta* format) that has to be upload as input by biologists.

The user can select either of the abiotic stresses, (i.e., heat/cold/salt/drought) followed by uploading the sequence. Once the raw protein sequence is uploaded in *fasta* format, the output classifies the sequences to the predicted category. This web server is user-friendly and freely accessible at http://login1.cabgrid.res.in:5500/. Figure 3 shows the interface of this web-implemented server and its usage. This web-based tool helps the biologist to classify the unknown protein sequence to the respective class of abiotic stress. Also, the developed mobile app can be popularized for easy and quick handling of data for

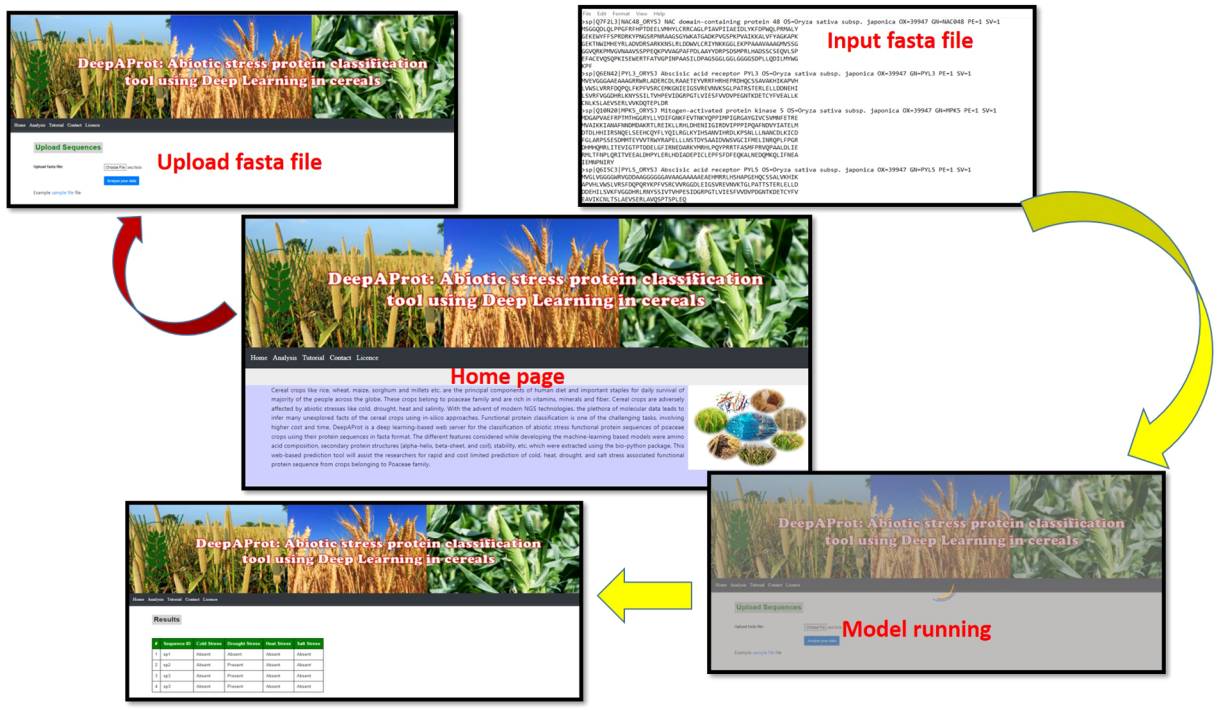


FIGURE 3
Interface for use of DeepAProt.

the identification of stress. It can be downloaded from the Homepage.

As classification and prediction of proper abiotic stress protein sequences help the biologist to implement it in crop improvement. Machine learning and deep learning models help to find out the abiotic stress protein sequences in a cost and effective manner. However, most biologists do not have enough knowledge about machine learning and deep learning to predict the proper abiotic stress protein sequences. Therefore, our models help them to distinguish between the abiotic stress and non-abiotic stress protein sequence that comes from the sequencing laboratory directly.

## 4 Conclusion

In this study, we proposed a novel activation function name SIELU which was used to build the DL model along with other hyperparameters. The performance of this novel activation function has been studied using public domain data to predict stress-responsive proteins under four abiotic stresses, *namely*, cold, heat, salinity, and drought from the major crops of the Poaceae family. Further, a comparative analysis was carried out between *SVM, RF*, and *LSTM* with *GELU*, and *SIELU* activation functions. It has been observed that LSTM with *SIELU* activation function outperformed as compared to other competitive models used in this study. Hence, LSTM with *SIELU* models was implemented in the form of web servers for the classification of unknown protein sequences into different abiotic stresses of crops from the Poaceae family. This work can be of immense use for plant breeders for *in silico* identification of the stress-responsive proteins in crops of the Poaceae family, leading to the rapid development of abiotic stress-resistant varieties.

**Resource used:** The research was carried out using python programming packages, version 3.7.8. Also, for the graphical user interface (GUI), Anaconda Repository was used for coding these models in a Jupyter notebook with necessary python libraries. All these model buildings have been carried out in HP-Z400-Workstation dual booting system where Linux - Ubuntu version with 16.04 LTS is used with the memory of 99.3 GB. The RAM of the system was 16 BGB with a processor of Intel® Xeon(R) CPU W3565 at 3.20GHz × 4 having NVC1 graphics.

## Data availability statement

The original contributions presented in the study are publicly available. This data can be found here: Python library: PyPi (https://pypi.org/project/sielu/). Web-based application:

http://login1.cabgrid.res.in:5500/ Mobile Application: download from http://login1.cabgrid.res.in:5500/.

## Author contributions

SJ, AR, and DK conceived the theme of the study. BA, MI, SJ, and AR developed the methodology, BA collected the data. BA, MH, SJ, MI, and UA were involved in the computational analysis and development of web resources and mobile applications. SJ, MI, and AR supervised the study. BA wrote the original draft. DK and AR reviewed and edited the manuscript. All authors contributed to the article and approved the submitted version.

## Funding

The authors are thankful to the CABin grant, Indian Council of Agricultural Research, Ministry of Agriculture and Farmers' Welfare, Govt. of India (F. no. Agril. Edn. 4–1/2013-AandP) for providing financial support. The grant of the IARI Merit scholarship to BA is duly acknowledged.

## Acknowledgments

The financial grants, ICAR- CABin and IARI Merit scholarship to BA are duly acknowledged. The authors further acknowledge the supportive role of the Director, ICAR-IASRI, New Delhi.

## Conflict of interest

The authors declare that the research was conducted in the absence of any commercial or financial relationships that could be construed as a potential conflict of interest.

## Publisher's note



## Supplementary material

The Supplementary Material for this article can be found online at: https://www.frontiersin.org/articles/10.3389/fpls.2022.1008756/full#supplementary-material

SUPPLEMENTARY FIGURE 1
Precision-Recall curve of different abiotic stress data.

SUPPLEMENTARY FIGURE 2
Receiver Operating Characteristics curve of different abiotic stress data.

## References

Agarap, A. F. M. (2018). Deep learning using rectified linear units (ReLU). *ArXiv* 1, 2–8.

Ahsan, M., Mahmud, M., Saha, P., Gupta, K., and Siddique, Z. (2021). Effect of data scaling methods on machine learning algorithms and model performance. *Technologies* 9 (3), 52. doi: 10.3390/technologies9030052

Akarsh, S., Poornachandran, P., Menon, V. K., and Soman, K. P. (2019). "A detailed investigation and analysis of deep learning architectures and visualization techniques for malware family identification," in *Advanced sciences and technologies for security applications* (Springer International Publishing). doi: 10.1007/978-3-030-16837-7_12

An, J., Li, W., Li, M., Cui, S., and Yue, H. (2019). Identification and classification of maize drought stress using deep convolutional neural network. *Symmetry* 11, 256. doi: 10.3390/sym11020256

Armenteros, J. J. A., Salvatore, M., Emanuelsson, O., Winther, O., Von Heijne, G., Elofsson, A., et al. (2019). Detecting sequence signals in targeting peptides using deep learning. *Life Sci. Alliance.* 2 (5), 1–14. doi: 10.26508/lsa.201900429

Bagby, R. J. (1995). Calculating normal probabilities. *Am. Math. monthly.* 102, 46–49. doi: 10.1080/00029890.1995.11990532

Beljkas, Z., Knezevic, M., Rutesic, S., and Ivanisevic, N. (2020). Application of artificial intelligence for the estimation of concrete and reinforcement consumption in the construction of integral bridges. *Adv. Civil Eng.* 2020, 1–8. doi: 10.1155/2020/8645031

Benvenuto, N., and Piazza, F. (1992). On the complex back-propagation algorithm. *IEEE Trans. Signal Process.* 40 (4), 967–969. doi: 10.1109/78.127967

Bileschi, M., Belanger, D., Bryant, D., Sanderson, T., Carter, B., DePristo, M., et al. (2022). Using deep learning to annotate the protein universe. *Nat Biotechnol* 40, 932–937. doi: 10.1038/s41587-021-01179-w

Boyd, K., Costa, V. S., Davis, J., and Page, C. D. (2012). "Unachievable region in precision-recall space and its effect on empirical evaluation," in *Proceedings of the 29th International Conference on Machine Learning, ICML 2012*, (Edinburgh, Scotland, UK: The International Conference on Machine Learning (ICML)) Vol. 1639–646.

Boyer, J. S. (1982). Plant Productivity and Environment. Science 218, 443–448.

Brophy, A. L. (1985). Approximation of the inverse normal distribution function. *Behav. Res. Methods Instrum. Comput.* 17 (3), 415–417. doi: 10.3758/bf03200956

Cai, Y., Wang, J., and Deng, L. (2020). SDN2GO : An integrated deep learning model for protein function prediction 8, April, 1–11. doi: 10.3389/fbioe.2020.00391

Cai, C., Xu, Y., Ke, D., and Su, K. (2015). Deep neural networks with multistate activation functions. *Comput. Intell. Neurosci.* 721367, 1–10. doi: 10.1155/2015/721367

Cha, J., and Bae, G. (2022). Deep learning based infant cry analysis utilizing computer vision 17, 1, 30–35.

Chen, J., Xu, W., Velten, J., Xin, Z., and Stout, J. (2012). Characterization of maize inbred lines for drought and heat tolerance. *J. Soil Water Conserv.* 67 (5), 354–364. doi: 10.2489/jswc.67.5.354

Cobb, J. N., DeClerck, G., Greenberg, A., Clark, R., and McCouch, S. (2013). Next-generation phenotyping: requirements and strategies for enhancing our understanding of genotype–phenotype relationships and its relevance to crop

improvement. *Theor. Appl. Genet.* 126 (4), 867–887. doi: 10.1007/s00122-013-2066-0

Cock, P. J. A., Antao, T., Chang, J. T., Chapman, B. A., Cox, C. J., Dalke, A., et al. (2009). Biopython: Freely available python tools for computational molecular biology and bioinformatics. *Bioinformatics* 25 (11), 1422–1423. doi: 10.1093/bioinformatics/btp163

Dao, P. D., He, Y., and Proctor, C. (2021). Plant drought impact detection using ultra-high spatial resolution hyperspectral images and machine learning. *Int. J. Appl. Earth Obs. Geoinformation* 102, 102364. doi: 10.1016/j.jag.2021.102364

Das, B., Manohara, K. K., Mahajan, G. R., and Sahoo, R. N. (2020). Spectroscopy based novel spectral indices, PCA- and PLSR-coupled machine learning models for salinity stress phenotyping of rice. *Spectrochim. Acta Part A Mol. Biomol. Spectrosc.* 229, 117983. doi: 10.1016/j.saa.2019.117983

Delcev, S., and Draskovic, D. (2018). "Modern JavaScript frameworks: A survey study," in *2018 Zooming Innovation in Consumer Technologies Conference (ZINC)*. (Novi Sad, Serbia) 106–109 (IEEE). doi: 10.1109/ZINC.2018.8448444

Ding, W., Nakai, K., and Gong, H. (2022). Protein design *via* deep learning. *Briefings Bioinf.* 23 (3), 1–16. doi: 10.1093/bib/bbac102

Dunn, A. M., Hofmann, O. S., Waters, B., and Witchel, E. (2011). "Cloaking malware with the trusted platform module," in *Proceedings of the 20th USENIX Security Symposium*. (San Francisco, CA: USENIX Security Symposium) 395–410.

Elaraby, N. M., and Elmogy, M. (2016). Deep Learning : Effective tool for big data analytics. *Int. J. Comput. Sci. Eng.* 5 (05), 254–262.

Emerson, P. L. (1979). Computer approximation of the inverse of the normal distribution function. *Behav. Res. Methods Instrum.* 11, 397–398. doi: 10.3758/BF03205685

Erenstein, O., Jaleta, M., Mottaleb, K. A., Sonder, K., Donovan, J., and Braun, H. J. (2022). "Global trends in wheat production, consumption and trade," in *Wheat improvement*. Eds. M. P. Reynolds and H. J. Braun (Springer, Cham). doi: 10.1007/978-3-030-90673-3_4

Etminan, A., Pour-Aboughadareh, A., Mohammadi, R., Shooshtari, L., Yousefiazarkhanian, M., and Moradkhani, H. (2019). Determining the best drought tolerance indices using artificial neural network (ANN): Insight into application of intelligent agriculture in agronomy and plant breeding. *Cereal Res. Commun.* 47 (1), 170–181. doi: 10.1556/0806.46.2018.057

Fenu, G., and Malloci, F. M. (2021). Review forecasting plant and crop disease: An explorative study on current algorithms. *Big Data Cogn. Computing* 5 (1), 1–24. doi: 10.3390/bdcc5010002

Flach, P. A., and Kull, M. (2015). Precision-Recall-Gain curves: PR analysis done right. *Adv. Neural Inf. Process. Syst.*, 1838–846.

Gelman, S., Fahlberg, S. A., Heinzelman, P., Romero, P. A., and Gitter, A. (2021). Neural networks to learn protein sequence-function relationships from deep mutational scanning data. *Proc. Natl. Acad. Sci. United States America* 118 (48), e2104878118. doi: 10.1073/pnas.2104878118

Genevès, P., Layaïda, N., and Quint, V. (2012). "On the analysis of cascading style sheets," in *WWW'12 - Proceedings of the 21st Annual Conference on World Wide Web*, (New York, United States: Springer Link) 809–818.

Gholamy, A., Kreinovich, V., and Kosheleva, O. (2018). Why 70/30 or 80/20 relation between training and testing Sets : A pedagogical explanation. *Departmental Tech. Rep. (CS)* 1209, 1–6.

Ghosal, S., Blystone, D., Singh, A. K., Ganapathysubramanian, B., Singh, A., and Sarkar, S. (2018). An explainable deep machine vision framework for plant stress phenotyping. *Proc Natl Acad Sci U S A* 115 (18), 4613–4618. doi: 10.1073/pnas.1716999115

Gill, M., Anderson, R., Hu, H., Bennamoun, M., Petereit, J., Valliyodan, B., et al. (2022). Machine learning models outperform deep learning models, provide interpretation and facilitate feature selection for soybean trait prediction. *BMC Plant Biol.* 22, 180. doi: 10.1186/s12870-022-03559-z

Gupta, C., Ramegowda, V., Basu, S., and Pereira, A. (2021). Using network-based machine learning to predict transcription factors involved in drought resistance. *Front. Genet.* 943. doi: 10.3389/fgene.2021.652189

Gu, Z., Sharma, S., Riley, D., Pantawane, M., Joshi, S., Fu, S., et al. (2022). A universal predictor-based machine learning model for optimal process maps in laser powder bed fusion process. *J. Intell. Manuf.*, 1–23. doi: 10.1007/s10845-022-02004-0

Hasan, M. M., Basith, S., Khatun, M. S., Lee, G., Manavalan, B., and Kurata, H. (2021). Meta-i6mA: Deepm5C N6-methyladenine sites of plant genomes by exploiting informative features in an integrative machine-learning framework. *Briefings Bioinf.* 22 (3), bbaa202. doi: 10.1093/bib/bbaa202

Hasan, M. M., Tsukiyama, S., Cho, J. Y., Kurata, H., Alam, M. A., Liu, X., et al. (2022). Deepm5C: A deep-learning-based hybrid framework for identifying human RNA N5-methylcytosine sites using a stacking strategy. *Mol. Ther.* 30 (8), 2856–2867. doi: 10.1016/j.ymthe.2022.05.001

Hastings, C. J. (1955). *Approximations for digital computers* (Princeton, NJ: Princeton University Press). Available at: https://books.google.co.in/books?hl=enandlr=andid=IRTWCgAAQBAJandoi=fndandpg=PP1andots=UKUd8hGL3Landsig=-cTtzuSYIcORnRC1Co6f1vkMesandredir_esc=y#v=onepageandqandf=false.

Hendrycks, D., and Gimpel, K. (2016). Gaussian Error linear units (gelus). *arXiv*, 1–9.

Huang, Y., Niu, B., Gao, Y., Fu, L., and Li, W.. (2010). CD-HIT suite: A web server for clustering and comparing biological sequences. *Bioinformatics* 26, 680–682. doi: 10.1093/bioinformatics/btq003

Ingole, K., and Patil, N. (2020). Performance analysis of various activation function on a shallow neural network. *Int. J. Emerging Technol. Innovative Res.* 7 (6), 269–276. doi: 10.1729/Journal.24670

Jansen, M. A., and Potters, G. (2017). "Plant stress physiology," in *Stress: The way of life*, *2nd ed* (London, UK: CABI), ix–xiv.

Jiang, X., Zhu, Z., and Chen, L. (2020). An intelligent deep feature learning method with improved activation functions for machine fault diagnosis. *IEEE Access.* 8, 1975–1985. doi: 10.1109/ACCESS.2019.2962734

Kanai, S., Fujiwara, Y., Yamanaka, Y., and Adachi, S. (2018). "Sigsoftmax: Reanalysis of the softmax bottleneck," in *NIPS'18: Proceedings of the 32nd International Conference on Neural Information Processing Systems*. (CA, USA: Neural Information Processing Systems Foundation, Inc. (NeurIPS)) 284–294. doi: 10.5555/3326943.3326970

Kang, D., Ahn, H., Lee, S., Lee, C. J., Hur, J., Jung, W., et al. (2018). "Identifying stress-related genes and predicting stress types in arabidopsis using logical correlation layer and CMCL loss through time-series data," in *Proceedings - 2018 IEEE International Conference on Bioinformatics and Biomedicine, BIBM 2018*, (Madrid, Spain: Institute of Electrical and Electronics Engineers (IEEE)) December 2018. 399–404. doi: 10.1109/BIBM.2018.8621581

Karlaš, B., Dao, D., Interlandi, M., Li, B., Schelter, S., Wu, W., et al. (2022). Data debugging with shapley importance over end-to-End machine learning pipelines. arXiv:2204.11131 [cs.LG], 1–43.

Karlik, B., and Olgac, A. V. (2011). Performance analysis of various activation functions in generalized MLP architectures of neural networks. *Int. J. Artif. Intell. Expert Syst.* 1 (4), 111–122.

Khaki, S., Khalilzadeh, Z., and Wang, L. (2019). Classification of crop tolerance to heat and drought–a deep convolutional neural networks approach. *Agronomy* 9 (12), 833. doi: 10.3390/agronomy9120833

Kiani, M., Panaretos, J., Psarakis, S., and Saleem, M. (2008). Approximations to the normal distribution function and an extended table for the mean range of the normal variables. *J. Iranian Stat. Soc. (Jirss)* 7 (12), 57–72.

Landi, S., Hausman, J. F., Guerriero, G., and Esposito, S. (2017). Poaceae vs. abiotic stress: focus on drought and salt stress, recent insights and perspectives. *Front. Plant science.* 8, 1214.

LeCun, Y. A., Bottou, L., Orr, G. B., and Müller, K. R. (2012). "Efficient backprop," in *Neural networks:Tricks of the trade, lecture notes in computer science*, vol. 7700 . Eds. G. Montavon, G. B. Orr and K. R. Müller (Berlin, Heidelberg: Springer), 375–405. doi: 10.1007/978-3-642-35289-8_3

Li, Y., Wang, S., Umarov, R., Xie, B., Fan, M., Li, L., et al. (2018). DEEPre: Sequence-based enzyme EC number prediction by deep learning. *Bioinformatics* 34 (5), 760–769. doi: 10.1093/bioinformatics/btx680

Lobell, D. B., Schlenker, W., and Costa-Roberts, J. (2011). Climate trends and global crop production since 1980. *Science* 333, 616–620. doi: 10.1126/science.1204531

Majnik, M., and Bosnić, Z. (2013). ROC analysis of classifiers in machine learning: A survey. *Intell. Data Anal.* 17 (3), 531–558. doi: 10.3233/IDA-130592

Moghimi, A., Yang, C., and Marchetto, P. M. (2018). Ensemble feature selection for plant phenotyping: A journey from hyperspectral to multispectral imaging. *IEEE Access* 6, 56870–56884. doi: 10.1109/ACCESS.2018.2872801

Nguyen, Q. H., Ly, H. B., Ho, L. S., Al-Ansari, N., Van Le, H., Tran, V. Q., et al. (2021). Influence of data splitting on performance of machine learning models in prediction of shear strength of soil. *Math. Problems Eng.* 2021. doi: 10.1155/2021/4832864

Niu, Y., Han, W., Zhang, H., Zhang, L., and Chen, H. (2021). Estimating fractional vegetation cover of maize under water stress from UAV multispectral imagery using machine learning algorithms. *Comput. Electron. Agric.* 189 (106414). doi: 10.1016/j.compag.2021.106414

Otoom, A. F., Abdallah, E. E., Kilani, Y., Kefaye, A., and Ashour, M. (2015). Effective diagnosis and monitoring of heart disease. *Int. J. software Eng. its Appl.* 9 (1), 143–156. doi: 10.14257/ijseia.2015.9.1.12

Palanog, A. D., Swamy, B. P. M., Shamsudin, N. A. A., Dixit, S., Hernandez, J. E., Boromeo, T. H., Cruz, P. C. S., et al (2014). Grain yield QTLs with consistent-effect under reproductive-stage drought stress in rice. *Field Crops Res* 161, 46–54.

Peroni, S., Osborne, F., Di Iorio, A., Nuzzolese, A. G., Poggi, F., Vitali,, et al. (2017). Research articles in simplified HTML: a web-first format for HTML-based scholarly articles. *PeerJ Comput. Sci.* 3, e132. doi: 10.7717/peerj-cs.132

Pham, B. T., Qi, C., Ho, L. S., Nguyen-Thoi, T., Al-Ansari, N., Nguyen, M. D., et al. (2020). A novel hybrid soft computing model using random forest and particle swarm optimization for estimation of undrained shear strength of soil. *Sustain. (Switzerland)* 12 (6), 1–16. doi: 10.3390/su12062218

Pratiwi, H., Windarto, A. P., Susliansyah, S., Aria, R. R., Susilowati, S., Rahayu, L. K., et al. (2020). Sigmoid activation function in selecting the best model of artificial neural networks. *J. Physics: Conf. Ser.* 1471 (1), 12010. doi: 10.1088/1742-6596/1471/1/012010

Rico-Chávez, A. K., Franco, J. A., Fernandez-Jaramillo, A. A., Contreras-Medina, L. M., Guevara-González, R. G., and Hernandez-Escobedo, Q. (2022). Machine learning for plant stress modeling: A perspective towards hormesis management. *Plants* 11 (7), 1–22. doi: 10.3390/plants11070970

Salman, S., and Liu, X. (2019). Overfitting mechanism and avoidance in deep neural networks. *arXiv*:1901.06566 [cs.LG].

Sarker, I. H. (2021). Deep learning: A comprehensive overview on techniques, taxonomy, applications and research directions. *SN Comput. Sci.* 2 (6), 1–20. doi: 10.1007/s42979-021-00815-1

Sridevi, S., and Kanimozhi, T. (2021). "Classification of protein sequences using hybrid recurrent deep learning models," in *IEEE International Conference on Technology, Research, and Innovation for Betterment of Society (TRIBES), 2021*. (Raipur, India: Institute of Electrical and Electronics Engineers (IEEE)) 1–4. doi: 10.1109/TRIBES52498.2021.9751666

Srinivasan, K., Cherukuri, A. K., Vincent, D. R., Garg, A., and Chen, B. Y. (2019). An efficient implementation of artificial neural networks with K-fold cross-validation for process optimization. *J. Internet Technol.* 20 (4), 1213–1225. doi: 10.3966/160792642019072004020

Sue Wing, I., De Cian, E., and Mistry, M. N. (2021). Global vulnerability of crop yields to climate change. *J. Environ. Econ. Manage.* 109, 102462. doi: 10.1016/j.jeem.2021.102462

Szandała, T. (2021). Review and comparison of commonly used activation functions for deep neural networks. In: A. Bhoi, P. Mallick, C. M. Liu and V. Balas eds. *Bio-inspired Neurocomputing. Studies in Computational Intelligence* Singapore: Springer, 903. doi: 10.1007/978-981-15-5495-7_11

Tauber, L., and Sánchez, V. (2002). "Introducing the normal distribution in a data analysis course: specific meaning contributed by the use of computers," in *Proceedings of Seventh International Congress for Teaching Statistics, Citeseer*. (Brazil: IEEE) 1–6.

Venal, M. C. A., Fajardo, A. C., and Hernandez, A. A. (2019). "Plant stress classification for smart agriculture utilizing convolutional neural network-support vector machine," in *Proceeding - 2019 International Conference on ICT for Smart Society: Innovation and Transformation Toward Smart Region, ICISS 2019*, (Indonesia: School of Electrical Engineering and Informatics ITB) February 2020. doi: 10.1109/ICISS48059.2019.8969799

Wang, A. (2022). Deep learning methods for protein family classification on PDB sequencing data. ArXiv, abs/1505.00853.

Wang, Y., Li, Y., Song, Y., and Rong, X. (2020). The influence of the activation function in a convolution neural network model of facial expression recognition. *Appl. Sci.* 10 (5). doi: 10.3390/app10051897

Wen, M., Cong, P., Zhang, Z., Lu, H., and Li, T. (2018). DeepMirTar: a deep learning approach for predicting human miRNA targets. *Bioinformatics* 34 (22), 3781–3787. doi: 10.1093/bioinformatics/bty424

Xu, Y., Verma, D., Sheridan, R. P., Liaw, A., Ma, J., Marshall, N. M., et al. (2020). Deep dive into machine learning models for protein engineering. *J. Chem. Inf. Modeling* 60 (6), 2773–2790. doi: 10.1021/acs.jcim.0c00073

Xu, B., Wang, N., Chen, T., and Li, M. (2015). Empirical evaluation of rectified activations in convolutional network. *arXiv*, abs/1505.00853.

Zahid, A., Dashtipour, K., Abbas, H. T., Mabrouk, I.B., Al-Hasan, M., Ren, A., et al. (2022). Machine learning enabled identification and real-time prediction of living plants' stress using terahertz waves. *Defence Technol.* 18 (8), 1330–1339. doi: 10.1016/j.dt.2022.01.003

Zelen, M., and Severo, N. C. (1964). "Probability functions," in *Handbook of mathematical functions with formulas, graphs, and mathematical tables*. Eds. M. Abramowitz and I. A. Stegun (Washington DC: Government Printing Office).

frontiers | Frontiers in Plant Science

TYPE Original Research
PUBLISHED 16 January 2023
DOI 10.3389/fpls.2022.1082513



OPEN ACCESS

EDITED BY
Nabin Bhusal,
Agriculture and Forestry University, Nepal

REVIEWED BY
Anuj Kumar,
Dalhousie University, Canada
Ruilian Jing,
Institute of Crop Sciences (CAAS), China

*CORRESPONDENCE
Hari Krishna
harikrishna.agri@gmail.com
Pradeep Kumar Singh
pksinghiari@gmail.com

SPECIALTY SECTION
This article was submitted to Plant Abiotic Stress, a section of the journal Frontiers in Plant Science

RECEIVED 28 October 2022
ACCEPTED 15 December 2022
PUBLISHED 16 January 2023

CITATION
Devate NB, Krishna H, Mishra CN, Manjunath KK, Sunilkumar VP, Chauhan D, Singh S, Sinha N, Jain N, Singh GP and Singh PK (2023) Genetic dissection of marker trait associations for grain micro-nutrients and thousand grain weight under heat and drought stress conditions in wheat. *Front. Plant Sci.* 13:1082513. doi: 10.3389/fpls.2022.1082513



# Genetic dissection of marker trait associations for grain micro-nutrients and thousand grain weight under heat and drought stress conditions in wheat

Narayana Bhat Devate[1], Hari Krishna[1]*, Chandra Nath Mishra[2], Karthik Kumar Manjunath[1], V. P. Sunilkumar[1], Divya Chauhan[1], Shweta Singh[1], Nivedita Sinha[1], Neelu Jain[1], Gyanendra Pratap Singh[2] and Pradeep Kumar Singh[1]*

[1]Division of Genetics, ICAR-Indian Agricultural research institute, New Delhi, India, [2]ICAR- Indian Institute of Wheat and Barley Research, Karnal, India

**Introduction:** Wheat is grown and consumed worldwide, making it an important staple food crop for both its calorific and nutritional content. In places where wheat is used as a staple food, suboptimal micronutrient content levels, especially of grain iron (Fe) and zinc (Zn), can lead to malnutrition. Grain nutrient content is influenced by abiotic stresses, such as drought and heat stress. The best method for addressing micronutrient deficiencies is the biofortification of food crops. The prerequisites for marker-assisted varietal development are the identification of the genomic region responsible for high grain iron and zinc contents and an understanding of their genetics.

**Methods:** A total of 193 diverse wheat genotypes were evaluated under drought and heat stress conditions across the years at the Indian Agricultural Research Institute (IARI), New Delhi, under timely sown irrigated (IR), restricted irrigated (RI) and late sown (LS) conditions. Grain iron content (GFeC) and grain zinc content (GZnC) were estimated from both the control and treatment groups. Genotyping of all the lines under study was carried out with the single nucleotide polymorphisms (SNPs) from Breeder's 35K Axiom Array.

**Result and Discussion:** Three subgroups were observed in the association panel based on both principal component analysis (PCA) and dendrogram analysis. A large whole-genome linkage disequilibrium (LD) block size of 3.49 Mb was observed. A genome-wide association study identified 16 unique stringent marker trait associations for GFeC, GZnC, and 1000-grain weight (TGW). *In silico* analysis demonstrated the presence of 28 potential candidate genes in the flanking region of 16 linked SNPs, such as

synaptotagmin-like mitochondrial-lipid-binding domain, HAUS augmin-like complex, di-copper center-containing domain, protein kinase, chaperonin Cpn60, zinc finger, NUDIX hydrolase, etc. Expression levels of these genes in vegetative tissues and grain were also found. Utilization of identified markers in marker-assisted breeding may lead to the rapid development of biofortified wheat genotypes to combat malnutrition.

KEYWORDS

**wheat, grain iron, and zinc content, drought and heat stress, GWAS, SNPs**

## Introduction

Wheat (*Triticum aestivum* L.) is one of the most extensively cultivated crops in the world and contributes a major portion of the calories in the global diet. Wheat provides up to 60% of daily energy needs in developing and underdeveloped nations (Wang et al., 2011). Farming of the crop has undergone significant improvements in productivity and production over the past 50 years, under the moniker "green revolution" (Pingali, 2012; Yadav et al., 2019). As a result, we are in a reasonably secure position to satisfy the demand for food. However, a major emphasis was placed on productivity to hasten the food supply rather than giving importance to the wheat's quality. Compared with naturally occurring wheat, our improved cultivars have a lower level of micronutrients in their grains (Gupta et al., 2021), which is referred to as the "dilution effect" (Murphy et al., 2008; Khoshgoftarmanesh et al., 2011; Amiri et al., 2015).

In areas that are severely affected by micronutrient deficiencies, cereals make up the majority of daily dietary intake. The micronutrient content of staple cereals like wheat and rice, especially the amount of iron (Fe) and zinc (Zn), is not at its optimal level, and milling further decreases this concentration (Rathan et al., 2022). Enhancing the nutritional qualities of crop plants is a strategy known as biofortification that can be used to fight micronutrient deficiencies in food (Bouis et al., 2011). Agronomic biofortification is based on optimized fertilizer applications, whereas genetic biofortification is based on traditional plant breeding and/or genetic engineering to improve nutrient concentrations (Cakmak, 2008; Borrill et al., 2014). Out of these two strategies, genetic biofortification has been identified as an effective and affordable technique to enhance food nutrition content in a sustainable long-lasting way to combat mineral nutrition deficiencies (Krishnappa et al., 2022).

Among the most common human micronutrient deficiencies worldwide, iron and zinc deficiencies are important ones (Welch and Graham, 1999). Hemoglobin, a vital substance for the transportation of oxygen and carbon dioxide, preserves the acid–base balance in the blood and contains a significant amount of iron. Iron deficiency results in anemia, which negatively impacts hemoglobin function and impairs the physical and mental development of children, and can cause maternal mortality in undernourished pregnant women. Zinc promotes growth, controls the body's immune response, and participates in the production of numerous enzymes (Liu et al., 2014). Inadequate intake of zinc increases the risk of developing cancer, impaired immune function, defective bone formation, and contagious infection (Brown et al., 2004; Gibson, 2006).

The majority of wheat-growing land is affected by sporadic rains, rising temperatures, and heat waves on a regular basis. Heat and drought stress have an impact on grain-filling time, starch accumulation, and seed size. In addition, during heat and drought stress, the grain sink capacity reduces to a greater extent (Zahra et al., 2021). Food and nutritional security will worsen as a result of rising temperatures brought on by climate change and declining water availability in the majority of spring wheat growing regions (Velu et al., 2016). Grain iron and zinc content are complex characteristics affected by multiple genes, with a complicated genetic inheritance, and is significantly influenced by environmental factors (Krishnappa et al., 2017). Drought and heat stress often change the expression of genes involved in nutrient accumulation and translocation owing to polygenic inheritance and genotype-by-environment interactions.

The direct uptake of minerals from the soil and/or the remobilization of minerals held in vegetative tissues during grain filling are the two main sources of grain mineral supply (Kutman et al., 2012). According to research, the vegetative tissues of wheat plants hold the majority of the reserves of grain micronutrients, with more than 70% of these reserves being remobilized during grain filling (Erenoglu et al., 2011; Cu et al., 2020). Abiotic stress influences the vegetative growth and osmotic regulation of plants, indirectly influencing mineral nutrients in the food grains. Heat and drought stress shortens grain-filling durations, decreases starch accumulation, and leads

to smaller and shriveled seeds. In addition, heat and drought stress reduce grain sink capacity (Zahra et al., 2021). To breed stable nutrient-containing grain varieties under drought and heat stress, a thorough understanding of the genetic regulation of nutritional traits and its relationship with grain yield is necessary (Samineni et al., 2022). Introgression and mobilization of the genes underlying the desired traits into locally adapted cultivars could result in the genetic improvement of grain nutritional state under abiotic stress.

Recent improvements in high-throughput genotyping and phenotyping have boosted the feasibility of discovering the genetic basis of complex traits (Devate et al., 2022a), such as grain nutrient content. This has led to the popularization of whole-genome-marker-based techniques such as Quantitative trait loci (QTL) mapping, genome-wide association studies (GWASs), and genomic selection (Krishnappa et al., 2021; Anilkumar et al., 2022; Harikrishna et al., 2022). Previous research has been conducted to find grain iron- and zinc-associated QTLs in order to identify potential candidate genomic loci (Xu et al., 2012; Crespo-Herrera et al., 2017; Krishnappa et al., 2017; Velu et al., 2017; Wang et al., 2021). However, QTL mapping requires a long time to establish biparental mapping populations when compared with genome-wide association studies (Edae et al., 2014).

The precise modulation of a complex quantitative trait for adaptation to a specific environmental condition, such as drought or heat stress, necessitates the identification of relevant genetic regions, such as QTLs (Puttamadanayaka et al., 2020; Sunil et al., 2020). GWAS is one of the most effective strategies for identifying genes/QTLs based on linkage disequilibrium (LD). The extent of LD across the genome is greater in self-pollinated crops, such as wheat (Roncallo et al., 2021), providing high resolution and power of association. High-density SNP markers, which are employed in GWASs, may screen large gene pools of breeding material. GWASa have been widely utilized in numerous crops to predict candidate genes using genome-wide-dense markers for various complex traits (Sukumaran et al., 2015; Liu et al., 2018; Srivastava et al., 2020; Alseekh et al., 2021; Danakumara et al., 2021; Devate et al., 2022a; Khan et al., 2022; Tiwari et al., 2022). The benefits of GWASs include the ability to identify Marker trait association (MTAs) with high resolution utilizing diverse germplasm, making the method more efficient and less expensive than biparental QTL mapping (Jin et al., 2016). GWAS is one of the best methods to identify robust QTLs that have an effect in both normal and stress environments (Jamil et al., 2019; Ahmed et al., 2021; Saini et al., 2022). As a result, GWASs have evolved into a potent and widely used method for studying complex traits (Tibbs Cortes et al., 2021).

There have been attempts to identify the genomic regions targeting grain nutrient content such as iron and zin using GWASs (Bhatta et al., 2018; Kumar et al., 2018; Velu et al., 2018; Krishnappa et al., 2022; Rathan et al., 2022). However, all of them are conducted under stress-free ideal conditions for wheat growth, with a few exceptions (Devate et al., 2022b). Most of the wheat-growing area is impacted by drought and heat stress, influencing the quality and quantity of wheat production. Hence, in this study, our focus is on the identification of a candidate genomic region for grain iron and zinc content in wheat grown under drought and heat stress.

## Materials and methods

### Plant material and field experimentation

The association panel under investigation included 193 genetically diverse bread wheat genotypes (Supplementary Table 1) consisting of advanced breeding lines, commercial cultivars, elite varieties, germplasm Core-set, and synthetic derivatives. The plant material collections were available at the Division of Genetics, Indian Agricultural Research Institute (IARI), New Delhi. Field experiments were carried out at the field station of the ICAR–Indian Council Agricultural Research Institute, New Delhi (28.6550° N, 77.1888° E, mean sea level 228.61 m) for 2 years, during the rabi seasons of 2020–2021 and 2021–2022. Weather data during the growing season of wheat (November to March) in 2020–2021 and 2021–2022 are included in Supplementary Table 2. In each year genotypes were evaluated under three conditions, that is, irrigated (IR), restricted irrigated (RI), and late sown (LS) to impose stress. Irrigated trials received a total of six irrigations, whereas restricted irrigated trials received only one irrigation (i.e., 21 days after sowing in addition to pre-sowing irrigation) to induce terminal drought stress. Terminal heat stress was introduced by planting the crop (late sown; LS) in the second fortnight of December to expose it to high temperatures during flowering and grain filling, rather than the ideal sowing time, which is the first fortnight of November [followed for the control (IR) and drought (RI) treatments]. The genotypes were evaluated under augmented Augmented -Randomized complete block design (Augmented RCBD) (Federer, 1956; Federer, 1961; Searle, 1965), with 193 genotypes and four checks (HD-3271, HD-3086, HD-3237, and HD-2967) replicated twice in each of the six blocks. Each plot consisted of three 1-m lines sown 25 cm apart. Recommended agronomic practices for the given geographical area were carried out in both years. All four check varieties are popular wheat varieties of the northeastern plain zone where experimentation was conducted. HD 3086 and HD 2967 were recommended varieties for timely sown irrigated conditions, whereas HD 3237 and HD 3271 were recommended varieties for RI and LS conditions, respectively. Furthermore, they are non-

segregating homozygous lines, hence suitable to evaluate as checks. For a better understanding of the methods followed in the study, see the flow chart in Figure 1.

## Phenotyping

In both years, the collection of grain for grain iron content (GFeC) analysis, grain zinc content (GZnC) analysis, and 1000-grain weight (TGW) estimation was carried out by hand picking 20 random spikes from each line into polythene bags. Hand threshing was done to avoid contamination in machines. GFeC and GZnC were estimated using around 20 g of the grain sample from each genotype. A high-throughput energy-dispersive X-ray fluorescence (ED-XRF) spectrometric, bench-top, non-destructive machine (model X-Supreme 8000; Oxford Instruments plc, Abingdon, United Kingdom) (Paltridge et al., 2012), located at ICAR–Indian Institute of Wheat and Barley Research, Karnal, was used for phenotyping. The concentration of grain iron and zinc was measured in mg/kg. The TGW was measured from manual hand sampling of random representative grains from each genotype. The TGW was recorded in grams using an electronic balance.

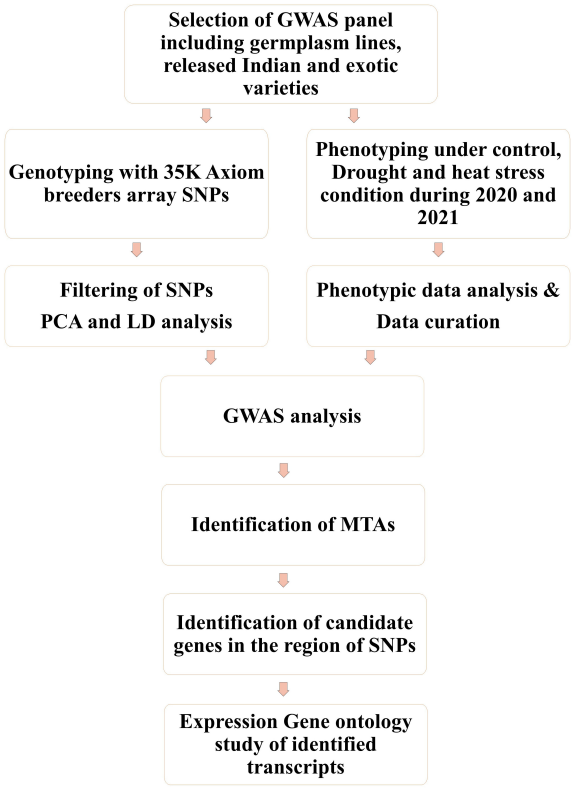


FIGURE 1
Flow chart of the genome-wide association studies (GWASs) conducted.

## Genotyping

Genomic DNA from leaf samples of all 193 genotypes was isolated with the cetyltrimethylammonium bromide (CTAB) extraction method (Murray and Thompson, 1980) followed by a DNA quality check through 0.8% agarose gel electrophoresis. Genotyping was carried out using the Axiom Wheat Breeder's Genotyping Array (Affymetrix, Santa Clara, CA, United States) with 35,143 SNPs following standard protocols. Allele calling was carried out using the Affymetrix proprietary software package Axiom Analysis Suite, following the Axiom® Best Practices genotyping work flow (https://media.affymetrix.com/support/downloads/manuals/axiom_analysis_suite_user_guide.pdf). SNPs were filtered, and monomorphic markers and markers with a minor allele frequency (MAF) of 5%, missing data of more than 10%, and heterozygote frequency greater than 50% were eliminated from the study. The remaining 13,947 SNPs were analyzed further.

## Phenotypic data analysis

Analysis of variance, descriptive statistics (mean, SD, range, CV, coefficient of variation $H^2$, heritability), and adjusted means of phenotypic data were calculated by year and by treatment (2020–2021 or 2021–2022, and IR, RI, or LS) using the R package 'augmentedRCBD' (Aravind et al., 2021). Individual best linear unbiased predictions (BLUP), combined best linear unbiased predictions (BLUP) values of IR, RI, and LS across two seasons (denoted as IR_BLUP, RI_BLUP, LS_BLUP), and overall BLUP (C_BLUP) across the six environments were estimated using ACBD-R software (Rodríguez et al., 2018) with the following model:

$$Yij = \mu + Gen\ j + Envi + Envi \times Genj + Blocki(Envi) + eij.$$

$$Yij = \mu + Blocki + IdCheckj + Genj + Checkj + Envi + Envi \times IdCheckj + Envi \times Genj + Envi \times Checkj + Blocki(Envi) + eij.$$

$IdCheck_j$, $Gen_j$, and $Check_j$ correspond to the effects of the identifier of checks, the unreplicated genotypes, and the checks that are repeated in each block ($Block_i$), respectively. $Env_i$ is the effect of $i$th environment and $Env_i \times Gen_j$, $Env_i \times IdCheck_j$, $Env_i \times Gen_j$, and $Env_i \times Check_j$ are the interaction effects. μ is the mean and e is the error component (as described in ACBD-R User Manual, Rodríguez et al., 2018).

Graphical representations of the phenotypic data with frequency distribution and box plot were generated using "ggplot2" package from R software. SNP distribution by chromosome with an SNP density plot was generated using the web tool SR-Plots (https://www.bioinformatics.com.cn/en). Pearson correlation coefficient values among the traits in each environment were also calculated.

## Diversity, linkage disequilibrium, and association analysis

Diversity in the GWAS panel was identified by marker-based principal component analysis (PCA) and neighbor-joining (NJ) dendrogram analysis using Genome Association and Prediction Integrated Tool (GAPIT) v3 (Lipka et al., 2012) and trait analysis by association, evolution, and linkage (TASSEL v5.0) (Bradbury et al., 2007), respectively, with default parameters. For cluster analysis, the distance matrix was calculated from TASSEL v5.0 and the NJ tree file in Newick format was exported to iTOL version 6.5.2 (https://itol.embl.de/) to draw the dendrogram.

Intrachromosomal linkage disequilibrium (LD) was calculated from the pairwise $r^2$-value, between markers were calculated from TASSEL 5.0, and the LD decay curve was drawn for each A, B, and D genome along with the whole genome. Pairwise $r^2$-values were plotted against the distance in base pairs (BP) to estimate LD block size and the distance at the half-LD decay point was noted (Remington et al., 2001).

A total of 13,947 Filtered SNPs and adjusted means for each environment, BLUPs calculated from the two-season data for IR, RI, and LS (separately and overall), and A total of 13,947 Filtered SNPs and best linear unbiased predictions (BLUPs) across the six environments were used to decipher the associated markers with traits using 'BLINK' (Bayesian-information and linkage-disequilibrium iteratively nested keyway) (Huang et al., 2019) under GAPIT v3 in R. In the model, PCA-based population structure was applied as a fixed effect to eliminate the effect of population structure in the analysis. A Q–Q plot was drawn to determine association model fitting, by plotting the expected vs. observed *-log10(p)* values. Marker trait associations (MTAs) in all six environments for GFeC, GZnC, and TGW were found to have a significant *p*-value of< 0.0001. For stringent selection, a Bonferroni correction was applied ($p$ = 0.05/total number of markers).

## *In silico*, gene ontology and expression analysis

Associated markers identified using GWAS were subjected to a basic local alignment search tool (BLAST) search using the sequence information of the markers. The BLAST search was carried out using the data web service Ensembl Plants (Yates et al., 2022) (https://plants.ensembl.org/Triticum_aestivum/Tools/Blast) against the bread wheat reference genome IWGSC (RefSeq v1.0). Putative candidate transcripts within a 100-kb flanking region of SNPs were identified by region comparison followed by protein produced (or coded) by them using InterPro Classification of protein families (Blum et al., 2021) (https://www.ebi.ac.uk/interpro/). A further gene ontology study of identified genes was carried out to know their biological process, cellular components, and molecular functions from Expression Atlas (Papatheodorou et al., 2020) (https://www.ebi.ac.uk/gxa/home). Expression analysis of putative candidate genes linked to the identified SNPs was carried out in the Wheat Expression Browser by expVIP (Ramírez-González et al., 2018) (http://www.wheat-expression.com/). Expression of genes in high-level tissue, that is, root, shoot/leaves, spike, and grains, was noted down in the transcript per million (TPM). A heat map based on expression data was generated using the 'ggplot2' package in R. Genes with a higher expression level were identified.

# Results

## Phenotypic evaluation

Descriptive statistics were studied for all three traits, i.e., GFeC, GZnC, and TGW, across IR, RI, and LS treatments from both years and are given in Table 1. A frequency distribution histogram demonstrates that all the studied traits were distributed normally in the population (Figure 2). Box plots demonstrated that GFeC and GZnC had a higher mean value under RI (Fe 44.29 mg/kg; Zn 48.09 mg/kg) and LS (Fe 44.79 mg/kg; Zn 53.9 mg/kg) treatment than the control (Fe 33.47 mg/kg; Zn 45.13 mg/kg) in the year 2020, and a similar pattern was observed for LS in 2021. Whereas in 2021, under RI, grain iron content (40.87 mg/kg) was higher than the control, but grain zinc content was observed to be lower (39.24 mg/kg). There was a slight increase in TGW upon drought stress, and a significant decrease under heat stress in both the 2020 and 2021 growing periods, compared with control (Figure 3).

Analysis of variance (given as a MSS "Mean sum of squares" ; Table 1) demonstrated that all the studied traits in all the treatments across the years showed significant variation, except for GFeC under IR in 2021. The coefficient of variation (CV) ranged from 4.89% to 12.64% for GZnC under LS in 2020 and RI in 2021, respectively. For GFeC and TGW the CV ranged from 5.14% to 7.27% and 6.72% to 11.46% respectively. All the studied traits depicted medium-to-high broad sense heritability, with the highest heritability by GZnC under LS in 2020. The range of heritability of GFeC, GZnC, and TGW was 19.42% to 61.43%, 41.57 to 88.89%, and 58.13% to 80.08%, respectively (Table 1).

TABLE 1 Descriptive statistics, analysis of variance (ANOVA) and heritability for GFeC, GZnC, and TGW across the six environments timely sown irrigated (IR), restricted irrigated (RI) and late sown (LS) treatments evaluated in New Delhi during the 2020 and 2021 growing periods.

| Trait | Env | Mean ± SD (range) | MSS | CV | hBS |
|---|---|---|---|---|---|
| Fe | IR_20 | 33.47 ± 2.49 (27.01–40.9) | 6.4 ** | 5.28 | 51.14 |
| | RI_20 | 44.29 ± 3.65 (35.49–54.59) | 14.7 ** | 5.67 | 46.54 |
| | LS_20 | 44.79 ± 3.87 (34.63–57.9) | 11.77 ** | 5.65 | 56.51 |
| | IR_21 | 39.57 ± 3.23 (29.3–49.89) | 10.2 $^{ns}$ | 7.27 | 19.42 |
| | RI_21 | 40.87 ± 3.62 (30.34–53.22) | 10.25 * | 5.14 | 61.43 |
| | LS_21 | 42.41 ± 3.19 (35.96–56.87) | 11.32 ** | 6.10 | 34.88 |
| Zn | IR_20 | 45.13 ± 5.27 (33.13–63.73) | 27.43 ** | 7.8 | 55.87 |
| | RI_20 | 48.09 ± 5.44 (30.64–64.97) | 60.02 ** | 7.11 | 69.59 |
| | LS_20 | 53.9 ± 7.77 (30.86–82.92) | 37.68 ** | 4.89 | 88.89 |
| | IR_21 | 45.01 ± 6.04 (31.91–65.97) | 37.35 ** | 6.94 | 74.39 |
| | RI_21 | 39.24 ± 6.75 (24.98–68.67) | 97.03 ** | 12.64 | 41.57 |
| | LS_21 | 53.82 ± 9.42 (32.64–87.69) | 40.82 * | 9.91 | 71.38 |
| TGW | IR_20 | 40.16 ± 5.18 (24.61–55.11) | 31.19 ** | 7.31 | 72.88 |
| | RI_20 | 41.67 ± 6.03 (25.36–58.11) | 23.5 ** | 6.72 | 79.19 |
| | LS_20 | 35.95 ± 4.82 (19.14–50.02) | 37.12 ** | 7.07 | 72.37 |
| | IR_21 | 34.91 ± 5.95 (20.25–50.53) | 37.06 ** | 7.9 | 80.08 |
| | RI_21 | 36.58 ± 4.7 (26.19–49.99) | 27.38 ** | 7.49 | 66.47 |
| | LS_21 | 29.91 ± 4.88 (19.04–41.28) | 22.09 ** | 11.46 | 58.13 |

* p<0.05; **p< 0.01; ns, non-significant.
Env, environment; SD, Standered deviation; MSS, Mean sum of squares; CV, coefficient of variation; hBS, heritability broad sense.

The Pearson correlation coefficient among the traits in each treatment across the year demonstrated a significant positive correlation between GFeC and GZnC under all environments ($p$<0.001), except under RI in 2020, which showed a non-significant correlation. The correlation of TGW with GFeC and GZnC was non-significant in 2020 under all three treatments. However, in 2021, TGW showed a positive correlation with GFeC under the IR and RI conditions, and a negative correlation with GZnC under IR and LS (Table 2). Correlation among the observations across the three treatments and the years for each trait separately demonstrated all positive correlations with high correlation coefficient values for TGW (Supplementary Figure 1).

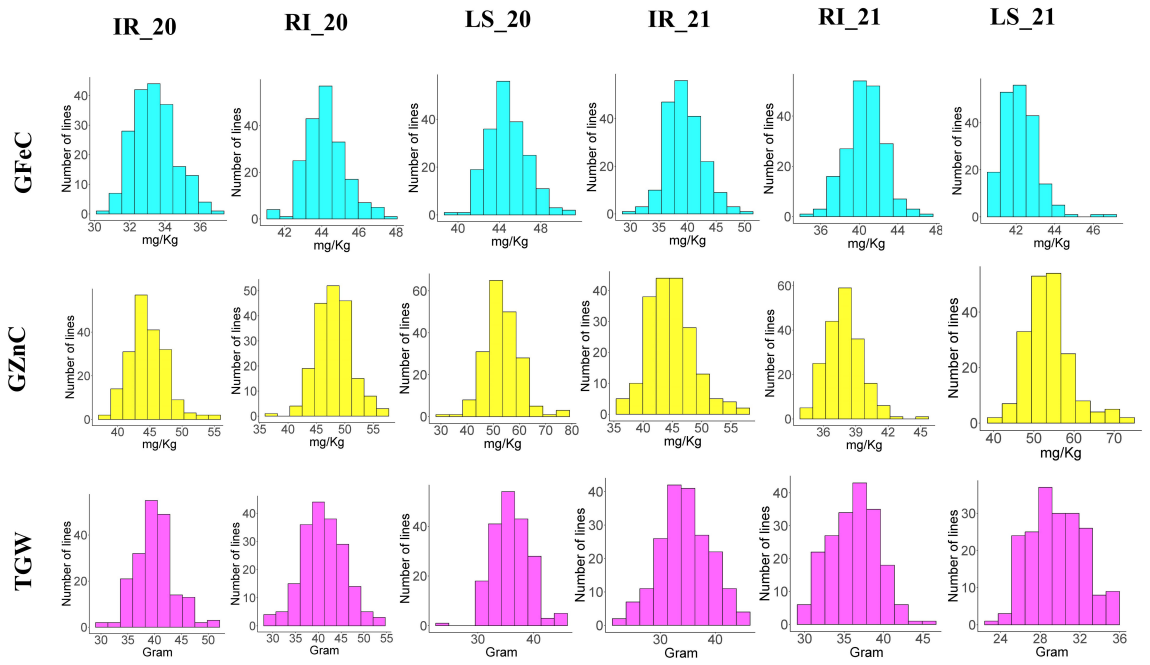


FIGURE 2
Histogram showing the frequency distribution of all the studied traits across the six environments.

## SNP markers distribution, population diversity and linkage disequilibrium

Out of the 35,143 SNPs from the 35K array, a total of 13,947 genome-wide SNPs were retained after filtering for a MAF of<0.05, a heterozygote frequency of<0.5, and missing data<0.1 for quality processing. These SNPs were distributed over the genomes A, B, and D, with 4,307, 5,246, and 4,394 SNPs, respectively. The numbers of SNPs distributed over each chromosome are given in Table 3 and are graphically depicted through an SNP density plot (Figure 4).

Molecular marker-based PCA demonstrated that PC1 and PC2 corresponded to 54.56% and 25.03% of the variation, and the population was grouped into three subgroups (Figure 5). A neighbor-joining dendrogram drawn based on the distance matrix among the genotypes from the GWAS panel inferred three main clusters branching into many clusters in the population (Figure 5). PCA-based population grouping was used as a covariate in association analysis to avoid false associations occurring as a result of the population structure.

Linkage disequilibrium (LD) between the marker pairs was calculated as $r^2$. The LD decay plot was drawn using the $r^2$-value

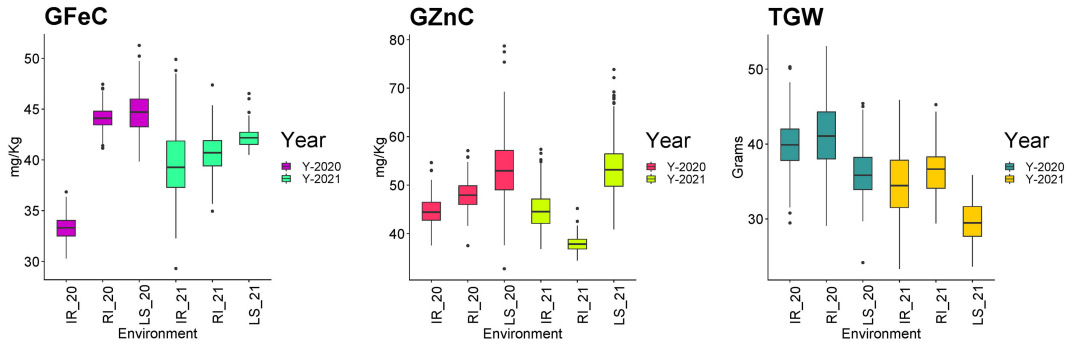


FIGURE 3
Box plot depicting the distribution of grain iron content (GFeC), grain zinc content (GZnC)p, and the 1000-grain weight (TGW) under timely sown irrigated (IR), restricted irrigated (RI) and late sown (LS) conditions across the years 2020–2021 and 2021–2022.

10.3389/fpls.2022.1082513

TABLE 2 Correlation among the traits of grain iron content (GFeC), grain zinc content (GZnC), and 1000-grain weight (TGW) in each environment.

| Treatment | Traits | Season 2020–21 rabi | | | Season 2021–22 rabi | | |
|---|---|---|---|---|---|---|---|
| | | GFeC | GZnC | TGW | GFeC | GZnC | TGW |
| IR | GFeC | 1 | **0.24*** ** | 0.13 | 1 | **0.49*** ** | **0.21** ** |
| | GZnC | | 1 | –0.02 | | 1 | **–0.17*** |
| | TGW | | | 1 | | | 1 |
| RI | GFeC | 1 | 0.07 | 0.08 | 1 | **0.40*** ** | **0.21** ** |
| | GZnC | | 1 | –0.04 | | 1 | 0.03 |
| | TGW | | | 1 | | | 1 |
| LS | GFeC | 1 | **0.30*** ** | 0.11 | 1 | **0.37*** ** | 0.12 |
| | GZnC | | 1 | 0.1 | | 1 | **–0.29*** ** |
| | TGW | | | 1 | | | 1 |

Significant correlations are given in bold text, *** p < 0.001, **P < 0.01, *p < 0.05.

against genetic distance in base pairs (bps). A large LD block size of 3.49 Mb was observed for the whole genome indicating that SNPs at this block act as inheritance blocks, whereas subgenomes A, B, and D had block sizes of 2.48 Mb, 4.29 Mb, and 3.82 Mb, respectively (Figure 6).

## Genome-wide association study

The GWAS for all three traits, with a BLUP value for each treatment in both of the years separately, across all the years, and the overall BLUP, revealed 36 unique marker trait associations (MTAs) for all three traits put together at the cut-off *p*-value of<0.0001. Among them, five, six, and 10 unique, treatment-specific SNPs were linked to GFeC, GZnC, and TGW, respectively. Similarly, based on combined BLUPs, five SNPs were linked to GFeC, and 10 were linked to TGW (Supplementary Table 3). To enhance the stringency of the selection a Bonferroni correction was applied ($-\log_{10}(p) > 5.45$) and 16 MTAs (five for GFeC, one for GZnC, and 10 for TGW) were retained and they were depicted with Manhattan and quantile–quantile (Q–Q) plots (Figures 7 and 8). SNP AX-94926681 located on 6A at 610.4 Mb was linked with TGW, and was identified under more than one treatment and also under combined BLUPs. Similarly, SNP AX-94393306 was linked with GFeC under LS in 2020 and LS_BLUP across the years. Only one linked SNP AX-95095792 was located on chromosome 4B at 660.4 Mb and was identified for GZnC under IR in 2020. A total of five different SNPs were linked to GFeC and were identified on four different chromosomes: 6D, 3A, 7B, and 3B (Table 4; Figure 9).

## *In silico* analysis

A total of 16 MTAs were retained after stringent selection and were further searched for their candidate genes in a 100-kb

TABLE 3 Distribution of 13,947 filtered SNPs over chromosomes and three subgenomes A, B, and D.

| Chromosome | Subgenome | | | |
|---|---|---|---|---|
| | A | B | D | |
| 1 | 687 | 998 | 890 | |
| 2 | 707 | 927 | 920 | |
| 3 | 623 | 717 | 626 | |
| 4 | 446 | 435 | 274 | |
| 5 | 623 | 762 | 609 | |
| 6 | 495 | 727 | 463 | |
| 7 | 726 | 680 | 612 | |
| Total number of SNPs | 4,307 | 5,246 | 4,394 | 13,947 |

10.3389/fpls.2022.1082513

TABLE 4 Significant marker trait associations (MTAs) with a Bonferroni-corrected *p*-value ($-\log_{10}(p) > 5.45$) for traits under study at each environment.

| Trait | Environment | SNP | Chromosome | Position | *p*-value | $-\log_{10}(p)$ |
|---|---|---|---|---|---|---|
| **Fe** | IR_20 | AX-94877284 | 6D | 4.68E+08 | 5.77E-09 | 8.238789 |
| | RI_ BLUP | AX-95168777 | 3A | 4.02E+08 | 1.29E-07 | 6.890502 |
| | LS_20 | **AX-94393306** | 7B | 6.28E+08 | 3.39E-06 | 5.470092 |
| | LS_21 | AX-94565216 | 3A | 5.72E+08 | 8.49E-08 | 7.071115 |
| | LS_BLUP | **AX-94393306** | 7B | 6.28E+08 | 1.74E-11 | 10.75943 |
| | C_BLUP | AX-94850629 | 3B | 4.74E+08 | 4.63E-09 | 8.334826 |
| **Zn** | IR_20 | AX-95095792 | 4B | 6.6E+08 | 1.17E-07 | 6.929969 |
| **TGW** | IR_20 | **AX-94926681** | 6A | 6.1E+08 | 3.96E-08 | 7.401876 |
| | | AX-94888039 | 4A | 6.82E+08 | 4.15E-07 | 6.381996 |
| | | AX-95133680 | 1D | 3.28E+08 | 7.11E-07 | 6.148171 |
| | IR_BLUP | **AX-94926681** | 6A | 6.1E+08 | 5.05E-10 | 9.296763 |
| | | AX-94488007 | 1B | 5.63E+08 | 3.29E-07 | 6.483375 |
| | | AX-94937080 | 5A | 5.68E+08 | 5.12E-07 | 6.290645 |
| | | AX-95189725 | 6D | 3.86E+08 | 1.98E-06 | 5.702482 |
| | RI_21 | **AX-94926681** | 6A | 6.1E+08 | 5.35E-12 | 11.27166 |
| | | AX-94546067 | 6A | 5.3E+08 | 1.79E-07 | 6.746621 |
| | | AX-94981340 | 3B | 3.96E+08 | 6.07E-07 | 6.217013 |
| | | AX-94950047 | 2B | 2.33E+08 | 1.90E-06 | 5.720823 |
| | RI_BLUP | **AX-94926681** | 6A | 6.1E+08 | 8.73E-11 | 10.05904 |
| | LS_BLUP | **AX-94926681** | 6A | 6.1E+08 | 7.50E-08 | 7.125002 |
| | C_BLUP | **AX-94926681** | 6A | 6.1E+08 | 8.56E-11 | 10.06758 |
| | | AX-94824733 | 3B | 1.95E+08 | 5.82E-08 | 7.235218 |

MTAs identified more than once are given in bold text.

flanking region using sequence information from the SNPs identified with the BLAST search in Ensembl Plants. The SNP AX-94393306, which was present on chromosome 7B, was linked to GFeC and was BLASTed to gene codes for HAUS augmin–like complex subunit 2. A gene ontology study found that the gene was an integral part of the microtubule organizing center, as it plays a role in spindle assembly during cell division. In a 100-kb flanking region of this SNP, there is another transcript coding for the P-loop-containing nucleoside triphosphate hydrolase. Similarly, SNP AX-94850629 was within the region coding for a serine–threonine/tyrosine-protein kinase, which is a catalytic domain with a major role in protein phosphorylation. Two other transcripts coding for the glycoside hydrolase superfamily and the bifunctional inhibitor/plant lipid transfer protein/seed storage helical domain were present in the flanking region of the SNP. Only one MTA AX-95095792 was found to be linked to GZnC at a –log10(*p*) value of 6.92. This MTA was present in the transcribing region codes for restriction endonuclease type II-like protein. In the flanking region of this SNP another two transcribing regions (TraesCS4B02G378800, TraesCS4B02G378500) were identified as coding for cyclophilin-type peptidyl-prolyl cis–trans isomerase domain and tRNA/rRNA methyltransferase, with them having a potential role in protein peptidyl-prolyl isomerization and RNA processing, respectively. A stably identified SNP AX-94926681, linked to TGW, was present in the region coding for ribonuclease H, exonuclease, and RNase T/DNA polymerase III, all of which have crucial roles in nucleic acid binding. Similarly, the location of the transcripts within or near the region of identified MTAs were searched, and are presented in Table 5. Two MTAs namely, AX-94950047 and AX-94824733, were located in the non-genic region.

An expression study of candidate genes using wheat expression data revealed several transcripts, that is, TraesCS4A02G409100, TraesCS6A02G296400, TraesCS3B02G248500, TraesCS1B02G336000 and TraesCS6D02G277900, which had

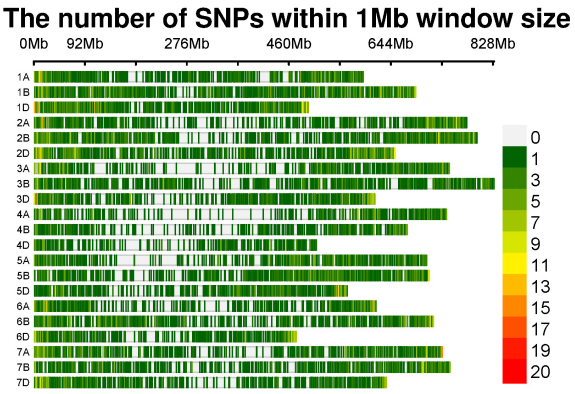


FIGURE 4
SNP density plot indicating the distribution of filtered SNPs across chromosomes.

very high expression in root and shoots, compared with grains and genes, and mainly belonged to MTAs linked to the TGW. The ranges of expression in root, shoot, spike, and grains were 0.03–37.58 TPM, 0.01–24.51 TPM, 0.02–29.37 TPM, and 0–9.18 TPM, respectively. Among the transcripts expressed in grains, TraesCS6D02G394800, TraesCS6D02G278100, TraesCS4A02G409000, and TraesCS1B02G336000 had higher expression than others. Transcript TraesCS1B02G336000 was linked with higher expression in both vegetative tissues and grain (Figure 10). The transcript producing secretory carrier membrane proteins (SCAMPs) was found to be important in subcellular localization and trafficking (Law et al., 2012).

## Discussion

Wheat has nutritional importance in combatting hidden hunger; however, the grain is deficient in iron and zinc. Environmental influence often affects the quality, quantity, and nutritional status of the grain because of environmental influences, such as heat and drought stress, during the growth phase (Sehgal et al., 2018). It is necessary to have a deep knowledge of the genomic region influencing grain iron and zinc content under drought and heat stress in order to develop specific varieties with a high micronutrient status along with a higher yield. Previously identified drought- and its component trait-related QTLs were utilized to improve drought tolerance of varieties through marker-assisted back crossbreeding (Sunilkumar et al., 2022). For such implications, the identification of a marker linked with the trait of interest is a prerequisite. Hence, the use of a diverse mapping panel for the identification of MTAs linked to GFeC, GZnC, and TKW in wheat grown under heat and drought stress along with control plants was attempted in this study.

Analysis of variance for all the studied traits (except GFeC under IR in 2021) in both years showed significant variation among the traits. The trait variations are a prerequisite for genetic studies and a breeding program of the nutrient status of the grain (Cu et al., 2020). Trait values of GFeC and GZnC were enhanced under drought and heat stress, as compared to the control, due to a lower yield, which is called the concentration effect (Oury et al., 2006; Morgounov et al., 2007; Fan et al., 2008; Liu et al., 2014). A greater yield lowers the grain nutrient content due to the dilution effect (Gupta et al., 2021).

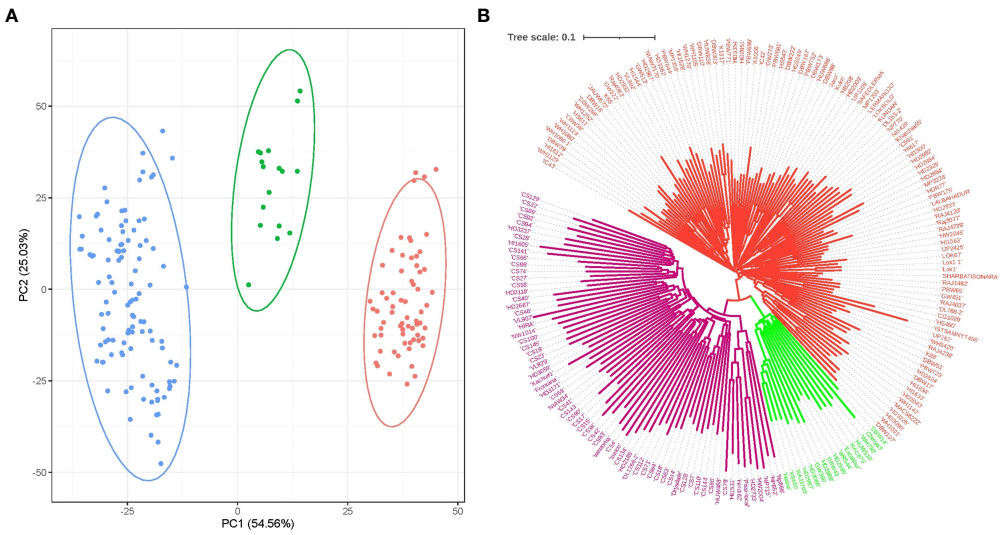


FIGURE 5
Population groupings in the GWAS panel from different models. **(A)** Principal component-based grouping based on PC1 vs. PC2; and **(B)** neighbor-joining tree based on a distance matrix.

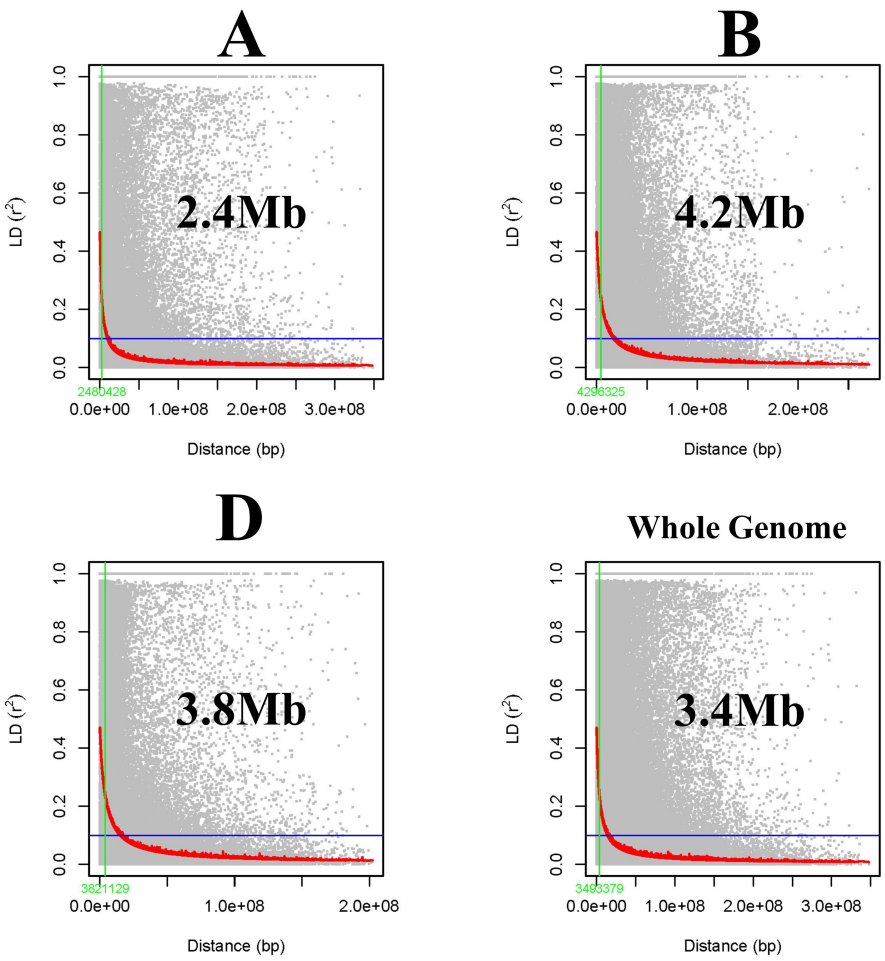


FIGURE 6
Subgenome **(A, B, D)** and whole-genome-wide linkage disequilibrium (LD) decay in the GWAS panel.

However, grain iron and zinc contents were higher in stress conditions, except for GZnC under RI in 2021 (39.24 mg/kg), compared with the control. Given that GFeC and GZnC are complex traits, with a quantitative pattern of inheritance and environmental influence, their expression levels might differ with the season, treatment, and soil nutrient condition, etc.

The coefficient of variation (CV) and broad-sense heritability for GZnC and TKW were higher compared with GFeC. TGW was having high heritability throughout the six environments followed by GZnC, which was similar to previous reports by Krishnappa et al., 2022. Heritability of GFeC was low to medium, having a wide range from 19.42% to 61.43%. Higher heritability indicates the greater contribution of genetic variance to the total variance and indicates the possibility of genetic improvement of traits through marker-assisted selection (Rathan et al., 2022). Inter-season correlation among TGW measured under three different treatments across two years had a strong positive correlation, indicating the higher heritability of the trait. Inter-season correlation for GFeC and GZnC was positive, but the strength was low, similar to a previous report on GZnC (Alomari et al., 2018); this might be because of environmental influence.

We observed that the Pearson correlation coefficient was positive between GFeC and GZnC under all the treatments (except RI in 2020), which was similar to the results reported by Liu et al. (2014); Rathan et al. (2022); Krishnappa et al. (2022). However, Cu et al. (2020) reported both positive and non-significant correlations between GFeC and GZnC in matured and immature grains. TGW had no correlation with GFeC and GZnC in 2020–2021, whereas it showed a positive correlation with GFeC in 2021–2022. Correlation between TGW and GFeC showed positive (Rathan et al., 2022), negative, and no correlations (Cu et al., 2020) in previous studies. Traits harbored by additive gene action and with positive correlation can be improved together efficiently despite environmental influences (Borah et al., 2018).

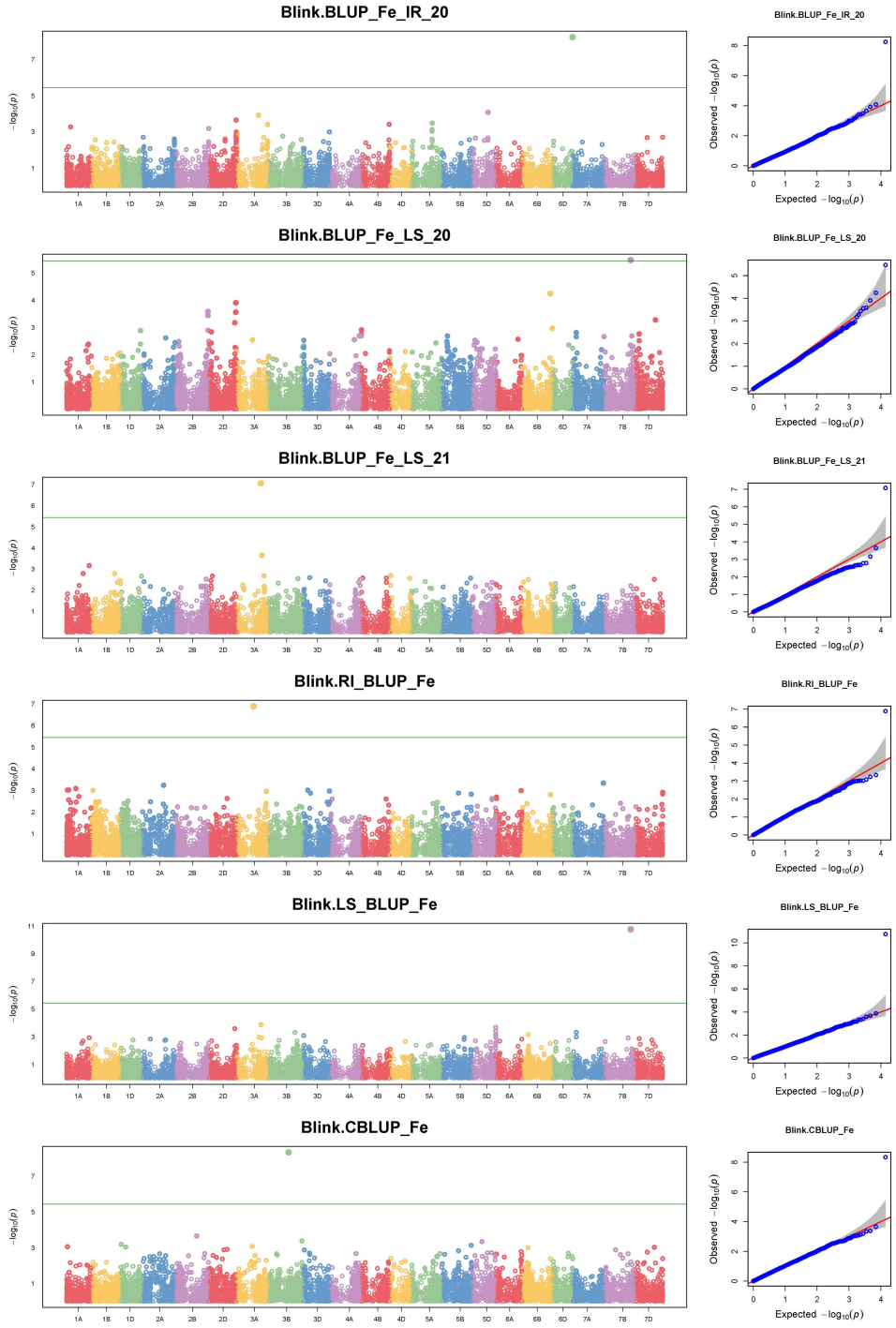


FIGURE 7
Manhattan and respective quantile–quantile (Q–Q) plots of significant associations for GFeC under IR, RI, LS, and combined BLUPs.

The use of structured populations influences the identification of MTAs through GWASs (Pritchard et al., 2000). To nullify this effect, population structure is used as a covariate in the analysis. The present material had three subpopulations, as identified by marker-based PCA. PCA is one of the popular approaches for inferring the population structure of the genome-wide association panel using high-density SNPs (Abraham and Inouye, 2014; Devate et al., 2022a). A diversity tree, based on the genetic distance, confirms that there was sufficient diversity by having three

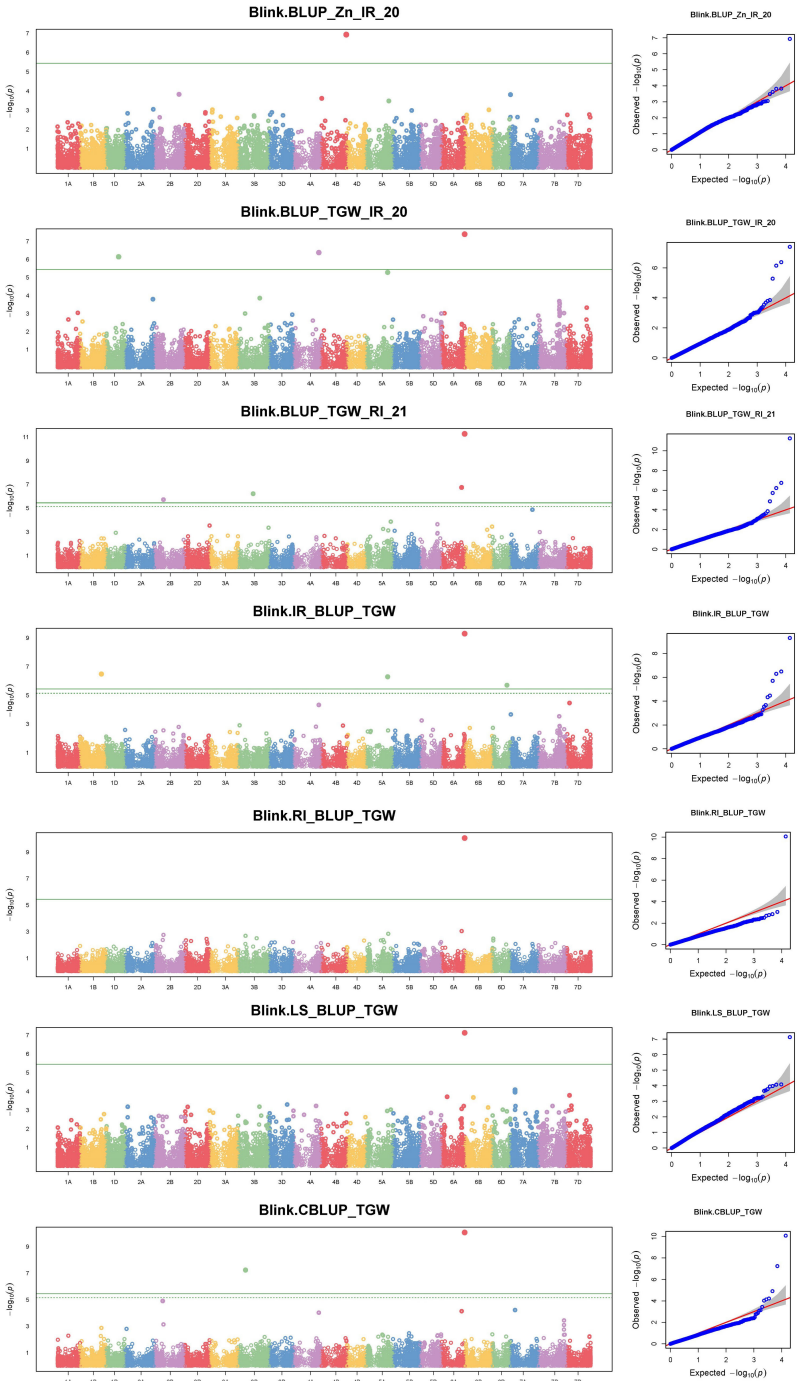


FIGURE 8
Manhattan and respective Q–Q plots of significant associations for GZnC and TGW under IR, RI, LS, and combined BLUPs.

main clusters and many subclusters branching further. The grouping pattern seemed to correlate with the origin of materials. All the core-set lines in the GWAS panel were grouped in one group and the varieties of Indian origin were in another.

The linkage disequilibrium (LD) decay over genetic distance in a population determines the density of marker coverage needed to perform GWASs. A faster LD decay indicates the requirement of a higher marker density to capture the markers close enough to the causal loci (Flint-Garcia et al., 2003). In the

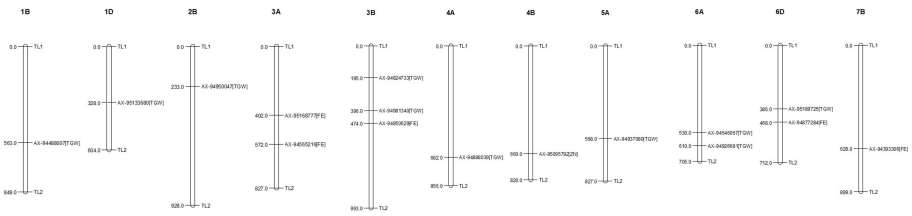


FIGURE 9
Distribution and position (in Mb) of identified marker trait associations (MTAs) at their respective chromosome with associated trait.

present study, a large LD block size was found with 3.49 Mb for the whole genome. The LD for the subgenomes was found to be 2.48 Mb, 4.29 Mb, and 3.82 Mb for A, B, and D genomes, respectively. Similarly, a large LD block size of 4.4 Mb was observed by Pang et al., 2020. In the current study, a low rate of LD decay was observed for the B genome followed by D and A, whereas faster LD decay (Ledesma-Ramírez et al., 2019), as well as slow decay in the D genome, were reported in previous studies (Ogbonnaya et al., 2017; Jamil et al., 2019; Li et al., 2019; Pang et al., 2020; Devate et al., 2022a). The LD may vary in different populations because of population size, genetic drift, admixtures, selection, mutation, non-random mating, pollination behavior, and recombination frequency (Gupta et al., 2005; Vos et al., 2017).

A genome-wide association study was carried out with the BLINK model under GAPIT, which is presumed to be superior for identifying QTNs and avoiding false positives to decipher true associations (Huang et al., 2019). A total of 36 MTAs were identified to be linked to the studied traits at a *p*-value of<0.0001. However, to enhance the stringency of selection to avoid false positives, a Bonferroni correction was applied. A total of 16 stringent markers were found: five for GFeC, one for GZnC, and 10 for TGW. Bonferroni correction is a method to counteract the multiple comparisons problem to reduce type 1 error, i.e., false positives (Kaler and Purcell, 2019).

Recent advances in wheat genome sequencing and annotation made it possible to decipher the candidate genes in the genomic region identified with GWAS, which may be responsible for the variation of the grain nutrient content directly or indirectly by influencing the nutrient metabolism (Cu et al., 2020). Candidate genes located near 100-kb regions of identified MTAs were tabulated with their transcript ID and the probable proteins they code for. Tissue specific expression of genes, responsible for stress management and nutrient content in the grains were identified in the genomic region of linked SNP markers. Stress-related expression of genes in roots, as well as in seed, were identified based on the expression study using the Wheat Expression Database and the Expression Atlas.

Marker trait associations (MTAs) with GFeC were found on chromosomes 3A, 3B, 4B, 6B, and 7D; there have been similar reports on chromosome 3B (Crespo-Herrera et al., 2017; Liu et al., 2019; Cu et al., 2020; Liu et al., 2021; Krishnappa et al., 2022), whereas the rest of the MTAs were novel to this study. The grain iron content-linked SNP marker AX-94877284 was identified to be present near the candidate regions coding for NB-ARC, the winged helix-like DNA-binding domain, and the synaptotagmin-like mitochondrial-lipid-binding domain. The coding regions were identified through *in silico* analysis. Furthermore, the expression study revealed their expression in the grain as well as in the root, and they are an integral part of the membrane, acting as a lipid transporter. These three important proteins have a crucial role in plant disease resistance (Van Ooijen et al., 2008), iron deficiency response (Colangelo and Guerinot, 2004), and homeostasis during abiotic stress (Ruiz-Lopez et al., 2021). As wheat is a hexaploid with three homeologous genomes there is a high chance that similar genes on the respective homeologous chromosomes would be found. An elaborate study of iron deficiency-specific clone 3 (Ids3)-like genes in hexaploid wheat was conducted by Mathpal et al., 2018. The authors found an ortholog on the telomeric region of chromosome 7A and its homolog ranged from 78% to 88% on chromosomes 7D and 7B. Similarly, we found a novel region related to GFeC on chromosome 7B linked to MTA AX-94393306. The region was found to be present near the gene region that encodes the HAUS augmin–like complex subunit. This subunit has an influence on microtubule development during mitosis (Uehara et al., 2009) and on the P-loop-containing nucleoside triphosphate hydrolase whose homologs have the property to bind divalent cation (Tan et al., 2010). Iron has both divalent and trivalent valency. However, the majority of its uptake and assimilation only take place in its divalent status (Tsai and Schmidt, 2017). There is evidence to influence transporters on more than one kind of ions (Pinilla-Tenas et al., 2011; Wang et al., 2012). The candidate region coding for the tyrosinase copper-binding domain, which performs a metal-binding activity (Solano, 2018), was identified in the vicinity of the marker AX-94565216. SNP marker AX-94850629 was linked with the candidate genes coding for the serine–threonine/tyrosine-protein kinase catalytic domain and the bifunctional inhibitor/plant lipid transfer protein/seed

TABLE 5 Putative candidate genes in the 100-kb region of the linked marker with protein produced and gene ontology studies.

| Trait | SNP | Chromosome | TrasID | SNP position on the gene | Protein | Gene ontology | | |
|---|---|---|---|---|---|---|---|---|
| | | | | | | Biological process | Cellular component | Molecular function |
| GFeC | AX-94877284 | 6D | TraesCS6D02G394700 | Exon 3 | P-loop-containing nucleoside triphosphate hydrolase | | | |
| | | | TraesCS6D02G394800 | Flanking | Synaptotagmin-like mitochondrial-lipid-binding domain | Lipid transport | Integral component of membrane | Lipid binding |
| | AX-94393306 | 7B | TraesCS7B02G365000 | 5' UTR | HAUS augmin–like complex subunit 2 | Spindle assembly | Microtubule organizing center organization | |
| | | | TraesCS7B02G365100 | Flanking | P-loop-containing nucleoside triphosphate hydrolase | ADP binding | | |
| | AX-94565216 | 3A | TraesCS3A02G326700 | 5' UTR | Protein coding | | | |
| | | | TraesCS3A02G326600 | Flanking | Di-copper center-containing domain superfamily | | | |
| | AX-94850629 | 3B | TraesCS3B02G295000 | Exon 1 | Serine–threonine/tyrosine-protein kinase, catalytic domain | Protein phosphorylation | ATP binding/ polysaccharide binding | Protein kinase activity |
| | | | TraesCS3B02G294900 | Flanking | Glycoside hydrolase superfamily | Protein phosphorylation, | ATP binding/ hydrolyzing *O*-glycosyl compounds | Hydrolase activity/carbohydrate metabolic process/protein kinase activity |
| | | | TraesCS3B02G294800 | Flanking | Bifunctional inhibitor/plant lipid transfer protein/seed storage helical domain superfamily | Lipid transport | | |
| | AX-95168777 | 3A | TraesCS3A02G219000 | Intron 1 | C-5 cytosine methyltransferase | Negative regulation of gene expression/ epigenetic | Nucleus | Methyltransferase activity |
| GZnC | AX-95095792 | 4B | TraesCS4B02G378700 | Exon 1 | Restriction endonuclease type II like | | | |
| | | | TraesCS4B02G378800 | Flanking | Cyclophilin-type peptidyl-prolyl cis–trans isomerase domain | Protein peptidyl-prolyl isomerization | | Peptidyl-prolyl cis–trans isomerase activity |
| | | | TraesCS4B02G378500 | Flanking | tRNA/rRNA methyltransferase, SpoU type | RNA processing | RNA binding | RNA methyltransferase activity |
| TGW | AX-94926681 | 6A | TraesCS6A02G402600 | 5'UTR | Ribonuclease H-like superfamily | Nucleic acid binding | Integral component of membrane | |
| | | | | | Exonuclease, RNase T/DNA polymerase III | | | |
| | | 4A | TraesCS4A02G409100 | Exon 4 | Chaperonin Cpn60/GroEL | ATP binding | Cytoplasm | Protein folding and re folding |

*(Continued)*





10.3389/fpls.2022.1082513

TABLE 5 Continued

| Trait | SNP | Chromosome | TrasID | SNP position on the gene | Protein | Gene ontology | | |
|---|---|---|---|---|---|---|---|---|
| | | | | | | Biological process | Cellular component | Molecular function |
| | AX-94888039 | | TraesCS4A02G409000 | Flanking | Zinc finger, FYVE/PHD-type | Metal ion binding | Nucleus | Chromatin organization |
| | AX-95133680 | 1D | TraesCS1D02G238600 | Exon 5 | *S*-adenosyl-*L*-methionine-dependent methyltransferase | Methyltransferase activity | | |
| | | | TraesCS1D02G238700 | Flanking | Conserved oligomeric Golgi complex subunit 5 | Intra-Golgi vesicle-mediated transport | Golgi transport complex | |
| | | | TraesCS1D02G238500 | Flanking | DNA-directed RNA polymerase, insert domain superfamily | Transcription, RNA polymerase I and III activity | | DNA binding/protein dimerization activity |
| | AX-94546067 | 6A | TraesCS6A02G296400 | 3'UTR | NUDIX hydrolase domain | Hydrolase activity | | |
| | AX-94981340 | 3B | TraesCS3B02G248500 | Exon 15 | ABC transporter-like, ATP-binding domain | ATPase activity | ATP binding/membrane | Coupled to transmembrane movement of substances |
| | AX-94488007 | 1B | TraesCS1B02G336000 | Intron 7 | Secretory carrier membrane proteins (SCAMPs) | Protein transport | Integral component of membrane | |
| | AX-94937080 | 5A | TraesCS5A02G367700 | Exon 4 | Protein kinase domain | Protein phosphorylation | | ATP binding/protein kinase activity/ protein binding |
| | | | TraesCS5A02G367600 | Flanking | UDP-3-*O*-[3-hydroxymyristoyl] glucosamine *N*-acyltransferase LpxD | Lipid A biosynthetic process | | *N*-acyltransferase activity |
| | AX-95189725 | 6D | TraesCS6D02G277900 | Exon 3 | Ankyrin repeat-containing domain superfamily | Protein binding | Plasma membrane | |
| | | | TraesCS6D02G278000 | Flanking | Pentatricopeptide repeat | Protein binding | | |
| | | | TraesCS6D02G278100 | Flanking | Zinc finger, RING type | | Integral component of membrane | |
| | AX-94950047 | 2B | NA | | | | | |
| | AX-94824733 | 3B | NA | | | | | |





10.3389/fpls.2022.1082513

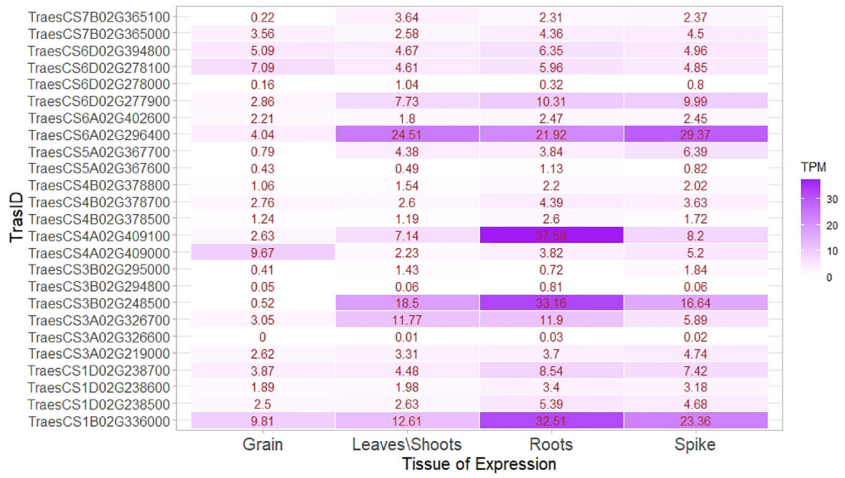


FIGURE 10
Expression heat map of identified genes in important tissues, that is, root, shoot/leaves, spikes, and grain.

storage helical domain. The first gene influences plant responses to stress signals and developmental processes involving modifications in protein Tyr phosphorylation (Shankar et al., 2015). The second gene is a seed storage proteins homolog such as napin from *Brassica napus* (Rico et al., 1996) and 2S albumin from *Ricinus communis* (Pantoja-Uceda et al., 2003). Furthermore, their cellular function was found to be protein phosphorylation and regulation of protein kinase activity. A differential regulation of the transcript during drought and heat stress (Gahlaut et al., 2020) was maintained by a candidate gene near AX-95168777, i.e., C-5 cytosine methyltransferase under the RI condition. Differential regulation of genes may have an influence on nutrient homeostasis in plants.

Stringent selection for MTAs left only one marker AX-95095792 on chromosome 4B linked with grain zinc content. The candidate region is mainly responsible for gene regulation and translation-related activities. Cyclophilin-type peptidyl-prolyl cis–trans isomerase domain, tRNA/rRNA methyltransferase, and SpoU-type proteins were reported in the candidate region. They have functions in the isomerization of the prolyl–peptide bond (Singh et al., 2021) and tRNA modification linked to protein synthesis (Hori, 2017). However, for GZnC, as a quantitative trait, the study revealed its low level of expression in the root as well as the grain and demonstrated it to be a minor gene, which is a common feature of quantitative traits governed by many genes. As housekeeping genes are expressed regularly and have importance in various metabolic and physiological activities of plants, this region might have an indirect influence on the zinc content of grains.

A total of eight unique MTAs were identified for TGW located on chromosomes 1B, 1D, 2B, 3B, 4A, 5A, 6A, and 6D. Similarly, previous studies reported TGW-related QTLs/MTAs on chromosomes 6A (Godoy et al., 2018; Ward et al., 2019; Goel et al., 2019), 5A (Liu et al., 2019; Krishnappa et al., 2022), and 1D (Goel et al., 2019). Stably identified MTA for TGW under different treatments and combined BLUP, AX-94926681 located on chromosome 6A, was identified with transcript TraesCS6A02G402600. The locus codes for three major enzymes ribonuclease H-like and exonuclease and RNase T/DNA polymerase III were identified and are related to the enzymes responsible for nucleic acid metabolism, replication, homologous recombination, DNA repair, transposition (Majorek et al., 2014), epigenetic changes at RNAPIII (Hummel and Liu, 2022), and the repair of double-stranded breaks in *Arabidopsis thaliana* (Peralta-Castro et al., 2020). Their presence as an integral part of the membrane and property of DNA binding further confirms the results based on gene ontology. Another marker, AX-94888039, located in the region responsible for stress management, had candidate genes expressed in the cytoplasm and nucleus. These genes encode chaperonin Cpn60/GroEL, which is involved in abiotic stress-induced expression (Nagaraju et al., 2021), and the zinc finger FYVE/PHD type, which has a role in abiotic stress tolerance by regulating sodium and potassium homeostasis, reactive oxygen species scavenging, and osmotic potential (Zang et al., 2016). Chaperonin Cpn60/GroEL was found to have a very high expression of up to 37.58 TPM in root tissue under abiotic stress conditions. Two MTAs were found to be linked to TGW under RI conditions, that is, AX-94546067 and AX-94981340. Their transcripts code for the NUDIX hydrolase domain and the ABC transporter-like, ATP-binding domain, with their function being related to plant immune responses as found in *Arabidopsis*

*thaliana* (Fonseca and Dong, 2014), the negative regulator in response to drought stress in peach (He et al., 2022), and the transport of substrates into and out of the cytoplasm in plants (Locher, 2016). A secretory pathway, subcellular localization, and trafficking-related secretory carrier membrane proteins (SCAMPs) were found in the region of SNP AX-94488007. The location of marker AX-94488007 was in the seventh intronic region of the gene coding for secretory carrier membrane proteins (SCAMPs) and was found to have very high levels of expression in the root (i.e., 32.51 TPM), as well as in grain (i.e., 9.81 TPM), suggesting the importance of this gene in grain filling. It was also found to have higher levels of expression under abiotic stress conditions of up to 17.81 TPM from the wheat expression database. Photosynthate mobilization and accumulation are key factors that determine the source–sink relationship and, hence, may influence grain filling (Chang and Zhu, 2017). However, further study is required to elucidate the role of candidate genes in determining the TGW. The transcript TraesCS5A02G367700 was linked with a TGW-related SNP, AX-94937080. This was found to code for a protein kinase domain and a G-protein beta WD-40 repeat. WD40 repeat proteins were found to have a role in plant cell wall formation (Guerriero et al., 2015), a unique property of the plant cell. The genomic region of AX-95189725 was located in the third exonic region of gene coding for ankyrin and pentatricopeptide repeat proteins, which are found to be responsible for drought and salt tolerance in *Arabidopsis* and soybean (i.e., gene GmANK114) (Zhao et al., 2020), and pollen development in rice (Zhang et al., 2020). Most of the genes identified in the candidate region were found to play a crucial role in plant development. Many of their homologs have been studied extensively in other species, giving us a broad idea of their role. Expression analysis and gene ontology identified genes with higher expression along with their biological role in the cell organelles. Further study of each of the identified locations could be carried out to gain a better understanding of the genomic region and its potential role in a breeding program.

## Conclusion

The development of biofortified wheat varieties through the transfer of genomic regions associated with higher concentrations of micronutrients in grain will aid in the health of millions of malnourished people suffering from hidden hunger. Genetic biofortification is easy, economical, and sustainable in the long term. Identification of genomic regions using linked markers is a prerequisite to transfer them into the popular cultivars to develop a variety with a higher grain nutrient content. The association mapping panel used in this study with 193 wheat genotypes revealed that GFeC, GZnC, and TGW are complex traits that are quantitatively inherited and strongly influenced by abiotic stress, such as drought and heat stress. The significant positive correlation between the GFeC and GZnC, as well as their high heritability, suggests that simultaneous improvement of both traits can be possible. Five of the 16 stringent MTAs identified were linked to GFeC, one to GZnC, and 10 to TGW, and were located near novel candidate genes that have a direct or indirect effect on traits. Several putative candidate genes identified were found to encode proteins that have important molecular functions in plant ionic balance, protein and enzyme metabolism, and abiotic stress responsiveness, etc. Furthermore, identified MTAs could be subjected to validation and utilized in marker-assisted breeding programs to create biofortified varieties.

## Data availability statement

All the raw data used in this study is available at https://doi.org/10.5061/dryad.0cfxpnw6c.

## Author contributions

PS, NJ, GS, and HK conceptualized the investigation and edited the manuscript. ND conducted the investigation and prepared the draft of the manuscript. ND, CM, and KM generated the phenotypic data. ND, HK, PS, SS, and DC contributed to the generation of genotyping data. ND and HK did the statistical and GWAS analysis. All authors contributed to the article and approved the submitted version.

## Funding

Part of the research was supported by a grant from the Bill and Melinda Gates Foundation (Grant number # OPP1215722) through a sub-grant to the India for Zn Mainstreaming Project and the ICAR -BMGF Project (Grant Number: OPP1194767).

## Acknowledgments

ND acknowledges the Council of Scientific and Industrial Research (CSIR), New Delhi, and the ICAR-Indian Agricultural Research Institute (IARI), New Delhi for scholarships to complete this work as part of their Ph.D. thesis.

## Conflict of interest

The authors declare that the research was conducted in the absence of any commercial or financial relationships that could be construed as a potential conflict of interest.

## Publisher's note

All claims expressed in this article are solely those of the authors and do not necessarily represent those of their affiliated organizations, or those of the publisher, the editors and the reviewers. Any product that may be evaluated in this article, or claim that may be made by its manufacturer, is not guaranteed or endorsed by the publisher.

## Supplementary material

The Supplementary Material for this article can be found online at: https://www.frontiersin.org/articles/10.3389/fpls.2022.1082513/full#supplementary-material

## References


Abraham, G., and Inouye, M. (2014). Fast principal component analysis of large-scale genome-wide data. *PloS One* 9 (4), e93766. doi: 10.1371/journal.pone.0093766

Ahmed, H. G. M. D., Iqbal, M. N., Iqbal, M. A., Zeng, Y., Ullah, A., Iqbal, M., et al. (2021). Genome-wide association mapping for stomata and yield indices in bread wheat under water limited conditions. *Agronomy* 11 (8), 1646. doi: 10.3390/agronomy11081646

Alomari, D. Z., Eggert, K., Von Wiren, N., Alqudah, A. M., Polley, A., Plieske, J., et al. (2018). Identifying candidate genes for enhancing grain zn concentration in wheat. *Front. Plant Sci.* 9, 1313. doi: 10.3389/fpls.2018.01313

Alseekh, S., Kostova, D., Bulut, M., and Fernie, A. R. (2021). Genome-wide association studies: assessing trait characteristics in model and crop plants. *Cell. Mol. Life Sci.* 78 (15), 5743–5754. doi: 10.1007/s00018-021-03868-w

Amiri, R., Bahraminejad, S., Sasani, S., Jalali-Honarmand, S., and Fakhri, R. (2015). Bread wheat genetic variation for grain's protein, iron and zinc concentrations as uptake by their genetic ability. *Eur. J. Agron.* 67, 20–26. doi: 10.1016/j.eja.2015.03.004

Anilkumar, C., Sunitha, N. C., Devate, N. B., and Ramesh, S. (2022). Advances in integrated genomic selection for rapid genetic gain in crop improvement: a review. *Planta* 256 (5), 1–20. doi: 10.1007/s00425-022-03996-y

Aravind, J., Mukesh Sankar, S., Wankhede, D. P., and Kaur, V. (2021). AugmentedRCBD: Analysis of augmented randomised complete block designs. *R Package version* 0.1.5.9000.

Bhatta, M., Baenziger, P. S., Waters, B. M., Poudel, R., Belamkar, V., Poland, J., et al. (2018). Genome-wide association study reveals novel genomic regions associated with 10 grain minerals in synthetic hexaploid wheat. *Int. J. Mol. Sci.* 19 (10), 3237. doi: 10.3390/ijms19103237

Blum, M., Chang, H. Y., Chuguransky, S., Grego, T., Kandasaamy, S., Mitchell, A., et al. (2021). The InterPro protein families and domains database: 20 years on. *Nucleic Acids Res.* 49 (D1), D344–D354. doi: 10.1093/nar/gkaa977

Borah, J., Singode, A., Talukdar, A., Yadav, R. R., and Sarma, R. N. (2018). Genome-wide association studies (GWAS) reveal candidate genes for plant height and number of primary branches in soybean [Glycine max (L.) Merrill]. *Indian J. Genet. Plant Breed.* 78 (04), 460–469.

Borrill, P., Connorton, J. M., Balk, J., Miller, A. J., Sanders, D., and Uauy, C. (2014). Biofortification of wheat grain with iron and zinc: integrating novel genomic resources and knowledge from model crops. *Front. Plant Sci.* 5, 53. doi: 10.3389/fpls.2014.00053

Bouis, H. E., Hotz, C., McClafferty, B., Meenakshi, J. V., and Pfeiffer, W. H. (2011). Biofortification: a new tool to reduce micronutrient malnutrition. *Food Nutr. Bull.* 32 (1_suppl1), S31–S40. doi: 10.1177/15648265110321S105

Bradbury, P. J., Zhang, Z., Kroon, D. E., Casstevens, T. M., Ramdoss, Y., and Buckler, E. S. (2007). TASSEL: Software for association mapping of complex traits in diverse samples 23, 2633–2635. doi: 10.1093/bioinformatics/btm308

Brown, K. H., Rivera, J. A., Bhutta, Z., Gibson, R. S., King, J. C., Lönnerdal, B., et al. (2004). International zinc nutrition consultative group (IZiNCG) technical document 1. assessment of the risk of zinc deficiency in populations and options for its control. *Food Nutr. Bull.* 25 (1 Suppl 2), S99–S203.

Cakmak, I. (2008). Enrichment of cereal grains with zinc: agronomic or genetic biofortification? *Plant Soil* 302 (1), 1–17. doi: 10.1007/s11104-007-9466-3

Chang, T. G., and Zhu, X. G. (2017). Source–sink interaction: a century old concept under the light of modern molecular systems biology. *J. Exp. Bot.* 68 (16), 4417–4431. doi: 10.1093/jxb/erx002

Colangelo, E. P., and Guerinot, M. L. (2004). The essential basic helix-loop-helix protein FIT1 is required for the iron deficiency response. *Plant Cell* 16 (12), 3400–3412. doi: 10.1105/tpc.104.024315

Crespo-Herrera, L. A., Govindan, V., Stangoulis, J., Hao, Y., and Singh, R. P. (2017). QTL mapping of grain zn and fe concentrations in two hexaploid wheat RIL populations with ample transgressive segregation. *Front. Plant Sci.* 8, 1800. doi: 10.3389/fpls.2017.01800

Cu, S. T., Guild, G., Nicolson, A., Velu, G., Singh, R., and Stangoulis, J. (2020). Genetic dissection of zinc, iron, copper, manganese and phosphorus in wheat (Triticum aestivum l.) grain and rachis at two developmental stages. *Plant Sci.* 291, 110338.

Danakumara, T., Kumari, J., Singh, A. K., Sinha, S. K., Pradhan, A. K., Sharma, S., et al. (2021). Genetic dissection of seedling root system architectural traits in a diverse panel of hexaploid wheat through multi-locus genome-wide association mapping for improving drought tolerance. *Int. J. Mol. Sci.* 22 (13), 7188. doi: 10.3390/ijms22137188

Devate, N. B., Krishna, H., Parmeshwarappa, S. K. V., Manjunath, K. K., Chauhan, D., Singh, S., et al. (2022a). Genome wide association mapping for component traits of drought and heat tolerance in wheat. *Front. Plant Sci.* 13, 943033. doi: 10.3389/fpls.2022.943033

Devate, N. B., Krishna, H., Sunilkumar, V. P., Manjunath, K. K., Mishra, C. N., Jain, N., et al. (2022b). Identification of genomic regions of wheat associated with grain fe and zn content under drought and heat stress using genome-wide association study. *Front. Genet.* 13, 1034947. doi: 10.3389/fgene.2022.1034947

Edae, E. A., Byrne, P. F., Haley, S. D., Lopes, M. S., and Reynolds, M. P. (2014). Genome-wide association mapping of yield and yield components of spring wheat under contrasting moisture regimes. *Theor. Appl. Genet.* 127 (4), 791–807. doi: 10.1007/s00122-013-2257-8

Erenoglu, E. B., Kutman, U. B., Ceylan, Y., Yildiz, B., and Cakmak, I. (2011). Improved nitrogen nutrition enhances root uptake, root-to-shoot translocation and remobilization of zinc (65Zn) in wheat. *New Phytol.* 189 (2), 438–448. doi: 10.1111/j.1469-8137.2010.03488.x

Fan, M. S., Zhao, F. J., Fairweather-Tait, S. J., Poulton, P. R., Dunham, S. J., and McGrath, S. P. (2008). Evidence of decreasing mineral density in wheat grain over the last 160 years. *J. Trace Elements Med. Biol.* 22 (4), 315–324. doi: 10.1016/j.jtemb.2008.07.002

Federer, W. T. (1956). "Augmented (or hoonuiaku) designs". *LV(2)* 191–208.

Federer, W. T. (1961). "Augmented designs with one-way elimination of heterogeneity". *Biometrics* 17 (3), 447–473. doi: 10.2307/2527837

Flint-Garcia, S. A., Thornsberry, J. M., and Buckler, E. S.IV (2003). Structure of linkage disequilibrium in plants. *Annu. Rev. Plant Biol.* 54 (1), 357–374. doi: 10.1146/annurev.arplant.54.031902.134907

Fonseca, J. P., and Dong, X. (2014). Functional characterization of a nudix hydrolase AtNUDX8 upon pathogen attack indicates a positive role in plant immune responses. *PloS One* 9 (12), e114119. doi: 10.1371/journal.pone.0114119

Gahlaut, V., Samtani, H., and Khurana, P. (2020). Genome-wide identification and expression profiling of cytosine-5 DNA methyltransferases during drought and heat stress in wheat (Triticum aestivum). *Genomics* 112 (6), 4796–4807. doi: 10.1016/j.ygeno.2020.08.031

Gibson, R. S. (2006). Zinc: the missing link in combating micronutrient malnutrition in developing countries. *Proc. Nutr. Soc.* 65 (1), 51–60. doi: 10.1079/PNS2005474

Godoy, J., Gizaw, S., Chao, S., Blake, N., Carter, A., Cuthbert, R., et al. (2018). Genome-wide association study of agronomic traits in a spring-planted north American elite hard red spring wheat panel. *Crop Sci.* 58 (5), 1838–1852. doi: 10.2135/cropsci2017.07.0423

Goel, S., Singh, K., Singh, B., Grewal, S., Dwivedi, N., Alqarawi, A. A., et al. (2019). Analysis of genetic control and QTL mapping of essential wheat grain quality traits in a recombinant inbred population. *PloS One* 14 (3), e0200669. doi: 10.1371/journal.pone.0200669

Guerriero, G., Hausman, J. F., and Ezcurra, I. (2015). WD40-repeat proteins in plant cell wall formation: Current evidence and research prospects. *Front. Plant Sci.* 6, 1112. doi: 10.3389/fpls.2015.01112

Gupta, P. K., Balyan, H. S., Sharma, S., and Kumar, R. (2021). Biofortification and bioavailability of zn, fe and Se in wheat: present status and future prospects. *Theor. Appl. Genet.* 134 (1), 1–35. doi: 10.1007/s00122-020-03709-7

Gupta, P. K., Rustgi, S., and Kulwal, P. L. (2005). Linkage disequilibrium and association studies in higher plants: present status and future prospects. *Plant Mol. Biol.* 57 (4), 461–485. doi: 10.1007/s11103-005-0257-z

Harikrishna, S., Gajghate, R., Devate, N. B., Shiv, A., Mehta, B. K., Sunilkumar, V. P., et al. (2022). "Breaking the yield barriers to enhance genetic gains in wheat," in *New horizons in wheat and barley research* (Singapore: Springer), pp179–pp226.

He, H., Zhang, Y., Wen, B., Meng, X., Wang, N., Sun, M., et al. (2022). PpNUDX8, a peach NUDIX hydrolase, plays a negative regulator in response to drought stress. *Front. Plant Sci.* 12, 831883. doi: 10.3389/fpls.2021.831883

Hori, H. (2017). Transfer RNA methyltransferases with a SpoU-TrmD (SPOUT) fold and their modified nucleosides in tRNA. *Biomolecules* 7 (1), 23. doi: 10.3390/biom7010023

Huang, M., Liu, X., Zhou, Y., Summers, R. M., and Zhang, Z. (2019). BLINK: a package for the next level of genome wide association studies with both individuals and markers in the millions. *Gigascience* 8 (2), giy154. doi: 10.1093/gigascience/giy154

Hummel, G., and Liu, C. (2022). Organization and epigenomic control of RNA polymerase III-transcribed genes in plants. *Curr. Opin. Plant Biol.* 67, 102199. doi: 10.1016/j.pbi.2022.102199

Jamil, M., Ali, A., Gul, A., Ghafoor, A., Napar, A. A., Ibrahim, A. M., et al. (2019). Genome-wide association studies of seven agronomic traits under two sowing conditions in bread wheat. *BMC Plant Biol.* 19 (1), 1–18. doi: 10.1186/s12870-019-1754-6

Jin, H., Wen, W., Liu, J., Zhai, S., Zhang, Y., Yan, J., et al. (2016). Genome-wide QTL mapping for wheat processing quality parameters in a gaocheng 8901/Zhoumai 16 recombinant inbred line population. *Front. Plant Sci.* 7, 1032. doi: 10.3389/fpls.2016.01032

Kaler, A. S., and Purcell, L. C. (2019). Estimation of a significance threshold for genome-wide association studies. *BMC Genomics* 20 (1), 1–8. doi: 10.1186/s12864-019-5992-7

Khan, H., Krishnappa, G., Kumar, S., Mishra, C. N., Krishna, H., Devate, N. B., et al. (2022). Genome-wide association study for grain yield and component traits in bread wheat (Triticum aestivum l.). *Front. Genet.* 13, 982589. doi: 10.3389/fgene.2022.982589

Khoshgoftarmanesh, A. H., Schulin, R., Chaney, R. L., Daneshbakhsh, B., and Afyuni, M. (2011). Micronutrient-efficient genotypes for crop yield and nutritional quality in sustainable agriculture. *Sustain. Agric.* Volume 2, 219–249. doi: 10.1007/978-94-007-0394-0_13

Krishnappa, G., Khan, H., Krishna, H., Kumar, S., Mishra, C. N., Parkash, O., et al. (2022). Genetic dissection of grain iron and zinc, and thousand kernel weight in wheat (Triticum aestivum l.) using genome-wide association study. *Sci. Rep.* 12 (1), 1–14.

Krishnappa, G., Savadi, S., Tyagi, B. S., Singh, S. K., Mamrutha, H. M., Kumar, S., et al. (2021). Integrated genomic selection for rapid improvement of crops. *Genomics* 113 (3), 1070–1086. doi: 10.1016/j.ygeno.2021.02.007

Krishnappa, G., Singh, A. M., Chaudhary, S., Ahlawat, A. K., Singh, S. K., Shukla, R. B., et al. (2017). Molecular mapping of the grain iron and zinc concentration, protein content and thousand kernel weight in wheat (Triticum aestivum l.). *PloS One* 12 (4), e0174972. doi: 10.1371/journal.pone.0174972

Kumar, J., Saripalli, G., Gahlaut, V., Goel, N., Meher, P. K., Mishra, K. K., et al. (2018). Genetics of fe, zn, β-carotene, GPC and yield traits in bread wheat (Triticum aestivum l.) using multi-locus and multi-traits GWAS. *Euphytica* 214 (11), 1–17.

Kutman, U. B., Kutman, B. Y., Ceylan, Y., Ova, E. A., and Cakmak, I. (2012). Contributions of root uptake and remobilization to grain zinc accumulation in wheat depending on post-anthesis zinc availability and nitrogen nutrition. *Plant Soil* 361 (1), 177–187. doi: 10.1007/s11104-012-1300-x

Law, A. H.Y., Chow, C. M., and Jiang, L. (2012). Secretory carrier membrane proteins. *Protoplasma*, 249(2), 269–283.

Ledesma-Ramírez, L., Solís-Moya, E., Iturriaga, G., Sehgal, D., Reyes-Valdes, M. H., Montero-Tavera, V., et al. (2019). GWAS to identify genetic loci for resistance to yellow rust in wheat pre-breeding lines derived from diverse exotic crosses. *Front. Plant Sci.* 1390. doi: 10.3389/fpls.2019.01390

Lipka, A. E., Tian, F., Wang, Q., Peiffer, J., Li, M., et al. (2012). GAPIT: genome association and prediction integrated tool. *Bioinformatics* 28, 2397–2399. doi: 10.1093/bioinformatics/bts444

Liu, Y., Chen, Y., Yang, Y., Zhang, Q., Fu, B., Cai, J., et al. (2021). A thorough screening based on QTLs controlling zinc and copper accumulation in the grain of different wheat genotypes. *Environ. Sci. pollut. Res.* 28 (12), 15043–15054. doi: 10.1007/s11356-020-11690-3

Liu, J., Feng, B., Xu, Z. B., Fan, X. L., Jiang, F., Jin, X. F., et al. (2018). A genomewide association study of wheat yield and quality-related traits in southwest China. *Mol. Breed.* 38, 1. doi: 10.1007/s11032-017-0759-9

Liu, H., Wang, Z. H., Li, F., Li, K., Yang, N., Yang, Y., et al. (2014). Grain iron and zinc concentrations of wheat and their relationships to yield in major wheat production areas in China. *Field Crops Res.* 156, 151–160. doi: 10.1016/j.fcr.2013.11.011

Liu, J., Wu, B., Singh, R. P., and Velu, G. (2019). QTL mapping for micronutrients concentration and yield component traits in a hexaploid wheat mapping population. *J. Cereal Sci.* 88, 57–64. doi: 10.1016/j.jcs.2019.05.008

Li, G., Xu, X., Tan, C., Carver, B. F., Bai, G., Wang, X., et al. (2019). Identification of powdery mildew resistance loci in wheat by integrating genome-wide association study (GWAS) and linkage mapping. *Crop J.* 7 (3), 294–306. doi: 10.1016/j.cj.2019.01.005

Locher, K. P. (2016). Mechanistic diversity in ATP-binding cassette (ABC) transporters. *Nat. Struct. Mol. Biol.* 23 (6), 487–493. doi: 10.1038/nsmb.3216

Majorek, K. A., Dunin-Horkawicz, S., Steczkiewicz, K., Muszewska, A., Nowotny, M., Ginalski, K., et al. (2014). The RNase h-like superfamily: new members, comparative structural analysis and evolutionary classification. *Nucleic Acids Res.* 42 (7), 4160–4179. doi: 10.1093/nar/gkt1414

Mathpal, P., Kumar, U., Kumar, A., Kumar, S., Malik, S., Kumar, N., et al. (2018). Identification, expression analysis, and molecular modeling of iron-deficiency-specific clone 3 (Ids3)-like gene in hexaploid wheat. *3 Biotech.* 8 (4), 1–11. doi: 10.1007/s13205-018-1230-2

Morgounov, A., Gómez-Becerra, H. F., Abugalieva, A., Dzhunusova, M., Yessimbekova, M., Muminjanov, H., et al. (2007). Iron and zinc grain density in common wheat grown in central Asia. *Euphytica* 155 (1), 193–203. doi: 10.1007/s10681-006-9321-2

Murphy, K. M., Reeves, P. G., and Jones, S. S. (2008). Relationship between yield and mineral nutrient concentrations in historical and modern spring wheat cultivars. *Euphytica* 163 (3), 381–390. doi: 10.1007/s10681-008-9681-x

Murray, M. G., and Thompson, W. F. (1980). Rapid isolation of high molecularweight plant DNA. *Nucleic Acids Res.* 8, 4321–4325. doi: 10.1093/nar/8.19.4321

Nagaraju, M., Kumar, A., Jalaja, N., Rao, D. M., and Kishor, P. B. (2021). Functional exploration of chaperonin (HSP60/10) family genes and their abiotic stress-induced expression patterns in sorghum bicolor. *Curr. Genomics* 22 (2), 137–152. doi: 10.2174/1389202922666210324154336

Ogbonnaya, F. C., Rasheed, A., Okechukwu, E. C., Jighly, A., Makdis, F., Wuletaw, T., et al. (2017). Genome-wide association study for agronomic and physiological traits in spring wheat evaluated in a range of heat prone environments. *Theor. Appl. Genet.* 130 (9), 1819–1835. doi: 10.1007/s00122-017-2927-z

Oury, F. X., Leenhardt, F., Remesy, C., Chanliaud, E., Duperrier, B., Balfourier, F., et al. (2006). Genetic variability and stability of grain magnesium, zinc and iron concentrations in bread wheat. *Eur. J. Agron.* 25 (2), 177–185. doi: 10.1016/j.eja.2006.04.011

Paltridge, N. G., Milham, P. J., Ortiz-Monasterio, J. I., Velu, G., Yasmin, Z., Palmer, L. J., et al. (2012). Energy-dispersive X-ray fluorescence spectrometry as a tool for zinc, iron and selenium analysis in whole grain wheat. *Plant Soil* 361 (1), 261–269. doi: 10.1007/s11104-012-1423-0

Pang, Y., Liu, C., Wang, D., Amand, P. S., Bernardo, A., Li, W., et al. (2020). High-resolution genome-wide association study identifies genomic regions and candidate genes for important agronomic traits in wheat. *Mol. Plant* 13 (9), 1311–1327. doi: 10.1016/j.molp.2020.07.008

Pantoja-Uceda, D., Bruix, M., Giménez-Gallego, G., Rico, M., and Santoro, J. (2003). Solution structure of RicC3, a 2S albumin storage protein from ricinus communis. *Biochemistry* 42 (47), 13839–13847. doi: 10.1021/bi0352217

Papatheodorou, I., Moreno, P., Manning, J., Fuentes, A. M. P., George, N., Fexova, S., et al. (2020). Expression atlas update: from tissues to single cells. *Nucleic Acids Res.* 48 (D1), D77–D83.

Peralta-Castro, A., García-Medel, P. L., Baruch-Torres, N., Trasviña-Arenas, C. H., Juarez-Quintero, V., Morales-Vazquez, C. M., et al. (2020). Plant organellar DNA polymerases evolved multifunctionality through the acquisition of novel amino acid insertions. *Genes* 11 (11), 1370. doi: 10.3390/genes11111370

Pingali, P. L. (2012). Green revolution: impacts, limits, and the path ahead. *Proc. Natl. Acad. Sci.* 109 (31), 12302–12308. doi: 10.1073/pnas.0912953109

Pinilla-Tenas, J. J., Sparkman, B. K., Shawki, A., Illing, A. C., Mitchell, C. J., Zhao, N., et al. (2011). Zip14 is a complex broad-scope metal-ion transporter whose functional properties support roles in the cellular uptake of zinc and nontransferrin-bound iron. *Am. J. Physiology-Cell Physiol.* 301 (4), C862–C871. doi: 10.1152/ajpcell.00479.2010

Pritchard, J. K., Stephens, M., Rosenberg, N. A., and Donnelly, P. (2000). Association mapping in structured populations. *Am. J. Hum. Genet.* 67 (1), 170–181. doi: 10.1086/302959

Puttamadanayaka, S., Harikrishna,, Balaramaiah, M., Biradar, S., Parmeshwarappa, S. V., Sinha, N., et al. (2020). Mapping genomic regions of moisture deficit stress tolerance using backcross inbred lines in wheat (Triticum aestivum l.). *Sci. Rep.* 10 (1), 1–17. doi: 10.1038/s41598-020-78671-x

Ramírez-González, R. H., Borrill, P., Lang, D., Harrington, S. A., Brinton, J., Venturini, L., et al. (2018). The transcriptional landscape of polyploid wheat. *Science* 361 (6403), eaar6089.

Rathan, N. D., Krishna, H., Ellur, R. K., Sehgal, D., Govindan, V., Ahlawat, A. K., et al. (2022). Genetic dissection of grain zinc and iron concentration, protein content, test weight and thousand kernel weight in wheat (Triticum aestivum l.) through genome wide association study.

Remington, D. L., Thornsberry, J. M., Matsuoka, Y., Wilson, L. M., Whitt, S. R., Doebley, J., et al. (2001). Structure of linkage disequilibrium and phenotypic associations in the maize genome. *Proc. Natl. Acad. Sci.* 98 (20), 11479–11484. doi: 10.1073/pnas.201394398

Rico, M., Bruix, M., González, C., Monsalve, R. I., and Rodríguez, R. (1996). 1H NMR assignment and global fold of napin BnIb, a representative 2S albumin seed protein. *Biochemistry* 35 (49), 15672–15682. doi: 10.1021/bi961748q

Rodríguez, F., Alvarado, G., Pacheco, Á., and Burgueño, J. (2018). ACBD-r augmented complete block design with r for windows, version 4.0. *CIMMYT Res. Data Software Repository Network*.

Roncallo, P. F., Larsen, A. O., Achilli, A. L., Pierre, C. S., Gallo, C. A., Dreisigacker, S., et al. (2021). Linkage disequilibrium patterns, population structure and diversity analysis in a worldwide durum wheat collection including Argentinian genotypes. *BMC Genomics* 22 (1), 1–17. doi: 10.1186/s12864-021-07519-z

Ruiz-Lopez, N., Pérez-Sancho, J., Del Valle, A. E., Haslam, R. P., Vanneste, S., Catalá, R., et al. (2021). Synaptotagmins at the endoplasmic reticulum–plasma membrane contact sites maintain diacylglycerol homeostasis during abiotic stress. *Plant Cell* 33 (7), 2431–2453. doi: 10.1093/plcell/koab122

Saini, D. K., Chopra, Y., Singh, J., Sandhu, K. S., Kumar, A., Bazzer, S., et al. (2022). Comprehensive evaluation of mapping complex traits in wheat using genome-wide association studies. *Mol. Breed.* 42 (1), 1–52. doi: 10.1007/s11032-021-01272-7

Samineni, S., Mahendrakar, M. D., Hotti, A., Chand, U., Rathore, A., and Gaur, P. M. (2022). Impact of heat and drought stresses on grain nutrient content in chickpea: Genome-wide marker-trait associations for protein, fe and zn. *Environ. Exp. Bot.* 194, 104688. doi: 10.1016/j.envexpbot.2021.104688

Searle, S. R. (1965). "Computing formulae for analyzing augmented randomized complete block designs," in *Technical report BU-207-M* (New York: Cornell University).

Sehgal, A., Sita, K., Siddique, K. H., Kumar, R., Bhogireddy, S., Varshney, R. K., et al. (2018). Drought or/and heat-stress effects on seed filling in food crops: impacts on functional biochemistry, seed yields, and nutritional quality. *Front. Plant Sci.* 9, 1705. doi: 10.3389/fpls.2018.01705

Shankar, A., Agrawal, N., Sharma, M., Pandey, A., and K Pandey, G. (2015). Role of protein tyrosine phosphatases in plants. *Curr. Genomics* 16 (4), 224–236. doi: 10.2174/1389202916666150424234300

Singh, M., Kaur, K., Sharma, A., Kaur, R., Joshi, D., Chatterjee, M., et al. (2021). Genome-wide characterization of peptidyl-prolyl cis–trans isomerases in penicillium and their regulation by salt stress in a halotolerant p. oxalicum. *Sci. Rep.* 11 (1), 1–19. doi: 10.1038/s41598-021-91602-8

Solano, F. (2018). On the metal cofactor in the tyrosinase family. *Int. J. Mol. Sci.* 19 (2), 633. doi: 10.3390/ijms19020633

Srivastava, R. K., Singh, R. B., Pujarula, V. L., Bollam, S., Pusuluri, M., Chellapilla, T. S., et al. (2020). Genome-wide association studies and genomic selection in pearl millet: Advances and prospects. *Front. Genet.* 10, 1389. doi: 10.3389/fgene.2019.01389

Sukumaran, S., Dreisigacker, S., Lopes, M., Chavez, P., and Reynolds, M. P. (2015). Genome-wide association study for grain yield and related traits in an elite spring wheat population grown in temperate irrigated environments. *Theor. Appl. Genet.* 128 (2), 353–363. doi: 10.1007/s00122-014-2435-3

Sunilkumar, V. P., Krishna, H., Devate, N. B., Manjunath, K. K., Chauhan, D., Singh, S., et al. (2022). Marker assisted improvement for leaf rust and moisture deficit stress tolerance in wheat variety HD3086. *Front. Plant Science.* 13, 1035016. doi: 10.3389/fpls.2022.1035016

Sunil, H., Upadhyay, D., Gajghate, R., Shashikumara, P., Chouhan, D., Singh, S., et al. (2020). QTL mapping for heat tolerance related traits using backcross inbred lines in wheat (Triticum aestivum l.). *Indian J. Genet. Plant Breed.* 80 (3), 242–249.

Tan, Y. F., O'Toole, N., Taylor, N. L., and Millar, A. H. (2010). Divalent metal ions in plant mitochondria and their role in interactions with proteins and oxidative stress-induced damage to respiratory function. *Plant Physiol.* 152 (2), 747–761. doi: 10.1104/pp.109.147942

Tibbs Cortes, L., Zhang, Z., and Yu, J. (2021). Status and prospects of genome-wide association studies in plants. *Plant Genome* 14 (1), e20077.

Tiwari, A., Choudhary, S., Padiya, J., Ubale, A., Mikkilineni, V., and Char, B. (2022). Recent advances and applicability of GBS, GWAS, and GS in maize. *Genotyping by Sequencing Crop Improvement*, 188–217. doi: 10.1002/9781119745686.ch9

Tsai, H. H., and Schmidt, W. (2017). One way. or another? iron uptake in plants. *New Phytol.* 214 (2), 500–505.

Uehara, R., Nozawa, R. S., Tomioka, A., Petry, S., Vale, R. D., Obuse, C., et al. (2009). The augmin complex plays a critical role in spindle microtubule generation for mitotic progression and cytokinesis in human cells. *Proc. Natl. Acad. Sci.* 106 (17), 6998–7003. doi: 10.1073/pnas.0901587106

Van Ooijen, G., Mayr, G., Kasiem, M. M., Albrecht, M., Cornelissen, B. J., and Takken, F. L. (2008). Structure–function analysis of the NB-ARC domain of plant disease resistance proteins. *J. Exp. Bot.* 59 (6), 1383–1397. doi: 10.1093/jxb/ern045

Velu, G., Guzman, C., Mondal, S., Autrique, J. E., Huerta, J., and Singh, R. P. (2016). Effect of drought and elevated temperature on grain zinc and iron concentrations in CIMMYT spring wheat. *J. Cereal Sci.* 69, 182–186. doi: 10.1016/j.jcs.2016.03.006

Velu, G., Singh, R. P., Crespo-Herrera, L., Juliana, P., Dreisigacker, S., Valluru, R., et al. (2018). Genetic dissection of grain zinc concentration in spring wheat for mainstreaming biofortification in CIMMYT wheat breeding. *Sci. Rep.* 8 (1), 1–10. doi: 10.1038/s41598-018-31951-z

Velu, G., Tutus, Y., Gomez-Becerra, H. F., Hao, Y., Demir, L., Kara, R., et al. (2017). QTL mapping for grain zinc and iron concentrations and zinc efficiency in a tetraploid and hexaploid wheat mapping populations. *Plant Soil* 411 (1), 81–99. doi: 10.1007/s11104-016-3025-8

Vos, P. G., Paulo, M. J., Voorrips, R. E., Visser, R. G., van Eck, H. J., and van Eeuwijk, F. A. (2017). Evaluation of LD decay and various LD-decay estimators in simulated and SNP-array data of tetraploid potato. *Theor. Appl. Genet.* 130 (1), 123–135. doi: 10.1007/s00122-016-2798-8

Wang, C. Y., Jenkitkasemwong, S., Duarte, S., Sparkman, B. K., Shawki, A., Mackenzie, B., et al. (2012). ZIP8 is an iron and zinc transporter whose cell-surface expression is up-regulated by cellular iron loading. *J. Biol. Chem.* 287 (41), 34032–34043. doi: 10.1074/jbc.M112.367284

Wang, Y., Xu, X., Hao, Y., Zhang, Y., Liu, Y., Pu, Z., et al. (2021). QTL mapping for grain zinc and iron concentrations in bread wheat. *Front. Nutr.* 229. doi: 10.3389/fnut.2021.680391

Wang, S., Yin, L., Tanaka, H., Tanaka, K., and Tsujimoto, H. (2011). Wheat-aegilops chromosome addition lines showing high iron and zinc contents in grains. *Breed. Sci.* 61 (2), 189–195. doi: 10.1270/jsbbs.61.189

Ward, B. P., Brown-Guedira, G., Kolb, F. L., Van Sanford, D. A., Tyagi, P., Sneller, C. H., et al. (2019). Genome-wide association studies for yield-related traits in soft red winter wheat grown in Virginia. *PloS One* 14 (2), e0208217. doi: 10.1371/journal.pone.0208217

Welch, R. M., and Graham, R. D. (1999). A new paradigm for world agriculture: meeting human needs: productive, sustainable, nutritious. *Field Crops Res.* 60 (1-2), 1–10.

Xu, Y., An, D., Liu, D., Zhang, A., Xu, H., and Li, B. (2012). Molecular mapping of QTLs for grain zinc, iron and protein concentration of wheat across two environments. *Field Crops Res.* 138, 57–62. doi: 10.1016/j.fcr.2012.09.017

Yadav, O. P., Singh, D. V., Dhillon, B. S., and Mohapatra, T. (2019). India's evergreen revolution in cereals. *Curr. Sci.* 116 (11), 1805–1808. doi: 10.18520/cs/v116/i11/1805-1808

Yates, A. D., Allen, J., Amode, R. M., Azov, A. G., Barba, M., Becerra, A., et al. (2022). Ensembl genomes 2022: an expanding genome resource for non-vertebrates. *Nucleic Acids Res.* 50 (D1), D996–D1003. doi: 10.1093/nar/gkab1007

Zahra, N., Wahid, A., Hafeez, M. B., Ullah, A., Siddique, K. H., and Farooq, M. (2021). Grain development in wheat under combined heat and drought stress: Plant responses and management. *Environ. Exp. Bot.* 188, 104517. doi: 10.1016/j.envexpbot.2021.104517

Zang, D., Li, H., Xu, H., Zhang, W., Zhang, Y., Shi, X., et al. (2016). An arabidopsis zinc finger protein increases abiotic stress tolerance by regulating sodium and potassium homeostasis, reactive oxygen species scavenging and osmotic potential. *Front. Plant Sci.* 7, 1272. doi: 10.3389/fpls.2016.01272

Zhang, Q., Xu, Y., Huang, J., Zhang, K., Xiao, H., Qin, X., et al. (2020). The rice pentatricopeptide repeat protein PPR756 is involved in pollen development by affecting multiple RNA editing in mitochondria. *Front. Plant Sci.* 11, 749. doi: 10.3389/fpls.2020.00749

Zhao, J. Y., Lu, Z. W., Sun, Y., Fang, Z. W., Chen, J., Zhou, Y. B., et al. (2020). The ankyrin-repeat gene GmANK114 confers drought and salt tolerance in arabidopsis and soybean. *Front. Plant Sci.* 11, 584167. doi: 10.3389/fpls.2020.584167

# Frontiers in
# Plant Science

**Cultivates the science of plant biology and its applications**

The most cited plant science journal, which advances our understanding of plant biology for sustainable food security, functional ecosystems and human health.

---

## Discover the latest Research Topics

See more →

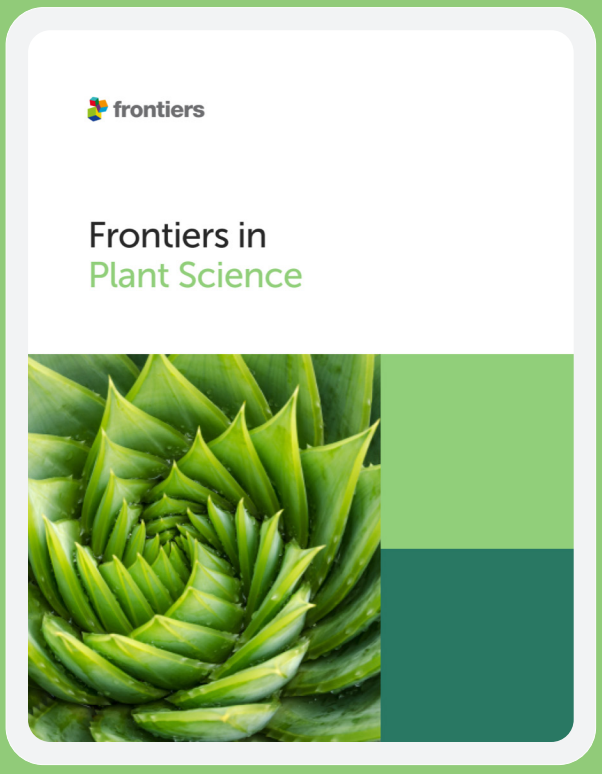


**Frontiers**

Avenue du Tribunal-Fédéral 34
1005 Lausanne, Switzerland
frontiersin.org

**Contact us**

+41 (0)21 510 17 00
frontiersin.org/about/contact